

World Journal of *Gastroenterology*

World J Gastroenterol 2012 August 21; 18(31): 4071-4242



Editorial Board

2010-2013

The *World Journal of Gastroenterology* Editorial Board consists of 1352 members, representing a team of worldwide experts in gastroenterology and hepatology. They are from 64 countries, including Albania (1), Argentina (8), Australia (33), Austria (15), Belgium (14), Brazil (13), Brunei Darussalam (1), Bulgaria (2), Canada (21), Chile (3), China (82), Colombia (1), Croatia (2), Cuba (1), Czech (6), Denmark (9), Ecuador (1), Egypt (4), Estonia (2), Finland (8), France (29), Germany (87), Greece (22), Hungary (11), India (32), Indonesia (2), Iran (10), Ireland (6), Israel (13), Italy (124), Japan (140), Jordan (2), Kuwait (1), Lebanon (4), Lithuania (2), Malaysia (1), Mexico (11), Morocco (1), Moldova (1), Netherlands (32), New Zealand (2), Norway (13), Pakistan (2), Poland (11), Portugal (6), Romania (4), Russia (1), Saudi Arabia (3), Serbia (3), Singapore (11), Slovenia (1), South Africa (3), South Korea (46), Spain (43), Sri Lanka (1), Sweden (17), Switzerland (12), Thailand (1), Trinidad and Tobago (1), Turkey (30), United Arab Emirates (2), United Kingdom (95), United States (285), and Uruguay (1).

HONORARY EDITORS-IN-CHIEF

James L Boyer, *New Haven*
Ke-Ji Chen, *Beijing*
Martin H Floch, *New Haven*
Bo-Rong Pan, *Xi'an*
Eamonn M Quigley, *Cork*
Rafiq A Sheikh, *Sacramento*
Nicholas J Talley, *Rochester*

EDITOR-IN-CHIEF

Ferruccio Bonino, *Pisa*
Myung-Hwan Kim, *Seoul*
Kjell Öberg, *Uppsala*
Matt Rutter, *Stockton-on-Tees*
Andrzej S Tarnawski, *Long Beach*

STRATEGY ASSOCIATE EDITORS-IN-CHIEF

You-Yong Lu, *Beijing*
Peter Draganov, *Florida*
Hugh J Freeman, *Vancouver*
Maria Concepción Gutiérrez-Ruiz, *México*
Kazuhiro Hanazaki, *Kochi*
Akio Inui, *Kagoshima*
Kalpesh Jani, *Baroda*
Javier San Martin, *Punta del Este*
Natalia A Osna, *Omaha*
Wei Tang, *Tokyo*
Alan BR Thomson, *Edmonton*
Harry Hua-Xiang Xia, *Livingston*
John M Luk, *Hong Kong*
Hiroshi Shimada, *Yokohama*

GUEST EDITORIAL BOARD MEMBERS

Jiunn-Jong Wu, *Tainan*

Cheng-Shyong Wu, *Chia-Yi*
Ta-Sen Yeh, *Taoyuan*
Tsung-Hui Hu, *Kaohsiung*
Chuah Seng-Kee, *Kaohsiung*
I-Rue Lai, *Taipei*
Jin-Town Wang, *Taipei*
Ming-Shiang Wu, *Taipei*
Teng-Yu Lee, *Taichung*
Yang-Yuan Chen, *Changhua*
Po-Shiuan Hsieh, *Taipei*
Chao-Hung Hung, *Kaohsiung*
Hon-Yi Shi, *Kaohsiung*
Hui-kang Liu, *Taipei*
Jen-Hwey Chiu, *Taipei*
Chih-Chi Wang, *Kaohsiung*
Wan-Long Chuang, *Kaohsiung*
Wen-Hsin Huang, *Taichung*
Hsu-Heng Yen, *Changhua*
Ching Chung Lin, *Taipei*
Chien-Jen Chen, *Taipei*
Jaw-Ching Wu, *Taipei*
Ming-Chih Hou, *Taipei*
Kevin Cheng-Wen Hsiao, *Taipei*
Chiun Hsu, *Taipei*
Yu-Jen Chen, *Taipei*
Chen Hsiu-Hsi Chen, *Taipei*
Liang-Shun Wang, *Taipei*
hun-Fa Yang, *Taichung*
Min-Hsiung Pan, *Kaohsiung*
Chun-Hung Lin, *Taipei*
Ming-Whei Yu, *Taipei*
Chuen Hsueh, *Taoyuan*
Hsiu-Po Wang, *Taipei*
Lein-Ray Mo, *Tainan*
Ming-Lung Yu, *Kaohsiung*

MEMBERS OF THE EDITORIAL BOARD



Albania

Bashkim Resuli, *Tirana*



Argentina

Julio H Carri, *Córdoba*
Bernabe Matias Quesada, *Buenos Aires*
Bernardo Frider, *Buenos Aires*
Maria Ines Vaccaro, *Buenos Aires*
Eduardo de Santibañes, *Buenos Aires*
Adriana M Torres, *Rosario*
Carlos J Pirola, *Buenos Aires*
Silvia Sookoian, *Buenos Aires*



Australia

Finlay A Macrae, *Victoria*
David Ian Watson, *Bedford Park*
Jacob George, *Sydney*
Leon Anton Adams, *Nedlands*
Minoti V Apte, *Liverpool*
Andrew V Biankin, *Sydney*
Filip Braet, *Sydney*
Guy D Eslick, *Sydney*
Michael A Fink, *Melbourne*
Mark D Gorrell, *Sydney*
Michael Horowitz, *Adelaide*
John E Kellow, *Sydney*
Daniel Markovich, *Brisbane*

Phillip S Oates, *Perth*
 Ross C Smith, *Sydney*
 Kevin J Spring, *Brisbane*
 Philip G Dinning, *Koagarah*
 Christopher Christophi, *Melbourne*
 Cuong D Tran, *North Adelaide*
 Shan Rajendra, *Tasmania*
 Rajvinder Singh, *Adelaide*
 William Kemp, *Melbourne*
 Phil Sutton, *Melbourne*
 Richard Anderson, *Victoria*
 Vance Matthews, *Melbourne*
 Alexander G Heriot, *Melbourne*
 Debbie Trinder, *Fremantle*
 Ian C Lawrance, *Perth*
 Adrian G Cummins, *Adelaide*
 John K Olynyk, *Fremantle*
 Alex Boussioutas, *Melbourne*
 Emilia Prakoso, *Sydney*
 Robert JL Fraser, *Daw Park*



Austria

Wolfgang Mikulits, *Vienna*
 Alfred Gangl, *Vienna*
 Dietmar Öfner, *Salzburg*
 Georg Roth, *Vienna*
 Herwig R Cerwenka, *Graz*
 Ashraf Dahaba, *Graz*
 Markus Raderer, *Vienna*
 Alexander M Hirschl, *Wien*
 Thomas Wild, *Kapellerfeld*
 Peter Ferenci, *Vienna*
 Valentin Fuhrmann, *Vienna*
 Kurt Lenz, *Linz*
 Markus Peck-Radosavljevic, *Vienna*
 Michael Trauner, *Vienna*
 Stefan Riss, *Vienna*



Belgium

Rudi Beyaert, *Gent*
 Inge I Depoortere, *Leuven*
 Olivier Detry, *Liège*
 Benedicte Y De Winter, *Antwerp*
 Etienne M Sokal, *Brussels*
 Marc Peeters, *De Pintelaan*
 Eddie Wisse, *Keerbergen*
 Jean-Yves L Reginster, *Liège*
 Mark De Ridder, *Brussel*
 Freddy Penninckx, *Leuven*
 Kristin Verbeke, *Leuven*
 Lukas Van Oudenhove, *Leuven*
 Leo van Grunsven, *Brussels*
 Philip Meuleman, *Ghent*



Brazil

Heitor Rosa, *Goiania*
 Roberto J Carvalho-Filho, *Sao Paulo*
 Damiao Carlos Moraes Santos, *Rio de Janeiro*
 Marcelo Lima Ribeiro, *Braganca Paulista*
 Eduardo Garcia Vilela, *Belo Horizonte*
 Jaime Natan Eisig, *São Paulo*
 Andre Castro Lyra, *Salvador*
 José Liberato Ferreira Caboclo, *Brazil*
 Yukie Sato-Kuwabara, *São Paulo*
 Raquel Rocha, *Salvador*

Paolo R Salvalaggio, *Sao Paulo*
 Ana Cristina Simões e Silva, *Belo Horizonte*
 Joao Batista Teixeira Rocha, *Santa Maria*



Brunei Darussalam

Vui Heng Chong, *Bandar Seri Begawan*



Bulgaria

Zahariy Krastev, *Sofia*
 Mihaela Petrova, *Sofia*



Canada

Eldon Shaffer, *Calgary*
 Nathalie Perreault, *Sherbrooke*
 Philip H Gordon, *Montreal*
 Ram Prakash Galwa, *Ottawa*
 Baljinder Singh Salh, *Vancouver*
 Claudia Zwingmann, *Montreal*
 Alain Bitton, *Montreal*
 Pingchang Yang, *Hamilton*
 Michael F Byrne, *Vancouver*
 Andrew L Mason, *Alberta*
 John K Marshall, *Hamilton Ontario*
 Kostas Pantopoulos, *Montreal*
 Waliul Khan, *Ontario*
 Eric M Yoshida, *Vancouver*
 Geoffrey C Nguyen, *Toronto*
 Devendra K Amre, *Montreal*
 Tedros Bezabeh, *Winnipeg*
 Wangxue Chen, *Ottawa*
 Qiang Liu, *Saskatoon*



Chile

De Aretxabala Xabier, *Santiago*
 Marcelo A Beltran, *La Serena*
 Silvana Zanlungo, *Santiago*



China

Chi-Hin Cho, *Hong Kong*
 Chun-Qing Zhang, *Jinan*
 Ren Xiang Tan, *Nanjing*
 Fei Li, *Beijing*
 Hui-Jie Bian, *Xi'an*
 Xiao-Peng Zhang, *Beijing*
 Xing-Hua Lu, *Beijing*
 Fu-Sheng Wang, *Beijing*
 An-Gang Yang, *Xi'an*
 Xiao-Ping Chen, *Wuhan*
 Zong-Jie Cui, *Beijing*
 Ming-Liang He, *Hong Kong*
 Yuk-Tong Lee, *Hong Kong*
 Qin Su, *Beijing*
 Jian-Zhong Zhang, *Beijing*
 Paul Kwong-Hang Tam, *Hong Kong*
 Wen-Rong Xu, *Zhenjiang*
 Chun-Yi Hao, *Beijing*
 San-Jun Cai, *Shanghai*
 Simon Law, *Hong Kong*
 Yuk Him Tam, *Hong Kong*
 De-Liang Fu, *Shanghai*
 Eric WC Tse, *Hong Kong*

Justin CY Wu, *Hong Kong*
 Nathalie Wong, *Hong Kong*
 Jing Yuan Fang, *Shanghai*
 Yi-Min Mao, *Shanghai*
 Wei-Cheng You, *Beijing*
 Xiang-Dong Wang, *Shanghai*
 Xuan Zhang, *Beijing*
 Zhao-Shen Li, *Shanghai*
 Guang-Wen Cao, *Shanghai*
 En-min Li, *Shantou*
 Yu-Yuan Li, *Guangzhou*
 Fook Hong Ng, *Hong Kong*
 Hsiang-Fu Kung, *Hong Kong*
 Wai Lun Law, *Hong Kong*
 Eric CH Lai, *Hong Kong*
 Jun Yu, *Hong Kong*
 Ze-Guang Han, *Shanghai*
 Bian zhao-xiang, *Hong Kong*
 Wei-Dong Tong, *Chongqing*



Colombia

Germán Campuzano-Maya, *Medellín*



Croatia

Tamara Cacev, *Zagreb*
 Marko Duvnjak, *Zagreb*



Cuba

Damian C Rodriguez, *Havana*



Czech

Milan Jirsa, *Praha*
 Pavel Trunečka, *Prague*
 Jan Bures, *Hradec Kralove*
 Marcela Kopacova, *Hradec Kralove*
 Ondrej Slaby, *Brno*
 Radan Bruha, *Prague*



Denmark

Asbjørn M Drewes, *Aalborg*
 Leif Percival Andersen, *Copenhagen*
 Jan Mollenhauer, *Odense C*
 Morten Frisch, *Copenhagen S*
 Jorgen Rask-Madsen, *Skodsborg*
 Morten Hylander Møller, *Holte*
 Søren Rafaelsen, *Vejle*
 Vibeke Andersen, *Aabenraa*
 Ole Haagen Nielsen, *Herlev*



Ecuador

Fernando E Sempértegui, *Quito*



Egypt

Zeinab Nabil Ahmed Said, *Cairo*
 Hussein M Atta, *El-Minia*
 Asmaa Gaber Abdou, *Shebein Elkom*

Maha Maher Shehata, *Mansoura*



Estonia

Riina Salupere, *Tartu*
Tamara Vorobjova, *Tartu*



Finland

Saila Kauhanen, *Turku*
Pauli Antero Puolakkainen, *Turku*
Minna Nyström, *Helsinki*
Juhani Sand, *Tampere*
Jukka-Pekka Mecklin, *Jyväskylä*
Lea Veijola, *Helsinki*
Kaija-Leena Kolho, *Helsinki*
Thomas Kietzmann, *Oulu*



France

Boris Guiu, *Dijon*
Baumert F Thomas, *Strasbourg*
Alain L Servin, *Châtenay-Malabry*
Patrick Marcellin, *Paris*
Jean-Jacques Tuech, *Rouen*
Francoise L Fabiani, *Angers*
Jean-Luc Faucheron, *Grenoble*
Philippe Lehours, *Bordeaux*
Stephane Supiot, *Nantes*
Lionel Bueno, *Toulouse*
Flavio Maina, *Marseille*
Paul Hofman, *Nice*
Abdel-Majid Khatib, *Paris*
Annie Schmid-Alliana, *Nice cedex 3*
Frank Zerbib, *Bordeaux Cedex*
Rene Gerolami Santandera, *Marseille*
Sabine Colnot, *Paris*
Catherine Daniel, *Lille Cedex*
Thabut Dominique, *Paris*
Laurent Huwart, *Paris*
Alain Braillon, *Amiens*
Bruno Bonaz, *Grenoble*
Evelyne Schvoerer, *Strasbourg*
M Coeffier, *Rouen*
Mathias Chamailard, *Lille*
Hang Nguyen, *Clermont-Ferrand*
Veronique Vitton, *Marseille*
Alexis Desmoulière, *Limoges*
Juan Iovanna, *Marseille*



Germany

Hans L Tillmann, *Leipzig*
Stefan Kubicka, *Hannover*
Elke Cario, *Essen*
Hans Scherubl, *Berlin*
Harald F Teutsch, *Ulm*
Peter Konturek, *Erlangen*
Thilo Hackert, *Heidelberg*
Jurgen M Stein, *Frankfurt*
Andrej Khandoga, *Munich*
Karsten Schulmann, *Bochum*
Jutta Elisabeth Lüttges, *Riegelsberg*
Wolfgang Hagmann, *Heidelberg*
Hubert Blum, *Freiburg*
Thomas Bock, *Berlin*

Christa Buechler, *Regensburg*
Christoph F Dietrich, *Bad Mergentheim*
Ulrich R Fölsch, *Kiel*
Nikolaus Gassler, *Aachen*
Markus Gerhard, *Munich*
Dieter Glebe, *Giessen*
Klaus R Herrlinger, *Stuttgart*
Eberhard Hildt, *Berlin*
Joerg C Hoffmann, *Ludwigshafen*
Joachim Labenz, *Siegen*
Peter Malfertheiner, *Magdeburg*
Sabine Mihm, *Göttingen*
Markus Reiser, *Bochum*
Steffen Rickes, *Magdeburg*
Andreas G Schreyer, *Regensburg*
Henning Schulze-Bergkamen, *Heidelberg*
Ulrike S Stein, *Berlin*
Wolfgang R Stremmel, *Heidelberg*
Fritz von Weizsäcker, *Berlin*
Stefan Wirth, *Wuppertal*
Dean Bogoevski, *Hamburg*
Bruno Christ, *Halle/Saale*
Peter N Meier, *Hannover*
Stephan Johannes Ott, *Kiel*
Arndt Vogel, *Hannover*
Dirk Haller, *Freising*
Jens Standop, *Bonn*
Jonas Mudter, *Erlangen*
Jürgen Büning, *Lübeck*
Matthias Ocker, *Erlangen*
Joerg Trojan, *Frankfurt*
Christian Trautwein, *Aachen*
Jorg Kleeff, *Munich*
Christian Rust, *Munich*
Claus Hellerbrand, *Regensburg*
Elke Roeb, *Giessen*
Erwin Biecker, *Siegburg*
Ingmar Königsrainer, *Tübingen*
Jürgen Borlak, *Hannover*
Axel M Gressner, *Aachen*
Oliver Mann, *Hamburg*
Marty Zdichavsky, *Tübingen*
Christoph Reichel, *Bad Brückenau*
Nils Habbe, *Marburg*
Thomas Wex, *Magdeburg*
Frank Ulrich Weiss, *Greifswald*
Manfred V Singer, *Mannheim*
Martin K Schilling, *Homburg*
Philip D Hard, *Giessen*
Michael Linnebacher, *Rostock*
Ralph Graeser, *Freiburg*
Rene Schmidt, *Freiburg*
Robert Obermaier, *Freiburg*
Sebastian Mueller, *Heidelberg*
Andrea Hille, *Goettingen*
Klaus Mönkemüller, *Bottrop*
Elfriede Bollschweiler, *Köln*
Siegfried Wagner, *Deggendorf*
Dieter Schilling, *Mannheim*
Joerg F Schlaak, *Essen*
Michael Keese, *Frankfurt*
Robert Grützmann, *Dresden*
Ali Canbay, *Essen*
Dirk Domagk, *Muenster*
Jens Hoepfner, *Freiburg*
Frank Tacke, *Aachen*
Patrick Michl, *Marburg*
Alfred A Königsrainer, *Tübingen*
Kilian Weigand, *Heidelberg*
Mohamed Hassan, *Duesseldorf*
Gustav Paumgartner, *Munich*

Philippe N Khalil, *Munich*
Martin Storr, *Munich*



Greece

Andreas Larentzakis, *Athens*
Tsianos Epameinondas, *Ioannina*
Elias A Kouroumalis, *Heraklion*
Helen Christopoulou-Aletra, *Thessaloniki*
George Papatheodoridis, *Athens*
Ioannis Kanellos, *Thessaloniki*
Michael Koutsilieris, *Athens*
T Choli-Papadopoulou, *Thessaloniki*
Emanuel K Manesis, *Athens*
Evangelos Tsiambas, *Ag Paraskevi Attiki*
Konstantinos Mimidis, *Alexandroupolis*
Spilios Manolakopoulos, *Athens*
Spiros Sgouros, *Athens*
Ioannis E Koutroubakis, *Heraklion*
Stefanos Karagiannis, *Athens*
Spiros Ladas, *Athens*
Elena Vezali, *Athens*
Dina G Tiniakos, *Athens*
Ekaterini Chatzaki, *Alexandroupolis*
Dimitrios Roukos, *Ioannina*
George Sgourakis, *Athens*
Maroulio Talieri, *Athens*



Hungary

Peter L Lakatos, *Budapest*
Yvette Mándi, *Szeged*
Ferenc Sipos, *Budapest*
György M Buzás, *Budapest*
László Czákó, *Szeged*
Peter Hegyi, *Szeged*
Zoltan Rakonczay, *Szeged*
Gyula Farkas, *Szeged*
Zsuzsa Szondy, *Debrecen*
Gabor Veres, *Budapest*
Zsuzsa Schaff, *Budapest*



India

Philip Abraham, *Mumbai*
Sri P Misra, *Allahabad*
Ramesh Roop Rai, *Jaipur*
Nageshwar D Reddy, *Hyderabad*
Rakesh Kumar Tandon, *New Delhi*
Jai Dev Wig, *Chandigarh*
Uday C Ghoshal, *Lucknow*
Pramod Kumar Garg, *New Delhi*
Barjesh Chander Sharma, *New Delhi*
Gopal Nath, *Varanasi*
Bhupendra Kumar Jain, *Delhi*
Devinder Kumar Dhawan, *Chandigarh*
Ashok Kumar, *Lucknow*
Benjamin Perakath, *Tamil Nadu*
Debidas Ghosh, *Midnapore*
Pankaj Garg, *Panchkula*
Samiran Nundy, *New Delhi*
Virendra Singh, *Chandigarh*
Bikash Medhi, *Chandigarh*
Radha K Dhiman, *Chandigarh*
Vandana Panda, *Mumbai*
Vineet Ahuja, *New Delhi*
SV Rana, *Chandigarh*

Deepak N Amarapurkar, *Mumbai*
Abhijit Chowdhury, *Kolkata*
Jasbir Singh, *Kurukshetra*
B Mittal, *Lucknow*
Sundeep Singh Saluja, *New Delhi*
Pradyumna Kumar Mishra, *Mumbai*
Runu Chakravarty, *Kolkata*
Nagarajan Perumal, *New Delhi*



Indonesia

David handoyo Muljono, *Jakarta*
Andi Utama, *Tangerang*



Iran

Seyed-Moayed Alavian, *Tehran*
Reza Malekzadeh, *Tehran*
Peyman Adibi, *Isfahan*
Alireza Mani, *Tehran*
Seyed Mohsen Dehghani, *Shiraz*
Mohammad Abdollahi, *Tehran*
Majid Assadi, *Bushehr*
Arezoo Aghakhani, *Tehran*
Marjan Mohammadi, *Tehran*
Fariborz Mansour-Ghanaei, *Rasht*



Ireland

Ross McManus, *Dublin*
Billy Bourke, *Dublin*
Catherine Greene, *Dublin*
Ted Dinan, *Cork*
Marion Rowland, *Dublin*



Israel

Abraham R Eliakim, *Haifa*
Simon Bar-Meir, *Tel Hashomer*
Ami D Sperber, *Beer-Sheva*
Boris Kirshtein, *Beer Sheva*
Mark Pines, *Bet Dagan*
Menachem Moshkowitz, *Tel-Aviv*
Ron Shaoul, *Haifa*
Shmuel Odes, *Beer Sheva*
Sigal Fishman, *Tel Aviv*
Alexander Becker, *Afula*
Assy Nimer, *Safed*
Eli Magen, *Ashdod*
Amir Shlomain, *Tel-Aviv*



Italy

Mauro Bortolotti, *Bologna*
Gianlorenzo Dionigi, *Varese*
Fiorucci Stefano, *Perugia*
Roberto Berni Canani, *Naples*
Ballarin Roberto, *Modena*
Bruno Annibale, *Roma*
Vincenzo Stanghellini, *Bologna*
Giovanni B Gaeta, *Napoli*
Claudio Bassi, *Verona*
Mauro Bernardi, *Bologna*
Giuseppe Chiarioni, *Valeggio*
Michele Cicala, *Rome*

Dario Conte, *Milano*
Francesco Costa, *Pisa*
Giovanni D De Palma, *Naples*
Giammarco Fava, *Ancona*
Francesco Feo, *Sassari*
Edoardo G Giannini, *Genoa*
Fabio Grizzi, *Milan*
Salvatore Gruttadauria, *Palermo*
Pietro Invernizzi, *Milan*
Ezio Laconi, *Cagliari*
Giuseppe Montalto, *Palermo*
Giovanni Musso, *Torino*
Gerardo Nardone, *Napoli*
Valerio Nobili, *Rome*
Raffaele Pezzilli, *Bologna*
Alberto Piperno, *Monza*
Anna C Piscaglia, *Roma*
Piero Portincasa, *Bari*
Giovanni Tarantino, *Naples*
Cesare Tosetti, *Porretta Terme*
Alessandra Ferlini, *Ferrara*
Alessandro Ferrero, *Torino*
Donato F Altomare, *Bari*
Giovanni Milito, *Rome*
Giuseppe Sica, *Rome*
Guglielmo Borgia, *Naples*
Giovanni Latella, *L'Aquila*
Salvatore Auricchio, *Naples*
Alberto Biondi, *Rome*
Alberto Tommasini, *Trieste*
Antonio Basoli, *Roma*
Giuliana Decorti, *Trieste*
Marco Silano, *Roma*
Michele Reni, *Milan*
Pierpaolo Sileri, *Rome*
Achille Iolascon, *Naples*
Alessandro Granito, *Bologna*
Angelo A Izzo, *Naples*
Giuseppe Currò, *Messina*
Pier Mannuccio Mannucci, *Milano*
Marco Vivarelli, *Bologna*
Massimo Levvero, *Rome*
Massimo Rugge, *Padova*
Paolo Angeli, *Padova*
Silvio Danese, *Milano*
Antonello Trecca, *Rome*
Antonio Gasbarrini, *Rome*
Cesare Ruffolo, *Treviso*
Massimo Falconi, *Verona*
Fausto Catena, *Bologna*
Francesco Manguso, *Napoli*
Giancarlo Mansueto, *Verona*
Luca Morelli, *Trento*
Marco Scarpa, *Padova*
Mario M D'Elios, *Florence*
Francesco Luzzza, *Catanzaro*
Franco Roviello, *Siena*
Guido Torzilli, *Rozzano Milano*
Luca Frulloni, *Verona*
Lucia Malaguarnera, *Catania*
Lucia Ricci Vitiani, *Rome*
Mara Massimi, *L'Aquila*
Mario Pescatori, *Rome*
Mario Rizzetto, *Torino*
Mirko D'Onofrio, *Verona*
Nadia Peparini, *Rome*
Paola De Nardi, *Milan*
Paolo Aurelio, *Rome*
Piero Amodio, *Padova*
Riccardo Nascimbeni, *Brescia*

Vincenzo Villanacci, *Brescia*
Vittorio Ricci, *Pavia*
Silvia Fargion, *Milan*
Luigi Bonavina, *Milano*
Oliviero Riggio, *Rome*
Fabio Pace, *Milano*
Gabrio Bassotti, *Perugia*
Giulio Marchesini, *Bologna*
Roberto de Franchis, *Milano*
Giovanni Monteleone, *Rome*
C armelo Scarpignato, *Parma*
Luca VC Valenti, *Milan*
Urgesi Riccardo, *Rome*
Marcello Persico, *Naples*
Antonio Moschetta, *Bari*
Luigi Muratori, *Bologna*
Angelo Zullo, *Roma*
Vito Annese, *Florence*
Simone Lanini, *Rome*
Alessandro Grasso, *Savona*
Giovanni Targher, *Verona*
Domenico Girelli, *Verona*
Alessandro Cucchetti, *Bologna*
Fabio Marra, *Florence*
Michele Milella, *Rome*
Francesco Franceschi, *Rome*
Giuseppina De Petro, *Brescia*
Salvatore Leonardi, *Catania*
Cristiano Simone, *Santa Maria Imbaro*
Bernardino Rampone, *Salerno*
Francesco Crea, *Pisa*
Walter Fries, *Messina*
Antonio Craxi, *Palermo*
Gerardo Rosati, *Potenza*
Mario Guslandi, *Milano*
Gianluigi Giannelli, *Bari*
Paola Loria, *Modena*
Paolo Sorrentino, *Avellino*
Armando Santoro, *Rozzano*
Gabriele Grassi, *Trieste*
Antonio Orlicchio, *Rome*



Japan

Tsuneo Kitamura, *Chiba*
Katsutoshi Yoshizato, *Higashihiroshima*
Masahiro Arai, *Tokyo*
Shinji Tanaka, *Hiroshima*
Keiji Hirata, *Kitakyushu*
Yoshio Shirai, *Niigata*
Susumu Ohmada, *Maebashi*
Kenichi Ikejima, *Tokyo*
Masatoshi Kudo, *Osaka*
Yoshiaki Murakami, *Hiroshima*
Masahiro Tajika, *Nagoya*
Kentaro Yoshika, *Toyoake*
Kyoichi Adachi, *Izumo*
Yasushi Adachi, *Sapporo*
Takafumi Ando, *Nagoya*
Akira Andoh, *Otsu*
Hitoshi Asakura, *Tokyo*
Mitsuhiro Fujishiro, *Tokyo*
Toru Hiyama, *Higashihiroshima*
Yutaka Inagaki, *Kanagawa*
Hiromi Ishibashi, *Nagasaki*
Shunji Ishihara, *Izumo*
Toru Ishikawa, *Niigata*
Yoshiaki Iwasaki, *Okayama*
Terumi Kamisawa, *Tokyo*

Norihiko Kokudo, *Tokyo*
 Shin Maeda, *Tokyo*
 Yasushi Matsuzaki, *Ibaraki*
 Kenji Miki, *Tokyo*
 Hiroto Miwa, *Hyogo*
 Yoshiharu Motoo, *Kanazawa*
 Kunihiko Murase, *Tusima*
 Atsushi Nakajima, *Yokohama*
 Yuji Naito, *Kyoto*
 Hisato Nakajima, *Tokyo*
 Hiroki Nakamura, *Yamaguchi*
 Shotaro Nakamura, *Fukuoka*
 Mikio Nishioka, *Niihama*
 Hirohide Ohnishi, *Akita*
 Kazuichi Okazaki, *Osaka*
 Morikazu Onji, *Ehime*
 Satoshi Osawa, *Hamamatsu*
 Hidetsugu Saito, *Tokyo*
 Yutaka Saito, *Tokyo*
 Yasushi Sano, *Kobe*
 Tomohiko Shimatani, *Kure*
 Yukihiko Shimizu, *Toyama*
 Shinji Shimoda, *Fukuoka*
 Masayuki Sho, *Nara*
 Hidekazu Suzuki, *Tokyo*
 Shinji Togo, *Yokohama*
 Satoshi Yamagiwa, *Niigata*
 Takayuki Yamamoto, *Yokkaichi*
 Hiroshi Yoshida, *Tokyo*
 Norimasa Yoshida, *Kyoto*
 Akihito Nagahara, *Tokyo*
 Hiroaki Takeuchi, *Kochi*
 Keiji Ogura, *Tokyo*
 Kotaro Miyake, *Tokushima*
 Mitsunori Yamakawa, *Yamagata*
 Naoaki Sakata, *Sendai*
 Naoya Kato, *Tokyo*
 Satoshi Mamori, *Hyogo*
 Shogo Kikuchi, *Aichi*
 Shoichiro Sumi, *Kyoto*
 Susumu Ikehara, *Osaka*
 Taketo Yamaguchi, *Chiba*
 Tokihiko Sawada, *Tochigi*
 Tomoharu Yoshizumi, *Fukuoka*
 Toshiyuki Ishiwata, *Tokyo*
 Yasuhiro Fujino, *Akashi*
 Yasuhiro Koga, *Isehara city*
 Yoshihisa Takahashi, *Tokyo*
 Yoshitaka Takuma, *Okayama*
 Yutaka Yata, *Maebashi-city*
 Itaru Endo, *Yokohama*
 Kazuo Chijiwa, *Miyazaki*
 Kouhei Fukushima, *Sendai*
 Masahiro Iizuka, *Akita*
 Mitsuyoshi Urashima, *Tokyo*
 Munechika Enjoji, *Fukuoka*
 Takashi Kojima, *Sapporo*
 Takumi Kawaguchi, *Kurume*
 Yoshiyuki Ueno, *Sendai*
 Yuichiro Eguchi, *Saga*
 Akihiro Tamori, *Osaka*
 Atsushi Masamune, *Sendai*
 Atsushi Tanaka, *Tokyo*
 Hitoshi Tsuda, *Tokyo*
 Takashi Kobayashi, *Tokyo*
 Akimasa Nakao, *Nagoya*
 Hiroyuki Uehara, *Osaka*
 Masahito Uemura, *Kashihara*
 Satoshi Tanno, *Sapporo*
 Toshinari Takamura, *Kanazawa*
 Yohei Kida, *Kainan*

Masanori Hatakeyama, *Tokyo*
 Satoru Kakizaki, *Gunma*
 Shuhei Nishiguchi, *Hyogo*
 Yuichi Yoshida, *Osaka*
 Manabu Morimoto, *Japan*
 Mototsugu Kato, *Sapporo*
 Naoki Ishii, *Tokyo*
 Noriko Nakajima, *Tokyo*
 Nobuhiro Ohkohchi, *Tsukuba*
 Takanori Kanai, *Tokyo*
 Kenichi Goda, *Tokyo*
 Mitsugi Shimoda, *Mibu*
 Zenichi Morise, *Nagoya*
 Hitoshi Yoshiji, *Kashihara*
 Takahiro Nakazawa, *Nagoya*
 Utaroh Motosugi, *Yamanashi*
 Nobuyuki Matsuhashi, *Tokyo*
 Yasuhiro Kodera, *Nagoya*
 Takayoshi Ito, *Tokyo*
 Yasuhito Tanaka, *Nagoya*
 Haruhiko Sugimura, *Hamamatsu*
 Hiroki Yamaue, *Wakayama*
 Masao Ichinose, *Wakayama*
 Takaaki Arigami, *Kagoshima*
 Nobuhiro Zaima, *Nara*
 Naoki Tanaka, *Matsumoto*
 Satoru Motoyama, *Akita*
 Tomoyuki Shibata, *Toyoake*
 Tatsuya Ide, *Kurume*
 Tsutomu Fujii, *Nagoya*
 Osamu Kanauchi, *Tokyo*
 Atsushi Irisawa, *Aizuwakamatsu*
 Hikaru Nagahara, *Tokyo*
 Keiji Hanada, *Onomichi*
 Keiichi Mitsuyama, *Fukuoka*
 Shin Maeda, *Yokohama*
 Takuya Watanabe, *Niigata*
 Toshihiro Mitaka, *Sapporo*
 Yoshiki Murakami, *Kyoto*
 Tadashi Shimoyama, *Hirosaki*



Jordan

Ismail Matalka, *Irbid*
 Khaled Jadallah, *Irbid*



Kuwait

Islam Khan, *Safat*



Lebanon

Bassam N Abboud, *Beirut*
 Rami Moucari, *Beirut*
 Ala I Sharara, *Beirut*
 Rita Slim, *Beirut*



Lithuania

Giedrius Barauskas, *Kaunas*
 Limas Kupcinskas, *Kaunas*



Malaysia

Andrew Seng Boon Chua, *Ipo*



Mexico

Saúl Villa-Trevio, *México*
 Omar Vergara-Fernandez, *Mexico*
 Diego Garcia-Compean, *Monterrey*
 Arturo Panduro, *Jalisco*
 Miguel Angel Mercado, *Distrito Federal*
 Richard A Awad, *Mexico*
 Aldo Torre Delgadillo, *México*
 Paulino Martínez Hernández Magro, *Celaya*
 Carlos A Aguilar-Salinas, *Mexico*
 Jesus K Yamamoto-Furusho, *Mexico*



Morocco

Samir Ahboucha, *Khoubra*



Moldova

Igor Mishin, *Kishinev*



Netherlands

Ulrich Beuers, *Amsterdam*
 Albert Frederik Pull ter Gunne, *Tilburg*
 Jantine van Baal, *Heidelberglaan*
 Wendy Wilhelmina Johanna de Leng, *Utrecht*
 Gerrit A Meijer, *Amsterdam*
 Lee Bouwman, *Leiden*
 J Bart A Crusius, *Amsterdam*
 Frank Hoentjen, *Haarlem*
 Servaas Morré, *Amsterdam*
 Chris JJ Mulder, *Amsterdam*
 Paul E Sijens, *Groningen*
 Karel van Erpecum, *Utrecht*
 BW Marcel Spanier, *Arnhem*
 Misha Luyer, *Sittard*
 Pieter JF de Jonge, *Rotterdam*
 Robert Christiaan Verdonk, *Groningen*
 John Plukker, *Groningen*
 Maarten Tushuizen, *Amsterdam*
 Wouter de Herder, *Rotterdam*
 Erwin G Zoetendal, *Wageningen*
 Robert J de Negt, *Rotterdam*
 Albert J Bredenoord, *Nieuwegein*
 Annemarie de Vries, *Rotterdam*
 Astrid van der Velde, *Ede*
 Lodewijk AA Brosens, *Utrecht*
 James CH Hardwick, *Leiden*
 Loes van Keimpema, *Nijmegen*
 WJ de Jonge, *Amsterdam*
 Zuzana Zelinkova, *Rotterdam*
 LN van Steenberghe, *Eindhoven*
 Frank G Schaap, *Amsterdam*
 Jeroen Maljaars, *Leiden*



New Zealand

Andrew S Day, *Christchurch*
 Max S Petrov, *Auckland*



Norway

Espen Melum, *Oslo*

Trine Olsen, *Tromsø*
 Eyvind J Paulssen, *Tromsø*
 Rasmus Goll, *Tromsø*
 Asle W Medhus, *Oslo*
 Jon Arne Søreide, *Stavanger*
 Kjetil Soreide, *Stavanger*
 Reidar Fossmark, *Trondheim*
 Trond Peder Flaten, *Trondheim*
 Olav Dalgard, *Oslo*
 Ole Høie, *Arendal*
 Magdy El-Salhy, *Bergen*
 Jørgen Valeur, *Oslo*



Pakistan

Shahab Abid, *Karachi*
 Syed MW Jafri, *Karachi*



Poland

Beata Jolanta Jabłońska, *Katowice*
 Halina Cichoż-Lach, *Lublin*
 Tomasz Brzozowski, *Cracow*
 Hanna Gregorek, *Warsaw*
 Marek Hartleb, *Katowice*
 Stanislaw J Konturek, *Krakow*
 Andrzej Dabrowski, *Bialystok*
 Jan Kulig, *Kraków*
 Julian Swierczynski, *Gdansk*
 Marek Bebenek, *Wroclaw*
 Dariusz M Lebensztejn, *Bialystok*



Portugal

Ricardo Marcos, *Porto*
 Guida Portela-Gomes, *Estoril*
 Ana Isabel Lopes, *Lisboa Codex*
 Raquel Almeida, *Porto*
 Rui Tato Marinho, *Lisbon*
 Ceu Figueiredo, *Porto*



Romania

Dan L Dumitrascu, *Cluj*
 Adrian Saftoiu, *Craiova*
 Andrada Seicean, *Cluj-Napoca*
 Anca Trifan, *Iasi*



Russia

Vasiliy I Reshetnyak, *Moscow*



Saudi Arabia

Ibrahim A Al Mofleh, *Riyadh*
 Abdul-Wahed Meshikhes, *Qatif*
 Faisal Sanai, *Riyadh*



Serbia

Tamara M Alempijevic, *Belgrade*
 Dusan M Jovanovic, *Sremska Kamenica*
 Zoran Krivokapic, *Belgrade*



Singapore

Brian Kim Poh Goh, *Singapore*
 Khek-Yu Ho, *Singapore*
 Fock Kwong Ming, *Singapore*
 Francis Seow-Choen, *Singapore*
 Kok Sun Ho, *Singapore*
 Kong Weng Eu, *Singapore*
 Madhav Bhatia, *Singapore*
 London Lucien Ooi, *Singapore*
 Wei Ning Chen, *Singapore*
 Richie Soong, *Singapore*
 Kok Ann Gwee, *Singapore*



Slovenia

Matjaz Homan, *Ljubljana*



South Africa

Rosemary Joyce Burnett, *Pretoria*
 Michael Kew, *Cape Town*
 Roland Ndip, *Alice*



South Korea

Byung Chul Yoo, *Seoul*
 Jae J Kim, *Seoul*
 Jin-Hong Kim, *Suwon*
 Marie Yeo, *Suwon*
 Jeong Min Lee, *Seoul*
 Eun-Yi Moon, *Seoul*
 Joong-Won Park, *Goyang*
 Hoon Jai Chun, *Seoul*
 Myung-Gyu Choi, *Seoul*
 Sang Kil Lee, *Seoul*
 Sang Yeoup Lee, *Gyeongsangnam-do*
 Won Ho Kim, *Seoul*
 Dae-Yeul Yu, *Daejeon*
 Donghee Kim, *Seoul*
 Sang Geon Kim, *Seoul*
 Sun Pyo Hong, *Geonggi-do*
 Sung-Gil Chi, *Seoul*
 Yeun-Jun Chung, *Seoul*
 Ki-Baik Hahm, *Incheon*
 Ji Kon Ryu, *Seoul*
 Kyu Taek Lee, *Seoul*
 Yong Chan Lee, *Seoul*
 Seong Gyu Hwang, *Seongnam*
 Seung Woon Paik, *Seoul*
 Sung Kim, *Seoul*
 Hong Joo Kim, *Seoul*
 Hyoung-Chul Oh, *Seoul*
 Nayoung Kim, *Seongnam-si*
 Sang Hoon Ahn, *Seoul*
 Seon Hahn Kim, *Seoul*
 Si Young Song, *Seoul*
 Young-Hwa Chung, *Seoul*
 Hyo-Cheol Kim, *Seoul*
 Kwang Jae Lee, *Swon*
 Sang Min Park, *Seoul*
 Young Chul Kim, *Seoul*
 Do Hyun Park, *Seoul*
 Dae Won Jun, *Seoul*
 Dong Wan Seo, *Seoul*
 Soon-Sun Hong, *Incheon*

Hoguen Kim, *Seoul*
 Ho-Young Song, *Seoul*
 Joo-Ho Lee, *Seoul*
 Jung Eun Lee, *Seoul*
 Jong H Moon, *Bucheon*



Spain

Eva Vaquero, *Barcelona*
 Andres Cardenas, *Barcelona*
 Laureano Fernández-Cruz, *Barcelona*
 Antoni Farré, *Spain*
 Maria-Angeles Aller, *Madrid*
 Raul J Andrade, *Málaga*
 Fernando Azpiroz, *Barcelona*
 Josep M Bordas, *Barcelona*
 Antoni Castells, *Barcelona*
 Vicente Felipo, *Valencia*
 Isabel Fabregat, *Barcelona*
 Angel Lanas, *Zaragoza*
 Juan-Ramón Larrubia, *Guadalajara*
 María IT López, *Jaén*
 Jesús M Prieto, *Pamplona*
 Mireia Miquel, *Sabadell*
 Ramon Bataller, *Barcelona*
 Fernando J Corrales, *Pamplona*
 Julio Mayol, *Madrid*
 Matias A Avila, *Pamplona*
 Juan Macías, *Seville*
 Juan Carlos Laguna Egea, *Barcelona*
 Juli Busquets, *Barcelona*
 Belén Beltrán, *Valencia*
 José Manuel Martin-Villa, *Madrid*
 Lisardo Boscá, *Madrid*
 Luis Grande, *Barcelona*
 Pedro Lorenzo Majano Rodriguez, *Madrid*
 Adolfo Benages, *Valencia*
 Domínguez-Muñoz JE, *Santiago de Compostela*
 Gloria González Aseguinolaza, *Navarra*
 Javier Martin, *Granada*
 Luis Bujanda, *San Sebastián*
 Matilde Bustos, *Pamplona*
 Luis Aparisi, *Valencia*
 José Julián calvo Andrés, *Salamanca*
 Benito Velayos, *Valladolid*
 Javier Gonzalez-Gallego, *León*
 Ruben Ciria, *Córdoba*
 Francisco Rodriguez-Frias, *Barcelona*
 Manuel Romero-Gómez, *Sevilla*
 Albert Parés, *Barcelona*
 Joan Roselló-Catafau, *Barcelona*



Sri Lanka

Arjuna De Silva, *Kelaniya*



Sweden

Stefan G Pierzynowski, *Lund*
 Hanns-Ulrich Marschall, *Stockholm*
 Lars A Pahlman, *Uppsala*
 Helena Nordenstedt, *Stockholm*
 Bobby Tingstedt, *Lund*
 Evangelos Kalaitzakis, *Gothenburg*
 Lars Erik Agréus, *Huddinge*
 Annika Lindblom, *Stockholm*

Roland Andersson, *Lund*
Zongli Zheng, *Stockholm*
Mauro D'Amato, *Huddinge*
Greger Lindberg, *Stockholm*
Pär Erik Myrelið, *Linköping*
Sara Lindén, *Göteborg*
Sara Regné, *Malmö*
Åke Nilsson, *Lund*



Switzerland

Jean L Frossard, *Geneva*
Andreas Geier, *Zürich*
Bruno Stieger, *Zürich*
Pascal Gervaz, *Geneva*
Paul M Schneider, *Zurich*
Felix Stickel, *Berne*
Fabrizio Montecucco, *Geneva*
Inti Zlobec, *Basel*
Michelangelo Foti, *Geneva*
Pascal Bucher, *Geneva*
Andrea De Gottardi, *Berne*
Christian Toso, *Geneva*



Thailand

Weekitt Kittisupamongkol, *Bangkok*



Trinidad and Tobago

Shivananda Nayak, *Mount Hope*



Turkey

Tarkan Karakan, *Ankara*
Yusuf Bayraktar, *Ankara*
Ahmet Tekin, *Mersin*
Aydin Karabacakoglu, *Konya*
Osman C Ozdogan, *Istanbul*
Özlem Yilmaz, *Izmir*
Bülent Salman, *Ankara*
Can GONEN, *Kutahya*
Cuneyt Kayaalp, *Malatya*
Ekmel Tezel, *Ankara*
Eren Ersoy, *Ankara*
Hayrullah Derici, *Balıkesir*
Mehmet Refik Mas, *Etilik-Ankara*
Sinan Akay, *Tekirdag*
A Mithat Bozdayi, *Ankara*
Metin Basaranoglu, *Istanbul*
Mesut Tez, *Ankara*
Orhan Sezgin, *Mersin*
Mukaddes Esrefoglu, *Malatya*
Ilker Tasci, *Ankara*
Kemal Kismet, *Ankara*
Selin Kapan, *Istanbul*
Seyfettin Köklü, *Ankara*
Murat Sayan, *Kocaeli*
Sabahattin Kaymakoglu, *Istanbul*
Yucel Ustundag, *Zonguldak*
Can Gonen, *Istanbul*
Yusuf Yilmaz, *Istanbul*
Müge Tecder-Ünal, *Ankara*
İlhami Yüksel, *Ankara*



United Arab Emirates

Fikri M Abu-Zidan, *Al-Ain*
Sherif M Karam, *Al-Ain*



United Kingdom

Anastasios Koulaouzidis, *Edinburgh*
Sylvia LF Pender, *Southampton*
Hong-Xiang Liu, *Cambridge*
William Dickey, *Londonderry*
Simon D Taylor-Robinson, *London*
James Neuberger, *Birmingham*
Frank I Tovey, *London*
Kevin Robertson, *Glasgow*
Chew Thean Soon, *Manchester*
Geoffrey Burnstock, *London*
Vamsi R Velchuru, *United Kingdom*
Simon Afford, *Birmingham*
Navneet K Ahluwalia, *Stockport*
Lesley A Anderson, *Belfast*
Anthony TR Axon, *Leeds*
Jim D Bell, *London*
Alastair D Burt, *Newcastle*
Tatjana Crnogorac-Jurcevic, *London*
Daniel R Gaya, *Edinburgh*
William Greenhalf, *Liverpool*
Indra N Guha, *Southampton*
Stefan G Hübscher, *Birmingham*
Robin Hughes, *London*
Pali Hungin, *Stockton*
Janusz AZ Jankowski, *Oxford*
Peter Karayiannis, *London*
Patricia F Lalor, *Birmingham*
Giorgina Mieli-Vergani, *London*
D Mark Pritchard, *Liverpool*
Marco Senzolo, *Padova*
Roger Williams, *London*
M H Ahmed, *Southampton*
Christos Paraskeva, *Bristol*
Emad M El-Omar, *Aberdeen*
A M El-Tawil, *Birmingham*
Anne McCune, *Bristol*
Charles B Ferguson, *Belfast*
Chin Wee Ang, *Liverpool*
Clement W Imrie, *Glasgow*
Dileep N Lobo, *Nottingham*
Graham MacKay, *Glasgow*
Guy Fairbairn Nash, *Poole*
Ian Lindsey, *Oxford*
Jason CB Goh, *Birmingham*
Jeremy FL Cobbold, *London*
Julian RF Walters, *London*
Jamie Murphy, *London*
John Beynon, *Swansea*
John B Schofield, *Kent*
Anil George, *London*
Aravind Suppiah, *East Yorkshire*
Basil Ammori, *Salford*
Catherine Walter, *Cheltenham*
Chris Briggs, *Sheffield*
Jeff Butterworth, *Shrewsbury*
Nawfal Hussein, *Nottingham*
Patrick O'Dwyer, *Glasgow*
Rob Glynne-Jones, *Northwood*
Sharad Karandikar, *Birmingham*
Venkatesh Shanmugam, *Derby*

Yeng S Ang, *Wigan*
Alberto Quaglia, *London*
Andrew Fowell, *Southampton*
Gianpiero Gravante, *Leicester*
Piers Gatenby, *London*
Kondragunta Rajendra Prasad, *Leeds*
Sunil Dolwani, *Cardiff*
Andrew McCulloch Veitch, *Wolverhampton*
Brian Green, *Belfast*
Noriko Suzuki, *Middlesex*
Richard Parker, *North Staffordshire*
Shahid A Khan, *London*
Akhilesh B Reddy, *Cambridge*
Jean E Crabtree, *Leeds*
John S Leeds, *Sheffield*
Paul Sharp, *London*
Sumita Verma, *Brighton*
Thamara Perera, *Birmingham*
Donald Campbell McMillan, *Glasgow*
Kathleen B Bamford, *London*
Helen Coleman, *Belfast*
Eyad Elkord, *Manchester*
Mohammad Ilyas, *Nottingham*
Simon R Carding, *Norwich*
Ian Chau, *Sutton*
Claudio Nicoletti, *Norwich*
Hendrik-Tobias Arkenau, *London*
Muhammad Imran Aslam, *Leicester*
Giuseppe Orlando, *Oxford*
John S Leeds, *Aberdeen*
S Madhusudan, *Nottingham*
Amin Ibrahim Amin, *Dunfermline*
David C Hay, *Edinburgh*
Alan Burns, *London*



United States

Tauseef Ali, *Oklahoma City*
George Y Wu, *Farmington*
Josef E Fischer, *Boston*
Thomas Clancy, *Boston*
John Morton, *Stanford*
Luca Stocchi, *Cleveland*
Kevin Michael Reavis, *Orange*
Shiu-Ming Kuo, *Buffalo*
Gary R Lichtenstein, *Philadelphia*
Natalie J Torok, *Sacramento*
Scott A Waldman, *Philadelphia*
Georgios Papachristou, *Pittsburgh*
Carla W Brady, *Durham*
Robert CG Martin, *Louisville*
Eugene P Ceppa, *Durham*
Shashi Bala, *Worcester*
Imran Hassan, *Springfield*
Klaus Thaler, *Columbia*
Andreas M Kaiser, *Los Angeles*
Shawn D Safford, *Norfolk*
Massimo Raimondo, *Jacksonville*
Kazuaki Takabe, *Richmond VA*
Stephen M Kavic, *Baltimore*
T Clark Gamblin, *Pittsburgh*
BS Anand, *Houston*
Ananthanarayanan M, *New York*
Anthony J Bauer, *Pittsburgh*
Edmund J Bini, *New York*
Xian-Ming Chen, *Omaha*
Ramsey Chi-man Cheung, *Palo Alto*
Parimal Chowdhury, *Arkansas*
Mark J Czaja, *New York*

Conor P Delaney, *Cleveland*
Sharon DeMorrow, *Temple*
Bijan Eghtesad, *Cleveland*
Alessandro Fichera, *Chicago*
Glenn T Furuta, *Aurora*
Jean-Francois Geschwind, *Baltimore*
Shannon S Glaser, *Temple*
Ajay Goel, *Dallas*
James H Grendell, *New York*
Anna S Gukovskaya, *Los Angeles*
Jamal A Ibdah, *Columbia*
Atif Iqbal, *Omaha*
Hajime Isomoto, *Rochester*
Hartmut Jaeschke, *Kansas*
Leonard R Johnson, *Memphis*
Rashmi Kaul, *Tulsa*
Ali Keshavarzian, *Chicago*
Miran Kim, *Providence*
Burton I Korelitz, *New York*
Richard A Kozarek, *Seattle*
Alyssa M Krasinskas, *Pittsburgh*
Ming Li, *New Orleans*
Zhiping Li, *Baltimore*
Chen Liu, *Gainesville*
Michael R Lucey, *Madison*
James D Luketich, *Pittsburgh*
Patrick M Lynch, *Houston*
Willis C Maddrey, *Dallas*
Mercedes Susan Mandell, *Aurora*
Wendy M Mars, *Pittsburgh*
Laura E Matarese, *Pittsburgh*
Lynne V McFarland, *Washington*
Stephan Menne, *New York*
Didier Merlin, *Atlanta*
George Michalopoulos, *Pittsburgh*
James M Millis, *Chicago*
Pramod K Mistry, *New Haven*
Emiko Mizoguchi, *Boston*
Peter L Moses, *Burlington*
Masaki Nagaya, *Boston*
Robert D Odze, *Boston*
Stephen JD O'Keefe, *Pittsburgh*
Zhiheng Pei, *New York*
Raymund R Razonable, *Minnesota*
Basil Rigas, *New York*
Richard A Rippe, *Chapel Hill*
Philip Rosenthal, *San Francisco*
Stuart Sherman, *Indianapolis*
Christina Surawicz, *Seattle*
Wing-Kin Syn, *Durham*
Yvette Taché, *Los Angeles*
K-M Tchou-Wong, *New York*
George Triadafilopoulos, *Stanford*
Chung-Jyi Tsai, *Lexington*
Andrew Ukleja, *Florida*
Arnold Wald, *Wisconsin*
Irving Waxman, *Chicago*
Steven D Wexner, *Weston*
Jackie Wood, *Ohio*
Jian Wu, *Sacramento*
Zobair M Younossi, *Virginia*
Liqing Yu, *Winston-Salem*
Ruben Zamora, *Pittsburgh*
Michael E Zenilman, *New York*
Michael A Zimmerman, *Colorado*
Beat Schnüriger, *California*
Clifford S Cho, *Madison*

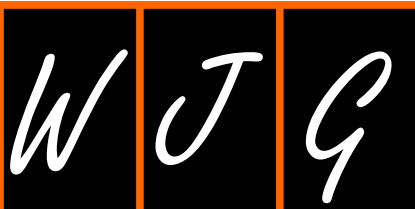
R Mark Ghobrial, *Texas*
Anthony T Yeung, *Philadelphia*
Chang Kim, *West Lafayette*
Balamurugan N Appakalai, *Minneapolis*
Aejaz Nasir, *Tampa*
Ashkan Farhadi, *Irvine*
Kevin E Behrns, *Gainesville*
Joseph J Cullen, *Iowa City*
David J McGee, *Shreveport*
Anthony J Demetris, *Pittsburgh*
Dimitrios V Avgerinos, *New York*
Dong-Hui Li, *Houston*
Eric S Hungness, *Chicago*
Giuseppe Orlando, *Winston Salem*
Hai-Yong Han, *Phoenix*
Huanbiao Mo, *Denton*
Jong Park, *Tampa*
Justin MM Cates, *Nashville*
Charles P Heise, *Madison*
Craig D Logsdon, *Houston*
Ece A Mutlu, *Chicago*
Jessica A Davila, *Houston*
Rabih M Salloum, *Rochester*
Amir Maqbul Khan, *Marshall*
Bruce E Sands, *Boston*
Chakshu Gupta, *Saint Joseph*
Ricardo Alberto Cruciani, *New York*
Mariana D Dabeva, *Bronx*
Edward L Bradley III, *Sarasota*
Martín E Fernández-Zapico, *Rochester*
Henry J Binder, *New Haven*
John R Grider, *Richmond*
Ronnie Fass, *Tucson*
Dinesh Vyas, *Washington*
Wael El-Rifai, *Nashville*
Craig J McClain, *Louisville*
Christopher Mantyh, *Durham*
Daniel S Straus, *Riverside*
David A Brenner, *San Diego*
Eileen F Grady, *San Francisco*
Ekihiro Seki, *La Jolla*
Fang Yan, *Nashville*
Fritz Francois, *New York*
Giamila Fantuzzi, *Chicago*
Guang-Yin Xu, *Galveston*
Jianyuan Chai, *Long Beach*
JingXuan Kang, *Charlestown*
Le Shen, *Chicago*
Lin Zhang, *Pittsburgh*
Mitchell L Shiffman, *Richmond*
Douglas K Rex, *Indianapolis*
Bo Shen, *Cleveland*
Edward J Ciaccio, *New York*
Jean S Wang, *Saint Louis*
Bao-Ting Zhu, *Kansas*
Tamir Miloh, *Phoenix*
Eric R Kallwitz, *Chicago*
Yujin Hoshida, *Cambridge*
C Chris Yun, *Atlanta*
Alan C Moss, *Boston*
Oliver Grundmann, *Gainesville*
Linda A Feagins, *Dallas*
Chanjuan Shi, *Nashville*
Xiaonan Han, *Cincinnati*
William R Brugge, *Boston*
Richard W McCallum, *El Paso*
Lisa Ganley-Leal, *Boston*
Lin-Feng Chen, *Urbana*

Elaine Y Lin, *New York*
Julian Abrams, *New York*
Arun Swaminath, *New York*
Huiping Zhou, *Richmond*
Korkut Uygun, *Boston*
Anupam Bishayee, *Signal Hill*
C Bart Rountree, *Hershey*
Avinash Kambadakone, *Boston*
Courtney W Houchen, *Oklahoma*
Joshua R Friedman, *Philadelphia*
Justin H Nguyen, *Jacksonville*
Sophoclis Alexopoulos, *Los Angeles*
Suryakanth R Gurudu, *Scottsdale*
Wei Jia, *Kannapolis*
Yoon-Young Jang, *Baltimore*
Ourania M Andrisani, *West Lafayette*
Roderick M Quiros, *Bethlehem*
Timothy R Koch, *Washington*
Adam S Cheifetz, *Boston*
Lifang Hou, *Chicago*
Thiru vengadam Muniraj, *Pittsburgh*
Dhiraj Yadav, *Pittsburgh*
Ying Gao, *Rockville*
John F Gibbs, *Buffalo*
Aaron Vinik, *Norfolk*
Charles Thomas, *Oregon*
Robert Jensen, *Bethesda*
John W Wiley, *Ann Arbor*
Jonathan Strosberg, *Tampa*
Randeep Singh Kashyap, *New York*
Kaye M Reid Lombardo, *Rochester*
Lygia Stewart, *San Francisco*
Martin D Zielinski, *Rochester*
Matthew James Schuchert, *Pittsburgh*
Michelle Lai, *Boston*
Million Mulugeta, *Los Angeles*
Patricia Sylla, *Boston*
Pete Muscarella, *Columbus*
Raul J Rosenthal, *Weston*
Robert V Rege, *Dallas*
Roberto Bergamaschi, *New York*
Ronald S Chamberlain, *Livingston*
Alexander S Rosemurgy, *Tampa*
Run Yu, *Los Angeles*
Samuel B Ho, *San Diego*
Sami R Achem, *Florida*
Sandeep Mukherjee, *Omaha*
Santhi Swaroop Vege, *Rochester*
Scott Steele, *Fort Lewis*
Steven Hochwald, *Gainesville*
Udayakumar Navaneethan, *Cincinnati*
Radha Krishna Yellapu, *New York*
Rupjyoti Talukdar, *Rochester*
Shi-Ying Cai, *New Haven*
Thérèse Tuohy, *Salt Lake City*
Tor C Savidge, *Galveston*
William R Parker, *Durham*
Xiaofa Qin, *Newark*
Zhang-Xu Liu, *Los Angeles*
Adeel A Butt, *Pittsburgh*
Dean Y Kim, *Detroit*
Denesh Chitkara, *East Brunswick*
Mohamad A Eloubeidi, *Alabama*
JiPing Wang, *Boston*
Oscar Joe Hines, *Los Angeles*
Jon C Gould, *Madison*
Kirk Ludwig, *Wisconsin*
Mansour A Parsi, *Cleveland*

Perry Shen, *Winston-Salem*
Piero Marco Fisichella, *Maywood*
Marco Giuseppe Patti, *Chicago*
Michael Leitman, *New York*
Parviz M Pour, *Omaha*
Florencia Georgina Que, *Rochester*
Richard Hu, *Los Angeles*
Robert E Schoen, *Pittsburgh*
Valentina Medici, *Sacramento*
Wojciech Blonski, *Philadelphia*
Yuan-Ping Han, *Los Angeles*
Grigoriy E Gurvits, *New York*
Robert C Moesinger, *Ogden*
Mark Bloomston, *Columbus*

Bronislaw L Slomiany, *Newark*
Laurie DeLeve, *Los Angeles*
Michel M Murr, *Tampa*
John Marshall, *Columbia*
Wilfred M Weinstein, *Los Angeles*
Jonathan D Kaunitz, *Los Angeles*
Josh Korzenik, *Boston*
Kareem M Abu-Elmagd, *Pittsburgh*
Michael L Schilsky, *New Haven*
John David Christein, *Birmingham*
Mark A Zern, *Sacramento*
Ana J Coito, *Los Angeles*
Golo Ahlenstiel, *Bethesda*
Smruti R Mohanty, *Chicago*

Victor E Reyes, *Galveston*
CS Pitchumoni, *New Brunswick*
Yoshio Yamaoka, *Houston*
Sukru H Emre, *New Haven*
Branko Stefanovic, *Tallahassee*
Jack R Wands, *Providence*
Wen Xie, *Pittsburgh*
Robert Todd Striker, *Madison*
Shivendra Shukla, *Columbia*
Laura E Nagy, *Cleveland*
Fei Chen, *Morgantown*
Kusum K Kharbanda, *Omaha*
Pal Pacher, *Rockville*
Pietro Valdastrì, *Nashville*



EDITORIAL	4071	Inflammation- and stress-related signaling pathways in hepatocarcinogenesis <i>Nakagawa H, Maeda S</i>
FIELD OF VISION	4082	Indomethacin for post-endoscopic retrograde cholangiopancreatography pancreatitis prophylaxis: Is it the magic bullet? <i>Yang D, Draganov PV</i>
	4086	Three-dimensional image reconstruction in capsule endoscopy <i>Koulaouzidis A, Karargyris A</i>
	4091	Colorectal cancer in patients with inflammatory bowel disease: Can we predict risk? <i>Andersen V, Halfvarson J, Vogel U</i>
TOPIC HIGHLIGHT	4095	Is enteroscopy necessary for diagnosis of celiac disease? <i>Kav T, Sivri B</i>
REVIEW	4102	Diffusion-weighted imaging of biliopancreatic disorders: Correlation with conventional magnetic resonance imaging <i>Lee NK, Kim S, Kim GH, Kim DU, Seo HI, Kim TU, Kang DH, Jang HJ</i>
ORIGINAL ARTICLE	4118	Efficacy of MK615 for the treatment of patients with liver disorders <i>Hokari A, Ishikawa T, Tajiri H, Matsuda T, Ishii O, Matsumoto N, Okuse C, Takahashi H, Kurihara T, Kawahara K, Maruyama I, Zeniya M</i>
	4127	siRNA-mediated downregulation of TC21 sensitizes esophageal cancer cells to cisplatin <i>Hasan MR, Chauhan SS, Sharma R, Ralhan R</i>
	4136	Double contrast-enhanced two-dimensional and three-dimensional ultrasonography for evaluation of gastric lesions <i>Shi H, Yu XH, Guo XZ, Guo Y, Zhang H, Qian B, Wei ZR, Li L, Wang XC, Kong ZX</i>
BRIEF ARTICLE	4145	A comparison of survival and pathologic features of non-alcoholic steatohepatitis and hepatitis C virus patients with hepatocellular carcinoma <i>Hernandez-Alejandro R, Croome KP, Drage M, Sela N, Parfitt J, Chandok N, Marotta P, Dale C, Wall W, Quan D</i>
	4150	Adjusting CA19-9 values to predict malignancy in obstructive jaundice: Influence of bilirubin and C-reactive protein <i>La Greca G, Sofia M, Lombardo R, Latteri S, Ricotta A, Puleo S, Russello D</i>

- 4156 Intrahepatic expression of genes related to metabotropic receptors in chronic hepatitis
Cieśla A, Kuśmider M, Faron-Górecka A, Dziedzicka-Wasylewska M, Bociąga-Jasik M, Owczarek D, Ciećko-Michalska I, Cibor D, Mach T
- 4162 Growth inhibitory effects of *Phyllanthus niruri* extracts in combination with cisplatin on cancer cell lines
Araújo Júnior RF, Soares LAL, da Costa Porto CR, de Aquino RGF, Guedes HG, Petrovick PR, de Souza TP, Araújo AA, Guerra GCB
- 4169 Sensitivity of the suspected blood indicator: An experimental study
Park SC, Chun HJ, Kim ES, Keum B, Seo YS, Kim YS, Jeon YT, Lee HS, Um SH, Kim CD, Ryu HS
- 4175 Impact of surgical volume on nationwide hospital mortality after pancreaticoduodenectomy
Kim CG, Jo S, Kim JS
- 4182 Diabetes but not insulin is associated with higher colon cancer mortality
Tseng CH
- 4191 Role of body mass index in colon cancer patients in Taiwan
Chin CC, Kuo YH, Yeh CY, Chen JS, Tang R, Changchien CR, Wang JY, Huang WS
- 4199 Oxymatrine liposome attenuates hepatic fibrosis *via* targeting hepatic stellate cells
Chai NL, Fu Q, Shi H, Cai CH, Wan J, Xu SP, Wu BY
- 4207 X-ray repair cross-complementing group 1 polymorphisms and hepatocellular carcinoma: A meta-analysis
Xie T, Wang ZG, Zhang JL, Liu H
- 4215 Metabolic syndrome and gallstone disease
Chen LY, Qiao QH, Zhang SC, Chen YH, Chao GQ, Fang LZ
- CASE REPORT**
- 4221 Eosinophilic esophagitis-endoscopic distinguishing findings
Caetano AC, Gonçalves R, Rolanda C
- 4224 Dehiscence following successful endoscopic closure of gastric perforation during endoscopic submucosal dissection
Sekiguchi M, Suzuki H, Oda I, Yoshinaga S, Nonaka S, Saka M, Katai H, Taniguchi H, Kushima R, Saito Y
- 4228 Autoimmune pancreatitis complicated by gastric varices: A report of 3 cases
Goto N, Mimura J, Itani T, Hayashi M, Shimada Y, Matsumori T

- 4233 Ischemic colitis during interferon-ribavirin therapy for chronic hepatitis C: A case report
Baik SJ, Kim TH, Yoo K, Moon IH, Cho MS
- 4237 Spontaneous hemoperitoneum from hepatic metastatic trophoblastic tumor
Liu YH, Ma HX, Ji B, Cao DB

LETTERS TO THE EDITOR 4241 Non-steroidal anti-inflammatory drugs-induced small intestinal injury and probiotic agents
Guslandi M

ACKNOWLEDGMENTS I Acknowledgments to reviewers of *World Journal of Gastroenterology*

APPENDIX I Meetings
I-VI Instructions to authors

ABOUT COVER Editorial Board Member of *World Journal of Gastroenterology*, Julio H Carri, Professor, Internal Medicine-Gastroenterology, National University of Córdoba, Av. Estrada 160-P 5-Department D, Córdoba 5000, Argentina

FLYLEAF I-IX Editorial Board

EDITORS FOR THIS ISSUE

Responsible Assistant Editor: *Yuan Zhou*
Responsible Electronic Editor: *Dan-Ni Zhang*
Proofing Editor-in-Chief: *Lian-Sheng Ma*
Responsible Science Editor: *Ling Jiang*
Proofing Editorial Office Director: *Jian-Xia Cheng*

NAME OF JOURNAL
World Journal of Gastroenterology

ISSN AND EISSN
ISSN 1007-9327 (print)
ISSN 2219-2840 (online)

LAUNCH DATE
October 1, 1995

FREQUENCY
Weekly

RESPONSIBLE INSTITUTION
Department of Science and Technology of Shanxi Province

SPONSOR
Taiyuan Research and Treatment Center for Digestive Diseases, 77 Shuangta Xijie, Taiyuan 030001, Shanxi Province, China

EDITING
Editorial Board of *World Journal of Gastroenterology*
Room 903, Building D, Ocean International Center, No. 62 Dongsihuan Zhonglu, Chaoyang District, Beijing 100025, China
Telephone: +86-10-59080039
Fax: +86-10-85381893
E-mail: wjg@wjgnet.com
<http://www.wjgnet.com>

EDITOR-IN-CHIEF
Ferruccio Bonino, MD, PhD, Professor of Gastroenterology, Director of Liver and Digestive Disease Division, Department of Internal Medicine, University

of Pisa, Director of General Medicine 2 Unit University Hospital of Pisa, Via Roma 67, 56124 Pisa, Italy

Myung-Hwan Kim, MD, PhD, Professor, Head, Department of Gastroenterology, Director, Center for Biliary Diseases, University of Ulsan College of Medicine, Asan Medical Center, 388-1 Pungnap-2dong, Songpa-gu, Seoul 138-736, South Korea

Kjell Öberg, MD, PhD, Professor, Department of Endocrine Oncology, Uppsala University Hospital, SE-751 85 Uppsala, Sweden

Matt D Rutter, MBBS, MD, FRCP, Consultant Gastroenterologist, Senior Lecturer, Director, Tees Bowel Cancer Screening Centre, University Hospital of North Tees, Durham University, Stockton-on-Tees, Cleveland TS19 8PE, United Kingdom

Andrzej S Tarnawski, MD, PhD, DSc (Med), Professor of Medicine, Chief Gastroenterology, VA Long Beach Health Care System, University of California, Irvine, CA, 5901 E. Seventh Str., Long Beach, CA 90822, United States

EDITORIAL OFFICE
Jian-Xia Cheng, Director
Jin-Lei Wang, Vice Director
World Journal of Gastroenterology
Room 903, Building D, Ocean International Center, No. 62 Dongsihuan Zhonglu, Chaoyang District, Beijing 100025, China
Telephone: +86-10-59080039
Fax: +86-10-85381893
E-mail: wjg@wjgnet.com
<http://www.wjgnet.com>

PUBLISHER
Baishideng Publishing Group Co., Limited
Room 1701, 17/F, Henan Building,
No.90 Jaffe Road, Wanchai, Hong Kong, China
Fax: +852-31158812
Telephone: +852-58042046
E-mail: bpg@baishideng.com
<http://www.wjgnet.com>

PRINT SUBSCRIPTION
RMB 300 Yuan for each issue, RMB 14400 Yuan for one year.

PUBLICATION DATE
August 21, 2012

COPYRIGHT
© 2012 Baishideng. Articles published by this Open-Access journal are distributed under the terms of the Creative Commons Attribution Non-commercial License, which permits use, distribution, and reproduction in any medium, provided the original work is properly cited, the use is non commercial and is otherwise in compliance with the license.

SPECIAL STATEMENT
All articles published in this journal represent the viewpoints of the authors except where indicated otherwise.

INSTRUCTIONS TO AUTHORS
Full instructions are available online at http://www.wjgnet.com/1007-9327/g_info_20100315215714.htm

ONLINE SUBMISSION
<http://www.wjgnet.com/esp/>

Inflammation- and stress-related signaling pathways in hepatocarcinogenesis

Hayato Nakagawa, Shin Maeda

Hayato Nakagawa, Department of Gastroenterology, University of Tokyo, Tokyo 113-8655, Japan

Shin Maeda, Department of Gastroenterology, Yokohama City University, Yokohama 236-0004, Japan

Author contributions: Nakagawa H drafted of the article; Maeda S was contributed to the critical revision of the manuscript.

Supported by A fellowship from the Daiichi Sankyo Foundation of Life Science, to Nakagawa H

Correspondence to: Shin Maeda, Professor, Department of Gastroenterology, Yokohama City University, 3-9 Fukuura, Kanazawa-ku, Yokohama 236-0004,

Japan. smaeda@med.yokohama-cu.ac.jp

Telephone: +81-45-7872326 Fax: +81-45-7872327

Received: February 15, 2012 Revised: May 28, 2012

Accepted: June 8, 2012

Published online: August 21, 2012

Abstract

It has been established that cancer can be promoted and exacerbated by inflammation. Hepatocellular carcinoma (HCC) is the fifth most common cancer worldwide, and its long-term prognosis remains poor. Although HCC is a complex and heterogeneous tumor with several genomic mutations, it usually develops in the context of chronic liver damage and inflammation, suggesting that understanding the mechanism(s) of inflammation-mediated hepatocarcinogenesis is essential for the treatment and prevention of HCC. Chronic liver damage induces a persistent cycle of necroinflammation and hepatocyte regeneration, resulting in genetic mutations in hepatocytes and expansion of initiated cells, eventually leading to HCC development. Recently, several inflammation- and stress-related signaling pathways have been identified as key players in these processes, which include the nuclear factor- κ B, signal transducer and activator of transcription, and stress-activated mitogen-activated protein kinase pathways. Although these pathways may suggest potential therapeutic targets, they have a wide range of functions and complex crosstalk occurs among them.

This review focuses on recent advances in our understanding of the roles of these signaling pathways in hepatocarcinogenesis.

© 2012 Baishideng. All rights reserved.

Key words: Hepatocellular carcinoma; Inflammation; Nuclear factor- κ B; Mitogen-activated protein kinase; Signal transducer and activator of transcription; c-Jun NH₂-terminal kinase; p38; Transforming growth factor-activated kinase 1; Apoptosis signal-regulating kinase 1

Peer reviewers: Dr. Richard A Rippe, National Institutes of Health, 5635 Fishers Lane, Room 2109 NIH/NIAAA, Rockville, MD 20852, United States; Dr. Xian-Ming Chen, Department of Med Microbiol and Immunol, Creighton University Medical Center, 2500 California Plaza, Omaha, NE 68178, United States; Rudi Beyaert, Professor, Department of Molecular Biomedical Research, Flanders Interuniversity Institute for Biotechnology and Ghent University, Technologiepark 927, B-9052 Gent, Belgium

Nakagawa H, Maeda S. Inflammation- and stress-related signaling pathways in hepatocarcinogenesis. *World J Gastroenterol* 2012; 18(31): 4071-4081 Available from: URL: <http://www.wjgnet.com/1007-9327/full/v18/i31/4071.htm> DOI: <http://dx.doi.org/10.3748/wjg.v18.i31.4071>

INTRODUCTION

Various types of cancer arise in the setting of chronic inflammation, suggesting a strong link between inflammation and carcinogenesis^[1,2]. Although Virchow first suggested this relationship in the 19th century, clear evidence for it has been obtained only during the last decade^[3]. The development of hepatocellular carcinoma (HCC) is one of the most extensively investigated inflammation-based carcinogenic processes because more than 90% of HCCs develop in the context of chronic liver damage and inflammation.

HCC is diagnosed in more than half a million people each year and is the third most common cause of cancer mortality worldwide^[4]. The short-term prognosis of patients with HCC has improved recently due to advances in early diagnosis and treatment, but long-term prognosis remains unsatisfactory, as indicated by the low overall survival of 22%-35% at 10 years after curative treatment^[5,6]. Thus, understanding the molecular carcinogenic mechanisms and the unique pathogenic biology of HCC has become an important issue worldwide.

HCC is a complex and heterogeneous tumor with several genomic mutations, but even the most frequent genetic mutations, such as those in p53 and β -catenin, are seen in 30%-50% of HCC cases at most^[7]. On the other hand, as mentioned above, more than 90% of HCC develops based on chronic inflammation, indicating that understanding the mechanism(s) of inflammation-mediated hepatocarcinogenesis is necessary for the treatment and prevention of HCC.

The main cause of HCC is viral hepatitis caused by the hepatitis B virus (HBV) or hepatitis C virus (HCV); other major etiologies include hemochromatosis, alcoholic hepatitis, and non-alcoholic steatohepatitis (NASH)^[7]. Most of these diseases are known to cause chronic inflammation in the liver, which plays a critical role in hepatocarcinogenesis. For example, in chronic viral hepatitis, the host immune responses to HBV or HCV are often insufficiently strong to completely clear the infection, resulting in chronic stimulation of an antigen-specific immune response^[8]. Virus-infected hepatocytes are killed by host immune cells as well as the intrinsic cytopathic effects of the hepatitis viruses, triggering the production of various cytokines and growth factors and subsequently inducing compensatory hepatocyte regeneration. This persistent cycle of necro-inflammation and hepatocyte regeneration is thought to increase the risk of genetic mutation in hepatocytes, and, furthermore, to promote survival and expansion of initiated cells^[9-11]. Additionally, reactive oxygen species (ROS) and nitrogen oxygen species, generated by both initiated cells and inflammatory cells, could accelerate hepatocarcinogenesis through several mechanisms, such as the induction of oxidative DNA damage, DNA methylation, and hepatocyte injury^[11].

Multiple signaling pathways are involved in these processes. Among them, recent *in vivo* studies have shown that several inflammation- and stress-related signaling pathways are key players in hepatocarcinogenesis, including the nuclear factor- κ B (NF- κ B), signal transducer and activator of transcription (STAT), and stress-activated mitogen-activated protein kinase (MAPK) pathways. Mutations in genes involved in these signaling pathways are currently thought to be rare. Nevertheless, constitutive activation of these pathways is frequently seen in the tumor and surrounding liver tissues, and may be due to the inflammatory microenvironment. Interestingly, these signaling pathways do not act independently, but are linked through extensive crosstalk. This review highlights

advances in the understanding of these interesting but complex signaling pathways in hepatocarcinogenesis.

INFLAMMATION-RELATED SIGNALING IN HEPATOCARCINOGENESIS

Role of the I κ B kinase/NF- κ B pathway in hepatocytes

The NF- κ B family of transcription factors consists of five members: p65/RelA, c-Rel, RelB, p50/NF- κ B1, and p52/NF- κ B2. Two of the five members dimerize and are held in the cytoplasm by the inhibitor of NF- κ B (I κ B) proteins^[12]. In response to many kinds of proinflammatory stimuli, the I κ B kinase (IKK) complex, which consists of two catalytic subunits, IKK α and IKK β , and a regulatory component, IKK γ /I κ B kinase (NEMO), phosphorylates I κ B and subsequently induces degradation of it. Once activated, NF- κ B dimers translocate into the nucleus and stimulate the transcription of various genes, such as those encoding cytokines and anti-apoptotic factors^[13]. Mice lacking RelA, IKK β , or NEMO reveal embryonic lethality with extensive liver apoptosis and degeneration^[14-16]. This liver apoptosis is induced by tumor necrosis factor (TNF)- α , and intercrossing with TNF receptor 1 knockout mice prevents liver damage and the lethal phenotype^[14,17,18]. Furthermore, hepatocyte-specific IKK β or NEMO knockout mice are not embryonic-lethal, but are more sensitive to TNF- α -mediated liver injury^[19,20]. Thus, NF- κ B plays a key role in liver homeostasis by preventing hepatocyte death.

The role of IKK β in hepatocarcinogenesis has been examined using the diethylnitrosamine (DEN)-induced mouse HCC model^[21]. DEN is the most commonly used genotoxic chemical carcinogen to investigate the mechanism of hepatocarcinogenesis, because it is easy to induce HCC and DEN-induced HCC shows histology and gene expression similar to human HCC, especially with a poor prognosis^[22,23]. A single dose of DEN given to 2-wk-old male mice is sufficient to induce HCC. However, when DEN is administered to mice older than 4 wk of age, it cannot induce HCC and requires assistance from tumor promoters, such as phenobarbital, because hepatocyte proliferation is rare in adult mice^[24]. Thus, some stimulation that induces hepatocyte proliferation is indispensable as a tumor promoter in this model.

Strikingly, DEN-induced HCC was markedly increased in hepatocyte-specific IKK β knockout mice^[21]. Hepatocyte-specific knockout of IKK β induced a greater extent of hepatocyte death with ROS accumulation after DEN administration, because NF- κ B activation is required for the up-regulation of antioxidative genes, such as ferritin heavy chain and manganese-dependent superoxide dismutase. Excess ROS accumulation promotes cell death through various mechanisms, including prolonged c-Jun NH₂ terminal kinase (JNK) activation^[25]. Cell death is accompanied by an inflammatory reaction, and the elevated hepatocyte death rate enhances compensatory proliferation. Thus, the hepatocyte-specific deletion of

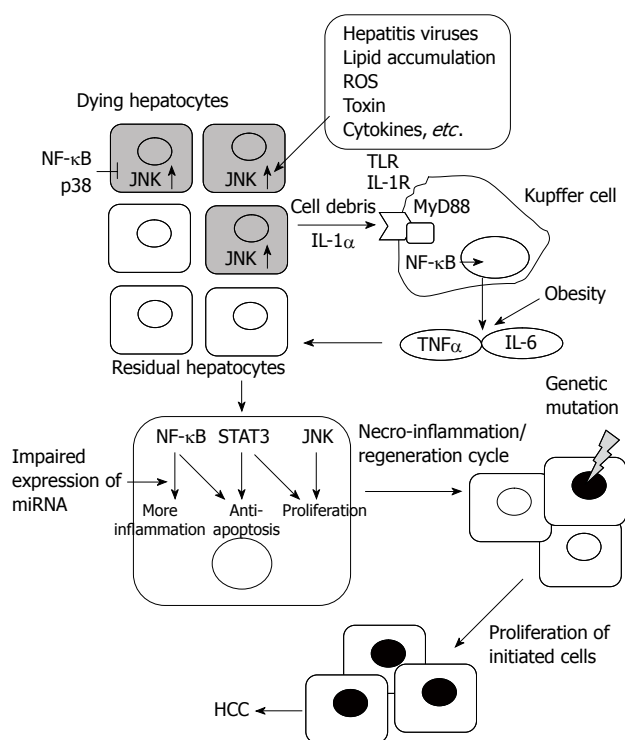


Figure 1 Role of inflammation- and stress-related signaling pathways in hepatocarcinogenesis. Chronic liver damage induces a persistent cycle of necro-inflammation and hepatocyte regeneration, resulting in genetic mutations in hepatocytes and expansion of initiated cells, eventually leading to hepatocellular carcinoma (HCC) development. As shown in the figure, nuclear factor- κ B, signal transducer and activator of transcription 3, and stress-activated mitogen-activated protein kinase pathways play critical roles in these processes. Furthermore, other factors, such as obesity and impaired expression of microRNA, can modify these inflammatory processes and accelerate HCC development. ROS: Reactive oxygen species; TLR: Toll-like receptor; NF- κ B: Nuclear factor- κ B; TNF: Tumor necrosis factor; IL: Interleukin; JNK: c-Jun NH₂ terminal kinase; STAT: Signal transducer and activator of transcription.

IKK β augments DEN-induced hepatocyte death and cytokine-driven compensatory proliferation, which acts as a tumor promoter and eventually leads to increased HCC development (Figure 1). Similar findings were obtained in mice lacking IKK γ /NEMO, the hepatocyte-specific deletion of which results in spontaneous liver damage, hepatosteatosis, fibrosis, and HCC development^[20].

Although the experiments described above demonstrate a tumor-suppressive role of NF- κ B in the hepatocyte, hepatocyte NF- κ B has been also identified to have tumor-promoting roles in other HCC models that depend on chronic inflammation rather than liver damage and death-driven compensatory proliferation. Experiments crossing transgenic mice expressing a non-degradable I κ B α mutant in hepatocytes with *MDR2* knockout mice, which show low-grade chronic inflammation in the portal area and subsequent cancer development, revealed that the inhibition of NF- κ B activation resulted in reduced HCC development^[26]. In this model, NF- κ B activation in the hepatocyte promoted a low degree of TNF- α production and paracrine TNF- α signaling maintained NF- κ B activation in the malignant cells, leading to

the expression of anti-apoptotic genes and the survival of malignant cells. Notably, NF- κ B activation is more important in the progression of hepatocarcinogenesis than in the initiation step in this model. A similar tumor-promoting role of NF- κ B in the hepatocyte has been reported in hepatocyte-specific lymphotoxin $\alpha\beta$ transgenic mice^[27]. Lymphotoxin $\alpha\beta$ transgenic hepatocytes produce chemokines, such as CCL2, CCL7, CXCL1, and CXCL10, in an IKK β -dependent manner, recruiting inflammatory cells into the liver and inducing spontaneous chronic inflammation and the subsequent development of HCC. These findings suggest that NF- κ B activation in the hepatocyte is involved in the production of cytokines and chemokines that maintain the inflammatory environment as a tumor promoter. Thus, the NF- κ B pathway in the hepatocyte plays dual roles in hepatocarcinogenesis, according to the disease model and the carcinogenesis stage.

Role of the IKK/NF- κ B pathway in myeloid cells

The role of the NF- κ B pathway in myeloid cells has also been investigated using a DEN-induced HCC model^[21]. In contrast to hepatocyte-specific IKK β knockout mice, deletion of IKK β in both hepatocytes and myeloid cells, including Kupffer cells, strongly inhibited DEN-induced HCC development. This phenotype was derived from the markedly reduced production of cytokines, such as TNF- α , interleukin-6 (IL-6), and hepatocyte growth factor, which are secreted by non-parenchymal cells in response to dying hepatocytes and induce compensatory proliferation of residual hepatocytes. Thus, IKK β /NF- κ B in myeloid cells is required for the production of liver growth factors and subsequent hepatocarcinogenesis. Furthermore, IKK β in myeloid cells, especially in Kupffer cells, has also been implicated in the development of metastatic liver tumors through IL-6 production^[28]. Thus, the IKK β /NF- κ B pathway orchestrates inflammatory crosstalk between hepatocytes and myeloid cells in liver cancer development (Figure 1).

Role of inflammatory cytokines in hepatocarcinogenesis

As mentioned above, NF- κ B activation-mediated production of inflammatory cytokines plays an important role in the inflammation-carcinogenesis axis of the liver. Various inflammatory cytokines, including TNF- α , IL-1 α , IL-1 β , IL-6, and IL-8, have been implicated in chronic liver inflammation, among which IL-6 is thought to be one of the most important^[8,29,30]. In chronic hepatitis, IL-6 is considered to be produced mainly by activated Kupffer cells and to intensify local inflammatory responses, and then induce compensatory hepatocyte proliferation, facilitating malignant transformation of hepatocytes^[30]. Hepatocytes express high amounts of the IL-6 receptor and a signal-transducing element (gp130) that, upon IL-6 binding, activates two signaling pathways, Janus activated kinase (JAK)-STAT and MAPK, which are important in the regulation of cell survival and proliferation^[31]. In fact, serum IL-6 levels are elevated in patients with chronic liv-

er diseases, including alcoholic hepatitis, HBV and HCV infections, and NASH^[32-34]. Additionally, a higher serum IL-6 level correlates with future HCC development in patients with chronic hepatitis B or C^[35,36]. These findings suggest that IL-6 plays a role linking chronic inflammation and hepatocarcinogenesis in humans.

In a mouse HCC model, IL-6 knockout mice showed a marked reduction in DEN-induced HCC development, indicating that IL-6 signaling is directly involved in hepatocarcinogenesis^[37]. This study also demonstrated the key role played by the toll-like receptor (TLR) adapter protein MyD88. Necrotic hepatocyte-induced IL-6 production was reduced significantly in MyD88-deficient Kupffer cells. Furthermore, deletion of MyD88 suppresses DEN-induced carcinogenesis, indicating that IL-6 production through the TLR/MyD88/NF- κ B pathway in Kupffer cells is essential for HCC development. Another study showed that the DEN-induced acute inflammatory response is triggered by IL-1 α release from necrotic hepatocytes, and IL-1 α subsequently induces IL-6 production by Kupffer cells^[38]. Indeed, IL-1 receptor knockout mice showed significantly reduced DEN-induced IL-6 production and subsequent HCC development^[38]. Of note, a clinical study revealed that higher serum IL-6 levels correlated with higher aspartate aminotransferase levels in chronic hepatitis C, suggesting that IL-6 may be produced in response to HCV-induced hepatocyte injury^[36].

HCC develops much more frequently in males than in females in almost all populations, with a male-to-female ratio of 2:1-4:1^[39]. Interestingly, although this sex disparity is also found in this DEN-induced HCC model, ablation of IL-6 abolished the sex differences in hepatocarcinogenesis^[37]. However, ovariectomized female mice revealed enhanced IL-6 production and aggravated HCC development. Furthermore, estrogen administration to Kupffer cells inhibits necrotic hepatocyte-induced IL-6 production. These results suggest that estrogen-mediated down-regulation of IL-6 may partly explain the sex disparity in HCC development. However, more recently, Li *et al*^[40] reported that transcription factors Foxa1 and Foxa2 in the hepatocyte played important roles in the sex disparity in hepatocarcinogenesis through an interaction with the estrogen and androgen receptors, independent of IL-6 signaling. Thus, the sex disparity in hepatocarcinogenesis may have several causes in addition to estrogen-mediated down-regulation of IL-6.

Several epidemiologic studies have shown that obesity and metabolic syndrome increase the risk of HCC^[41-43]. Although the mechanism by which obesity and metabolic syndrome promote hepatocarcinogenesis is not fully understood, it seems likely to be mediated, in part, by a state of chronic inflammation. A recent report by Park *et al*^[44] demonstrated that dietary- or genetically induced obesity promoted DEN-induced HCC along with low-grade inflammation, and ablation of IL-6 or the TNF receptor 1 abrogated their tumor-promoting effects, suggesting that IL-6 and TNF- α are required for the promotion of obesity-associated HCC. IL-6 and TNF- α produced by

adipose tissue or Kupffer cells activate hepatocyte STAT3 and NF- κ B, respectively, promoting cell proliferation and survival of initiated hepatocytes. In fact, recent clinical studies have suggested that visceral fat accumulation, insulin resistance, and dysregulation of adipokines, which induce the activation of the inflammatory response, play important roles in hepatocarcinogenesis^[45-47]. As the incidence rate of such obesity-associated hepatocarcinogenesis is likely to increase in the near future, inflammatory cytokines have also attracted considerable attention as a mediator of the association between obesity and hepatocarcinogenesis^[48].

Role of JAK-STAT signaling

JAK/STAT signaling pathways are important components of many cytokine receptor systems. Cytokines function by specifically recognizing their receptors, which, as a result of binding to their ligand, undergo conformational changes, resulting in the displacement of JAKs, and subsequently JAKs phosphorylate and activate STATs. The STAT protein family consists of seven members encoded by distinct genes. Among them, STAT3 is the most important IL-6 signaling pathway molecule and is recognized as a key player linking inflammation and cancer^[49,50]. In response to IL-6 signaling through gp130/JAK, STAT3 forms homodimers that translocate to the nucleus. STAT3 is constitutively active in many tumor cells, but not in normal cells, and regulates the expression of genes involved in tumor progression, such as cell survival, proliferation, invasion, and angiogenesis^[51].

Clinical and experimental evidence suggest the involvement of the STAT3 signaling pathway in hepatocarcinogenesis. Activated nuclear STAT3 is found in 60% of HCC and is more pronounced in aggressive tumors^[52]. In contrast, suppressors of this pathway, such as suppressor of cytokine signaling 3 (SOCS3), are down-regulated in HCC^[53]. In a mouse model, hepatocyte-specific STAT3 ablation prevented DEN-induced HCC development^[52], whereas hepatocyte-specific SOCS3 knockout mice were susceptible to HCC development through the enhanced activation of JAK/STAT and MAPK signaling^[53]. Hepatocyte-specific IL-6 and IL-6R transgenic mice spontaneously develop hepatocellular hyperplasia and adenomas, which are considered precancerous lesions in humans, accompanying STAT3 activation^[54]. Furthermore, in a human study, gain-of-function mutations in gp130 have been identified in 60% of benign hepatocellular adenomas with an inflammatory phenotype, and when combined with β -catenin-activating mutation, lead to HCC development^[55]. Thus, the IL-6-gp130-JAK-STAT3 signaling axis is an important contributor to HCC development, making it an attractive target for the treatment and/or prevention of hepatocarcinogenesis.

Interaction between STAT3 and NF- κ B has been reported at several levels in tumors. Some studies showed that STAT3 and NF- κ B co-regulate numerous oncogenic and inflammatory genes^[50]. Additionally, STAT3 directly interacts with RelA, trapping it in the nucleus, thereby

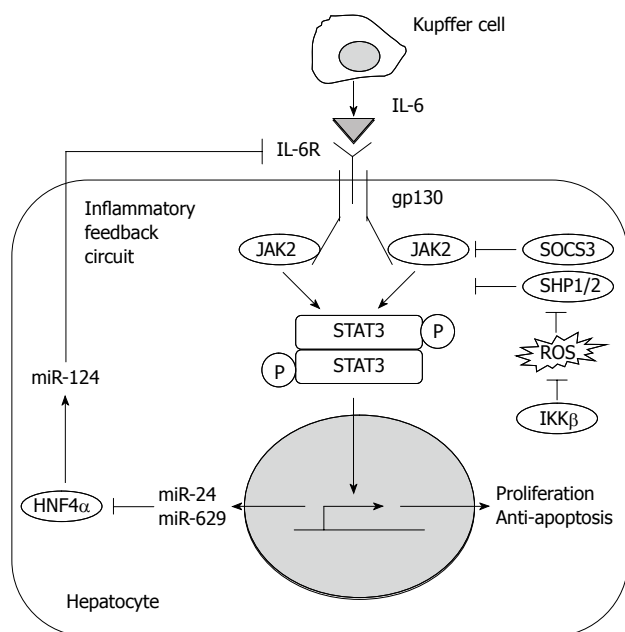


Figure 2 Implications and regulatory system of interleukin-6/gp130/janus activated kinase/signal transducer and activator of transcription 3 signaling in hepatocarcinogenesis. Interleukin (IL)-6 secreted by Kupffer cells activates signal transducer and activator of transcription (STAT) 3, which promotes the proliferation and survival of initiated hepatocytes. STAT3 activation is suppressed by I κ B kinase β through the prevention of reactive oxygen species. However, once STAT3 is activated, STAT3 activation becomes sustained through a microRNA feedback inflammatory loop. JAK: Janus activated kinase; SOCS3: Suppressor of cytokine signaling 3; IKK: I κ B kinase; HNF: Hepatocyte nuclear factor; ROS: Reactive oxygen species.

contributing to constitutive NF- κ B activation^[56]. On the other hand, a recent *in vivo* study revealed that IKK β /NF- κ B in the hepatocyte negatively regulated STAT3 activation in a DEN-induced HCC model^[52]. Inactivation of IKK β caused ROS accumulation and ROS were found to oxidize protein tyrosine phosphatases, including SHP1 and SHP2, which dephosphorylated JAK2 and STAT3. Oxidation of SHP1 and SHP2 results in the loss of their catalytic activity and the constitutive activation of STAT3. In fact, an inverse correlation between NF- κ B and STAT3 has been found in human HCC samples. This crosstalk may be a reason for the aggravation of DEN-induced HCC in hepatocyte-specific IKK β knock-out mice. Furthermore, Bard-Chapeau *et al.*^[57] showed that hepatocyte-specific SHP2 knockout mice revealed spontaneous liver inflammation and tumorigenesis, accompanied by STAT3 activation. These mice also showed enhanced DEN-induced HCC, which was decreased significantly by intercrossing with hepatocyte-specific STAT3 knockout mice. These results suggest that the inhibition of STAT3 activation by SHP2 plays an important tumor-suppressing role in hepatocarcinogenesis (Figure 2).

Implications of microRNA in inflammatory signaling

MicroRNAs (miRNAs) are endogenous 20-23-nucleotide RNAs that play important gene-regulatory roles by pairing with the messenger RNAs of protein-coding genes to

direct their post-translational repression^[58]. Recently, miRNAs have been reported to be implicated in hepatocarcinogenesis through modulating inflammatory signaling pathways. Ji *et al.*^[59] found that miR-26 was significantly reduced in human HCC tissues, compared with surrounding non-tumor tissues, and a gene network analysis revealed that miR-26 expression was inversely correlated with the activation of NF- κ B and IL-6 signaling pathways. Although a causal relationship between miR-26 and hepatocarcinogenesis could not be evaluated in this study, Kota *et al.*^[60] showed that low miR-26 expression played a causal role in hepatocarcinogenesis using a myc-induced mouse HCC model, and induction of miR-26 by gene therapy suppressed HCC development.

More recently, hepatocyte nuclear factor 4 α (HNF4 α), a transcription factor that is essential for the development of hepatocytes, was reported to play a key role in hepatocarcinogenesis, linking miRNAs and inflammatory signaling pathways^[61]. Transient suppression of HNF4 α induces decreased miR-124 expression, leading to increased IL-6R expression and subsequent STAT3 activation. STAT3 activation not only plays the tumor-promoting roles described above, but also up-regulates HNF4 α -targeting miRNAs, miR-24 and miR-629, resulting in continued suppression of HNF4 α . Thus, transient suppression of HNF4 α initiates an IL-6/STAT3-mediated hepatocarcinogenesis process through a miRNA feedback loop circuit (Figure 2). The authors also showed that systemic administration of miR-124 prevented hepatocarcinogenesis by inhibiting the feedback loop and inducing tumor-specific apoptosis in mice. Thus, a therapeutic strategy targeting miRNA may be useful for the prevention and treatment of HCC.

STRESS-RELATED SIGNALING IN HEPATOCARCINOGENESIS

Stress-activated MAPK

MAPK cascades are signaling systems that transmit intracellular signals initiated by extracellular stimuli to the nucleus^[62,63]. The MAPK family consists of three major MAPK cascades, converging on extracellular signal-regulated kinases (ERKs), JNKs, and p38 MAPKs. Each MAPK signaling system comprises at least three components: MAPK, MAPK kinase (MAPKK), and MAPKK kinase (MAP3K). MAP3K phosphorylates, and thereby activates, MAPKK, and activated MAPKK, in turn, phosphorylates and activates MAPK. Among the three MAPKs, ERKs are activated predominantly by growth factors, whereas JNKs and p38 MAPKs, also called stress-activated MAPKs, are activated by stresses. We discuss the function and regulation of the stress-activated MAPKs in hepatocarcinogenesis in detail below.

Role of JNK signaling

JNK has three isoforms (JNK1, JNK2, JNK3) encoded by three loci. JNK1 and JNK2 are expressed ubiquitously, including in the liver, whereas JNK3 is expressed primar-

ily in the brain^[64]. JNK is phosphorylated and activated by two MAPKs, MKK4 and MKK7, and subsequently phosphorylates transcription factors, such as c-Jun and JunD, which compose the AP-1 complex^[65]. Additionally, JNK phosphorylates other proteins, such as Bcl-2 family members, and exerts various kinds of functions, depending on the cell type and stimuli^[66]. Furthermore, although JNK1 and JNK2 isoforms play redundant roles in many physiological processes, they also have distinct biological activities in some situations^[67,68].

The major functions of JNK in the liver are thought to be the induction of hepatocyte proliferation and cell death. JNK is involved in cell cycle progression, mostly through the activation of c-Jun. In this function, JNK1 is considered to be more important than JNK2, because proliferation of hepatocytes after partial hepatectomy is significantly impaired in JNK1 knockout mice, but not in JNK2 knockout mice^[69]. Additionally, hepatocyte death due to TNF- α , lipotoxicity, ER stress, ischemia-reperfusion, and drug toxicity, such as that from acetaminophen, are also considered to be JNK-dependent^[19,70-73]. JNK1 and JNK2 are, to some extent, redundant in this function. Although the downstream targets of JNK are not fully understood, most studies have demonstrated that JNK is required for the activation of the mitochondrial apoptotic pathway, through the activation of pro-apoptotic Bcl-2 family members^[74,75].

The role of JNK in hepatocarcinogenesis has been investigated using the DEN-induced HCC model^[76]. As mentioned above, hepatocyte-specific knockout of IKK β markedly promotes DEN-induced HCC, through enhanced hepatocyte death and compensatory proliferation^[21]. These phenomena can be partly explained by enhanced JNK activation in the setting of IKK β depletion. Because prolonged JNK activation is closely related to cell death, systems for the regulation of JNK activity are needed for tissue homeostasis. In this regard, NF- κ B plays an important role. Although several mechanisms have been proposed in the NF- κ B-mediated inhibition of JNK activation, ROS is one of the most important mediators^[25,77-79]. ROS accumulation, caused by the reduced expression of NF- κ B-dependent antioxidative enzymes, extends JNK activation by inactivating MAPK phosphatases that are essential for the dephosphorylation of activated JNK^[25]. In fact, the administration of antioxidants to hepatocyte-specific IKK β knockout mice decreased sustained JNK activation and hepatocyte death after DEN injection, and furthermore, intercrossing hepatocyte-specific IKK β knockout mice with JNK1 knockout mice significantly reduced DEN-induced hepatocyte death and compensatory proliferation, eventually suppressing HCC development^[21,76]. Additionally, JNK1 knockout mice showed a significant reduction of DEN-induced HCC, compared with wild-type controls. Thus, JNK1 is involved in hepatocarcinogenesis through hepatocyte death and proliferation, which are key components of necro-inflammatory cycles (Figure 1). Furthermore, in addition to the initial phase, JNK1 plays a tumor-

promoting role by enhancing cancer cell proliferation and neovascularization through the increased expression of cyclin D1 and vascular endothelial growth factor, respectively^[76]. Another study showed that JNK1 promoted HCC cell proliferation *in vivo* through the up-regulation of c-myc expression and the down-regulation of p21 expression^[69]. This study, however, also showed that JNK2 was not involved in hepatocarcinogenesis. In fact, JNK1, but not JNK2, is activated in approximately half of human HCC tissues, compared with adjacent non-tumor tissues^[69,80]. These results suggest that JNKs, especially JNK1, play an important role in the development of HCC. Notably, the pharmacological inhibition of JNK suppressed DEN-induced HCC and the growth of xenografted human HCC cells, suggesting that JNK may be a promising therapeutic target for HCC^[69].

On the other hand, a recent study using conditional JNK knockout mice showed that the ablation of both JNK isoforms, JNK1 and JNK2, in hepatocytes increased DEN-induced HCC, whereas the ablation of JNK1 and JNK2 in both hepatocytes and myeloid cells reduced hepatic inflammation and the development of HCC, indicating that JNK plays dual roles in hepatocarcinogenesis, depending on cell type and carcinogenesis stage^[81].

JNK plays a pivotal role in the development of metabolic syndrome-related disorders, including NASH^[41]. Inflammatory cytokines and ROS accumulation in the liver caused by obesity and fatty liver disease induce JNK activation, leading to insulin resistance by increasing inhibitory insulin receptor substrate 1 ser307 phosphorylation^[82]. As a clinical study showed that insulin resistance was a major contributor to obesity-mediated hepatocarcinogenesis, JNK may be a candidate therapeutic target in such situations^[83]. Furthermore, ROS-mediated JNK activation in the liver is linked not only to liver disease, but also to systemic disorders, such as atherosclerotic cerebrovascular diseases; thus, further elucidation of this process is important^[84,85].

Role of p38 signaling

The p38 MAPK family consists of four members: p38 α , p38 β , p38 γ , and p38 δ ^[86]. Among them, p38 α is abundant in most cell types, and its function has been investigated in most published studies of p38 MAPKs. p38 is activated through phosphorylation, primarily by MKK3 and MKK6, but phosphorylation by MKK4 and autophosphorylation are also involved in some stimuli^[87]. p38 can activate not only transcription factors, such as ATF2, p53, and Mitf, but also protein kinases, such as MAPKAP kinase 2 (MK2) and MK5^[88]. Although p38 was initially discovered as a regulator of inflammatory cytokine production, recent studies have revealed that it has tumor-suppressing properties. p38 inhibits tumorigenesis by the down-regulation of cyclins, up-regulation of cyclin-dependent kinase inhibitors, and modulation of the tumor suppressor p53, resulting in cell cycle arrest, oncogene-induced senescence, apoptosis induction, and contact inhibition^[86].

Although the roles of p38 in the liver have yet to be clarified, compared with JNK, major roles reported to date are the inhibition of hepatocyte death and proliferation. These effects of p38 are partially mediated by negative regulation of the JNK/c-Jun pathway. For example, hepatocyte-specific p38 α knockout mice showed much stronger lipopolysaccharide (LPS)-induced JNK activation in the liver, and intercrossing with hepatocyte specific IKK β knockout mice induced severe liver injury after LPS administration, suggesting that p38 α and IKK β act synergistically to protect the liver from TNF- α -induced hepatocyte death^[89].

The role of p38 in hepatocarcinogenesis has also been investigated using the DEN-induced HCC model^[38]. Similar to hepatocyte-specific IKK β knockout mice, hepatocyte-specific p38 α knockout mice showed enhancement of DEN-induced ROS accumulation, JNK activation, liver damage, and compensatory hepatocyte proliferation, eventually resulting in enhanced carcinogenesis. Another study showed the tumor-suppressing role of p38 through interaction with the JNK/c-Jun pathway by focusing on the antiproliferative effects in the advanced stage^[90]. However, in contrast to IKK β knockout mice, enhanced activation of the JNK pathway in p38 α knockout mice was accompanied by MAPKK activation, suggesting that the targets of p38 α may be upstream of JNK, such as MAPKKs and MAP3Ks^[38]. Consistent with these animal experiments, in human samples, the activity of the MKK6/p38 pathway is decreased in HCC tissues, compared with adjacent non-tumor tissues, and is significantly lower in larger HCC tissues^[91]. These findings suggest that the p38 pathway may play an anti-proliferative role in human HCC.

Regulatory system of stress-activated MAPK signaling by MAP3Ks

The evidence presented above suggests that JNK acts generally as a tumor promoter and p38 acts generally as a tumor suppressor in hepatocarcinogenesis, but some studies have shown opposite roles in HCC and other cancers. For example, JNK plays tumor-suppressing roles in mouse skin cancer and mammalian cancer models^[92,93]. Additionally, JNK has been reported to act as a tumor suppressor by inducing cancer cell apoptosis in HCC^[94]. As mentioned above, JNK was also reported to play dual roles in hepatocarcinogenesis, depending on cell type and carcinogenesis stage^[81]. p38 may also have oncogenic effects, facilitating cell invasion, inflammation, and angiogenesis^[95,96]. Furthermore, crosstalk among JNK, p38, and molecules involved in other signaling pathways, such as NF- κ B, further complicates their roles^[97]. Thus, understanding of the regulatory system of stress-activated MAPK signaling is necessary for the potential use of these molecules as therapeutic targets. Importantly, only two molecules, JNK and p38, are downstream in this pathway, whereas more than 10 molecules have been identified for upstream MAP3Ks^[98]. Each MAP3K is activated by several different kinds of stimuli, and integrated

into a unique pattern of MAPK activation and substrate phosphorylation, leading to a specific cellular response to the stimulus. Thus, the activities of JNK and p38 are tightly regulated by MAP3Ks. Several recent studies have uncovered roles of MAP3Ks in the regulation of stress-activated MAPK signaling in hepatocarcinogenesis.

Role of apoptosis signal-regulating kinase 1

Apoptosis signal-regulating kinase 1 (ASK1), one of the most important MAP3Ks, selectively activates JNK and p38 signaling in response to a variety of stimuli, including ROS and cytokines^[99]. In particular, ASK1 plays a key role in oxidative stress-induced cell death. In the absence of oxidative stress, thioredoxin (Trx), a reduction/oxidation regulatory protein, inhibits ASK1 kinase activity *via* direct binding to the N-terminal region of ASK1. However, once oxidative stress occurs in the cell, Trx is converted to its oxidized form and dissociates from ASK1, resulting in ASK1 kinase activation^[100]. ASK1 is considered to induce cell death through stress-activated MAPK-mediated activation of the mitochondrial cell death pathway^[101]. In fact, ASK1 is involved in acetaminophen-induced hepatocyte death, a typical ROS-mediated liver injury, through mechanisms involving Trx-ASK1 dissociation^[102]. Furthermore, ASK1 is involved in hepatocyte death mediated by death receptors, such as TNF-R and Fas^[75].

ASK1 knockout mice showed significantly increased DEN-induced HCC, suggesting that ASK1 plays tumor-suppressing roles in hepatocarcinogenesis in this model^[75]. Activation of JNK and the pro-apoptotic Bcl-2 family member Bim, which are required for death receptor-mediated apoptosis, are attenuated in ASK1 knockout HCC, resulting in decreased cancer cell apoptosis. On the other hand, ASK1 plays a minor role in the tumor-promoting effects of JNK, such as the DEN-induced acute phase reaction, cancer cell proliferation, and neovascularization. Thus, ASK1 is considered to play major roles in the tumor-suppressing part of JNK activity in hepatocarcinogenesis. Furthermore, DNA damage-induced p38 activation and subsequent p21 up-regulation is impaired in ASK1 knockout mice. Thus, ASK1 controls the tumor-suppressing function in stress-activated MAPK signaling through the induction of apoptosis and the DNA damage response.

Another study indicated that ASK1 and Bim are also required for sorafenib-induced apoptosis in HCC cells^[103]. Sorafenib is a small-molecule multikinase inhibitor that is currently the sole therapeutic drug effective for the treatment of HCC^[104]. Most recently, somatic mutations in the ASK1 gene, which reduce the kinase activity of ASK1, have been identified in melanoma^[105]. Thus, it may be important to clarify whether similar mutations are found in HCC, from the point of view of not only the carcinogenesis mechanism, but also possible therapeutic effects of anticancer drugs.

Role of transforming growth factor β -activated kinase 1

Another major MAP3K, activated kinase 1 (TAK1), is

activated through TNF receptor, TLR, IL-1 receptor, and transforming growth factor β receptor signaling, and then activates the JNK and NF- κ B pathways, which play opposing roles in cell death^[106]. Interestingly, hepatocyte-specific TAK1 knockout mice show spontaneous hepatocyte death, and this phenotype is partially rescued by crossing with TNF receptor 1 knockout mice, suggesting that TAK1 knockout hepatocytes are highly sensitive to endogenous TNF- α -induced apoptosis^[107]. This spontaneous cell death subsequently causes compensatory hepatocyte proliferation, inflammation, fibrosis, and the eventual development of HCC in aged mice^[107,108]. These phenomena resemble the phenotype observed in hepatocyte-specific NF- κ B knockout mice. Furthermore, JNK activation is rather enhanced in TAK1 knockout mice, indicating that TAK1 in the hepatocytes acts as a tumor suppressor, mainly by regulating the activation of the NF- κ B pathway. However, enhanced JNK activation in TAK1 knockout mice occurs partially through the activation of another MAP3K, TAO2, suggesting that TAK1 may interact with other MAP3Ks^[108]. Interestingly, crossing hepatocyte-specific TAK1 knockout mice with NEMO knockout mice attenuated JNK activation and prevented hepatocyte death and the development of HCC, suggesting that NEMO has a tumor-promoting function in the setting of TAK1 deletion^[108]. Additionally, this function of NEMO is considered to be independent of NF- κ B. Furthermore, a recent study showed that TAK1 inhibits ASK1-mediated apoptosis through a direct interaction between the C-terminal domain of TAK1 and the N-terminal or C-terminal domain of ASK1 in HEK 293 cells^[109]. Thus, in the setting of TAK1 deletion, ASK1 may play a tumor-promoting role by accelerating hepatocyte apoptosis and subsequent inflammation. Because crosstalk among MAP3Ks is less well understood, further studies are needed to clarify the whole picture of stress-activated MAPK signaling pathways.

CONCLUSION

One of the most important reasons for the poor prognosis of HCC is its frequent recurrence. Once HCC has developed, the recurrence rate does not decline with time, suggesting that most cases of late-phase recurrence are due to metachronous multicentric carcinogenesis caused by persistent chronic inflammation^[110]. Thus, determining the molecular mechanism(s) of inflammation-mediated hepatocarcinogenesis is important in preventing not only the occurrence, but also the recurrence, of HCC. As discussed in this review, recent studies have indicated that NF- κ B, STAT3, and stress-activated MAPK signaling pathways play key roles in inflammation-mediated hepatocarcinogenesis. These findings may prompt their introduction into the clinical setting as therapeutic targets. However, these pathways have a wide range of functions and exhibit complex crosstalk, and furthermore, may play opposing roles, depending on the cell type and carcinogenesis stage. Thus, alternative strategies, such as

targeting particular isoforms, including JNK1; upstream regulators, including MAP3K; and other modulators, including miRNA; may be more beneficial than targeting the entire pathway. In this regard, further studies clarifying the entire picture of the signaling network are needed to translate these signaling pathways into clinical practice.

REFERENCES

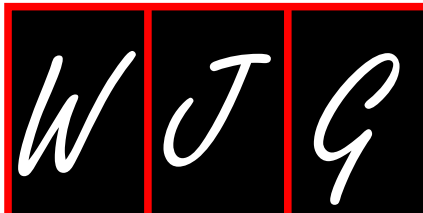
- 1 **Grivennikov SI**, Greten FR, Karin M. Immunity, inflammation, and cancer. *Cell* 2010; **140**: 883-899
- 2 **Maeda S**, Omata M. Inflammation and cancer: role of nuclear factor-kappaB activation. *Cancer Sci* 2008; **99**: 836-842
- 3 **Balkwill F**, Mantovani A. Inflammation and cancer: back to Virchow? *Lancet* 2001; **357**: 539-545
- 4 **El-Serag HB**. Hepatocellular carcinoma. *N Engl J Med* 2011; **365**: 1118-1127
- 5 **Masuzaki R**, Yoshida H, Tateishi R, Shiina S, Omata M. Hepatocellular carcinoma in viral hepatitis: improving standard therapy. *Best Pract Res Clin Gastroenterol* 2008; **22**: 1137-1151
- 6 **Shiina S**, Tateishi R, Arano T, Uchino K, Enooku K, Nakagawa H, Asaoka Y, Sato T, Masuzaki R, Kondo Y, Goto T, Yoshida H, Omata M, Koike K. Radiofrequency ablation for hepatocellular carcinoma: 10-year outcome and prognostic factors. *Am J Gastroenterol* 2012; **107**: 569-577; quiz 578
- 7 **El-Serag HB**, Rudolph KL. Hepatocellular carcinoma: epidemiology and molecular carcinogenesis. *Gastroenterology* 2007; **132**: 2557-2576
- 8 **Budhu A**, Wang XW. The role of cytokines in hepatocellular carcinoma. *J Leukoc Biol* 2006; **80**: 1197-1213
- 9 **Levrero M**. Viral hepatitis and liver cancer: the case of hepatitis C. *Oncogene* 2006; **25**: 3834-3847
- 10 **Maeda S**. NF- κ B, JNK, and TLR Signaling Pathways in Hepatocarcinogenesis. *Gastroenterol Res Pract* 2010; **2010**: 367694
- 11 **He G**, Karin M. NF- κ B and STAT3 - key players in liver inflammation and cancer. *Cell Res* 2011; **21**: 159-168
- 12 **Hoffmann A**, Baltimore D. Circuitry of nuclear factor kappaB signaling. *Immunol Rev* 2006; **210**: 171-186
- 13 **Ghosh S**, Karin M. Missing pieces in the NF-kappaB puzzle. *Cell* 2002; **109** Suppl: S81-S96
- 14 **Beg AA**, Sha WC, Bronson RT, Ghosh S, Baltimore D. Embryonic lethality and liver degeneration in mice lacking the RelA component of NF-kappa B. *Nature* 1995; **376**: 167-170
- 15 **Li Q**, Van Antwerp D, Mercurio F, Lee KF, Verma IM. Severe liver degeneration in mice lacking the IkappaB kinase 2 gene. *Science* 1999; **284**: 321-325
- 16 **Rudolph D**, Yeh WC, Wakeham A, Rudolph B, Nallainathan D, Potter J, Elia AJ, Mak TW. Severe liver degeneration and lack of NF-kappaB activation in NEMO/IKKgamma-deficient mice. *Genes Dev* 2000; **14**: 854-862
- 17 **Doi TS**, Marino MW, Takahashi T, Yoshida T, Sakakura T, Old LJ, Obata Y. Absence of tumor necrosis factor rescues RelA-deficient mice from embryonic lethality. *Proc Natl Acad Sci USA* 1999; **96**: 2994-2999
- 18 **Rosenfeld ME**, Prichard L, Shiojiri N, Fausto N. Prevention of hepatic apoptosis and embryonic lethality in RelA/TNFR-1 double knockout mice. *Am J Pathol* 2000; **156**: 997-1007
- 19 **Maeda S**, Chang L, Li ZW, Luo JL, Leffert H, Karin M. IKKbeta is required for prevention of apoptosis mediated by cell-bound but not by circulating TNFalpha. *Immunity* 2003; **19**: 725-737
- 20 **Luedde T**, Beraza N, Kotsikoris V, van Loo G, Nenci A, De Vos R, Roskams T, Trautwein C, Pasparakis M. Deletion of NEMO/IKKgamma in liver parenchymal cells causes steatohepatitis and hepatocellular carcinoma. *Cancer Cell* 2007; **11**: 119-132
- 21 **Maeda S**, Kamata H, Luo JL, Leffert H, Karin M. IKKbeta

- couples hepatocyte death to cytokine-driven compensatory proliferation that promotes chemical hepatocarcinogenesis. *Cell* 2005; **121**: 977-990
- 22 **Lee JS**, Chu IS, Mikaelyan A, Calvisi DF, Heo J, Reddy JK, Thorgeirsson SS. Application of comparative functional genomics to identify best-fit mouse models to study human cancer. *Nat Genet* 2004; **36**: 1306-1311
- 23 **Leenders MW**, Nijkamp MW, Borel Rinkes IH. Mouse models in liver cancer research: a review of current literature. *World J Gastroenterol* 2008; **14**: 6915-6923
- 24 **Fausto N**. Mouse liver tumorigenesis: models, mechanisms, and relevance to human disease. *Semin Liver Dis* 1999; **19**: 243-252
- 25 **Kamata H**, Honda S, Maeda S, Chang L, Hirata H, Karin M. Reactive oxygen species promote TNF α -induced death and sustained JNK activation by inhibiting MAP kinase phosphatases. *Cell* 2005; **120**: 649-661
- 26 **Pikarsky E**, Porat RM, Stein I, Abramovitch R, Amit S, Kasem S, Gutkovich-Pyest E, Urieli-Shoval S, Galun E, Ben-Neriah Y. NF- κ B functions as a tumour promoter in inflammation-associated cancer. *Nature* 2004; **431**: 461-466
- 27 **Haybaeck J**, Zeller N, Wolf MJ, Weber A, Wagner U, Kurrer MO, Bremer J, Iezzi G, Graf R, Clavien PA, Thimme R, Blum H, Nedospasov SA, Zatloukal K, Ramzan M, Ciesek S, Pietschmann T, Marche PN, Karin M, Kopf M, Browning JL, Aguzzi A, Heikenwalder M. A lymphotoxin-driven pathway to hepatocellular carcinoma. *Cancer Cell* 2009; **16**: 295-308
- 28 **Maeda S**, Hikiba Y, Sakamoto K, Nakagawa H, Hirata Y, Hayakawa Y, Yanai A, Ogura K, Karin M, Omata M. Ikappa B kinase β /nuclear factor- κ B activation controls the development of liver metastasis by way of interleukin-6 expression. *Hepatology* 2009; **50**: 1851-1860
- 29 **Berasain C**, Castillo J, Perugorria MJ, Latasa MU, Prieto J, Avila MA. Inflammation and liver cancer: new molecular links. *Ann N Y Acad Sci* 2009; **1155**: 206-221
- 30 **Naugler WE**, Karin M. The wolf in sheep's clothing: the role of interleukin-6 in immunity, inflammation and cancer. *Trends Mol Med* 2008; **14**: 109-119
- 31 **Gao B**. Cytokines, STATs and liver disease. *Cell Mol Immunol* 2005; **2**: 92-100
- 32 **Devriere J**, Content J, Denys C, Vandebussche P, Schandene L, Wybran J, Dupont E. High interleukin-6 serum levels and increased production by leucocytes in alcoholic liver cirrhosis. Correlation with IgA serum levels and lymphokines production. *Clin Exp Immunol* 1989; **77**: 221-225
- 33 **Lee Y**, Park US, Choi I, Yoon SK, Park YM, Lee YI. Human interleukin 6 gene is activated by hepatitis B virus-X protein in human hepatoma cells. *Clin Cancer Res* 1998; **4**: 1711-1717
- 34 **Wieckowska A**, Papouchado BG, Li Z, Lopez R, Zein NN, Feldstein AE. Increased hepatic and circulating interleukin-6 levels in human nonalcoholic steatohepatitis. *Am J Gastroenterol* 2008; **103**: 1372-1379
- 35 **Wong VW**, Yu J, Cheng AS, Wong GL, Chan HY, Chu ES, Ng EK, Chan FK, Sung JJ, Chan HL. High serum interleukin-6 level predicts future hepatocellular carcinoma development in patients with chronic hepatitis B. *Int J Cancer* 2009; **124**: 2766-2770
- 36 **Nakagawa H**, Maeda S, Yoshida H, Tateishi R, Masuzaki R, Ohki T, Hayakawa Y, Kinoshita H, Yamakado M, Kato N, Shiina S, Omata M. Serum IL-6 levels and the risk for hepatocarcinogenesis in chronic hepatitis C patients: an analysis based on gender differences. *Int J Cancer* 2009; **125**: 2264-2269
- 37 **Naugler WE**, Sakurai T, Kim S, Maeda S, Kim K, Elsharkawy AM, Karin M. Gender disparity in liver cancer due to sex differences in MyD88-dependent IL-6 production. *Science* 2007; **317**: 121-124
- 38 **Sakurai T**, He G, Matsuzawa A, Yu GY, Maeda S, Hardiman G, Karin M. Hepatocyte necrosis induced by oxidative stress and IL-1 α release mediate carcinogen-induced compensatory proliferation and liver tumorigenesis. *Cancer Cell* 2008; **14**: 156-165
- 39 **Ruggieri A**, Barbati C, Malorni W. Cellular and molecular mechanisms involved in hepatocellular carcinoma gender disparity. *Int J Cancer* 2010; **127**: 499-504
- 40 **Li Z**, Tuteja G, Schug J, Kaestner KH. Foxa1 and Foxa2 are essential for sexual dimorphism in liver cancer. *Cell* 2012; **148**: 72-83
- 41 **Gregor MF**, Hotamisligil GS. Inflammatory mechanisms in obesity. *Annu Rev Immunol* 2011; **29**: 415-445
- 42 **Muto Y**, Sato S, Watanabe A, Moriwaki H, Suzuki K, Kato A, Kato M, Nakamura T, Higuchi K, Nishiguchi S, Kumada H, Ohashi Y. Overweight and obesity increase the risk for liver cancer in patients with liver cirrhosis and long-term oral supplementation with branched-chain amino acid granules inhibits liver carcinogenesis in heavier patients with liver cirrhosis. *Hepatology* 2006; **35**: 204-214
- 43 **Ioannou GN**, Splan MF, Weiss NS, McDonald GB, Beretta L, Lee SP. Incidence and predictors of hepatocellular carcinoma in patients with cirrhosis. *Clin Gastroenterol Hepatol* 2007; **5**: 938-945, 945.e1-4
- 44 **Park EJ**, Lee JH, Yu GY, He G, Ali SR, Holzer RG, Osterreicher CH, Takahashi H, Karin M. Dietary and genetic obesity promote liver inflammation and tumorigenesis by enhancing IL-6 and TNF expression. *Cell* 2010; **140**: 197-208
- 45 **Ohki T**, Tateishi R, Shiina S, Goto E, Sato T, Nakagawa H, Masuzaki R, Goto T, Hamamura K, Kanai F, Yoshida H, Kawabe T, Omata M. Visceral fat accumulation is an independent risk factor for hepatocellular carcinoma recurrence after curative treatment in patients with suspected NASH. *Gut* 2009; **58**: 839-844
- 46 **Marra F**, Bertolani C. Adipokines in liver diseases. *Hepatology* 2009; **50**: 957-969
- 47 **Arano T**, Nakagawa H, Tateishi R, Ikeda H, Uchino K, Enooku K, Goto E, Masuzaki R, Asaoka Y, Kondo Y, Goto T, Shiina S, Omata M, Yoshida H, Koike K. Serum level of adiponectin and the risk of liver cancer development in chronic hepatitis C patients. *Int J Cancer* 2011; **129**: 2226-2235
- 48 **Toffanin S**, Friedman SL, Llovet JM. Obesity, inflammatory signaling, and hepatocellular carcinoma-an enlarging link. *Cancer Cell* 2010; **17**: 115-117
- 49 **Yoshimura A**. Signal transduction of inflammatory cytokines and tumor development. *Cancer Sci* 2006; **97**: 439-447
- 50 **Yu H**, Pardoll D, Jove R. STATs in cancer inflammation and immunity: a leading role for STAT3. *Nat Rev Cancer* 2009; **9**: 798-809
- 51 **Aggarwal BB**, Kunnumakkara AB, Harikumar KB, Gupta SR, Tharakan ST, Koca C, Dey S, Sung B. Signal transducer and activator of transcription-3, inflammation, and cancer: how intimate is the relationship? *Ann N Y Acad Sci* 2009; **1171**: 59-76
- 52 **He G**, Yu GY, Temkin V, Ogata H, Kuntzen C, Sakurai T, Sieghart W, Peck-Radosavljevic M, Leffert HL, Karin M. Hepatocyte IKK β /NF- κ B inhibits tumor promotion and progression by preventing oxidative stress-driven STAT3 activation. *Cancer Cell* 2010; **17**: 286-297
- 53 **Ogata H**, Kobayashi T, Chinen T, Takaki H, Sanada T, Minoda Y, Koga K, Takaesu G, Maehara Y, Iida M, Yoshimura A. Deletion of the SOCS3 gene in liver parenchymal cells promotes hepatitis-induced hepatocarcinogenesis. *Gastroenterology* 2006; **131**: 179-193
- 54 **Maione D**, Di Carlo E, Li W, Musiani P, Modesti A, Peters M, Rose-John S, Della Rocca C, Tripodi M, Lazzaro D, Taub R, Savino R, Ciliberto G. Coexpression of IL-6 and soluble IL-6R causes nodular regenerative hyperplasia and adenomas of the liver. *EMBO J* 1998; **17**: 5588-5597
- 55 **Rebouisson S**, Amessou M, Couchy G, Poussin K, Imbeaud S, Pilati C, Izard T, Balabaud C, Bioulac-Sage P, Zucman-Rossi J. Frequent in-frame somatic deletions activate gp130 in inflammatory hepatocellular tumours. *Nature* 2009; **457**: 200-204

- 56 **Lee H**, Herrmann A, Deng JH, Kujawski M, Niu G, Li Z, Forman S, Jove R, Pardoll DM, Yu H. Persistently activated Stat3 maintains constitutive NF-kappaB activity in tumors. *Cancer Cell* 2009; **15**: 283-293
- 57 **Bard-Chapeau EA**, Li S, Ding J, Zhang SS, Zhu HH, Princen F, Fang DD, Han T, Bailly-Maitre B, Poli V, Varki NM, Wang H, Feng GS. Ptpn11/Shp2 acts as a tumor suppressor in hepatocellular carcinogenesis. *Cancer Cell* 2011; **19**: 629-639
- 58 **Bartel DP**. MicroRNAs: target recognition and regulatory functions. *Cell* 2009; **136**: 215-233
- 59 **Ji J**, Shi J, Budhu A, Yu Z, Forgues M, Roessler S, Ambs S, Chen Y, Meltzer PS, Croce CM, Qin LX, Man K, Lo CM, Lee J, Ng IO, Fan J, Tang ZY, Sun HC, Wang XW. MicroRNA expression, survival, and response to interferon in liver cancer. *N Engl J Med* 2009; **361**: 1437-1447
- 60 **Kota J**, Chivukula RR, O'Donnell KA, Wentzel EA, Montgomery CL, Hwang HW, Chang TC, Vivekanandan P, Torbenson M, Clark KR, Mendell JR, Mendell JT. Therapeutic microRNA delivery suppresses tumorigenesis in a murine liver cancer model. *Cell* 2009; **137**: 1005-1017
- 61 **Hatziaepostolou M**, Polytaichou C, Aggelidou E, Drakaki A, Poultsides GA, Jaeger SA, Ogata H, Karin M, Struhl K, Hadzopoulou-Cladaras M, Iliopoulos D. An HNF4c-miRNA inflammatory feedback circuit regulates hepatocellular oncogenesis. *Cell* 2011; **147**: 1233-1247
- 62 **Kyriakis JM**, Avruch J. Mammalian mitogen-activated protein kinase signal transduction pathways activated by stress and inflammation. *Physiol Rev* 2001; **81**: 807-869
- 63 **Chang L**, Karin M. Mammalian MAP kinase signalling cascades. *Nature* 2001; **410**: 37-40
- 64 **Davis RJ**. Signal transduction by the JNK group of MAP kinases. *Cell* 2000; **103**: 239-252
- 65 **Shaulian E**, Karin M. AP-1 as a regulator of cell life and death. *Nat Cell Biol* 2002; **4**: E131-E136
- 66 **Weston CR**, Davis RJ. The JNK signal transduction pathway. *Curr Opin Genet Dev* 2002; **12**: 14-21
- 67 **Sabapathy K**, Hochedlinger K, Nam SY, Bauer A, Karin M, Wagner EF. Distinct roles for JNK1 and JNK2 in regulating JNK activity and c-Jun-dependent cell proliferation. *Mol Cell* 2004; **15**: 713-725
- 68 **Shen HM**, Liu ZG. JNK signaling pathway is a key modulator in cell death mediated by reactive oxygen and nitrogen species. *Free Radic Biol Med* 2006; **40**: 928-939
- 69 **Hui L**, Zatloukal K, Scheuch H, Stepniak E, Wagner EF. Proliferation of human HCC cells and chemically induced mouse liver cancers requires JNK1-dependent p21 down-regulation. *J Clin Invest* 2008; **118**: 3943-3953
- 70 **Malhi H**, Bronk SF, Werneburg NW, Gores GJ. Free fatty acids induce JNK-dependent hepatocyte lipoapoptosis. *J Biol Chem* 2006; **281**: 12093-12101
- 71 **Malhi H**, Gores GJ. Molecular mechanisms of lipotoxicity in nonalcoholic fatty liver disease. *Semin Liver Dis* 2008; **28**: 360-369
- 72 **Uehara T**, Bennett B, Sakata ST, Satoh Y, Bilter GK, Westwick JK, Brenner DA. JNK mediates hepatic ischemia reperfusion injury. *J Hepatol* 2005; **42**: 850-859
- 73 **Gunawan BK**, Liu ZX, Han D, Hanawa N, Gaarde WA, Kaplowitz N. c-Jun N-terminal kinase plays a major role in murine acetaminophen hepatotoxicity. *Gastroenterology* 2006; **131**: 165-178
- 74 **Kaufmann T**, Jost PJ, Pellegrini M, Puthalakath H, Gugasyan R, Gerondakis S, Cretney E, Smyth MJ, Silke J, Hakem R, Bouillet P, Mak TW, Dixit VM, Strasser A. Fatal hepatitis mediated by tumor necrosis factor TNFalpha requires caspase-8 and involves the BH3-only proteins Bid and Bim. *Immunity* 2009; **30**: 56-66
- 75 **Nakagawa H**, Hirata Y, Takeda K, Hayakawa Y, Sato T, Kinoshita H, Sakamoto K, Nakata W, Hikiba Y, Omata M, Yoshida H, Koike K, Ichijo H, Maeda S. Apoptosis signal-regulating kinase 1 inhibits hepatocarcinogenesis by controlling the tumor-suppressing function of stress-activated mitogen-activated protein kinase. *Hepatology* 2011; **54**: 185-195
- 76 **Sakurai T**, Maeda S, Chang L, Karin M. Loss of hepatic NF-kappa B activity enhances chemical hepatocarcinogenesis through sustained c-Jun N-terminal kinase 1 activation. *Proc Natl Acad Sci USA* 2006; **103**: 10544-10551
- 77 **De Smaele E**, Zazzeroni F, Papa S, Nguyen DU, Jin R, Jones J, Cong R, Franzoso G. Induction of gadd45beta by NF-kappaB downregulates pro-apoptotic JNK signalling. *Nature* 2001; **414**: 308-313
- 78 **Kaur S**, Wang F, Venkatraman M, Arsuru M. X-linked inhibitor of apoptosis (XIAP) inhibits c-Jun N-terminal kinase 1 (JNK1) activation by transforming growth factor beta1 (TGF-beta1) through ubiquitin-mediated proteosomal degradation of the TGF-beta1-activated kinase 1 (TAK1). *J Biol Chem* 2005; **280**: 38599-38608
- 79 **Lee EG**, Boone DL, Chai S, Libby SL, Chien M, Lodolce JP, Ma A. Failure to regulate TNF-induced NF-kappaB and cell death responses in A20-deficient mice. *Science* 2000; **289**: 2350-2354
- 80 **Chang Q**, Zhang Y, Beezhold KJ, Bhatia D, Zhao H, Chen J, Castranova V, Shi X, Chen F. Sustained JNK1 activation is associated with altered histone H3 methylations in human liver cancer. *J Hepatol* 2009; **50**: 323-333
- 81 **Das M**, Garlick DS, Greiner DL, Davis RJ. The role of JNK in the development of hepatocellular carcinoma. *Genes Dev* 2011; **25**: 634-645
- 82 **Hirosumi J**, Tuncman G, Chang L, Görgün CZ, Uysal KT, Maeda K, Karin M, Hotamisligil GS. A central role for JNK in obesity and insulin resistance. *Nature* 2002; **420**: 333-336
- 83 **Nkontchou G**, Bastard JP, Ziol M, Aout M, Cosson E, Ganne-Carrie N, Grando-Lemaire V, Roulot D, Capeau J, Trinchet JC, Vicaute E, Beaugrand M. Insulin resistance, serum leptin, and adiponectin levels and outcomes of viral hepatitis C cirrhosis. *J Hepatol* 2010; **53**: 827-833
- 84 **Kaneto H**, Katakami N, Matsuhisa M, Matsuoka TA. Role of reactive oxygen species in the progression of type 2 diabetes and atherosclerosis. *Mediators Inflamm* 2010; **2010**: 453892
- 85 **Nakagawa H**, Isogawa A, Tateishi R, Tani M, Yoshida H, Yamakado M, Koike K. Serum gamma-glutamyltransferase level is associated with serum superoxide dismutase activity and metabolic syndrome in a Japanese population. *J Gastroenterol* 2011; Epub ahead of print
- 86 **Han J**, Sun P. The pathways to tumor suppression via route p38. *Trends Biochem Sci* 2007; **32**: 364-371
- 87 **Ge B**, Gram H, Di Padova F, Huang B, New L, Ulevitch RJ, Luo Y, Han J. MAPKK-independent activation of p38alpha mediated by TAB1-dependent autophosphorylation of p38alpha. *Science* 2002; **295**: 1291-1294
- 88 **Hui L**, Bakiri L, Stepniak E, Wagner EF. p38alpha: a suppressor of cell proliferation and tumorigenesis. *Cell Cycle* 2007; **6**: 2429-2433
- 89 **Heinrichsdorff J**, Luedde T, Perdiguero E, Nebreda AR, Pasparakis M. p38 alpha MAPK inhibits JNK activation and collaborates with IkkappaB kinase 2 to prevent endotoxin-induced liver failure. *EMBO Rep* 2008; **9**: 1048-1054
- 90 **Hui L**, Bakiri L, Mairhorfer A, Schweifer N, Haslinger C, Kenner L, Komnenovic V, Scheuch H, Beug H, Wagner EF. p38alpha suppresses normal and cancer cell proliferation by antagonizing the JNK-c-Jun pathway. *Nat Genet* 2007; **39**: 741-749
- 91 **Iyoda K**, Sasaki Y, Horimoto M, Toyama T, Yakushiji T, Sakakibara M, Takehara T, Fujimoto J, Hori M, Wands JR, Hayashi N. Involvement of the p38 mitogen-activated protein kinase cascade in hepatocellular carcinoma. *Cancer* 2003; **97**: 3017-3026
- 92 **She QB**, Chen N, Bode AM, Flavell RA, Dong Z. Deficiency of c-Jun-NH(2)-terminal kinase-1 in mice enhances skin tumor development by 12-O-tetradecanoylphorbol-13-acetate. *Cancer Res* 2002; **62**: 1343-1348

- 93 **Cellurale C**, Weston CR, Reilly J, Garlick DS, Jerry DJ, Sluss HK, Davis RJ. Role of JNK in a Trp53-dependent mouse model of breast cancer. *PLoS One* 2010; **5**: e12469
- 94 **Saxena NK**, Fu PP, Nagalingam A, Wang J, Handy J, Cohen C, Tighiouart M, Sharma D, Anania FA. Adiponectin modulates C-jun N-terminal kinase and mammalian target of rapamycin and inhibits hepatocellular carcinoma. *Gastroenterology* 2010; **139**: 1762-1763
- 95 **Hsieh YH**, Wu TT, Huang CY, Hsieh YS, Hwang JM, Liu JY. p38 mitogen-activated protein kinase pathway is involved in protein kinase C α -regulated invasion in human hepatocellular carcinoma cells. *Cancer Res* 2007; **67**: 4320-4327
- 96 **Kim MS**, Lee EJ, Kim HR, Moon A. p38 kinase is a key signaling molecule for H-Ras-induced cell motility and invasive phenotype in human breast epithelial cells. *Cancer Res* 2003; **63**: 5454-5461
- 97 **Wagner EF**, Nebreda AR. Signal integration by JNK and p38 MAPK pathways in cancer development. *Nat Rev Cancer* 2009; **9**: 537-549
- 98 **Runchel C**, Matsuzawa A, Ichijo H. Mitogen-activated protein kinases in mammalian oxidative stress responses. *Antioxid Redox Signal* 2011; **15**: 205-218
- 99 **Ichijo H**, Nishida E, Irie K, ten Dijke P, Saitoh M, Moriguchi T, Takagi M, Matsumoto K, Miyazono K, Gotoh Y. Induction of apoptosis by ASK1, a mammalian MAPKKK that activates SAPK/JNK and p38 signaling pathways. *Science* 1997; **275**: 90-94
- 100 **Saitoh M**, Nishitoh H, Fujii M, Takeda K, Tobiume K, Sawada Y, Kawabata M, Miyazono K, Ichijo H. Mammalian thioredoxin is a direct inhibitor of apoptosis signal-regulating kinase (ASK) 1. *EMBO J* 1998; **17**: 2596-2606
- 101 **Hatai T**, Matsuzawa A, Inoshita S, Mochida Y, Kuroda T, Sakamaki K, Kuida K, Yonehara S, Ichijo H, Takeda K. Execution of apoptosis signal-regulating kinase 1 (ASK1)-induced apoptosis by the mitochondria-dependent caspase activation. *J Biol Chem* 2000; **275**: 26576-26581
- 102 **Nakagawa H**, Maeda S, Hikiba Y, Ohmae T, Shibata W, Yanai A, Sakamoto K, Ogura K, Noguchi T, Karin M, Ichijo H, Omata M. Deletion of apoptosis signal-regulating kinase 1 attenuates acetaminophen-induced liver injury by inhibiting c-Jun N-terminal kinase activation. *Gastroenterology* 2008; **135**: 1311-1321
- 103 **Huynh H**, Choo SP, Toh HC, Tai WM, Chung AY, Chow PK, Ong R, Soo KC. Comparing the efficacy of sunitinib with sorafenib in xenograft models of human hepatocellular carcinoma: mechanistic explanation. *Curr Cancer Drug Targets* 2011; **11**: 944-953
- 104 **Llovet JM**, Ricci S, Mazzaferro V, Hilgard P, Gane E, Blanc JF, de Oliveira AC, Santoro A, Raoul JL, Forner A, Schwartz M, Porta C, Zeuzem S, Bolondi L, Greten TF, Galle PR, Seitz JF, Borbath I, Häussinger D, Giannaris T, Shan M, Moscovici M, Voliotis D, Bruix J. Sorafenib in advanced hepatocellular carcinoma. *N Engl J Med* 2008; **359**: 378-390
- 105 **Stark MS**, Woods SL, Gartside MG, Bonazzi VF, Dutton-Regester K, Aoude LG, Chow D, Sereduk C, Niemi NM, Tang N, Ellis JJ, Reid J, Zismann V, Tyagi S, Muzny D, Newsham I, Wu Y, Palmer JM, Pollak T, Youngkin D, Brooks BR, Lanagan C, Schmidt CW, Kobe B, MacKeigan JP, Yin H, Brown KM, Gibbs R, Trent J, Hayward NK. Frequent somatic mutations in MAP3K5 and MAP3K9 in metastatic melanoma identified by exome sequencing. *Nat Genet* 2012; **44**: 165-169
- 106 **Rincón M**, Davis RJ. Regulation of the immune response by stress-activated protein kinases. *Immunol Rev* 2009; **228**: 212-224
- 107 **Inokuchi S**, Aoyama T, Miura K, Osterreicher CH, Kodama Y, Miyai K, Akira S, Brenner DA, Seki E. Disruption of TAK1 in hepatocytes causes hepatic injury, inflammation, fibrosis, and carcinogenesis. *Proc Natl Acad Sci USA* 2010; **107**: 844-849
- 108 **Bettermann K**, Vucur M, Haybaeck J, Koppe C, Janssen J, Heymann F, Weber A, Weiskirchen R, Liedtke C, Gassler N, Müller M, de Vos R, Wolf MJ, Boege Y, Seleznik GM, Zeller N, Erny D, Fuchs T, Zoller S, Cairo S, Buendia MA, Prinz M, Akira S, Tacke F, Heikenwalder M, Trautwein C, Luedde T. TAK1 suppresses a NEMO-dependent but NF- κ B-independent pathway to liver cancer. *Cancer Cell* 2010; **17**: 481-496
- 109 **Kim SY**, Shim JH, Chun E, Lee KY. Reciprocal inhibition between the transforming growth factor- β -activated kinase 1 (TAK1) and apoptosis signal-regulating kinase 1 (ASK1) mitogen-activated protein kinase kinases and its suppression by TAK1-binding protein 2 (TAB2), an adapter protein for TAK1. *J Biol Chem* 2012; **287**: 3381-3391
- 110 **Masuzaki R**, Yoshida H, Omata M. Does chemotherapy prevent HCV-related hepatocellular carcinoma? *Pros. Dig Liver Dis* 2010; **42** Suppl 3: S281-S286

S- Editor Gou SX L- Editor A E- Editor Zhang DN



Indomethacin for post-endoscopic retrograde cholangiopancreatography pancreatitis prophylaxis: Is it the magic bullet?

Dennis Yang, Peter V Draganov

Dennis Yang, Peter V Draganov, Division of Gastroenterology, Hepatology and Nutrition, Department of Medicine, University of Florida, Gainesville, FL 32610, United States

Author contributions: Yang D performed the literature search and wrote the first draft of the manuscript; Draganov PV provided the concept for the manuscript, contributed new articles to the literature search, reviewed the article and provided critical appraisal.

Correspondence to: Peter V Draganov, MD, Division of Gastroenterology, Hepatology and Nutrition, Department of Medicine, University of Florida, 1600 SW Archer Road, Room HD 602, PO Box 100214, Gainesville, FL 32610, United States. dragapv@medicine.ufl.edu

Telephone: +1-352-2739474 Fax: +1-352-3923618

Received: June 20, 2012 Revised: July 10, 2012

Accepted: July 18, 2012

Published online: August 21, 2012

© 2012 Baishideng. All rights reserved.

Key words: Non-steroidal anti-inflammatory drugs; Indomethacin; Post-endoscopic retrograde cholangiopancreatography pancreatitis; Acute pancreatitis

Peer reviewer: Ferruccio Bonino, MD, PhD, Professor of Gastroenterology, Director of Liver and Digestive Disease Division, Department of Internal Medicine, University of Pisa, Director of General Medicine 2 Unit, University Hospital of Pisa, Via Roma 67, 56124 Pisa, Italy

Yang D, Draganov PV. Indomethacin for post-endoscopic retrograde cholangiopancreatography pancreatitis prophylaxis: Is it the magic bullet? *World J Gastroenterol* 2012; 18(31): 4082-4085 Available from: URL: <http://www.wjgnet.com/1007-9327/full/v18/i31/4082.htm> DOI: <http://dx.doi.org/10.3748/wjg.v18.i31.4082>

Abstract

Acute pancreatitis is a common complication of endoscopic retrograde cholangiopancreatography (ERCP). Pancreatic duct stent insertion after ERCP has been widely accepted as the standard of care for the prevention of this complication in high-risk patients. Unfortunately, the placement of pancreatic stents requires higher level of endoscopic expertise and is not always feasible due to anatomic considerations. Therefore, effective non-invasive pharmacologic prophylaxis remains appealing, particularly if it is inexpensive, easily administered, has a low risk side effect profile and is widely available. There have been multiple studies evaluating potential pharmacologic candidates for post-ERCP pancreatitis (PEP) prophylaxis, most of them yielding disappointing results. A recently published large, multi-center, randomized controlled trial reported that in high risk patients a single dose of rectal indomethacin administered immediately after the ERCP significantly decreased the incidence of PEP compare to placebo.

INVITED COMMENTARY ON HOT ARTICLES

Acute pancreatitis is the most frequent complication of endoscopic retrograde cholangiopancreatography (ERCP). The incidence of post-ERCP pancreatitis (PEP) varies between 1%-10%, with incidence exceeding 25% being reported in certain high-risk patient populations^[1,2]. The wide range for this incidence is mostly due to the heterogeneous interplay of patient characteristics, procedure-related, and operator-related factors^[3,4].

Numerous agents and interventions have been studied so far in the prevention of PEP. These can be divided into sphincter relaxants, protease inhibitors, types of contrast, anti-inflammatory/anti-oxidant agents, anti-secretory agents, electrosurgical techniques, and placement of various types of pancreatic stents^[5]. The results have generally been disappointing and at present the only fea-

sible option to decrease the rate of PEP is the insertion of pancreatic stent in high risk patients. Unfortunately, the placement of pancreatic stents requires higher level of endoscopic expertise and is not always feasible due to anatomic considerations. Indeed, a recent survey reported that more than 20% of physicians performing ERCP never place pancreatic stents^[6]. Therefore, effective pharmacologic prophylaxis remains appealing, particularly if it is inexpensive, easily administered, has a low risk side effect profile and is widely available. Intravenous gabexate, a protease inhibitor, and somatostatin, an anti-secretory agent, have been shown to prevent PEP^[7]. However, both of these therapies are not readily available and require continuous intravenous infusion. As such, the search for effective, cheap and feasible pharmacologic prophylaxis for PEP has been continued.

Phospholipase A₂ is presumed to play a pivotal role in the inflammatory cascade associated with acute pancreatitis^[8]. This has been the basis for several prospective placebo-controlled randomized controlled trials (RCTs) evaluating non-steroidal anti-inflammatory drugs (NSAIDs), potent inhibitors of phospholipase A₂ activity, in the prevention of PEP. In 2003, Murray *et al*^[9] showed that rectal diclofenac given immediately after ERCP reduced the incidence of PEP in a high-risk patient population. These findings were corroborated by Khoshbaten *et al*^[10], who also demonstrated that immediate administration of rectal diclofenac after ERCP reduced the incidence of acute pancreatitis in patients undergoing pancreatogram. Studies evaluating rectal indomethacin have also suggested a protective effect against PEP in patients undergoing pancreatography or ERCP for biliary obstruction^[11,12]. In spite of these promising findings, the relatively small sample size of each of these studies and the heterogeneous study groups, have yielded overall inconclusive results.

A meta-analysis published in 2008 attempted to further validate the role of prophylactic rectal NSAIDs on PEP^[13]. Assuming a two-tailed $\alpha = 0.05$, a power of 0.9 and PEP incidences of 12.06% and 4.38% in the placebo and NSAID groups respectively, the authors concluded that a total of 586 patients would be required to demonstrate the intended decrease in the incidence of PEP. By compiling the results of four previous RCTs, an adequate pooled sample size was achieved to detect a statistically significant 64% (95% CI: 0.22-0.60) reduction in acute pancreatitis in patients who received NSAIDs immediately after ERCP when compared to placebo. The results of this meta-analysis further emphasized the apparent benefit of rectal administered NSAIDs for PEP prophylaxis and the need of large prospective multi-center trials to confirm these findings.

On the background of these promising results, Elmunzer *et al*^[14], report the results of a multi-center, randomized, placebo-controlled, double-blind clinical trial conducted to determine the effect of a single dose of rectal indomethacin administered immediately after ERCP in patients at elevated risk for PEP. Inclusion cri-

teria selected patients with an elevated baseline risk of PEP as defined by one or more of the following major criteria: clinical suspicion of sphincter of Oddi dysfunction (SOD), a history of PEP, pancreatic sphincterotomy, precut sphincterotomy, more than eight cannulation attempts, pneumatic dilatation of an intact biliary sphincter, or ampullectomy. Patients were also eligible if they met two or more of the following minor criteria: an age of less than 50 years and female sex, history of recurrent pancreatitis (≥ 2 episodes), three or more injections of contrast agent into the pancreatic duct with at least one injection to the tail of the pancreas, excessive injection of contrast agent into the pancreatic duct resulting in opacification of pancreatic acini, or the acquisition of a cytologic specimen from the pancreatic duct with the use of a brush. The study design consisted of patients randomly assigned to receive either two 50 mg indomethacin suppositories or two identical-appearing placebo suppositories immediately after ERCP. The randomization was concealed by using centralized location and stratified by study center. The primary and secondary outcomes of the study were the development of PEP^[15] and moderate or severe PEP, respectively. Patients with post-ERCP abdominal pain were hospitalized, followed clinically, and had their serum amylase and lipase measured at least once 24 h after the procedure. Patients discharged after uneventful ERCP were contacted within 5 d and again at 30 d to capture delayed occurrence of primary outcome and to assess for any delayed adverse events.

The study enrolled a total of 602 subjects from February 2009 through July 2011. An interim analysis recommended the study to be terminated early on the basis of the benefit of indomethacin compared with placebo. A total of 295 patients received indomethacin, and 307 patients received placebo. Baseline characteristics were similar in the two study groups. The majority of patients (82%) had a clinical suspicion of sphincter of Oddi dysfunction. The overall incidence of PEP was 13.1% (79 of 602 patients). The incidence of PEP was 9.2% (27 of 295 patients) in the indomethacin group compared to 16.9% (52 of 307) in the placebo group ($P = 0.005$), corresponding to an absolute risk reduction of 7.7 percentage points, relative risk reduction of 46%, with a number needed to treat to prevent one additional episode of PEP of 13. The secondary outcome of moderate or severe PEP occurred in 40 patients, 13 (4.4%) in the indomethacin group compared to 27 (8.8%) in the placebo group ($P = 0.03$). Among patients hospitalized for PEP, the median length of hospital stay was 0.5 d shorter in the indomethacin group (3.5 d) than in the placebo group (4 d) ($P < 0.001$). A persistent protective effect of indomethacin against PEP was noted in the post-hoc analysis of patients stratified based on their pre-treatment risk of PEP^[16], regardless of whether patients had undergone pancreatic stenting, clinical suspicion of SOD, and in all subtypes of SOD. The authors concluded that among patients at high risk for post-ERCP pancreatitis, rectal indomethacin significantly reduced the incidence of the

condition.

Acute pancreatitis remains the most common major complication of ERCP. NSAIDs represent an attractive pharmacological agent for PEP prophylaxis because they are inexpensive, can be easily administered and have a relatively low risk profile. Previous efforts to endorse NSAIDs for PEP prophylaxis have been limited by small single-center studies with conflicting results.

This study by Elmunzer *et al*^[14] is the first large multi-center, randomized, controlled trial that demonstrates the protective effects of a single dose rectal indomethacin against PEP in high-risk patients. The validity of the conclusions is supported by a number of the study methodological strengths including double blinded randomized design, adequate allocation concealment, strict clinically meaningful definition of PEP, thorough follow up with very low lost-to-follow-up rate and intention-to-treat analysis. The authors should also be commended for following the patients thirty days post-procedure to evaluate for any delayed pancreatitis or adverse events. A reduction in the incidence of PEP with rectal NSAIDs in the study group consisting primarily of patients with clinical suspicion of SOD (82%) confirms the benefit of this prophylactic agent in this challenging patient population. This finding is congruent with previous trials suggesting a maximal benefit from prophylactic NSAIDs in high-risk patients. Moreover, this study showed that the relative treatment effect of indomethacin remained across the spectrum of patient's risk of PEP. These results, in conjunction with a trend toward benefit with respect to rates of PEP in patients without clinical suspicion of SOD treated with indomethacin, suggest the need of additional studies to confirm a potential protective effect even in low-risk patients. The very high prevalence of patients with suspected SOD in this trial should be considered when interpreting the external validity of the results and applying them to other high risk PEP patients.

Prophylactic temporary pancreatic duct stenting has been widely accepted for PEP prophylaxis^[17]. One of the main limitations of previous prospective trials regarding the effects of NSAIDs for PEP prophylaxis is their failure to report the use of prophylactic pancreatic stents in their study population. A particular strength of this study is that the majority of patients (> 80%) underwent pancreatic stent placement in addition to the study intervention (indomethacin or placebo). Indomethacin reduced the risk of PEP to a similar degree irrespective to whether the patient received a pancreatic stent or not. These findings highlight the additive protective effect of NSAIDs for PEP prophylaxis in high-risk patients receiving temporary pancreatic duct stenting. Furthermore, it suggests that NSAIDs may be an alternate non-invasive prophylactic measure for PEP in those patients in whom pancreatic stenting may not be feasible or not recommended; however, this requires further investigation.

Elmunzer *et al*^[14] also reported that prophylactic indomethacin was associated with decreased severity of PEP, which is congruent with previous findings by

Sotoudehmanesh and colleagues. In the subgroup of patients that were hospitalized post-ERCP, the indomethacin group also had a shorter hospital stay when compared to placebo. These results suggest that the benefits of NSAIDs are not limited to reducing the incidence of PEP; but potentially also includes disease severity modulation presumably by regulating the inflammatory response and clinical manifestation of PEP. If further validated, these findings have both clinical as well as economic implications, given the substantial morbidity with increasing severity of PEP and associated health care expenditures.

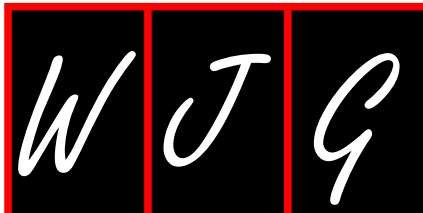
In summary, this multi-center double blinded randomized controlled trial further supports the use of prophylactic rectal NSAIDs in the prevention of PEP and addresses several limitations of previous studies that have been met with general skepticism. This study demonstrates that rectal indomethacin can reduce the incidence and severity of PEP in high-risk population consisting mostly of patients with suspected SOD and could potentially have a benefit even in low-risk patients. The low cost and risk profile associated with a single standard dose of rectal indomethacin makes this an attractive prophylactic pharmacological agent in those patients in whom this medication is not otherwise contraindicated. While clinical judgment in selecting patients with appropriate indications for ERCP remains the most important measure in preventing PEP, rectal indomethacin is a safe, easily administered, widely available pharmacological prophylactic measure that could change how we address this serious ERCP-associated complication.

REFERENCES

- 1 **Rabenstein T**, Hahn EG. Post-ERCP pancreatitis: new momentum. *Endoscopy* 2002; **34**: 325-329
- 2 **Freeman ML**, Guda NM. Prevention of post-ERCP pancreatitis: a comprehensive review. *Gastrointest Endosc* 2004; **59**: 845-864
- 3 **Wagh MS**, Sherman S. Indomethacin for post-ERCP pancreatitis prophylaxis: another attempt at the Holy Grail. *Am J Gastroenterol* 2007; **102**: 984-986
- 4 **Freeman ML**, DiSario JA, Nelson DB, Fennerty MB, Lee JG, Bjorkman DJ, Overby CS, Aas J, Ryan ME, Bochna GS, Shaw MJ, Snady HW, Erickson RV, Moore JP, Roel JP. Risk factors for post-ERCP pancreatitis: a prospective, multicenter study. *Gastrointest Endosc* 2001; **54**: 425-434
- 5 **Lieb JG**, Draganov PV. Early successes and late failures in the prevention of post endoscopic retrograde cholangiopancreatography. *World J Gastroenterol* 2007; **13**: 3567-3574
- 6 **Dumonceau JM**, Rigaux J, Kahaleh M, Gomez CM, Vandermeeren A, Devière J. Prophylaxis of post-ERCP pancreatitis: a practice survey. *Gastrointest Endosc* 2010; **71**: 934-939
- 7 **Andriulli A**, Clemente R, Solmi L, Terruzzi V, Suriani R, Sigillito A, Leandro G, Leo P, De Maio G, Perri F. Gabexate or somatostatin administration before ERCP in patients at high risk for post-ERCP pancreatitis: a multicenter, placebo-controlled, randomized clinical trial. *Gastrointest Endosc* 2002; **56**: 488-495
- 8 **Gross V**, Leser HG, Heinisch A, Schölmerich J. Inflammatory mediators and cytokines--new aspects of the pathophysiology and assessment of severity of acute pancreatitis? *Hepato gastroenterology* 1993; **40**: 522-530

- 9 **Murray B**, Carter R, Imrie C, Evans S, O'Suilleabhain C. Diclofenac reduces the incidence of acute pancreatitis after endoscopic retrograde cholangiopancreatography. *Gastroenterology* 2003; **124**: 1786-1791
- 10 **Khoshbaten M**, Khorram H, Madad L, Ehsani Ardakani MJ, Farzin H, Zali MR. Role of diclofenac in reducing post-endoscopic retrograde cholangiopancreatography pancreatitis. *J Gastroenterol Hepatol* 2008; **23**: e11-e16
- 11 **Sotoudehmanesh R**, Khatibian M, Kolahdoozan S, Ainechi S, Malboosbaf R, Nouriae M. Indomethacin may reduce the incidence and severity of acute pancreatitis after ERCP. *Am J Gastroenterol* 2007; **102**: 978-983
- 12 **Montaño Loza A**, Rodríguez Lomelí X, García Correa JE, Dávalos Cobián C, Cervantes Guevara G, Medrano Muñoz F, Fuentes Orozco C, González Ojeda A. [Effect of the administration of rectal indomethacin on amylase serum levels after endoscopic retrograde cholangiopancreatography, and its impact on the development of secondary pancreatitis episodes]. *Rev Esp Enferm Dig* 2007; **99**: 330-336
- 13 **Elmunzer BJ**, Waljee AK, Elta GH, Taylor JR, Fehmi SM, Higgins PD. A meta-analysis of rectal NSAIDs in the prevention of post-ERCP pancreatitis. *Gut* 2008; **57**: 1262-1267
- 14 **Elmunzer BJ**, Scheiman JM, Lehman GA, Chak A, Mosler P, Higgins PD, Hayward RA, Romagnuolo J, Elta GH, Sherman S, Waljee AK, Repaka A, Atkinson MR, Cote GA, Kwon RS, McHenry L, Piraka CR, Wamsteker EJ, Watkins JL, Korsnes SJ, Schmidt SE, Turner SM, Nicholson S, Fogel EL. A randomized trial of rectal indomethacin to prevent post-ERCP pancreatitis. *N Engl J Med* 2012; **366**: 1414-1422
- 15 **Cotton PB**, Lehman G, Vennes J, Geenen JE, Russell RC, Meyers WC, Liguory C, Nickl N. Endoscopic sphincterotomy complications and their management: an attempt at consensus. *Gastrointest Endosc* 1991; **37**: 383-393
- 16 **Kent DM**, Rothwell PM, Ioannidis JP, Altman DG, Hayward RA. Assessing and reporting heterogeneity in treatment effects in clinical trials: a proposal. *Trials* 2010; **11**: 85
- 17 **Singh P**, Das A, Isenberg G, Wong RC, Sivak MV, Agrawal D, Chak A. Does prophylactic pancreatic stent placement reduce the risk of post-ERCP acute pancreatitis? A meta-analysis of controlled trials. *Gastrointest Endosc* 2004; **60**: 544-550

S- Editor Gou SX L- Editor A E- Editor Zhang DN



Three-dimensional image reconstruction in capsule endoscopy

Anastasios Koulaouzidis, Alexandros Karargyris

Anastasios Koulaouzidis, Centre for Liver and Digestive Disorders, The Royal Infirmary of Edinburgh, Scotland EH16 4SA, United Kingdom

Alexandros Karargyris, National Library of Medicine, National Institutes of Health, Bethesda, MD 20814, United States

Author contributions: Koulaouzidis A and Karargyris A collected the material, discussed the topic and wrote the manuscript.

Correspondence to: Dr. Anastasios Koulaouzidis, MD, MRCP, FEBG, Centre for Liver and Digestive Disorders, The Royal Infirmary of Edinburgh, 51 Little France Crescent, Edinburgh, Scotland EH16 4SA,

United Kingdom. akoulaouzidis@hotmail.com

Telephone: +44-131-2421126 Fax: +44-131-2421618

Received: June 20, 2012 Revised: July 13, 2012

Accepted: July 18, 2012

Published online: August 21, 2012

troenterology, Department of Internal Medicine, University Hospital of Pisa, University Hospital of Pisa, University of Pisa, Via Roma 67, 56124 Pisa, Italy; Naoaki Sakata, MD, PhD, Division of Hepato-Biliary Pancreatic Surgery, Tohoku University Graduate School of Medicine, 1-1 Seiryomachi, Aoba-ku, Sendai, Miyagi 980-8574, Japan; Andrzej S Tarnawski, MD, PhD, DSc (Med), Professor of Medicine, Chief Gastroenterology, VA Long Beach Health Care System, University of California, Irvine, CA, 5901 E. Seventh Str., Long Beach, CA 90822, United States

Koulaouzidis A, Karargyris A. Three-dimensional image reconstruction in capsule endoscopy. *World J Gastroenterol* 2012; 18(31): 4086-4090 Available from: URL: <http://www.wjgnet.com/1007-9327/full/v18/i31/4086.htm> DOI: <http://dx.doi.org/10.3748/wjg.v18.i31.4086>

Abstract

To date, limited research has been carried out in developing methods and materials that offer three-dimensional (3-D) representation of the digestive tract. In the field of capsule endoscopy (CE), hardware approaches have been developed that provide real time both 3-D information and texture using an infrared projector and a complementary metal oxide semiconductor camera. The major drawbacks of this system are its size, power consumption and packaging issues. A software approach to approximate a 3-D representation of digestive tract surface utilising current CE technology has been proposed. The algorithm utilizes the Shape from Shading technique and seem to provide promising results for polypoid structures and angioectasias. Further clinical evaluation is currently under way.

© 2012 Baishideng. All rights reserved.

Key words: Capsule endoscopy; Three-dimensional; Reconstruction; Angioectasias; Software

Peer reviewers: Ferruccio Bonino, MD, PhD, Professor of Gas-

INVITED COMMENTARY ON HOT ARTICLES

I read with great interest the recent paper by Karargyris *et al*^[1] on the use of elastic video interpolation in the three-dimensional (3-D) reconstruction of the digestive wall in capsule endoscopy (CE) videos. The article presents promising 3-D approaches in CE; due to its technical nature though it may be slightly difficult for the general gastroenterologist. Therefore, I invited its first author to help me present the clinically relevant points. These authors believe that proper consideration should be given for its further clinical application in CE.

Wireless CE, a milestone in minimally invasive investigation of the gastrointestinal tract, was made possible by the advent of power efficient/low cost image sensors based on complementary metal oxide semiconductor (CMOS) technology^[2,3]. Upon the 1950's debut of the world's first gastro-camera, few could have envisaged that, just half a century later, imaging of the human digestive tract would become wireless^[4-6]. However, this spectacular advent in medical endoscopy is not without its limitations. Let us not forget that a complete capsule platform



Figure 1 Various sensors which are commercially available^[12]. A: Miniature magnetometers offer orientation and acceleration information, [Bertda Services (SEA) Pte. Ltd.]; B: Three-dimensional (3-D) range camera used in a widely commercial product; C: 3-D guidance system used in endoscopy devices (inition).

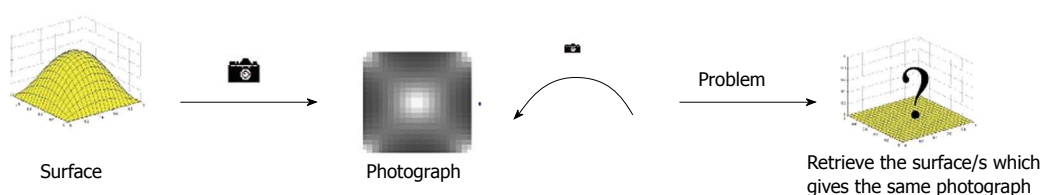


Figure 2 The Shape from Shading flow^[12,13]. Capturing a surface using a camera removes depth information. Shape from Shading techniques try to reproduce the missing depth information from a given image.

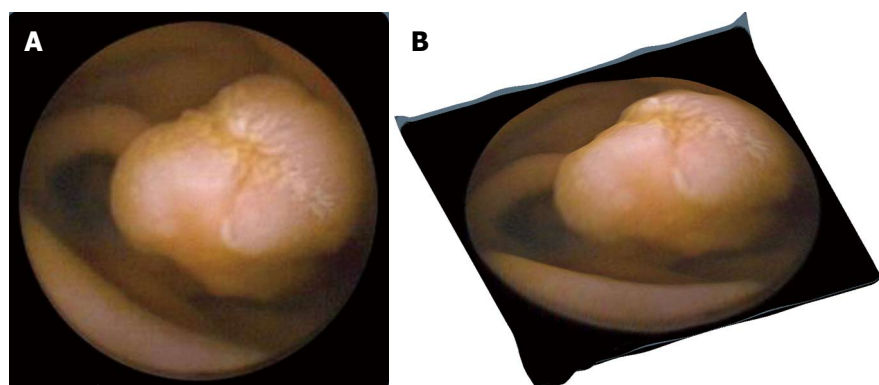


Figure 3 Original capsule endoscopy and 3-D represented image depicting a protrusion. A: Original capsule endoscopy image depicting a protrusion (polyp); B: Its 3-D represented image processed by the proposed Shape from Shading approach.

comprises six fundamental modules: locomotion, vision, telemetry, localisation, power and diagnostic/tissue manipulation tools^[7]. To present, due to space constraints, the majority of commercially available capsules include only a subset of the aforementioned modules^[7]. Furthermore, power limitation is a major hurdle which current CE technology has yet to overcome^[1,5,7].

Since the capsule needs 6-8 h to traverse through the small-bowel^[7,8], cameras within the currently marketed capsule endoscopes work at a capture rate of 2-3 frames per second (fps) in order to comply with power requirements^[7]. Nonetheless, this has an adverse effect on the smoothness of motion between consecutive frames and creates a visually unpleasant effect to the human eye^[1,7]. Furthermore, shape is an important element in human perception, yet CE suffers, unlike other diagnostic modalities i.e., Computed tomography, magnetic resonance imaging, from lack of 3-D information^[1]. Practically, this

can only be feasible with the use of new generation devices that have yet to be realised.

3-D technology is currently in use e.g., a magnetometer can provide not only acceleration values on the three axes but also the 3-D orientation of the device (Figure 1A)^[9]. Commercial time-of-flight range cameras (i.e., Microsoft's Kinect Project, Figure 1B)^[10] already exist in the market and in the near future this may be further improved and miniaturised for use inside a capsule endoscope. These cameras offer information on depth and colour. We should not forget that 3-D guidance systems are already used for endoscopic surgeries offering 3-D position information of the sensor (Figure 1C). Therefore, using the acquired information (orientation, acceleration, depth values, position *etc.*) from these miniature sensors in conjunction with sophisticated registration software algorithms, an accurate 3-D representation of the digestive tract could be created successfully.

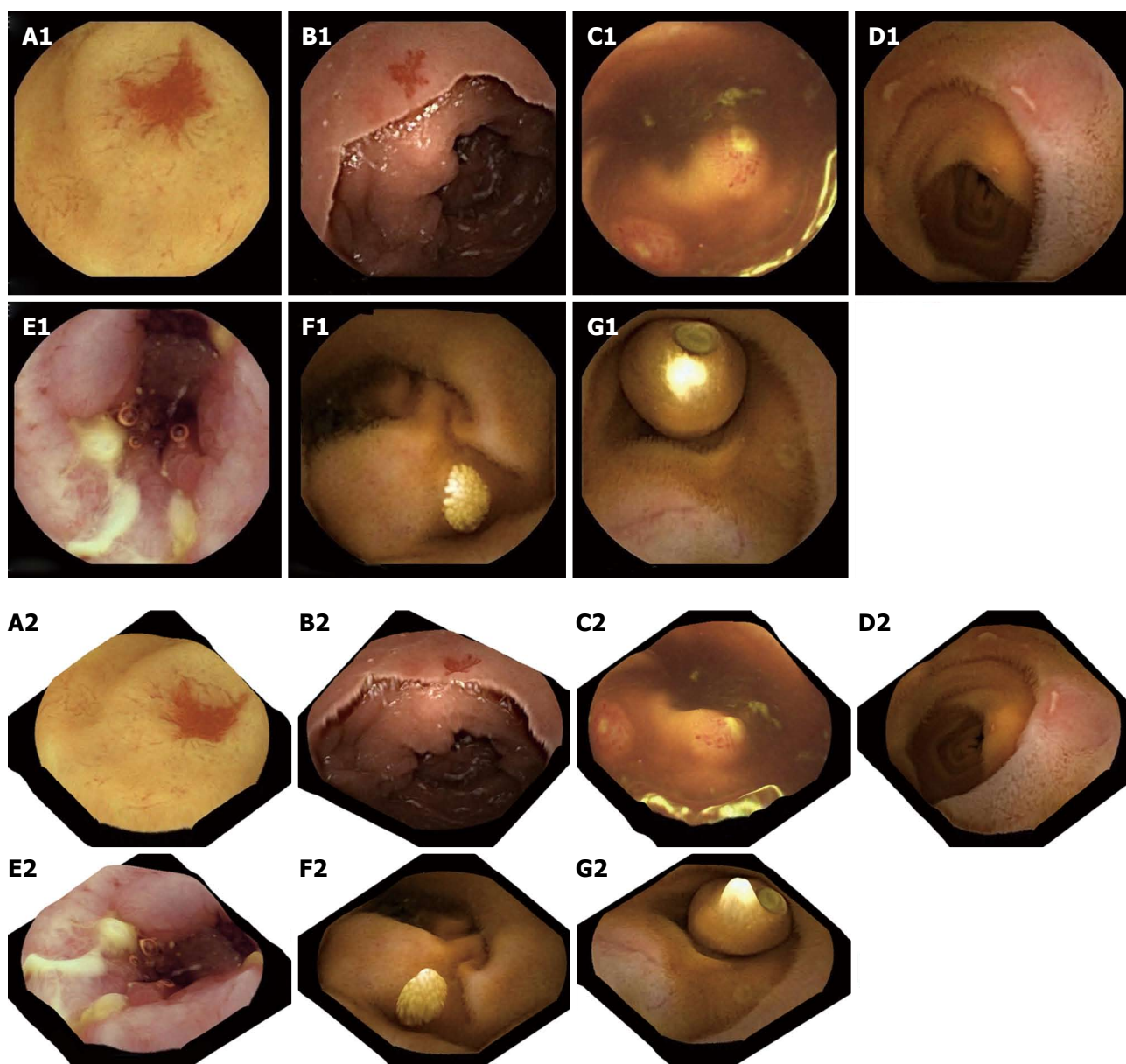


Figure 4 Two-dimensional capsule endoscopy images (upper panel) and three-dimensional representation of above structures is seen (lower panel). A1, A2: P2 angiectasia; B1, B2: P1 angiectasia; C1, C2: Lymphoid hyperplasia with superficial ulceration; D1, D2: Aphthous ulcers; E1, E2: Serpiginous ulcers; F1, F2: Nodular lymphangiectasia; G1, G2: Another capsule endoscope still inside the small-bowel.

Highlights removal

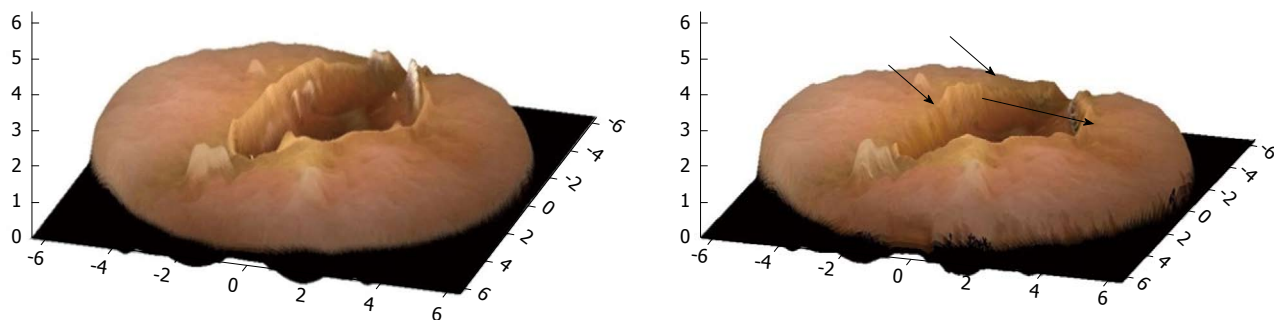


Figure 5 3-D representation of a single video capsule image with highlights removal (arrows).

3-D representation for endoscopy

To date, limited research has been carried out in developing methods and materials that offer 3-D representation of the digestive tract. For conventional endoscopy systems, stereo technology has been introduced to capture stereo images and to create depth information and therefore 3-D reconstruction of digestive structures. However, due to issues with size, such systems have not been widely accepted^[1,5]. Likewise, in CE there has been a hardware approach that provides in real time both 3-D information and texture using an infrared projector and a CMOS camera. The major drawbacks of this system are its size, power consumption and packaging issues^[11]. Therefore, in order to tackle the problem of the current hardware limitations, Karargyris *et al.*^[1,12] proposed the use of a software approach to approximate a 3-D representation of digestive tract surface utilising current CE technology.

Shape from shading

The Shape from Shading (SfS) technique is a member of a family of “shape recovery” algorithms called shape-from-X techniques^[1,13]. Essentially, SfS algorithms try to recover the shape of objects by using the gradual variation of shading (Figure 2)^[14]. SfS techniques can be divided into four groups or approaches: minimisation, propagation, local, and linear approaches^[13,14].

Karargyris *et al.*^[1] propose using a specific sub-category of SfS methods: the Tsai’s method (or linear approach)^[1,15] because (1) it produces good results for spherical surfaces, which in fact is the case with most shapes of digestive tract pathology e.g., polyps; (2) it is very fast; and (3) it “behaves” relatively well with specular surfaces (surfaces with mirror-like reflection of light). Of note, in CE the light source axis and the miniature camera are basically aligned. Tsai’s method works well on smooth objects and spherical structures^[15]. Additionally, Tsai’s method takes into consideration only the light direction, which in our case is 0° degrees (since the lighting direction and that of the camera are parallel).

A correction on the camera distortion is not performed because there is insufficient data on the capsule camera optics’ specifications. The result of applying Tsai’s method in a CE frame is given in Figure 3. Figure 3A shows a polyp in a conventional 2-D CE frame, whereas in Figure 3B the same polyp is presented using the 3-D software. The SfS approach gives promising outcomes, especially for visualizing polyps and vascular lesions, but less so for ulcers or lymphangiectasia (Figure 4). In the first 2 cases, the 3-D result is rather exciting, supporting the argument for further evaluation of this technique for use in clinical practice. Additionally, a 3-D representation may be helpful in the design of more accurate and robust computer-aided detection algorithms, incorporating other image enhancement tools e.g., virtual chromoendoscopy (FICE)^[16] or colour (blue) mode^[17] analysis of CE videos instead of still CE frames. However, prior to any software integration, further qualitative assessment and accuracy assessment should take place (work currently undertaken by

these authors).

Conversely, in cases of sudden large intensity change, Tsai’s method fails because it takes into consideration the preservation of intensity gradient. However, in non-artificial images such as CE frames, the brightness (image pixel values) transitions smoothly with no abrupt changes. Technically however, one can notice in Figure 5 the presence of highlights, hence false information about the shape. Highlights are essentially linear combinations of specular and diffuse reflection (light reflected at various angles) components of the surface.

Many objects in the real world are dielectric and homogeneous, hence displaying both types of reflections. Most digestive structures fall into this category^[18]. When the light beams fall on to such an object, some of them reflect back immediately creating the specular reflection, while the rest of the beams first penetrate the object and then reflect creating the diffuse reflection. Along with 3-D representation algorithm a highlight suppression scheme is applied to the original CE images to produce desired better results, whilst maintaining the shapes and structures of the digestive tract. Figure 5 shows the successful highlight removal without affecting the shapes of other objects. It has to be mentioned that highlights from light reflections on the surface of the digestive tract are still an open problem not only for a 3-D representation but also for traditional CE review.

In conclusion, the software by Karargyris *et al.*^[1] offers a new potential to reform and enhance the currently existing reading software in capsule endoscopy by improving lesion demarcation and highlighting the textural features of ulcers, angioectasias and polyps^[5,19]. Further work is needed to prove its clinical validity but the idea of a 3-D aid (with the present level of CE technology) seems, at least for this author, not only captivating but promising as well. However, it should not be forgotten that true 3-D capability requires dual video images, although the inclusion of two cameras within the shell of a capsule endoscopy might be unwieldy at present^[5].

REFERENCES

- 1 **Karargyris A**, Bourbakis N. Three-dimensional reconstruction of the digestive wall in capsule endoscopy videos using elastic video interpolation. *IEEE Trans Med Imaging* 2011; **30**: 957-971
- 2 **Liedlgruber M**, Uhl A. Computer-aided decision support systems for endoscopy in the gastrointestinal tract: a review. *IEEE Rev Biomed Eng* 2011; **4**: 73-88
- 3 **Muñoz-Navas M**. Capsule endoscopy. *World J Gastroenterol* 2009; **15**: 1584-1586
- 4 **Fireman Z**. Capsule endoscopy: Future horizons. *World J Gastrointest Endosc* 2010; **2**: 305-307
- 5 **Fisher LR**, Hasler WL. New vision in video capsule endoscopy: current status and future directions. *Nat Rev Gastroenterol Hepatol* 2012; **9**: 392-405
- 6 **Swain P**. At a watershed? Technical developments in wireless capsule endoscopy. *J Dig Dis* 2010; **11**: 259-265
- 7 **Ciuti G**, Menciassi A, Dario P. Capsule endoscopy: from current achievements to open challenges. *IEEE Rev Biomed Eng* 2011; **4**: 59-72
- 8 **Westerhof J**, Koornstra JJ, Hoedemaker RA, Sluiter WJ,

- Kleibeuker JH, Weersma RK. Diagnostic yield of small bowel capsule endoscopy depends on the small bowel transit time. *World J Gastroenterol* 2012; **18**: 1502-1507
- 9 Magnetometer. Available from: URL: <http://en.wikipedia.org/wiki/Magnetometer>
- 10 Kinect. Available from: URL: <http://en.wikipedia.org/wiki/Kinect>
- 11 **Kolar A**, Romain O, Ayoub J, Faura D, Viateur S, Granado B, Graba T. A system for an accurate 3D reconstruction in Video Endoscopy Capsule. *EURASIP J on Emb Sys* 2009; **2009**: 716317
- 12 **Karagyris A**, Karagyris O, Bourbakis N. 3D Representation of the Digestive Tract Surface in Wireless Capsule Endoscopy Videos. In: Proceedings of the 2010 IEEE International Conference on Bioinformatics and BioEngineering (BIBE); 2010 May 31-Jun 3; Philadelphia, United States. New Jersey: IEEE xplore, 2010: 279-280
- 13 **Prados E**, Faugeras OF. A rigorous and realistic Shape from Shading method and some of its applications. France: INRIA, 2004
- 14 **Zhang R**, Tsai PS, Cryer JE, Shah M. Shape-from-Shading: A Survey. *IEEE Trans Pattern Anal Mach Intell* 1999; **21**: 690-706
- 15 **Tsai PS**, Shah M. Shape from shading using linear approximation. *Image and Vision Computing* 1994; **12**: 487-498
- 16 **Gupta T**, Ibrahim M, Deviere J, Van Gossum A. Evaluation of Fujinon intelligent chromo endoscopy-assisted capsule endoscopy in patients with obscure gastroenterology bleeding. *World J Gastroenterol* 2011; **17**: 4590-4595
- 17 **Krystallis C**, Koulaouzidis A, Douglas S, Plevris JN. Chromoendoscopy in small bowel capsule endoscopy: Blue mode or Fuji Intelligent Colour Enhancement? *Dig Liver Dis* 2011; **43**: 953-957
- 18 **van der Zee P**. Measurement and modeling of the optical properties of human tissue in the near infrared. London: University of London, 1992
- 19 **Lewis BS**. Expanding role of capsule endoscopy in inflammatory bowel disease. *World J Gastroenterol* 2008; **14**: 4137-4141

S- Editor Gou SX L- Editor A E- Editor Zhang DN

Colorectal cancer in patients with inflammatory bowel disease: Can we predict risk?

Vibeke Andersen, Jonas Halfvarson, Ulla Vogel

Vibeke Andersen, Medical Department, Sygehus Sønderjylland Aabenraa, DK-6200 Aabenraa, Denmark

Vibeke Andersen, Institute of Regional Health Services Research, University of Southern Denmark, DK-5000 Odense, Denmark

Jonas Halfvarson, Department of Internal Medicine, Örebro University Hospital, Örebro University, Örebro 70185, Sweden

Ulla Vogel, National Research Centre for the Working Environment, DK-2100 Copenhagen, Denmark

Author contributions: Andersen V collected the material and wrote the manuscript; Halfvarsson J discussed the topic; and Vogel U supervised the manuscript.

Correspondence to: Vibeke Andersen, Consultant, Specialist, Medical Department, Sygehus Sønderjylland Aabenraa, Kresten Philipsens Vej 15, DK-6200 Aabenraa, Denmark. vandersen@health.sdu.dk

Telephone: +45-2-1157790 Fax: +45-8-8834488

Received: June 27, 2012 Revised: July 10, 2012

Accepted: July 18, 2012

Published online: August 21, 2012

Abstract

The inflammatory bowel diseases (IBD), Crohn's disease (CD) and ulcerative colitis (UC), may be complicated by colorectal cancer (CRC). In a recent population-based cohort study of 47 347 Danish patients with IBD by Tine Jess and colleagues 268 patients with UC and 70 patients with CD developed CRC during 30 years of observation. The overall risk of CRC among patients with UC and CD was comparable with that of the general population. However, patients diagnosed with UC during childhood or as adolescents, patients with long duration of disease and those with concomitant primary sclerosing cholangitis were at increased risk. In this commentary, we discuss the mechanisms underlying carcinogenesis in IBD and current investigations of genetic susceptibility in IBD patients. Further advances will depend on the cooperative work by epidemiologist and molecular geneticists in order to identify genetic polymorphisms involved in IBD-associated CRC. The ultimate goal is to incorporate genotypes and clinical

parameters into a predictive model that will refine the prediction of risk for CRC in colonic IBD. The challenge will be to translate these new findings into clinical practice and to determine appropriate preventive strategies in order to avoid CRC in IBD patients. The achieved knowledge may also be relevant for other inflammation-associated cancers.

© 2012 Baishideng. All rights reserved.

Key words: Inflammatory bowel disease; Crohn's disease; Ulcerative colitis; Colorectal cancer; Inflammation-associated cancer; Genetics; Preventive strategies

Peer reviewers: Andrzej S Tarnawski, Professor, Gastroenterology Section, VA Medical Center, University of California, Irvine, CA 90822, United States; Ferruccio Bonino, Professor, Liver and Digestive Division, Department of Internal Medicine, University of Pisa, Lungarno Bruno Buozzi 13, 56125 Pisa, Italy

Andersen V, Halfvarson J, Vogel U. Colorectal cancer in patients with inflammatory bowel disease: Can we predict risk? *World J Gastroenterol* 2012; 18(31): 4091-4094 Available from: URL: <http://www.wjgnet.com/1007-9327/full/v18/i31/4091.htm> DOI: <http://dx.doi.org/10.3748/wjg.v18.i31.4091>

INVITED COMMENTARY ON HOT ARTICLES

Incidence of colorectal cancer in inflammatory bowel diseases

The inflammatory bowel diseases (IBD), Crohn's disease (CD) and ulcerative colitis (UC), may be complicated by colorectal cancer (CRC). In a new population-based cohort study encompassing 47 347 Danish patients with IBD, 268 patients with UC and 70 patients with CD developed CRC during 30 years of observation^[1]. The authors concluded that the overall risk of CRC among patients with UC was comparable with that of the general

population [relative risk (RR), 1.07; 95% confidence interval (CI): 0.95-1.21]. The observed risk estimate persisted even after exclusion of patients with hemorrhagic proctitis (RR, 1.04; 95% CI: 0.91-1.18). When adjusted for age at diagnosis and duration of UC, a decreased risk of CRC among UC patients diagnosed in 1999-2008 was observed compared to UC patients diagnosed in 1989-1998 (RR, 0.59; 95% CI: 0.39-0.90). However, patients diagnosed with UC during childhood or adolescents (age 0-19 years; RR, 43.8; 95% CI: 27.2-70.7, age 20-39 years; RR, 2.65; 95% CI: 1.97-3.56) may be at increased risk as well as those with long duration of disease. Thirteen years after diagnosis, the CRC risk was significantly increased over background, and with longer follow-up the risk remained 50% above the risk in non-IBD individuals. The risk of CRC in patients with CD was similar to that of the non-IBD population. RR for CRC was 0.85 (95% CI: 0.67-1.07) among patients with CD and 0.80 (95% CI: 0.43-1.49) among patients with colonic CD.

Risk of CRC in IBD has been assessed previously in a Swedish population-based study^[2]. In agreement with the present study there was a trend towards lowered risk with shorter observation period^[2]. During 198 227 person-years follow-up for 7607 IBD cases, 188 cases of CRC were observed from 1954 to 2004^[2]. After adjusting for sex, age, duration of disease, type and extent of IBD, the authors found a decline in relative risk from a 5-fold increased risk in the 1960s to a doubled risk of CRC in the time-period 2000-2004 (*P* for trend 0.006). The overall risk of CRC among the patients with IBD, UC and CD colitis was found to be increased compared with the general population (standardized incidence ratio 2.3; 95% CI: 2.0-2.6, 2.7; 95% CI: 2.3-3.2, and 2.1; 95% CI: 1.2-3.4, respectively). The CRC risk among patients with colonic CD has also been estimated in hospital-based or community-based case-control studies^[3-5] and the overall relative risk estimate over the past 30 years was found to be 4.5 (range: 1.3-14.9) in a meta-analysis, with declining risk estimate over the past 30 years^[3]. On the other hand, a recent study by Herrington *et al*^[6] which was also published in *Gastroenterology* assessed time changes in risk of CRC within the Kaiser Permanente Medical Care Program, a community-based health care delivery system, from 1998 to 2010. The authors identified 29 and 53 CRC cases among CD and UC patients, respectively, corresponding to an incidence of CRC in patients with IBD which was 60% higher than in the general population. Furthermore, the incidence was found to be essentially constant over time. The study design may have some drawbacks such as missing detailed data on the study participants, selection bias, and too short observation period to detect the impact of optimizing IBD management on CRC risks which were discussed in the Editorials^[7].

There is general agreement that patients with UC diagnosed at a young age, with primary sclerosing cholangitis, and with long disease duration are at increased risk of CRC^[8-10]. Most cancers arise in extensive colitis and pancolitis and there is little or no increased risk associated

with proctitis while left sided colitis is associated with an intermediate cancer risk^[11,12]. The Danish study found no risk associated with having UC even after excluding cases with proctitis compared to the general population^[1].

According to the British Society of Gastroenterology (BSG) "It is now widely accepted that patients with ulcerative colitis have a similar risk to those with Crohn's colitis for a similar extent and duration of colonic involvement"^[13]. The Danish population-based study covered 30 years follow-up of all UC and CD patients and is by far the largest study to date on IBD and CRC risk^[1]. This study found no risk of CRC among patients with colonic CD compared to the general population which the authors speculated could be due to the medical treatment and follow-up leading to control of the intestinal inflammation^[1].

Surveillance colonoscopy is considered to be the gold standard in diagnosing early dysplastic alterations. The recent years new and emerging endoscopic imaging techniques have improved neoplasia detection rate^[14]. The existing recommendation is, however, based on evidence level IV: Evidence obtained from expert committee reports, opinions or clinical experiences of respected authorities^[13]. The study by Jess and colleagues constitutes a basis for future evidence-based guidelines.

Understanding the mechanism(s) of CRC in IBD

The relationship between inflammation and cancer has been well established in the gastro-intestinal system. Colitis-associated cancer has been investigated in mouse models^[15-17]. These studies have highlighted the role of toll-like receptors (TLR) and tumour necrosis factor- α (TNF- α) in the activation of nuclear factor κ B (NF κ B), which induces transcription of genes involved in tumorigenesis, including COX-2^[15-17]. Defect signalling via p53 may be an early event in the progression of colitis-induced dysplasia to cancer^[18]. Without p53-induced apoptosis, aberrant cells are not eliminated and cancer may ensue^[18]. Probiotic bacteria may prevent carcinogenesis in mouse models of cancer by producing conjugated linoleic acid which activates PPAR γ , inhibits COX-2 and induces apoptosis^[19,20].

Current strategies to identify genetic predictors of CRC in IBD

It is increasingly recognized that CRC consists of many entities having similar phenotypic appearance. This heterogeneity may at least in part be due to differences in genetic susceptibility which may act in combination with various environmental factors such as diet and intestinal microbes. Patients with IBD and CRC constitute 1%-2% of all cases of CRC^[21]. As a group, patients with IBD-associated CRC are characterized by intestinal inflammation and may thus represent a model with a relatively homogeneous mechanism for developing CRC. Indeed, distinct characteristics have been found for IBD-associated CRC. For example, a Norwegian study found that cancer was more often widespread than localized at diag-

nosis, age at diagnosis of CRC was lower, and prognosis poorer in IBD-associated CRC compared to CRC in the background population^[22]. Thus, "IBD-associated cancer serves as an excellent model of inflammation-associated cancer and might provide many important clues to understanding the pathogenesis of sporadic colorectal cancer"^[23]. On the other hand, a Swedish population-based study of more than 30 000 IBD cases identified 560 CRCs cases among first-degree relatives, giving no increased risk of CRC among first-degree relatives^[24]. The authors concluded that the study did not suggest a common cause of IBD and CRC in general and the risk of CRC in IBD seemed to be the result of the disease rather than genetic predisposition^[23].

The International IBD Genetics Consortium is a network of researchers working on the genetics of IBD^[25]. This group has initiated a case-control study to determine if genetic polymorphisms associated with IBD and other immune disorders related to IBD are more prevalent in patients with colonic IBD and CRC/dysplasia than in patients with colonic IBD alone. For each case with IBD-associated CRC/dysplasia, two IBD non-cancer cases from the same centre will be included. Analyses are carried out using the Immunochip, an Illumina Infinium genotyping chip containing 196 524 polymorphisms (718 small insertion deletions, 195 806 SNPs). The Immunochip was initiated by the Wellcome Trust Case-Control Consortium and designed to perform deep replication of major autoimmune and inflammatory pathways^[26]. Phenotypic information includes age at IBD and CRC/dysplasia diagnosis, gender, disease location, family history of CRC/dysplasia, medication, history of hospitalizations, and smoking habits.

Another approach may be based on utilizing existing pathological samples. For example, in Denmark, individual-based registration-systems have been developed along with the introduction of information technology and since 1978 nation-wide reporting of clinical diagnosis has been implemented^[27]. Due to the introduction of DNA changes (e.g., mutations and polyploidy) during carcinogenesis, pathological samples with signs of CRC should be avoided. Samples with signs of IBD which precede CRC development, may be used for DNA extraction and assessment of genetic polymorphisms^[28-31]. Furthermore, data may be linked to other registers such as Danish National Patient Register and The Danish Prescription Database for further investigations^[32]. The validity of the diagnoses of IBD and CRC, respectively, in the Danish National Patient Register are more than 90%^[33,34]. Thereby, candidate gene analyses of genetic polymorphisms in inflammatory pathways and associations found by genome-wide association studies may be performed and sought replicated.

Future research directions to predict the risk for CRC in IBD

A major challenge is now to identify the patients who would benefit from preventive strategies. Large and well-

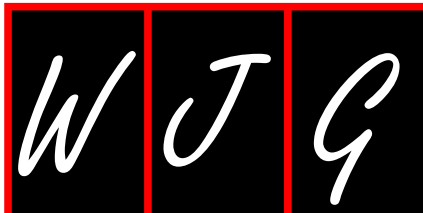
designed cohorts, such as population-based cohorts, with prospectively recorded data are required for the assessment of patients at risk. Provided that genetic susceptibility contributes to the risk of CRC in IBD, investigating genetic susceptibility in IBD patients may be particularly rewarding due to the expected relatively homogeneous biological mechanism(s) of action in this group. This may imply that associations may be identified in relatively small groups of well-characterized patients. The further advance will depend on the cooperative work of e.g., epidemiologists and molecular geneticists. The ultimate goal is to incorporate genotypes and clinical parameters into a predictive model that will refine the risk for CRC in colonic IBD. The challenge will be to translate these new findings into clinical practice and to determine appropriate preventive strategies in order to avoid CRC in IBD patients.

REFERENCES

- 1 **Jess T**, Simonsen J, Jørgensen KT, Pedersen BV, Nielsen NM, Frisch M. Decreasing risk of colorectal cancer in patients with inflammatory bowel disease over 30 years. *Gastroenterology* 2012; **143**: 375-381.e1
- 2 **Söderlund S**, Brandt L, Lapidus A, Karlén P, Broström O, Löfberg R, Ekblom A, Askling J. Decreasing time-trends of colorectal cancer in a large cohort of patients with inflammatory bowel disease. *Gastroenterology* 2009; **136**: 1561-1567; quiz 1818-1819
- 3 **Canavan C**, Abrams KR, Mayberry J. Meta-analysis: colorectal and small bowel cancer risk in patients with Crohn's disease. *Aliment Pharmacol Ther* 2006; **23**: 1097-1104
- 4 **Ekblom A**, Helmick C, Zack M, Adami HO. Increased risk of large-bowel cancer in Crohn's disease with colonic involvement. *Lancet* 1990; **336**: 357-359
- 5 **Jess T**, Gamborg M, Matzen P, Munkholm P, Sørensen TI. Increased risk of intestinal cancer in Crohn's disease: a meta-analysis of population-based cohort studies. *Am J Gastroenterol* 2005; **100**: 2724-2729
- 6 **Herrinton LJ**, Liu L, Levin TR, Allison JE, Lewis JD, Velayos F. Incidence and mortality of colorectal adenocarcinoma in persons with inflammatory bowel disease from 1998 to 2010. *Gastroenterology* 2012; **143**: 382-389
- 7 **Nguyen GC**, Bressler B. A tale of two cohorts: are we overestimating the risk of colorectal cancer in inflammatory bowel disease? *Gastroenterology* 2012; **143**: 288-290
- 8 **Baars JE**, Looman CW, Steyerberg EW, Beukers R, Tan AC, Weusten BL, Kuipers EJ, van der Woude CJ. The risk of inflammatory bowel disease-related colorectal carcinoma is limited: results from a nationwide nested case-control study. *Am J Gastroenterol* 2011; **106**: 319-328
- 9 **Rutter MD**, Saunders BP, Wilkinson KH, Rumbles S, Schofield G, Kamm MA, Williams CB, Price AB, Talbot IC, Forbes A. Thirty-year analysis of a colonoscopic surveillance program for neoplasia in ulcerative colitis. *Gastroenterology* 2006; **130**: 1030-1038
- 10 **Eaden JA**, Abrams KR, Mayberry JF. The risk of colorectal cancer in ulcerative colitis: a meta-analysis. *Gut* 2001; **48**: 526-535
- 11 **Ekblom A**, Helmick C, Zack M, Adami HO. Ulcerative colitis and colorectal cancer. A population-based study. *N Engl J Med* 1990; **323**: 1228-1233
- 12 **Jess T**, Loftus EV, Velayos FS, Harmsen WS, Zinsmeister AR, Smyrk TC, Schleck CD, Tremaine WJ, Melton LJ, Munkholm P, Sandborn WJ. Risk of intestinal cancer in inflammatory bowel disease: a population-based study from olmsted

- county, Minnesota. *Gastroenterology* 2006; **130**: 1039-1046
- 13 Cairns SR, Scholefield JH, Steele RJ, Dunlop MG, Thomas HJ, Evans GD, Eaden JA, Rutter MD, Atkin WP, Saunders BP, Lucassen A, Jenkins P, Fairclough PD, Woodhouse CR. Guidelines for colorectal cancer screening and surveillance in moderate and high risk groups (update from 2002). *Gut* 2010; **59**: 666-689
 - 14 Neumann H, Vieth M, Langner C, Neurath MF, Mudter J. Cancer risk in IBD: how to diagnose and how to manage DALM and ALM. *World J Gastroenterol* 2011; **17**: 3184-3191
 - 15 Westbrook AM, Szakmary A, Schiestl RH. Mechanisms of intestinal inflammation and development of associated cancers: lessons learned from mouse models. *Mutat Res* 2010; **705**: 40-59
 - 16 Goel GA, Kandiel A, Achkar JP, Lashner B. Molecular pathways underlying IBD-associated colorectal neoplasia: therapeutic implications. *Am J Gastroenterol* 2011; **106**: 719-730
 - 17 McConnell BB, Yang VW. The Role of Inflammation in the Pathogenesis of Colorectal Cancer. *Curr Colorectal Cancer Rep* 2009; **5**: 69-74
 - 18 Dirisina R, Katzman RB, Goretsky T, Managlia E, Mittal N, Williams DB, Qiu W, Yu J, Chandel NS, Zhang L, Barrett TA. p53 and PUMA independently regulate apoptosis of intestinal epithelial cells in patients and mice with colitis. *Gastroenterology* 2011; **141**: 1036-1045
 - 19 Bassaganya-Riera J, Viladomiu M, Pedragosa M, De Simone C, Hontecillas R. Immunoregulatory mechanisms underlying prevention of colitis-associated colorectal cancer by probiotic bacteria. *PLoS One* 2012; **7**: e34676
 - 20 Bassaganya-Riera J, Viladomiu M, Pedragosa M, De Simone C, Carbo A, Shaykhtudinov R, Jobin C, Arthur JC, Corl BA, Vogel H, Storr M, Hontecillas R. Probiotic bacteria produce conjugated linoleic acid locally in the gut that targets macrophage PPAR γ to suppress colitis. *PLoS One* 2012; **7**: e31238
 - 21 Munkholm P. Review article: the incidence and prevalence of colorectal cancer in inflammatory bowel disease. *Aliment Pharmacol Ther* 2003; **18** Suppl 2: 1-5
 - 22 Brackmann S, Aamodt G, Andersen SN, Roald B, Langmark F, Clausen OP, Aadland E, Fausa O, Rydning A, Vatn MH. Widespread but not localized neoplasia in inflammatory bowel disease worsens the prognosis of colorectal cancer. *Inflamm Bowel Dis* 2010; **16**: 474-481
 - 23 Rhodes JM, Campbell BJ. Inflammation and colorectal cancer: IBD-associated and sporadic cancer compared. *Trends Mol Med* 2002; **8**: 10-16
 - 24 Askling J, Dickman PW, Karlén P, Broström O, Lapidus A, Löfberg R, Ekblom A. Colorectal cancer rates among first-degree relatives of patients with inflammatory bowel disease: a population-based cohort study. *Lancet* 2001; **357**: 262-266
 - 25 International inflammatory bowel disease genetics consortium (IIBDGC). Hinxton (UK): Trust Sanger Institute; [updated 2012 Jul 3; cited 2012]. Available from: URL: <http://www.ibdgenetics.org/>
 - 26 Cortes A, Brown MA. Promise and pitfalls of the Immuno-chip. *Arthritis Res Ther* 2011; **13**: 101
 - 27 The danish pathology data bank (Patologidatabank). [updated Jul 3 2009; cited 2012]. Available from: URL: <http://www.patobank.dk/>
 - 28 Vangsted AJ, Klausen TW, Ruminski W, Gimsing P, Andersen NF, Gang AO, Abildgaard N, Knudsen LM, Nielsen JL, Gregersen H, Vogel U. The polymorphism IL-1beta T-31C is associated with a longer overall survival in patients with multiple myeloma undergoing auto-SCT. *Bone Marrow Transplant* 2009; **43**: 539-545
 - 29 Vangsted AJ, Klausen TW, Gimsing P, Andersen NF, Abildgaard N, Gregersen H, Vogel U. A polymorphism in NFKB1 is associated with improved effect of interferon- α maintenance treatment of patients with multiple myeloma after high-dose treatment with stem cell support. *Haematologica* 2009; **94**: 1274-1281
 - 30 Vangsted AJ, Klausen TW, Abildgaard N, Andersen NF, Gimsing P, Gregersen H, Nexø BA, Vogel U. Single nucleotide polymorphisms in the promoter region of the IL1B gene influence outcome in multiple myeloma patients treated with high-dose chemotherapy independently of relapse treatment with thalidomide and bortezomib. *Ann Hematol* 2011; **90**: 1173-1181
 - 31 Pikor LA, Enfield KS, Cameron H, Lam WL. DNA extraction from paraffin embedded material for genetic and epigenetic analyses. *J Vis Exp* 2011; (**49**): 2763
 - 32 Pedersen CB, Gøtzsche H, Møller JO, Mortensen PB. The Danish Civil Registration System. A cohort of eight million persons. *Dan Med Bull* 2006; **53**: 441-449
 - 33 Fonager K, Sørensen HT, Rasmussen SN, Møller-Petersen J, Vyberg M. Assessment of the diagnoses of Crohn's disease and ulcerative colitis in a Danish hospital information system. *Scand J Gastroenterol* 1996; **31**: 154-159
 - 34 Helqvist L, Erichsen R, Gammelager H, Johansen MB, Sørensen HT. Quality of ICD-10 colorectal cancer diagnosis codes in the Danish National Registry of Patients. *Eur J Cancer Care (Engl)* 2012; Epub ahead of print

S- Editor Gou SX L- Editor A E- Editor Zhang DN



Yusuf Bayraktar, Professor, Series Editor

Is enteroscopy necessary for diagnosis of celiac disease?

Taylan Kav, Bulent Sivri

Taylan Kav, Bulent Sivri, Hacettepe University School of Medicine, Department of Medicine, Division of Gastroenterology, Sıhhiye, Ankara 06100, Turkey

Author contributions: Kav T and Sivri B contributed equally to this work.

Correspondence to: Taylan Kav, MD, Associate Professor of Gastroenterology, Hacettepe University School of Medicine, Department of Medicine, Division of Gastroenterology, Sıhhiye, Ankara 06100, Turkey. tkav@hacettepe.edu.tr

Telephone: +90-312-3051712 Fax: +90-312-4429429

Received: October 28, 2011 Revised: March 26, 2012

Accepted: April 9, 2012

Published online: August 21, 2012

© 2012 Baishideng. All rights reserved.

Key words: Celiac disease; Diagnosis; Enteroscopy; Single balloon enteroscopy; Capsule enteroscopy

Peer reviewer: Dr. Ron Shaoul, Pediatric Gastroenterology, Rambam Medical Center, Haifa 31096, Israel

Kav T, Sivri B. Is enteroscopy necessary for diagnosis of celiac disease? *World J Gastroenterol* 2012; 18(31): 4095-4101
Available from: URL: <http://www.wjgnet.com/1007-9327/full/v18/i31/4095.htm> DOI: <http://dx.doi.org/10.3748/wjg.v18.i31.4095>

Abstract

Celiac disease (CD) is an autoimmune inflammatory disease of the small intestine as a result of reaction to wheat protein, gluten. Exclusion of dietary gluten is the mainstay of the treatment that necessitates a precise diagnosis of the disease. Serological screening may aid in identifying patients with suspected CD, which should be confirmed by intestinal biopsy. It has been shown that duodenal biopsies are good for detection of the disease in most patients. However, there is a group of patients with positive serology and inconclusive pathology. As a result of the widespread use of serology, many patients with equivocal findings grow quickly. Unfortunately current endoscopic methods can only diagnose villous atrophy, which can be present in the later grades of disease (i.e., Marsh III). To diagnose CD correctly, going deeper in the intestine may be necessary. Enteroscopy can reveal changes in CD in the intestinal mucosa in 10%-17% of cases that have negative histology at initial workup. Invasiveness of the method limits its use. Capsule endoscopy may be a good substitute for enteroscopy. However, both techniques should be reserved for patients with suspected diagnosis of complications. This paper reviews the current literature in terms of the value of enteroscopy for diagnosis of CD.

INTRODUCTION

Celiac disease (CD) is the most common inflammatory disease of the small bowel with a prevalence of 1%-2.1% in different countries^[1]. CD was previously thought to be a pediatric malabsorption syndrome, but it is now primarily recognized as an adult disease that resembles a multisystem disorder with a range of clinical manifestations that vary according to age of presentation. The clinical presentation among adults has clearly changed over time. Typical presentation should not be expected in the adult population; fewer patients present with diarrhea or a malabsorption syndrome. Instead, silent symptoms such as anemia, osteoporosis or dyspepsia are the most common manifestations, and interestingly, patients are frequently overweight or even obese at presentation. Patients may also present with vague dyspeptic symptoms or esophageal reflux, irritable bowel syndrome, iron deficiency, or neurological disorders. In fact, over time there has been a substantial increase in prevalence of the disease, and serological testing for CD has affected the rate of diagnosis^[1-4].

Widespread use and availability of serology and awareness of the disease have led to a surge in the diagnosis of CD from a very rare disease to a common one.

In fact, screening of asymptomatic and at-risk individuals has contributed to this high prevalence^[3]. The majority of CD patients detected by screening (> 80%) are clinically silent or so called “oligosymptomatic”^[4]. Mainstay vehicles for screening are autoantibodies to tissue transglutaminase and endomysial antibody (EMA), which are highly sensitive and specific^[4-7].

Despite these effective tools, small bowel biopsy should be performed in suspected patients, and histopathological examination of the small intestine must show any of the following: villous atrophy, crypt hyperplasia and elevated intraepithelial lymphocytes (IELs). Although small bowel mucosal changes are not specific for CD, abnormal biopsy findings can confirm the diagnosis in the context of the clinical setting that includes symptoms, serology and exclusion of other disorders. The only current and effective treatment is dietary restriction of the gluten in affected individuals, which necessitates the correct diagnosis.

CD AT A GLANCE

Characteristic pathological changes of the small bowel found in CD have been classified by Marsh and further modified by Oberhuber^[8,9]. It is believed that small-bowel mucosal damage has three phases. In phase 1, the infiltrative phase, there are increased numbers of IELs. In phase 2, the hyperplastic phase, there is crypt hypertrophy. The destructive phase 3 of the disease is associated with varying degrees of villous atrophy that can be assessed during endoscopy^[8,9]. The mucosal changes associated with CD can be patchy with parts of the mucosa appearing normal and nearby parts severely affected in children and adults. This patchy villous atrophy or disease poses a significant sampling error that leads to the possibility of missing the diagnosis, which can be detrimental for a young patient with long life expectancy, because the course of untreated CD is not always benign. Delay in diagnosis in patients with severe presentation is associated with increased mortality, primarily because of malignancy. A major question is the ultimate outcome of undiagnosed, presumed silent CD? It has been suggested that there is a significantly increased risk of mortality in patients with undiagnosed CD. However, the association with increased mortality is not universal nor is the association with increased malignancy^[10-12]. Early diagnosis and treatment of CD has the potential to decrease risks of lymphoma, gastrointestinal cancer, bone disease, endocrine abnormalities, infertility and other autoimmune diseases^[13].

As a consequence of an intensified screening policy, individuals with positive antibodies but without diagnostic small-bowel mucosal villous atrophy frequently are found. The condition often is considered false-positive, but there also is evidence to suggest that such a finding is indicative of early stage CD. Randomized clinical trials on the natural history and treatment of CD patients with mild mucosal changes and positive antibodies are lacking, and there is no consensus whether these patients should be treated at all with a gluten-free diet before villous atro-

phy has developed^[2,10,13-15].

Despite recent advances in endoscopic imaging and serological tests, the accurate diagnosis of CD remains challenging. The site and number of biopsies to diagnose CD correctly have been the focus of recent research. Newly introduced technologies may carry a high yield but availability may limit their widespread use.

The gold standard of diagnosis relies on duodenal biopsy^[16]; however, the reliability of duodenal biopsy is not straightforward. Patients come to biopsy because of the result of positive serological tests, a high index of suspicion for a mucosal disease process, or because of routine duodenal biopsy at endoscopy^[17]. Biopsies from different sites of the duodenum in patients with positive celiac serology undergoing biopsy showed that none of the biopsies were considered normal. Moreover, in only 50% of patients was the degree of villous atrophy present in all sites the same; consistent with the patchy nature of the degree of villous atrophy. An interesting observation is that total villous atrophy significantly increased in a distal direction. Although more severe degrees of villous atrophy have been found distally, the diagnosis has mostly been confirmed in any location in the duodenum or jejunum^[2,9,10,15].

INTESTINAL INVOLVEMENT

CD involves the proximal small intestine including duodenum and upper jejunum and extends distally for a variable length into the ileum. Damaged small bowel mucosa heals in a distal to proximal direction. Mucosal atrophy is continuous in most patients as a diffuse proximal enteropathy, which can be seen by any means of endoscopy. Autopsy studies on CD patients have also confirmed the involvement of the duodenum and jejunum in most cases and occasional extension into the ileum. However, distribution and extent of the CD are variable^[13,18].

Dickey *et al*^[19] have evaluated terminal ileal biopsies of 30 patients with CD and control patients and found that IEL counts were significantly higher in the CD group. They concluded that increased IELs in the terminal ileum correlated with duodenal atrophy, and that this finding should alert physicians to consider CD.

Although evaluation of the extent of the bowel involvement is not possible by conventional methods, capsule endoscopy (CE) can give an estimation about whether the whole of the small bowel is affected. It has been reported that 66.6% of patients with CD had an extension of the mucosal changes beyond the proximal small intestine and 11.1% had entire small bowel involvement^[20]. According to Murray *et al*^[21], in the majority of patients, the abnormal findings seen in the CE started in the proximal duodenum and extended into the jejunum. Findings of atrophy were seen in a continuous pattern in the duodenum, but features of atrophy were seen less obviously and were patchy in the jejunum. Extensive enteropathy was seen in 59% of the patients, denoting that CD affected the small bowel more than we think.

Mucosal specimens can be obtained using radiographically guided suction capsule (Crosby capsule) biopsy, which has disadvantages such as long procedure time, high failure rate, discomfort and radiation exposure during the procedure, although it is possible to take large biopsy specimens. Perforation, intramural hematoma of the small bowel and pancreatitis are reported complications^[22]. Nowadays, Crosby capsule biopsy is not performed due to comparable efficacy of the duodenal biopsy to detect villous atrophy. Another important fact to take into account is the patchy nature of CD, which necessitates multiple biopsy approach to minimize sampling errors^[23].

There are no clear-cut recommendations for the exact number of biopsy specimens to confirm or exclude diagnosis of CD, although the American Gastroenterological Association technical review recommends 4-6 biopsies^[24]. Unfortunately, there is a gap between evidence-based data and real-life practice. A survey has shown that 63% of patients had fewer than four duodenum biopsies, which may indicate the reluctance of the endoscopists to take an adequate number of biopsies^[25].

Site of the biopsy is another object of the debate. Pais *et al*^[26] have found that duodenal biopsy specimens show some variability in terms of histological changes, and a minority of patients may have a discrepancy of more than two Marsh grades between biopsy sites. Ravelli *et al*^[15] have found no cases of normal histology and coexisting villous atrophy in the same patient. This observation was supported by another study by Thijs *et al*^[22] in which no discrepancy between jejunal and duodenal biopsies was found. Biopsies from the duodenum have been demonstrated to be useful for the diagnosis of CD and almost replaced the need for the jejunal biopsy.

Unfortunately, biopsy specimens from the duodenum harbor some problems and may not be a good place for the diagnosis of CD, given the nature of the disease and necessity of a strict diet. Not only is there more natural irregularity of the proximal duodenal mucosa, but specifically, the influence of nutrients mixed with gastric acid from the stomach and digestive fluids released into the duodenum in reaction to a meal may induce a chronic mild inflammatory response^[27,28]. This may alter the appearance of mucosal inflammation and villous architectural changes, and therefore, disqualify duodenal biopsies for diagnostic use, especially when minor architectural changes and intraepithelial lymphocytosis must be considered^[29].

All of the current endoscopic imaging techniques rely on the morphological changes of the mucosa associated with CD, which may direct the endoscopist for sampling. The value of endoscopy in the diagnosis of CD is limited to villous atrophy (Marsh grade 3). Celiac patients with villous atrophy are easily diagnosed, and most of them have positive serology, thus making this group of patients non-challenging. Histological changes in this group are so characteristic that they cannot be mistaken for other diseases. In contrast, patients with milder enteropathy,

which is the most prevalent form of the disease at present, may show increased IELs that cannot be identified under white light or even with narrow band imaging or magnification endoscopy.

Diagnostic accuracy of biopsy specimens can be improved with advanced endoscopic technologies. Magnification endoscopy with narrow band imaging is a useful tool for obtaining biopsies at diseased sites^[30]. These white light or blue-green light endoscopies are not capable of detecting increased IELs, which in turn limits us to the advanced stage of the disease with apparent atrophy and changes, but the problem is to detect the patients with subtle changes (i.e., Marsh grades 1 and 2). Confocal endomicroscopy (CEM) may aid in diagnosis in theory. However, fact is a little different from theory; CEM is good at detecting atrophy, although it cannot differentiate subgrades, and increased IELs, but falls short at detecting crypt hyperplasia, topical acriflavine use is helpful for quantification of IELs but fluorescein is not helpful. Very limited availability and safety issues on acriflavine use are the major drawbacks of CEM, and some imaging improvements should be done before its prime time use in CD^[31].

ENDOSCOPIC FEATURES OF CD

The opportunity to make a correct diagnosis of CD might, therefore, also depend on the endoscopic appearance of the small bowel mucosa. Several endoscopic markers related but not specific to CD have been identified. These endoscopic markers are useful to determine whether duodenal biopsies are indicated and possibly to target from where biopsies should be taken. Endoscopic markers of CD are as follows: a reduction or absence of duodenal folds; scalloping, which is a notched appearance of the duodenal folds; visible submucosal vasculature; a mosaic pattern, which is the micronodular or cobblestone appearance of the mucosal surface; and mucosal fissures, crevices or grooves^[17] (Figure 1). These indirect signs of villous atrophy have been helpful for predicting the presence or absence of duodenal villi and for targeting duodenal biopsies during upper endoscopy for diagnosing CD. Nevertheless, the sensitivity of these signs has been demonstrated to be variable in the different studies, and therefore, multiple endoscopic biopsies from descending duodenum and bulbar mucosa are recommended to ameliorate the diagnostic accuracy and to avoid underdiagnosis of patchy forms of CD^[32,33].

Contradictory results concerning the value of these endoscopic markers of villous atrophy have been reported. Among several studies, the overall sensitivity and specificity of endoscopic markers of CD vary from 6% to 94% and from 83% to 100%, respectively. Several possible explanations exist for the absence of endoscopic markers in patients with CD. For example, such markers might actually be absent for degrees of enteropathy milder than subtotal or total villous atrophy (e.g., partial villous atrophy) and absent in cases in which the histo-

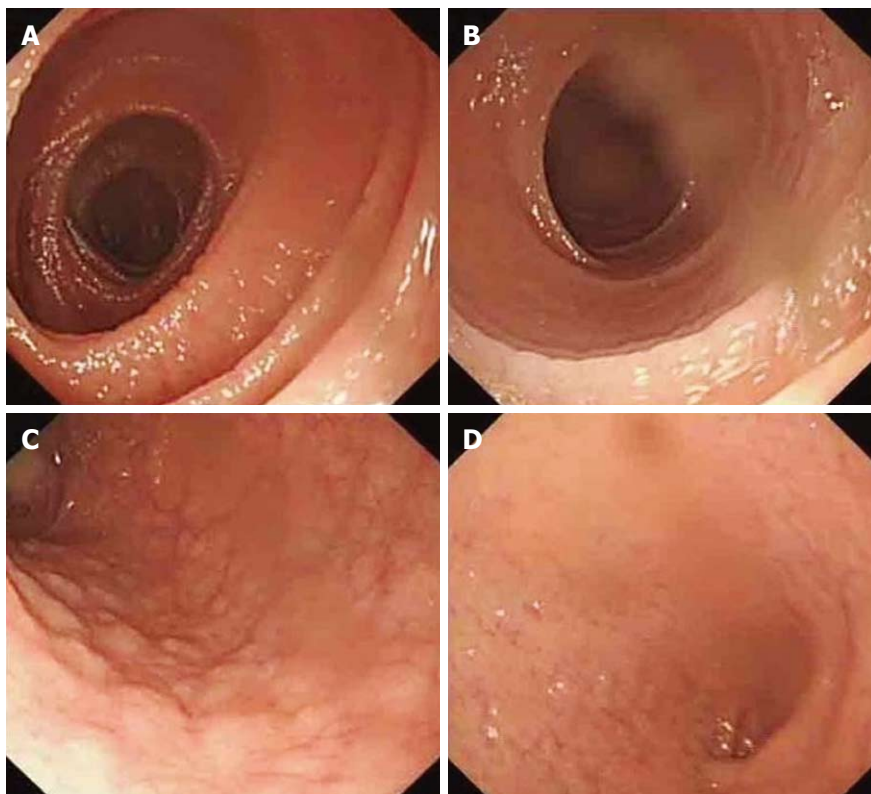


Figure 1 Proximal jejunum mucosa showing scalloping (A), reduced loss of mucosal folds (B), nodularity and mosaic appearance (C) and total mucosal atrophy (D), seen in patients with celiac disease during enteroscopy.

pathological involvement of the duodenum is patchy. In contrast, scalloping of duodenal folds has been reported in some patients who have moderate-to-severe enteropathy that is unrelated to CD; scalloping has a positive predictive value of 69% for CD and 96% for any duodenal mucosal pathology^[34]. Scalloping is not specific for CD but rather a predictor of mucosal disease as evidenced by villous atrophy, widening, and edema^[35].

It is possible to augment the villous changes by a simple procedure of underwater examination of the mucosa, which is called the water-immersion technique (WIT), which consists of the instillation of water into the duodenum after removal of air and adds only a few seconds to the examination time. WIT-assisted duodenoscopy has been demonstrated as reliable in distinguishing accurately the presence or absence of villi in the duodenal bulb and the descending duodenum^[32,33]. However, no study has specifically addressed the value of WIT during enteroscopy. We usually perform WIT to assess the villi structure in the jejunum during the enteroscopy examination of patients with diarrhea and malabsorption and find it useful for diagnosis of CD.

MAKING THE CASE FOR ENTEROSCOPY

CD is a gluten-dependent enteropathy characterized by chronic small intestinal inflammation and villous atrophy. However, CD is not the only cause of an inflammatory cell infiltrate with or without villous atrophy in duodenal

mucosa. Other causes include postviral enteritis, cow or soy milk enteritis, Crohn's disease, common variable immunodeficiency, autoimmune enteropathy, nonsteroidal anti-inflammatory drugs, giardiasis, tropical sprue, and tuberculosis. It is more likely that the normal state of the bulb mucosa is not as free of inflammation as is mucosa of the second or third part of the duodenum, nor does it have a villous/crypt ratio the same as these zones. It has been proposed that the anatomical location of the bulb makes it more vulnerable than the more distal duodenum to injury by gluten. However, similar reasoning applies also to potential injury of the bulbar mucosa by aforementioned causes and gastric acid. In addition, Brunner's glands and lymphoid nodules can give a common endoscopic finding of nodularity in the duodenal bulb, which can also distort the overlying architecture. On biopsy, lymphoid aggregates are also commonly found in the duodenal bulb of younger children. That is why some findings in the bulb may be a part of life rather than disease. Biopsy samples from the duodenal bulb may be difficult to interpret, in fact, the duodenal bulb is not considered a useful site for the diagnosis of CD, even though this site has rarely been reported to be the only one showing reliable histological changes in adults and children with CD. Taking biopsy samples more distally may decrease the likelihood of confusing histological findings^[34].

CD has many atypical manifestations, and endoscopic findings alone are not considered sensitive or specific for the diagnosis of CD. Pais *et al*^[20] examined 247 patients

to determine how many duodenal biopsy specimens were needed to diagnose CD. They concluded that only two specimens led to confirmation of CD in 90% of cases and that four descending duodenal biopsy specimens led to 100% confidence in the diagnosis. Comparison of biopsy specimens from the second, third, and fourth parts of the duodenum, the ligament of Treitz, and the proximal jejunum has shown that each site is suitable for diagnosing CD^[7]. Mucosal specimens taken from the distal duodenal or jejunal mucosa are strongly correlated, therefore, biopsy samples from the second or third part of the duodenum are considered adequate to obtain material for histological interpretation^[29]. Thus, biopsy of the other parts of the small intestine may be needed for precise diagnosis of CD, which is an indication for enteroscopy.

ENTEROSCOPY

We have long been aware that complete examination of the small bowel is crucial for evaluation of refractory disease or its complications. However, conventional endoscopy has limited value for evaluation of complications like ulcerative jejunoileitis and lymphoma that may be located deep in the small bowel, which necessitates deep enteroscopy techniques such as push enteroscopy (PE), balloon-assisted enteroscopy (BAE) and CE. Invasiveness of the enteroscopy technique limits its use. Two studies have explored the value of PE for the diagnosis of complicated CD.

Höroldt *et al.*^[36] have searched the possible role of PE with jejunal biopsies. They prospectively recruited 31 patients who had symptoms suggestive of CD and positive serology, but non-diagnostic duodenal biopsies that were either normal or showed increased IELs. Enteroscopy with duodenal and additional jejunal biopsies was performed in all of the patients, who continued a normal gluten containing diet, 6-12 wk after index endoscopy. Repeat biopsies confirmed CD in five of the eight patients who were positive for EMA. Moreover, in 60% of cases, these changes were diagnostic in the jejunal biopsies only. De Vitis *et al.*^[37] also studied a similar group of 23 patients, and in their group, only four patients were diagnosed with CD according to jejunal biopsies alone. According to these enteroscopy studies, CD can be further diagnosed in 10%-17% of patients with equivocal findings in the previous studies of patients who were presumed to have CD. A limitation of PE is that it evaluates a fraction of the small bowel, leaving the majority of the small bowel uninvestigated.

Cellier *et al.*^[38] demonstrated that PE detected jejunal ulcerations in 62.5% of CD patients, in whom no duodenal lesions were observed. They found that PE with jejunal biopsies has diagnostic value only in patients with refractory CD but not in those with uncomplicated CD. However PE requires expertise and takes longer than standard esophagogastroduodenoscopy (EGD). Nowadays, it has mostly been replaced by BAE, which enables concise investigation of the small bowel. However, is it

worth digging deeper? BAE makes it possible to evaluate the entire small bowel with biopsy capability. After the introduction of BAE into clinical practice, it has been used to evaluate the small bowel in various diseases, with a high success rate for complete bowel examination^[39]. Unfortunately, there is no study specially addressing the value of BAE in the diagnosis of uncomplicated CD. According to a report by Hadithi *et al.*^[40], who performed double balloon enteroscopy (DBE) in refractory CD, DBE had a significant diagnostic yield and revealed complications such as ulcerative jejunoileitis and lymphoma in 30% of patients. A further important result of the study was that DBE successfully ruled out T cell lymphoma in 25% of patients. Potential risks of BAE limit its use in every patient, which makes it difficult to recommend the procedure to every single CD patient, and it should be reserved for those patients with unequivocal findings or abnormal imaging results. Enteroscopy should be considered in patients with refractory CD and in those with a high clinical or serological suspicion of CD but inconclusive duodenal biopsies. Although this group of patients will always remain small, it is important to bear in mind that enteroscopy can sometimes be of value to diagnose CD^[41]. It should be emphasized that BAE is an effective way for the evaluation of the complications of CD and should be utilized early in the diagnostic algorithm.

Another way of examining the small intestine is CE, which may be a possible substitute for EGD because of its minimal invasiveness, however, its cost and limited availability make it insufficient to replace EGD. CE has an eightfold magnification capacity and therefore is able to assess the small bowel mucosa. For this reason, CE could offer an alternative in patients who are unable or unwilling to undergo endoscopic examination. CE is done without air inflation, with the round dome-shaped edge housing the optical system close to the mucosa. It allows examination of the entire small bowel and facilitates diagnosis of complications^[42]. CE studies have failed to demonstrate any correlation between clinical presentation and the length of involvement. Diagnostic yield of CE increases significantly when a CD patient is under the risk of having a complication or malignancy, such as patients with iron deficiency anemia or refractory disease. In these high probability patients, ulcerations or other positive findings can be revealed in up to half the patients^[43]. CE is not superior to the conventional EGD in the case of new diagnosis of CD patients^[44]. Another point to remember is that CE is a poor modality for examination of the duodenum due to rapid transfer of the capsule in this area. That is why, if there is limited proximal enteropathy, CE may miss the mucosal changes; even Marsh grade 3c changes can be missed. Addition of Fuji Intelligent Color Enhancement - capability or post-processing of the acquired images may aid discrimination of villous atrophy^[45]. When should we use CE for the diagnosis of uncomplicated CD? Patients who have less than four duodenal biopsies should be directed for repeat endoscopy with at least four biopsies and CE should be performed in those patients

who still have normal duodenal histology and are positive for celiac serology and HLA-DQ2 or HLA-DQ8^[46]. Similar reasoning may also apply to BAE with biopsy of the jejunum or deep intestine, and in this case, BAE with biopsy could be superior to CE in terms of biopsy and histological confirmation of the disease. Otherwise, both methods rely on white light visible morphological changes. Therefore, it should be stressed that CE is not a substitute for histological examination, however, CE can detect complications missed by routine EGD^[44]. That is why the use of both BAEs and CE to evaluate the entire small bowel at the time of initial diagnosis does not seem to be justified^[47].

CONCLUSION

Is enteroscopy needed for the diagnosis of the CD? We can answer “yes” to this question, with reserve. Based on these findings, enteroscopy examination for CD should be reserved for patients with positive serology and negative histopathology at initial EGD, and in the search for complications during follow-up. Enteroscopy cannot be recommended at the initial work-up of CD patients. CE may find a place for the diagnosis of complications of CD because of its noninvasiveness and ease of use. The main problem is to diagnose the early forms of the disease by simple examination, for which the current endoscopy methods have failed in terms of detection, because these methods successfully detect atrophy, which is the only visible sign of the disease. We believe that addition of water immersion, even during enteroscopy, is helpful, easy and incurs no cost, and should be performed in every suspected patient to minimize unnecessary biopsies.

REFERENCES

- 1 **Tjon JM**, van Bergen J, Koning F. Celiac disease: how complicated can it get? *Immunogenetics* 2010; **62**: 641-651
- 2 **Schuppan D**, Junker Y, Barisani D. Celiac disease: from pathogenesis to novel therapies. *Gastroenterology* 2009; **137**: 1912-1933
- 3 **Vilppula A**, Kaukinen K, Luostarinen L, Krekelä I, Patrikainen H, Valve R, Mäki M, Collin P. Increasing prevalence and high incidence of celiac disease in elderly people: a population-based study. *BMC Gastroenterol* 2009; **9**: 49
- 4 **Murray JA**, Herlein J, Mitros F, Goeken JA. Serologic testing for celiac disease in the United States: results of a multilaboratory comparison study. *Clin Diagn Lab Immunol* 2000; **7**: 584-587
- 5 **Zintzaras E**, Germenis AE. Performance of antibodies against tissue transglutaminase for the diagnosis of celiac disease: meta-analysis. *Clin Vaccine Immunol* 2006; **13**: 187-192
- 6 **Rampertab SD**, Pooran N, Brar P, Singh P, Green PH. Trends in the presentation of celiac disease. *Am J Med* 2006; **119**: 355.e9-355.14
- 7 **Dandalides SM**, Carey WD, Petras R, Achkar E. Endoscopic small bowel mucosal biopsy: a controlled trial evaluating forceps size and biopsy location in the diagnosis of normal and abnormal mucosal architecture. *Gastrointest Endosc* 1989; **35**: 197-200
- 8 **Oberhuber G**. Histopathology of celiac disease. *Biomed Pharmacother* 2000; **54**: 368-372
- 9 **Cammarota G**, Fedeli P, Gasbarrini A. Emerging technologies in upper gastrointestinal endoscopy and celiac disease. *Nat Clin Pract Gastroenterol Hepatol* 2009; **6**: 47-56
- 10 **Rubio-Tapia A**, Murray JA. Celiac disease. *Curr Opin Gastroenterol* 2010; **26**: 116-122
- 11 **Lohi S**, Mäki M, Montonen J, Knekt P, Pukkala E, Reunanen A, Kaukinen K. Malignancies in cases with screening-identified evidence of coeliac disease: a long-term population-based cohort study. *Gut* 2009; **58**: 643-647
- 12 **Lohi S**, Mäki M, Rissanen H, Knekt P, Reunanen A, Kaukinen K. Prognosis of unrecognized coeliac disease as regards mortality: a population-based cohort study. *Ann Med* 2009; **41**: 508-515
- 13 **Oberhuber G**, Granditsch G, Vogelsang H. The histopathology of coeliac disease: time for a standardized report scheme for pathologists. *Eur J Gastroenterol Hepatol* 1999; **11**: 1185-1194
- 14 **Kurppa K**, Collin P, Viljamaa M, Haimila K, Saavalainen P, Partanen J, Laurila K, Huhtala H, Paasikivi K, Mäki M, Kaukinen K. Diagnosing mild enteropathy celiac disease: a randomized, controlled clinical study. *Gastroenterology* 2009; **136**: 816-823
- 15 **Ravelli A**, Bolognini S, Gambarotti M, Villanacci V. Variability of histologic lesions in relation to biopsy site in gluten-sensitive enteropathy. *Am J Gastroenterol* 2005; **100**: 177-185
- 16 **Bonamico M**, Thanasi E, Mariani P, Nenna R, Luparia RP, Barbera C, Morra I, Lerro P, Guariso G, De Giacomo C, Scotta S, Pontone S, Carpino F, Magliocca FM. Duodenal bulb biopsies in celiac disease: a multicenter study. *J Pediatr Gastroenterol Nutr* 2008; **47**: 618-622
- 17 **Lee SK**, Green PH. Endoscopy in celiac disease. *Curr Opin Gastroenterol* 2005; **21**: 589-594
- 18 **Ensari A**. Gluten-sensitive enteropathy (celiac disease): controversies in diagnosis and classification. *Arch Pathol Lab Med* 2010; **134**: 826-836
- 19 **Dickey W**, Hughes DF. Histology of the terminal ileum in coeliac disease. *Scand J Gastroenterol* 2004; **39**: 665-667
- 20 **Rondonotti E**, Spada C, Cave D, Pennazio M, Riccioni ME, De Vitis I, Schneider D, Sprujevnik T, Villa F, Langelier J, Arrigoni A, Costamagna G, de Franchis R. Video capsule enteroscopy in the diagnosis of celiac disease: a multicenter study. *Am J Gastroenterol* 2007; **102**: 1624-1631
- 21 **Murray JA**, Rubio-Tapia A, Van Dyke CT, Brogan DL, Knipschild MA, Lahr B, Rumalla A, Zinsmeister AR, Gostout CJ. Mucosal atrophy in celiac disease: extent of involvement, correlation with clinical presentation, and response to treatment. *Clin Gastroenterol Hepatol* 2008; **6**: 186-193; quiz 125
- 22 **Thijs WJ**, van Baarlen J, Kleibeuker JH, Kolkman JJ. Duodenal versus jejunal biopsies in suspected celiac disease. *Endoscopy* 2004; **36**: 993-996
- 23 **Evans KE**, Sanders DS. What is the use of biopsy and antibodies in coeliac disease diagnosis? *J Intern Med* 2011; **269**: 572-581
- 24 **Rostom A**, Murray JA, Kagnoff MF. American Gastroenterological Association (AGA) Institute technical review on the diagnosis and management of celiac disease. *Gastroenterology* 2006; **131**: 1981-2002
- 25 **Rostami K**, Kasturi R, Villanacci V, Bassotti G, Zambelli A. Challenges in endoscopy and histological diagnosis of celiac disease. *Endoscopy* 2011; **43**: 375; author reply 376
- 26 **Pais WP**, Duerksen DR, Pettigrew NM, Bernstein CN. How many duodenal biopsy specimens are required to make a diagnosis of celiac disease? *Gastrointest Endosc* 2008; **67**: 1082-1087
- 27 **Schmitz-Moormann P**, Schmidt-Slördahl R, Peter JH, Massarrat S. Morphometric studies of normal and inflamed duodenal mucosa. *Pathol Res Pract* 1980; **167**: 313-321
- 28 **Gonzalez S**, Gupta A, Cheng J, Tennyson C, Lewis SK, Bha-

- gat G, Green PH. Prospective study of the role of duodenal bulb biopsies in the diagnosis of celiac disease. *Gastrointest Endosc* 2010; **72**: 758-765
- 29 **Meijer JW**, Wahab PJ, Mulder CJ. Small intestinal biopsies in celiac disease: duodenal or jejunal? *Virchows Arch* 2003; **442**: 124-128
- 30 **Singh R**, Nind G, Tucker G, Nguyen N, Holloway R, Bate J, Shetti M, George B, Tam W. Narrow-band imaging in the evaluation of villous morphology: a feasibility study assessing a simplified classification and observer agreement. *Endoscopy* 2010; **42**: 889-894
- 31 **Günther U**, Daum S, Heller F, Schumann M, Loddenkemper C, Grünbaum M, Zeitz M, Bojarski C. Diagnostic value of confocal endomicroscopy in celiac disease. *Endoscopy* 2010; **42**: 197-202
- 32 **Cammarota G**, Cazzato A, Genovese O, Pantanella A, Ianiro G, Giorgio V, Montalto M, Vecchio FM, Larocca LM, Gasbarrini G, Fundarò C. Water-immersion technique during standard upper endoscopy may be useful to drive the biopsy sampling of duodenal mucosa in children with celiac disease. *J Pediatr Gastroenterol Nutr* 2009; **49**: 411-416
- 33 **Cammarota G**, Cesaro P, Cazzato A, Cianci R, Fedeli P, Ojetti V, Certo M, Sparano L, Giovannini S, Larocca LM, Vecchio FM, Gasbarrini G. The water immersion technique is easy to learn for routine use during EGD for duodenal villous evaluation: a single-center 2-year experience. *J Clin Gastroenterol* 2009; **43**: 244-248
- 34 **Hassall E**. Not everything is celiac disease. *Gastrointest Endosc* 2010; **72**: 569-571
- 35 **Shah VH**, Rotterdam H, Kotler DP, Fasano A, Green PH. All that scallops is not celiac disease. *Gastrointest Endosc* 2000; **51**: 717-720
- 36 **Höroldt BS**, McAlindon ME, Stephenson TJ, Hadjivassiliou M, Sanders DS. Making the diagnosis of coeliac disease: is there a role for push enteroscopy? *Eur J Gastroenterol Hepatol* 2004; **16**: 1143-1146
- 37 **De Vitis I**, Spada C, Pirozzi PA, Guidi L, Fedeli G, Gasbarini G. Role of enteroscopy in the diagnosis of coeliac disease [Abstract]. *Gastrointest Endosc* 2003; **58**: AB147
- 38 **Cellier C**, Cuillierier E, Patey-Mariaud de Serre N, Marteau P, Verkarre V, Brière J, Brousse N, Barbier JP, Schmitz J, Landi B. Push enteroscopy in celiac sprue and refractory sprue. *Gastrointest Endosc* 1999; **50**: 613-617
- 39 **Neumann H**, Fry LC, Bellutti M, Malfertheiner P, Mönkemüller K. Double-balloon enteroscopy-assisted virtual chromoendoscopy for small-bowel disorders: a case series. *Endoscopy* 2009; **41**: 468-471
- 40 **Hadithi M**, Al-toma A, Oudejans J, van Bodegraven AA, Mulder CJ, Jacobs M. The value of double-balloon enteroscopy in patients with refractory celiac disease. *Am J Gastroenterol* 2007; **102**: 987-996
- 41 **Frenz MB**, Mee AS. Making the diagnosis of coeliac disease: is there a role for push enteroscopy? *Eur J Gastroenterol Hepatol* 2004; **16**: 1127-1129
- 42 **Spada C**, Riccioni ME, Urgesi R, Costamagna G. Capsule endoscopy in celiac disease. *World J Gastroenterol* 2008; **14**: 4146-4151
- 43 **Culliford A**, Daly J, Diamond B, Rubin M, Green PH. The value of wireless capsule endoscopy in patients with complicated celiac disease. *Gastrointest Endosc* 2005; **62**: 55-61
- 44 **Maiden L**, Elliott T, McLaughlin SD, Ciclitira P. A blinded pilot comparison of capsule endoscopy and small bowel histology in unresponsive celiac disease. *Dig Dis Sci* 2009; **54**: 1280-1283
- 45 **Ciaccio EJ**, Tennyson CA, Lewis SK, Krishnareddy S, Bhagat G, Green PH. Distinguishing patients with celiac disease by quantitative analysis of videocapsule endoscopy images. *Comput Methods Programs Biomed* 2010; **100**: 39-48
- 46 **Lidums I**, Cummins AG, Teo E. The role of capsule endoscopy in suspected celiac disease patients with positive celiac serology. *Dig Dis Sci* 2011; **56**: 499-505
- 47 **Rondonotti E**, Villa F, Saladino V, de Franchis R. Enteroscopy in the diagnosis and management of celiac disease. *Gastrointest Endosc Clin N Am* 2009; **19**: 445-460

S- Editor Gou SX L- Editor Kerr C E- Editor Zheng XM

Diffusion-weighted imaging of biliopancreatic disorders: Correlation with conventional magnetic resonance imaging

Nam Kyung Lee, Suk Kim, Gwang Ha Kim, Dong Uk Kim, Hyung Il Seo, Tae Un Kim, Dae Hwan Kang, Ho Jin Jang

Nam Kyung Lee, Suk Kim, Department of Radiology, Biomedical Research Institute, Pusan National University Hospital, School of Medicine, Pusan National University, Busan 602-739, South Korea

Gwang Ha Kim, Dong Uk Kim, Department of Internal Medicine, Biomedical Research Institute, Pusan National University Hospital, School of Medicine, Pusan National University, Busan 602-739, South Korea

Hyung Il Seo, Department of Surgery, Biomedical Research Institute, Pusan National University Hospital, School of Medicine, Pusan National University, Busan 602-739, South Korea

Tae Un Kim, Department of Radiology, Yangsan Pusan National University Hospital, School of Medicine, Pusan National University, Yangsan 626-770, South Korea

Dae Hwan Kang, Department of Internal Medicine, Yangsan Pusan National University Hospital, School of Medicine, Pusan National University, Yangsan 626-770, South Korea

Ho Jin Jang, Department of Obstetrics and Gynecology, Armed Forces Seoul Hospital, Seoul 110-200, South Korea

Author contributions: Kim S contributed conception and design; Lee NK, Kim GH, Kim DU, Seo HI, Kim TU, Kang DH and Jang HJ acquired and interpreted data; Lee NK and Kim S wrote the article and revised it critically for important intellectual content; Kim S finally approved the revision to be published.

Supported by Clinical research grant from Pusan National University Hospital

Correspondence to: Suk Kim, MD, Department of Radiology, Biomedical Research Institute, Pusan National University Hospital, School of Medicine, Pusan National University, No.1-10, Ami-Dong, Seo-Gu, Busan 602-739, South Korea. kimsuk@medimail.co.kr

Telephone: +82-51-2407354 Fax: +82-51-2447534

Received: December 9, 2011 Revised: April 26, 2012

Accepted: May 6, 2012

Published online: August 21, 2012

Abstract

Diffusion-weighted magnetic resonance imaging (DWI)

is a well established method for the evaluation of intracranial diseases, such as acute stroke. DWI for extracranial application is more difficult due to physiological motion artifacts and the heterogeneous composition of the organs. However, thanks to the newer technical development of DWI, DWI has become increasingly used over the past few years in extracranial organs including the abdomen and pelvis. Most previous studies of DWI have been limited to the evaluation of diffuse parenchymal abnormalities and focal lesions in abdominal organs, whereas there are few studies about DWI for the evaluation of the biliopancreatic tract. Although further studies are needed to determine its performance in evaluating bile duct, gallbladder and pancreas diseases, DWI has potential in the assessment of the functional information on the biliopancreatic tract concerning the status of tissue cellularity, because increased cellularity is associated with impeded diffusion, as indicated by a reduction in the apparent diffusion coefficient. The detection of malignant lesions and their differentiation from benign tumor-like lesions in the biliopancreatic tract could be improved using DWI in conjunction with findings obtained with conventional magnetic resonance cholangiopancreatography. Additionally, DWI can be useful for the assessment of the biliopancreatic tract in patients with renal impairment because contrast-enhanced computed tomography or magnetic resonance scans should be avoided in these patients.

© 2012 Baishideng. All rights reserved.

Key words: Magnetic resonance imaging; Diffusion-weighted imaging; Biliary tract; Gallbladder; Pancreas

Peer reviewer: Xiao-Peng Zhang, Professor, Department of Radiology, Beijing Cancer Hospital and Institute, Peking University School of Oncology, No.52 Haidian District, Beijing 100142, China

Lee NK, Kim S, Kim GH, Kim DU, Seo HI, Kim TU, Kang DH, Jang HJ. Diffusion-weighted imaging of biliopancreatic disorders: Correlation with conventional magnetic resonance imaging. *World J Gastroenterol* 2012; 18(31): 4102-4117 Available from: URL: <http://www.wjgnet.com/1007-9327/full/v18/i31/4102.htm> DOI: <http://dx.doi.org/10.3748/wjg.v18.i31.4102>

INTRODUCTION

Diffusion-weighted magnetic resonance imaging (DWI) provides information on the random (Brownian) motion of water molecules in the body. It is well established that DWI is a useful tool for the evaluation of intracranial diseases, such as acute stroke. The development of phased-array surface coils, high-gradient amplitudes, and rapid imaging techniques such as echo planar imaging (EPI) and parallel imaging have been instrumental in allowing the extracranial application of DWI^[1-3].

The degree of restriction to water diffusion in biological tissues is directly proportional to tissue cellularity and the integrity of cell membranes. In tissues with a high cell density and associated with many intact cell membranes, such as malignant tumors, the motion of water molecules is more restricted than in less cellular tissue. The degree of water motion is found to be proportional to the degree of signal attenuation in DWI. Thus, more cellular solid tumors show relatively higher signal intensities and exhibit lower apparent diffusion coefficient (ADC, expressed in mm²/s) values on DWI using two or more b values than do less cellular tissues. Recently, this utility of DWI has been expanded to examination of abdominal organs; the ADC values of malignant masses are significantly lower than those of benign masses in the liver, pancreas, kidney, and prostate, although there is a small degree of overlap^[4-9]. Most previous studies on DWI have been limited to the evaluation of diffuse parenchymal abnormalities and focal lesions in abdominal organs, whereas there are few studies about DWI for the evaluation of the biliopancreatic tract^[10].

To date, contrast-enhanced magnetic resonance imaging (MRI) combined with magnetic resonance cholangiopancreatography (MRCP) has been found to be accurate for diagnosis of biliopancreatic diseases. The role of DWI for the evaluation of biliopancreatic diseases is not yet well established. However, because DWI yields qualitative and quantitative information reflecting cell membrane integrity and tissue cellularity, DWI can be used to differentiate normal and abnormal structures of tissues better, and thus may help in the characterization of various abnormalities in the biliopancreatic tract when added to conventional MRI.

In this article, we briefly review the basic concepts for the biological basis of DWI and its technical considerations. Additionally, we illustrate clinical applications of DWI for the following: evaluation of the biliopancreatic tract, including stone-related complications such as

acute cholangitis, hepatic abscesses, and acute gallstone pancreatitis; characterization and diagnosis of gallbladder lesions, including cholecystitis, gallbladder empyema, and gallbladder carcinoma; characterization of intrahepatic biliary lesions and diagnosis of malignant lesions in the intrahepatic bile ducts; and characterization of extrahepatic biliary lesions and diagnosis of malignant lesions in the extrahepatic bile ducts, including extrahepatic cholangiocarcinoma, pancreatic carcinoma, and focal pancreatitis. We also describe pitfalls of DWI misinterpretation.

BASIC CONCEPTS

In biological tissue, the diffusion of water molecules is impeded or restricted by natural barriers, such as cell membranes, large protein molecules, and tissue cellularity. Pathological conditions, such as tumors, cytotoxic edema, abscesses, and fibrosis, in which the physical nature of the intracellular and extracellular spaces changes, result in increased restriction of the diffusion of water molecules. In tissues of low cellularity or where the cellular membranes have been disrupted, the diffusion of water molecules is relatively free or less restricted (Figure 1)^[1-3,8,11].

DWI is typically obtained using an ultrafast T2-weighted single-shot spin-echo EPI sequence by applying a symmetric pair diffusion-sensitizing gradient, known as the Stejskal-Tanner sequence. It provides information on the random (Brownian) motion of water molecules in tissues between the first dephasing (diffusion-sensitizing) gradient and the second rephasing gradient on either side of the 180° refocusing pulse. Static molecules acquire phase information from the first diffusion-sensitizing gradient, but information will be cancelled out by the second gradient. As a result, signal intensity is preserved, with the exception of T2 decay. In contrast, less restricted water molecules move a considerable distance between the first dephasing (diffusion-sensitizing) and second rephasing gradients. The moving water molecules are not entirely rephased, resulting in reduction of the overall T2 signal intensity (Figure 2)^[1-3].

The sensitivity of a DWI sequence to water diffusion can be altered by changing the parameter known as the b value, which represents the diffusion factor (measured in s/mm²) and the strength of the diffusion gradients. DWI is obtained with at least two different b values. DWI using lower b values (50-100 s/mm²) is sensitive only to fast motion of water molecules. On DWI using lower b values, water molecules in vessels are depicted as dark blood flow (black-blood images). DWI using higher b values (> 500 s/mm²) is sensitive to both fast and slow motion of water molecules. Water movements in highly cellular tissue are restricted and retain their signals even at higher b values. The images obtained at different b values allow the quantification of the ADC of tissues, which is usually displayed as a parametric (ADC) map. The mean or median ADC value can be measured by drawing regions of interest (ROIs) on the ADC map. Tissues with restricted

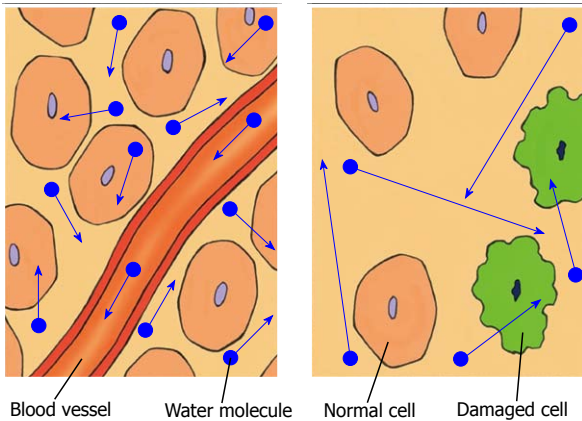


Figure 1 Diffusion of water molecules. Highly cellular tissues with intact cell membrane restrict the movement of water molecules within intravascular, intracellular, and extracellular space. In contrast, relatively less cellular tissues or damaged cells with defective cellular membrane increase extracellular space, which allow greater water molecule movement.

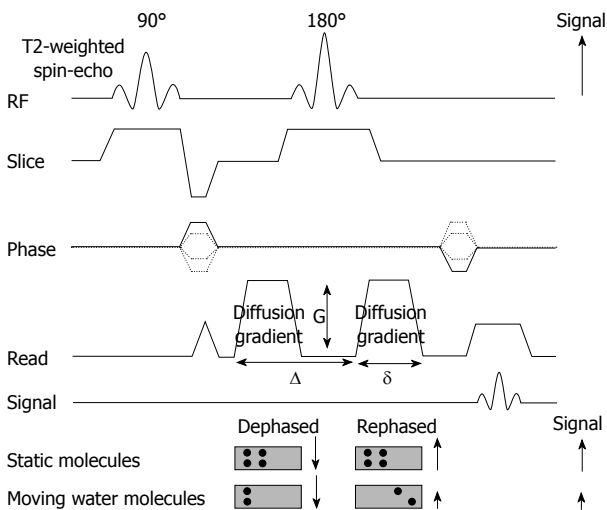


Figure 2 Diagram of diffusion-weighted sequence. DWI is based on T2-weighted spin-echo sequencing with application of two equal gradient pulses (a dephasing gradient and a rephasing gradient) on each side of the 180° radiofrequency pulse. Static molecules are dephased by the first diffusion gradient and rephased perfectly by the second diffusion gradient; therefore measured high signal intensity is preserved. In contrast, moving molecules undergo dephasing but are not entirely rephased by the second gradient because of their motion, thereby resulting in signal loss. DWI: Diffusion-weighted magnetic resonance imaging; RF: Radiofrequency.

diffusion and high cellular density show low ADC values, whereas tissues with less cellular density show higher ADC values^[1,2].

TECHNICAL CONSIDERATIONS

The signal intensity on DWI is dependent on diffusion of water molecules and T2 relaxation time. Thus, an area with a very long T2 relaxation time (e.g., bile in the biliary tract) maintains high signals on high-b-value DWI, and can be mistaken for restricted diffusion. This phenomenon is known as the “T2 shine-through” effect (Figure 3). The T2 shine-through effect inevitably

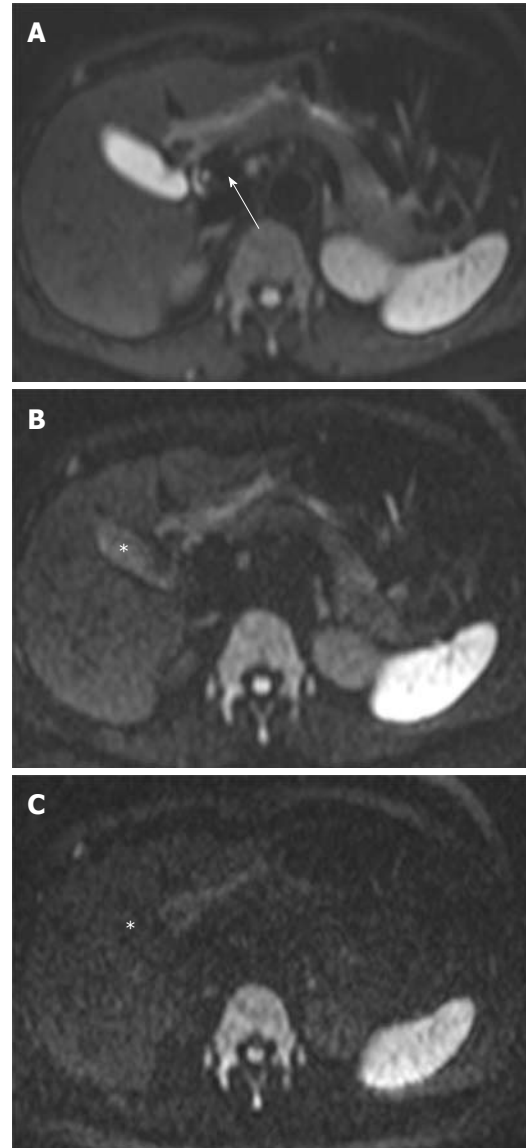


Figure 3 DWI of the normal liver, pancreas, and biliary tract. A: DWI at $b = 50 \text{ s/mm}^2$ shows that the liver is hypointense compared to the kidney and spleen, and isointense compared to the pancreas; there is a signal void within the portal vein (arrow). DWI using low b values results in decreasing signals of fast motion of water molecules, such as that occurring within vessels. Such images are referred to as black-blood images; B: DWI at $b = 500 \text{ s/mm}^2$ shows that the signal intensity of bile is decreased (asterisk) and the wall of the gallbladder is not identified. The liver is isointense compared to the pancreas; C: DWI at $b = 1000 \text{ s/mm}^2$ shows a significant reduction in the signal intensity of bile in the gallbladder (asterisk). DWI: Diffusion-weighted magnetic resonance imaging.

confounds DWI images, and the ADC map eliminates this effect. In clinical practice, higher-b-value DWI (usually $800\text{-}1000 \text{ s/mm}^2$) results in a reduction of the signal from moving protons in the bile ducts, cyst, vessels, and fluid in the bowel. This leads to a reduction in the T2 shine-through effect, resulting in increased contrast between lesions and visceral organs such as the liver or gallbladder. However, the tradeoffs of higher-b-value DWI are a lower signal-to-noise ratio, the possibility of ADC error, and increased image distortion due to the longer echo time required^[1,2,8,12].

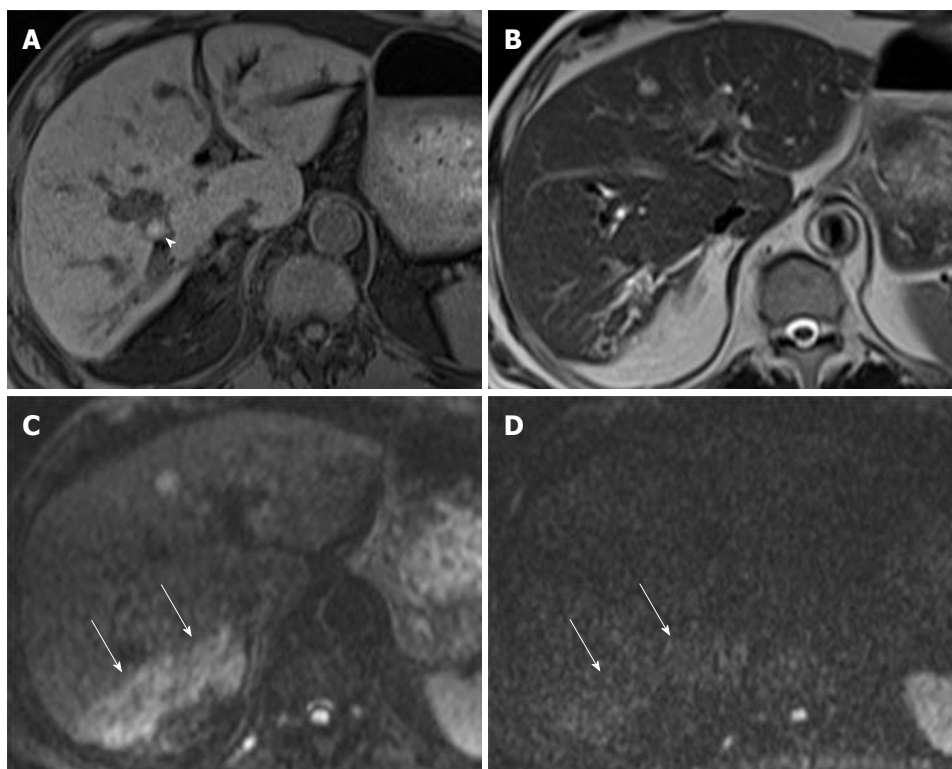


Figure 4 Parenchymal changes in acute cholangitis in a 76-year-old man. A: Axial fat-saturated T1-weighted image shows a hyperintense stone (arrowhead) with upstream bile duct dilation; B: Axial T2-weighted rapid acquisition relaxation enhancement image shows mild bile duct dilatation in the right lobe of the liver, but no definite area of increased parenchymal signal intensity; C: DWI at $b = 50 \text{ s/mm}^2$ shows wedge-shaped areas of increased parenchymal signal intensity in segment 6 (arrows). Parenchymal changes are more conspicuous on black-blood images than on routine T2-weighted images; D: DWI at $b = 800 \text{ s/mm}^2$ shows that most areas of increased parenchymal signal intensity usually return to isointensity (arrows). Such a finding can be a clue for differentiating parenchymal changes due to cholangitis from abscesses. DWI: Diffusion-weighted magnetic resonance imaging.

DWI performed during free breathing can lead to substantial signal loss. Thus, breath-hold or respiration-triggered DWI would be necessary to prevent signal loss as a result of respiratory movement. Breath-hold DWI is generally used because of its short acquisition time. However, only a limited number of image sections of relatively large section thicknesses can be acquired. Moreover, because this technique is usually performed using a single-shot EPI technique, the signal-to-noise ratio and lesion conspicuity is reduced. In contrast, respiration-triggered DWI provides higher signal-to-noise and contrast-to-noise ratios, although its acquisition time is longer than that of breath-hold DWI^[13,14].

Fat suppression is necessary to increase the dynamic range of DWI and reduce the chemical shift artifacts that are prevalent in EPI. Inversion recovery sequence is preferred when performing DWI over a large area of the body, because it is likely to produce more uniform fat suppression^[13].

Unlike brain imaging where b values are well established, b values in other parts of the body vary widely between investigators. Thus, b values for body imaging require optimization. Biexponential signal intensity in the abdominal organs has been shown in DWI with increasing b values; the initial rapid decrease in signal intensity is noted with a small increase in b value, and is followed by a more gradual decrease of signal intensity

beyond approximately $b = 100 \text{ s/mm}^2$. ADC measurement using at least three b values adequately reflects this biexponential behavior, compared with the use of only two b values. Low b values are sensitive to capillary perfusion, which can increase the amount of perfusion contamination in ADC measurement. In contrast, high b values enable less perfusion contamination in the ADC measurement and reflect tissue sensitivity^[13].

In our institution, MRI is performed with a superconductive 1.5-T imaging unit (Magnetom Avanto; Siemens Medical Solutions, Erlangen, Germany), and a 3.0-T imaging unit (Magnetom Trio; Siemens Medical Solutions) by using a phased-array multicoil. For DWI, respiration-triggered, fat-suppressed, single-shot EPI is performed in the transverse plane with a parallel imaging (generalized autocalibrating partially parallel acquisition) acceleration factor of two. DWI is performed prior to the intravenous injection of gadolinium chelates. Pre-contrast DWI is usually preferred because gadolinium chelates may affect the ADC values by decreasing the signal intensity on these T2-sequences due to shortening of the T1 and T2 relaxation time. However, it has been reported that DWI after administration of gadolinium chelates does not appear to affect ADC values significantly^[15]. The imaging parameters of DWI in the 1.5-T unit are as follows: 5000/103 (repetition time ms/echo time ms), 90° flip angle, 4-mm section thickness, 1-mm

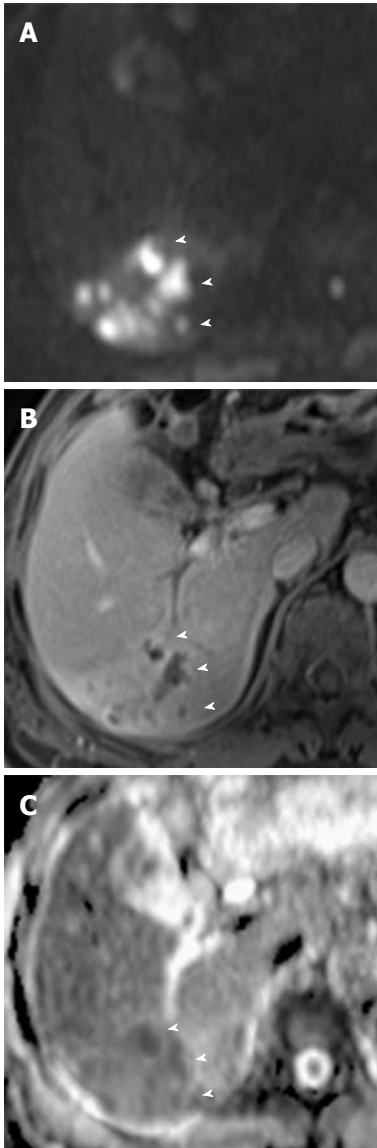


Figure 5 Liver abscesses complicating acute cholangitis in a 79-year-old man. A: DWI at $b = 1000 \text{ s/mm}^2$ shows multiple liver abscesses with high signal intensity (arrowheads); B: Multiple abscesses with peripheral rim enhancement (arrowheads) are less conspicuous on contrast-enhanced fat-saturated T1-weighted images (B) than on DWI (A); C: On an ADC map, multiple abscesses appear as low signal intensity (arrowheads) due to restriction of diffusion. DWI: Diffusion-weighted magnetic resonance imaging; ADC: Apparent diffusion coefficient.

intersection gap, 964-Hz/pixel bandwidth, 20 slices, 230-mm field of view, 192×192 matrix, and 85-s acquisition time. Imaging parameters in the 3.0-T unit are as follows: 3900/92 (repetition time ms/echo time ms), 90° flip angle, 5-mm section thickness, 0.5-mm intersection gap, 1184-Hz/pixel bandwidth, 24 slices, 230-mm field of view, 192×192 matrix, and 85-s acquisition time. Each acquisition is obtained using five different b values including low values (0 s/mm^2 and 50 s/mm^2) and high values (500 s/mm^2 , 800 s/mm^2 and 1000 s/mm^2)^[16,17]. The ADC map is generated automatically with the built-in software of the MRI unit.

The signal intensity of the normal liver on DWI is

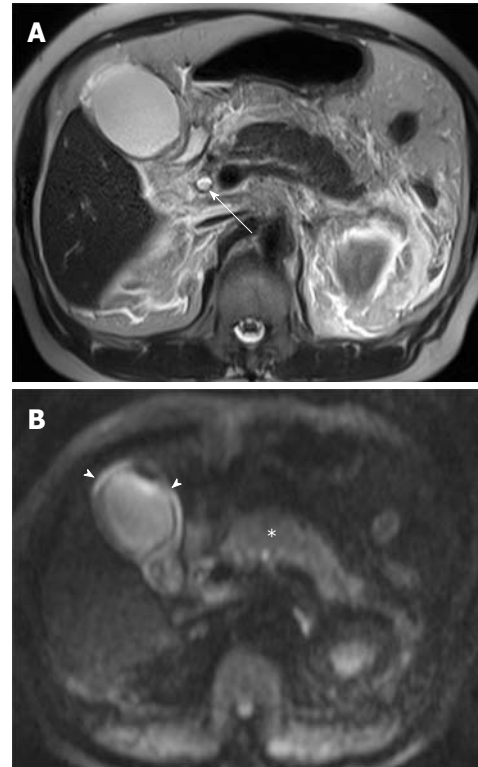


Figure 6 Acute pancreatitis and cholecystitis due to a bile duct stone in a 72-year-old woman. A: Axial T2-weighted rapid acquisition relaxation enhancement image demonstrates stones in the distal common bile duct (arrow), a distended gallbladder with pericholecystic fluid, and pancreatic edema with peripancreatic fluid, findings suggestive of cholecystitis and pancreatitis; B: DWI at $b = 800 \text{ s/mm}^2$ shows that the pancreas is slightly hyperintense (asterisk) compared to the liver, and the presence of a peripancreatic fluid collection; findings indicative of pancreatitis. A distended gallbladder with diffuse and symmetric high signal intensity in the wall (arrowheads), due to the restriction of water diffusion in the inflamed gallbladder wall, is also seen. DWI: Diffusion-weighted magnetic resonance imaging.

the same as on T2-weighted images. The liver is hypointense compared to the kidney and spleen, and isointense or hypointense compared to the pancreas (Figure 3). The reported ADC value of the normal liver ranges from $1.02 \times 10^{-3} \text{ mm}^2/\text{s}$ to $1.83 \times 10^{-3} \text{ mm}^2/\text{s}$ ^[4,18-20]. Yoshikawa *et al.*^[18] have reported that the mean ADC value of the pancreas ranges from $1.02 \times 10^{-3} \text{ mm}^2/\text{s}$ to $1.94 \times 10^{-3} \text{ mm}^2/\text{s}$ using DWI with two values (0 s/mm^2 and 600 s/mm^2). On higher DWI (usually $800\text{-}1000 \text{ s/mm}^2$), the walls of the bile duct and gallbladder are not identified (Figure 3).

CLINICAL APPLICATIONS OF DWI FOR EVALUATION OF THE BILIOPANCREATIC TRACT

DWI for evaluation of gallstone-related complications

Acute cholangitis is the most frequently encountered benign inflammatory lesion and is usually related to bile duct stones. Acute cholangitis usually manifests as a dilated bile duct, due to bile duct obstruction, mild and diffuse bile duct wall thickening, and hepatic paren-

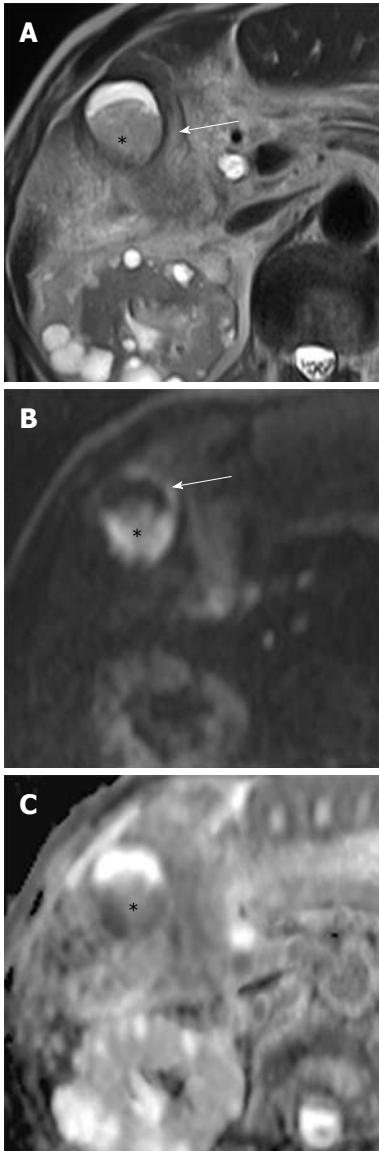


Figure 7 Gallbladder empyema in a 92-year-old man. A: Axial T2-weighted rapid acquisition relaxation enhancement image demonstrates a fluid-fluid level with low signal intensity in the dependent portion (asterisk) of an inflamed gallbladder (arrow); B: DWI at $b = 1000 \text{ s/mm}^2$ shows purulent bile with high signal intensity (asterisk), and diffuse, symmetric high signal intensity in the wall of the gallbladder (arrow); C: On an ADC map, pus in the dependent portion of the gallbladder appears with low signal intensity (asterisk) due to restriction of diffusion. Empyema was confirmed by aspiration of pus during percutaneous cholecystostomy. DWI: Diffusion-weighted magnetic resonance imaging; ADC: Apparent diffusion coefficient.

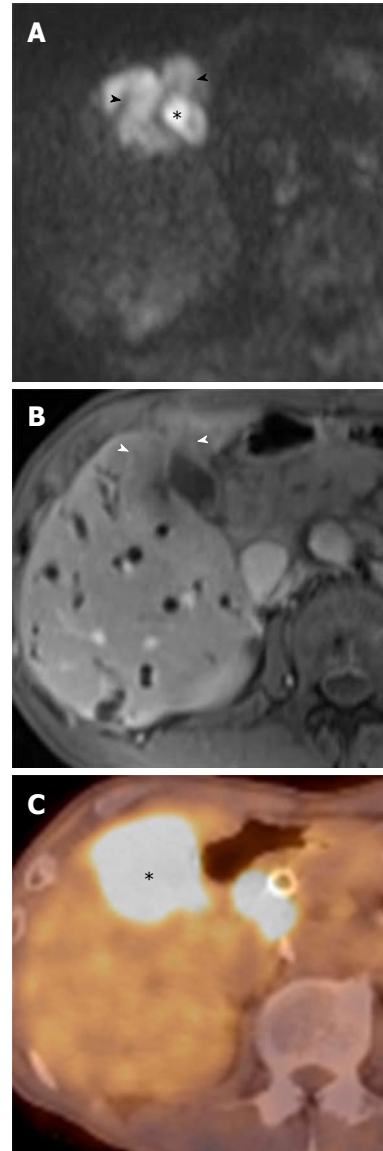


Figure 8 Gallbladder carcinoma in a 70-year-old man. A: DWI at $b = 1000 \text{ s/mm}^2$ shows high signal intensity in the mass occupying the entire gallbladder (asterisk), which invades the hepatic parenchyma adjacent to the gallbladder (arrowheads); B: Gallbladder carcinoma with direct liver invasion (arrowheads) is less conspicuous on contrast-enhanced, fat-saturated T1-weighted images than on DWI; C: Fused positron emission tomography-CT image confirms intense hypermetabolism (asterisk) in the gallbladder carcinoma with direct liver invasion adjacent to the gallbladder. DWI: Diffusion-weighted magnetic resonance imaging; CT: Computed tomography.

chymal changes on MRI. Hepatic parenchymal changes appear as patchy or wedge-shaped areas of increased parenchymal signal intensity on T2-weighted images and transient inhomogeneous parenchymal enhancement in arterial dominant phase imaging^[21,22].

In a recent study, DWI using low b values ($< 100 \text{ s/mm}^2$), giving black-blood images, detected focal hepatic lesions more clearly than routine turbo spin-echo T2-weighted images, and can potentially replace the routine turbo spin-echo T2-weighted images for lesion detection^[23]. In our experience, the increased parenchymal signal inten-

sity is more conspicuous on black-blood images than on routine T2-weighted images in patients with acute cholangitis. On DWI using high b values, areas of increased parenchymal signal intensity usually return to signal isointensity, and infrequently remain at high signal intensity (Figure 4). This may suggest the differentiation of parenchymal changes due to cholangitis from abscesses, which remain at very high signal intensity on DWI using high b values. The causes for signal changes on DWI in the setting of acute inflammation have not been studied extensively. On DWI using low b values, signal changes in cholangitis are influenced by both perfusion and dif-

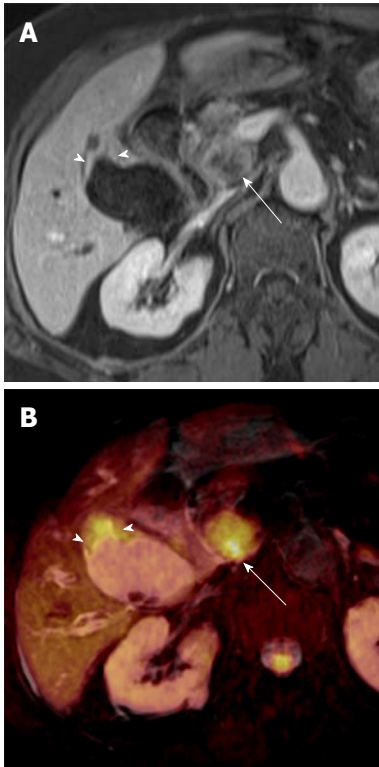


Figure 9 Gallbladder carcinoma (focal wall-thickening type) in a 77-year-old woman. A: Axial contrast-enhanced, fat-saturated, T1-weighted image shows focal wall thickening (arrowheads) in the gallbladder with a metastatic lymph node in the portocaval space (arrow); B: Fusion image of T2-weighted image and DWI at $b = 800 \text{ s/mm}^2$ shows focal, asymmetric high signal intensity in the fundal portion of the gallbladder (arrowheads) with a hyperintense metastatic lymph node in the portocaval space (arrow). DWI: Diffusion-weighted magnetic resonance imaging.

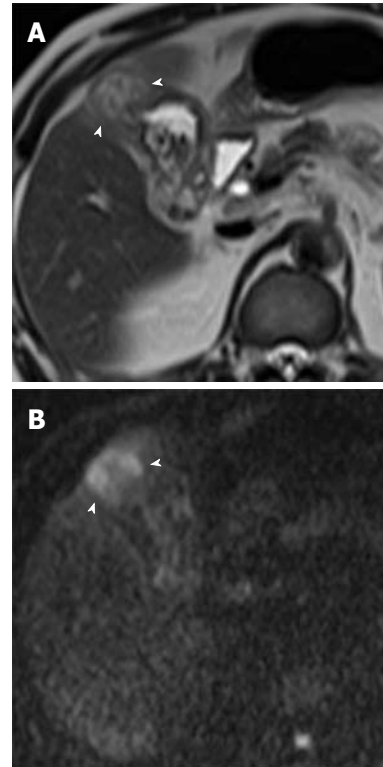


Figure 10 Xanthogranulomatous cholecystitis in a 55-year-old man. A: Axial T2-weighted rapid acquisition relaxation enhancement image shows focal wall thickening with a fundal mass (arrowheads). There is focal high signal intensity within the thickened wall of the gallbladder; a finding that is consistent with an intramural collection; B: DWI at $b = 800 \text{ s/mm}^2$ shows focal high signal intensity in the fundal portion of the gallbladder (arrowheads). Xanthogranulomatous cholecystitis was confirmed by laparoscopic cholecystectomy. DWI: Diffusion-weighted magnetic resonance imaging.

fusion; perfusion effects may be attributed to vasodilatation involving both arterioles and capillary beds, leading to increase blood flow, and diffusion effects may be explained by increases in the size and numbers of inflammatory cells, leading to restriction of water molecules. However, when going to higher b values, the perfusion effect is decreased, leading to decreased signal intensity on DWI. Increased parenchymal signal intensity on DWI may be reversible after treatment, although further studies are needed to confirm this.

Hepatic abscesses are defined as intrahepatic single or multiple collections of pus within the liver. They result from infectious cholangitis and are usually seen in patients with suppurative cholangitis. Pyogenic abscesses have variable signal intensities on T1- and T2-weighted images. However, most lesions appear hypointense on T1-weighted images and hyperintense on T2-weighted images. Peripheral rim enhancement and transient hepatic intensity differences associated with abscesses can be seen after administration of gadolinium. Abscesses can be a life-threatening emergency if not recognized and treated promptly^[24].

DWI is helpful in the early detection of abscesses and their differentiation from cystic or necrotic tumors. On DWI using high b values, abscesses appear hyperin-

tense with low ADC values (Figure 5). This appearance is explained by the dense viscous content of the abscess and the presence of cellular infiltrates within the abscess. In comparison, cystic or necrotic tumors have a greater degree of signal attenuation on higher-b-value DWI and return higher ADC values^[25].

In a recent study, there was no difference in the ability to detect acute pancreatitis between DWI and computed tomography (CT)^[26]. However, DWI can be useful to detect gallstone pancreatitis more clearly than can nonenhanced CT in the setting of contrast contraindications. Acute pancreatitis has restricted diffusion because of acute inflammation, and thus may appear as hyperintense on high-b-value DWI (Figure 6). Peripancreatic fluid usually has no restricted diffusion on high-b-value DWI, but infected fluid may have restricted diffusion. Signal changes in pancreatitis on DWI may be also reversible after treatment.

DWI for characterization and diagnosis of gallbladder lesions

Cholecystitis: Cholecystitis is defined as inflammation of the gallbladder and is usually related to the presence of gallstones. In patients clinically suspected to have acute cholecystitis, ultrasonography (US) is usually favored

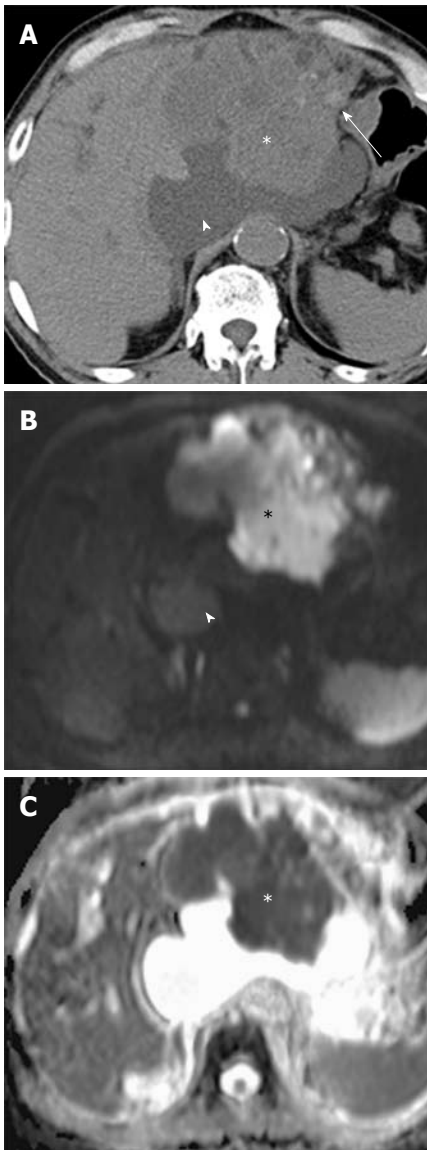


Figure 11 Intrahepatic cholangiocarcinoma (mass-forming type) in a 71-year-old man. A: Nonenhanced CT image shows intrahepatic cholangiocarcinoma in the left lobe of the liver (asterisk), stones in the dilated left bile ducts (arrow), and a fluid collection in the lesser sac (arrowhead); B: DWI at $b = 1000 \text{ s/mm}^2$ shows intrahepatic cholangiocarcinoma with high signal intensity (asterisk). Note a fluid collection (arrowhead) in the lesser sac, which appears as significant attenuation of the signal intensity reduction at a high b value; C: On the ADC map, cholangiocarcinoma appears as low signal intensity (asterisk) due to restriction of diffusion. DWI: Diffusion-weighted magnetic resonance imaging; CT: Computed tomography; ADC: Apparent diffusion coefficient.

as the initial imaging technique. CT and MRI usually provide morphological information similar to that provided by US, and can be performed initially if the clinical presentation is atypical. Increased wall enhancement of the gallbladder and increased pericholecystic hepatic parenchymal enhancement are frequent and specific CT and MRI findings of acute cholecystitis. In acute cholecystitis, the wall of the distended gallbladder is typically thickened due to inflammatory edema, inflammatory exudates, and hemorrhage^[21]. DWI can provide additional important information in cholecystitis when

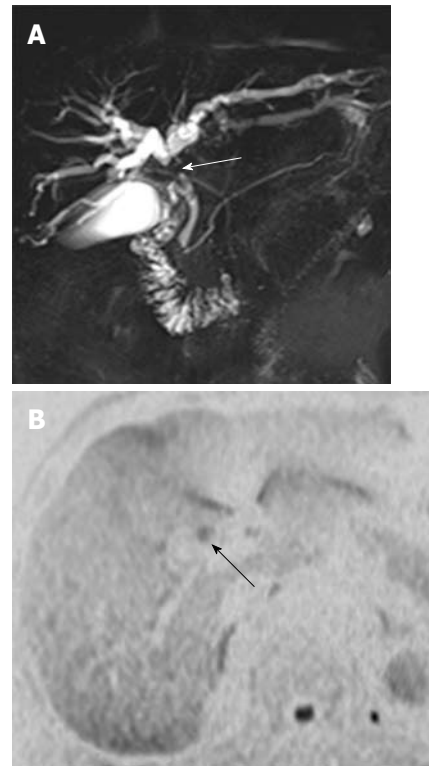


Figure 12 Cholangiocarcinoma (periductal-infiltrating type) in a 70-year-old man. A: Coronal image from thick-slab, single-shot MRCP shows marked dilatation of the intrahepatic ducts and abrupt narrowing at the confluence of the hepatic duct (arrow); B: DWI at $b = 800 \text{ s/mm}^2$ with inverted black-and-white image contrast clearly depicts the mass (arrow) at the confluence of the hepatic duct. DWI: Diffusion-weighted magnetic resonance imaging; MRCP: Magnetic resonance cholangiopancreatography.

added to conventional MRI or MRCP. On DWI using high b values, diffuse and symmetric hyperintensity in the wall of the gallbladder is seen in acute cholecystitis, because of restricted diffusion in the inflamed gallbladder wall (Figure 6). However, restricted diffusion in the gallbladder wall can be also seen in malignant lesions of the gallbladder.

Pus in the gallbladder (empyema) occurs in approximately 2%-3% of patients with acute cholecystitis. Empyema carries a high risk of sepsis and perforation. Thus, urgent drainage or surgical resection with systemic antibiotic coverage is required as soon as the diagnosis is suspected. A diagnosis of empyema may be suggested by the identification of pus as a fluid-fluid level in the dependent portion of the gallbladder on T2-weighted images. However, a fluid-fluid level of the bile in the gallbladder is not specific for empyema; this can be seen in other conditions, such as concentrated bile, sludge, or hemobilia^[21]. It has been reported that DWI is a reliable imaging technique for differentiating pyonephrosis from hydronephrosis. The pus in pyonephrosis has high viscosity and cellularity, thus leading to impeded diffusion and a low ADC value^[27]. DWI findings of gallbladder empyema on DWI may be similar to those of pyonephrosis (Figure 7). Thus, DWI may be helpful

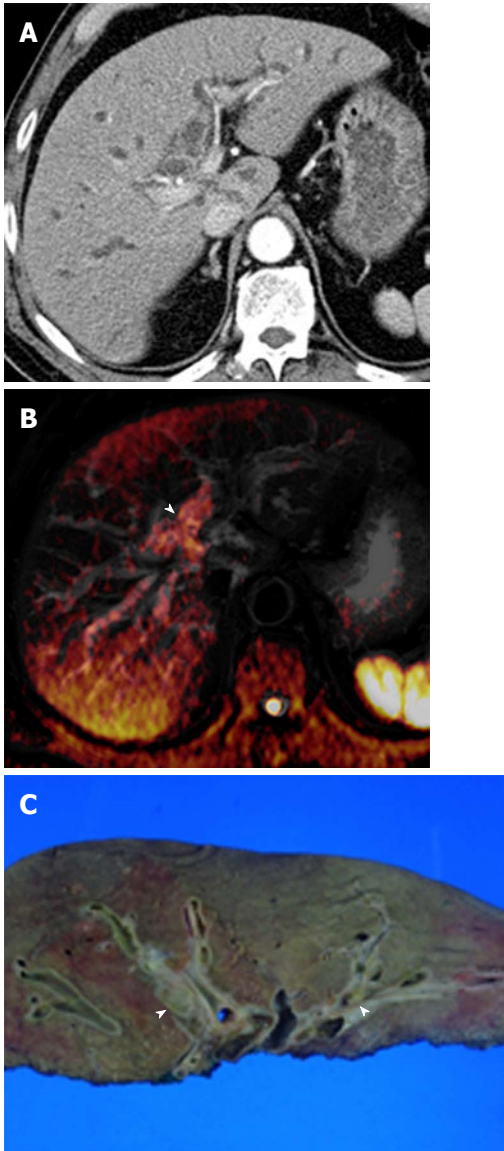


Figure 13 Hilar cholangiocarcinoma (intraductal-growing type) in a 67-year-old man. A: Contrast-enhanced CT shows mild intrahepatic duct dilatation. However, intraductal masses are not clearly depicted on CT; B: Fusion image of T2-weighted and diffusion-weighted images at $b = 800 \text{ s/mm}^2$ shows high signal intensity (arrowhead) at the first branch of the intrahepatic duct; C: Photograph of the gross specimen shows intraductal growing masses (arrowheads) in the bile duct. Histological analysis revealed biliary intraepithelial neoplasia with high grade dysplasia. CT: Computed tomography.

in differentiating pus from concentrated bile, sludge, or hemobilia in the gallbladder.

Gallbladder carcinoma: Imaging findings of focal or diffuse wall thickening or a mass replacing the gallbladder mimics the appearance of acute cholecystitis. DWI can be helpful in the diagnosis of gallbladder carcinoma, the detection of liver and lymph node metastasis, and differentiation from inflammatory conditions of the gallbladder. A hyperintense mass occupying the entire gallbladder lumen or focal and asymmetric high signal intensity in or around the gallbladder wall is more common in malignant lesions of the gallbladder (Figures 8 and 9)^[28]. In contrast, diffuse and smooth high signal intensity in

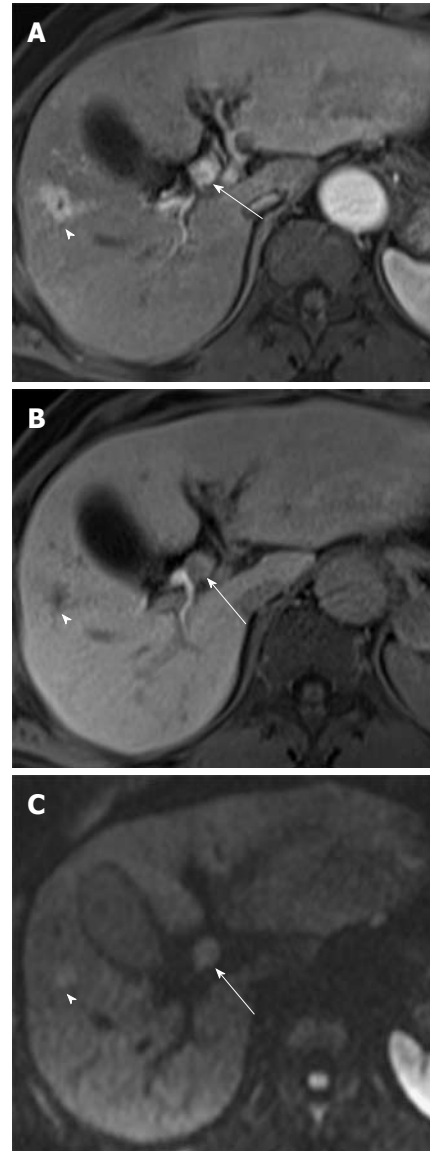


Figure 14 Hepatocellular carcinoma with tumor thrombus in bile duct in a 62-year-old man. A: Gadoteric acid-enhanced T1-weighted image obtained during the arterial phase shows a hypervascular HCC in the right lobe of the liver (arrowhead) and an intraluminal enhancing mass (arrow) in the common hepatic duct; B: On gadoteric acid-enhanced T1-weighted image obtained 20 min after injection, a small HCC (arrowhead) is hypointense relative to the surrounding liver. Contrast material filling the left intrahepatic duct is delayed owing to a partial bile duct obstruction caused by tumor thrombus in the bile duct (arrow); C: DWI at $b = 800 \text{ s/mm}^2$ shows a hyperintense small HCC (arrowhead) and tumor thrombus in the bile duct (arrow). HCC: Hepatocellular carcinoma.

the wall of the gallbladder due to acute inflammation is more common in cholecystitis on DWI using high b values. In our experience, however, focal and irregular high signal intensities in the gallbladder wall on DWI are also seen in xanthogranulomatous cholecystitis and papillary adenomatous polyps (Figure 10). Thus, differentiating gallbladder carcinoma from some adenomatous polyps or xanthogranulomatous cholecystitis may be difficult, even with DWI. Additionally, the presence of associated findings on DWI, such as direct invasion of the liver or adjacent structures, hematogenous liver metastasis, and nodal

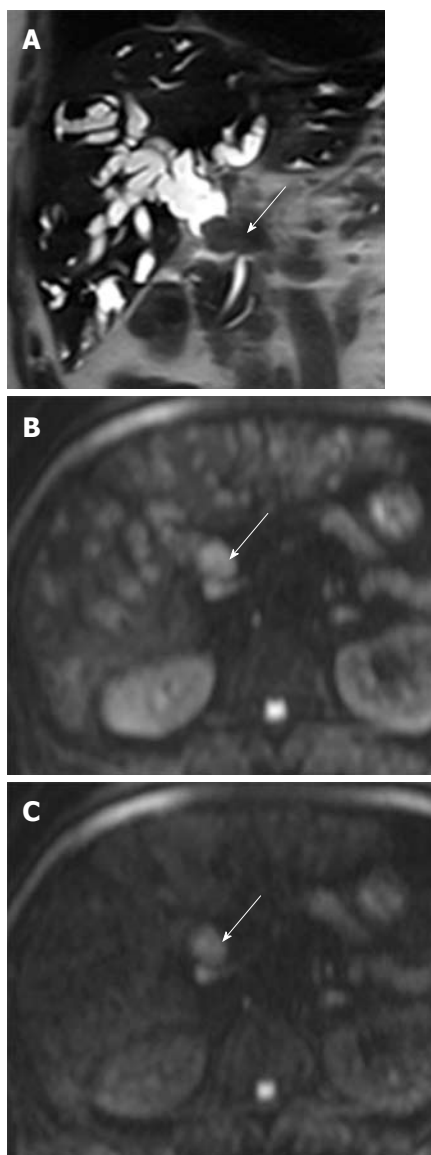


Figure 15 Extrahepatic cholangiocarcinoma in a 62-year-old man. A: Coronal T2-weighted rapid acquisition relaxation enhancement image shows a mass (arrow) in the distal common bile duct and marked upstream bile duct dilatation; B: DWI at $b = 800 \text{ s/mm}^2$ shows a mass with high signal intensity (arrow), but the signal intensity of bile is also increased; C: DWI at $b = 1000 \text{ s/mm}^2$ shows a mass with high signal intensity (arrow). Note that the signal intensity of bile in the bile duct is significantly reduced. DWI: Diffusion-weighted magnetic resonance imaging.

metastasis, favor the diagnosis of gallbladder carcinoma rather than benign gallbladder lesions (Figures 8 and 9).

DWI for characterization of intrahepatic biliary lesions and diagnosis of malignant lesions in the intrahepatic bile duct

Depending on their sites of origin, cholangiocarcinoma is classified as intrahepatic or extrahepatic. Based on its growth pattern, it is also classified as mass-forming, periductal-infiltrating, or intraductal-growing type. Intrahepatic cholangiocarcinoma originates from second-order or greater peripheral branches of the intrahepatic bile duct. The mass-forming cholangiocarcinoma is the



Figure 16 Pancreatic adenocarcinoma in a 50-year-old woman. A: Coronal reformatted contrast-enhanced CT image shows a double duct sign secondary to a pancreatic head cancer (arrow); B: On DWI at $b = 800 \text{ s/mm}^2$, pancreatic adenocarcinoma (arrow) shows hyperintensity; C: DWI at $b = 800 \text{ s/mm}^2$ superior to (B) shows high signal intensity of the remaining pancreas (arrowheads) due to obstructive pancreatitis. However, the remaining pancreas is less hyperintense relative to pancreatic adenocarcinoma. The ADC value of pancreatic cancer ($1.23 \pm 0.32 \text{ mm}^2/\text{s}$) is significantly lower than that of the remaining pancreas ($1.85 \pm 0.45 \text{ mm}^2/\text{s}$). DWI: Diffusion-weighted magnetic resonance imaging; CT: Computed tomography; ADC: Apparent diffusion coefficient.

most common type of intrahepatic cholangiocarcinoma, but periductal-infiltrating and intraductal-growing intrahepatic cholangiocarcinoma is also seen^[29,30].

Mass-forming intrahepatic cholangiocarcinoma appears as a single, predominantly homogeneous mass with well-circumscribed lobulated margins. Satellite nodules are frequent and vary in size. They usually appear as noncapsulated tumors, hypointense on T1-weighted images, and mild-to-moderately hyperintense on T2-weighted images, depending on the amount of fibrous tissue, necrosis, and mucin content. Dynamic-enhanced

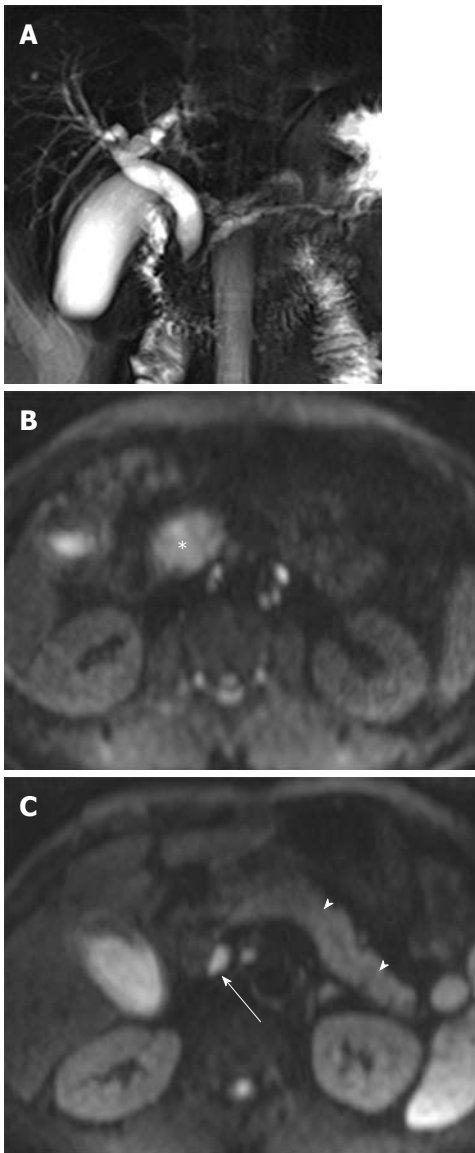


Figure 17 Focal pancreatitis in a 52-year-old man. A: Coronal image from thick-slab single-shot MRCP shows a double duct sign with tapered narrowing of pancreatic duct in the head of the pancreas; B: On DWI at $b = 800 \text{ s/mm}^2$ focal pancreatitis (asterisk) shows hyperintensity; C: DWI at $b = 800 \text{ s/mm}^2$ superior to (B) shows high signal intensity of the remaining pancreas due to obstructive pancreatitis. The remaining pancreas is slightly hypointense (arrowheads) relative to pancreatic adenocarcinoma. The ADC value of focal pancreatitis ($1.48 \pm 0.16 \text{ mm}^2/\text{s}$) is similar to that of the remaining pancreas ($1.54 \pm 0.28 \text{ mm}^2/\text{s}$). Note a hyperintense reactive lymph node (arrow). DWI: Diffusion-weighted magnetic resonance imaging; MRCP: Magnetic resonance cholangiopancreatography; ADC: Apparent diffusion coefficient.

MRI reveals minimal-to-moderate initial peripheral rim enhancement followed by progressive and concentric incomplete filling of the tumor with contrast material^[29].

In several studies, DWI is useful for detection of focal hepatic lesions, differentiation of cystic and solid hepatic lesions, and differentiation of benign and malignant focal hepatic lesions^[4,19,31]. In one investigation using two b values (0 and 500 s/mm^2), there were significant differences between the ADCs of benign and malignant focal hepatic lesions ($2.45 \pm 0.96 \times 10^{-3}$ and $1.08 \pm 0.50 \times 10^{-3} \text{ mm}^2/\text{s}$ for $b = 0$ and 500 s/mm^2 , respectively; $P < 0.001$),

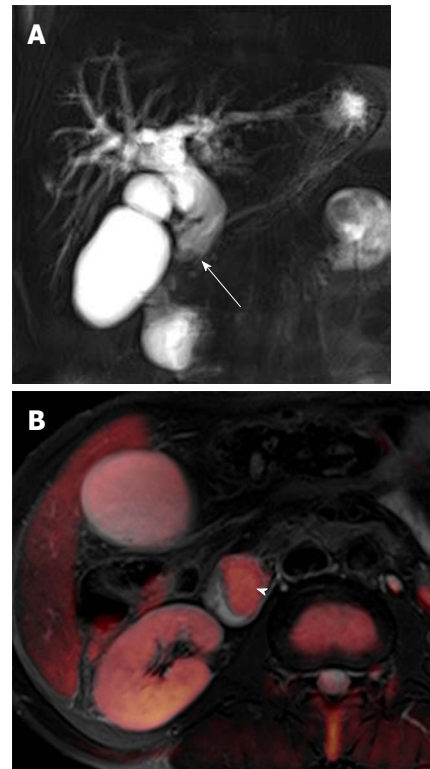


Figure 18 Ampullary carcinoma in a 63-year-old man. A: Coronal image from thick-slab single-shot MRCP shows marked bile duct dilatation with abrupt narrowing (arrow) at the distal common bile duct; B: Fusion image of T2-weighted and diffusion-weighted imaging at $b = 800 \text{ s/mm}^2$ shows an ampullary mass with hyperintensity (arrowhead). MRCP: Magnetic resonance cholangiopancreatography.

although there was some overlap^[4].

Mass-forming intrahepatic cholangiocarcinoma is usually large, achieving a diameter of up to 15 cm because early symptoms are rarely present. Thus, it is readily depicted on DWI and remains hyperintense on DWI using high b values with low ADC values; similar to values of other malignant focal hepatic lesions (Figure 11). Central hypointensity of the mass lesion may be seen on T2-weighted images and DWI using high b values, which may reflect fibrotic tissue in the central portion of the tumor. Peripheral hyperintensity can be demonstrated on DWI using high b values, corresponding to the more highly cellular region. As mentioned earlier, it is, however, difficult to distinguish mass-forming intrahepatic cholangiocarcinoma, hepatocellular carcinoma (HCC), and metastasis. Thus, DWI should be used along with conventional MRI sequences, such as dynamic-enhanced MRI, to differentiate mass-forming intrahepatic cholangiocarcinoma from other hepatic malignancies.

Cholangiocarcinoma tends to occur in atrophied or heavily stone-burdened segments. On cross-sectional images, it is difficult to diagnose cholangiocarcinoma associated with hepatolithiasis. A diagnosis of cholangiocarcinoma associated with hepatolithiasis should be considered when a mass involving or surrounding the bile duct is seen, or when focal nodular biliary wall thickening with increased enhancement is present in the



Figure 19 Papillitis due to a recently passed stone in a 75-year-old man. A: Coronal image from thick-slab single-shot MRCP shows mild bile duct dilatation; B: DWI at $b = 50 \text{ s/mm}^2$ shows a papilla with high signal intensity (arrow); C: On DWI at $b = 800 \text{ s/mm}^2$, the signal intensity of the papilla returns to the isosignal intensity (arrow). DWI: Diffusion-weighted magnetic resonance imaging; MRCP: Magnetic resonance cholangiopancreatography.

region of the stricture^[32]. DWI using high b values can be useful for the detection of cholangiocarcinoma associated with hepatolithiasis (Figure 11).

Diffuse periductal thickening along the bile duct in the periductal-infiltrating type, causing mild-to-marked bile duct dilatation, is seen in intrahepatic cholangiocarcinoma^[29]. DWI may be helpful for the detection of malignant bile duct lesions causing a variable degree of intrahepatic bile duct dilatation, as well as for differentiating between intrahepatic malignant and benign bile duct lesions (Figure 12).

Intraductal-growing cholangiocarcinoma appears as hyperintense intraluminal filling defects on DWI using high b values with low ADC values (Figure 13). However, detection of small malignant bile duct lesions is

limited on DWI because tumor detection with DWI is affected by variable causes, such as low spatial resolution of higher- b -value DWI, tumor cellularity, bowel peristalsis, and artifacts.

Invasion of the intrahepatic bile duct is infrequent in HCC, and seen in approximately 3.3%-9.0% of cases^[33]. Obstruction of the bile duct in patients with HCC is caused by invasion of the intrahepatic bile duct, blood clots from the tumor, and tumor fragments. HCC with bile duct tumor thrombi can be distinguished from hematomas in the bile duct based on the presence of mass enhancement on dynamic-enhanced CT or MRI^[34,35]. DWI can be useful for the differentiation of HCC and bile duct tumor thrombi from blood clots within the bile on the basis of identification of restricted diffusion of the mass lesion in the bile duct. They appear as hyperintense intraluminal filling defects on DWI using high b values with low ADC values (Figure 14). However, because imaging findings of HCC with bile duct thrombi are similar to those of intraductal-growing cholangiocarcinoma, conventional MRI findings of a mass outside the ductal system, hypervascularity on dynamic imaging, and underlying cirrhosis favor the diagnosis of HCC with bile duct tumor thrombi rather than intraductal cholangiocarcinoma.

DWI for characterization of extrahepatic biliary lesions and diagnosis of malignant lesions in the extrahepatic bile duct

Approximately two-thirds of extrahepatic bile duct cancer arises at the hepatic hilum (known as hilar cholangiocarcinoma or Klatskin tumor), and approximately one-third originates from the distal common bile duct. The most common pattern of tumor growth is focal infiltration of the ductal wall or the periductal-infiltrating type, resulting in focal strictures. Other tumor growth patterns include the mass-forming and intraductal-growing types^[29].

Extrahepatic bile duct carcinoma causes varying degrees of upstream bile duct dilatation. MRCP is highly accurate in identifying the presence and level of bile duct obstruction. Although differentiation between benign and malignant biliary lesions by MRCP is sometimes difficult, inspection of the bile duct lumen and wall on thin-section images helps to identify malignancies, which often cause an eccentric, abrupt change in the bile duct caliber, with irregular shouldering at the transition point from large obstructed to small-caliber decompressed ducts. Benign strictures tend to show short-segment involvement with smooth, gradual, and concentric narrowing^[36].

It has been reported that DWI is useful for the detection of extrahepatic cholangiocarcinoma and differentiation between malignant and benign biliary lesions. In a study using two b values (0 s/mm^2 and 500 s/mm^2), the sensitivity, specificity and accuracy of the detection of extrahepatic carcinoma were 94.3%, 100% and 96.4%, respectively^[10]. On DWI using high b values, a high signal intensity with a low ADC value at the transition point

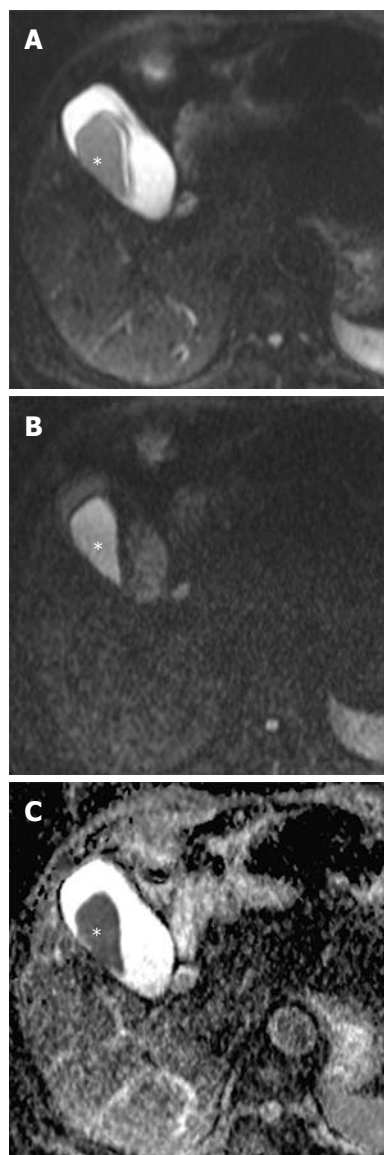


Figure 20 Hemobilia secondary to percutaneous liver biopsy in a 55-year-old man. A: DWI at $b = 50 \text{ s/mm}^2$ shows a hypointense hematoma in the gallbladder (asterisk); B: On DWI at $b = 800 \text{ s/mm}^2$, signal intensity of the hematoma changes to high signal (asterisk). C: On the ADC map, the hematoma in the gallbladder appears as low signal intensity (asterisk), which is associated with intact RBC membranes (i.e., hyperacute, acute, and early subacute hematomas). DWI: Diffusion-weighted magnetic resonance imaging; ADC: Apparent diffusion coefficient; RBC: Red blood cell.

from large obstructed to small-caliber decompressed ducts is a highly suggestive finding for malignant, rather than benign, biliary lesions because benign lesions usually show no hyper- or isointensity to the surrounding structures in the transitional area (Figure 15). Thus, this finding can be a clue for differentiating between malignant and benign biliary lesions. However, there is some degree of overlap; benign active inflammatory conditions rarely have hyperintensity, and some malignant lesions are not demonstrated on DWI using high b values^[10].

Pancreatic carcinoma, cholangiocarcinoma, or chronic pancreatitis should be considered when a bile duct stricture is limited to the distal (intrapancreatic) common

bile duct. Pancreatitis remains difficult to distinguish from pancreatic carcinoma on the basis of MRI findings, particularly in cases of acute or chronic mass-forming pancreatitis, because both appear as hypointense masses or mass-like lesions in the pancreas on T1-weighted images and are associated with ductal obstruction^[37].

In a study using b values (0 s/mm^2 and 600 s/mm^2), DWI is helpful in detecting focal pancreatic lesions and differentiating between pancreatic carcinoma and mass-forming pancreatitis. Mass-forming pancreatitis has either lower or higher ADC values than pancreatic carcinoma, but ultimately follows the ADC values of the remaining pancreatic parenchyma, whereas the focal lesion in pancreatic carcinoma is invariably lower than the remaining parenchyma (Figures 16 and 17)^[7]. In a study using a high b value (1000 s/mm^2), the sensitivity and specificity for the detection of pancreatic adenocarcinoma was 96.2% and 98.6%, respectively^[38]. ADC values in pancreatic carcinoma tend to be lower than in the normal pancreas in most studies, although there is some degree of overlap^[7,38]. Pancreatic carcinoma invokes a fibrotic response similar to desmoplastic reaction, therefore, ADC values are correlated with the degree of fibrosis; the ADC value of pancreatic carcinoma with loose fibrosis is higher than that of pancreatic carcinoma with dense fibrosis^[39]. In a recent study, ADC at lower b values ($< 500 \text{ s/mm}^2$) was higher in mass-forming pancreatitis than in pancreatic carcinoma, whereas ADC at high b values was not significantly different between mass-forming pancreatitis and pancreatic carcinoma^[17]. This was attributed to increasing perfusion effects at lower b values, which was correlated with high vascularity in chronic pancreatitis. Thus, DWI alone is suboptimal for the differentiation of pancreatic masses and mass-like lesions, and should be interpreted in conjunction with conventional MRI.

Periampullary lesions have one or more of the following MRI features: the presence of biliary dilatation at the level of the ampulla of Vater with or without a dilated pancreatic duct, bulging of the papilla, a mass lesion in or around the ampulla of Vater, and abnormal enhancement of the papilla. It is not always easy to distinguish between neoplastic and non-neoplastic conditions in or around the ampulla of Vater using conventional MRI, because of the confusing or overlapping findings^[40].

In our experience, ampullary or periampullary carcinoma displays mild-to-moderately high signal intensity on DWI using high b values with low ADC values, reflecting the high cellularity of tumors, whereas benign lesions, such as sphincter of Oddi dysfunction or papillary stenosis, show no high signal intensity in or around the ampulla of Vater (Figures 18 and 19). Thus, DWI can be helpful for detecting highly cellular malignant lesions and distinguishing between malignant and benign conditions in or around the ampulla of Vater. However, as mentioned earlier, some small malignant lesions in or around the ampulla of Vater are not identified on DWI using high b values.

Table 1 Characteristic diffusion-weighted magnetic resonance imaging features in the various biliopancreatic tract disorders

Categories	Diagnosis	Characteristic DWI features
DWI for the evaluation of gallstone-related complications	Acute cholangitis	Hyperintense parenchyma on low b values usually returns to isointense on high b values
	Hepatic abscess	Hyperintense on high b values with low ADC values
	Acute pancreatitis	Hyperintense on high b values
DWI for the characterization and diagnosis of gallbladder lesions	Cholecystitis	Diffuse and symmetric hyperintensity in the gallbladder wall on high b values Pus in the dependent portion: hyperintense on high b values with low ADC values
	Gallbladder carcinoma	Hyperintense mass occupying the entire gallbladder lumen or focal and asymmetric hyperintensity in or around the gallbladder wall on high b values
DWI for the characterization of intrahepatic biliary lesions and diagnosis of malignant lesions in the intrahepatic bile duct	Mass-forming cholangiocarcinoma	Hyperintense on high b values with low ADC values, similar to that of other malignant hepatic masses
	Periductal-infiltrative cholangiocarcinoma	Hyperintense periductal thickening along the bile duct on high b values with low ADC values
	Intraductal-growing cholangiocarcinoma	Hyperintense intraluminal filling defect on high b values with low ADC values
DWI for characterization of extrahepatic biliary lesions and diagnosis of malignant lesions in the extrahepatic bile duct	HCC with bile duct thrombi	Similar to that of intraductal-growing cholangiocarcinoma
	Extrahepatic cholangiocarcinoma	Hyperintense on high b values with low ADC values, at the transition point from large obstructed to small-caliber decompressed ducts
	Pancreatic carcinoma	Lower ADC values than those of the remaining pancreas
	Mass-forming pancreatitis	Similar ADC values to those of remaining pancreas
	Ampullary or periampullary carcinoma	Mild to moderate hyperintensity in or around ampulla of Vater on high b values with low ADC values
	Sphincter Oddi dysfunction or papillary stenosis	Isointensity in or around ampulla of vater on high b values

DWI: Diffusion-weighted magnetic resonance imaging; HCC: Hepatocellular carcinoma; ADC: Apparent diffusion coefficient.

PITFALLS

DWI is susceptible to a variety of artifacts that arise from motion, use of strong gradient pulses, and EPI technique. Physiological motion artifacts such as respiratory motion, cardiac pulsation, movement of the diaphragm, and motility of the bowel lead to ghosting images and blurring. The pulsatile motion of the heart and aorta obscure or diminish visualization of and increase ADC in the left lobe of the liver. These artifacts can be overcome using respiratory or electrocardiographic triggering. The EPI technique produces a low spatial resolution and signal-to-noise ratio. The rapid on-and-off switching of the high-intensity gradient field easily produce eddy currents, leading to geometrical distortion and image shearing artifacts that may become more pronounced with increased b values. DWI is also highly sensitive to magnetic field inhomogeneity. Susceptibility artifacts caused by field inhomogeneity are prevalent at air-tissue interfaces or around tissue-metal interfaces^[13,41].

Although restricted diffusion is generally considered to be associated with malignant lesions, some malignant lesions may not be detected on DWI. Some malignant tumors are too small for the DWI signal change to be obvious, or restriction to water diffusion is likely to be limited in malignant tumors with low cellularity, such as tumors with large cystic components. In contrast, some benign lesions sometimes exhibit restricted diffusion on imaging with high b values. The highly cellular tissue in reactive lymph nodes may show restricted diffusion (Figure 17). Thus, the role of DWI and ADC in distinguish-

ing between benign and malignant lymph nodes remains unclear^[42]. Additionally, diffusion of water in hematoma may be significantly restricted. Decreased ADC values in hemorrhage with intact red blood cell (RBC) membranes (i.e., hyperacute, acute, and early subacute hematoma) and increased ADCs after lysis of RBC membranes (i.e., "free" methemoglobin in subacute-to-chronic hematoma) have been reported (Figure 20). This may be mistaken for malignant lesions on DWI or the ADC map, causing erroneous detection or characterization of lesions^[43].

Thus, the radiologists have to be aware of potential pitfalls and limitation of the technique, and it should be kept in mind that DWI should be interpreted in conjunction with other conventional MRI.

CONCLUSION

DWI results for evaluating biliopancreatic diseases are still preliminary, and further studies are needed to determine its performance in the biliopancreatic tract. Additionally, correlation of DWI with pathological findings is required to define better the pathophysiology of various biliopancreatic diseases. Nevertheless, DWI can complement morphological information obtained by conventional MRCP by providing additional functional information concerning the alteration of tissue cellularity due to pathological processes. The detection of abnormal lesions and the differentiation of malignant from benign tumor-like lesions in the biliopancreatic tract can be improved by combined evaluation using both DWI and conventional MRI (Table 1). Moreover, DWI can

be a reasonable alternative technique for the assessment of the biliopancreatic tract in the setting of a contraindication to contrast agents such as renal insufficiency or contrast allergy.

REFERENCES

- 1 **Koh DM**, Collins DJ. Diffusion-weighted MRI in the body: applications and challenges in oncology. *AJR Am J Roentgenol* 2007; **188**: 1622-1635
- 2 **Qayyum A**. Diffusion-weighted imaging in the abdomen and pelvis: concepts and applications. *Radiographics* 2009; **29**: 1797-1810
- 3 **Thoeny HC**, De Keyzer F. Extracranial applications of diffusion-weighted magnetic resonance imaging. *Eur Radiol* 2007; **17**: 1385-1393
- 4 **Taouli B**, Vilgrain V, Dumont E, Daire JL, Fan B, Menu Y. Evaluation of liver diffusion isotropy and characterization of focal hepatic lesions with two single-shot echo-planar MR imaging sequences: prospective study in 66 patients. *Radiology* 2003; **226**: 71-78
- 5 **Parikh T**, Drew SJ, Lee VS, Wong S, Hecht EM, Babb JS, Taouli B. Focal liver lesion detection and characterization with diffusion-weighted MR imaging: comparison with standard breath-hold T2-weighted imaging. *Radiology* 2008; **246**: 812-822
- 6 **Matsuki M**, Inada Y, Nakai G, Tatsugami F, Tanikake M, Narabayashi I, Masuda D, Arisaka Y, Takaori K, Tanigawa N. Diffusion-weighted MR imaging of pancreatic carcinoma. *Abdom Imaging* 2007; **32**: 481-483
- 7 **Fattahi R**, Balci NC, Perman WH, Hsueh EC, Alkaade S, Havlioglu N, Burton FR. Pancreatic diffusion-weighted imaging (DWI): comparison between mass-forming focal pancreatitis (FP), pancreatic cancer (PC), and normal pancreas. *J Magn Reson Imaging* 2009; **29**: 350-356
- 8 **Saremi F**, Knoll AN, Bendavid OJ, Schultze-Haakh H, Narula N, Sarlati F. Characterization of genitourinary lesions with diffusion-weighted imaging. *Radiographics* 2009; **29**: 1295-1317
- 9 **Zhang J**, Tehrani YM, Wang L, Ishill NM, Schwartz LH, Hricak H. Renal masses: characterization with diffusion-weighted MR imaging--a preliminary experience. *Radiology* 2008; **247**: 458-464
- 10 **Cui XY**, Chen HW. Role of diffusion-weighted magnetic resonance imaging in the diagnosis of extrahepatic cholangiocarcinoma. *World J Gastroenterol* 2010; **16**: 3196-3201
- 11 **Patterson DM**, Padhani AR, Collins DJ. Technology insight: water diffusion MRI--a potential new biomarker of response to cancer therapy. *Nat Clin Pract Oncol* 2008; **5**: 220-233
- 12 **Whittaker CS**, Coady A, Culver L, Rustin G, Padwick M, Padhani AR. Diffusion-weighted MR imaging of female pelvic tumors: a pictorial review. *Radiographics* 2009; **29**: 759-774; discussion 774-778
- 13 **Koh DM**, Takahara T, Imai Y, Collins DJ. Practical aspects of assessing tumors using clinical diffusion-weighted imaging in the body. *Magn Reson Med Sci* 2007; **6**: 211-224
- 14 **Kandpal H**, Sharma R, Madhusudhan KS, Kapoor KS. Respiratory-triggered versus breath-hold diffusion-weighted MRI of liver lesions: comparison of image quality and apparent diffusion coefficient values. *AJR Am J Roentgenol* 2009; **192**: 915-922
- 15 **Chiu FY**, Jao JC, Chen CY, Liu GC, Jaw TS, Chiou YY, Hsu FO, Hsu JS. Effect of intravenous gadolinium-DTPA on diffusion-weighted magnetic resonance images for evaluation of focal hepatic lesions. *J Comput Assist Tomogr* 2005; **29**: 176-180
- 16 **Thoeny HC**, De Keyzer F, Oyen RH, Peeters RR. Diffusion-weighted MR imaging of kidneys in healthy volunteers and patients with parenchymal diseases: initial experience. *Radiology* 2005; **235**: 911-917
- 17 **Klauss M**, Lemke A, Grünberg K, Simon D, Re TJ, Wente MN, Laun FB, Kauczor HU, Delorme S, Grenacher L, Stieltjes B. Intravoxel incoherent motion MRI for the differentiation between mass forming chronic pancreatitis and pancreatic carcinoma. *Invest Radiol* 2011; **46**: 57-63
- 18 **Yoshikawa T**, Kawamitsu H, Mitchell DG, Ohno Y, Ku Y, Seo Y, Fujii M, Sugimura K. ADC measurement of abdominal organs and lesions using parallel imaging technique. *AJR Am J Roentgenol* 2006; **187**: 1521-1530
- 19 **Briegel M**, Holzapfel K, Gaa J, Woertler K, Waldt S, Kiefer B, Stemmer A, Ganter C, Rummeny EJ. Characterization of focal liver lesions by ADC measurements using a respiratory triggered diffusion-weighted single-shot echo-planar MR imaging technique. *Eur Radiol* 2008; **18**: 477-485
- 20 **Kim T**, Murakami T, Takahashi S, Hori M, Tsuda K, Nakamura H. Diffusion-weighted single-shot echoplanar MR imaging for liver disease. *AJR Am J Roentgenol* 1999; **173**: 393-398
- 21 **Watanabe Y**, Nagayama M, Okumura A, Amoh Y, Katsube T, Suga T, Koyama S, Nakatani K, Dodo Y. MR imaging of acute biliary disorders. *Radiographics* 2007; **27**: 477-495
- 22 **Bader TR**, Braga L, Beavers KL, Semelka RC. MR imaging findings of infectious cholangitis. *Magn Reson Imaging* 2001; **19**: 781-788
- 23 **Hussain SM**, De Becker J, Hop WC, Dwarkasing S, Wielopolski PA. Can a single-shot black-blood T2-weighted spin-echo echo-planar imaging sequence with sensitivity encoding replace the respiratory-triggered turbo spin-echo sequence for the liver? An optimization and feasibility study. *J Magn Reson Imaging* 2005; **21**: 219-229
- 24 **Méndez RJ**, Schiebler ML, Outwater EK, Kressel HY. Hepatic abscesses: MR imaging findings. *Radiology* 1994; **190**: 431-436
- 25 **Chan JH**, Tsui EY, Luk SH, Fung AS, Yuen MK, Szeto ML, Cheung YK, Wong KP. Diffusion-weighted MR imaging of the liver: distinguishing hepatic abscess from cystic or necrotic tumor. *Abdom Imaging* 2001; **26**: 161-165
- 26 **Shinya S**, Sasaki T, Nakagawa Y, Guiquing Z, Yamamoto F, Yamashita Y. The efficacy of diffusion-weighted imaging for the detection and evaluation of acute pancreatitis. *Hepatogastroenterology* 2009; **56**: 1407-1410
- 27 **Chan JH**, Tsui EY, Luk SH, Fung SL, Cheung YK, Chan MS, Yuen MK, Mak SF, Wong KP. MR diffusion-weighted imaging of kidney: differentiation between hydronephrosis and pyonephrosis. *Clin Imaging* 2001; **25**: 110-113
- 28 **Sugita R**, Yamazaki T, Furuta A, Itoh K, Fujita N, Takahashi S. High b-value diffusion-weighted MRI for detecting gallbladder carcinoma: preliminary study and results. *Eur Radiol* 2009; **19**: 1794-1798
- 29 **Chung YE**, Kim MJ, Park YN, Choi JY, Pyo JY, Kim YC, Cho HJ, Kim KA, Choi SY. Varying appearances of cholangiocarcinoma: radiologic-pathologic correlation. *Radiographics* 2009; **29**: 683-700
- 30 **Lim JH**. Cholangiocarcinoma: morphologic classification according to growth pattern and imaging findings. *AJR Am J Roentgenol* 2003; **181**: 819-827
- 31 **Moteki T**, Horikoshi H, Oya N, Aoki J, Endo K. Evaluation of hepatic lesions and hepatic parenchyma using diffusion-weighted reordered turboFLASH magnetic resonance images. *J Magn Reson Imaging* 2002; **15**: 564-572
- 32 **Park HS**, Lee JM, Kim SH, Jeong JY, Kim YJ, Lee KH, Choi SH, Han JK, Choi BI. CT Differentiation of cholangiocarcinoma from periductal fibrosis in patients with hepatolithiasis. *AJR Am J Roentgenol* 2006; **187**: 445-453
- 33 **Wang HJ**, Kim JH, Kim JH, Kim WH, Kim MW. Hepatocellular carcinoma with tumor thrombi in the bile duct. *Hepatogastroenterology* 1999; **46**: 2495-2499
- 34 **Jung AY**, Lee JM, Choi SH, Kim SH, Lee JY, Kim SW, Han JK, Choi BI. CT features of an intraductal polypoid mass:

- Differentiation between hepatocellular carcinoma with bile duct tumor invasion and intraductal papillary cholangiocarcinoma. *J Comput Assist Tomogr* 2006; **30**: 173-181
- 35 **Gabata T**, Terayama N, Kobayashi S, Sanada J, Kadoya M, Matsui O. MR imaging of hepatocellular carcinomas with biliary tumor thrombi. *Abdom Imaging* 2007; **32**: 470-474
- 36 **Park MS**, Kim TK, Kim KW, Park SW, Lee JK, Kim JS, Lee JH, Kim KA, Kim AY, Kim PN, Lee MG, Ha HK. Differentiation of extrahepatic bile duct cholangiocarcinoma from benign stricture: findings at MRCP versus ERCP. *Radiology* 2004; **233**: 234-240
- 37 **Johnson PT**, Outwater EK. Pancreatic carcinoma versus chronic pancreatitis: dynamic MR imaging. *Radiology* 1999; **212**: 213-218
- 38 **Ichikawa T**, Erturk SM, Motosugi U, Sou H, Iino H, Araki T, Fujii H. High-b value diffusion-weighted MRI for detecting pancreatic adenocarcinoma: preliminary results. *AJR Am J Roentgenol* 2007; **188**: 409-414
- 39 **Muraoka N**, Uematsu H, Kimura H, Imamura Y, Fujiwara Y, Murakami M, Yamaguchi A, Itoh H. Apparent diffusion coefficient in pancreatic cancer: characterization and histopathological correlations. *J Magn Reson Imaging* 2008; **27**: 1302-1308
- 40 **Kim TU**, Kim S, Lee JW, Woo SK, Lee TH, Choo KS, Kim CW, Kim GH, Kang DH. Ampulla of Vater: comprehensive anatomy, MR imaging of pathologic conditions, and correlation with endoscopy. *Eur J Radiol* 2008; **66**: 48-64
- 41 **Le Bihan D**, Poupon C, Amadon A, Lethimonnier F. Artifacts and pitfalls in diffusion MRI. *J Magn Reson Imaging* 2006; **24**: 478-488
- 42 **Feuerlein S**, Pauls S, Juchems MS, Stuber T, Hoffmann MH, Brambs HJ, Ernst AS. Pitfalls in abdominal diffusion-weighted imaging: how predictive is restricted water diffusion for malignancy. *AJR Am J Roentgenol* 2009; **193**: 1070-1076
- 43 **Atlas SW**, DuBois P, Singer MB, Lu D. Diffusion measurements in intracranial hematomas: implications for MR imaging of acute stroke. *AJNR Am J Neuroradiol* 2000; **21**: 1190-1194

S-Editor Gou SX **L-Editor** Kerr C **E-Editor** Zhang DN

Efficacy of MK615 for the treatment of patients with liver disorders

Atsushi Hokari, Tomohisa Ishikawa, Hisao Tajiri, Takahide Matsuda, Osamu Ishii, Nobuyuki Matsumoto, Chiaki Okuse, Hideaki Takahashi, Takeshi Kurihara, Ko-ichi Kawahara, Ikuro Maruyama, Mikio Zeniya

Atsushi Hokari, Tomohisa Ishikawa, Hisao Tajiri, Mikio Zeniya, Department of Internal Medicine, Division of Gastroenterology and Hepatology, The Jikei University School of Medicine, Tokyo 1058471, Japan

Takahide Matsuda, Osamu Ishii, Department of Internal Medicine, Division of General Internal Medicine, St. Marianna University School of Medicine, Kawasaki 2168511, Japan

Nobuyuki Matsumoto, Chiaki Okuse, Hideaki Takahashi, Department of Internal Medicine, Division of Gastroenterology and Hepatology, St. Marianna University School of Medicine, Kawasaki 2168511, Japan

Takeshi Kurihara, Keio University, Graduate School of Media and Governance, Fujisawa 2520882, Japan

Ko-ichi Kawahara, Department of Biomedical Engineering, Osaka Institute of Technology, Osaka 5358585, Japan

Ikuro Maruyama, Department of Systems Biology in Thromboregulation, Kagoshima University Graduate School of Medical and Dental Sciences, Kagoshima 8908580, Japan

Author contributions: Kawahara K, Maruyama I, Zeniya M designed the research; Hokari A, Ishikawa T, Tajiri H, Matsuda T, Ishii O, Matsumoto N, Okuse C, Takahashi H, Kurihara T, Zeniya M performed the research; Hokari A, Zeniya M analyzed the data; and Hokari A and Zeniya M wrote the paper.

Correspondence to: Dr. Mikio Zeniya, Department of Internal Medicine, Division of Gastroenterology and Hepatology, The Jikei University School of Medicine, Nishi-shimbashi 3-25-8, Minato-ku, Tokyo 1058471, Japan. zeniya@jikei.ac.jp

Telephone: +81-3-34331111 Fax: +81-3-34350569

Received: December 8, 2011 Revised: May 10, 2012

Accepted: May 26, 2012

Published online: August 21, 2012

Abstract

AIM: To investigate the hepatoprotective effect of MK615, a Japanese apricot extract, in an animal model, and its clinical therapeutic effect.

METHODS: Wistar rats were administered physiological saline (4 mL/kg) or MK615 solution (4 mL/kg) for 7 d. On the sixth d, acute hepatic injury was induced by

administering a single intraperitoneal injection (*ip*) of D-galactosamine hydrochloride (D-GalN) (600 mg/kg). Plasma levels of alanine aminotransferase (ALT) and aspartate aminotransferase (AST) were determined, and liver tissues were used for histopathological analysis. Fifty-eight patients with liver disorders [hepatitis C ($n = 40$), non-alcoholic fatty liver disease ($n = 15$), and autoimmune liver disease ($n = 3$)] were orally administered commercially available Misatol ME-containing MK615 (13 g/d) daily for 12 wk. Blood and urine were sampled immediately before and 6 wk, 12 wk, and 16 wk after the start of intake to measure various biochemical parameters. The percentage change in ALT and AST levels after 12 wk from the pre-intake baseline served as a primary endpoint.

RESULTS: D-GalN effectively induced acute hepatic injury in the rats. At 48 h after the *ip* injection of D-GalN, the plasma levels of ALT (475.6 ± 191.5 IU/L *vs* 225.3 ± 194.2 IU/L, $P < 0.05$) and AST (1253.9 ± 223.4 IU/L *vs* 621.9 ± 478.2 IU/L, $P < 0.05$) in the MK615 group were significantly lower than the control group. Scattered single cell necrosis, loss of hepatocytes, and extensive inflammatory cell infiltration were observed in hepatic tissue samples collected from the control group. However, these findings were less pronounced in the group receiving MK615. At the end of the clinical study, serum ALT and AST levels were significantly decreased compared with pre-intake baseline levels from 103.5 ± 58.8 IU/L to 71.8 ± 39.3 IU/L ($P < 0.05$) and from 93.5 ± 55.6 IU/L to 65.5 ± 34.8 IU/L ($P < 0.05$), respectively. A reduction of $\geq 30\%$ from the pre-study baseline ALT level was observed in 26 (45%) of the 58 patients, while 25 (43%) patients exhibited similar AST level reductions. The chronic hepatitis C group exhibited significant ALT and AST level reductions from 93.4 ± 51.1 IU/L to 64.6 ± 35.1 IU/L ($P < 0.05$) and from 94.2 ± 55.5 IU/L to 67.2 ± 35.6 IU/L ($P < 0.05$), respectively. A reduction of $\geq 30\%$ from the pre-study baseline ALT level was observed in 20 (50%) of the 40 patients.

ALT levels in both the combined ursodeoxycholic acid (UDCA) treatment and the UDCA uncombined groups were significantly lower after Misatol ME administration. MK615 protected hepatocytes from D-GalN-induced cytotoxicity in rats. Misatol ME decreased elevated ALT and AST levels in patients with liver disorders.

CONCLUSION: These results suggest that MK615 and Misatol ME are promising hepatoprotective agents for patients with liver disorders.

© 2012 Baishideng. All rights reserved.

Key words: *Prunus mume*; MK615; Liver damage; Hepatitis C; Non-alcoholic fatty liver disease

Peer reviewer: Marek Hartleb, Department of Gastroenterology and Hepatology, Medical University of Silesia, 70-111 Szczecin, Poland

Hokari A, Ishikawa T, Tajiri H, Matsuda T, Ishii O, Matsumoto N, Okuse C, Takahashi H, Kurihara T, Kawahara K, Maruyama I, Zeniya M. Efficacy of MK615 for the treatment of patients with liver disorders. *World J Gastroenterol* 2012; 18(31): 4118-4126 Available from: URL: <http://www.wjgnet.com/1007-9327/full/v18/i31/4118.htm> DOI: <http://dx.doi.org/10.3748/wjg.v18.i31.4118>

INTRODUCTION

Japanese apricot (*Prunus mume* Sieb. et Zucc.), hereinafter referred to as *ume*, was brought to Japan from China around the eighth century. The flesh of this fruit has been used not only as food but also as medicine. *Ishinbo*, the oldest medical monograph in Japan, which was written in AD 984, indicates that both *umeboshi* (pickled *ume*) and *ubai* (smoke-dried *ume*) were used as medicines (e.g., as anti-diarrheal agents and for detoxification in food or drug poisoning). *Shokokukodenbiho*, published in 1817, also refers to the effectiveness of *ume* extracts. It is thus evident that *ume* was used extensively as a folk remedy in Japan. Syringaresinol, a lignan in *ume*, was recently shown to control infection by inhibiting the migration of *Helicobacter pylori*^[1]. MK615, an extract from Japanese apricot, contains triterpenoids such as ursolic acid (UA)^[2], oleanolic acid (OA)^[2,4], lupeol^[2,4], α -amyrin^[2], and β -sitosterol^[4]. These substances have been shown to exert various biological actions. Reports have described diverse effects, including anti-tumor activity (against tumor cell lines such as those of gastric cancer^[5], leukemia^[5], breast cancer^[4,6], hepatocellular carcinoma^[7,8], colon cancer^[9], pancreatic cancer^[10], and malignant melanoma^[11]) and immunopotentiality in experimental animals exposed to X-rays^[4]. MK615 was previously reported to inhibit the release of high-mobility group box 1 (HMGB1) from lipopolysaccharide (LPS)-stimulated macrophage-like RAW264.7 cells and to activate the transcription factor nuclear factor erythroid 2-related factor 2 (Nrf2), resulting in the

induction of heme oxygenase-1 (HO-1). MK615 was also shown to suppress the formation of inflammation-inducing cytokines [tumor necrosis factor α (TNF- α) and interleukin-6 (IL-6)] by inactivating mitogen-activated protein kinases (MAPKs) and the transcription factor nuclear factor- κ B (NF- κ B)^[3,12]. It is thus evident that *ume* extracts exert anti-inflammatory and antioxidative actions. However, the significance of these actions in the liver has not been adequately clarified.

Given the anti-inflammatory and antioxidative actions of MK615, we investigated the hepatoprotective effects of MK615. In addition, the effects of Misatol ME, a beverage containing MK615 that is approved as a health food product in Japan, were clinically evaluated in patients with liver disorders that included hepatitis C, chronic inflammation of the liver, as well as fatty liver disease, which is closely involved in oxidative stress.

MATERIALS AND METHODS

Effect of MK615 on D-galactosamine hydrochloride-induced acute hepatic injury in rats

Preparation of MK615 solution: MK615 solution was prepared from a condensed extract of *ume*. In brief, *ume* were squeezed using a press, and the *ume* juice was then heated and concentrated 20-fold^[5]. The condensed extract was neutralized using NaOH and was then heat-sterilized. The MK615 solution contained the neutral, condensed *ume* extract.

D-galactosamine hydrochloride-induced hepatic injury in rats: Seven-week-old male Wistar rats (Crj:WI) weighing 200-240 g were purchased from Charles River Laboratories Japan (Yokohama, Japan). All rats were maintained under controlled temperature and lighting conditions (12/12-h dark/light cycle), and water and standard diet were provided ad libitum in accordance with the institute's guidelines for care and use of laboratory animals in research.

Acute hepatic injury was induced by administering a single intraperitoneal (*ip*) injection of D-galactosamine hydrochloride (D-GalN) (600 mg/kg; Wako Pure Chemical Industries, Osaka, Japan). In this study, rats were divided into 3 experimental groups. In group I (the vehicle control group), rats were administered physiological saline (4 mL/kg per day) *via* gavage for 7 d and injected with D-GalN (*ip*) 2 h after the sixth oral administration of saline (6 d from the first oral administration). In group II (the MK615 group), rats received MK615 solution (4 mL/kg per day) *via* gavage for 7 d and were injected with D-GalN (*ip*) 2 h after the sixth oral administration of MK615 solution. In group III, rats were administered the neutral MK615 solution (4 mL/kg per day) *via* gavage for 7 d and were injected with saline (*ip*) 2 h after the sixth oral administration of MK615 solution. group III served as a negative experimental control without D-GalN-induced hepatic injury (Figure 1). Treatments involving oral administration by gavage were conducted between

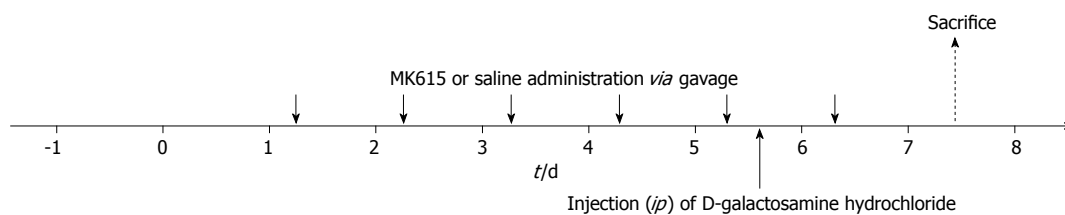


Figure 1 Experiment protocol of D-galactosamine hydrochloride-induced acute hepatic injury in rats.

9:00 and 10:00 AM and *ip* injections were administered between 11:00 AM and 12:00 noon. All rats were sacrificed by exsanguination under anesthesia 48 h after the *ip* injection of D-GalN or saline (8 d after the first oral administration). Blood samples from the abdominal aorta were immediately heparinized, and plasma samples were isolated by centrifugation. Plasma samples were frozen and stored at -80°C until used, and subsequently analyzed to determine the levels of alanine aminotransferase (ALT) and aspartate aminotransferase (AST). Liver tissue samples were also obtained from each rat and used for histopathological analysis. The plasma levels of ALT and AST were determined using a commercially available analytical kit (Transaminase CII-Test; Wako Pure Chemical Industries).

Evaluation of the effects of MK615 in patients with liver disorder

Subjects: This study involved patients who were definitively diagnosed with a liver disorder at the Jikei University School of Medicine Hospital, the St. Marianna University School of Medicine Hospital, or the Kurihara Clinic between December 2007 and December 2009 and who met the following requirements: (1) ALT level exceeding reference limits when tested within 3 mo before the start of this study, indicating the presence of hepatopathy; (2) serum hepatitis C virus (HCV)-RNA positivity (determined by real-time polymerase chain reaction) in patients with chronic hepatitis C; and (3) presence of fatty liver confirmed by diagnostic imaging in cases of non-alcoholic fatty liver disease (NAFLD). The following patients were excluded from the study: (1) those receiving treatment for liver cirrhosis, hepatocellular carcinoma, or other malignant tumors; (2) patients receiving treatment with Stronger Neo-Minophagen C; (3) those receiving treatment with interferon (IFN); and (4) habitual drinkers (alcohol consumption, > 30 g/d) or occasional heavy drinkers. Concomitant use of drugs or any treatment with antiviral, immunomodulating, or marrow-suppressive activity was prohibited during the study period, but continued use of drugs that had been initiated before the study was permitted. No patients were heavy drinkers. The ethics committee of each participating facility approved the study protocol. Informed consent to participate in the study was obtained in writing from all patients.

Methods: In Japan, MK615 solution is commercially available as Misatol ME (AdaBio Co. Ltd., Takasaki, Japan). For the clinical study, Misatol ME was used as the

MK615 solution and was ingested orally every d (2×6.5 g packs/d) for 12 wk. Blood and urine were sampled immediately before and 6 wk, 12 wk, and 16 wk after the start of MK615 intake to measure the following parameters: white blood cell (WBC) count, differential leukocyte count, red blood cell (RBC) count, hemoglobin, hematocrit, platelet count, ALT, AST, γ -glutamyl transpeptidase (γ -GTP), alkaline phosphatase (ALP), total protein, albumin, total cholesterol, cholinesterase, and total bilirubin, as well as urinalysis parameters. The percentage change in ALT and AST levels after 12 wk of intake from the pre-intake baseline served as primary and secondary endpoints, respectively. In the analysis of these endpoints, an improvement of $\geq 50\%$ from the pre-intake baseline was regarded “markedly effective”, $\geq 30\%$ was regarded “effective”, $\leq 30\%$ as “ineffective”, and an aggravation of $\geq 30\%$ as “worsened”. The response rate was defined as the percentage of “markedly effective” plus “effective” cases.

Statistical analysis

Data are expressed as mean \pm SD. Statistical analyses were performed using Stat View for Windows Version 5.0 (SAS Institute Inc., North Carolina, United States). Differences between 2 groups were analyzed using the Mann-Whitney *U* test. Comparisons between baseline and each time point were performed using Dunnett’s test. $P < 0.05$ was considered significant.

RESULTS

The effect of MK615 on D-galactosamine hydrochloride-induced acute hepatic injury in rats

ALT and AST plasma levels in control rats were elevated 48 h after D-GalN induction, with mean values of 475.6 ± 191.5 IU/L ($n = 8$) and 1253.9 ± 223.4 IU/L ($n = 8$), respectively. In the MK615 group, the ALT and AST levels were 225.3 ± 194.2 IU/L ($n = 9$) and 621.9 ± 478.2 IU/L ($n = 9$), respectively. The levels of ALT and AST in the MK615 group rats were significantly lower than in those of the control group ($P = 0.0433$ for ALT, $P = 0.0124$ for AST by Mann-Whitney *U* test) (Figure 2A and B).

Liver tissues were obtained from both control group rats and MK615 group rats at 48 h after D-GalN injection. Scattered single cell necrosis (swollen eosinophilic hepatocytes) and loss of hepatocytes was observed in hepatic tissue samples from the control group. Extensive inflammatory cell infiltration was also noted (Figure 2C). Figure 2D shows that these features of D-GalN-induced

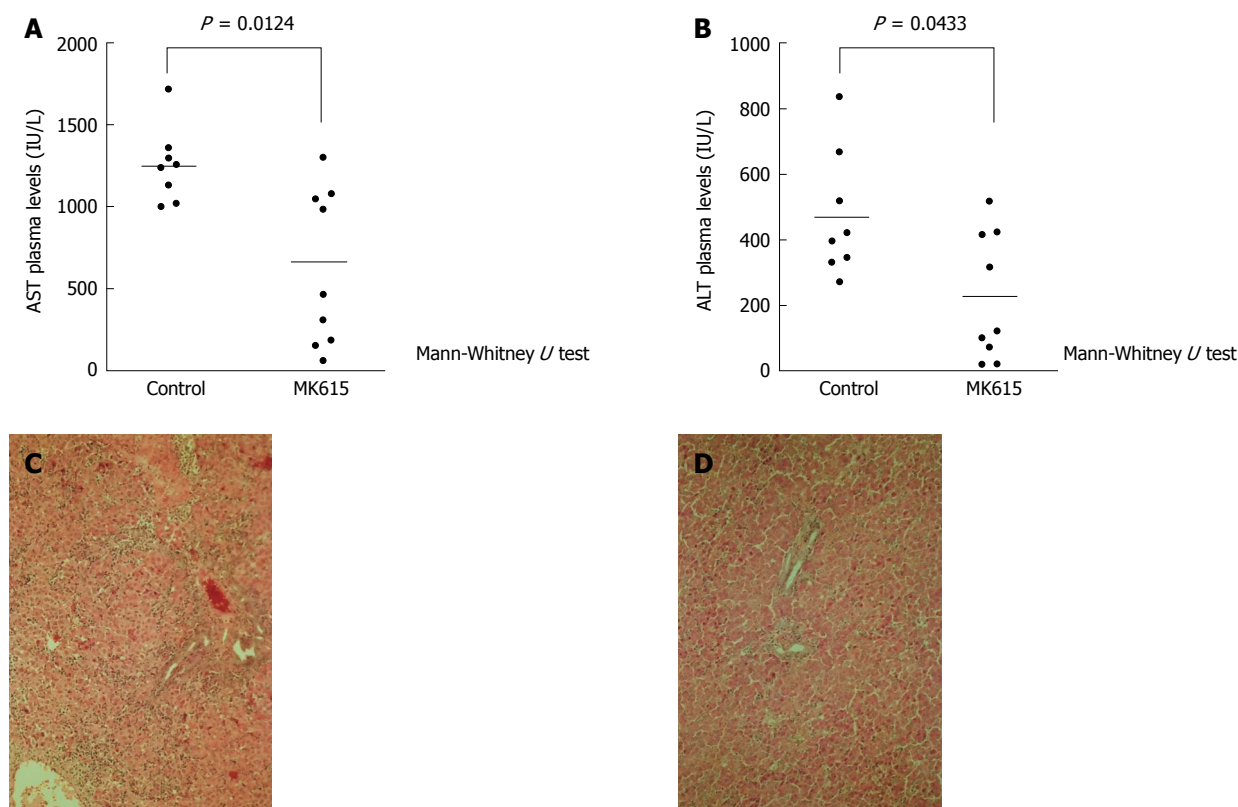


Figure 2 Effect of MK615 in D-galactosamine hydrochloride-induced acute hepatic injury in rats. A: AST plasma levels; B: ALT plasma levels; C: Control group (liver); D: MK615 group (liver). AST:Aspartate aminotransferase; ALT: Alanine aminotransferase.

Table 1 Background of patients with liver disorders

	Chronic hepatitis C	NAFLD	Autoimmune liver disease
Number	40	15	3
Gender (M/F)	25/15	14/1	1/2
Age (yr)	64.4 ± 11.3	52.5 ± 13.7	65.7 ± 4.0
HCV viral load(10^6 /mL)	6.2 ± 0.8		
≥ 5log/< 5log/ND	35/3/2		
WBC count (/μL)	4153 ± 994	6800 ± 1578	3967 ± 723
RBC count (10^4 /μL)	415 ± 59	490 ± 51	448 ± 48
Hemoglobin (g/dL)	13.1 ± 1.8	15.5 ± 1.1	12.5 ± 1.7
Platelet count (10^4 /μL)	13.8 ± 5.7	20.3 ± 8.4	17.2 ± 5.1
AST (IU/L)	94.2 ± 55.5	84.5 ± 50.0	129.3 ± 90.5
ALT (IU/L)	93.4 ± 51.1	131.9 ± 72.5	96.7 ± 50.1
γ-GTP (IU/L)	72.9 ± 60.5	181.9 ± 197.5	120.3 ± 74.2
LDH (IU/L)	237.8 ± 54.8	228.9 ± 44.4	270 ± 44.3
ALP (IU/L)	318.1 ± 116.8	303.4 ± 106.8	391 ± 293.1
Total bilirubin (mg/dL)	0.84 ± 0.29	0.8 ± 0.44	0.67 ± 0.15
Total cholesterol (mg/dL)	162 ± 35.2	188.5 ± 49.1	174.7 ± 40.1
Total protein (g/dL)	7.5 ± 0.6	7.7 ± 0.3	7.9 ± 0.9
Albumin (g/dL)	3.9 ± 0.4	4.4 ± 0.3	3.9 ± 0.9
BUN (mg/dL)	16.2 ± 4.0	13.6 ± 3.2	15.3 ± 3.1
Creatinine (mg/dL)	0.76 ± 0.16	0.75 ± 0.1	0.62 ± 0.06

Data are expressed as the mean ± standard deviation. NAFLD: Non-alcoholic fatty liver disease; ND: Not done; M: Male; F: Female; HCV: Hepatitis C virus; WBC: White blood cell; RBC: Red blood cell; AST: Aspartate aminotransferase; ALT: Alanine aminotransferase; γ-GTP: γ guanosine triphosphate; LDH: Lactate dehydrogenase; ALP: Alkaline phosphatase; BUN: Blood urea nitrogen.

hepatic injury were reduced in the treatment group re-

ceiving the MK615 solution.

The effects of MK615 in patients with liver disorders

We enrolled 58 patients in this clinical study (mean age, 61.4 ± 12.7 years; range: 29-82 years; 40 men and 18 women). The diagnosis was chronic hepatitis C in 40 patients, NAFLD in 15 patients, and autoimmune liver disease in 3 patients (2 with autoimmune hepatitis and 1 with primary sclerosing cholangitis). Table 1 lists the background variables in relation to the diseases diagnosed.

Analysis of the entire study population determined that ALT levels had decreased significantly from 103.5 ± 58.8 IU/L before the start of the study to 81.3 ± 45.7 IU/L ($P < 0.05$) at 6 wk, 71.8 ± 39.3 IU/L ($P < 0.05$) at 12 wk, and 72.3 ± 40.3 IU/L ($P < 0.05$) at 16 wk (Figure 3A). AST levels decreased significantly from 93.5 ± 55.6 IU/L before the start of the study to 77.6 ± 47.1 IU/L ($P < 0.05$) at 6 wk, 65.5 ± 34.8 IU/L ($P < 0.05$) at 12 wk, and 68.3 ± 37.8 IU/L ($P < 0.05$) at 16 wk (Figure 3B). A reduction of ≥ 30% from pre-study baseline ALT levels was observed in 26 (45%) of the 58 patients, whereas 25 (43%) patients exhibited a similar reduction in AST levels (Table 2).

When the effects of Misatol ME were analyzed in relation to the disease diagnosed, the chronic hepatitis C group exhibited significant ALT level reductions from the pre-study baseline of 93.4 ± 51.1 IU/L to 75.3 ± 46.6 IU/L ($P < 0.05$) at 6 wk, 64.6 ± 35.1 IU/L ($P < 0.05$) at 12 wk, and 64.6 ± 33.8 IU/L ($P < 0.05$) at 16 wk (Figure

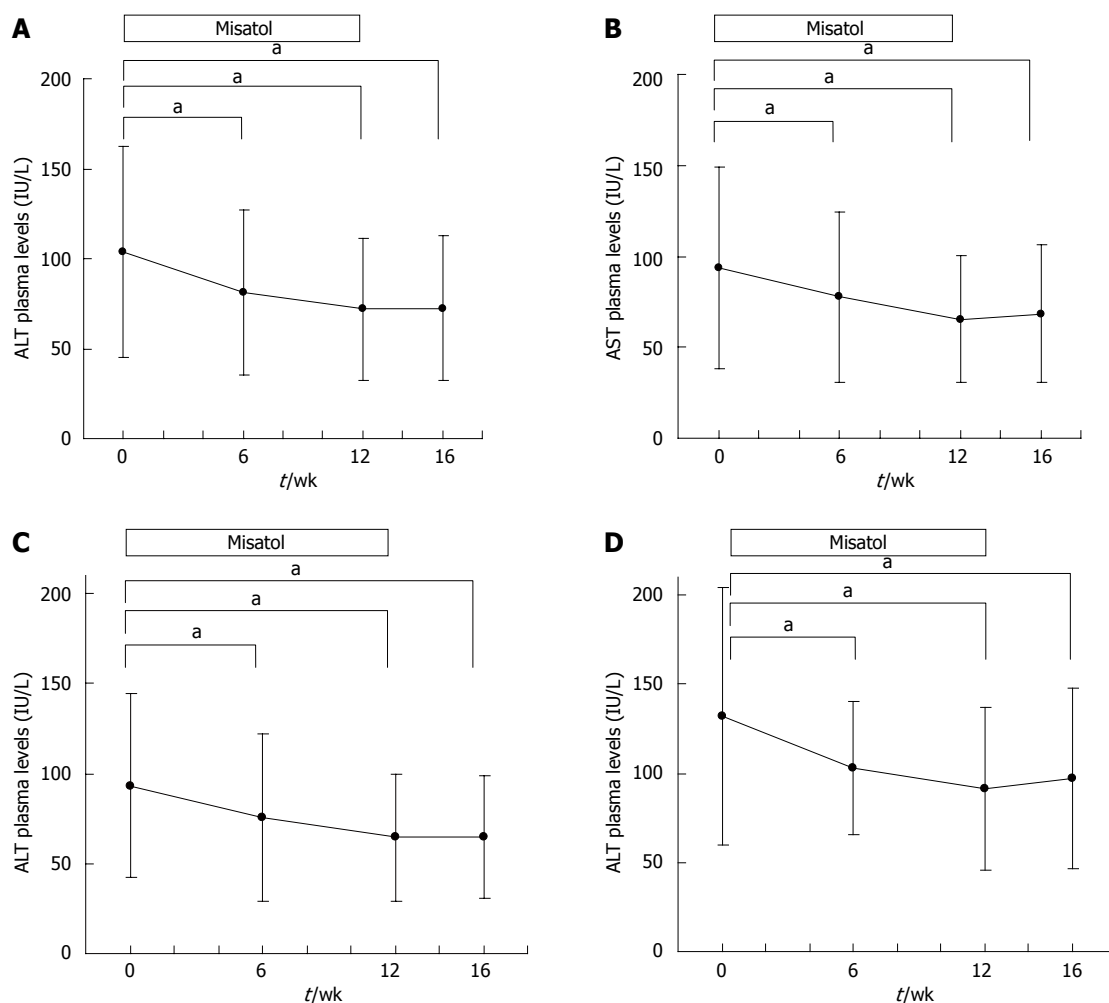


Figure 3 Effects of MK615 in patients with liver disorder, chronic hepatitis C and non-alcoholic fatty liver disease. A: Alanine aminotransferase (ALT); B: Aspartate aminotransferase (AST); C: Chronic hepatitis C group (ALT); D: Non-alcoholic fatty liver disease group (ALT). ^a*P* < 0.05 vs 0 wk group. Dunnett's test.

Table 2 Response rate of MK615 therapy in patients with liver disorder (%)		
	ALT	AST
Chronic hepatitis C	20/40 (50)	16/40 (40)
NAFLD	5/15 (33)	6/15 (40)
Autoimmune liver disease	1/3 (33)	3/3 (100)
Total	26/58 (45)	25/58 (43)

NAFLD: Non-alcoholic fatty liver disease; AST: Aspartate aminotransferase; ALT: Alanine aminotransferase.

3C). This same group of patients exhibited significant AST level reductions from the pre-study baseline of 94.2 ± 55.5 IU/L to 78.8 ± 49.5 IU/L (*P* < 0.05) at 6 wk, 67.2 ± 35.6 IU/L (*P* < 0.05) at 12 wk, and 66.6 ± 33.7 IU/L (*P* < 0.05) at 16 wk. In the chronic hepatitis C group, a reduction of $\geq 30\%$ from the pre-study baseline ALT level was observed in 20 (50%) of the 40 patients, while 16 (40%) patients exhibited similar AST level reductions (Table 2). Among the patients with chronic hepatitis C, ALT data before the start of test beverage intake (24 wk before starting intake) were available for 32 patients. These patients were subdivided into combined ursode-

oxycholic acid (UDCA) treatment (*n* = 20) (Figure 4A) and UDCA uncombined (*n* = 12) groups (Figure 4B). In both the combined UDCA treatment and UDCA uncombined groups, ALT levels were significantly lower after the intake of Misatol ME compared with those before intake.

The NAFLD group exhibited significant ALT level reductions from 131.9 ± 72.5 IU/L before the start of the study to 102.8 ± 37.6 IU/L (*P* < 0.05) at 6 wk, 90.9 ± 45.6 IU/L (*P* < 0.05) at 12 wk, and 96.9 ± 50.8 IU/L (*P* < 0.05) at 16 wk (Figure 3D). This group also exhibited significant AST level reductions during the Misatol ME intake period compared with the pre-start baseline level; levels were 84.5 ± 50.0 IU/L before the start of the study, 66.7 ± 24.2 IU/L (*P* < 0.05) at 6 wk, 58.1 ± 26.0 IU/L (*P* < 0.05) at 12 wk, and 69.8 ± 41.9 IU/L (NS) at 16 wk. In the NAFLD group, a reduction of $\geq 30\%$ from the pre-study baseline ALT level was observed in 5 (33%) of the 15 patients, whereas similar AST level reductions were observed in 6 (40%) patients (Table 2).

The levels of γ -GTP in the entire study population also decreased significantly after Misatol ME intake compared with pre-intake baseline levels (data not shown).

Table 3 presents the hematological and biochemical

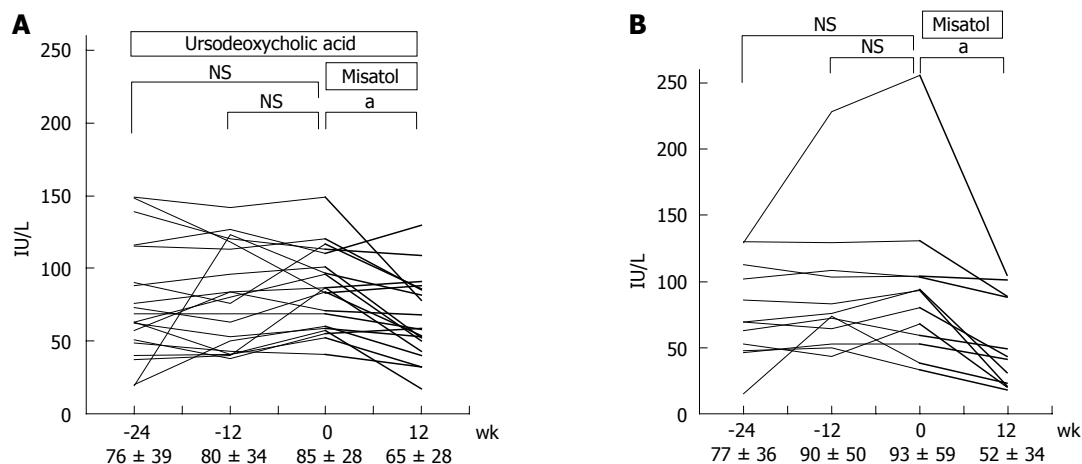


Figure 4 Effects of MK615 in patients with chronic hepatitis C (alanine aminotransferase). A: Misatol was added on ursodeoxycholic acid; B: Only Misatol was used. ^a $P < 0.05$ vs 0 wk group. Dunnett's test. NS: Not significant.

Table 3 Changes of serum level during MK615 therapy in patients with liver disorders

	Before therapy	During therapy 12 wk	P value ¹
WBC count (/ μ L)	4828 \pm 1640	4977 \pm 1855	NS
RBC count (10^4 / μ L)	436 \pm 65	435 \pm 65	NS
Hemoglobin (g/dL)	13.7 \pm 2.0	13.8 \pm 1.9	NS
Platelet count (10^3 / μ L)	15.7 \pm 7.0	15.6 \pm 6.6	NS
AST (IU/L)	94 \pm 56	66 \pm 35	< 0.05
ALT (IU/L)	104 \pm 59	72 \pm 39	< 0.05
γ -GTP (IU/L)	104 \pm 121	74 \pm 93	< 0.05
LDH (IU/L)	237 \pm 52	227 \pm 52	< 0.05
ALP (IU/L)	318 \pm 124	298 \pm 126	< 0.05
Total bilirubin (mg/dL)	0.8 \pm 0.3	0.8 \pm 0.3	NS
Total cholesterol (mg/dL)	170 \pm 40	171 \pm 43	NS
Total protein (g/dL)	7.6 \pm 0.6	7.6 \pm 0.5	NS
Albumin (g/dL)	4.0 \pm 0.5	4.1 \pm 0.4	NS
BUN (mg/dL)	15.5 \pm 3.9	14.7 \pm 3.5	NS
Creatinine (mg/dL)	0.75 \pm 0.15	0.74 \pm 0.15	NS

Data are expressed as the mean \pm standard deviation. ¹Dunnett's test. NS: Not significant; WBC: White blood cell; RBC: Red blood cell; AST: Aspartate aminotransferase; ALT: Alanine aminotransferase; γ -GTP: γ -guanosine triphosphate; LDH: Lactate dehydrogenase; ALP: Alkaline phosphatase; BUN: Blood urea nitrogen; NS: Not significant.

data obtained for the clinical study. No change associated with Misatol ME intake was noted in any hematological or biochemical parameter other than in the indicators of liver function, which improved after MK615 intake. An unexplained eruption was observed in 1 patient with NAFLD, which was the only adverse event observed during this study, and was not found to have a causal relationship with the intake of Misatol ME.

DISCUSSION

This is the first study demonstrating that Misatol ME (a beverage containing MK615, an *ume* extract) lowers blood transaminase levels in patients with liver disorders such as chronic hepatitis C and NAFLD. *ume* has been used as traditional medicine and food in Japan since ancient

times^[5]. The clinical effects of *ume* have been attributed to the biological activity of MK615. MK615 contains triterpenoids such as OA, UA, lupeol, α -amyrin, and β -sitosterol^[2-4], and has been shown to exert anti-tumor activity against various tumor cell lines, including those of gastric cancer^[5], leukemia^[5], breast cancer^[4,6], hepatocellular carcinoma^[7,8], colorectal cancer^[9], pancreatic cancer^[10], esophageal cancer^[2], and malignant melanoma^[11]. The possible mechanisms underlying the anti-tumor activity of MK615 include induction of apoptosis^[2,6,9,11], induction of autophagy^[9], cell cycle arrest^[2,6,7,10], reduced expression of receptors for advanced glycation end products (RAGE) on membrane surfaces of cancer cells^[8,11], and immunopotentialiation following exposure to X-rays^[4]. MK615 inhibits the release of HMGB1 from mouse macrophage-like RAW264.7 cells^[5]. This inhibitory activity is mediated by Nrf2 activation and HO-1 induction, suggesting that MK615 possesses antioxidative activity^[3]. The authors also previously demonstrated that MK615 suppressed the release of the inflammatory cytokines TNF- α and IL-6 in RAW264.7 cells^[12]. This suppression was mediated by the inactivation of MAPKs and NF- κ B, thus indicating an anti-inflammatory effect of MK615^[12].

The present study reveals that MK615 also exerts hepatoprotective activity in a rat model of D-GalN-induced hepatopathy, given that treatment with MK615 resulted in lower plasma ALT and AST levels accompanied by histological evidence of suppressed destruction of hepatic parenchymal cells when compared with untreated controls. Therefore, MK615 protected the rats from D-GalN-induced hepatopathy.

Previous studies using animal models of D-GalN-induced hepatopathy revealed the activation of MAPKs in the liver^[13], suggesting that liver protection might be achieved by the induction of HO-1^[14] or by the inhibition of NF- κ B in Kupffer cells^[15]. In the present study, the effects of MK615 in suppressing MAPK phosphorylation, inducing HO-1, and inhibiting NF- κ B activation may have protected the rats from D-GalN-induced hepatopathy.

Additionally, it was shown that the intake of Misatol

ME, which contains MK615, lowered the elevated levels of AST and ALT in patients with hepatic impairment. This effect was observed in patients with etiologically different hepatic diseases, i.e., those with hepatitis C and those with NAFLD. No adverse event was associated with the intake of Misatol ME during this study. Furthermore, add-on Misatol ME in combination with UDCA, which had been initiated before the start of Misatol ME intake, resulted in further AST and ALT level reductions in patients with hepatitis C. Moreover, the reduction in ALT levels was also noted in patients who were previously resistant to UDCA therapy.

A major approach to treating HCV infection is antiviral therapy using a combination of IFN and ribavirin^[16]. In cases in which the virus cannot be eradicated or IFN is not indicated, it is important to prevent the progression of HCV infection to liver cirrhosis or liver cancer^[17]. In practice, the progression of HCV infection to liver fibrosis is accelerated by higher levels of ALT^[18-21]. Therefore, when dealing with cases in which virus eradication is difficult, therapeutic interventions that result in lower ALT levels are important for delaying disease progression. In the present study, Misatol ME was shown to significantly reduce ALT levels in patients with chronic hepatitis C, and further reductions in ALT levels were also observed in patients refractory or poorly responsive to UDCA. Given the significance of these findings, Misatol ME warrants further evaluation as a potential treatment for liver disease, including an evaluation of its efficacy during prolonged use. Because Misatol ME is a functional food, conducting the same controlled study to investigate its potential as a medicine was difficult. Nevertheless, the usefulness of Misatol ME as a functional food was clarified. A future investigation is required in which a detailed analysis of the active principal component of Misatol ME should be conducted to elucidate the mechanism underlying its effectiveness as a functional food.

The mechanism underlying the hepatoprotective activity of Misatol ME in patients with chronic hepatitis C appears to involve the anti-inflammatory and antioxidative actions of the MK615 component of Misatol ME. Patients with chronic hepatitis C have high levels of inflammatory cytokines such as TNF- α and IL-6^[22-25]. MK615 inhibits the phosphorylation of MAPKs in LPS-stimulated macrophage-like RAW264.7 cells and suppresses the formation of TNF- α and IL-6 by inhibiting NF- κ B activation^[12]; these findings suggest that the effect of MK615 in suppressing cytokine formation contributes to the suppression of hepatocyte damage in patients with hepatic impairment. Given that Nrf2 activation^[26-29] and HO-1 induction^[14,30-32] are known to be hepatoprotective, the authors previously demonstrated that MK615 and its component OA activate the transcription factor Nrf2 in LPS-stimulated macrophage-like RAW264.7 cells and induce HO-1, one of the target genes^[3]. Whether MK615 also activates Nrf2 and induces HO-1 in clinical cases is unknown. However, it appears highly probable that the antioxidative action of MK615 protects the liver.

MK615 was also effective in patients with NAFLD,

reducing serum AST and ALT levels in these patients, as well as in those with hepatitis C. The involvement of factors such as oxidative stress, insulin resistance, and TNF- α in the progression of NAFLD into non-alcoholic steatohepatitis (NASH) has been suggested^[33-35]. Diet and exercise are the standard therapies for the treatment of such cases^[36,37]. However, the outcomes of these treatments are often unsatisfactory. The effects of MK615 on oxidative stress and insulin resistance in patients with NAFLD are most likely based on the antioxidative effect and the inflammatory cytokine-suppressive action of MK615. Therefore, MK615 therapy may be a promising new means of treating such cases clinically. Obesity is considered a major factor associated with NAFLD. The livers of obese individuals display disturbances in autophagy, with upregulation of autophagy reducing insulin resistance^[38]. Since MK615 has been demonstrated to induce autophagy in colorectal carcinoma cell lines^[9], this effect is also expected to be useful for treatment^[39]. More recently, it was reported that a rat model of NASH exhibited increased expression of RAGE in the liver, suggesting that inhibiting RAGE expression can protect the liver^[40]. MK615 reduces the expression of RAGE on the cell membranes of the high-RAGE expression hepatocellular carcinoma cell line HuH7^[8]. This RAGE suppression may also play a role in the hepatoprotective effects of Misatol ME.

In the present study, MK615 and Misatol ME, which contains MK615, were shown to potentially alleviate various types of hepatic impairment caused by different factors. MK615 contains multiple triterpenoids (OA, UA, lupeol, *etc.*); previous *in vitro* and *in vivo* studies have shown that these triterpenoids protect the liver from various hepatotoxic substances, such as D-galactosamine, acetaminophen, carbon tetrachloride, and ethanol^[27-29,41-47]. As a result of these diverse actions, Misatol ME may exert extensive hepatoprotective effects in patients with hepatic impairments of differing etiologies. Therefore, further studies are required to elucidate the diverse actions of Misatol ME and to assess the significance of its long-term use and its clinical efficacy in suppressing the onset and progression of cancer, as previously demonstrated at experimental level.

COMMENTS

Background

MK615, an extract from Japanese apricot, contains triterpenoids. These substances have been shown to exert various biological actions. In the present study, MK615 (a beverage containing MK615, an *ume* extract) was found to protect hepatocytes from D-galactosamine hydrochloride-induced cytotoxicity in rats. MK615 decreased the elevated alanine aminotransferase (ALT) and aspartate aminotransferase levels in the patients with liver disorder.

Research frontiers

The mechanism underlying the hepatoprotective activity of MK615 in patients with chronic hepatitis C appears to involve the anti-inflammatory and antioxidative actions of the MK615 component of MK615.

Innovations and breakthroughs

This is the first study to indicate that MK615 lowers blood transaminase levels in patients with liver disorders such as chronic hepatitis C and non-alcoholic

fatty liver disease.

Applications

In treating hepatitis C virus infection, therapeutic interventions that result in lower ALT levels are important for delaying disease progression. In the present study, MK615 was shown to significantly reduce the ALT levels in the patients with chronic hepatitis C, and further reductions in ALT levels were observed in the patients refractory or poorly responsive to ursodeoxycholic acid. Given the significance of these findings, MK615 warrants further evaluation as a potential treatment for liver disease, including an evaluation of its efficacy during prolonged use.

Terminology

MK615, an extract from Japanese apricot, contains triterpenoids such as ursolic acid, oleanolic acid, lupeol, α -amyrin, and -sitosterol. Ume extracts exert anti-inflammatory and antioxidative actions.

Peer review

The strongest point of this study should be the histological comparison of the rat livers with galactosamine-induced injury pretreated with MK615 and those not pretreated with MK615. The result is interesting and suggest that MK615 are promising hepatoprotective agents for patients with liver disorders.

REFERENCES

- Miyazawa M, Utsunomiya H, Inada K, Yamada T, Okuno Y, Tanaka H, Tatematsu M. Inhibition of *Helicobacter pylori* motility by (+)-Syringaresinol from unripe Japanese apricot. *Biol Pharm Bull* 2006; **29**: 172-173
- Yamai H, Sawada N, Yoshida T, Seike J, Takizawa H, Kenzaki K, Miyoshi T, Kondo K, Bando Y, Ohnishi Y, Tangoku A. Triterpenes augment the inhibitory effects of anticancer drugs on growth of human esophageal carcinoma cells in vitro and suppress experimental metastasis in vivo. *Int J Cancer* 2009; **125**: 952-960
- Kawahara K, Hashiguchi T, Masuda K, Saniabadi AR, Kikuchi K, Tancharoen S, Ito T, Miura N, Morimoto Y, Biswas KK, Nawa Y, Meng X, Oyama Y, Takenouchi K, Shrestha B, Sameshima H, Shimizu T, Adachi T, Adachi M, Maruyama I. Mechanism of HMGB1 release inhibition from RAW264.7 cells by oleanolic acid in *Prunus mume* Sieb. et Zucc. *Int J Mol Med* 2009; **23**: 615-620
- Al-Jahdari WS, Sakurai H, Yoshida Y, Mobaraki A, Suzuki Y, Nakano T. MK615, a prospective anti-proliferative agent, enhances CD4/CD8 ratio after exposure to irradiation. *Int J Radiat Biol* 2011; **87**: 81-90
- Adachi M, Suzuki Y, Mizuta T, Osawa T, Adachi T, Osaka K, Suzuki K, Shiojima K, Arai Y, Masuda K, Uchiyama M, Oyamada T, Clerici M. The "Prunus mume Sieb. et Zucc" (Ume) is a Rich Natural Source of Novel Anti-Cancer Substance. *Int J Food Prop* 2007; **10**: 375-384
- Nakagawa A, Sawada T, Okada T, Ohsawa T, Adachi M, Kubota K. New antineoplastic agent, MK615, from UME (a Variety of) Japanese apricot inhibits growth of breast cancer cells in vitro. *Breast J* 2007; **13**: 44-49
- Okada T, Sawada T, Osawa T, Adachi M, Kubota K. A novel anti-cancer substance, MK615, from ume, a variety of Japanese apricot, inhibits growth of hepatocellular carcinoma cells by suppressing Aurora A kinase activity. *Hepatogastroenterology* 2007; **54**: 1770-1774
- Sakuraoka Y, Sawada T, Okada T, Shiraki T, Miura Y, Hiraiishi K, Ohsawa T, Adachi M, Takino J, Takeuchi M, Kubota K. MK615 decreases RAGE expression and inhibits TAGE-induced proliferation in hepatocellular carcinoma cells. *World J Gastroenterol* 2010; **16**: 5334-5341
- Mori S, Sawada T, Okada T, Ohsawa T, Adachi M, Keiichi K. New anti-proliferative agent, MK615, from Japanese apricot "Prunus mume" induces striking autophagy in colon cancer cells in vitro. *World J Gastroenterol* 2007; **13**: 6512-6517
- Okada T, Sawada T, Osawa T, Adachi M, Kubota K. MK615 inhibits pancreatic cancer cell growth by dual inhibition of Aurora A and B kinases. *World J Gastroenterol* 2008; **14**: 1378-1382
- Matsushita S, Tada K, Kawahara K, Kawai K, Hashiguchi T, Maruyama I, Kanekura T. Advanced malignant melanoma responds to *Prunus mume* Sieb. Et Zucc (Ume) extract: Case report and in vitro study. *Exp and Ther Med* 2010; **1**: 569-574
- Morimoto Y, Kikuchi K, Ito T, Tokuda M, Matsuyama T, Noma S, Hashiguchi T, Torii M, Maruyama I, Kawahara K. MK615 attenuates Porphyromonas gingivalis lipopolysaccharide-induced pro-inflammatory cytokine release via MAPK inactivation in murine macrophage-like RAW264.7 cells. *Biochem Biophys Res Commun* 2009; **389**: 90-94
- Nishioka H, Kishioka T, Iida C, Fujii K, Ichi I, Kojo S. Activation of mitogen activated protein kinase (MAPK) during D-galactosamine intoxication in the rat liver. *Bioorg Med Chem Lett* 2006; **16**: 3019-3022
- Wen T, Wu ZM, Liu Y, Tan YF, Ren F, Wu H. Upregulation of heme oxygenase-1 with hemin prevents D-galactosamine and lipopolysaccharide-induced acute hepatic injury in rats. *Toxicology* 2007; **237**: 184-193
- Hoffmann F, Sass G, Zillies J, Zahler S, Tiegs G, Hartkorn A, Fuchs S, Wagner J, Winter G, Coester C, Gerbes AL, Vollmar AM. A novel technique for selective NF-kappaB inhibition in Kupffer cells: contrary effects in fulminant hepatitis and ischaemia-reperfusion. *Gut* 2009; **58**: 1670-1678
- Fried MW, Shiffman ML, Reddy KR, Smith C, Marinos G, Gonçales FL, Häussinger D, Diago M, Carosi G, Dhumeaux D, Craxi A, Lin A, Hoffman J, Yu J. Peginterferon alfa-2a plus ribavirin for chronic hepatitis C virus infection. *N Engl J Med* 2002; **347**: 975-982
- Fassio E. Hepatitis C and hepatocellular carcinoma. *Ann Hepatol* 2010; **9** Suppl: 119-122
- Tarao K, Rino Y, Ohkawa S, Shimizu A, Tamai S, Miyakawa K, Aoki H, Imada T, Shindo K, Okamoto N, Totsuka S. Association between high serum alanine aminotransferase levels and more rapid development and higher rate of incidence of hepatocellular carcinoma in patients with hepatitis C virus-associated cirrhosis. *Cancer* 1999; **86**: 589-595
- Toyoda H, Kumada T, Kiriyama S, Sone Y, Tanikawa M, Hisanaga Y, Hayashi K, Honda T, Kuzuya T. Influence of age, sex, and degree of liver fibrosis on the association between serum alanine aminotransferase levels and liver inflammation in patients with chronic hepatitis C. *Dig Dis Sci* 2004; **49**: 295-299
- Rino Y, Tarao K, Morinaga S, Ohkawa S, Miyakawa K, Hirokawa S, Masaki T, Tarao N, Yukawa N, Saeki H, Takanashi Y, Imada T. Reduction therapy of alanine aminotransferase levels prevent HCC development in patients with HCV-associated cirrhosis. *Anticancer Res* 2006; **26**: 2221-2226
- Kurokawa M, Hiramatsu N, Oze T, Mochizuki K, Yakushijin T, Kurashige N, Inoue Y, Igura T, Imanaka K, Yamada A, Oshita M, Hagiwara H, Mita E, Ito T, Inui Y, Hijioka T, Yoshihara H, Inoue A, Imai Y, Kato M, Kiso S, Kanto T, Takehara T, Kasahara A, Hayashi N. Effect of interferon alpha-2b plus ribavirin therapy on incidence of hepatocellular carcinoma in patients with chronic hepatitis. *Hepatol Res* 2009; **39**: 432-438
- Nelson DR, Lim HL, Marousis CG, Fang JW, Davis GL, Shen L, Urdea MS, Kolberg JA, Lau JY. Activation of tumor necrosis factor-alpha system in chronic hepatitis C virus infection. *Dig Dis Sci* 1997; **42**: 2487-2494
- Gochee PA, Jonsson JR, Clouston AD, Pandeya N, Purdie DM, Powell EE. Steatosis in chronic hepatitis C: association with increased messenger RNA expression of collagen I, tumor necrosis factor-alpha and cytochrome P450 2E1. *J Gastroenterol Hepatol* 2003; **18**: 386-392
- Malaguarnera M, Di Fazio I, Romeo MA, Restuccia S, Laurino A, Trovato BA. Elevation of interleukin 6 levels in patients with chronic hepatitis due to hepatitis C virus. *J Gastroenterol* 1997; **32**: 211-215
- Oyanagi Y, Takahashi T, Matsui S, Takahashi S, Boku S, Takahashi K, Furukawa K, Arai F, Asakura H. Enhanced

- expression of interleukin-6 in chronic hepatitis C. *Liver* 1999; **19**: 464-472
- 26 **Okada K**, Shoda J, Taguchi K, Maher JM, Ishizaki K, Inoue Y, Ohtsuki M, Goto N, Takeda K, Utsunomiya H, Oda K, Warabi E, Ishii T, Osaka K, Hyodo I, Yamamoto M. Ursodeoxycholic acid stimulates Nrf2-mediated hepatocellular transport, detoxification, and antioxidative stress systems in mice. *Am J Physiol Gastrointest Liver Physiol* 2008; **295**: G735-G747
- 27 **Liu J**, Wu Q, Lu YF, Pi J. New insights into generalized hepatoprotective effects of oleanolic acid: key roles of metallothionein and Nrf2 induction. *Biochem Pharmacol* 2008; **76**: 922-928
- 28 **Reisman SA**, Aleksunes LM, Klaassen CD. Oleanolic acid activates Nrf2 and protects from acetaminophen hepatotoxicity via Nrf2-dependent and Nrf2-independent processes. *Biochem Pharmacol* 2009; **77**: 1273-1282
- 29 **Wang X**, Ye XL, Liu R, Chen HL, Bai H, Liang X, Zhang XD, Wang Z, Li WL, Hai CX. Antioxidant activities of oleanolic acid in vitro: possible role of Nrf2 and MAP kinases. *Chem Biol Interact* 2010; **184**: 328-337
- 30 **Zhu Z**, Wilson AT, Mathahs MM, Wen F, Brown KE, Luxon BA, Schmidt WN. Heme oxygenase-1 suppresses hepatitis C virus replication and increases resistance of hepatocytes to oxidant injury. *Hepatology* 2008; **48**: 1430-1439
- 31 **Roller J**, Laschke MW, Scheuer C, Menger MD. Heme oxygenase (HO)-1 protects from lipopolysaccharide (LPS)-mediated liver injury by inhibition of hepatic leukocyte accumulation and improvement of microvascular perfusion. *Langenbecks Arch Surg* 2010; **395**: 387-394
- 32 **Immenschuh S**, Baumgart-Vogt E, Mueller S. Heme oxygenase-1 and iron in liver inflammation: a complex alliance. *Curr Drug Targets* 2010; **11**: 1541-1550
- 33 **Day CP**, James OF. Steatohepatitis: a tale of two "hits"? *Gastroenterology* 1998; **114**: 842-845
- 34 **Ekstedt M**, Franzén LE, Mathiesen UL, Thorelius L, Holmqvist M, Bodemar G, Kechagias S. Long-term follow-up of patients with NAFLD and elevated liver enzymes. *Hepatology* 2006; **44**: 865-873
- 35 **Tomita K**, Tamiya G, Ando S, Ohsumi K, Chiyo T, Mizutani A, Kitamura N, Toda K, Kaneko T, Horie Y, Han JY, Kato S, Shimoda M, Oike Y, Tomizawa M, Makino S, Ohkura T, Saito H, Kumagai N, Nagata H, Ishii H, Hibi T. Tumour necrosis factor alpha signalling through activation of Kupffer cells plays an essential role in liver fibrosis of non-alcoholic steatohepatitis in mice. *Gut* 2006; **55**: 415-424
- 36 **Suzuki A**, Lindor K, St Saver J, Lymp J, Mendes F, Muto A, Okada T, Angulo P. Effect of changes on body weight and lifestyle in nonalcoholic fatty liver disease. *J Hepatol* 2005; **43**: 1060-1066
- 37 **Omagari K**, Morikawa S, Nagaoka S, Sadakane Y, Sato M, Hamasaki M, Kato S, Masuda J, Osabe M, Kadota T, Sera K. Predictive factors for the development or regression of Fatty liver in Japanese adults. *J Clin Biochem Nutr* 2009; **45**: 56-67
- 38 **Rautou PE**, Mansouri A, Lebrec D, Durand F, Valla D, Moreau R. Autophagy in liver diseases. *J Hepatol* 2010; **53**: 1123-1134
- 39 **Amir M**, Czaja MJ. Autophagy in nonalcoholic steatohepatitis. *Expert Rev Gastroenterol Hepatol* 2011; **5**: 159-166
- 40 **Wu J**, Zhao MY, Zheng H, Zhang H, Jiang Y. Pentoxifylline alleviates high-fat diet-induced non-alcoholic steatohepatitis and early atherosclerosis in rats by inhibiting AGE and RAGE expression. *Acta Pharmacol Sin* 2010; **31**: 1367-1375
- 41 **Liu J**, Liu Y, Klaassen CD. Protective effect of oleanolic acid against chemical-induced acute necrotic liver injury in mice. *Zhongguo Yao Li Xue Bao* 1995; **16**: 97-102
- 42 **Liu Y**, Kreppel H, Liu J, Choudhuri S, Klaassen CD. Oleanolic acid protects against cadmium hepatotoxicity by inducing metallothionein. *J Pharmacol Exp Ther* 1993; **266**: 400-406
- 43 **Liu J**, Liu Y, Madhu C, Klaassen CD. Protective effects of oleanolic acid on acetaminophen-induced hepatotoxicity in mice. *J Pharmacol Exp Ther* 1993; **266**: 1607-1613
- 44 **Tang XH**, Gao J, Fang F, Chen J, Xu LZ, Zhao XN, Xu Q. Hepatoprotection of oleanolic acid is related to its inhibition on mitochondrial permeability transition. *Am J Chin Med* 2005; **33**: 627-637
- 45 **Saravanan R**, Viswanathan P, Pugalendi KV. Protective effect of ursolic acid on ethanol-mediated experimental liver damage in rats. *Life Sci* 2006; **78**: 713-718
- 46 **Martin-Aragón S**, de las Heras B, Sanchez-Reus MI, Benedi J. Pharmacological modification of endogenous antioxidant enzymes by ursolic acid on tetrachloride-induced liver damage in rats and primary cultures of rat hepatocytes. *Exp Toxicol Pathol* 2001; **53**: 199-206
- 47 **Sunitha S**, Nagaraj M, Varalakshmi P. Hepatoprotective effect of lupeol and lupeol linoleate on tissue antioxidant defence system in cadmium-induced hepatotoxicity in rats. *Fitoterapia* 2001; **72**: 516-523

S- Editor Gou SX L- Editor A E- Editor Zhang DN

siRNA-mediated downregulation of TC21 sensitizes esophageal cancer cells to cisplatin

Md. Raghibul Hasan, Shyam Singh Chauhan, Rinu Sharma, Ranju Ralhan

Md. Raghibul Hasan, Shyam Singh Chauhan, Department of Biochemistry, All India Institute of Medical Sciences, New Delhi 110029, India

Rinu Sharma, Department of Biotechnology, School of Biotechnology, Guru Gobind Singh Indraprastha University, New Delhi 110075, India

Ranju Ralhan, Department of Otolaryngology-Head and Neck Surgery, Joseph and Mildred Sonshine Family Centre for Head and Neck Diseases, Mount Sinai Hospital, Toronto, ON M5G 1X5, Canada

Ranju Ralhan, Department of Pathology and Laboratory Medicine, Alex Simona Shnaider Laboratory for Molecular Oncology, Mount Sinai Hospital, Toronto, ON M5G 1X5, Canada

Author contributions: Hasan MR designed the study and carried out the experimental procedures, and significantly contributed to the analysis of data and manuscript preparation; Chauhan SS contributed to drafting the manuscript; Sharma R conceptualized and designed the study, contributed in the initial standardization of the RNAi experiments and was involved in interpretation of data and drafting the manuscript; Ralhan R was involved in drafting the manuscript, revising it critically for important intellectual content, and has given approval for the final version; all authors approve the final manuscript.

Supported by Department of Science and Technology, Government of India

Correspondence to: Dr. Rinu Sharma, Assistant Professor, School of Biotechnology, Guru Gobind Singh Indraprastha University, Sector 16 C, Dwarka, New Delhi 110075, India. rinusharma@gmail.com

Telephone: +91-11-25302312 Fax: +91-11-25302111

Received: November 24, 2011 Revised: May 7, 2012

Accepted: May 26, 2012

Published online: August 21, 2012

We demonstrated the effect of TC21 downregulation of cell signaling in esophageal cancer cells by assessing the phosphorylation status of its downstream targets, phosphoinositide 3-kinase (PI3K), phosphatase and tensin homolog (PTEN), protein kinase B (pAkt), nuclear factor- κ B (NF- κ B) and cyclinD1 using specific antibodies. Cell survival analysis after cisplatin treatment was carried out by cell viability assay and cell cycle analysis using flow cytometry.

RESULTS: TC21 knockdown in human ESCC cell line TE13 cells, showed only a marginal increase (14.2%) in cell death compared with control cells. The expressions of the signaling proteins PI3K and pAkt, transcription factor NF- κ B, and cell cycle protein cyclin D1 were markedly decreased in response to TC21 downregulation, whereas the level of pPTEN, an antagonist of PI3K, was increased. In addition, we evaluated the potential of TC21 as a putative target for sensitizing ESCC cells to the chemotherapeutic agent cisplatin. Increased cell death (38.4%) was observed in cells treated with cisplatin after TC21 knockdown compared with cells which were treated with cisplatin alone (20% cell death).

CONCLUSION: Results suggest that TC21 mediates its effects *via* the PI3K-Akt pathway, NF- κ B and cyclin D1, and enhances chemoresistance in esophageal cancer cells.

© 2012 Baishideng. All rights reserved.

Key words: TC21; Esophageal squamous cell carcinoma; siRNA; Cisplatin; Chemosensitivity

Peer reviewer: Itaru Endo, Professor, Gastroenterological Surgery, Graduate School of Medicine, Yokohama City University, 3-9 Fukuura, Kanazawa-ku, Yokohama 2360004, Japan

Hasan MR, Chauhan SS, Sharma R, Ralhan R. siRNA-mediated downregulation of TC21 sensitizes esophageal cancer cells to cisplatin. *World J Gastroenterol* 2012; 18(31): 4127-4135 Available from: URL: <http://www.wjgnet.com/1007-9327/full/v18/i31/4127.htm> DOI: <http://dx.doi.org/10.3748/wjg.v18.i31.4127>

Abstract

AIM: To determine the functional significance of TC21 in esophageal squamous cell carcinoma (ESCC).

METHODS: TC21 siRNA transfection was carried out using Hyperfectamine to knock down TC21, and transcripts were analyzed by reverse transcription-polymerase chain reaction and protein by Western blotting.

INTRODUCTION

Esophageal cancer is one of the most aggressive malignancies of the gastrointestinal tract, ranking as the sixth most common cancer among males and ninth most common cancer among females globally. Esophageal squamous cell carcinoma (ESCC) is the predominant histological subtype of esophageal cancer in India, characterized by a high mortality rate and strong association with dietary habits and lifestyle^[1,2]. It is the second most common cancer among males and fourth most common cancer among females in India^[3]. Despite advances in multimodality therapy, because of its insidious symptomatology, late stage of diagnosis and poor efficacy of treatment, the prognosis of patients with ESCC still remains poor, with an average 5-year survival of < 10% globally^[4,5] and 12% in India^[6,7].

TC21/R-Ras2 is the only member of the R-Ras subfamily for which overexpression or mutants were detected in human tumor cells, including cells derived from uterine sarcoma^[8], ovarian cancer^[9] and mammary tumors^[10]. Increased expression of TC21 was found in breast cancer cells^[11-13]. Our laboratory identified TC21 overexpression in human oral squamous cell carcinomas using differential display and verified its increased expressions independently in oral cancer^[14,15], as well as in esophageal carcinomas^[16]. These clinical studies suggested that deregulated TC21 activity might contribute to human oncogenesis, however like R-Ras, the functions of TC21 are not completely understood.

The R-Ras family of Ras-related proteins, including R-Ras, TC21 (R-Ras2), and M-Ras (R-Ras3), share 55% amino acid identity with H-Ras, including identical core effector regions^[17]. Besides H-, K-, and N-Ras, TC21 is the only Ras superfamily member known to transform epithelial and fibroblast cell lines^[18], and induce tumor formation *in vivo*^[9]. Despite their similarities, R-Ras and TC21/R-Ras2 exhibited differential transforming properties in a variety of cell lines. In NIH 3T3 fibroblasts, TC21/R-Ras2 induced foci formation and tumor growth more efficiently than R-Ras^[18]. TC21/R-Ras2 also potently transformed Rat-1 fibroblasts and various epithelial cell lines, including MCF-10A, RIE-1, and EpH4^[19,20]. In comparison, R-Ras was unable to transform Rat-1 fibroblasts, but promoted tumor growth in cervical epithelial cells^[21,22]. Phosphoinositide 3-kinase (PI3K) is the predominant effector of R-Ras and TC21/R-Ras2 transforming activity; however, these oncogenes also activate Raf1, Ral-GDS, extracellular signal-regulated kinase (ERK) 1/2, c-Jun NH2-terminal kinase, and p38 mitogen-activated protein kinase (MAPK) in a cell type-specific manner^[23-25]. Previous reports suggested that TC21 induces its effects in multiple ways in different cell types, for example TC21 has been shown to activate p38 MAPK in Cos7 cells^[18], and p38 MAPK activation is important for TC21-induced ureteric bud cell proliferation^[26], therefore, TC21-mediated signaling is tissue specific^[20-22,26,27]. We have earlier identified TC21 to be overexpressed in ESCC^[16], but its role in ESCC is not well understood. This study was designed to determine the

functional significance of TC21 protein in esophageal cancer. Further, we aimed to analyze the effect of TC21 downregulation on the sensitivity of ESCC cells to chemotherapeutic agents using cisplatin as a prototype.

MATERIALS AND METHODS

Reagents

Cisplatin, propidium iodide and protease inhibitor cocktail were procured from Sigma-Aldrich (St. Louis, MO, United States); protein assay reagent was obtained from Bio-Rad Laboratories (Hercules, CA, United States); lipofectamine, TC21 small interfering RNA (siRNA) and scrambled sequence siRNA from Qiagen, RPMI 1640 (Invitrogen); primary antibodies directed against protein kinase B [pAkt, (Ser 473)], pAkt (Thr 308), protein Glycogen synthase kinase 3β [pGSK3β (Ser9)], total Akt, phosphatase and tensin homolog [pPTEN, (Ser 380)], and protein Phosphoinositide-dependent kinase-1 [pPDK1 (Ser 241)] were procured from Cell Signaling Technology (Beverly, MA, United States); cyclin D1 and GSK3β were obtained from Santa Cruz Biotechnology Inc., (California, United States), β-actin (AC-15), GAPDH (Abcam Inc. Cambridge, MA, United States). Secondary antibodies, alkaline phosphatase conjugated goat anti-mouse IgG, goat anti rabbit IgG or rabbit anti-goat IgG, were from Cell Signaling Technology (Beverly, MA, United States). Enhanced chemiluminescence (ECL) Western blotting detection reagents were obtained from Santa Cruz Biotechnology Inc., CA, United States.

Cells and cell culture

A human ESCC line, TE13, were grown in RPMI-1640 supplemented with 10% heat inactivated fetal bovine serum, 100 units/mL penicillin and 100 μg/mL streptomycin. Cells were incubated at 37 °C in 5% humidified CO₂ enriched atmosphere and routinely sub-cultured every 2 d by trypsinization.

Cisplatin treatment and cell viability assay

Cells were seeded and grown to 60%-70% confluence in triplicates prior to addition of cisplatin. The cells were treated with varying doses of cisplatin (0-10 μg/mL) for 24 h. Thereafter, the cells were harvested and LD50 was determined by measuring the cell viability using 3-(4,5-dimethylthiazol-2-yl)-2,5-diphenyltetrazolium bromide (MTT) reagent according to the manufacturer's instructions. The conversion of MTT to formazan by mitochondrial dehydrogenases was measured at wavelength 570 nm in a microtiter plate reader. The percentage cell death was calculated individually for each dose as follows: $(A_{\text{control}} - A_{\text{treated}}) / A_{\text{control}} \times 100$, as described earlier^[28]. For further experiments, the cisplatin concentration required to inhibit cell growth by 50% (LD50) was determined by interpolation from dose-response curves.

RNA interference

TE13 cells were seeded and grown to 70% confluence

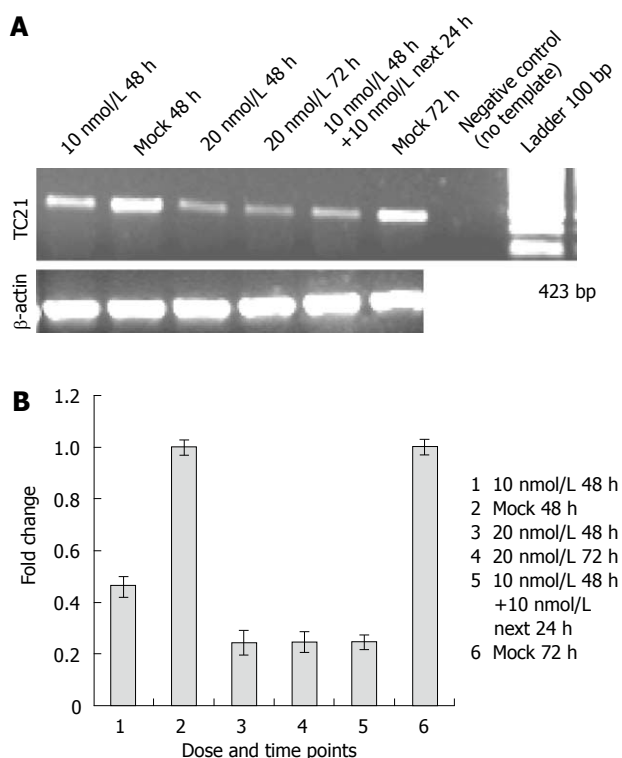


Figure 1 Small interfering RNA-targeting TC21/R-Ras2 was transfected in TE13 cells. A: Reverse transcriptase-polymerase chain reaction (RT-PCR) analysis: Small interfering RNA (siRNA)-targeting TC21/R-Ras2 was transfected in TE13 cells in a dose-dependent manner. After 48 h and 72 h, cells were lysed, RNA was isolated and the mRNA level was determined semiquantitatively by RT-PCR using TC21-specific primers; B: Bar diagram showing fold change in level of TC21 transcripts after TC21 knockdown.

in growth medium without antibiotics. Transfection was carried out using Hyperfectamine according to the manufacturer's instructions, using TC21 siRNA or scrambled sequence siRNA at final concentrations of 20 nmol/L and 10 nmol/L, respectively. After 24 h, 48 h and 72 h cells were harvested for reverse transcription-polymerase chain reaction (RT-PCR) and Western blotting analysis for detection of TC21. For cisplatin treatment the cells were transfected with TC21 siRNA for 48 h, followed by cisplatin treatment for 24 h and compared to untreated cells as controls, transfected with a scrambled sequence siRNA (negative control), or with the transfection reagent alone (mock). At least three independent experiments were performed with reproducible results. MAPK siRNA was used as a positive control and was detected by Western blotting for ERK.

RNA isolation

Total RNA was isolated from TE13 cells (untreated and TC21 siRNA transfected cells) using Qiagen kit following the manufacturer's instructions or the standard protocol. DNase I treatment of RNA was carried out using the Message Clean Kit (Gen Hunter Corp., Brookline, MASS, United States). RNA was quantified using formaldehyde agarose gel and by measuring spectrophotometrically the absorbance at 260 nm and 280 nm (ND-1000 UV-Vis Spectrophotometer from NanoDrop Technologies).

RT-PCR analysis

Briefly, cDNA was prepared using 1 µg of total RNA and Moloney murine leukemia virus reverse transcriptase (Gibco BRL, Life Technologies Inc., Gaithersburg, MD, United States) with oligo dT as the primer. Primers used for amplification of TC21-specific sequences were forward 5'-CCTTAGACCAAGAAGCTGGC-3' and reverse 5'-CAGGCATTTGGTATTTTGGC-3'. The PCR cycling parameters were initial denaturation at 94 °C for 5 min; 30 cycles of 94 °C for 1 min, 54 °C for 1 min and 72 °C for 2 min and final extension at 72 °C for 10 min. PCR for β-actin was reverse transcribed for all the samples to check for the quality and quantity of the initial RNA used. The PCR-amplified products were electrophoresed on 1.2% agarose gels and bands were visualized by ethidium bromide staining.

Protein extraction and Western blotting

After the above described TC21 siRNA treatment with or without cisplatin, TE13 cells were harvested and protein extracts were made by lysing cells in buffer, containing 50 mmol Tris-HCl, pH 7.5, 150 mmol NaCl, 1% Triton X-100, 10% glycerol, 1 mmol DTT, 10 mmol NaF, supplemented with 1 mmol activated Na₃VO₄ and 1 × protease inhibitor cocktail. Protein concentration was measured using Bradford reagent (Sigma) and bovine serum albumin as standard. Proteins were separated by Sodium Dodecyl Sulfate Polyacrylamide Gel Electrophoresis (SDS-PAGE) and transferred to polyvinylidene fluoride membranes by electroblotting. Membranes were blocked with phosphate-buffered saline containing 1% bovine serum albumin, followed by incubation with primary and secondary antibodies. Detection of antibody-protein complexes was done using an ECL Western blotting kit according to the manufacturer's instructions.

Flow cytometry

TE13 cells were transfected with TC21 siRNA, cisplatin alone, or a combination of siRNA and cisplatin for specific time intervals as described above, cells were harvested and resuspended in phosphate-buffered saline. For cell cycle analysis, cells were fixed in 70% ethanol overnight at -20 °C and stained with propidium iodide (20 µg/mL) and RNaseA (10 µg/mL). All flow cytometric analyses were done using a FACS Caliber flow cytometer (San Jose, CA, United States). The acquired data were analyzed using BD FACS Diva software. For each measurement 10 000 cells were analyzed.

Statistical analysis

The Western blotting data were subjected to statistical analyses using SPSS 10.0 software (Chicago). Densitometry analysis of Western blotting was carried out using ChemiImager 4400 software. The integrated density value was compared with the loading control. The protein expression of 4 different groups (mock, scrambled sequence, TC21siRNA 48 h treatment and TC21siRNA 72 h treatment) were compared using one-way analysis

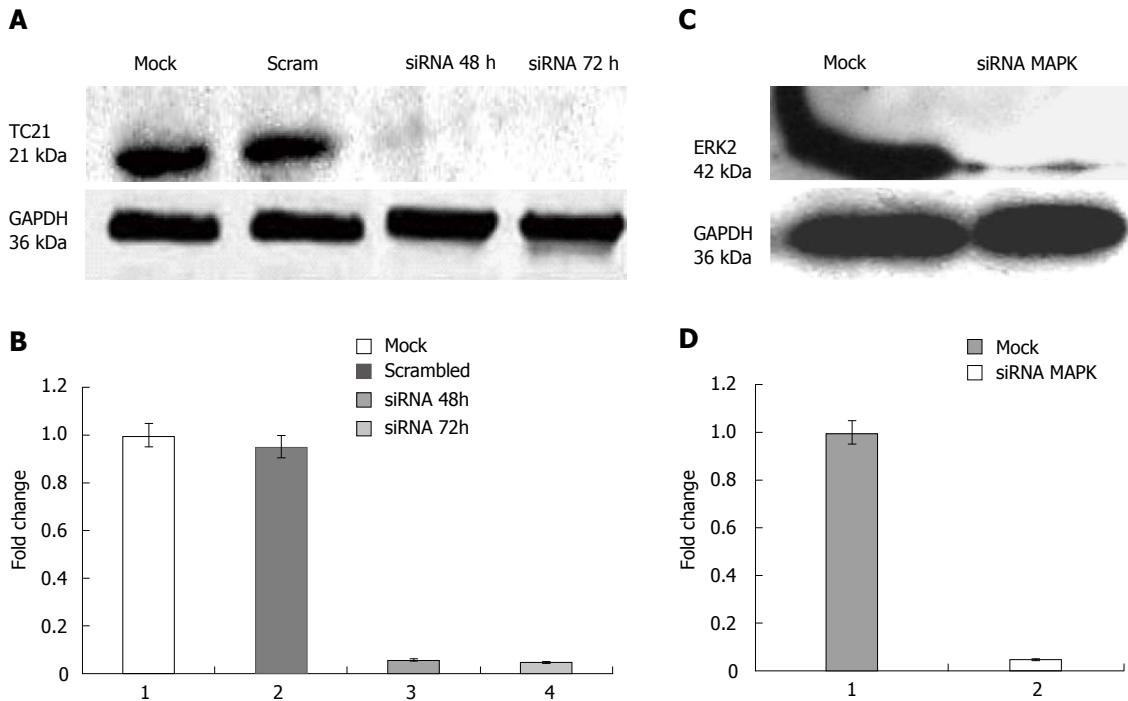


Figure 2 TC21 protein and extracellular signal-regulated kinase 2 level. A: Western blotting was carried out using specific antibody; the panel shows inhibition of TC21 protein compared with cells without transfection or transfection with a negative control siRNA (scrambled sequence); B: Bar diagram showing more than 95% decrease in TC21 protein level after TC21 knockdown compared with untreated mock and nonspecific scrambled sequence; C: Western blotting analyses show inhibition of ERK2 protein by targeted siRNA as positive control; D: Bar diagram showing more than 98% decrease in ERK2 level after MAPK knockdown compared with untreated mock and nonspecific scrambled siRNA sequence. ERK: Extracellular signal-regulated kinase; MAPK: Mitogen-activated protein kinase; GAPDH: Glyceraldehyde-3-phosphate dehydrogenase.

of variance (ANOVA). ANOVA was applied for statistical analysis with the *post hoc* (Bonferroni) multiple range test. $P < 0.05$ was considered to be significant.

RESULTS

TC21/R-Ras2 gene silencing using siRNA

Evaluation of TC21 mRNA and protein levels 48 h and 72 h post-transfection of TC21 siRNA revealed an 80% reduction in mRNA levels and a 95% reduction in TC21 protein levels as compared with the respective controls transfected with scrambled siRNA (negative control) or with transfection reagent alone (mock) as shown in Figure 1A, B and Figure 2A, B. MAPK siRNA was used as a positive control and its detection was carried out by Western blotting for ERK (Figure 2C, D).

TC21 activates the Akt pathway in ESCC

Since TC21 has been shown to activate PI3K, we investigated the role of the PI3K pathway in TC21-mediated esophageal tumorigenesis. siRNA-mediated TC21 down-regulation resulted in a significant decrease in the expression of phosphorylated Akt/PKB with $P < 0.001$ (Ser 473, Thr 308 showed equal reduction) and phosphorylated glycogen synthase kinase-3 β , pGSK3 β (Ser 9), without any change in the levels of total Akt (Figure 3A, B). A significant increase in expression of PTEN was observed in TC21 siRNA-treated TE13 cells compared with con-

trols ($P < 0.001$). Since PTEN is a PI3K antagonist and inhibits downstream signaling through Akt, its upregulation in siRNA-treated cells suggests the involvement of PI3K in TC21-mediated esophageal tumorigenesis. Moreover, knockdown of TC21 resulted in a significant decrease in PDK1 expression which may be responsible for the decrease in the expression of pAkt/PKB, resulting in reduced levels of pGSK3 β (Figure 3A, B).

TC21 activates the anti-apoptotic factor nuclear factor- κ B and cyclin D1

Western blotting analysis of whole cell lysates from TC21-knockdown TE13 cells probed with antibodies specific for the p65 subunit of nuclear factor- κ B (NF- κ B) and cyclin D1 showed significant decrease in NF- κ B and cyclin D1 proteins compared with untransfected controls (Figure 3A, B). Our results suggest that NF- κ B targeting the growth promoting protein cyclin D1, may be the downstream targets of TC21 signaling through the PI3-K/Akt pathway, thereby increasing survival of esophageal cancer cells.

TC21 knockdown does not affect P-Raf protein

There was no significant change in phosphorylated Raf protein expression observed in TC21-knockdown esophageal cancer cells for 72 h of transfection in comparison with control cells, but there was a decreased P-Raf protein level observed in TC21 siRNA treated for 48 h (Figure 3A, B).

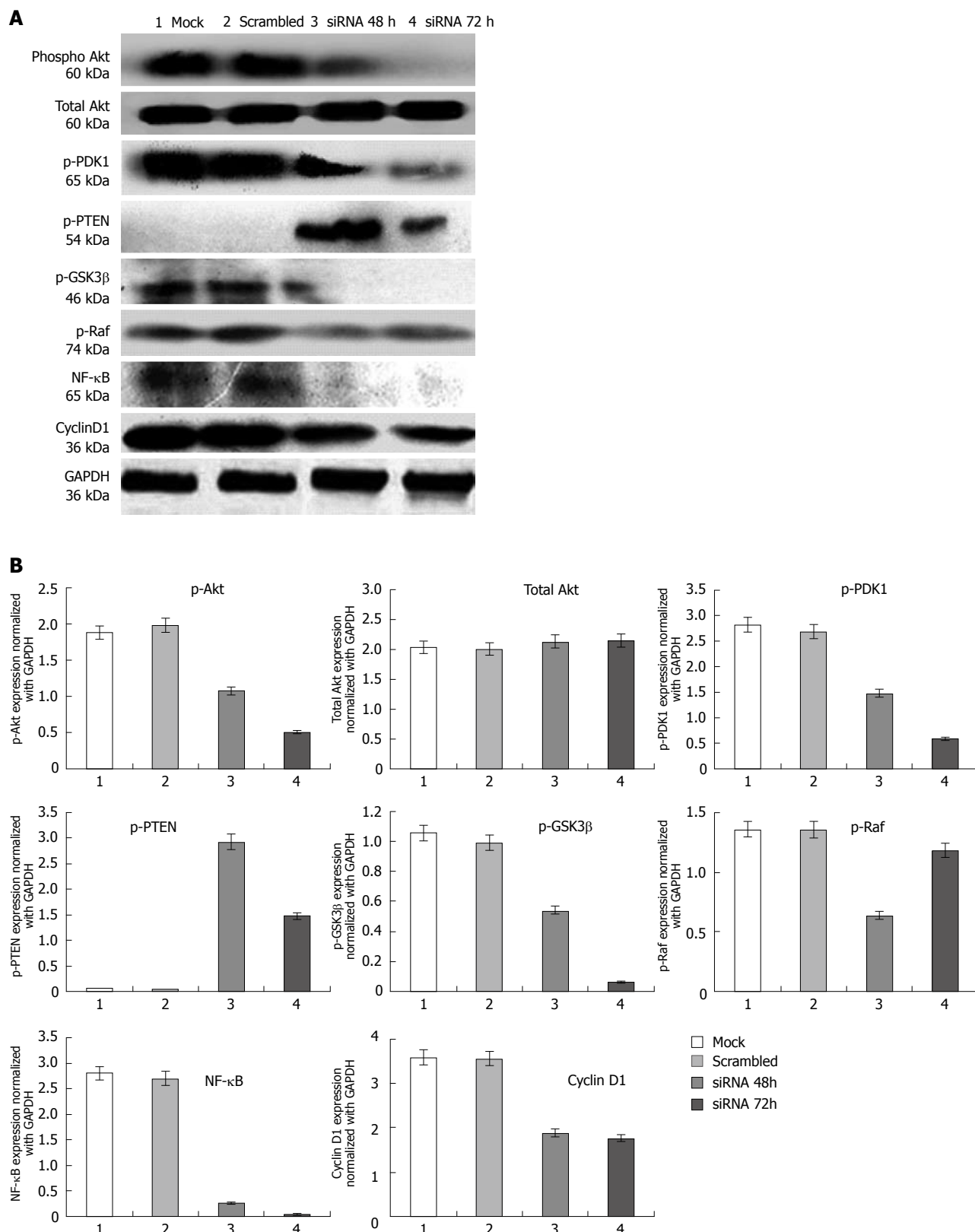


Figure 3 Expression of proteins in esophageal squamous cancer cells TE13 and compared with control. A: Expression analysis of protein kinase B (pAkt), total Akt, protein Glycogen synthase kinase 3β (pGSK3β), pRaf, protein Phosphoinositide-dependent kinase-1 (pPDK1), phosphatase and tensin homolog (pPTEN), nuclear factor-κB (NF-κB) and cyclin D1 proteins compared in esophageal squamous cancer cells TE13. Lane 1: Mock; Lane 2: Scrambled (non-target siRNA); Lane 3: TC21 siRNA transfected for 48 h; Lane 4: TC21 siRNA transfected for 72 h; B: Bar diagram showing relative levels of proteins in comparison with control protein GAPDH. GAPDH: Glyceraldehyde-3-phosphate dehydrogenase.

Table 1 Cell cycle analyses of siRNA-treated TE13 cells using flow cytometry

Experimental parameters	SubG0 (%)	G1 (%)	S (%)	G2/M (%)
Untreated TE13 ¹ cells for 24 h	5.7	37	21	34.8
Cisplatin treatment (8 µg/mL) for 24 h	17.8	30.6	11.8	38.2
Untreated TE13 cells for 48 h	7.9	34.7	10	41
TC21 siRNA ² (20 nmol) transfection for 48 h	14.2	22.8	12.2	42.3
Untreated TE13 cells for 72 h	10.3	36.7	27.7	25.8
TC21 siRNA transfection (20 nmol) for 48 h followed by cisplatin treatment for 24 h (total time of treatment is 72 h)	38.4	23.8	11.9	12.8

¹Esophageal squamous cell carcinoma cells; ²Small interfering RNA.

Knockdown of TC21 results in decreased G1/S population

TC21-knockdown TE13 cells resulted in a marginal increase (14.2%) in the subG0 population (cell death) compared with the mock control cells (7.9%), while the G1/S population decreased from 44% to 35% in the siRNA-treated cells (Figure 5A-2, B and Table 1).

Effect of cisplatin treatment on TE13 cells

The TE13 cells were treated with varying doses of cisplatin (0-10 µg/mL) for 24 h and LD50 was calculated by measuring the cell viability using MTT (Figure 4). LD50 was found to be 9 µg/mL. TE13 were treated with 8 µg/mL cisplatin for 24 h and flow cytometric analysis was performed to determine the cell cycle distribution. Cisplatin-treated TE13 cells showed a marginal increase in cell death (17.8%) compared with untreated cells (5.7%). There was a decrease in the S phase (11.8%) compared with 21% in the untreated control cells (Figure 5A-4, B and Table 1).

Knockdown of TC21 sensitizes TE13 cells to cisplatin treatment

The combined effect of TC21 siRNA and cisplatin treatment on TE13 cells was determined. In TC21 siRNA-transfected TE13 cells, 38.4% cell death was observed after exposure to 8 µg/mL cisplatin compared with 10.3% cell death in the untreated controls; 23.8% cells were found in the G₁ phase compared with 36.7% in the controls. Further, a decrease in S phase fraction (11.9%) was observed compared with the untreated control cells (27.7%) (Figure 5A-6, B and Table 1).

DISCUSSION

This study was focused on the effect of TC21 down-regulation on cell signaling in ESCC and its effect on the cisplatin response by downregulation of TC21 targets, both individually and in combination. In our study, TC21 protein expression correlated with cisplatin sensitivity. Earlier studies have shown that overexpression of TC21 resulted in cisplatin resistance to apoptosis^[29]. Therefore, we investigated whether TC21 downregulation would sensitize TE13 cells to cisplatin. Our results demonstrated that TC21 downregulation resulted in a

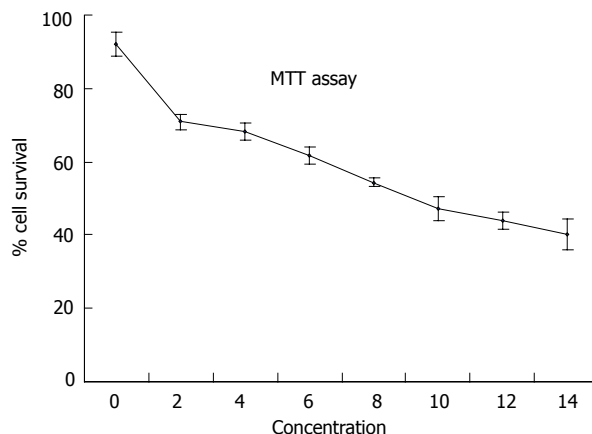


Figure 4 Cell viability assay. TE13 cells were treated with cisplatin in a dose-dependent manner for 24 h. Cell viability was determined using the MTT assay. LD50 was found to be 9 µg/mL. Further treatment with cisplatin was carried out at less than the LD50 dose.

significant reduction in the expression of the Akt pathway components, supporting that Akt pathway proteins serve as important downstream targets of TC21. Akt, an oncogenic protein implicated in human cancer development, is a key component of the PI3-K signaling pathway^[30,31]. Knockdown of TC21 decreased the expression of pAkt/PKB (antibodies specific for Ser 473 and Thr 308 showed similar effects), while the total Akt/PKB levels remained unaffected.

Furthermore, TC21 knockdown decreased the NF-κB levels. The TC21 oncogenic signals are mediated *via* the PI3K/Akt, NF-κB pathway, whereas the role of TC21 in activation of the extracellular signal-regulated kinase/MAPK pathway is less clear^[20].

Significant down-regulation of pGSK3β (Ser 9) in TC21-knockdown cells suggests a role of GSK3β downstream from Akt in TC21-mediated esophageal cancer. TC21 knockdown also suppressed the phosphorylation of the upstream kinase PDK1 (P-Serine 241). The phosphorylation of the p85 subunit of another upstream kinase, PI3K was also suppressed upon TC21 knockdown (data not shown). Suppression of Akt by TC21 siRNA led to the suppression of phosphorylation of GSK3β, the substrate for Akt. The serine/threonine kinase Akt, a key target of PIP3, is activated by TC21^[29], resulting in increased cell proliferation, transformation and survival

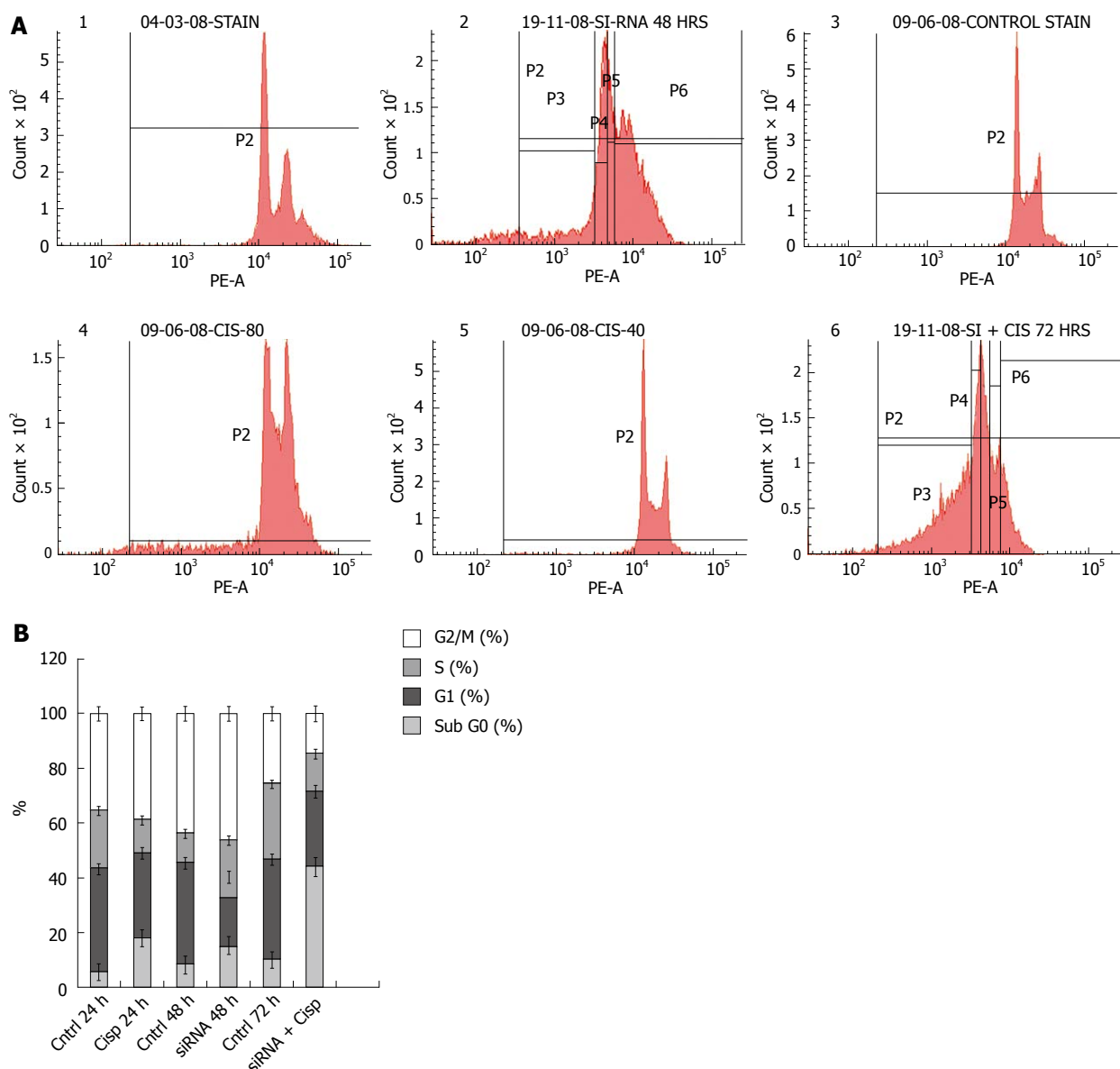


Figure 5 Cell cycle analyses. A: TC21-knockdown cells (20 nmol siRNA for 48 h) were treated with cisplatin (8 μg/mL) for 24 h and cell cycle analysis was performed by labeling cells with DNA binding dye propidium iodide. The panel shows 1: DNA histograms of mock-transfected TE13 cells for 48 h; 2: TE13 cells transfected with TC21 siRNA for 48 h showing increased cell death; 3: TE13 cells without transfection for 24 h; 4: TE13 cells were treated with cisplatin alone for 24 h; 5: TE13 cells without transfection for 72 h; 6: TE13 cells were transfected with TC21siRNA for 48 h for optimal knockdown followed by cisplatin at 8 μg/mL for 24 h; B: Stacked bar graph depicts the cell cycle distribution. Data presented here as mean of percentage events from 3 independent experiments.

through numerous effectors, including Bad, GSK-3β and mTOR^[32]. Notably, a significant increase in pPTEN expression was observed in TC21 siRNA-treated esophageal cancer cells compared with controls. Since pPTEN is a PI3K antagonist and inhibits downstream signaling through Akt, its upregulation in siRNA-treated cells suggests the involvement of PI3K in TC21-mediated esophageal tumorigenesis, suggesting that the PI3K/Akt is a downstream target of TC21.

TC21-knockdown esophageal cancer cells did not affect the level of P-Raf, suggesting that the TC21 pathway is independent of Raf. Our results support the previous report that TC21 is regulated similar to Ras except that it does not interact with full-length Raf 1, B raf, and A raf, suggesting that TC21 uses a Raf-independent

pathway to induce oncogenic transformation^[33]. It also interacts with Ral GDS *in vitro*, which may be responsible for the Raf-independent pathway^[34].

Cyclin D1 is a major regulator of the progression of cells into the proliferative stage of the cell cycle^[35]. Interestingly, TC21 knockdown resulted in reduced expression of cyclin D1, suggesting TC21 may increase cell survival of esophageal cancer by targeting cyclin D1. Thus cyclin D1 may be a target of TC21 signaling through the PI3K/Akt/NF-κB/cyclin D1 pathway. We observed that TC21 gene knockdown by RNAi alone induces an increase in the subG0 population of TE13 cells and a decrease in cyclin D1. Cell cycle progression from G0/G1 to the S phase requires cyclin/cyclin-dependent kinase (CDK) complexes and hyperphosphorylated reti-

noblastoma protein (Rb). In the early G1 phase, the cyclin D1/CDK 4 complex phosphorylates Rb, triggering a cascade of events, including the dissociation of E2F from hyperphosphorylated Rb, the activation of E2F transcription, and progression to the S phase^[36]. Keeping in view the above discussed facts it is possible that a TC21 knockdown-induced decrease in cyclin D1 expression may block transition from G1 to the S phase.

Overexpression of TC21 activated its downstream targets resulting in translocation of NF-κB to the nucleus and stimulated the transcription of anti-apoptotic genes including cyclin D1. Low cellular levels of cyclin D1 have been reported to potentially contribute to increased cisplatin sensitivity in human breast cancer cells CAL-148^[37]. Our results suggest that TC21 may enhance cell survival against cisplatin-induced cell death through activation of the PI3-K/Akt/NF-κB/cyclin D1 signaling pathway in esophageal cancer cells. Knockdown of TC21 sensitized TE-13 cells to cisplatin treatment and resulted in an increase in the subG0 population (cell death), a decrease in G1/S-phase and an increase in G2/M-phase populations. Further studies are needed to reveal new downstream targets of NF-κB responsible for TC21-mediated cell survival.

In summary, cyclin D1 is a downstream target for TC21 and TC21 may be a candidate marker for prediction of cisplatin treatment outcome in esophageal cancer patients. Our study draws attention to the relevance of TC21 in the context of cisplatin pharmacogenetics of esophageal cancer.

COMMENTS

Background

Esophageal cancer is one of the most aggressive malignancies of the gastrointestinal tract, ranking as the sixth most common cancer among males and ninth most common cancer among females globally. Esophageal squamous cell carcinoma (ESCC) is the predominant histological subtype of esophageal cancer in India, characterized by high mortality rate and strong association with dietary habits and lifestyle.

Research frontiers

TC21/R-Ras2 is the only member of the R-Ras subfamily for which overexpression or mutants were detected in human tumor cells, including cells derived from uterine sarcoma, ovarian cancer and mammary tumors. Increased expression of TC21 was found in breast cancer cells.

Innovations and breakthroughs

The effect of TC21 downregulation on cell signaling in esophageal cancer cells was determined by assessing the phosphorylation status of its downstream targets, phosphoinositide 3-kinase, phosphatase and tensin homolog, protein kinase B, nuclear factor-κB (NF-κB), and cyclin D1 using specific antibodies. Cell survival analysis after cisplatin treatment was carried out by a cell viability assay and cell cycle analysis using flow cytometry.

Applications

Cyclin D1 is a downstream target for TC21 and TC21 may be a candidate marker for prediction of cisplatin treatment outcome in esophageal cancer patients. The study draws attention to the relevance of TC21 in the context of cisplatin pharmacogenetics of esophageal cancer.

Peer review

This is a good descriptive study in which authors determine the functional significance of TC21 in ESCC. The results are interesting and suggest that TC21 mediates its effects *via* PI3K-Akt pathway, NF-κB and cyclin D1 and enhances chemoresistance in esophageal cancer cells.

REFERENCES

- 1 **Malkan G**, Mohandas KM. Epidemiology of digestive cancers in India. I. General principles and esophageal cancer. *Indian J Gastroenterol* 1997; **16**: 98-102
- 2 **Phukan RK**, Chetia CK, Ali MS, Mahanta J. Role of dietary habits in the development of esophageal cancer in Assam, the north-eastern region of India. *Nutr Cancer* 2001; **39**: 204-209
- 3 **Gajalakshmi V**, Swaminathan R, Shanta V. An Independent Survey to Assess Completeness of Registration: Population Based Cancer Registry, Chennai, India. *Asian Pac J Cancer Prev* 2001; **2**: 179-183
- 4 **Montesano R**, Hall J. Environmental causes of human cancers. *Eur J Cancer* 2001; **37** Suppl 8: S67-S87
- 5 **Parkin DM**, Moss SM. Lung cancer screening: improved survival but no reduction in deaths--the role of "overdiagnosis". *Cancer* 2000; **89**: 2369-2376
- 6 **Gupta D**, Boffetta P, Gaborieau V, Jindal SK. Risk factors of lung cancer in Chandigarh, India. *Indian J Med Res* 2001; **113**: 142-150
- 7 **Yeole BB**, Kumar AV. Population-based survival from cancers having a poor prognosis in Mumbai (Bombay), India. *Asian Pac J Cancer Prev* 2004; **5**: 175-182
- 8 **Huang J**, Roby KF, Pace JL, Russell SW, Hunt JS. Cellular localization and hormonal regulation of inducible nitric oxide synthase in cycling mouse uterus. *J Leukoc Biol* 1995; **57**: 27-35
- 9 **Chan LC**, Cheung A, Cheng D. Small cell carcinoma of the ovary associated with ins(10; 5)(p13; q31q13). *Cancer Genet Cytogenet* 1994; **77**: 89-90
- 10 **Barker KT**, Crompton MR. Ras-related TC21 is activated by mutation in a breast cancer cell line, but infrequently in breast carcinomas in vivo. *Br J Cancer* 1998; **78**: 296-300
- 11 **Clark GJ**, Kinch MS, Gilmer TM, Burridge K, Der CJ. Overexpression of the Ras-related TC21/R-Ras2 protein may contribute to the development of human breast cancers. *Oncogene* 1996; **12**: 169-176
- 12 **Movilla N**, Crespo P, Bustelo XR. Signal transduction elements of TC21, an oncogenic member of the R-Ras subfamily of GTP-binding proteins. *Oncogene* 1999; **18**: 5860-5869
- 13 **Rokavec M**, Schroth W, Amaral SM, Fritz P, Antoniadou L, Glavac D, Simon W, Schwab M, Eichelbaum M, Brauch H. A polymorphism in the TC21 promoter associates with an unfavorable tamoxifen treatment outcome in breast cancer. *Cancer Res* 2008; **68**: 9799-9808
- 14 **Arora S**, Matta A, Shukla NK, Deo SV, Ralhan R. Identification of differentially expressed genes in oral squamous cell carcinoma. *Mol Carcinog* 2005; **42**: 97-108
- 15 **Macha MA**, Matta A, Sriram U, Thakkar A, Shukla NK, Datta Gupta S, Ralhan R. Clinical significance of TC21 overexpression in oral cancer. *J Oral Pathol Med* 2010; **39**: 477-485
- 16 **Sharma R**, Sud N, Chattopadhyay TK, Ralhan R. TC21/R-Ras2 upregulation in esophageal tumorigenesis: potential diagnostic implications. *Oncology* 2005; **69**: 10-18
- 17 **Ehrhardt A**, Ehrhardt GR, Guo X, Schrader JW. Ras and relatives--job sharing and networking keep an old family together. *Exp Hematol* 2002; **30**: 1089-1106
- 18 **Graham SM**, Oldham SM, Martin CB, Drugan JK, Zohn IE, Campbell S, Der CJ. TC21 and Ras share indistinguishable transforming and differentiating activities. *Oncogene* 1999; **18**: 2107-2116
- 19 **Graham SM**, Cox AD, Drivas G, Rush MG, D'Eustachio P, Der CJ. Aberrant function of the Ras-related protein TC21/R-Ras2 triggers malignant transformation. *Mol Cell Biol* 1994; **14**: 4108-4115
- 20 **Erdogan M**, Pozzi A, Bhowmick N, Moses HL, Zent R. Signaling pathways regulating TC21-induced tumorigenesis. *J Biol Chem* 2007; **282**: 27713-27720
- 21 **Marte BM**, Rodriguez-Viciano P, Wennström S, Warne PH,

- Downward J. R-Ras can activate the phosphoinositide 3-kinase but not the MAP kinase arm of the Ras effector pathways. *Curr Biol* 1997; **7**: 63-70
- 22 **Rincon JC**, Haase HR, Bartold PM. Effect of Emdogain on human periodontal fibroblasts in an in vitro wound-healing model. *J Periodontal Res* 2003; **38**: 290-295
- 23 **Rosário M**, Paterson HF, Marshall CJ. Activation of the Raf/MAP kinase cascade by the Ras-related protein TC21 is required for the TC21-mediated transformation of NIH 3T3 cells. *EMBO J* 1999; **18**: 1270-1279
- 24 **Murphy GA**, Graham SM, Morita S, Reks SE, Rogers-Graham K, Vojtek A, Kelley GG, Der CJ. Involvement of phosphatidylinositol 3-kinase, but not RalGDS, in TC21/R-Ras2-mediated transformation. *J Biol Chem* 2002; **277**: 9966-9975
- 25 **Cox ME**, Deeble PD, Lakhani S, Parsons SJ. Acquisition of neuroendocrine characteristics by prostate tumor cells is reversible: implications for prostate cancer progression. *Cancer Res* 1999; **59**: 3821-3830
- 26 **Pozzi A**, Coffa S, Bulus N, Zhu W, Chen D, Chen X, Merzouk G, Su Y, Cai S, Singh A, Brissova M, Zent R. H-Ras, R-Ras, and TC21 differentially regulate ureteric bud cell branching morphogenesis. *Mol Biol Cell* 2006; **17**: 2046-2056
- 27 **Erdogan M**, Karadeniz M, Ozbek M, Ozgen AG, Berdeli A. Interleukin-10 gene polymorphism in patients with papillary thyroid cancer in Turkish population. *J Endocrinol Invest* 2008; **31**: 750-754
- 28 **Macha MA**, Matta A, Chauhan SS, Siu KW, Ralhan R. Guggulsterone targets smokeless tobacco induced PI3K/Akt pathway in head and neck cancer cells. *PLoS One* 2011; **6**: e14728
- 29 **Rong R**, He Q, Liu Y, Sheikh MS, Huang Y. TC21 mediates transformation and cell survival via activation of phosphatidylinositol 3-kinase/Akt and NF-kappaB signaling pathway. *Oncogene* 2002; **21**: 1062-1070
- 30 **Franke TF**, Kaplan DR, Cantley LC, Toker A. Direct regulation of the Akt proto-oncogene product by phosphatidylinositol-3,4-bisphosphate. *Science* 1997; **275**: 665-668
- 31 **Cantley LC**, Neel BG. New insights into tumor suppression: PTEN suppresses tumor formation by restraining the phosphoinositide 3-kinase/AKT pathway. *Proc Natl Acad Sci USA* 1999; **96**: 4240-4245
- 32 **Manning BD**, Cantley LC. AKT/PKB signaling: navigating downstream. *Cell* 2007; **129**: 1261-1274
- 33 **Wasylyk C**, Wasylyk B, Heidecker G, Huleihel M, Rapp UR. Expression of raf oncogenes activates the PEA1 transcription factor motif. *Mol Cell Biol* 1989; **9**: 2247-2250
- 34 **Westwick JK**, Cox AD, Der CJ, Cobb MH, Hibi M, Karin M, Brenner DA. Oncogenic Ras activates c-Jun via a separate pathway from the activation of extracellular signal-regulated kinases. *Proc Natl Acad Sci USA* 1994; **91**: 6030-6034
- 35 **Sherr CJ**. Cancer cell cycles. *Science* 1996; **274**: 1672-1677
- 36 **Vermeulen K**, Berneman ZN, Van Bockstaele DR. Cell cycle and apoptosis. *Cell Prolif* 2003; **36**: 165-175
- 37 **Yde CW**, Issinger OG. Enhancing cisplatin sensitivity in MCF-7 human breast cancer cells by down-regulation of Bcl-2 and cyclin D1. *Int J Oncol* 2006; **29**: 1397-1404

S-Editor Gou SX L-Editor Cant MR E-Editor Zhang DN

Double contrast-enhanced two-dimensional and three-dimensional ultrasonography for evaluation of gastric lesions

Hong Shi, Xiu-Hua Yu, Xin-Zhang Guo, Yuan Guo, Hong Zhang, Bin Qian, Zhang-Rui Wei, Li Li, Xian-Chen Wang, Zi-Xiang Kong

Hong Shi, Xiu-Hua Yu, Hong Zhang, Bin Qian, Zhang-Rui Wei, Li Li, Xian-Chen Wang, Zi-Xiang Kong, Department of Ultrasound, The 117th Hospital of PLA, Hangzhou 310013, Zhejiang Province, China

Xin-Zhang Guo, Department of Ultrasound, The Zhejiang Suichang Hospital, Suichang 323300, Zhejiang Province, China

Yuan Guo, Department of Cardiothoracic Surgery, Prince of Wales Hospital Randwick, Sydney NSW 2031, Australia

Author contributions: Shi H, Yu XH and Guo XZ designed the research, analyzed the ultrasonography, took care of patients, wrote and recruited the paper; Zhang H, Qian B, Li L, Wang XC and Kong ZX collected the data and took care of patients; Guo Y wrote the paper; Wei ZR did the statistical analysis of the data.

Supported by A key medical project in Nanjing Military District of the Chinese People's Liberation Army, No. 09Z039

Correspondence to: Hong Shi, MD, Department of Ultrasound, The 117th Hospital of PLA, Hangzhou 310013, Zhejiang Province, China. xuyyzh@hzcncc.com

Telephone: +86-571-87348842 Fax: +86-571-87348500

Received: October 15, 2011 Revised: February 10, 2012

Accepted: April 9, 2012

Published online: August 21, 2012

Abstract

AIM: To investigate the value of two-dimensional (2D) and three-dimensional (3D) double contrast-enhanced ultrasonography (DCUS) imaging for evaluation of gastric lesions.

METHODS: 2D and 3D DCUS imaging with both oral and intravenous administrations of contrast agents was used to assess gastroscopically-confirmed gastric lesions in 46 patients with benign and malignant diseases. Initially, liquid-based ultrasound contrast agent (Xinzhang®) was given orally at dose of 500-600 mL for conventional ultrasound examination of the gastric lesions, and then a microbubble-based contrast agent (SonoVue) was injected intravenously at dose of 1.2-2.4 mL in bolus fashion to assess the perfusion pattern of the lesions

using contrast imaging modes. The parameters derived from time-intensity curves including the arrival time (AT), time to peak (TTP), peak intensity (PI) and enhanced intensity (EI) were measured on the 2D DCUS imaging. 3D DCUS of the lesions was acquired to demonstrate the value of this imaging mode.

RESULTS: There were 22 cases with benign lesions including chronic gastritis ($n = 5$), gastric ulcer ($n = 9$), gastric polyps ($n = 3$), gastric stromal tumors ($n = 5$), and 24 cases with malignant lesions including gastric cancer ($n = 20$), gastric cardia carcinoma ($n = 3$) and post-operative recurrent gastric cancer ($n = 1$) in the study. The oral contrast-enhanced ultrasonography (CEUS) imaging of the stomach clearly demonstrated the anatomy of the stomach and morphologic features of gastric lesions. With optimal scanning window and imaging display under oral CEUS, intravenous CEUS clearly showed the perfusion of gastric lesions with various characteristic manifestations. Both 2D and 3D DCUS images clearly demonstrated normal gastric wall as a three-layer structure, from the inside out, hyperechoic mucosa, hypoechoic muscularis and hyperechoic serosa, respectively. There were statistical significant differences of AT (8.68 ± 2.06 vs 10.43 ± 2.75 , $P = 0.017$), PI (34.64 ± 6.63 vs 29.58 ± 8.22 , $P = 0.023$) and EI (29.72 ± 6.69 vs 22.66 ± 7.01 , $P = 0.001$) between malignant lesions and normal gastric wall. However, no differences of AT, PI and EI between benign lesions and normal gastric wall tissue were found. 3D DCUS could intuitively display morphological features and vascularities of the lesions with multiplanar and volume views. 3D DCUS imaging provided comprehensive information complementary to 2D imaging. The crater or wellhead appearances and feeding vessels as well as distorted nourishing vasculature of gastric carcinoma were better seen with 3D imaging than 2D imaging.

CONCLUSION: DCUS imaging can simultaneously

display the anatomic and perfusion features of gastric lesions. 3D DCUS can provide additional information to 2D DCUS for evaluation of gastric lesions.

© 2012 Baishideng. All rights reserved.

Key words: Contrast-enhanced ultrasonography; Gastric lesions; Two-dimensional imaging; Three-dimensional imaging; Contrast media

Peer reviewer: Ji-Bin Liu, Professor, Department of Radiology, Thomas Jefferson University Hospital, 132 S. 10th Street, 7th Main Building, Philadelphia, PA 19107, United States

Shi H, Yu XH, Guo XZ, Guo Y, Zhang H, Qian B, Wei ZR, Li L, Wang XC, Kong ZX. Double contrast-enhanced two-dimensional and three-dimensional ultrasonography for evaluation of gastric lesions. *World J Gastroenterol* 2012; 18(31): 4136-4144 Available from: URL: <http://www.wjgnet.com/1007-9327/full/v18/i31/4136.htm> DOI: <http://dx.doi.org/10.3748/wjg.v18.i31.4136>

INTRODUCTION

The common methods for examination of the upper gastrointestinal (GI) tract are x-ray with oral barium-based contrast agent and endoscopy. Their shortcomings include the fact that they often cannot delineate submucosal mural structures of the GI tract. Limitations to the sonographic assessment of the upper GI tract and adjacent organs include patient body habitus and the presence of gas-filled bowel, which can produce shadowing artifacts^[1,2]. Although ingestion of degassed water has been used to improve sonographic assessments of the GI tract and retroperitoneal structures, water simply displaces gas within the GI tract and can produce inconsistent results. Imaging water-filled stomach usually results in an increase in the wall through transmission, which may cause tissues of otherwise normal echogenicity to appear more echogenic than expected, creating a potential source of diagnostic error. Over the years, researchers attempted to develop oral contrast agents to improve the assessment of the GI tract and adjacent structures by absorbing and displacing bowel gas and provide an acoustic window for sonographic visualization of upper GI tract. One of such oral contrast agent Xinzhang[®] (Huqingyutang Pharmaceuticals Co., Hangzhou, China) has been developed and commercially available in China for ultrasound imaging of upper GI tract in clinical settings^[3-5].

During the last two decades, contrast-enhanced ultrasound imaging (CEUS) with intravascular contrast agents has been investigated and has gradually emerged in clinical settings. The rapid development of contrast agents for sonography is precipitated by the performance limits of grayscale imaging and Doppler techniques. As US Imaging is used to study smaller and deeper structures in the abdomen, the spatial resolution of grayscale imaging and Doppler sensitivity becomes critical to the degree

that it impacts the clinical utility of sonography. Contrast agents promise to improve the sensitivity and specificity of current sonographic diagnoses and have the potential to expand the already broad range of its applications.

Recently, we have explored new technique which combines both oral and intravenous CEUS imaging methods, so called Double contrast-enhanced ultrasound (DCUS), for evaluation of gastric abnormalities. The purpose of this study was to investigate the value of DCUS imaging using both two-dimensional (2D) and three-dimensional (3D) modes for the evaluation of gastric lesions.

MATERIALS AND METHODS

Patients

The study protocol was approved by our hospital ethical committee, and all patients gave informed consent and agreed to participate in the study. During a period from 2007 to 2011, 2D and 3D DCUS imaging with both oral and intravenous administrations of contrast agents was used to assess gastroscopically-detected gastric lesions in 46 patients with 22 benign cases and 24 malignant cases. All final diagnoses are confirmed by endoscopic biopsy or surgical pathological findings. There were 31 males and 15 females, aged from 23 years to 80 years with a mean age of 54.93 ± 12.49 years.

Equipment and contrast agents

The DCUS was performed using full digital ultrasound scanners iU22 (Philips Medical Systems, Bothell, WA) with a C5-2 probe or Sequoia-512 (Siemens Medical Solutions, Mountain View, CA) with a 4C1 probe for 2D imaging. Philips C6-2 volume probe was used for acquiring 3D DCUS imaging. Conventional ultrasound imaging mode was used for oral contrast imaging while contrast imaging modes (Philips Pulse inversion harmonic imaging and Siemens contrast pulse sequencing techniques) were used for intravascular contrast imaging.

The commercially available oral contrast agent Xinzhang[®] (Huqingyutang Pharmaceuticals Co., Hangzhou, China) was supplied as powder which is derived from rice and soya. The 48 g per package was reconstituted by adding 500-600 mL of cooled boiling water and gently agitating by hand to form a homogeneous thin paste.

The intravenous contrast agent SonoVue[®] (Bracco SpA, Milan, Italy) was injected in bolus fashion at doses of 1.2-2.4 mL through brachial vein, followed by 5 mL normal saline flush.

Double oral and intravenous contrast imaging

DCUS examination was performed after patient's fasting for at least 8 h on the day of the study. The stomach of all patients was scanned using real time gray-scale imaging when the patients swallowed the oral agent to expand the cavity of the stomach. Using contrast agent-filled gastric cavity with homogenous moderate echogenicity as an acoustic window, the location, shape and size of any possible lesions and the wall thickness of the stomach were

carefully imaged and recorded under dynamic scanning with patients in the supine and both decubitus positions. The scanning parameters (e.g., the depth, focus, and gain) were adjusted to achieve optimal imaging display as conventional ultrasound examination.

After oral contrast imaging localization of the gastric lesion, vascular CEUS of was performed with a bolus injection of 1.2-2.4 mL of SonoVue *via* a 20-gauge peripheral intravenous catheter under contrast imaging mode with a low mechanical index (0.09-0.21). Initially, each subject underwent 2D imaging to observe the perfusion pattern and measure the time-intensity curve of the lesions and adjacent normal wall of stomach as control. The CEUS parameters of arrival time (AT), time to peak (TTP), infusion time (IT, $IT = TTP - AT$), baseline intensity (BI), peak intensity (PI) and enhanced intensity (EI, $EI = PI - BI$) was obtained and calculated from the time-intensity curve. Next, the regions of interest were selected based on the 2D contrast imaging and 3D images of the region of interest were acquired using a 3D probe with additional contrast agent injection during the arterial phase of enhancement. The 3D imaging volume files was stored digitally with both on-line and off-line imaging process and analysis.

Statistical analysis

SPSS 13.0 (SPSS Inc., Chicago, United States) was used for statistical analysis. The values of measurements were expressed as (mean \pm SD). Two sample *t*-test was used to compare each parameter (AT, TTP, PI, EI and IT) between benign or malignant lesions and normal gastric walls. For all analyses, a *P* value of less than 0.05 was considered statistically significant.

RESULTS

A total of 46 pathologically-proved cases were enrolled in the study. There were 22 cases with benign lesions including chronic gastritis ($n = 5$), gastric ulcer ($n = 9$), gastric polyps ($n = 3$), gastric stromal tumors ($n = 5$), and 24 cases with malignant lesions including gastric cancer ($n = 20$), gastric cardia carcinoma ($n = 3$) and post-operative recurrent gastric cancer ($n = 1$). The 2D DCUS with oral and intravenous contrast enhancement was successfully performed in all 46 patients. While 43 out of 46 patients underwent 3D contrast imaging studies. Both 2D and 3D DCUS images clearly demonstrated normal gastric wall as a three-layer structure, from the inside out, hyperechoic mucosa, hypoechoic muscularis and hyperechoic serosa, respectively (Figure 1). DCUS characteristic findings of gastric lesions were visualized as follows.

Benign lesions

Gastric ulceration lesion: Gastric ulceration lesion appeared as a contrast agent-filled defect on the stomach wall with a spot-like mural hyperechogenic area in 9 cases. There was a lack of localized partial or prominent gastric wall thickening. Intravenous contrast 2D imaging shown

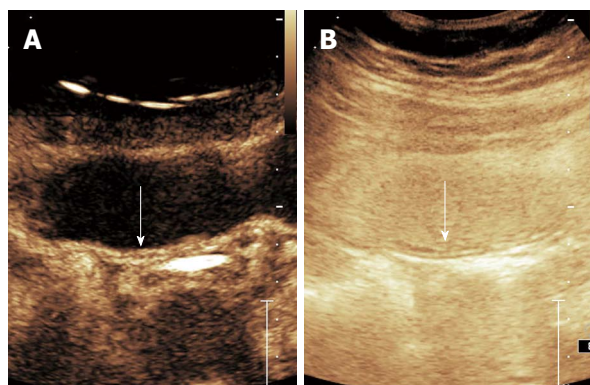


Figure 1 Two-dimensional double contrast-enhanced ultrasound imaging. A: The picture showing intravenous contrast harmonic imaging with the echo-free gastric cavity and three layers of normal gastric wall (arrow); B: The picture showing oral contrast imaging of normal gastric wall (arrow) and cavity filled with echogenic contrast agent.

uniformed enhancement of the gastric wall adjacent to the lesion and 3D DCUS imaging showed the gastric cavity and wall with a focal defect area consistent with an ulcer (Figure 2).

Gastric polyp: Gastric polyp appeared as a hyperechoic beansprout-shaped or a cone-shape mass projecting into the cavity of the stomach in 3 cases (Figure 3). Intravenous contrast 2D imaging shown simultaneous and equal enhancement of both lesions and normal gastric walls.

Gastric stromal tumor: Gastric stromal tumor shown as a hypoechoic or nearly anechoic mass within gastric wall under oral contrast imaging in 5 cases (Figure 4). These lesions had clear demarcation, regular around shape, and homogeneous echotexture. Larger ones protruded into the stomach cavity ($n = 3$) and have inhomogeneous echotexture ($n = 2$). Intravenous contrast 2D imaging demonstrated simultaneous or delayed enhancement of stromal tumors with homogeneous iso- or hypo-enhancement when compared with adjacent normal gastric wall. A ring enhancement appear in hypo-enhancement lesions ($n = 2$).

Gastric inflammatory lesion: Inflammatory thickening of the gastric wall was clearly seen under oral contrast displays in 5 chronic gastritis cases. The focal gastric inflammatory lesion appeared as homogeneous hypoechoic thickening associated with mild elevation of smooth surface of the wall. There was no remarkable change in the layers of the gastric wall. Intravenous contrast 2D imaging of the thickening wall shown uniform, simultaneous and iso- or hyper-enhancement compared to the normal gastric wall.

Malignant lesions

The characteristics of gastric carcinoma were demonstrated with oral contrast imaging in 24 cases. The features of malignant lesions included irregular shape, heterogeneous

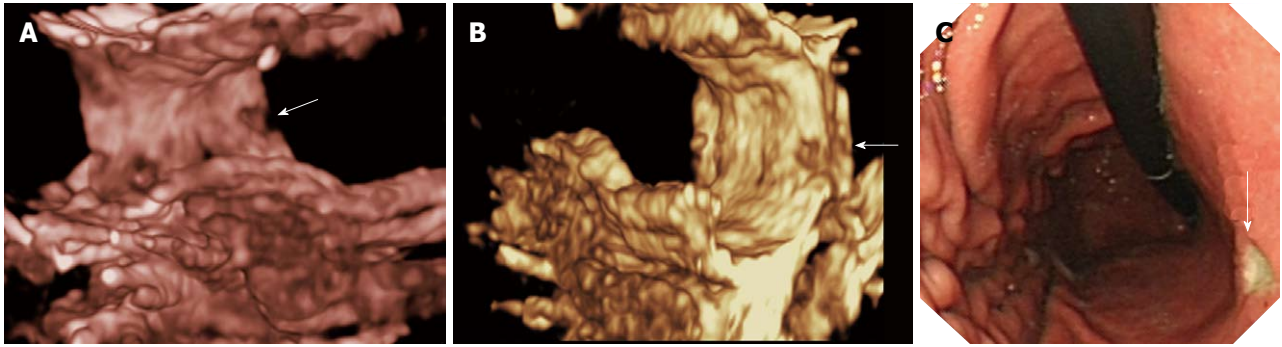


Figure 2 Double contrast-enhanced ultrasound imaging of gastric ulceration. A: Three-dimensional (3D) double contrast-enhanced ultrasound imaging showed the gastric cavity and wall with a focal defect area consistent with an ulcer (arrow); B: Another 3D imaging with different angle showed the ulcerative lesion (arrow) and the folds of gastric wall with pseudo-color which similar to gastroscopic imaging; C: The ulcerative lesion (arrow) is seen on gastroscopie imaging.

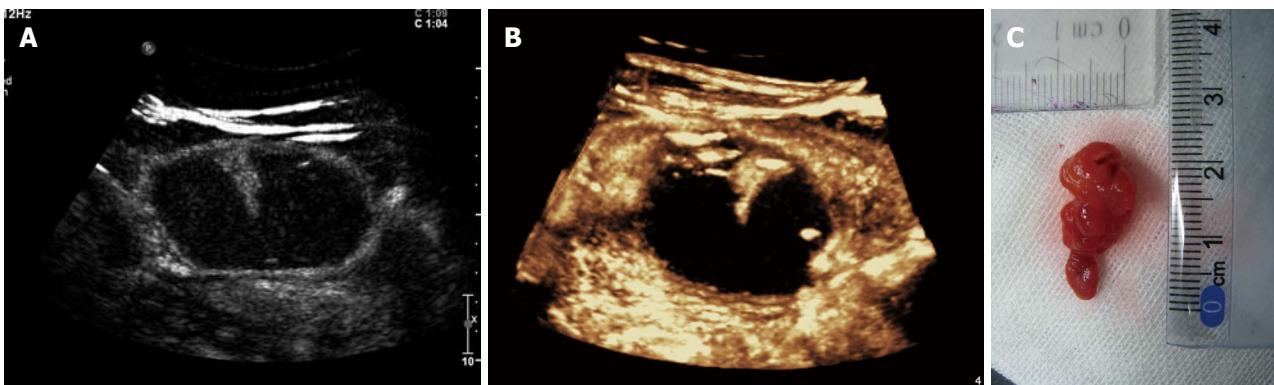


Figure 3 Double contrast-enhanced ultrasound imaging of gastric polyp. A: Two-dimensional double contrast-enhanced ultrasound (DCUS) imaging displayed a polyp with a wide base projecting into the gastric cavity. Contrast enhancement was seen on both polyp and gastric wall; B: Three-dimensional DCUS imaging of the polyp showed in figure A; C: The surgical specimen of the polyp confirmed the DCUS finding.

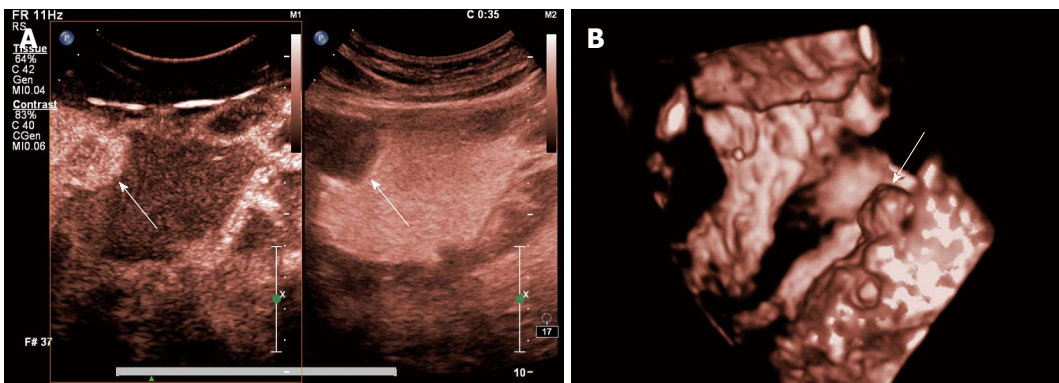


Figure 4 Double contrast-enhanced ultrasound imaging of gastric stromal tumor. A: Two-dimensional double contrast-enhanced ultrasound (DCUS) images displayed a anechoic mass into the gastric cavity in oral contrast ultrasonography (right figure), from which we hardly judged whether it was cystic or solid lesion; but the intravenous contrast imaging (left figure) showed there was contrast agent enhancement in the focus of infection (arrow); B: Three-dimensional DCUS imaging displayed the tumor elevated to the gastric cavity (arrow).

echotexture and disrupted layers of the gastric wall on the 2D oral contrast imaging. The mass-like lesion shown as a solid mass protruding into the cavity while the diffuse lesion appeared as a localized wall thickening and irregular surface of the lesions. The lesions with ulceration in 6 cases shown as filling defects within the lesions (Figure 5). Extensive infiltrative lesions in 9 cases shown diffuse het-

erogeneous thickening of the gastric wall which resulted in gastric cavity narrowing. The passage of oral contrast agent through the narrow gastric cavity can be seen with slow and stiff gastric peristalsis in real-time imaging. In 3 patients with carcinoma of gastric cardia, oral contrast imaging shown hypoechoic wall thickening of the distal esophageal and gastric cardia. Echogenic contrast agents

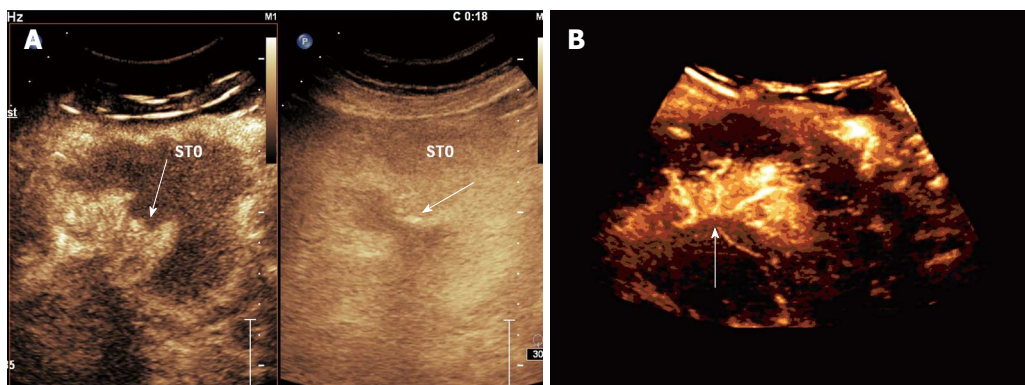


Figure 5 Double contrast-enhanced ultrasound imaging of ulcerative gastric cancer. A: Two-dimensional double contrast-enhanced ultrasound (DCUS) images (conventional imaging on the right and harmonic imaging on the left) showed a contrast-enhanced mass with crater-like ulcerative defect (arrow); B: Three-dimensional DCUS imaging showed distorted nourishing vasculature within the gastric cancer (arrow).

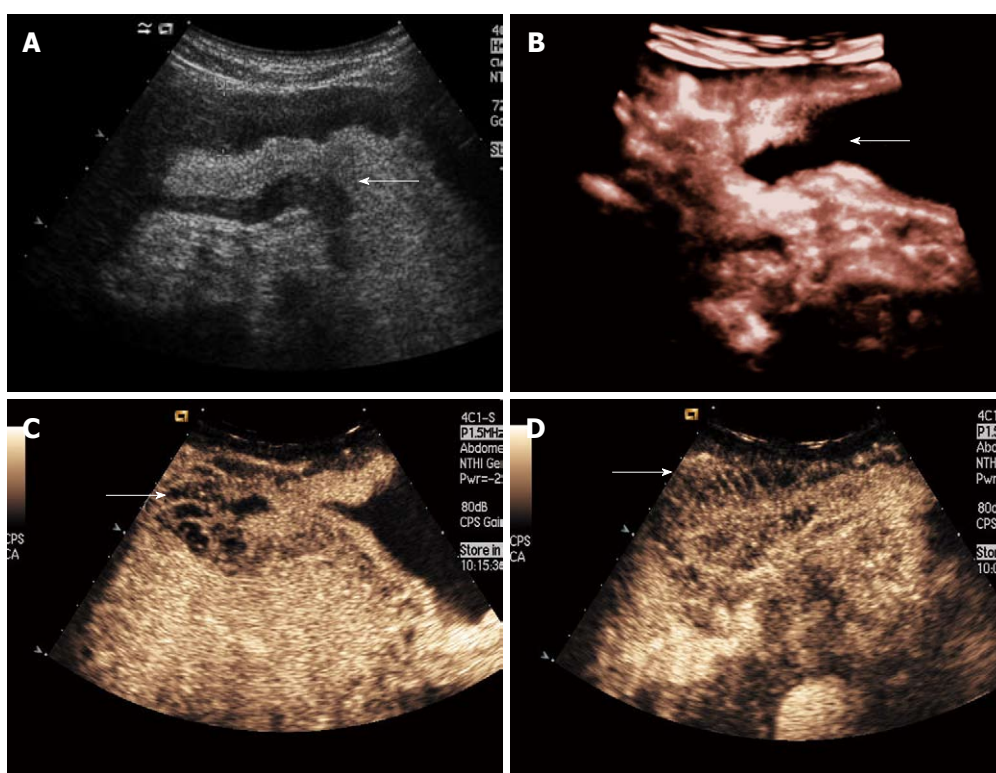


Figure 6 Double contrast-enhanced ultrasound imaging of infiltrative gastric cancer. A: An oral contrast image showed diffusely thickened gastric wall with narrowed gastric cavity (arrow) in a patient with gastric cancer; B: Three-dimensional double contrast-enhanced ultrasound (DCUS) imaging showed thickened gastric wall and narrowed echo-free gastric cavity (arrow); C, D: Two-dimensional DCUS images showed fence-like tumor vessels penetrating through thickened gastric wall in the arterial phase (arrows).

passing through the narrow lumen of gastroesophageal junction was seen during the swallowing of contrast agent. In 6 patients with gastric carcinoma, enlarged lymph nodes adjacent to gastric wall were identified with hypoechogenic and round-shape features.

Combining with oral contrast imaging, intravenous 2D contrast imaging demonstrated variable patterns of enhancement of the lesions. When compared to adjacent normal gastric wall, there were iso-enhancement in 2 lesions, hypo-enhancement in 1 lesions and hyper-enhancement in 21 lesions. The feeding vessels and dis-

torted tumor vasculature was clearly identified with 2D DCUS imaging (Figure 6). All lesions appeared as earlier enhancement in wash-in phase than the normal gastric wall. Under DCUS imaging condition, the enhancement parameters of time-intensity curves in both begin and malignant lesions shown in Table 1.

3D double contrast-enhanced ultrasonography imaging

Reconstructed 3D imaging demonstrated global rendering of DCUS imaging with different prospective of morphology for both normal structures and gastric le-

Table 1 Comparison between benign gastric lesions and normal gastric wall ($n = 22$), malignant gastric lesions and normal gastric wall ($n = 24$) from double contrast-enhanced ultrasound time-intensity curve

	Benign lesions	Normal gastric wall	<i>P</i> value	Malignant lesions	Normal gastric wall	<i>P</i> value
AT (s)	9.43 ± 2.25	9.22 ± 2.37	0.753	8.68 ± 2.06	10.43 ± 2.75	0.017
TTP (s)	16.24 ± 3.67	16.43 ± 3.32	0.862	15.86 ± 3.80	17.86 ± 4.19	0.089
IT (s)	6.85 ± 2.56	7.22 ± 2.57	0.643	7.17 ± 2.45	7.44 ± 3.03	0.344
BI (dB)	5.07 ± 3.49	5.29 ± 4.16	0.846	4.93 ± 3.25	6.92 ± 4.59	0.09
PI (dB)	31.36 ± 8.55	32.96 ± 8.58	0.538	34.64 ± 6.63	29.58 ± 8.22	0.023
EI (dB)	26.28 ± 9.90	27.64 ± 9.59	0.648	29.72 ± 6.69	22.66 ± 7.01	0.001

AT: Arrival time; TTP: Time to peak; IT: Infusion time; BI: Baseline intensity; PI: Peak intensity; EI: Enhanced intensity.

sions. 3D imaging displayed intuitive pictures of lesions and the gastric layers from multiple imaging angles and views, which corresponded well with surgical specimens (Figures 2, 3 and 7).

In cases with thickened wall bulging unevenly or a mass protruding into (or outward) the gastric cavity, 3D DCUS imaging provided comprehensive information to complementary to 2D imaging. The crater or wellhead appearances and feeding vessels as well as distorted nourishing vasculature of gastric carcinoma were better seen with 3D imaging than 2D imaging (Figures 5, 7).

DISCUSSION

Ultrasound imaging is a convenient and noninvasive diagnostic tool for evaluation of abdominal organs. However, its use in diagnosing gastric abnormalities is limited by the interference of the gas in the GI tract. In 1978, Warren first used hydrophilic methyl cellulose oral suspension in ultrasound examination to image retroperitoneal organs such as stomach, duodenum or pancreas^[6]. Since then, researchers have done many studies in oral contrast agent for gastric ultrasound imaging^[7-12]. Early-developed oral contrast agents have short emptying, large required quantity, and an unpalatable taste. The oral contrast agent Xinzhang[®] used in this study is vegetable-based with main components being beans and starch^[13], which is a uniform thin paste with pleasant taste and slow emptying feature without side effects, and thus is easily accepted by patients especially children and the elderly. The thin paste-based agent produces uniform moderate echogenic reflection within well-filled stomach, which clearly shows all normal layers of gastric wall, gastric lesions and surrounding structures under optimal contrast imaging. The gastric lesions revealed by oral contrast ultrasound in this study included mild thickening of the gastric wall, polypoid lesions and other stomach masses. Small lesions such as 0.5 cm diameter ulcer and 1.0 cm diameter stromal tumors can be identified. In addition, oral contrast gastric ultrasound imaging can be carried out using conventional ultrasound systems, which is easily applied in the clinical practice.

Although oral contrast imaging can show normal anatomy of the stomach and the location, shape and size of gastric lesions, its ability to determine internal structures and blood perfusion status of the lesion is limited. For example, gray-scale imaging cannot determine a very

hypoechoic mass (such as gastric stromal tumor) whether it is cystic or solid^[14-16]. Also, color Doppler ultrasound has a poor sensitivity in revealing small blood flow of the gastric wall or lesions. In previous study, intravenous contrast imaging has been used for the evaluation of gastric tumor in canine to determine the blood perfusion status of the tumors^[17-19]. However, without appropriated gray-scale imaging of the stomach, Intravenous contrast imaging cannot achieve useful information of blood perfusion for assessment of tumor vascularity and surrounding structures. Therefore, DCUS imaging is necessary for evaluation of gastric lesions in order to obtain comprehensive information.

Micro-bubble-based SonoVue is a second-generation intravenous ultrasound contrast agent. It has phospholipids as capsule, containing sulfur hexafluoride gas. Its diameter is similar to that of red blood cells, which enables it to reach microvessels of all peripheral organs through intravenous injection. This agent has an average half-life of 12 min *in vivo*. It is removed by lungs through respiration in 15 min and poses no obvious toxic effect to the liver and kidney. In term of the difference from CT contrast agents such as lipiodol, microbubble-based contrast agent does not penetrate vessel wall and leak into interstitial space. Its distribution in the lesion represents the distribution of the microvessels, and the intensity of the lesion enhancement represents the density of those vessels^[20-28]. Therefore, DCUS can be used to evaluate both the morphology and vascularity of gastric lesions.

In this study, we demonstrated that oral contrast imaging can provide excellent acoustic window for evaluation of a variety of gastric lesions by conventional gray-scale imaging. Furthermore, oral contrast imaging serves as important platform for assessment of blood perfusion of the lesions by intravascular contrast imaging. Thus, DCUS is able to demonstrate both morphologic appearances and perfusion status of both normal and abnormal structures, which improves the ability of differential diagnosis. For example, oral contrast imaging revealed 4 gastric stromal tumors as anechoic lesions which was difficult to decide whether they are cystic or solid lesions. However, the use of intravenous contrast imaging demonstrated internal blood perfusion of these tumor lesions, which confirmed they are solid lesions instead of cystic lesions. More important, DCUS can show the relationship of the lesion's vasculature and the gastric wall

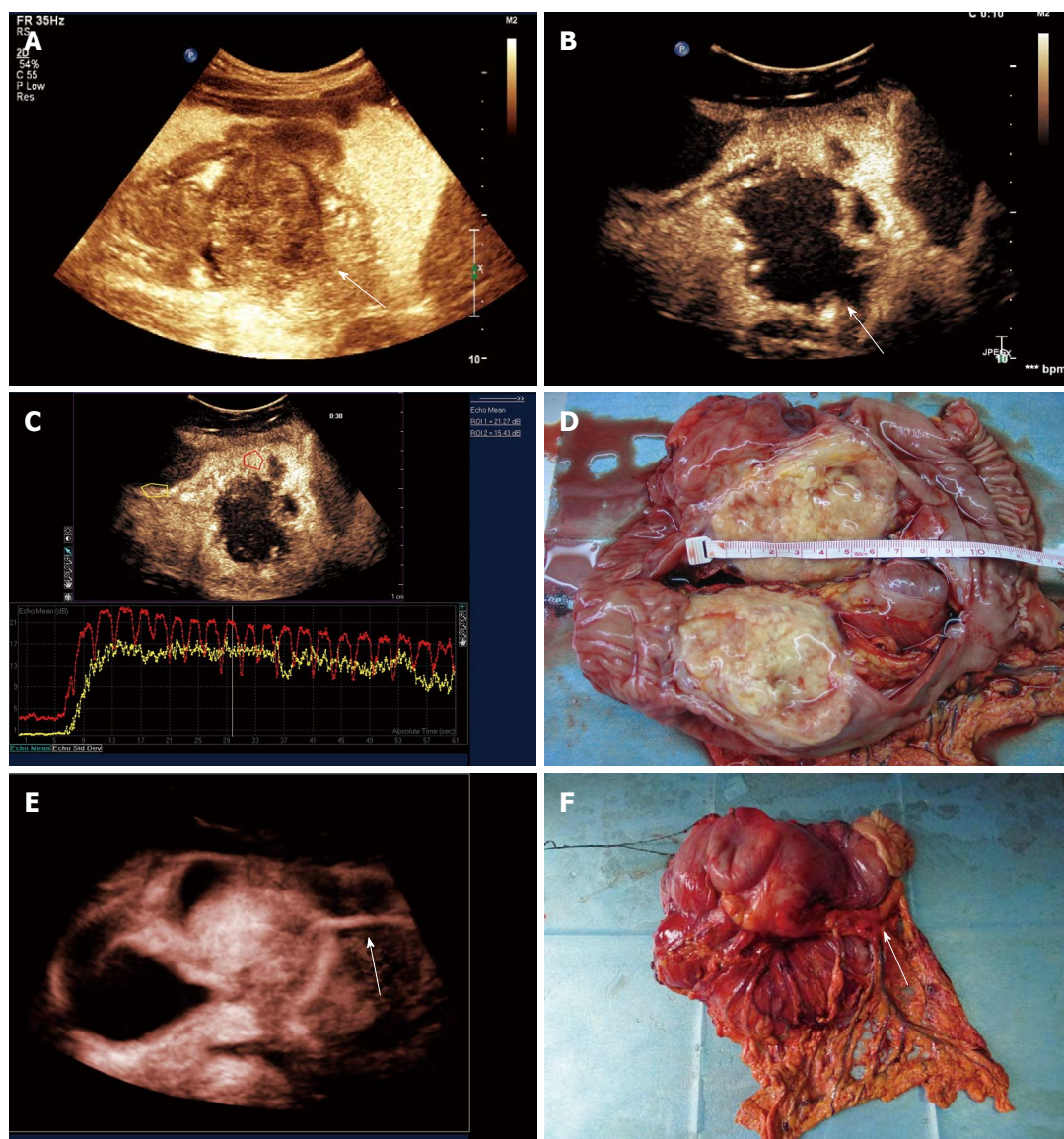


Figure 7 Double contrast-enhanced ultrasound imaging of mass-type gastric cancer. A: Oral contrast imaging revealed a tumor (arrow) extended into the back wall of stomach, which could not be seen by gastroscopy; B: Two-dimensional double contrast-enhanced ultrasound (DCUS) imaging showed the tumor attached to the posterior wall and enhanced in peripheral areas with the center of non-enhancement at early arterial phase; C: A contrast time-intensity curve of the lesion showed that the arrival time was shorter and the peak intensity was higher in the peripheral lesion (red curve) than those in normal gastric wall (yellow curve); D: The surgical specimen demonstrated the tumor with central necrosis which consistent to DCUS findings; E: Three-dimensional DCUS imaging showed the outer-growing lesion with a tumor feeding vessel (arrow); F: The feeding vessel on the gross specimen was seen and coincident with the DCUS imaging.

as well as their contours outlined by contrast imaging, which accentuates pathological features. Indeed, DCUS images can clearly show the pathological features of the lesions, which made sonographic diagnosis to fit with internationally wide adopted Borrmann's classification of advanced gastric cancer, i.e., polypoid lesion, ulcerated lesion, ulcerating infiltrative lesion, and infiltrative lesion.

Comparing malignant lesions with surrounding normal gastric tissue using contrast-enhanced time-intensity curve, values of AT, PI and EI parameters except TTP and IT were statistically significant ($P < 0.05$). Whereas comparing benign lesions with surrounding normal gastric tissue, all parameters including AT, TTP, IT, PI and EI are not statistically significant ($P > 0.05$). Thus, early AT and increased

PI, EI, can be used as potential indexes and indicators for evaluating gastric benign and malignant lesions^[29]. Since EI eliminated baseline intensity factor, it should reflect the actual intensity of the enhancement. Previous study have shown that, in gastric cancer, EI correlates well to the pathological microvessel density ($r = 0.921, P < 0.001$)^[30], which may reflect the density of microvessels with the lesion, and could be a new parameter for evaluating biological behavior and angiogenesis of gastric cancer.

3D DCUS imaging provides comprehensive and observational perspective for gastric wall and lesion morphology. It can show the intuitive appearance of the lesion relevant to the gastric wall which closely correlates to pathological specimen and increases the confidence

of clinical diagnosis. In malignant lesions, 3D imaging shown the dense, tortuous distorted and heavily cluttered vasculatures of the lesions, which is similar to the “tumor vascularity” seen in the liver and other organ malignancies^[31-35]. 3D DCUS imaging can supplement 2D imaging and provide more evidence for the diagnosis of benign and malignant gastric lesions.

It should be pointed out that this is preliminary observation of DCUS imaging applications. The limitations of this study include small number cases with various gastric abnormalities and no blinded comparison with endoscopic examinations. Prospective study design with larger clinical trial is needed for further investigations.

In conclusion, DCUS imaging is able to simultaneously display the sonographic features of various gastric lesions and its vasculatures as well as perfusion patterns. The parameters of AT, PI and EI could serve as potential indicators for differentiating benign and malignant gastric lesions. 3D DCUS could provide additional information to 2D DCUS for evaluation of gastric lesions.

COMMENTS

Background

The common methods for examination of the upper gastrointestinal (GI) tract are x-ray with oral barium-based contrast agent and endoscopy. Their shortcomings include the fact that they often cannot delineate submucosal mural structures of the GI tract. Over the years, oral contrast agents to improve the assessment of the GI tract and adjacent structures by absorbing and displacing bowel gas and provide an acoustic window for sonographic visualization of upper GI tract have been developed and commercially available in China, one of such oral contrast agent was Xinzhang®. Recently, the authors have explored new technique which combines both oral and intravenous contrast-enhanced ultrasonography (CEUS) imaging methods, called Double contrast-enhanced ultrasound, for evaluation both morphologic appearances and perfusion status of gastric abnormalities.

Research frontiers

Two-dimensional (2D) double contrast-enhanced ultrasound (DCUS) could clearly demonstrate normal gastric wall and differentiate normal gastric wall from benign and malignant lesions. Three-dimensional (3D) DCUS could intuitively display morphological features and vascularities of the lesions with multi-planar and volume views.

Innovations and breakthroughs

The oral contrast agent Xinzhang® used in this study is vegetable-based with main components being beans and starch, which is a uniform thin paste with pleasant taste and slow emptying feature without side effects, and thus is easily accepted by patients especially children and the elderly. DCUS is able to demonstrate both morphologic appearances and perfusion status of both normal and abnormal structures, which improves the ability of differential diagnosis. In the study, small lesions such as 0.5 cm diameter ulcer and 1.0 cm diameter stromal tumors can be identified.

Applications

The study results suggest that 2D and 3D double DCUS was safe, highly sensitive and specific and could be applied for evaluation of gastric lesions.

Peer review

This is an interesting and well written study aimed at assessing the role of contrast enhanced 2D and 3D US in the evaluation of gastric lesions. Even if it is a preliminary study and further prospective validation is needed, the manuscript is very clear and very well documented by images.

REFERENCES

- Gritzmann N, Hollerweger A, Macheiner P, Rettenbacher

- T. Transabdominal sonography of the gastrointestinal tract. *Eur Radiol* 2002; **12**: 1748-1761
- Badea R, Ciobanu L, Gomotirceanu A, Hagiuc C, Socaciu M. Contrast ultrasonography of the digestive tract lumen. Review of the literature and personal experience. *Med Ultrason* 2010; **12**: 52-61
- Guo XZ, Yao GC. [Examination of stomach and duodenum with oral ultrasonic contrast agent]. *Zhongguo Yixue Yingxiang Jishu* 1995; **11**: 56-57
- Guo XZ, Zhang W. A New Type of Acoustic Contrast for Visualizing the Upper Digestive Tract Walls and Pancreas. The 3rd Congress of Asian Federation of Societies for Ultrasound in Medicine and Biology; 1992; Seoul, Korea
- Wang XC, Shi H, Yu XH, Zhang H, Li L, Xu AF, Wei ZR, Kong ZX, Yao C, Xu JP, Guo XZ. [Comparison of contrast-enhanced ultrasound and gastroscopy in the diagnosis of gastric stromal tumor]. *Zhonghua Yixue Chaosheng Zazhi* 2011; **8**: 1033-1038
- Warren PS, Garrett WJ, Kossoff G. The liquid-filled stomach--an ultrasonic window to the upper abdomen. *J Clin Ultrasound* 1978; **6**: 315-320
- Weighall SL, Wolfman NT, Watson N. The fluid-filled stomach: a new sonic window. *J Clin Ultrasound* 1979; **7**: 353-356
- Sisler WJ, Tilcock C. Effect of cellulose concentration on the efficacy of a cellulose-based oral contrast agent for gastrointestinal ultrasonography. *J Ultrasound Med* 1995; **14**: 267-272
- Muradali D, Burns PN, Pron G, Hope-Simpson D, Wilson S. Improved retroperitoneal and gastrointestinal sonography using oral contrast agents in a porcine model. *AJR Am J Roentgenol* 1998; **171**: 475-481
- Lund PJ, Fritz TA, Unger EC, Hunt RK, Fuller E. Cellulose as a gastrointestinal US contrast agent. *Radiology* 1992; **185**: 783-788
- Liao SR, Dai Y, Huo L, Yan K, Zhang L, Zhang H, Gao W, Chen MH. Transabdominal ultrasonography in preoperative staging of gastric cancer. *World J Gastroenterol* 2004; **10**: 3399-3404
- Chaubal N, Dighe M, Shah M, Chaubal J. Sonography of the gastrointestinal tract. *J Ultrasound Med* 2006; **25**: 87-97
- Guo XZ, Zhang W. [Clinical application of oral contrast-enhanced gastrointestinal ultrasound]. *Zhonghua Yixue Chaosheng Zazhi*, 2010; **7**: 4-8
- Nishida T, Hirota S. Biological and clinical review of stromal tumors in the gastrointestinal tract. *Histol Histopathol* 2000; **15**: 1293-1301
- Fukuta N, Kitano M, Maekawa K, Chikugo T, Kudo M. Estimation of the malignant potential of gastrointestinal stromal tumors: the value of contrast-enhanced coded phase-inversion harmonics US. *J Gastroenterol* 2005; **40**: 247-255
- Pidhorecky I, Cheney RT, Kraybill WG, Gibbs JF. Gastrointestinal stromal tumors: current diagnosis, biologic behavior, and management. *Ann Surg Oncol* 2000; **7**: 705-712
- Kamino D, Hata J, Haruma K, Manabe N, Tanaka S, Chayama K. Real-time visualization and quantitation of canine gastric mucosal blood flow by contrast-enhanced ultrasonography. *Scand J Gastroenterol* 2006; **41**: 856-861
- Stock K, Hann von Weyhern C, Slotta-Huspenina J, Burian M, Clevert DA, Meining A, Prinz C, Pachmann C, Holzapfel K, Schmid RM, Lersch C. Microcirculation of subepithelial gastric tumors using contrast-enhanced ultrasound. *Clin Hemorheol Microcirc* 2010; **45**: 225-232
- Piscaglia F, Corradi F, Mancini M, Giangregorio F, Tambari S, Ugolini G, Cola B, Bazzocchi A, Righini R, Pini P, Fornari F, Bolondi L. Real time contrast enhanced ultrasonography in detection of liver metastases from gastrointestinal cancer. *BMC Cancer* 2007; **7**: 171
- Poon RT, Ng IO, Lau C, Yu WC, Yang ZF, Fan ST, Wong J. Tumor microvessel density as a predictor of recurrence after resection of hepatocellular carcinoma: a prospective study. *J*

- Clin Oncol* 2002; **20**: 1775-1785
- 21 **Sedelaar JP**, van Leenders GJ, Hulsbergen-van de Kaa CA, van der Poel HG, van der Laak JA, Debruyne FM, Wijkstra H, de la Rosette JJ. Microvessel density: correlation between contrast ultrasonography and histology of prostate cancer. *Eur Urol* 2001; **40**: 285-293
 - 22 **Ng IO**, Poon RT, Lee JM, Fan ST, Ng M, Tso WK. Microvessel density, vascular endothelial growth factor and its receptors Flt-1 and Flk-1/KDR in hepatocellular carcinoma. *Am J Clin Pathol* 2001; **116**: 838-845
 - 23 **Imao T**, Egawa M, Takashima H, Koshida K, Namiki M. Inverse correlation of microvessel density with metastasis and prognosis in renal cell carcinoma. *Int J Urol* 2004; **11**: 948-953
 - 24 **Yao DF**, Wu XH, Zhu Y, Shi GS, Dong ZZ, Yao DB, Wu W, Qiu LW, Meng XY. Quantitative analysis of vascular endothelial growth factor, microvascular density and their clinicopathologic features in human hepatocellular carcinoma. *Hepatobiliary Pancreat Dis Int* 2005; **4**: 220-226
 - 25 **Lim M**, Cheshier S, Steinberg GK. New vessel formation in the central nervous system during tumor growth, vascular malformations, and Moyamoya. *Curr Neurovasc Res* 2006; **3**: 237-245
 - 26 **Zhao HC**, Qin R, Chen XX, Sheng X, Wu JF, Wang DB, Chen GH. Microvessel density is a prognostic marker of human gastric cancer. *World J Gastroenterol* 2006; **12**: 7598-7603
 - 27 **Des Guetz G**, Uzzan B, Nicolas P, Cucherat M, Morere JF, Benamouzig R, Breau JL, Perret GY. Microvessel density and VEGF expression are prognostic factors in colorectal cancer. Meta-analysis of the literature. *Br J Cancer* 2006; **94**: 1823-1832
 - 28 **Du JR**, Jiang Y, Zhang YM, Fu H. Vascular endothelial growth factor and microvascular density in esophageal and gastric carcinomas. *World J Gastroenterol* 2003; **9**: 1604-1606
 - 29 **Wang GX**, Xu S, Wang W, Li T, Luo YY. [Clinical application of contrast-enhanced ultrasound in differential diagnosis of malignant and benign gastrointestinal neoplasms]. *Zhonghua Yixue Chaosheng Zazhi* 2007; **4**: 35-37
 - 30 **Shiyan L**, Pintong H, Zongmin W, Fuguang H, Zhiqiang Z, Yan Y, Cosgrove D. The relationship between enhanced intensity and microvessel density of gastric carcinoma using double contrast-enhanced ultrasonography. *Ultrasound Med Biol* 2009; **35**: 1086-1091
 - 31 **Ohto M**, Kato H, Tsujii H, Maruyama H, Matsutani S, Yamagata H. Vascular flow patterns of hepatic tumors in contrast-enhanced 3-dimensional fusion ultrasonography using plane shift and opacity control modes. *J Ultrasound Med* 2005; **24**: 49-57
 - 32 **Yukisawa S**, Ohto M, Masuya Y, Okabe S, Fukuda H, Yoshikawa M, Ebara M, Saisho H, Ohtsuka M, Miyazaki M, Kondo F. Contrast-enhanced three-dimensional fusion sonography of small liver metastases with pathologic correlation. *J Clin Ultrasound* 2007; **35**: 1-8
 - 33 **Coakley FV**, Schwartz LH. Imaging of hepatocellular carcinoma: a practical approach. *Semin Oncol* 2001; **28**: 460-473
 - 34 **Kudo M**. Imaging blood flow characteristics of hepatocellular carcinoma. *Oncology* 2002; **62** Suppl 1: 48-56
 - 35 **Shi H**, Yu XH, Zhang H, Li L. [Application of three-dimensional contrast-enhanced ultrasound in the vascular characteristics on display for abdominal tumors]. *Zhongguo Yixue Yingxiang Jishu* 2008; **24**: 1227-1230

S- Editor Lv S L- Editor A E- Editor Zheng XM

A comparison of survival and pathologic features of non-alcoholic steatohepatitis and hepatitis C virus patients with hepatocellular carcinoma

Roberto Hernandez-Alejandro, Kris P Croome, Martin Drage, Nathalie Sela, Jeremy Parfitt, Natasha Chandok, Paul Marotta, Cheryl Dale, William Wall, Douglas Quan

Roberto Hernandez-Alejandro, Kris P Croome, Martin Drage, Nathalie Sela, Natasha Chandok, Paul Marotta, Cheryl Dale, William Wall, Douglas Quan, Multi-Organ Transplant Program, Department of Surgery, London Health Sciences Centre, Ontario N6A 5A5, Canada

Jeremy Parfitt, Department of Pathology, London Health Sciences Centre, Ontario N6A 5A5, Canada

Author contributions: Hernandez-Alejandro R, Croome KP, Marotta P, Quan D, Wall W, Dale C Participated in research design; Hernandez-Alejandro R, Croome KP, Marotta P, Drage M participated in the writing of the paper; Hernandez-Alejandro R, Croome KP, Sela N, Parfitt J and Chandok N participated in the performance of the research; Hernandez-Alejandro R, Croome KP participated in data analysis.

Correspondence to: Roberto Hernandez-Alejandro, MD, Multi-Organ Transplant Program, Department of Surgery, London Health Sciences Centre, 339 Windermere Road London, Ontario N6A 5A5, Canada. roberto.hernandezalejandro@lhsc.on.ca
Telephone: +1-519-6632920 Fax: +1-519-6633858

Received: December 28, 2011 Revised: May 8, 2012

Accepted: May 13, 2012

Published online: August 21, 2012

Abstract

AIM: To compare the clinical outcome and pathologic features of non-alcoholic steatohepatitis (NASH) patients with hepatocellular carcinoma (HCC) and hepatitis C virus (HCV) patients with HCC (another group in which HCC is commonly seen) undergoing liver transplantation.

METHODS: Patients transplanted for HCV and NASH at our institution from January 2000 to April 2011 were analyzed. All explanted liver histology and pre-transplant liver biopsies were examined by two specialist liver histopathologists. Patient demographics, disease free survival, explant liver characteristics and HCC features (tumour number, cumulative tumour size, vascular invasion and differentiation) were compared between HCV

and NASH liver transplant recipients.

RESULTS: A total of 102 patients with NASH and 283 patients with HCV were transplanted. The incidence of HCC in NASH transplant recipients was 16.7% (17/102). The incidence of HCC in HCV transplant recipients was 22.6% (64/283). Patients with NASH-HCC were statistically older than HCV-HCC patients ($P < 0.001$). A significantly higher proportion of HCV-HCC patients had vascular invasion (23.4% vs 6.4%, $P = 0.002$) and poorly differentiated HCC (4.7% vs 0%, $P < 0.001$) compared to the NASH-HCC group. A trend of poorer recurrence free survival at 5 years was seen in HCV-HCC patients compared to NASH-HCC who underwent a Liver transplantation ($P = 0.11$).

CONCLUSION: Patients transplanted for NASH-HCC appear to have less aggressive tumour features compared to those with HCV-HCC, which likely in part accounts for their improved recurrence free survival.

© 2012 Baishideng. All rights reserved.

Key words: Hepatitis C virus; Liver transplant; Hepatocellular carcinoma; Non-alcoholic steatohepatitis; Comparison; Recurrence; Vascular invasion; Poorly differentiated; Survival

Peer reviewer: Wan-Long Chuang, Professor, Internal Medicine, Kaohsiung Medical University, No. 100, Shih-Chuan 1st Road, Kaohsiung 807, Taiwan, China

Hernandez-Alejandro R, Croome KP, Drage M, Sela N, Parfitt J, Chandok N, Marotta P, Dale C, Wall W, Quan D. A comparison of survival and pathologic features of non-alcoholic steatohepatitis and hepatitis C virus patients with hepatocellular carcinoma. *World J Gastroenterol* 2012; 18(31): 4145-4149 Available from: URL: <http://www.wjgnet.com/1007-9327/full/v18/i31/4145.htm>
DOI: <http://dx.doi.org/10.3748/wjg.v18.i31.4145>

INTRODUCTION

The prevalence of obesity in North American Society continues to rise^[1]. With this increasing rate of obesity there has been a concomitant increase in the prevalence of non-alcoholic fatty liver disease (NAFLD)^[2]. The natural history of NAFLD is quite variable. It includes a spectrum ranging from reversible steatosis to steatohepatitis with hepatic fibrosis (NASH), and ultimately cirrhosis^[3-5]. Up to 30% of adults in North America and Western Europe are known to have excess fat accumulation in the liver^[6]. Of these, nearly 10% have NASH, which represents 2%-3% of all adults. There is speculation that NASH may soon become one of the main causes of End Stage Liver Disease (ESLD) requiring liver transplantation in North America^[7].

Hepatitis C virus (HCV) is one of the most common underlying liver diseases in hepatocellular carcinoma (HCC), accounting for about one-third of the cases of HCC in the United States^[8]. It is well established that patients with NASH can progress to develop HCC with previous reports suggesting that the 5 year prevalence may be as high as 7.6%^[9]. However as increasing numbers of HCC cases arising from NASH are being seen, it is important to clarify the outcomes and recurrence by comparing the clinical and pathological features of HCC due to NASH with those of HCC caused by one the more common underlying liver diseases in HCC, HCV infection, as a benchmark.

Previous studies have suggested that patients with NASH cirrhosis are less likely than those with HCV to get transplanted^[10]. This may be in large part to a higher likelihood of being denied listing for co-morbid conditions. Previous authors have shown that NASH patients with diabetes, hypertension, body mass index (BMI) > 30 years and age > 60 years undergoing liver transplantation have a poor (50%) 1 year mortality^[11]. However in appropriately selected NASH patients post liver transplant survival can fair at least as well as individuals who undergo transplant for other etiologies. The outcome of NASH patients with underlying HCC undergoing a liver transplantation compared to HCV patients with underlying HCC (another group in which HCC is commonly seen) has not been thoroughly investigated. Specifically the tumour characteristics in explanted livers and disease free survival between these groups have not been compared. The goal of the present study was to compare the clinical and pathological parameters as well as disease free survival in the two groups.

MATERIALS AND METHODS

We performed a retrospective review on all patients who underwent liver transplantation (LT) for HCV or NASH cirrhosis from January 2000 to April 2011 at our institution. Patients less than 18 years of age were excluded. Data on these patients were prospectively entered in our transplant database. In order to confirm or refute the

original histological diagnoses, all explanted liver histology and pre-transplant liver biopsies were re-examined by two specialist liver histopathologists who were blinded to the original diagnoses.

The etiology of the original liver disease was diagnosed by set criteria. NASH was determined to be the cause of chronic liver disease in patients with histological evidence of steatohepatitis in pre-transplant liver biopsies or in liver explants (steatosis, portal and/or lobular inflammation, hepatocyte ballooning, pericellular fibrosis and the presence of Mallory bodies)^[12,13], in conjunction with no history of alcohol consumption. HCV-related liver disease was confirmed by explants pathology and the presence of HCV RNA.

All patients with a pre and post-transplant diagnosis of HCC were identified in both the NASH and HCV groups. Listed patients with known HCC all fell within Milan Criteria^[14]. Patients who received pre-transplant radiofrequency ablation were excluded. HCC was confirmed histologically in the explanted liver. All Donation after Cardiac Death (DCD) organs were procured from controlled DCD donors using techniques previously published by our group^[15]. Primary outcomes were patient survival as well as pathologic features of HCC (tumour number, cumulative tumour size, vascular invasion and differentiation). Level of differentiation of HCC tumours was graded using the Modified Edmondson-Steiner grading system^[16]. Additional variables investigated included age at diagnosis, gender and α -feto-protein (AFP) levels. Recurrence free survival was taken at the time point of maximal follow-up.

Statistical analysis

All data are presented as means \pm SD. Differences between groups were analyzed using the unpaired *t* test for continuous variables and by the χ^2 test or continuity correction method for categorical variables. Survival curves for patient and graft survival were generated using the Kaplan-Meier method and compared by the log-rank test. All statistical tests were two-sided and differences were considered significant when $P < 0.05$.

RESULTS

A total of 832 liver transplants were performed at the London Health Sciences Centre during the study period. Of these, 283 (34.0%) recipients were positive for HCV based on the aforementioned criteria. NASH was the indication for liver transplantation in 96 (11.5%) recipients, and 42 (5.1%) recipients were diagnosed with 'cryptogenic' or 'idiopathic' cirrhosis. The remaining 411 (49.4%) recipients had liver failure due to other identifiable causes. Of the 42 cases originally diagnosed as cryptogenic cirrhosis, 6 were re-designated as NASH associated cirrhosis based on current histologic and clinical definitions. Thus the final analysis of HCV and NASH liver transplant recipients was: 283 (34.0%), 102 (12.3%) respectively (Figure 1).

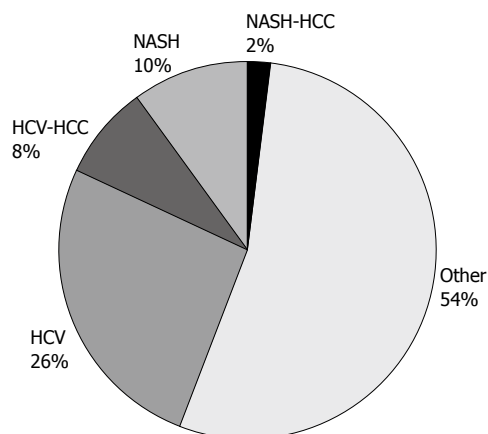


Figure 1 Diagnosis in patients undergoing liver transplantation. HCC: Hepatocellular carcinoma; HCV: Hepatitis C virus; NASH: Non-alcoholic steatohepatitis.

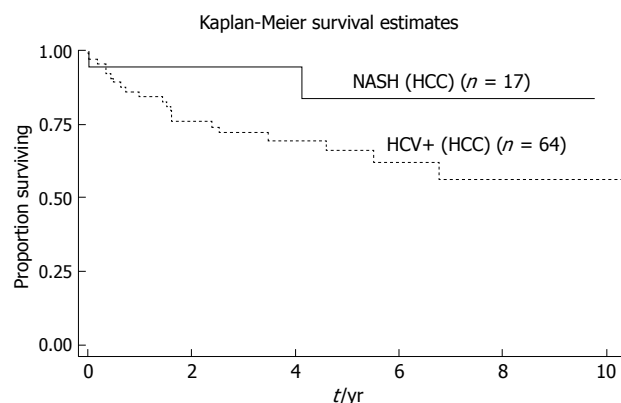


Figure 2 Recurrence free survival in non-alcoholic steatohepatitis-hepatocellular carcinoma vs hepatitis c virus-hepatocellular carcinoma groups. HCC: Hepatocellular carcinoma; HCV: Hepatitis C virus; NASH: Non-alcoholic steatohepatitis.

	HCV/HCC n = 64	NASH/HCC n = 17	P value
Age at transplant (mean ± SD)	52.6 ± 5.8	58.6 ± 4.2	< 0.001
Gender (% male)	94%	94%	1.000
Donor source (DBD/DCD/LD)	56/8/0	16/0/1	NA
AFP (mean ± SD)	93.1 ± 204.4	20.3 ± 34.0	0.149
Number of tumours (mean ± SD)	1.59 ± 0.81	1.64 ± 0.75	0.819
Cumulative size of tumours (mean ± SD)	3.98 ± 2.4	3.27 ± 2.1	0.270
Vascular invasion	23.40%	6.30%	0.002
Poorly differentiated	4.70%	0%	< 0.001

AFP: α -feto-protein; DBD: Donation after brain death; DCD: Donation after circulatory death; LD: Living donor; HCC: Hepatocellular carcinoma; HCV: Hepatitis C virus; NASH: Non-alcoholic steatohepatitis; NA: Not available.

The incidence of HCC in NASH recipients was 16.7% (17/102). Importantly, none of the re-categorized NASH patients who were originally designated cryptogenic were found to have HCC. The incidence of HCC in HCV liver transplant recipients at our centre was 22.6% (64/283).

Patients with NASH-HCC were statistically older than HCV-HCC patients (58.6 ± 4.2 years *vs* 52.6 ± 5.8 years, $P < 0.001$). There was no significant difference in gender or preoperative AFP level between the two groups. No patients with NASH-HCC received a DCD liver allograft (Table 1). The diagnosis of HCC was made before liver transplantation using multiple imaging techniques in 65% of NASH patients and 89% of HCV patients. HCC was more likely to be found incidentally in transplanted NASH patients (35%) than in transplanted HCV patients (11%) ($P = 0.015$).

Pathological characteristics of the NASH-HCC tumours were compared with those of HCV-HCC tumours (Table 1). A significantly higher proportion of HCV-HCC patients had vascular invasion (23.4% *vs* 6.4%, $P = 0.002$) as well as poorly differentiated tumours (4.7% *vs* 0%, $P < 0.001$) compared to the NASH-HCC. There was

no significant difference in the mean number of tumours or the mean cumulative size of the tumours between the two groups. In both groups, the tumours satisfied Milan criteria pre-transplantation.

Disease free survival at time of maximal follow-up was not statistically significant between the two groups however there was a clear trend towards lower disease free survival in the HCV-HCC group ($P = 0.11$, Figure 2).

DISCUSSION

The prevalence of NAFLD has continued to increase as the obesity epidemic continues. The rate of progression from NAFLD to the development of NASH or end stage liver disease is unknown. However, the frequency of NASH in patients listed for transplantation in North America has been previously determined to be 2.9%^[17]. This is likely an underestimate as this number was based on data collected from the 1990s, whereas in the last decade the rates of obesity and metabolic syndrome have increased dramatically. A more recent analysis of data from the Scientific Registry of Transplant Recipients (SRTR) reported that the rate had increased to 3.5%^[18]. In our series, 12.3% of patients have NASH as the diagnosis leading to liver failure requiring transplantation. NASH as a primary diagnosis in patients being listed or transplantation has continued to increase at our centre.

The natural history of NAFLD ranging from reversible steatosis to steatohepatitis with hepatic fibrosis (NASH), and ultimately the possibility of developing HCC has been previously described^[19]. In small previously published North American series of patients transplanted for NASH, HCC was found in 22% (2/9) of patients^[20]. In our series of 102 patients with NASH cirrhosis, 16.7% had HCC at the time of transplantation. This is a similar rate to the 22.6% of our HCV cirrhotic patients requiring transplantation, another well known high risk group for developing HCC. The high incidence of HCC in NASH patients undergoing liver transplantation suggests that these patients are at high risk of devel-

oping HCC and should undergo frequent ultrasound surveillance in a similar fashion to that performed in patients with HCV.

It has also been shown that patients with NASH are less likely to be listed for transplantation due to comorbidities, a justifiable practice given suboptimal results in NASH patients possessing these comorbidities^[10]. However in selected NASH patients receiving liver transplantation, others have shown that 5 year disease free survival after transplantation was significantly better than disease free survival in the C and B viral groups, 66%, 29% and 39% respectively^[21]. More recent studies have suggested there is no difference in 1 year and 3 year survival between patients transplanted for NASH and those transplanted for other indications^[22]. The outcome in patients with HCV is clearly affected by possible recurrence of HCV cirrhosis however NASH patients are also at risk for recurrence of NASH cirrhosis with some studies suggesting the incidence of recurrent NASH being as high as 25%^[23-25].

Patients with NASH and HCC post-transplant outcomes have not been previously investigated compared to patients with HCV and HCC (another group in which HCC is commonly seen). In previous studies looking at patients undergoing liver resection for HCC, cumulative survival after resection was comparable among HCV-HCC and NASH-HCC patient groups^[21].

In our study a significantly higher proportion of HCV-HCC patients had vascular invasion as well as poorly differentiated tumours compared to the NASH-HCC group. Vascular invasion is the strongest predictor of recurrence in patients with HCC^[26].

In the present study a trend of poorer recurrence free survival was seen in HCV-HCC patients compared to NASH-HCC who underwent a Liver transplantation. The higher proportion of patients with vascular invasion and poorly differentiated tumours may at least in part account for this difference in recurrence free survival. Based on our results it therefore appears that NASH associated HCC might be a less aggressive form of HCC compared with HCV associated HCC. It must also be entertained that some of the sickest NASH patients may not be listed for transplantation because of significant comorbidities or poor operative candidacy.

Limitations of the present study include its single centre nature as well as the lack of generalizability to non-transplant NASH and HCC populations due to the unique social and biologic factors of patients approved for transplantation.

In summary in those where NASH progresses to cirrhosis, there is a significant proportion that go on to develop HCC suggesting these individuals should undergo aggressive screening protocols directed toward the early detection of HCC, in a similar fashion to patients with HCV-cirrhosis. Patients with NASH-HCC undergoing liver transplantation also appear to be older than HCV-HCC patients undergoing liver transplantation. In appropriately selected patients with NASH and HCC post-transplant outcomes equal if not better than patients with

HCV-HCC (another group in which HCC is commonly seen). This may be related to less vascular invasion and less poorly differentiated pathology.

COMMENTS

Background

There is speculation that Non-alcoholic steatohepatitis (NASH) may soon become one of the main causes of end stage liver disease requiring liver transplantation in North America. The clinical outcome and pathologic features of NASH patients with hepatocellular carcinoma (HCC) undergoing liver transplantation compared with hepatitis c virus (HCV) patients with HCC (another group in which HCC is commonly seen) has not been thoroughly investigated.

Research frontiers

A significantly higher proportion of HCV-HCC patients had vascular invasion (23.4% vs 6.4%) and poorly differentiated HCC (4.7% vs 0%) compared to the NASH-HCC group. A trend of poorer recurrence free survival at 5 years was seen in HCV-HCC patients compared to NASH-HCC who underwent a Liver transplantation.

Innovations and breakthroughs

To knowledge, this represents the first study to compare the tumour characteristics in explanted livers and disease free survival between NASH-HCC and HCV-HCC patients undergoing liver transplantation.

Applications

In appropriately selected patients with NASH and HCC post-transplant outcomes equal if not better than patients with HCV HCC (another group in which HCC is commonly seen). This may be related to less vascular invasion and less poorly differentiated pathology.

Peer review

In this manuscript, the authors investigated the clinical outcome and pathologic features of NASH patients with HCC undergoing liver transplantation compared with HCV patients with HCC. This is a retrospective analysis. The originality of this study was not so high. Nonetheless, the data were properly presented and the manuscript was well prepared. The results of this study may provide useful information to the clinicians.

REFERENCES

- 1 **Ogden CL**, Carroll MD, Curtin LR, McDowell MA, Tabak CJ, Flegal KM. Prevalence of overweight and obesity in the United States, 1999-2004. *JAMA* 2006; **295**: 1549-1555
- 2 **Musso G**, Gambino R, Cassader M, Pagano G. Meta-analysis: natural history of non-alcoholic fatty liver disease (NAFLD) and diagnostic accuracy of non-invasive tests for liver disease severity. *Ann Med* 2011; **43**: 617-649
- 3 **Ong JP**, Younossi ZM. Nonalcoholic fatty liver disease (NAFLD)--two decades later: are we smarter about its natural history? *Am J Gastroenterol* 2003; **98**: 1915-1917
- 4 **Adams LA**, Sanderson S, Lindor KD, Angulo P. The histological course of nonalcoholic fatty liver disease: a longitudinal study of 103 patients with sequential liver biopsies. *J Hepatol* 2005; **42**: 132-138
- 5 **Harrison SA**, Torgerson S, Hayashi PH. The natural history of nonalcoholic fatty liver disease: a clinical histopathological study. *Am J Gastroenterol* 2003; **98**: 2042-2047
- 6 **Neuschwander-Tetri BA**, Caldwell SH. Nonalcoholic steatohepatitis: summary of an AASLD Single Topic Conference. *Hepatology* 2003; **37**: 1202-1219
- 7 **Charlton M**. Nonalcoholic fatty liver disease: a review of current understanding and future impact. *Clin Gastroenterol Hepatol* 2004; **2**: 1048-1058
- 8 **Shimada M**, Hashimoto E, Taniai M, Hasegawa K, Okuda H, Hayashi N, Takasaki K, Ludwig J. Hepatocellular carcinoma in patients with non-alcoholic steatohepatitis. *J Hepatol* 2002; **37**: 154-160
- 9 **Davila JA**, Morgan RO, Shaib Y, McGlynn KA, El-Serag HB. Hepatitis C infection and the increasing incidence of hepato-

- cellular carcinoma: a population-based study. *Gastroenterology* 2004; **127**: 1372-1380
- 10 **O'Leary JG**, Landaverde C, Jennings L, Goldstein RM, Davis GL. Patients with NASH and cryptogenic cirrhosis are less likely than those with hepatitis C to receive liver transplants. *Clin Gastroenterol Hepatol* 2011; **9**: 700-704.e1
 - 11 **Malik SM**, deVera ME, Fontes P, Shaikh O, Ahmad J. Outcome after liver transplantation for NASH cirrhosis. *Am J Transplant* 2009; **9**: 782-793
 - 12 **Nakano M**. Histological study on the resemblance and difference between non-alcoholic steatohepatitis (NASH) and alcoholic liver diseases (ALD). *Alcohol Clin Exp Res* 2005; **29**: 230S-235S
 - 13 **Hübscher SG**. Role of liver biopsy in the assessment of non-alcoholic fatty liver disease. *Eur J Gastroenterol Hepatol* 2004; **16**: 1107-1115
 - 14 **Mazzaferro V**, Regalia E, Doci R, Andreola S, Pulvirenti A, Bozzetti F, Montalto F, Ammatuna M, Morabito A, Gennari L. Liver transplantation for the treatment of small hepatocellular carcinomas in patients with cirrhosis. *N Engl J Med* 1996; **334**: 693-699
 - 15 **Hernandez-Alejandro R**, Croome KP, Quan D, Mawardi M, Chandok N, Dale C, McAlister V, Levstik MA, Wall W, Marotta P. Increased risk of severe recurrence of hepatitis C virus in liver transplant recipients of donation after cardiac death allografts. *Transplantation* 2011; **92**: 686-689
 - 16 **Edmondson HA**, Steiner PE. Primary carcinoma of the liver: a study of 100 cases among 48,900 necropsies. *Cancer* 1954; **7**: 462-503
 - 17 **Charlton M**, Kasparova P, Weston S, Lindor K, Maor-Kendler Y, Wiesner RH, Rosen CB, Batts KP. Frequency of nonalcoholic steatohepatitis as a cause of advanced liver disease. *Liver Transpl* 2001; **7**: 608-614
 - 18 **Angulo P**. Nonalcoholic fatty liver disease and liver transplantation. *Liver Transpl* 2006; **12**: 523-534
 - 19 **Vernon G**, Baranova A, Younossi ZM. Systematic review: the epidemiology and natural history of non-alcoholic fatty liver disease and non-alcoholic steatohepatitis in adults. *Aliment Pharmacol Ther* 2011; **34**: 274-285
 - 20 **Ayata G**, Gordon FD, Lewis WD, Pomfret E, Pomposelli JJ, Jenkins RL, Khettry U. Cryptogenic cirrhosis: clinicopathologic findings at and after liver transplantation. *Hum Pathol* 2002; **33**: 1098-1104
 - 21 **Wakai T**, Shirai Y, Sakata J, Korita PV, Ajioka Y, Hatakeyama K. Surgical outcomes for hepatocellular carcinoma in nonalcoholic fatty liver disease. *J Gastrointest Surg* 2011; **15**: 1450-1458
 - 22 **Charlton MR**, Burns JM, Pedersen RA, Watt KD, Heimbach JK, Dierkhising RA. Frequency and outcomes of liver transplantation for nonalcoholic steatohepatitis in the United States. *Gastroenterology* 2011; **141**: 1249-1253
 - 23 **El-Masry M**, Puig CA, Saab S. Recurrence of non-viral liver disease after orthotopic liver transplantation. *Liver Int* 2011; **31**: 291-302
 - 24 **Maor-Kendler Y**, Batts KP, Burgart LJ, Wiesner RH, Krom RA, Rosen CB, Charlton MR. Comparative allograft histology after liver transplantation for cryptogenic cirrhosis, alcohol, hepatitis C, and cholestatic liver diseases. *Transplantation* 2000; **70**: 292-297
 - 25 **Kim WR**, Poterucha JJ, Porayko MK, Dickson ER, Steers JL, Wiesner RH. Recurrence of nonalcoholic steatohepatitis following liver transplantation. *Transplantation* 1996; **62**: 1802-1805
 - 26 **Llovet JM**, Schwartz M, Mazzaferro V. Resection and liver transplantation for hepatocellular carcinoma. *Semin Liver Dis* 2005; **25**: 181-200

S- Editor Gou SX L- Editor A E- Editor Zhang DN

Adjusting CA19-9 values to predict malignancy in obstructive jaundice: Influence of bilirubin and C-reactive protein

Gaetano La Greca, Maria Sofia, Rosario Lombardo, Saverio Latteri, Agostino Ricotta, Stefano Puleo, Domenico Russello

Gaetano La Greca, Maria Sofia, Rosario Lombardo, Saverio Latteri, Agostino Ricotta, Stefano Puleo, Domenico Russello, Department of Surgical Sciences, Organ Transplantation and Advanced Technologies, University of Catania, 95125 Catania, Italy

Author contributions: La Greca G and Sofia M contributed equally to this work; La Greca G, Puleo S and Russello D designed research; Sofia M, Lombardo R, Latteri S and Ricotta A performed research; Puleo S and Latteri S contributed analytic tools; Sofia M and Lombardo R analyzed data; and Sofia M and La Greca G wrote the paper.

Correspondence to: Dr. Maria Sofia, Department of Surgical Sciences, Organ Transplantation and Advanced Technologies, University of Catania, Via Del Bosco, 324, 95125 Catania, Italy. mariasofia2002@libero.it

Telephone: +39-95-7263584 Fax: +39-95-7122221

Received: January 6, 2012 Revised: April 27, 2012

Accepted: May 5, 2012

Published online: August 21, 2012

Abstract

AIM: To find a possible relationship between inflammation and CA19-9 tumor marker by analyzing data from patients with benign jaundice (BJ) and malignant jaundice (MJ).

METHODS: All patients admitted for obstructive jaundice, in the period 2005-2009, were prospectively enrolled in the study, obtaining a total of 102 patients. On admission, all patients underwent complete standard blood test examinations including C-reactive protein (CRP), bilirubin, CA19-9. Patients were considered eligible for the study when they presented obstructive jaundice confirmed by instrumental examinations and increased serum bilirubin levels (total bilirubin > 2.0 mg/dL). The standard cut-off level for CA19-9 was 32 U/mL, whereas for CRP this was 1.5 mg/L. The CA19-9 level was adjusted by dividing it by the value of serum bilirubin or by the CRP value. The patients were divided

into 2 groups, MJ and BJ, and after the adjustment a comparison between the 2 groups of patients was performed. Sensitivity, specificity and positive predictive values were calculated before and after the adjustment.

RESULTS: Of the 102 patients, 51 were affected by BJ and 51 by MJ. Pathologic CA19-9 levels were found in 71.7% of the patients. In the group of 51 BJ patients there were 29 (56.9%) males and 22 (43.1%) females with a median age of 66 years (range 24-96 years), whereas in the MJ group there were 24 (47%) males and 27 (53%) females, with a mean age of 70 years (range 30-92 years). Pathologic CA19-9 serum level was found in 82.3% of MJ. CRP levels were pathologic in 66.6% of the patients with BJ and in 49% with MJ. Bilirubin and CA19-9 average levels were significantly higher in MJ compared with BJ ($P = 0.000$ and $P = 0.02$), while the CRP level was significantly higher in BJ ($P = 0.000$). Considering a CA19-9 cut-off level of 32 U/mL, 82.3% in the MJ group and 54.9% in the BJ group were positive for CA19-9 ($P = 0.002$). A CA19-9 cut-off of 100 U/mL increases the difference between the two groups: 35.3% in BJ and 68.6% in MJ ($P = 0.0007$). Adjusting the CA19-9 value by dividing it by serum bilirubin level meant that 21.5% in the BJ and 49% in the MJ group remained with a positive CA19-9 value ($P = 0.003$), while adjusting the CA19-9 value by dividing it by serum CRP value meant that 31.4% in the BJ group and 76.5% in the MJ group still had a positive CA19-9 value ($P = 0.000004$). Sensitivity, specificity, positive predictive values of CA19-9 > 32 U/mL were 82.3%, 45% and 59.1%; when the cut-off was CA19-9 > 100 U/mL they were, respectively, 68.6%, 64.7% and 66%. When the CA19-9 value was adjusted by dividing it by the bilirubin or CRP values, these became 49%, 78.4%, 69.4% and 76.5%, 68.6%, 70.9%, respectively.

CONCLUSION: The present study proposes CRP as a new and useful correction factor to improve the diag-

nostic value of the CA19-9 tumor marker in patients with cholestatic jaundice.

© 2012 Baishideng. All rights reserved.

Key words: Tumor marker; CA19-9; C-reactive protein; Bilirubin; Pancreato-biliary malignancy; Biliary stones

Peer reviewer: Dr. Ashok Kumar, Department of Surgical Gastroenterology, Sanjay Gandhi Post Graduate Institute of Medical Sciences, Raebareli Road, Lucknow 226014, India

La Greca G, Sofia M, Lombardo R, Latteri S, Ricotta A, Puleo S, Russello D. Adjusting CA19-9 values to predict malignancy in obstructive jaundice: Influence of bilirubin and C-reactive protein. *World J Gastroenterol* 2012; 18(31): 4150-4155 Available from: URL: <http://www.wjgnet.com/1007-9327/full/v18/i31/4150.htm> DOI: <http://dx.doi.org/10.3748/wjg.v18.i31.4150>

INTRODUCTION

CA19-9 is a tumor marker that increases in pancreatic and biliary malignancy and it has been promoted as a reliable test for the detection of pancreato-biliary malignancy. In pancreatic cancer, CA19-9 has been reported to have 70%-80% sensitivity and 80%-90% specificity in tumor diagnosis, whereas in cholangiocarcinoma without history of sclerosing cholangitis the sensitivity and specificity are, respectively, 77.9% and 76.3%^[1-2]. CA19-9 is unfortunately increased not only in patients with pancreatic or biliary cancers but also in benign biliary diseases which often present with jaundice and is therefore often misleading, reducing significantly the diagnostic accuracy of this marker^[3-5]. The relationship between CA19-9 and jaundice has been analyzed and studied to find possible adjustments to increase the sensitivity, specificity and predictive value of the test in differential diagnosis of hepatobiliary diseases associated with jaundice. Therefore, some authors have suggested to adjust CA19-9 value by dividing it empirically by the serum bilirubin value^[6,7]. Other factors that could influence and alter the values of this tumor marker have not been studied yet. Inflammation contributes to elevating the CA19-9 value and it can be assessed by monitoring the acute-phase proteins: one of these is the C-reactive protein (CRP) which rises in response to infection, injury and neoplasm.

This research was stimulated by our own experience of patients presenting with jaundice of benign etiology who were found to have grossly elevated CA19-9 levels. The purpose of this study was to clarify the clinical interpretation and diagnostic value of an elevated serum CA19-9 level, with special reference to coexistent obstructive jaundice. The present study, first in the literature, analyzes a possible relationship between CA19-9, bilirubin and inflammation, expressed as CRP value, aiming to find a ratio or a better corrective factor to increase predictivity of CA19-9 and reduce the number of misleading false positive results.

MATERIALS AND METHODS

All the patients admitted for obstructive jaundice to the Department of Emergency Surgery, Cannizzaro Hospital, University of Catania, Italy, between September 2005 and September 2009, were considered for the present study. The patients were enrolled prospectively, 51 for each group of benign jaundice (BJ) and malignant jaundice (MJ) patients, obtaining a total of 102 patients. At admission, all patients underwent complete standard blood test examinations, including serum bilirubin levels. Patients were considered eligible for the study when they presented obstructive jaundice confirmed by instrumental examinations and increased bilirubin serum levels (total bilirubin > 2.0 mg/dL). Serum levels of CA19-9 and CRP were also measured at the time of admission. The standard cut-off level of CA19-9 was 32 U/mL, whereas for CRP this was 1.5 mg/L. The definitive diagnosis was obtained by instrumental examinations, surgical exploration and pathology. Instrumental examinations included ultrasonography, computed tomography scan, magnetic resonance imaging, endoscopic ultrasound scan and endoscopic retrograde cholangiopancreatography. The CA19-9 level was adjusted by dividing it by the value of serum bilirubin firstly, and then by the CRP value. The patients were divided into 2 groups: MJ and BJ. After the adjustment a comparison between the serum levels in the 2 groups of patients was obtained by Wilcoxon two sample test. Differences for categorical variables were assessed using the chi-square test or Fisher's exact test when adequate. Spearman correlation between the 3 parameters of CA19-9, bilirubin and CRP in each group of patients was computed. The receiver operating characteristic curve was used to establish the probability that a patient with MJ has a high value of CA19-9. A *P* value less than 0.05 was considered statistically significant.

RESULTS

The present longitudinal study analyzed a total of 102 patients: 53 (52%) men and 49 (48%) women with a median age of 69 years (range 24-96 years). In the group of 51 BJ patients there were 29 (56.9%) males and 22 (43.1%) females with a median age of 66 years (range 24-96 years), whereas in the MJ group there were 24 (47%) males and 27 (53%) females, with a median age of 70 years (range 30-92 years). Causes of BJ included: common bile duct (CBD) stones (66.6%), gallbladder stones with cholangitis (15.7%), biliary pancreatitis (15.7%), papillitis (1.9%). Causes of MJ included: pancreatic cancer (49%), bile duct cancer (19.6%), gallbladder cancer (13.7%), ampullary cancer (9.8%), intrahepatic cholangiocarcinoma (1.9%) and other malignancy (5.8%; 2 patients with metastatic nodes in porta hepatis and one patient with peritoneal carcinomatosis from ovarian cancer). Pathologic CA19-9 serum level was found in 82.3% of MJ, but in two patients the CA19-9 was 2.5 U/mL. CA19-9 did not correlate directly with the grade of biliary obstruction either expressed as bilirubin level in BJ and MJ (Figure 1). CRP

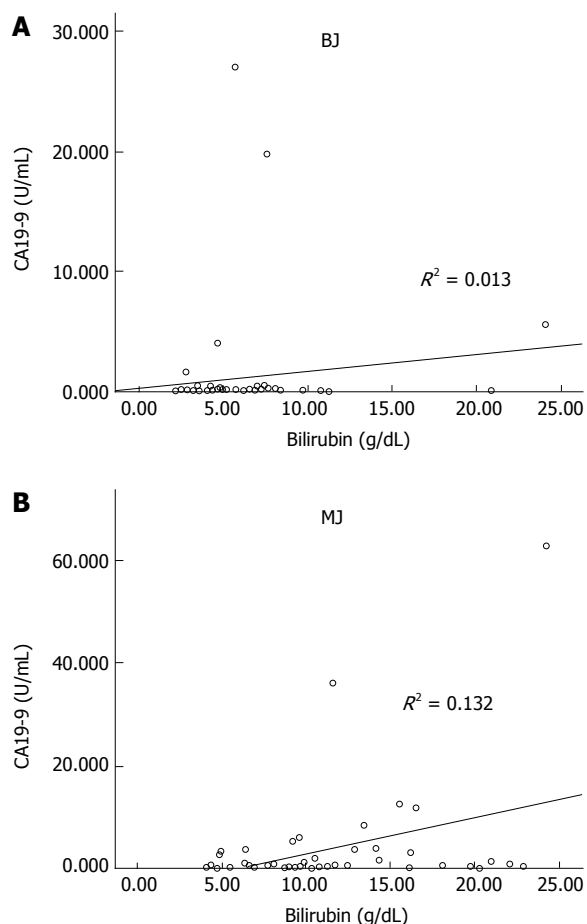


Figure 1 Correlation between total bilirubin and CA19-9 for benign jaundice (exponential line fit, $R^2 = 0.013$) (A) and malignant jaundice (exponential line fit, $R^2 = 0.132$) (B). BJ: Benign jaundice; MJ: Malignant jaundice.

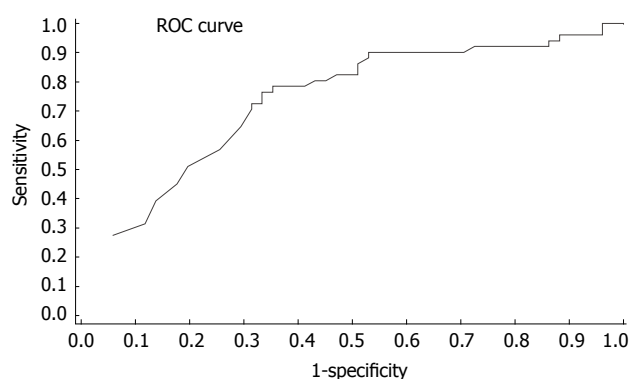


Figure 2 Receiver operating characteristic curve for biomarker CA19-9. ROC: Receiver operating characteristic.

levels were pathologic in 66.6% of the patients with BJ and in 49.0% with MJ. Mean bilirubin and CA19-9 levels were significantly higher in MJ compared to BJ, while the CRP level was significantly higher in BJ (Table 1). Table 2 reports the serum level of bilirubin, CA19-9 and CRP according to the cause of jaundice. There were no relevant differences in bilirubin according to the cause of jaundice. Comparing the CA19-9 value between patients with pancreatic cancer and patients with other causes of MJ and

	Benign	Malignant	P value
No. of patients	51	51	
Bilirubin serum level (median and range) (g/dL)	5.2 (2.12-24.03)	9.7 (4.07-24.25)	< 0.0001
CA19-9 serum level (median and range) (U/mL)	36 (2-27019)	405 (2.5-62974)	0.02
> 32 (%)	28/51 (54.9)	42/51 (82.3)	0.003
> 100 (%)	18/51 (35.3)	35/51 (68.6)	0.0007
CRP (median and range) (U/mL)	6.91 (0.1-30)	2.97 (0.1-13.2)	0.0002
> 1.5 (%)	34/51 (66.6)	25/51 (49.0)	0.005
> 5 (%)	21/51 (41.2)	7/51 (13.7)	0.004

CRP: C-reactive protein; CI: Confidence interval.

BJ, no difference was reported. CRP was significantly ($P = 0.04$) higher in patients with CBD stones than in pancreatic cancer, and patients with BJ and pancreatitis had the highest value of CRP. In MJ the average level of CRP was significantly higher in gallbladder cancer than in bile duct cancer, but not different from that in pancreatic cancer.

When considering the CA19-9 cut-off level of 32 U/mL, 42 of 51 patients (82.3%) in the malignant group and 28 of 51 (54.9%) in the benign group were positive for CA19-9 (Fisher's exact test: $P = 0.002$). Figure 2 shows that the area under the curve or probability that a patient diagnosed with MJ has a major value of CA19-9 compared to a patient diagnosed with BJ was 0.71. Increasing the cut-off level of CA19-9 to 100 U/mL, the difference between the two groups increases: 35.3% in BJ and 68.6% in MJ (Fisher's exact test: $P = 0.0007$). Changing the cut-off level alters the sensitivity and specificity as shown in Table 3, but by pushing up the cut-off level in spite of an increase of specificity we have obtained a reduction in the sensitivity of the test.

Adjusting the CA19-9 value by dividing it by serum bilirubin level, 11 of 51 patients (21.6%) in the BJ and 26 of 51 patients (51.0%) in the MJ group remained with a positive CA19-9 value (Fisher's exact test: $P = 0.003$), increasing the specificity to 78.4% but reducing the sensitivity to 49%.

The second mode of adjustment of the CA19-9 value was performed by dividing it by serum CRP value. Consequently, 16 of 51 patients (31.4%) in the BJ group and 39 of 51 patients (76.5%) in the MJ group remained with a positive CA19-9 value (Fisher's exact test: $P = 0.000004$). By this adjustment the sensitivity increases to 76.5%, the specificity to 68.6% and the positive predictive value (PPV) to 70.9%.

DISCUSSION

The diagnostic role of CA19-9 as a test for the detection of pancreato-biliary malignancy remains poorly defined, because, as in other diagnostic modalities, the utility of

Table 2 Bilirubin, CA19-9 and C-reactive protein levels according to jaundice cause at time of hospital admission *n* (%)

Cause	No. of cases	Bilirubin (g/dL), median	CA19-9 (U/mL)			CRP (U/mL)				
			Median	<i>P</i> value ¹	> 32	> 100	Median	<i>P</i> value ²	> 1.5	> 5
Malignant	51	9.7	405		42 (8.3)	35 (68.6)	2		25 (49)	7 (13.7)
Pancreatic cancer	25 (49)	11.29	461	-	23 (92)	19 (76)	1.96	0.04	12 (48)	3 (12)
Bile duct cancer	10 (19.6)	9.94	313	0.28	7 (70)	6 (60)	1.26	0.06	1 (10)	0
Gallbladder cancer	7 (13.7)	8.94	3361	0.59	6 (85.7)	5 (71.4)	4.13 ³	0.91	5 (71.4)	2 (28.5)
Ampullary cancer	5 (9.8)	6.49	196	0.42	4 (80)	3 (60)	4.5	0.69	4 (80)	1 (0.2)
Intrahepatic cholangio carcinoma	1 (1.9)	16.13	2600	NA	1	1	5.96	NA	1	1
Others	3 (5.8)	7.65	16	0.53	1	1	4.95	0.84	2 (66.6)	1 (33.3)
Benign	51	5.2	36		28 (54.9)	18 (35.3)	4.5		34 (66.6)	21 (41.2)
CBD stones	34 (66.6)	5.63	42	0.10	19 (55.8)	12 (35.2)	3.47	-	22 (64.7)	11 (32.3)
Gallbladder stones with cholangitis	8 (15.7)	5.26	55	0.54	4 (50)	3 (37.5)	2.31	0.73	5 (62.5)	3 (37.5)
Biliary pancreatitis	8 (15.7)	3.85	61	0.27	4 (50)	3 (37.5)	10.33	0.04	7 (87.5)	7 (87.5)
Chronic papillitis	1 (1.9)	6.6	35	NA	1	0	0.7	NA	0	0

¹*P* = 0.04 *vs* other cancers. ²Wilcoxon test compared to pancreatic cancer; ³Wilcoxon test compared to common bile duct (CBD) stones. CRP: C-reactive protein; NA: Not applicable.

Table 3 Adjustments of the value of CA19-9: Differences in sensitivity, specificity and positive predictive value (%)

	Sensitivity	Specificity	PPV
CA19-9 > 32 U/mL	82.3	45.0	59.1
CA19-9 > 100 U/mL	68.6	64.7	66.0
CA19-9/BIL	49.0	78.4	69.4
CA19-9/CRP	76.5	68.6	70.9

PPV: Positive predictive value; BIL: Bilirubin; CRP: C-reactive protein.

CA19-9 has several confounding limitations. Firstly, false positive elevations in CA19-9 exist in benign conditions such as liver diseases (primary sclerosing cholangitis, primary biliary cirrhosis, chronic hepatitis, acute liver failure), obstructive jaundice, pancreatitis^[3,5,8-11]. Even diseases not related to the hepatobiliary tract such as interstitial pulmonary disease^[12], collagen vascular diseases and, reportedly, heavy tea consumption^[4,13], suggest that CA19-9 may be expressed as a marker of a systemic inflammatory response. Furthermore, CA19-9 has also been shown to be upregulated in other malignant tumors including gastric, ovarian, and colorectal carcinoma^[14]. However, the most common cause of false positive CA19-9 is obstructive jaundice^[10]. Physiologically, biliary epithelial cells secrete mucins carrying the epitope of CA19-9, hence the high level of CA19-9 in serum during the obstructive jaundice, reflecting both inflammatory hypersecretion and leakage of biliary mucins into serum. This process can be reversed by resolution of the jaundice, which is often associated with a fall in CA19-9 greater in benign disease than in malignant^[3], because in malignant disease the synthesis of CA19-9 by proliferating cells contributes to the total level in a manner independent from any associated condition^[5,5]. In this series patient with malignant jaundice had higher mean levels of bilirubin than those with benign jaundice; additionally, the level of CA19-9 was significantly higher in malignant than in benign, especially if we considered a cut off level > 100 U/mL. Unfortunately, in our study,

CA19-9 does not correlate directly with the grade of biliary obstruction either in benign or in malignant jaundice (Figure 1), even if we observed that in patients with benign disease levels of CA19-9 decreased after relief of biliary obstruction (data not shown).

Secondly, the concentration of this tumor marker in the serum may be influenced by the patient's secretor status, because patients who are genotypically negative for the Lewis blood group antigen (a-, b-), approximately 4%-15% of the general population, do not synthesize CA19-9^[15]. As above in the present series the rate of MJ with a CA19-9 value less than 2 U/mL is 3.9%.

Furthermore, not only hyperbilirubinemia can obscure the clinical value of CA19-9, but inflammation can contribute and have a role. CRP, synthesized in hepatocytes, is one of the acute-phase proteins which are components of the innate immune responses that increase after infections, trauma, burns, tissue infarction, inflammatory process and tumors. In general, increased CRP levels in malignant disease could also be caused by an inflammatory response to tumor invasion^[16]. Padillo *et al*^[17], analysing CRP in 24 jaundice patients, found CRP levels significantly higher in patients with cancer. Differently from that study, this series showed the CRP serum levels are higher in benign obstructive jaundice than in malignant. Indeed, Table 2 reports that CRP is significantly (*P* = 0.04) higher in patients with CBD stones than those with pancreatic cancer; in particular, patients with BJ and pancreatitis have the highest value of CRP. Malignancy such as gallbladder cancer and intrahepatic cholangiocarcinoma present values of CRP comparable to BJ, probably due to an intensive inflammatory response to the tumor.

In our series, 54.9% of patients with benign jaundice had positive CA19-9 levels (cut-off 32 U/mL), and 35.5% had CA19-9 value over 100 U/mL; therefore, although the overall increase of the tumor marker in benign jaundice was inferior compared to that observed in malignancies, there was an overlap of values between cancer and non-cancer causes. This resulted in a low

accuracy of CA19-9 to diagnose pancreatic-biliary malignancies in patients with jaundice, especially since this marker is not able to distinguish pancreatic carcinoma from other malignancy or other benign causes of jaundice, as reported in Table 2, differing from what has been shown in other studies^[14,18]. Even when considering a cut-off level of 100 U/mL, the specificity is still 64.7%. As a result of this diagnostic overlap, the American Society of Clinical Oncology does not currently advocate its use for screening, evaluation of resectability or disease follow-up^[19]. For this reason some authors suggested to push up the cut-off level to 300 U/mL in presence of cholangitis and cholestasis to increase CA19-9 specificity, but this was associated with a significant decrease of sensitivity^[20]. To achieve a specificity of 100%, cut-off levels greater than 1000 U/mL should be considered^[21]. We recorded ten BJ patients with CA19-9 level greater than 300 U/mL and five BJ patients with more than 1000 U/mL, and all of them had serum bilirubin level lower than 8 mg/dL. These data can explain why there is no difference in the mean CA19-9 value between each cause of BJ and pancreatic cancer jaundice (Table 2). Indeed, multiple reports of patients with extremely high CA19-9 values in patients with BJ can be found in the literature^[22-24]. Several studies have shown that the association of elevated levels of CA19-9 with the diagnosis of cancer is significantly obscured in the face of obstructive jaundice, and because the bilirubin level correlates with CA19-9, they suggest that this value should be adjusted for hyperbilirubinemia^[10,11]. In our study CA19-9 does not correlate directly with the grade of biliary obstruction, either in BJ or in MJ.

Hence, based on the knowledge that in benign jaundice high levels of CA19-9 are an expression of obstruction and inflammation and CRP levels are higher in this group of patients, the most appropriate adjusting factor could be the CRP and not the bilirubin value. Indeed, 54.9% of patients with BJ had a CA19-9 level greater than 32 U/mL, and using a CA19-9 cut-off of 100 U/mL, the specificity of the test to detect malignancy is increased, with little decrease in the sensitivity. But the majority of benign jaundice patients have a CA19-9 value < 100 U/mL, so by adjusting this value with the CRP it is possible to increase the reliability of the test. As shown in Table 3 using the bilirubin as adjusting factor, even if the specificity reaches 78.4%, the sensitivity falls down to 49%; instead the CRP value better reflects the inflammatory status, obtaining 76.5% sensitivity, 68.6% specificity and 70.9% PPV. Certainly, the CA19-9 value has to be considered as an adjunctive value to the patient's history in the diagnosis of patients with obstructive jaundice, and its value, even after adjustment, should be helpful in planning the type and priority of further investigations with regard to the liver, bile ducts and pancreas.

In conclusion, the present study proposes adjusting to the CA19-9/CRP ratio as a new diagnostic tool in patients with cholestatic jaundice, which has not been reported in similar studies in the literature. This simple

ratio can significantly increase the specificity and the positive predictive value of CA19-9 in the differential diagnosis between malignant and benign jaundice. Other complementary studies of these markers are essential for diagnosis of malignant tumors when jaundice is present.

COMMENTS

Background

CA19-9 is a tumor marker which is increased in both benign and malignant hepatobiliary diseases. Previous studies have shown that CA19-9 has high sensitivity and specificity in pancreatic cancer. However, this tumor marker has been found to be elevated in benign biliary diseases as well. Hence the accuracy of CA19-9 is unreliable. The authors have tried to analyze the relationship between CA19-9, bilirubin and CRP levels to predict the accuracy of CA19-9 in malignant obstructive jaundice.

Research frontiers

After experiencing patients presenting with jaundice of benign etiology and having grossly elevated CA19-9 levels, the authors aimed to clarify the clinical interpretation and diagnostic value of an elevated serum CA19-9 level, with special reference to coexistent obstructive jaundice. CA19-9 is demonstrated to be influenced by bilirubin level, but other factors such as inflammation could influence and alter the values of this tumor marker. The research hotspot is how the inflammation influences the level of CA19-9.

Innovations and breakthroughs

In the past, the accuracy of CA19-9 level was improved by dividing it by bilirubin level, but the high level of CA19-9 in serum during obstructive jaundice reflects also an inflammatory hypersecretion. The inflammation can be assessed by monitoring the acute-phase proteins: one of these is the C-reactive protein (CRP). In this regard, in the present study, the CA19-9 level was adjusted by dividing it by the value of serum bilirubin and by the CRP value to look for a ratio or a better corrective factor to increase predictivity of CA19-9 and reduce the amount of misleading false positives. In fact, this adjustment increases the sensitivity to 76.5%, the specificity to 68.6% and the positive predictive value to 70.9%.

Applications

The study results suggest that considering inflammation as a reliable factor which increases the CA19-9 level in benign disease, abnormal tumor marker values in these patients can be corrected using the CRP in order to reduce the false positive results. In this way, it is possible to concentrate efforts in planning the type and priority of further investigations in the liver, bile ducts and pancreas in patients affected by malignancy.

Terminology

CA19-9: Tumor marker that increases in pancreatic and biliary malignancy, as physiologically biliary epithelial cells secrete mucins carrying the epitope of CA19-9; CRP: Synthesized in hepatocytes, is one of the acute-phase proteins, which are components of the innate immune responses that increase after infections, trauma, burns, tissue infarction, inflammatory process and tumors.

Peer review

This is a good longitudinal study in which authors analyze the relationship between CA19-9, bilirubin and CRP levels to predict the accuracy of CA19-9 in malignant obstructive jaundice. The results are interesting and suggest that the inflammation influences the CA19-9 value and reducing this confounding factor can help to better identify patients with malignant obstructive jaundice.

REFERENCES

- 1 **Goonetilleke KS**, Siriwardena AK. Systematic review of carbohydrate antigen (CA 19-9) as a biochemical marker in the diagnosis of pancreatic cancer. *Eur J Surg Oncol* 2007; **33**: 266-270
- 2 **John AR**, Haghghi KS, Taniere P, Esmat ME, Tan YM, Bramhall SR. Is a raised CA 19-9 level diagnostic for a cholangiocarcinoma in patients with no history of sclerosing cholangitis? *Dig Surg* 2006; **23**: 319-324
- 3 **Marrelli D**, Caruso S, Pedrazzani C, Neri A, Fernandes E,

- Marini M, Pinto E, Roviello F. CA19-9 serum levels in obstructive jaundice: clinical value in benign and malignant conditions. *Am J Surg* 2009; **198**: 333-339
- 4 **Kim HJ**, Kim MH, Myung SJ, Lim BC, Park ET, Yoo KS, Seo DW, Lee SK, Min YI. A new strategy for the application of CA19-9 in the differentiation of pancreaticobiliary cancer: analysis using a receiver operating characteristic curve. *Am J Gastroenterol* 1999; **94**: 1941-1946
 - 5 **Mann DV**, Edwards R, Ho S, Lau WY, Glazer G. Elevated tumour marker CA19-9: clinical interpretation and influence of obstructive jaundice. *Eur J Surg Oncol* 2000; **26**: 474-479
 - 6 **Kang CM**, Kim JY, Choi GH, Kim KS, Choi JS, Lee WJ, Kim BR. The use of adjusted preoperative CA 19-9 to predict the recurrence of resectable pancreatic cancer. *J Surg Res* 2007; **140**: 31-35
 - 7 **Ortiz-González J**, Alvarez-Aguila NP, Medina-Castro JM. Adjusted carbohydrate antigen 19-9. Correlation with histological grade in pancreatic adenocarcinoma. *Anticancer Res* 2005; **25**: 3625-3627
 - 8 **Patel AH**, Harnois DM, Klee GG, LaRusso NF, Gores GJ. The utility of CA 19-9 in the diagnoses of cholangiocarcinoma in patients without primary sclerosing cholangitis. *Am J Gastroenterol* 2000; **95**: 204-207
 - 9 **Qin XL**, Wang ZR, Shi JS, Lu M, Wang L, He QR. Utility of serum CA19-9 in diagnosis of cholangiocarcinoma: in comparison with CEA. *World J Gastroenterol* 2004; **10**: 427-432
 - 10 **Ong SL**, Sachdeva A, Garcea G, Gravante G, Metcalfe MS, Lloyd DM, Berry DP, Dennison AR. Elevation of carbohydrate antigen 19.9 in benign hepatobiliary conditions and its correlation with serum bilirubin concentration. *Dig Dis Sci* 2008; **53**: 3213-3217
 - 11 **Mery CM**, Duarte-Rojo A, Paz-Pineda F, Gómez E, Robles-Díaz G. [Does cholestasis change the clinical usefulness of CA 19-9 in pancreaticobiliary cancer?]. *Rev Invest Clin* 2001; **53**: 511-517
 - 12 **Kodama T**, Satoh H, Ishikawa H, Ohtsuka M. Serum levels of CA19-9 in patients with nonmalignant respiratory diseases. *J Clin Lab Anal* 2007; **21**: 103-106
 - 13 **Howaizi M**, Abboura M, Krespine C, Sbai-Idrissi MS, Marty O, Djabbari-Sobhani M. A new cause for CA19.9 elevation: heavy tea consumption. *Gut* 2003; **52**: 913-914
 - 14 **Morris-Stiff G**, Teli M, Jardine N, Puntis MC. CA19-9 antigen levels can distinguish between benign and malignant pancreaticobiliary disease. *Hepatobiliary Pancreat Dis Int* 2009; **8**: 620-626
 - 15 **Vestergaard EM**, Hein HO, Meyer H, Grunnet N, Jørgensen J, Wolf H, Orntoft TF. Reference values and biological variation for tumor marker CA 19-9 in serum for different Lewis and secretor genotypes and evaluation of secretor and Lewis genotyping in a Caucasian population. *Clin Chem* 1999; **45**: 54-61
 - 16 **Morley JJ**, Kushner I. Serum C-reactive protein levels in disease. *Ann N Y Acad Sci* 1982; **389**: 406-418
 - 17 **Padillo FJ**, Muntane J, Montero JL, Briceño J, Miño G, Solorzano G, Sitges-Serra A, Pera-Madrado C. Effect of internal biliary drainage on plasma levels of endotoxin, cytokines, and C-reactive protein in patients with obstructive jaundice. *World J Surg* 2002; **26**: 1328-1332
 - 18 **Fujioka S**, Misawa T, Okamoto T, Gocho T, Futagawa Y, Ishida Y, Yanaga K. Preoperative serum carcinoembryonic antigen and carbohydrate antigen 19-9 levels for the evaluation of curability and resectability in patients with pancreatic adenocarcinoma. *J Hepatobiliary Pancreat Surg* 2007; **14**: 539-544
 - 19 **Locker GY**, Hamilton S, Harris J, Jessup JM, Kemeny N, Macdonald JS, Somerfield MR, Hayes DF, Bast RC. ASCO 2006 update of recommendations for the use of tumor markers in gastrointestinal cancer. *J Clin Oncol* 2006; **24**: 5313-5327
 - 20 **Kim HR**, Lee CH, Kim YW, Han SK, Shim YS, Yim JJ. Increased CA 19-9 level in patients without malignant disease. *Clin Chem Lab Med* 2009; **47**: 750-754
 - 21 **Steinberg W**. The clinical utility of the CA 19-9 tumor-associated antigen. *Am J Gastroenterol* 1990; **85**: 350-355
 - 22 **Lowe D**, Lee J, Schade R, Chaudhary A. Patient with markedly elevated CA 19-9 not associated with malignancy. *South Med J* 2006; **99**: 306-308
 - 23 **Akdoğan M**, Saşmaz N, Kayhan B, Biyikoğlu I, Dişibeyaz S, Sahin B. Extraordinarily elevated CA19-9 in benign conditions: a case report and review of the literature. *Tumori* 2001; **87**: 337-339
 - 24 **Korkmaz M**, Ünal H, Selçuk H, Yılmaz U. Extraordinarily elevated serum levels of CA 19-9 and rapid decrease after successful therapy: a case report and review of literature. *Turk J Gastroenterol* 2010; **21**: 461-463

S- Editor Wu X L- Editor Logan S E- Editor Li JY

Intrahepatic expression of genes related to metabotropic receptors in chronic hepatitis

Andrzej Cieśla, Maciej Kuśmider, Agata Faron-Górecka, Marta Dziedzicka-Wasylewska, Monika Bociąga-Jasik, Danuta Owczarek, Irena Ciećko-Michalska, Dorota Cibor, Tomasz Mach

Andrzej Cieśla, Monika Bociąga-Jasik, Danuta Owczarek, Irena Ciećko-Michalska, Dorota Cibor, Tomasz Mach, Department of Gastroenterology, Hepatology and Infectious Diseases, Jagiellonian University Medical College, 31-521 Kraków, Poland

Maciej Kuśmider, Agata Faron-Górecka, Marta Dziedzicka-Wasylewska, Institute of Pharmacology, Polish Academy of Sciences, 31-343 Kraków, Poland

Author contributions: Cieśla A, Kuśmider M, Faron-Górecka A, Dziedzicka-Wasylewska M, Mach T designed the research; Cieśla A, Kuśmider M, Faron-Górecka A, Dziedzicka-Wasylewska M, Bociąga-Jasik M, Owczarek D, Ciećko-Michalska I, Cibor D performed the study; Kuśmider M, Faron-Górecka A, Dziedzicka-Wasylewska M performed the analytical part of study; Cieśla A, Kuśmider M, Faron-Górecka A, Dziedzicka-Wasylewska M analyzed the data; Cieśla A, Kuśmider M, Faron-Górecka A, Dziedzicka-Wasylewska M, Bociąga-Jasik M, Owczarek D, Ciećko-Michalska I, Cibor D, Mach T wrote the paper.

Correspondence to: Andrzej Cieśla, MD, Department of Gastroenterology, Hepatology and Infectious Diseases, Jagiellonian University Medical College, 31-521 Kraków, Poland. aciesla@su.krakow.pl

Telephone: +48-12-4247340 Fax: +48-12-42473480

Received: September 1, 2011 Revised: April 23, 2012

Accepted: April 27, 2012

Published online: August 21, 2012

Abstract

AIM: To screen for genes related to metabotropic receptors that might be involved in the development of chronic hepatitis.

METHODS: Assessment of 20 genes associated with metabotropic receptors was performed in liver specimens obtained by punch biopsy from 12 patients with autoimmune and chronic hepatitis type B and C. For this purpose, a microarray with low integrity grade and with oligonucleotide DNA probes complementary to target transcripts was used. Evaluation of gene ex-

pression was performed in relation to transcript level, correlation between samples and grouping of clinical parameters used in chronic hepatitis assessment. Clinical markers of chronic hepatitis included alanine and aspartate aminotransferase, γ -glutamyltranspeptidase, alkaline phosphatase and cholinesterase activity, levels of iron ions, total cholesterol, triglycerides, albumin, glucose, hemoglobin, platelets, histological analysis of inflammatory and necrotic status, fibrosis according to METAVIR score, steatosis, as well as anthropometric body mass index, waist/hip index, percentage of adipose tissue and liver size in ultrasound examination. Gender, age, concomitant diseases and drugs were also taken into account. Validation of oligonucleotide microarray gene expression results was done with the use of quantitative real-time polymerase chain reaction (qRT-PCR).

RESULTS: The highest ($0.002 < P < 0.046$) expression among genes encoding main components of metabotropic receptor pathways, such as the α subunit of G-coupled protein, phosphoinositol-dependent protein kinase or arrestin was comparable to that of angiotensinogen synthesized in the liver. Carcinogenesis suppressor genes, such as chemokine ligand 4, transcription factor early growth response protein 1 and lysophosphatidic acid receptor, were characterized by the lowest expression ($0.002 < P < 0.046$), while the factor potentially triggering hepatic cancer, transcription factor *JUN-B*, had a 20-fold higher expression. The correlation between expression of genes of protein kinases PDPK1, phosphoinositide 3-kinase and protein kinase A (Spearman's coefficient range: 0.762-0.769) confirmed a functional link between these enzymes. Gender ($P = 0.0046$) and inflammation severity, measured by alanine aminotransferase activity ($P = 0.035$), were characterized by diverse metabotropic receptor gene expression patterns. The Pearson's coefficient ranging from -0.35 to 0.99 from the results of qRT-PCR and microarray indicated that qRT-PCR had certain

limitations as a validation tool for oligonucleotide microarray studies.

CONCLUSION: A microarray-based analysis of hepatocyte metabotropic G-protein-related gene expression can reveal the molecular basis of chronic hepatitis.

© 2012 Baishideng. All rights reserved.

Key words: Metabotropic receptors; Gene expression; DNA oligonucleotides; Quantitative real-time polymerase chain reaction; Chronic hepatitis

Peer reviewer: Dr. Shashi Bala, Department of Medicine, UMass Medical School, 364 Plantation Street, LRB2701, Worcester, MA 01605, United States

Cieśla A, Kuśmider M, Faron-Górecka A, Dziedzicka-Wasyłowska M, Bociąga-Jasik M, Owczarek D, Ciećko-Michalska I, Cibor D, Mach T. Intrahepatic expression of genes related to metabotropic receptors in chronic hepatitis. *World J Gastroenterol* 2012; 18(31): 4156-4161 Available from: URL: <http://www.wjgnet.com/1007-9327/full/v18/i31/4156.htm> DOI: <http://dx.doi.org/10.3748/wjg.v18.i31.4156>

INTRODUCTION

The natural course of chronic viral hepatitis is affected by progression of fibrosis and the risk of hepatocellular carcinoma development^[1]. Current data indicate that intracellular signaling disturbances have an impact on progression of inflammation and fibrosis, as well as carcinogenesis, in the course of chronic hepatitis.

G-protein-coupled receptors (GPCRs) are a family of cell surface receptors which receive, integrate and enhance the majority of extracellular signals. After stimulation with different signals, GPCRs activate amplifying enzymatic cascades, regulatory proteins and ion channels. This activation regulates cellular responses, including growth, proliferation, and cell survival.

In the present study, using microarray DNA analysis, we attempt to define genes related to metabotropic receptors associated with progression of chronic hepatitis.

DNA technology with genomic profiling and cluster analysis allows determination of the role of genes in the pathogenesis of liver injury^[2]. We assessed the activity of 20 genes encoding metabotropic receptors, some of which have been documented to have probable significance in the progression of chronic hepatitis.

The assessment of expression of genes of the main component of GPCR, such as the G-protein α subunit (*GNAS*), 3-phosphoinositide-dependent protein kinase-1 (*PDPK1*), phosphoinositide 3-kinase (*PIK3CG*), protein kinase A (*AKT1*) and arrestin β (*ARRB2*) was performed. We determined transcription factor *JUN-B*, ETS-domain protein (*ELK4*), early growth response protein 1 (*EGR1*) activated as the result of GPCR stimulation, angiotensinogen (*AGT*), which is a GPCR-ligand,

dual-specificity protein phosphatases 14 (*DUSP14*), which is responsible for dephosphorylation of kinase products, calcitonin receptor proteins (*CALCR*), thyrotropin receptor (*TSHR*), colony stimulating factor-3 (*CSF3*), sphingosine-1-phosphate receptor 1 (*EDG1*), and lysophosphatidic acid receptor (*EDG2*) associated with G-protein. The selection of *EDG2*, *EGR1*, *JUN-B*, chemokine (C-C motif) ligand 4 (*CCL4*), *ELK4* genes was based on their association with cellular proliferation, differentiation and apoptosis^[3-6]. Additionally, the selected group represented genes involved in regulation of inflammatory response and liver fibrosis, which included genes for interleukin 1 β (*IL-1 β*) and its receptors IL1 type I (*IL1R1*), IL1 type II (*IL1R2*), *CALCR*, *EDG1*, *CCL4*, *AGT* and adhesion molecules vascular cell adhesion molecule 1 (*VCAM1*)^[7-14].

MATERIALS AND METHODS

In the group of 12 patients (7 men, 5 women; age 36 ± 10.8 years) with chronic hepatitis type B (2 patients) and C (8 patients) and autoimmune hepatitis (2 patients), according to clinical indications, a liver biopsy was performed by the Menghini technique. From the obtained liver sections, a sample of 2-3 mm in length was frozen at -75°C until the analysis of mRNA of 20 selected genes was performed (gene list Figure 1). During the histopathological investigation of the biopsies, the degree of inflammation and fibrosis was assessed by the METAVIR score and steatosis by the steatosis scoring system.

On the day of liver biopsy, the activity of serum alanine aminotransferase (ALT/GPT Cobas, Roche Diagnostics, Mannheim, Germany), aspartate aminotransferase (ASPART/GOT Cobas), γ -glutamyltransferase (GGT Cobas), alkaline phosphatase (ALP Cobas), cholinesterase (CHE Cobas), the level of iron (Fe Cobas), total cholesterol (CHOD-PAP Cobas), triglycerides (TG Cobas), albumin (ALB plus Cobas), glucose (GLU Cobas), hemoglobin and platelet (Sysmex XE-2100, Sysmex Europe GMBH, Norderstedt, Germany) were assessed. Anthropometric measurements, including body mass index, waist/hip index and the percentage of fatty mass was assessed by skin fold thickness. The size of the liver was measured during ultrasound examination of the abdomen. Patient characteristics included the presence of concomitant illnesses, drug history, as well as the use of such substances as alcohol and cigarettes (Figure 2). In women, the menstrual cycle phase and menopause were taken into account. Biochemical, histological and anthropometric parameters are presented in Figure 2. The gene expression studies were performed using microarray (with low integration level), with DNA oligonucleotides complementary to the investigated transcripts. Total RNA was isolated from liver samples using the TRI Reagent (Sigma-Aldrich, St. Louis, United States), and then purified using the RNeasy MiniElute spin columns with a DNA eliminator (Qiagen, Hilden, Germany). The quantity of isolated RNA was assessed by a spectrophotometer (NanoDrop, Wilmington, United States), and subsequently its degradation level was

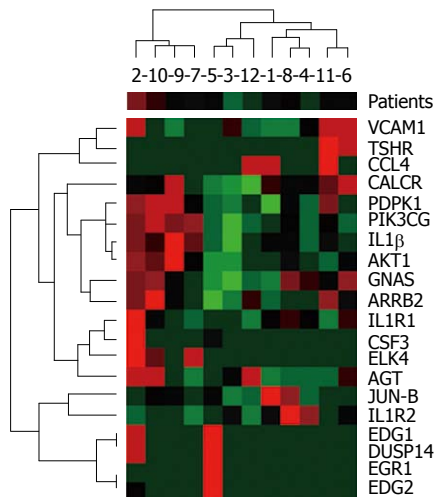


Figure 1 Agglomerative hierarchical clustering methods of genes expression. The dendrogram assigned to the numerical value on the horizontal axis describes the patients' correlation; the dendrogram assigned to individual genes on the vertical axis describes the genes' correlation. Figures on the x-axis denote patient order. *VCAM1*: Vascular cell adhesion molecule 1; *TSHR*: Thyroid stimulating hormone receptor; *CCL4*: Chemokine (C-C motif) ligand 4; *CALCR*: Calcitonin receptor; *PDPK1*: 3-phosphoinositide-dependent protein kinase-1; *PIK3CG*: Phosphoinositide 3-kinase; *IL1β*: Interleukin 1β; *AKT1*: Protein kinase A; *GNAS*: α subunit of G-coupled protein; *ARRB2*: Arrestin β; *IL1R1*: Interleukin 1 receptor, type I; *CSF3*: Colony stimulating factor-3; *ELK4*: ETS-domain protein; *AGT*: Angiotensinogen; *JUN-B*: Transcription factor jun-B; *IL1R2*: Interleukin 1 receptor, type II; *EDG1*: Sphingosine-1-phosphate receptor 1; *DUSP14*: Dual-specificity protein phosphatases 14; *EGR1*: Early growth response protein 1; *EDG2*: Lysophosphatidic acid receptor.

measured by a capillary electrophoresis system (Experion, Bio-Rad, Hercules, United States). For further analysis only samples without evidence of RNA degradation were qualified (RQI > 8.5 Rna Quality Index). Subsequently, based on the obtained RNA, probes were synthesized according to the manufacturer's instructions (SABiosciences, Frederick, United States), and then hybridized to a microarray. We used the Oligo GEArray Human GPCR Signaling Pathway Finder Microarray (OHS-071) supplied by SABiosciences. Detection of the array probes is achieved based on chemiluminescence, using the FujiLAS System (FujiFilm, Tokyo, Japan). The resulting images (the signal density) were quantified using the OligoAnalyser (SABiosciences). The obtained results describing the relative levels of gene expression (with respect to the reference gene) were further examined.

Diversification in gene expression was assessed by agglomerative hierarchical clustering methods. Using the Spearman's rank correlation coefficient for activity of the investigated genes, we searched for pairs of objects and then for clusters with the smallest distance (Figure 1). An analogous classification was carried out using biochemical, histological and anthropometric parameters (Figure 2). Determination of a direct correlation between gene expression and clinical features was done based on agglomerative hierarchical clustering of both the investigated indicators of chronic hepatitis. The genotype-phenotype distinction was analyzed using Fisher's exact test, to de-

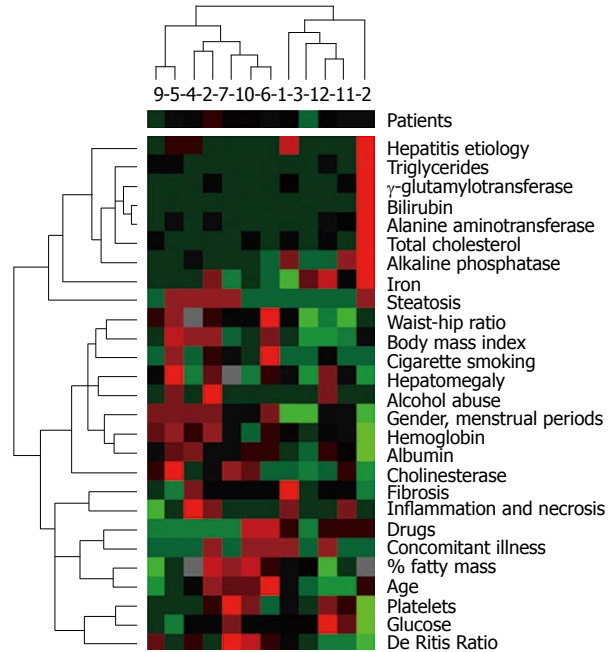


Figure 2 Agglomerative hierarchical clustering methods of clinical features expression. The dendrogram assigned to a numerical value on the horizontal axis describes the patients' correlation; the dendrogram assigned to individual clinical features on the vertical axis describes the clinical features' correlation. Figures on the x-axis denote patient order.

termine the difference between clustering of patients achieved on the basis of a dendrogram of clinical signs and a dendrogram of gene expression (Figures 1 and 2). Differentiation of clinical parameters between groups of patients with the biggest difference in gene expression was performed by the Mann-Whitney *U* test and Fisher's exact test. In the present study, these were patients number 2, 10, 9, 7 *vs* the rest (Figure 1). The Wilcoxon signed-rank test was used to assess differential expression between the selected genes, to determine the three groups of genes with the highest, moderate, and lowest activity (Figure 3).

The results of the microarray experiment were verified by means of quantitative real-time polymerase chain reaction (qRT-PCR) for *IL1B*, *VCAM1*, *PIK3CG*, *AGT*, *PDPK1*, *GNAS*, *JUN-B*, *EDG2*, *CCL4*, *EGR1*, *IL1R1*, *IL1R2*, *CALCR*, *AKT1* and *ARRB2*. Total RNA acquired from the tissues of interest was reverse-transcribed using the High-Capacity cDNA Archive Kit (Applied Biosystems, Foster City, United States) for the 2-step qRT-PCR assays. The qRT-PCR was performed on a Chromo 4 (Bio-Rad), using the ABI SYBR Green master mix (Applied Biosystems). Primer sets against sequences of genes are indicated by microarray. They are commercially available at OriGene (Rockville, United States), but were additionally checked for specificity with National Center for Biotechnology Information (NCBI) The Basic Local Alignment Search Tool (BLAST). The optimum annealing temperature for each primer set was determined prior to the analysis of experimental samples. Following amplification, dissociation curves were

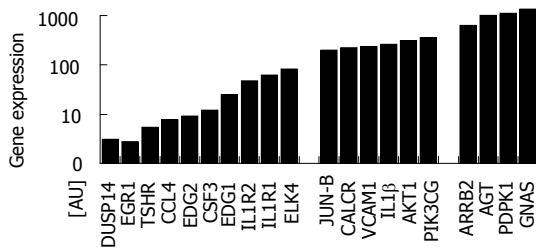


Figure 3 Arithmetic mean of gene activity. There was a statistically significant difference in the Wilcoxon signed-rank test between the genes with the highest expression, *GNAS*, *PDPK1*, *AGT*, and *ARRB2*, and moderate expression, *PIK3CG*, *AKT1*, *IL1 β* , *VCAM1*, *CALCR*, and *JUN-B*, and between the genes with moderate expression and the remaining genes with low expression.

analyzed for each reaction. A sample volume of 20 μ L was used for all assays which contained a 1X final concentration of SYBR green PCR master mix, 100 nmol gene specific primers, and 1 μ L of template. The assays were run using the following protocol: 95 $^{\circ}$ C for 10 min, 95 $^{\circ}$ C for 40 s, gene specific annealing temperature (58-62 $^{\circ}$ C) for 60 s for 40 cycles, followed by a gradual increase in temperature from 55 $^{\circ}$ C to 95 $^{\circ}$ C during the dissociation stage.

Following amplification, the instrument software was used to set the baseline and threshold for each reaction, as well as to determine the reaction efficiency. A cycle threshold (Ct) was assigned at the beginning of the logarithmic phase of PCR amplification and the difference in the Ct values [corrected for reaction efficiency: $Ct = Ct \times \log(\text{efficiency})/\log(2)$] of the housekeeping genes [mean Ct of glucuronidase (GUS) and beta-actin (BAKT)] and the gene of interest were used to determine the relative expression of the gene in each sample. Relative expression levels were then calculated as fold changes to the housekeeping genes, where each PCR cycle represented a 2-fold change.

The data of PCR and microarray experiments were then correlated using Pearson's coefficient.

The study was carried out in accordance with the Declaration of Helsinki (2000) of the World Medical Association.

RESULTS

Using the agglomerative hierarchical clustering methods we found statistically significant correlations between the *EDG1*, *DUSP14*, *EGR1* and *EDG2* genes and *PDPK1*, *PIK3CG*, *AKT1*, as well as clustering, though not statistically significant, for *GNAS* and *ARRB2* (Figure 1). Spearman's rank correlation coefficients were 0.762 for *PDPK1* and *AKT1*, 0.769 ($P < 0.05$) for *PDPK1* and *PIK3CG*, 0.769 ($P < 0.05$) for *AKT1* and *PIK3CG*, and 0.699 ($P < 0.05$) for *GNAS* and *ARRB2*. In case of *EDG1*, *DUSP14*, *EGR1* and *EDG2*, in 10 out of 12 patients there was no transcriptional activity. Except for the transcriptional factor *JUN-B* and the stage of fibrosis $r = 0.667$ ($P < 0.05$), we did not observe any correlation between the activity of the selected genes and the in-

vestigated clinical factors. Assessing patient distribution based on dendrograms of the investigated genotype and phenotype, a difference on the border of statistical significance was found in Fisher's exact test ($P = 0.08$). The patients with the highest diversity in gene expression (Figure 1) showed a statistically significant difference in gender and ALT activity ($P = 0.0046$ and $P = 0.035$, respectively). Based on expression activity, the genes were divided into a group with high activity, which included *GNAS*, *PDPK1*, *AGT* and *ARRB2* and statistically differed ($0.002 < P < 0.046$) from the genes with moderate and low expression. The group of genes with moderate activity of *AKT1*, *PIK3CG*, *IL1 β* , *VCAM1*, *JUN-B* and *CALCR* also showed a statistically significant difference ($0.002 < P < 0.041$) compared with genes which were classified as belonging to the group with low expression (Figure 3).

For the following genes: *JUN-B*, *EDG2*, *CCL4* and *EGR1*, estimated with the use of microarrays and qRT-PCR, there was a strong positive correlation, with Pearson's coefficient within the range of 0.61-0.99. For other genes, *IL1B*, *VCAM1*, *PIK3CG*, *AGT*, *PDPK1*, and *GNAS*, the correlation was weakly positive, with Pearson's coefficient ranging from 0.07 to 0.43; and for *IL1R1*, *IL1R2*, *CALCR*, *AKT1*, and *ARRB2* the correlation of expression estimated with the two methods was weakly negative (Pearson's coefficient ranging from -0.1 to -0.35).

DISCUSSION

With the exception of the correlation between *JUN-B* and fibrosis stage, we did not reveal any direct relationship between expression of genes related to metabotropic receptors in hepatocytes and anthropometric, histological and biochemical parameters that are commonly used for monitoring progression of chronic hepatitis. In assessing the connection between gene expression and the investigated clinical features, we found an impact of gender and concentration of ALT in the serum on changes in gene expression. The effect of these two factors was detected as the result of the analysis of not any single, but rather all the investigated genes. In the probability test, it was gender which better determined changes in gene activity rather than ALT. In chronic hepatitis C and B, gender is the factor which defines the course and prognosis of the disease^[1]. Changes in gene expression resulting from gender differences can influence the progression of liver disease.

In the present study, among different markers of inflammation and fibrosis in the liver parenchyma, only the ALT level differentiated the gene activity. Among the investigated genes, there were important mediators of inflammation, including IL-1 β , with their receptors, as well as chemokines and adhesion factors. Also protein products of such genes as *EDG1*, *EDG2*, *CALCR* are involved in the induction of the inflammatory response^[9,15]. In contrast to ALT, a small histological difference used to assess the inflammatory process in the

liver, classified in the majority of cases as score 1 or 2 according to METAVIR, were not useful in assessing gene expression.

The reported values of genes expression and their statistical diversity allow distinction between three groups of genes with high, moderate and low activity. Because there is no direct correlation between gene activity and clinical markers of chronic hepatitis, it is difficult to determine if the observed gene expression is induced or constitutional.

In the group of genes with the highest activity there were genes of the main metabotropic receptor proteins, *GNAS*, *PDPK1* and *ARRB2*. Their high transcriptional activity is related to their essential role in the metabotropic receptor system. *GNAS* expression, despite individual differences, showed the highest correlation with *ARRB2* among the investigated genes. Proportional to the level of stimulation of GPCR, *ARRB2* triggers the mechanism of receptor internalization, which is an adaptation to overstimulation^[16]. Also mRNA encoding AGT was characterized by high expression. This observation remains in accordance with current literature and is associated with the liver being the main site of AGT synthesis^[17]. Because AGT is incorporated only indirectly by the renin-angiotensin system in the progression of liver fibrosis^[18,19], its gene activity did not correlate with the histological assessment of this process.

In the group of genes with moderate activity, there were genes which encode products involved in the pathogenesis of liver injury. Disturbances of *PIK3CG* described in chronic hepatitis as caused by NS5 protein of hepatitis C virus and HBx protein of hepatitis B virus destabilize and damage hepatocytes^[20,21]. However, in the present study, expression of *PIK3CG* did not correlate with the markers of liver injury.

As there were no cases with advanced fibrosis among the investigated patients, we did not observe any increased expression of *VCAM1*, which is characteristic only for liver cirrhosis^[22].

The correlation of expression of phosphatidylinositol kinases observed in the study confirms the functional association of the investigated enzymes. A significantly higher expression of *PDPK1* compared with *PIK3CG* is due to the amplification of *PDPK1* during phosphorylation catalyzed by *PIK3CG*. *PDPK1* in turn activates *AKT1* correspondingly; therefore, the 3-fold higher activity of *PDPK1* is noteworthy.

Among the investigated phosphatases that dephosphorylate active kinases, *DUSP14* was measured. However, this phosphatase, which is not functionally associated with the presently studied kinases, showed low expression values and was not correlated with the expression of kinases. Interestingly, a statistically significant correlation was determined between the stage of fibrosis and expression of transcriptional factor *JUN-B*. This factor, in the malfunctioning of the liver, is responsible for reprogramming of hepatocyte genes to the phase of cell proliferation^[23,24]. Its increase is frequently observed

in liver injury and hepatic carcinogenesis^[25].

The higher expression of this factor linked to carcinogenesis correlated with a low activity of the genes *CCLA*, *EGR1*, *EDG2* involved in the induction of apoptosis and suppression of neoplasia^[26].

The results obtained in the present study indicate that qRT-PCR has certain limitations as a validation tool for oligonucleotide microarray studies. Only four genes have shown a similar expression pattern between results obtained with the use of both techniques. A weak positive and negative correlation observed for other genes might result from potential pitfalls inherent in both approaches, and might be a source of errors encountered while employing each method.

However, the range of differences in the correlation coefficient observed in the present study remains within the range described in the literature, from -0.48 to 0.94^[27,28]. The results obtained in this study reflect the debate over which methods produce the most accurate measurements of gene expression.

In conclusion, gender and inflammation activity, as determined by ALT level, were associated with a more diverse pattern of metabotropic receptor gene expression. The highest gene expression was observed for mRNA of the main components of the metabotropic receptor pathway, such as *GNAS*, *PDPK1*, *ARRB2*, and correlated with mRNA of angiotensinogen synthesized in the liver. The correlation of expression of protein kinases *PDPK1*, *PIK3CG* and *AKT1* points to a functional association of these enzymes. The genes suppressing carcinogenesis, *CCLA*, *EGR*, *EDG2*, were characterized by the lowest expression levels among the investigated genes. On the other hand, *JUN-B*, a factor potentially involved in the development of hepatocellular cancer, was characterized by a 20-fold higher level of expression.

COMMENTS

Background

Metabotropic G protein-coupled receptors activate various signaling pathways, which trigger multiple sub-cellular reactions. Microarray-based analysis of expression of hepatocyte genes related to metabotropic receptors can reveal the molecular basis of liver diseases.

Research frontiers

The natural course of chronic viral hepatitis is associated with progression of fibrosis and the risk of hepatocellular carcinoma development. Current data indicate that intracellular signaling disturbances have an impact on progression of inflammation and fibrosis as well as carcinogenesis in the course of chronic hepatitis.

Innovations and breakthroughs

The highest gene expression was in the mRNAs of the main components of the metabotropic receptor pathways, such as the α subunit of G-coupled protein, phosphoinositol-dependent protein kinase (*PDPK1*) and arrestin β and correlated with the mRNA for angiotensinogen synthesized in liver. Carcinogenesis suppressor genes such as chemokine *CCL4*, transcription factor *EGR1* and lysophosphatidic acid receptor were characterized by the lowest expression, while the factor potentially triggering hepatic cancer, *JUN-B*, had 20-fold higher expression. Comparable expression of genes encoding protein kinases *PDPK1*, phosphoinositide 3-kinase and protein kinase A confirms a functional link between these enzymes. Gender and inflammation severity, measured by alanine aminotransferase activity, were characterized by different expression patterns

of genes related to metabotropic receptors.

Applications

Results of the presented work enables better delineation of mechanisms governing the course of chronic hepatitis and form the basis for future investigations.

Terminology

G-protein-coupled receptors are a family of the cell surface receptors, which receive, integrate and enhance most of the extracellular signals implicated in cell growth, proliferation, and survival. Microarray DNA technology with genomic profiling and cluster analysis allows determination of the role of genes in the pathogenesis of liver injury.

Peer review

This is a good descriptive study in which authors screen for genes related to metabotropic receptors family that might be involved in the development of chronic hepatitis. The results are interesting and suggest that a microarray-based analysis of hepatocyte metabotropic G protein-related gene expression can reveal the molecular basis of chronic hepatitis.

REFERENCES

- 1 **Poynard T**, Bedossa P, Opolon P. Natural history of liver fibrosis progression in patients with chronic hepatitis C. The OBSVIRC, METAVIR, CLINIVIR, and DOSVIRC groups. *Lancet* 1997; **349**: 825-832
- 2 **Furuta K**, Sato S, Yamauchi T, Ozawa T, Harada M, Kakumu S. Intrahepatic gene expression profiles in chronic hepatitis B and autoimmune liver disease. *J Gastroenterol* 2008; **43**: 866-874
- 3 **van Meeteren LA**, Moolenaar WH. Regulation and biological activities of the autotaxin-LPA axis. *Prog Lipid Res* 2007; **46**: 145-160
- 4 **Cooper AB**, Wu J, Lu D, Maluccio MA. Is autotaxin (ENPP2) the link between hepatitis C and hepatocellular cancer? *J Gastrointest Surg* 2007; **11**: 1628-1634; discussion 1634-1635
- 5 **Martinez Martinez CM**, Hernandez Pando R. [Chemokines, a new family of cytokines in inflammatory cell recruitment]. *Rev Invest Clin* 1999; **51**: 255-268
- 6 **Goto T**, Kato N, Yoshida H, Otsuka M, Moriyama M, Shiratori Y, Koike K, Matsumura M, Omata M. Synergistic activation of the serum response element-dependent pathway by hepatitis B virus x protein and large-isoform hepatitis delta antigen. *J Infect Dis* 2003; **187**: 820-828
- 7 **Hay DL**, Christopoulos G, Christopoulos A, Poyner DR, Sexton PM. Pharmacological discrimination of calcitonin receptor: receptor activity-modifying protein complexes. *Mol Pharmacol* 2005; **67**: 1655-1665
- 8 **Zeremski M**, Petrovic LM, Talal AH. The role of chemokines as inflammatory mediators in chronic hepatitis C virus infection. *J Viral Hepat* 2007; **14**: 675-687
- 9 **Kroeger I**, Erhardt A, Abt D, Fischer M, Biburger M, Rau T, Neuhuber WL, Tiegs G. The neuropeptide calcitonin gene-related peptide (CGRP) prevents inflammatory liver injury in mice. *J Hepatol* 2009; **51**: 342-353
- 10 **Haruta I**, Tokushige K, Komatsu T, Ikeda I, Yamauchi K, Hayashi N. Clinical implication of vascular cell adhesion molecule-1 and very late activation antigen-4 interaction, and matrix metalloproteinase-2 production in patients with liver disease. *Can J Gastroenterol* 1999; **13**: 721-727
- 11 **Knittel T**, Dinter C, Kobold D, Neubauer K, Mehde M, Eichhorst S, Ramadori G. Expression and regulation of cell adhesion molecules by hepatic stellate cells (HSC) of rat liver: involvement of HSC in recruitment of inflammatory cells during hepatic tissue repair. *Am J Pathol* 1999; **154**: 153-167
- 12 **Watanabe Y**, Morita M, Ikematsu N, Akaike T. Tumor necrosis factor alpha and interleukin-1 beta but not interferon gamma induce vascular cell adhesion molecule-1 expression on primary cultured murine hepatocytes. *Biochem Biophys Res Commun* 1995; **209**: 335-342
- 13 **García-Monzón C**, Sánchez-Madrid F, García-Buey L, García-Arroyo A, García-Sánchez A, Moreno-Otero R. Vascular adhesion molecule expression in viral chronic hepatitis: evidence of neoangiogenesis in portal tracts. *Gastroenterology* 1995; **108**: 231-241
- 14 **Proost P**, Wuyts A, van Damme J. The role of chemokines in inflammation. *Int J Clin Lab Res* 1996; **26**: 211-223
- 15 **Kaneko T**, Murakami T, Kawana H, Takahashi M, Yasue T, Kobayashi E. Sphingosine-1-phosphate receptor agonists suppress concanavalin A-induced hepatic injury in mice. *Biochem Biophys Res Commun* 2006; **345**: 85-92
- 16 **Klaasse EC**, Ijzerman AP, de Grip WJ, Beukers MW. Internalization and desensitization of adenosine receptors. *Purinergic Signal* 2008; **4**: 21-37
- 17 **Takahashi D**, Tamura K, Ushikubo T, Moriya A, Yokoyama N, Nyui N, Chiba E, Hibi K, Ishigami T, Yabana M, Tomiyama M, Umemura S, Ishii M. Relationship between hepatic angiotensinogen mRNA expression and plasma angiotensinogen in patients with chronic hepatitis. *Life Sci* 1997; **60**: 1623-1633
- 18 **Forrest EH**, Thorburn D, Spence E, Oien KA, Inglis G, Smith CA, McCrudden EA, Fox R, Mills PR. Polymorphisms of the renin-angiotensin system and the severity of fibrosis in chronic hepatitis C virus infection. *J Viral Hepat* 2005; **12**: 519-524
- 19 **Xiao F**, Wei H, Song S, Li G, Song C. Polymorphisms in the promoter region of the angiotensinogen gene are associated with liver cirrhosis in patients with chronic hepatitis B. *J Gastroenterol Hepatol* 2006; **21**: 1488-1491
- 20 **Wang ZL**, Wu XH, Song LF, Wang YS, Hu XH, Luo YF, Chen ZZ, Ke J, Peng XD, He CM, Zhang W, Chen LJ, Wei YQ. Phosphoinositide 3-kinase gamma inhibitor ameliorates concanavalin A-induced hepatic injury in mice. *Biochem Biophys Res Commun* 2009; **386**: 569-574
- 21 **Mukherji A**, Janbandhu VC, Kumar V. HBx protein modulates PI3K/Akt pathway to overcome genotoxic stress-induced destabilization of cyclin D1 and arrest of cell cycle. *Indian J Biochem Biophys* 2009; **46**: 37-44
- 22 **Bruno CM**, Sciacca C, Cilio D, Bertino G, Marchese AE, Politi G, Chinnici L. Circulating adhesion molecules in patients with virus-related chronic diseases of the liver. *World J Gastroenterol* 2005; **11**: 4566-4569
- 23 **Beauchamp RD**, Papaconstantinou J, Henderson AM, Sheng HM, Townsend CM, Thompson JC. Activation of hepatic proliferation-associated transcription factors by lipopolysaccharide. *Surgery* 1994; **116**: 367-376; discussion 376-377
- 24 **Morello D**, Lavenu A, Babinet C. Differential regulation and expression of jun, c-fos and c-myc proto-oncogenes during mouse liver regeneration and after inhibition of protein synthesis. *Oncogene* 1990; **5**: 1511-1519
- 25 **Liao DZ**, Blanck A, Gustafsson JA, Hällström IP. Expression of the c-jun, jun-B, ets-2 and liver regeneration factor-1 (LRF-1) genes during promotion and progression of rat liver carcinogenesis in the resistant hepatocyte model. *Cancer Lett* 1996; **100**: 215-221
- 26 **Baek SJ**, Wilson LC, Hsi LC, Eling TE. Troglitazone, a peroxisome proliferator-activated receptor gamma (PPAR gamma) ligand, selectively induces the early growth response-1 gene independently of PPAR gamma. A novel mechanism for its anti-tumorigenic activity. *J Biol Chem* 2003; **278**: 5845-5853
- 27 **Etienne W**, Meyer MH, Peppers J, Meyer RA. Comparison of mRNA gene expression by RT-PCR and DNA microarray. *Biotechniques* 2004; **36**: 618-620, 622, 624-626
- 28 **Beckman KB**, Lee KY, Golden T, Melov S. Gene expression profiling in mitochondrial disease: assessment of microarray accuracy by high-throughput Q-PCR. *Mitochondrion* 2004; **4**: 453-470

S-Editor Gou SX L-Editor Cant MR E-Editor Zhang DN

Growth inhibitory effects of *Phyllanthus niruri* extracts in combination with cisplatin on cancer cell lines

Raimundo Fernandes de Araújo Júnior, Luiz Alberto Lira Soares, Cíntia Raquel da Costa Porto, Raniere Gurgel Furtado de Aquino, Hugo Gonçalo Guedes, Pedro Ros Petrovick, Tatiane Pereira de Souza, Aurigena Antunes de Araújo, Gerlane Coelho Bernardo Guerra

Raimundo Fernandes de Araújo Júnior, Raniere Gurgel Furtado de Aquino, Hugo Gonçalo Guedes, Department of Morphology/Postgraduate Program in Morphological Sciences, Federal University of Rio Grande do Norte, Natal 59072-970, Rio Grande do Norte, Brazil

Luiz Alberto Lira Soares, Postgraduate Program in Pharmaceutical Sciences, Federal University of Pernambuco, Recife 50670-901, Pernambuco, Brazil

Cíntia Raquel da Costa Porto, Postgraduate Program in Pharmaceutical Sciences, Federal University of Rio Grande do Norte, Natal 59012-570, Rio Grande do Norte, Brazil

Pedro Ros Petrovick, Department of Production and control of drugs, Federal University of Rio Grande do Sul, Porto Alegre 90610-000, Rio Grande do Sul, Brazil

Tatiane Pereira de Souza, Department of Food and Drug Administration, Federal University of Amazonas, Manaus 69077-000, Amazonas, Brazil

Aurigena Antunes de Araújo, Gerlane Coelho Bernardo Guerra, Department of Biophysics and Pharmacology, Federal University of Rio Grande do Norte, Natal 59072-970, Rio Grande do Norte, Brazil

Author contributions: Araújo Júnior RF and Guerra GCB designed the research; Araújo Júnior RF, Araújo AA and Guerra GCB performed the research; Soares LAL, Petrovick PR and de Souza TP contributed new reagents/analytic tools; Araújo Júnior RF, Guedes HG, da Costa Porto CR and de Aquino RGF analyzed the data; Araújo Júnior RF, Guedes HG, da Costa Porto CR, Araújo AA, Guerra GCB wrote the paper.

Supported by Conselho Nacional de Desenvolvimento Científico e Tecnológico (CNPq); CNPq (470179/2009-0) for financial support and Postgraduate Program in Pharmaceutical Sciences, Federal University of Rio Grande do Norte

Correspondence to: Gerlane Coelho Bernardo Guerra, PhD, Department of Biophysics and Pharmacology, Federal University of Rio Grande do Norte, Natal 59072-970, Rio Grande do Norte, Brazil. gerlaneguerra@hotmail.com

Telephone: +55-84-32153419 Fax: +55-84-33422200

Received: July 6, 2011 Revised: January 10, 2012

Accepted: May 12, 2012

Published online: August 21, 2012

Abstract

AIM: To investigate the cytotoxic effects of spray-dried extracts of *Phyllanthus niruri* in combination with cisplatin on two cancer cell lines.

METHODS: Colorectal carcinoma (HT29) and human hepatocellular carcinoma (HepG2) cells were treated with spray-dried extracts of *Phyllanthus niruri* (SDEPN) either alone or in combination with cisplatin at different concentrations (0.5 mg/mL and 1 mg/mL) for 4 h and 24 h. To verify and quantify cancer cells treated with these products as well as identify the cell cycle stage and cell viability, we stained the cells with propidium iodide and assessed them by flow cytometry. The percentage of cells in different cell cycle phases was quantified and data were expressed as histograms. Significant differences between groups were determined using analysis of variance and Bonferroni's test, as indicated. A value of $P < 0.05$ was considered to be statistically significant.

RESULTS: SDEPN had significantly different cytotoxic effects on HT29 (2.81 ± 0.11 vs 3.51 ± 1.13 , $P > 0.05$) and HepG2 (5.07 ± 0.3 vs 15.9 ± 1.04 , $P < 0.001$) cells when compared to control cells for 4 h. SDEPN also had significantly different cytotoxic effects on HT29 (1.91 ± 0.57 vs 4.53 ± 1.22 , $P > 0.05$) and HepG2 (14.56 ± 1.6 vs 35.67 ± 3.94 , $P < 0.001$) cells when compared to control cells for 24 h. Both cell lines were killed by cisplatin in a dose-dependent manner compared to control cells (HepG2 cells for 4 h: 10.78 ± 1.58 vs 53.89 ± 1.53 , $P < 0.001$; 24 h: 8.9 ± 1.43 vs 62.78 ± 1.87 , $P < 0.001$ and HT29 cells for 4 h: 9.52 ± 0.913 vs 49.86 ± 2.89 , $P < 0.001$; 24 h: 11.78 ± 1.05 vs 53.34 ± 2.65 , $P < 0.001$). In HT29 cells, pretreatment with SDEPN and subsequent treatment with cis-

platin resulted in a greater number of cells being killed (12.78 ± 1.01 vs 93.76 ± 1.6 , $P < 0.001$). HepG2 cells showed significant cell killing with treatment with SDEPN when combined with cisplatin (12.87 ± 2.78 vs 78.8 ± 3.02 , $P < 0.001$).

CONCLUSION: SDEPN is selectively toxic against two cancer cell lines. Moreover, SDEPN in combination with cisplatin induces a synergistic increase in the cell death of both HT29 and HepG2 cells.

© 2012 Baishideng. All rights reserved.

Key words: Cisplatin; Colorectal cancer; Liver cancer; *Phyllanthus niruri*; Cytotoxic effect

Peer reviewer: Chang-Qing Su, Professor, Department of Molecular Oncology, Eastern Hepatobiliary Surgical Hospital, Second Military Medical University, Changhai Rd. 225, Shanghai 200438, China

Araújo Júnior RF, Soares LAL, da Costa Porto CR, de Aquino RGF, Guedes HG, Petrovick PR, de Souza TP, Araújo AA, Guerra GCB. Growth inhibitory effects of *Phyllanthus niruri* extracts in combination with cisplatin on cancer cell lines. *World J Gastroenterol* 2012; 18(31): 4162-6168 Available from: URL: <http://www.wjgnet.com/1007-9327/full/v18/i31/4162.htm> DOI: <http://dx.doi.org/10.3748/wjg.v18.i31.4162>

INTRODUCTION

Phyllanthus niruri has many effective traditional uses for a wide variety of diseases. Some of the medicinal uses have been supported in experimental models, suggesting that the plant extracts possess various pharmacological properties. Due to its impressive preclinical therapeutic potential, extracts of species of the genus *Phyllanthus* have been evaluated to treat hypertension, jaundice, diabetes, hypercalciuria, and urolithiasis^[1]. Other studies revealed preclinical pharmacological activity and therapeutic potential of phytochemicals isolated from *Phyllanthus niruri*. The species has demonstrated an antimutagenic and anticarcinogenic action^[2], antitumor^[3], antioxidant^[4], hepatoprotective^[5,6] and antihyperuricemic properties^[7], as well as antihyperlipemic activity^[8,9].

Phytochemicals exhibit different structural characteristics with various pharmacological actions. For example, lignans have excellent hepatoprotective^[10,11] and anti-viral properties^[12], whereas terpenes exhibit anti-microbial activities^[13]. Flavonoids from *Phyllanthus niruri* have been shown to have antioxidant^[14], antileishmanial^[15], and anti-inflammatory properties^[16]. Phytochemical studies have shown that extracts of genus *Phyllanthus* contain a variety of components, including gallic acid^[11,17]. Furthermore, studies have demonstrated cytotoxic activity of gallic acid on the human promyelocytic leukemia HL-60 cell lines^[18,19]. Gallic acid has also been shown to induce apoptotic cell death in HSC-2 and HL-60 cells^[20].

More importantly, no side effects or toxicities have been reported for this herb after many years of research. Although extensive research has been conducted, there is still an abundance of unanswered questions regarding *Phyllanthus niruri*, particularly towards understanding the mechanism of biological activity of phytochemicals from the herb with emphasis on components that have anti-human immunodeficiency virus (HIV)^[21] and anti-hepatitis B^[22] properties. *Phyllanthus niruri* has been found to exhibit a marked inhibitory effect on the hepatitis B virus, as evidenced by its exhaustive utility in cases of chronic jaundice. However, to date, no research has focused on the identification and validation of active pharmacophores of *Phyllanthus niruri* that are responsible for the reported inhibitory effect of its aqueous extract on HIV^[21]. Investigations have examined anti-HIV effects of the alkaloidal extract from *Phyllanthus niruri* on human cell lines. An alkaloidal extract of *Phyllanthus niruri* showed suppressive activity on strains of HIV-1 cultured on the huT-4 cell line^[21].

Directed studies of botanical extracts may lead to the discovery of new agents with improved and intriguing pharmacological properties. This may be achieved by molecular modeling studies that assess the interactions of bioactive phytochemicals from *Phyllanthus niruri* with their respective molecular targets. Moreover, upon improvement of binding affinity to the specified target by virtual chemical modification of existing pharmacophores, new small molecules may be identified and synthesized in the laboratory^[23].

Other species of the genus *Phyllanthus*, such as *Phyllanthus polyphyllus* and *Phyllanthus emblica*, have demonstrated growth inhibitory activity with a certain degree of selectivity towards the two cancer cell lines tested. It has been previously shown that cisplatin can inhibit the growth of colorectal carcinoma (HT29) and human hepatocellular carcinoma (HepG2) cells in a dose-dependent manner^[20,24,25].

In this study, we investigated the antiproliferative or cell-killing activities of spray-dried extracts of *Phyllanthus niruri* on the human colorectal carcinoma HT29 and human hepatocellular HepG2 cell lines. In addition, we assessed the capacity of these extracts to potentiate the action of cis-diamminedichloroplatinum II (cisplatin).

MATERIALS AND METHODS

Preparation of *Phyllanthus niruri* spray dried extracts

A spray-dried extract of *Phyllanthus niruri* (SDEPN) containing 12.33 mg/g of gallic acid^[26] and 94.4 mg/g of total flavonoids^[27] was prepared following the manufacturer's instructions using a Spray Dryer Production Minor (GEA Niro, Denmark).

Cell culture

The human colorectal cancer cell line HT-29 and human hepatocellular carcinoma cell line HepG2 were

purchased from the Culture Collection of the Faculty of Medicine, University of São Paulo. The cells were maintained in Dulbecco's modified Eagle's medium (DMEM; Life Technologies, Inc., Grand Island, NY, United States) supplemented with 10% (v/v) heat-inactivated fetal bovine serum.

Flow cytometry

To verify and quantify cells treated with SDEPN extract and to identify the cell cycle stage and cell viability, we stained cells with propidium iodide (PI). PI emits different fluorescence intensities depending on the phase of the cell cycle, which in turn are captured by the photomultiplier detectors in a flow cytometer (BD FACSanto II). Cancer cells were plated in 6-well plates at a cell density of 5×10^5 cells/well in 2 mL of medium. Cells were treated with SDEPN alone, cisplatin alone, or SDEPN followed by cisplatin. After 24 h, the cells were treated with a series of SDEPN concentrations (0-75 mmol/L) for 4 h or 24 h. After this incubation, the medium containing SDEPN was replaced with medium containing 2.5 or 12 $\mu\text{mol/L}$ cisplatin. The cells were harvested by trypsinization when they reached approximately 80% confluence. The cells were placed in 70% ethanol and centrifuged for 5 min at 300 *g*. They were then resuspended in 200 μL of a PI solution (20 mL PBS, 20 μL 0.1% Triton X-100, 200 mg/mL RNase, and 20 $\mu\text{g/mL}$ PI), placed in FACS tubes, and incubated for 30 min at room temperature protected from light. The labeled cells were captured with a FACScalibur cytometer (BD Bioscience, Franklin Lakes, NJ, United States) and analyzed with the software CELLQuest™ (BD Biosciences). The percentage of cells in different cell cycle phases was quantified and data were expressed as histograms.

Statistical analysis

All experiments were performed at least in triplicate. The significance of differences between groups was calculated by applying analysis of variance and Bonferroni's test, as indicated. A value of $P < 0.05$ was considered to be statistically significant.

RESULTS

Cytotoxic effects of SDEPN on HT29 and HepG2 cells

The effects of SDEPN on cell killing in two cancer cell lines were determined by flow cytometry. All cell lines were killed in a dose-dependent manner after exposure to the plant extracts (Figure 1). SDEPN had significantly different cytotoxic effects on HT29 (2.81 ± 0.11 vs 3.51 ± 1.13 , $P > 0.05$) and HepG2 (5.07 ± 0.3 vs 15.9 ± 1.04 , $P < 0.001$) cells when compared to control cells for 4 h. SDEPN also had significantly different cytotoxic effects on HT29 (1.91 ± 0.57 vs 4.53 ± 1.22 , $P > 0.05$) and HepG2 (14.56 ± 1.6 vs 35.67 ± 3.94 , $P < 0.001$) cells when compared to control cells for 24 h. These results indicated that the plant extract was selectively toxic against the cancer cells tested. We therefore hypoth-

esized that the combination of these plant extracts with chemotherapeutic drugs may have a synergistic cytotoxic effect on these cells. Primary flow cytometry analyses are shown in Figure 2.

The effect of cisplatin on HT29 and HepG2 cells

Using flow cytometry, we assessed the effects of cisplatin on the proliferation of HepG2 and HT29 cells. Both cell lines were killed in a dose-dependent manner compared to control cells (HepG2 cells for 4 h: 10.78 ± 1.58 vs 53.89 ± 1.53 , $P < 0.001$; 24 h: 8.9 ± 1.43 vs 62.78 ± 1.87 , $P < 0.001$ and HT29 cells for 4 h: 9.52 ± 0.913 vs 49.86 ± 2.89 , $P < 0.001$; 24 h: 11.78 ± 1.05 vs 53.34 ± 2.65 , $P < 0.001$; Figure 1). Primary flow cytometry analyses are shown in Figure 2.

The combination of cisplatin and Phyllanthus niruri extracts has a synergistic cytotoxic effect on HT29 and HepG2 cells

HT29 cells did not undergo cell death when SDEPN was used alone ($P > 0.05$) but HepG2 cells ($P < 0.001$) showed significant cell killing with treatment with SDEPN alone (Figure 1), but also very significantly (12.87 ± 2.78 vs 78.8 ± 3.02 , $P < 0.001$) when combined with cisplatin (Figure 1). However, HT29 cells underwent cell death (12.78 ± 1.01 vs 93.76 ± 1.6 , $P < 0.001$) when treated with SDEPN for 24 h prior to cisplatin treatment (Figure 1). The primary images of flow cytometry analysis can be seen in Figure 2.

In HT29 cells, pretreatment with SDEPN and subsequent treatment with cisplatin resulted in a greater number of cells being killed compared to treatment with cisplatin or SDEPN alone (Figure 1A and B). This increase in the number of HepG2 cells killed in response to combination treatment was observed at the lower concentration of SDEPN (Figure 1C and D). Therefore, pretreatment with SDEPN allowed the cells (HT29) to be sensitized to killing induced by cisplatin. This suggests that this cell type is more able to adapt to stressful conditions.

DISCUSSION

In this study, the growth inhibitory activity of SDEPN extract alone and in combination with cisplatin was investigated in HT29 and HepG2 cells. Our results indicated that SDEPN extract significantly inhibited the growth of both cell lines in a dose-dependent manner when combined with cisplatin.

Cisplatin is a well-known cancer therapeutic agent that causes high toxicity to normal tissues during cancer therapy, inducing cell death through interaction of the platinum complex with DNA molecules which induces crosslinking in DNA^[28,29]. The platinum compound is used to treat various types of human solid tumors^[30]. The major limitation to clinical use of cisplatin is the adverse effects, mainly nephrotoxicity, caused by the compound^[31]. In addition to DNA interactions, cisplatin

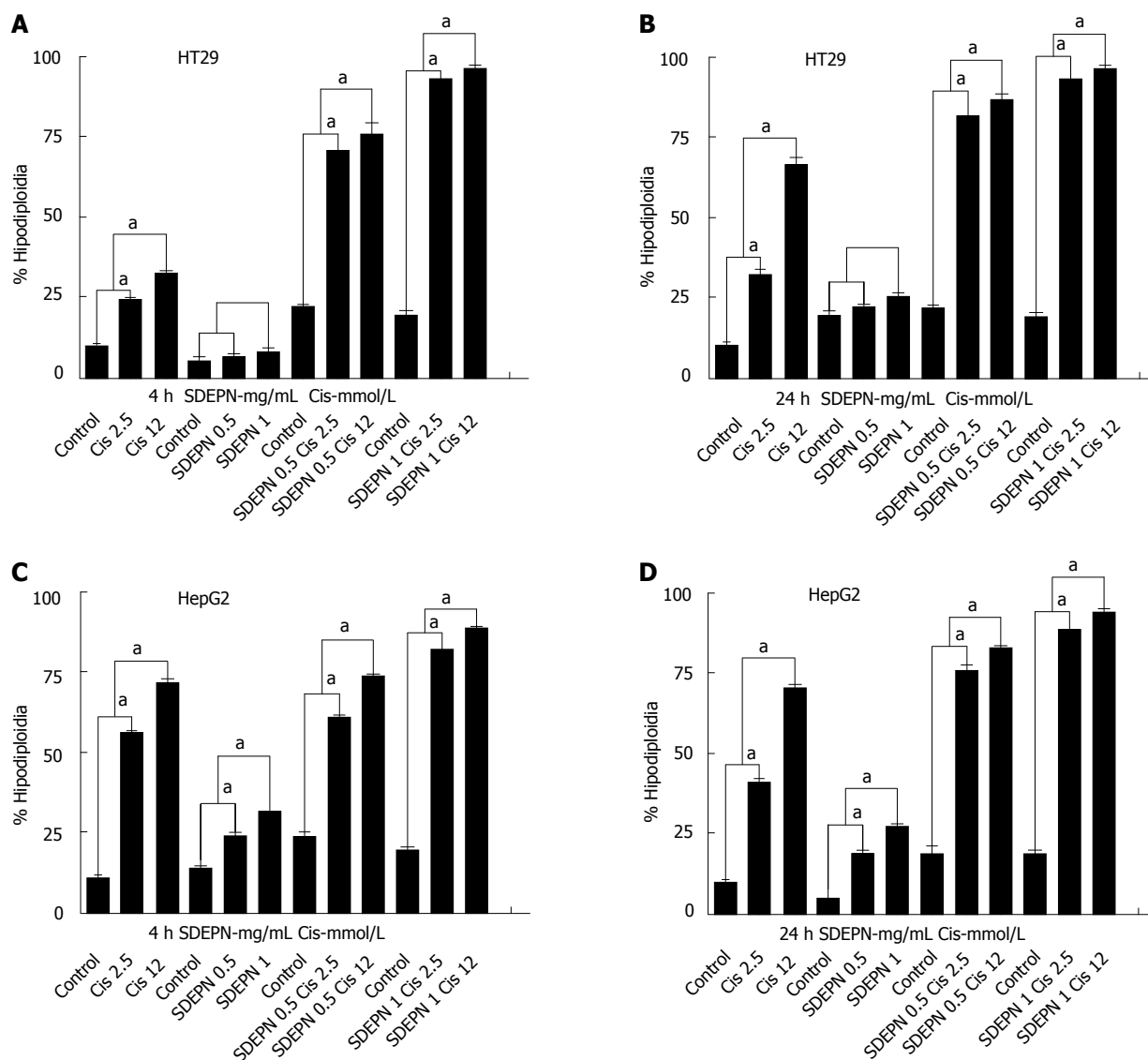


Figure 1 HT29 cells and HepG2 cells were treated for 4 h or 24 h with cisplatin alone, spray-dried extract of *Phyllanthus niruri* alone, or both. A, C: 4 h; B, D: 24 h. ^a $P < 0.05$ vs control group. SDEPN: Spray-dried extract of *Phyllanthus niruri*; Cis: Cisplatin; HT29: Colorectal carcinoma; HepG2: Human hepatocellular carcinoma.

is capable of generating oxidative stress through mitochondrial dysfunction, which results in the increased production of reactive oxygen species (ROS)^[32]. Therefore, our data show that HT29 cells are more resistant to SDEPN- or cisplatin-mediated cell death, and this resistance may be related to their ability to adapt to stressful conditions. In addition, HepG2 cells were more sensitive to both treatments, suggesting that these cells may be less adapted to stress. In this study we found that the combination of SDEPN with cisplatin induced growth inhibition and cell death at different dose levels in HT29 and HepG2 cell lines.

The mechanism of action of some plant extracts is still unclear, since they are not a single active ingredient but rather consist of multiple compounds that could potentially induce the observed effects^[1,23]. Plant-derived polyphenols, including gallic acid^[33,34] and tannins^[35], were reported to be the main components of *Phyllanthus*

niruri extracts^[1]. Therefore, the effects of SDEPN may induce apoptosis and cell death in the cell lines used in this study through multiple pathways due to the multiple components present in the extract. The active ingredients in *Phyllanthus niruri* that exert anticancer effects may include polyphenols, such as gallic acid, flavanoids or tannins, which are abundant in the herb. However, the detailed mechanism responsible for the anticancer effect of SDEPN extract and identification of the actual functional components require further elucidation.

It has been previously demonstrated that the effect of gallic acid on cancer cells, particularly lung cancer cells, involves caspase activation and oxidative processes^[33]. In addition, gallic acid has the capacity to induce apoptosis and increase the efficacy of cisplatin in LL-2 lung cancer cells^[34].

Our study provides corroborative evidence that SDEPN has selective cytotoxic effects against HT29 and HepG2

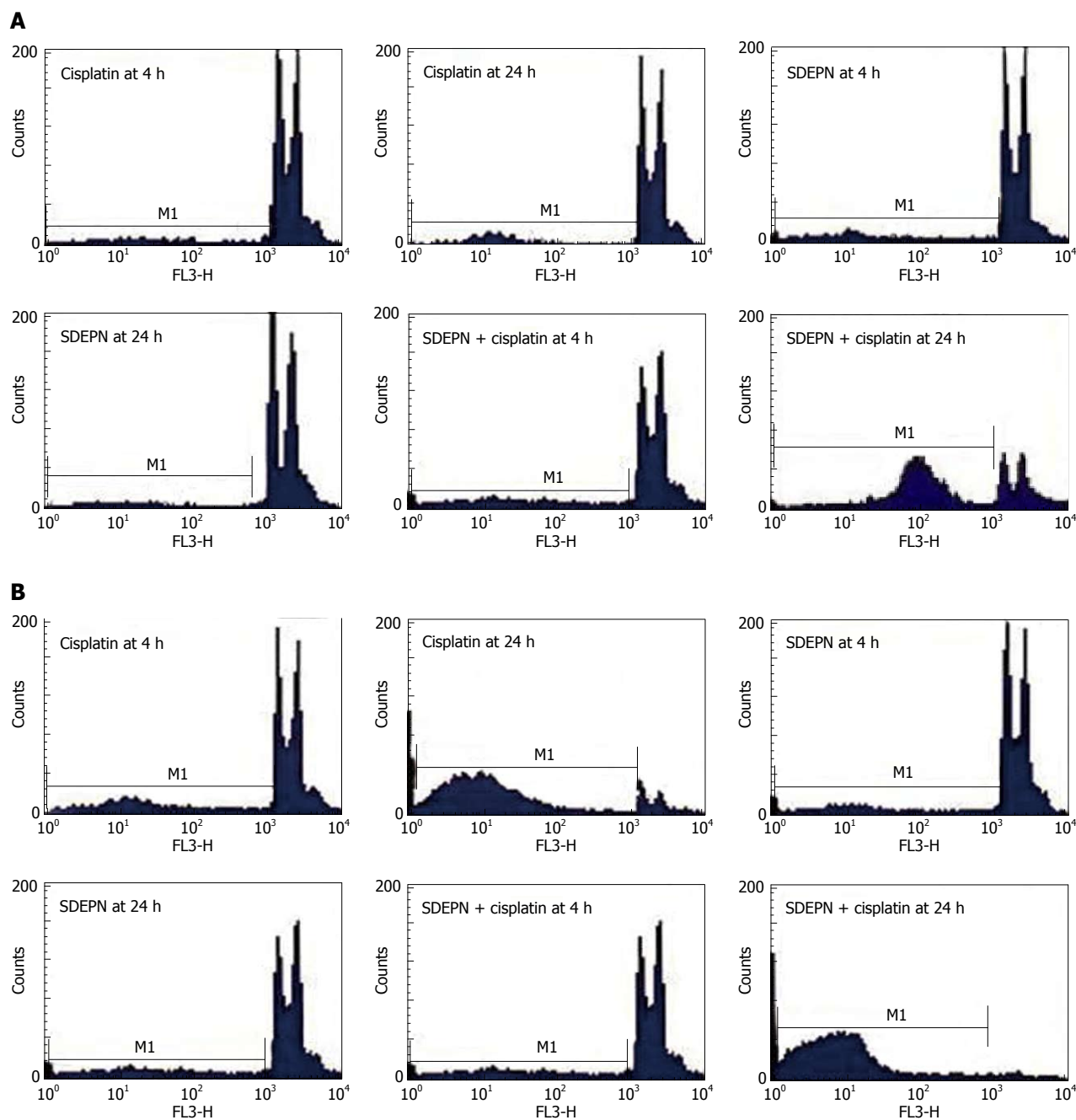


Figure 2 Effects of cisplatin, spray-dried extract of *Phyllanthus niruri*, or both on HT29 cells or HepG2 cells as assessed by flow cytometry. A: HT29 cells; B: HepG2 cells.

cells. Moreover, a synergistic effect was seen when the cells were treated with the extract in combination with cisplatin. This finding supports our hypothesis that combinations of plant extracts and chemotherapeutic agents may allow for a reduction in the dosage of the more toxic chemotherapeutic agent while retaining the therapeutic efficacy and minimizing toxicities. The induction of cell death by SDEPN may increase the sensitivity of HT29 cells to cisplatin-mediated cytotoxicity. Other species of the genus *Phyllanthus* have demonstrated growth inhibitory activity with a certain degree of selectivity towards the two cancer cell lines tested^[20].

The findings of this study support our hypothesis

that combinations of plant extracts and chemotherapeutic agents allow for a reduction in the dosage of the latter (i.e., cisplatin), while maintaining therapeutic efficacy. Moreover, the induction of cell death by SDEPN may be a strategy for increasing the sensitivity of HT29 cells to cisplatin-mediated cell death.

COMMENTS

Background

Phyllanthus niruri is a widespread tropical plant that is commonly found in coastal areas of Mexico, Argentina, and Brazil. In Brazil, some plant extracts have been distributed to patients by the Public Health Programme since 2010

as an adjunctive therapy for various diseases. The extract from aerial sections of *Phyllanthus niruri* was included in this list due to the long history of use in traditional medicine for the treatment of kidney and bladder diseases, intestinal infections, diabetes, and hepatitis B. Furthermore, this study has demonstrated an *in vitro* pro-death potential in cancer cells when *Phyllanthus niruri* is associated with cisplatin. *In vivo* studies are still needed to confirm our findings.

Research frontiers

Currently, a variety of effective phytochemicals have been tested in cancer treatment, which are used alone or in combination with chemotherapeutic agents for treatment. A spray-dried extract from *Phyllanthus niruri* (SDEPN) was found to be selectively toxic against two cancer cell lines and induced an increase in cell death of HT29 and HepG2 cells when used in combination with cisplatin. HT29 cells did not undergo cell death when SDEPN was used alone. The mechanism of this effect is currently unknown, but may involve apoptosis, since a major component of SDEPN extract is gallic acid, which has been shown to induce apoptotic pathways.

Innovations and breakthroughs

In this report, the authors have demonstrated that combinations of SDEPN with cisplatin in HT29 and HepG2 cell lines have a more potent effect than either agent alone.

Applications

Spray-dried extract of SDEPN appears to be cytotoxic against hepatocellular carcinoma and less toxic against colorectal carcinoma. A combination of SDEPN extract with a chemotherapeutic agent may therefore enhance the efficacy of each component against these cancers. Future *in vivo* studies will be performed by our group to study the anticancer activity of SDEPN alone and in combination with cisplatin as well as the toxicity against normal tissues.

Terminology

Dried herbal extracts are widely used as therapeutic products with improved pharmaceutical properties, such as stability and content uniformity. Additionally, dried extracts are successfully used to obtain solid dosage forms that contain a high dose of herbal extracts, such as capsules and tablets. Therefore, spray drying is the most commonly used procedure to obtain dried extracts (spray-dried extracts) in the herbal processing industry.

Peer review

The manuscript is well written and the findings are interesting to some extent. However, some concerns need to be addressed.

REFERENCES

- 1 Calixto JB, Santos AR, Cechinel Filho V, Yunes RA. A review of the plants of the genus *Phyllanthus*: their chemistry, pharmacology, and therapeutic potential. *Med Res Rev* 1998; **18**: 225-258
- 2 Sripanidkulchai B, Tattawasart U, Laupatarakasem P, Vinitketkumneun U, Sripanidkulchai K, Furihata C, Matsushima T. Antimutagenic and anticarcinogenic effects of *Phyllanthus amarus*. *Phytomedicine* 2002; **9**: 26-32
- 3 Rajeshkumar NV, Joy KL, Kuttan G, Ramsewak RS, Nair MG, Kuttan R. Antitumor and anticarcinogenic activity of *Phyllanthus amarus* extract. *J Ethnopharmacol* 2002; **81**: 17-22
- 4 Bhattacharjee R, Sil PC. The protein fraction of *Phyllanthus niruri* plays a protective role against acetaminophen induced hepatic disorder via its antioxidant properties. *Phytother Res* 2006; **20**: 595-601
- 5 Nassar AM, Helal EE, Ibrahim KA. Further observations on the ultrastructure of the schistosomal pigment in human liver. *J Egypt Soc Parasitol* 1986; **16**: 91-104
- 6 Manjrekar AP, Jisha V, Bag PP, Adhikary B, Pai MM, Hegde A, Nandini M. Effect of *Phyllanthus niruri* Linn. treatment on liver, kidney and testes in CCl₄ induced hepatotoxic rats. *Indian J Exp Biol* 2008; **46**: 514-520
- 7 Murugaiyah V, Chan KL. Mechanisms of antihyperuricemic effect of *Phyllanthus niruri* and its lignan constituents. *J Ethnopharmacol* 2009; **124**: 233-239
- 8 Khanna AK, Rizvi F, Chander R. Lipid lowering activity of *Phyllanthus niruri* in hyperlipemic rats. *J Ethnopharmacol* 2002; **82**: 19-22
- 9 Latha P, Chaitanya D, Rukkumani R. Protective effect of *Phyllanthus niruri* on alcohol and heated sunflower oil induced hyperlipidemia in Wistar rats. *Toxicol Mech Methods* 2010; **20**: 498-503
- 10 Chang CC, Lien YC, Liu KC, Lee SS. Lignans from *Phyllanthus urinaria*. *Phytochemistry* 2003; **63**: 825-833
- 11 Yan F, Zhang QY, Jiao L, Han T, Zhang H, Qin LP, Khalid R. Synergistic hepatoprotective effect of *Schisandrae* lignans with *Astragalus polysaccharides* on chronic liver injury in rats. *Phytomedicine* 2009; **16**: 805-813
- 12 Gnabre JN, Itob Y, Mab Y, Huanga RC. Isolation of anti-HIV-1 lignans from *Larrea tridentata* by counter-current chromatography. *Journal of Chromatography* 1996; **353**: 353-364
- 13 Popova MP, Chinou IB, Marekov IN, Bankova VS. Terpenes with antimicrobial activity from Cretan propolis. *Phytochemistry* 2009; **70**: 1262-1271
- 14 Hayashi Y, Matsushima M, Nakamura T, Shibasaki M, Hashimoto N, Imaizumi K, Shimokata K, Hasegawa Y, Kawabe T. Quercetin protects against pulmonary oxidant stress via heme oxygenase-1 induction in lung epithelial cells. *Biochem Biophys Res Commun* 2012; **417**: 169-174
- 15 Muzitano MF, Cruz EA, de Almeida AP, Da Silva SA, Kaiser CR, Guette C, Rossi-Bergmann B, Costa SS. Quercitrin: an antileishmanial flavonoid glycoside from *Kalanchoe pinnata*. *Planta Med* 2006; **72**: 81-83
- 16 Guardia T, Rotelli AE, Juarez AO, Pelzer LE. Anti-inflammatory properties of plant flavonoids. Effects of rutin, quercetin and hesperidin on adjuvant arthritis in rat. *Farmacologia* 2001; **56**: 683-687
- 17 Patel JR, Tripathi P, Sharma V, Chauhan NS, Dixit VK. *Phyllanthus amarus*: ethnomedicinal uses, phytochemistry and pharmacology: a review. *J Ethnopharmacol* 2011; **138**: 286-313
- 18 Ishihara M, Sakagami H. Application of semiempirical method to estimate the cytotoxic activity of gallic acid and its related compounds. *Anticancer Res* 2003; **23**: 2549-2552
- 19 Sakaguchi N, Inoue M, Isuzugawa K, Ogihara Y, Hosaka K. Cell death-inducing activity by gallic acid derivatives. *Biol Pharm Bull* 1999; **22**: 471-475
- 20 Pinmai K, Chunlaratthanabhorn S, Ngamkitidechakul C, Soonthornchareon N, Hahnvanjanawong C. Synergistic growth inhibitory effects of *Phyllanthus emblica* and *Terminalia bellerica* extracts with conventional cytotoxic agents: doxorubicin and cisplatin against human hepatocellular carcinoma and lung cancer cells. *World J Gastroenterol* 2008; **14**: 1491-1497
- 21 Naik AD, Juvekar AR. Effects of alkaloidal extract of *Phyllanthus niruri* on HIV replication. *Indian J Med Sci* 2003; **57**: 387-393
- 22 Sarkar MK, Sil PC. Hepatocytes are protected by herb *Phyllanthus niruri* protein isolate against thioacetamide toxicity. *Pathophysiology* 2007; **14**: 113-120
- 23 Bagalkotkar G, Sagineedu SR, Saad MS, Stanslas J. Phytochemicals from *Phyllanthus niruri* Linn. and their pharmacological properties: a review. *J Pharm Pharmacol* 2006; **58**: 1559-1570
- 24 Raj Kapoor B, Sankari M, Sumithra M, Anbu J, Harikrishnan N, Gobinath M, Suba V, Balaji R. Antitumor and cytotoxic effects of *Phyllanthus polyphyllus* on Ehrlich ascites carcinoma and human cancer cell lines. *Biosci Biotechnol Biochem* 2007; **71**: 2177-2183
- 25 Krishnaveni M, Mirunalini S. Therapeutic potential of *Phyllanthus emblica* (amla): the ayurvedic wonder. *J Basic Clin Physiol Pharmacol* 2010; **21**: 93-105
- 26 De Souza TP, Gómez-Amoza JL, Martínez-Pacheco R, Petrovick PR. Compression behavior of formulations from *Phyllanthus niruri* spray dried extract. *Pharmazie* 2006; **61**: 213-217
- 27 Uchiyama T, Kamio M, Kodaka T, Tamori S, Fukuhara S, Amakawa R, Uchino H, Araki K. Leukemic cells from some adult T-cell leukemia patients proliferate in response to interleukin-4. *Blood* 1988; **72**: 1182-1186

- 28 **Yunos NM**, Beale P, Yu JQ, Huq F. Synergism from sequenced combinations of curcumin and epigallocatechin-3-gallate with cisplatin in the killing of human ovarian cancer cells. *Anticancer Res* 2011; **31**: 1131-1140
- 29 **Gandara DR**, Perez EA, Weibe V, De Gregorio MW. Cisplatin chemoprotection and rescue: pharmacologic modulation of toxicity. *Semin Oncol* 1991; **18**: 49-55
- 30 **Ali BH**, Al Moundhri MS. Agents ameliorating or augmenting the nephrotoxicity of cisplatin and other platinum compounds: a review of some recent research. *Food Chem Toxicol* 2006; **44**: 1173-1183
- 31 **Baliga R**, Zhang Z, Baliga M, Ueda N, Shah SV. In vitro and in vivo evidence suggesting a role for iron in cisplatin-induced nephrotoxicity. *Kidney Int* 1998; **53**: 394-401
- 32 **Martins NM**, Santos NA, Curti C, Bianchi ML, Santos AC. Cisplatin induces mitochondrial oxidative stress with resultant energetic metabolism impairment, membrane rigidification and apoptosis in rat liver. *J Appl Toxicol* 2008; **28**: 337-344
- 33 **Ohno Y**, Fukuda K, Takemura G, Toyota M, Watanabe M, Yasuda N, Xinbin Q, Maruyama R, Akao S, Gotou K, Fujiwara T, Fujiwara H. Induction of apoptosis by gallic acid in lung cancer cells. *Anticancer Drugs* 1999; **10**: 845-851
- 34 **Kawada M**, Ohno Y, Ri Y, Ikoma T, Yuugetu H, Asai T, Watanabe M, Yasuda N, Akao S, Takemura G, Minatoguchi S, Gotoh K, Fujiwara H, Fukuda K. Anti-tumor effect of gallic acid on LL-2 lung cancer cells transplanted in mice. *Anticancer Drugs* 2001; **12**: 847-852
- 35 **Markom M**, Hasan M, Daud WRW, Singh H, Jahim JM. Extraction of hydrolysable tannins from *Phyllanthus niruri* Linn.: Effects of solvents and extraction methods. *Sep Purif Technol* 2007; **52**: 487-496

S- Editor Gou SX L- Editor Kerr C E- Editor Zhang DN

Sensitivity of the suspected blood indicator: An experimental study

Sung Chul Park, Hoon Jai Chun, Eun Sun Kim, Bora Keum, Yeon Seok Seo, Yong Sik Kim, Yoon Tae Jeon, Hong Sik Lee, Soon Ho Um, Chang Duck Kim, Ho Sang Ryu

Sung Chul Park, Division of Gastroenterology and Hepatology, Department of Internal Medicine, Kangwon National University School of Medicine, Chuncheon 200-722, South Korea

Hoon Jai Chun, Eun Sun Kim, Bora Keum, Yeon Seok Seo, Yong Sik Kim, Yoon Tae Jeon, Hong Sik Lee, Soon Ho Um, Chang Duck Kim, Ho Sang Ryu, Division of Gastroenterology and Hepatology, Department of Internal Medicine, Korea University College of Medicine, Seoul 136-705, South Korea

Author contributions: Park SC, Chun HJ, Kim ES, and Keum B performed the research; Seo YS, Kim YS, Jeon YT, Lee HS, Um SH, Kim CD, and Ryu HS analyzed the data; and Park SC and Chun HJ wrote the article.

Correspondence to: Hoon Jai Chun, MD, PhD, Division of Gastroenterology and Hepatology, Department of Internal Medicine, Korea University College of Medicine, 126-1, Anam-dong 5-ga, Seongbuk-gu, Seoul 136-705, South Korea. drchunhj@chol.com

Telephone: +82-2-9206555 Fax: +82-2-9531943

Received: February 11, 2012 Revised: May 2, 2012

Accepted: May 5, 2012

Published online: August 21, 2012

Abstract

AIM: To investigate whether suspected blood indicator (SBI) in capsule endoscopy (CE) is affected by background color and capsule passage velocity.

METHODS: Experimental models of the small intestine constructed from paper in a variety of colors were used to simulate the background colors observed in CE images. The background colors studied included very pale yellow, yellow, very pale magenta, light grayish pink, burnt sienna, and deep and dark brown, and red spots were attached inside them. An endoscopic capsule was manually passed through the models. The rate of detection of the red spots by the SBI was evaluated based on the colors of the models and the capsule passage velocities (0.5 cm/s, 1 cm/s, and 2 cm/s).

RESULTS: The rate of detection of the red spots by

the SBI differed significantly according to the background color of the model ($P < 0.001$). Detection rates were highest for backgrounds of very pale magenta, burnt sienna, and yellow, in that order. They were lowest for backgrounds of dark brown and very pale yellow. The rate of detection of red spots by the SBI tended to decrease at rapid capsule passage velocities (1-2 cm/s) compared to slow velocities (0.5 cm/s) for backgrounds of very pale yellow ($P = 0.042$), yellow ($P = 0.001$), very pale magenta ($P = 0.002$), and burnt sienna ($P = 0.001$). No significant differences in the rate of detection were observed according to velocity for light grayish pink ($P = 0.643$) or dark brown ($P = 0.396$).

CONCLUSION: SBI sensitivity was affected by background color and capsule passage velocity in the models. These findings may facilitate the rapid detection of bleeding lesions by CE.

© 2012 Baishideng. All rights reserved.

Key words: Capsule endoscopy; Suspected blood indicator; Sensitivity; Background color; Passage velocity

Peer reviewer: Dr. Josep M Bordas, Gastroenterology Unit, Hospital Clinic, Llusanes 11-13, 08022 Barcelona, Spain

Park SC, Chun HJ, Kim ES, Keum B, Seo YS, Kim YS, Jeon YT, Lee HS, Um SH, Kim CD, Ryu HS. Sensitivity of the suspected blood indicator: An experimental study. *World J Gastroenterol* 2012; 18(31): 4169-4174 Available from: URL: <http://www.wjgnet.com/1007-9327/full/v18/i31/4169.htm> DOI: <http://dx.doi.org/10.3748/wjg.v18.i31.4169>

INTRODUCTION

Capsule endoscopy (CE) is a useful method for the diagnosis of small bowel diseases, such as gastrointestinal bleeding of an unknown cause^[1-7]. However, it is relatively

time consuming to examine and interpret the results. To reduce the reading time of this procedure, the RAPID software (Given Imaging Ltd., Duluth, GA, United States) contains a suspected blood identification system, which identifies hemorrhages and suspicious vascular lesions by recognizing red-colored pixels against different colored backgrounds that may be encountered in the small intestine^[8].

Reports on the usefulness of the suspected blood indicator (SBI) generally show a low and variable overall sensitivity for lesions, ranging from 20% to 56.4%^[8-12]. Positive predictive values are also observed to be variable, from 24% to 90.3%. Therefore, SBI generates false-positive and false-negative results, and its clinical usefulness has not been verified.

Active bleeding is the most important factor affecting SBI sensitivity. The sensitivity increases to a range of 58.3% to 93% in cases of active bleeding. Additionally, the sensitivity of SBI may also be affected by other factors. However, not all of the factors that can affect SBI sensitivity have been fully assessed.

The RAPID software includes a tissue color bar function that represents the average color of the region of interest in the intestine and provides information to help determine the anatomical location of a lesion^[13]. When the small intestine is observed *via* CE, on-screen images are primarily composed of the intestinal mucosa and liquid present in the lumen. The background color behind a lesion may vary according to the color of the small intestinal mucosa, which is affected by patient factors, such as hemoglobin and bilirubin levels. Thus, very pale magenta, which is the normal mucous membrane color, can appear very pale yellow in patients with anemia or burnt sienna or deep brown in patients with jaundice. The background color can also be affected by the presence of intestinal fluid. The color and the degree of transparency of the fluid can vary depending on the presence of bile, debris, stool residue, and blood in the intestine. Therefore, a combination of these elements may produce many different colors that can be presented on screen during CE. The various background colors of lesions may influence the detection of SBI in CE images.

The velocity of the passage of a capsule through the small intestine can vary depending on the presence of underlying disease, such as diabetes and disorders of intestinal peristalsis^[14]. Furthermore, the passage velocity can vary in different sections of the small intestine. Capsule movement may be influenced regionally by the gastric emptying time, chronic intestinal motility disorders, small bowel obstruction, intestinal diverticulosis, and other factors^[15]. These differences in capsule passage velocity according to the clinical circumstances may also affect SBI sensitivity. It would be useful to examine the different factors that influence the sensitivity of the SBI for shortening the time required to interpret CE-generated video.

Therefore, we investigated the rate of detection of red spots using SBI according to the background colors of the screen image and the capsule passage velocity in experimental models of the small intestine to determine

the factors that affect SBI sensitivity in diverse clinical situations.

MATERIALS AND METHODS

Experimental small intestine model

To represent a variety of background colors that may be encountered in clinical situations, experimental small intestine models prepared with seven colors of paper were produced. The colors included very pale yellow, yellow, very pale magenta, light grayish pink, burnt sienna, deep brown, and dark brown (Figure 1). Very pale magenta corresponds to the color of a normal intestinal mucous membrane. Lighter colors can be observed in conditions such as anemia, and darker colors are visible in mucosae with concentrated bile. The Hue and Tone 120-color system that was developed by the Nippon Color and Design Institute was used to define the colors and hues used in this study, and all color saturation levels were uniform^[16]. Small bowel models that were 3 cm in diameter and 50 cm in length were constructed, and ten 6-mm red spots were attached inside the models at 5-cm intervals to simulate angiodysplasia.

Investigation of capsule passage

A CE device (M2A capsule; Given Imaging Ltd., Yoqneam, Israel) was fixed to a solid-line cardiac catheter and passed inside the cylinder of each small intestine model at a constant speed (0.5 cm/s). The screen image from the CE instrument as it passed through model was observed using a real-time viewer (Figure 2). To detect differences in the SBI sensitivity according to the background color, 150 red dots were required to achieve a power of 80% ($\alpha = 5\%$) according to a preliminary pilot study. Therefore, through repetition, the CE instrument was guided past 150 red spots on each of the background colors, and the number of red tags on the scroll bar was examined during the application of SBI.

Differences in the SBI sensitivity were examined when the CE was passed through the intestinal models at speeds of 0.5 cm/s, 1 cm/s, and 2 cm/s.

Statistical analysis

For all statistical analysis in this study, SPSS version 12.0 (SPSS Inc., Chicago, IL, United States) was used. Continuous variables were expressed as the mean \pm SD or as the median. For comparative analysis of continuous variables, the Student's *t*-test, the Mann-Whitney *U* test, or the Kruskal-Wallis test were used depending on the normality of the data. For the comparison of nominal variables, Fisher's exact test and a χ^2 test were used. A post-hoc Bonferroni's correction was applied for comparative analysis of the groups. All values with a *P* < 0.05 were considered statistically significant.

RESULTS

Detection according to background color

We compared the number of red tags recognized by the

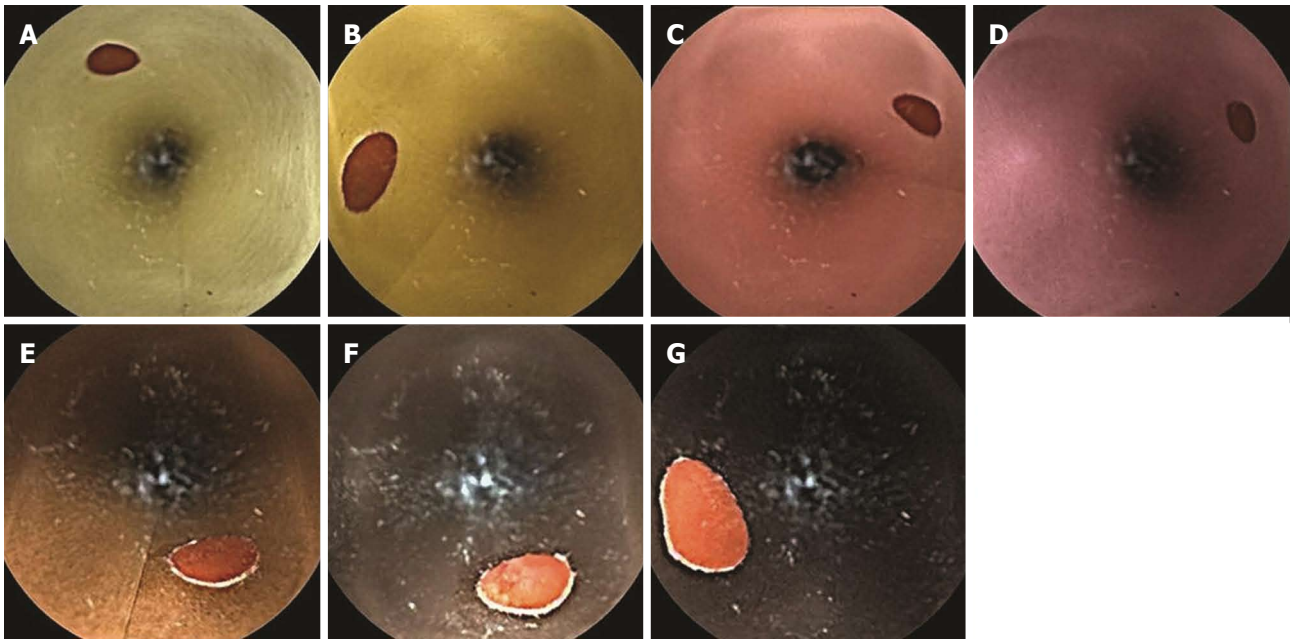


Figure 1 Endoscopic findings on backgrounds of different colors. A: Very pale yellow; B: Yellow; C: Very pale magenta; D: Light grayish pink; E: Burnt sienna; F: Deep brown; G: Dark brown.

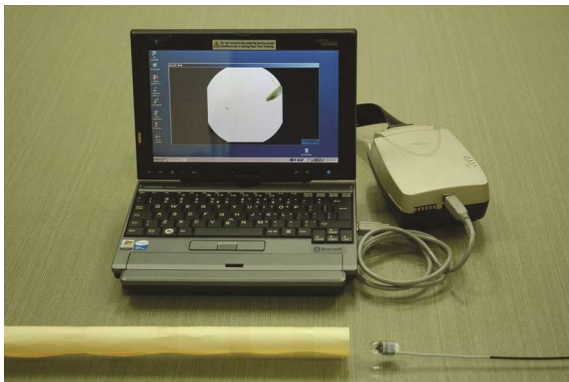


Figure 2 Experimental settings used for this study. A capsule endoscopy (CE) device was manually passed through models of the small bowel. The CE screen was observed using a real-time viewer.

SBI in the small intestine model for each background color. A significant difference was observed in the SBI detection rates on different background colors ($P < 0.001$, Table 1). The detection rates were highest for very pale magenta, burnt sienna, and yellow, in that order, and they were lowest for dark brown. Thus, the sensitivity of the SBI was the highest for a background of very pale magenta, which represented a normal mucosal color with good bowel cleansing, and the sensitivity was the lowest for dark brown, which represented concentrated bile. For a background of very pale yellow, which represented light bile, the detection rate of the red spots was low.

The sensitivity of the SBI for different background colors, analyzed with Bonferroni's correction, showed a significant difference for very pale magenta, for which the detection rate was the highest, compared to that of the other colors. The detection rate with a burnt sienna

Table 1 Detection rates of red spots by suspected blood indicator according to the background color

Color	Detection rate (%)	Rank
Very pale yellow	16/150 (10.7)	6
Yellow	28/150 (18.7)	3
Very pale magenta	64/150 (42.7)	1
Light grayish pink	19/150 (12.7)	4
Burnt sienna	36/150 (24.0)	2
Deep brown	18/150 (12.0)	5
Dark brown	5/150 (3.3)	7
Total	186/1050 (17.7)	$P < 0.001$

background was different from that with a very pale yellow and dark brown background, and the detection rate with a yellow background was different from that when a dark brown background was used (Table 2).

Detection according to capsule passage velocity

Generally, statistically significant differences were observed in the SBI detection rates of the red spots according to the capsule passage velocity in the small intestine models of some colors (Figure 3). Detection of the red spots by SBI tended to decrease at rapid capsule passage velocities (1-2 cm/s) compared to slow velocities (0.5 cm/s) for very pale yellow ($P = 0.042$), yellow ($P = 0.001$), very pale magenta ($P = 0.002$), and burnt sienna ($P = 0.001$) backgrounds. No significant differences were observed according to velocity for light grayish pink ($P = 0.643$) or dark brown ($P = 0.396$). Thus, differences according to velocity were highly pronounced in models constructed from colors that showed high SBI detection rates, and differences in sensitivity were not present for models with colors that had lower detection rates.

Table 2 Differences in detection rate among background colors using Bonferroni's correction

Color	Detection rate (%)	Dark brown	Very pale yellow	Deep brown	Light grayish pink	Yellow	Burnt sienna	Very pale magenta
Dark brown	3.3	1	0.0130	0.0049	0.0029	0.0000	0.0000	0.0000
Very pale yellow	10.7		1	0.7161	0.5901	0.0506	0.0023	0.0000
Deep brown	12.0			1	0.8609	0.1097	0.0069	0.0000
Light grayish pink	12.7				1	0.1535	0.0113	0.0000
Yellow	18.7					1	0.2603	0.0000
Burnt sienna	24.0						1	0.0006
Very pale magenta	42.7							1
Adjusted α	0.002381							

Table 3 Diagnostic accuracy of suspected blood indicator according to the literature (%)

	Liangpunsakul <i>et al.</i> ^[8]		Signorelli <i>et al.</i> ^[12]		D'Halluin <i>et al.</i> ^[10]		Buscaglia <i>et al.</i> ^[9]		Kim <i>et al.</i> ^[11]	
	OL	AB	OL	AB	OL	AB	OL	AB	OL	AB
Sensitivity	25.7	81.2	40.9	60.9	45	83	56.4	58.3	20	93
PPV	90.3	81.3	69.2	53.8	52	23	24	70	44	21

PPV: Positive predictive value; OL: Overall lesion; AB: Active bleeding.

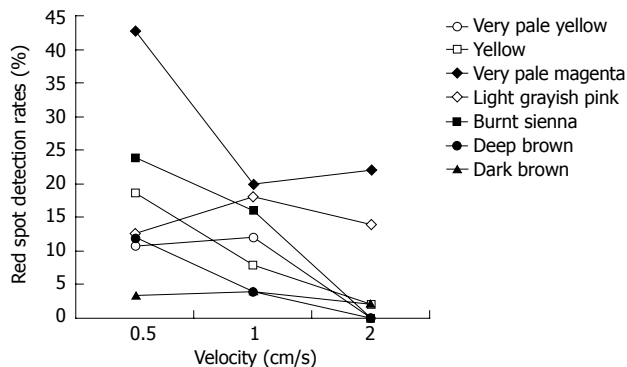


Figure 3 Detection rates of red spots by the suspected blood indicator according to the capsule endoscopy passage velocity.

DISCUSSION

CE was developed to diagnose lesions of the small intestine, and it is a useful method for diagnosing obscure gastrointestinal bleeding, Crohn's disease, polyposis syndrome, and small bowel tumors^[2-4,17-19]. CE has a higher diagnostic rate than radiological diagnosis methods and is less invasive and easier to perform than enteroscopy^[2-4,7,20]. However, CE has the disadvantage of requiring time to interpret multiple images^[21,22]. Usually, 45 min to two hours of viewing are required, although the reading time can be shortened using the multiview function, which allows the simultaneous observation of several images^[22]. To solve these problems, particularly in patients with suspected small intestine bleeding, SBI was developed^[10,23,24].

SBI can display frames that depict red zones during CE. The technique is activated in the first image frame of the duodenum and operates only in frames corresponding to the small intestine. The function is activated by an SBI view button within the software, resulting in the automatic identification of red pixels on the screen as

red hash marks on the scroll bar. Frame with suspected bleeding lesions can be selected in this way. Therefore, SBI helps physicians to review the video quickly, and bleeding lesions can be found easily. SBI provides supplementary information, but it does not replace the analysis of the video image. All frames recognized using the SBI feature should be later examined by a clinician in more detail.

In the first report on the accuracy of SBI in 24 patients by Liangpunsakul *et al.*^[8] in 2003, the sensitivity of the SBI was 25.7% (Table 3). However, when only active bleeding lesions were targeted, the sensitivity increased to 81.2%. In another study by Signorelli *et al.*^[12], the sensitivity was only 40.9% in 100 patients, although it increased to 60.9% in the presence of red blood or actively bleeding lesions. In another study, the overall sensitivity was 45%, with 83% for active bleeding^[10]. In a study by Buscaglia *et al.*^[9], the overall sensitivity was 56.4% and that in patients with active bleeding was 58.3%. According to a Korean report by Kim *et al.*^[11], SBI sensitivity of was as low as 20%; however, for actively bleeding lesions, such as angiodysplasia, a much higher sensitivity was observed (93%). SBI sensitivity showed large differences in these studies, ranging from 20% to 56.4%. The positive predictive value also varied from 24% to 90.3%. Even with active bleeding, sensitivity still differed from 58.3% to 93%. Therefore, SBI is thought to be useful as an adjunct method to screen for bleeding lesions using CE. Still, SBI cannot completely replace the reading of the CE-generated video.

Cases with no significant bleeding, but in which bleeding was still suspected, are problematic and clinically important^[25]. The cause of the variability in SBI sensitivity is likely to be due to the differences in CE images. The presence of bile, debris, stool residue, and blood in the small intestine can vary depending on the patient's condition and bowel preparation. The intestinal fluid may

be yellowish due to bile juices, light grayish pink due to blood, brownish due to stool residue, or dark brownish due to discolored stool. It can also vary according to the concentrations of bile and debris. That is, the intestinal fluid may be very pale yellow or yellow when clear of bile, or it may be burnt sienna or deep brown when thick bile is present. Therefore, the background colors may vary within the same patient depending on the area investigated. Additionally, the color of the intestinal mucosa may be different according to the underlying diseases of patients, such as anemia or jaundice.

The color contrast indicates that the presence of a combination of different colors can influence the detection of individual colors^[26]. The contrast is greatest when a color is combined with its complementary color in the color circle. The color contrast includes contrast related to lightness, hue, saturation, and square. In the color circle, the complementary color of red is blue-green, for which the contrast is greatest. Saturation contrast means that if other vivid colors are located close to the color of interest, the saturation of the color will be reduced. In this study, we investigated whether the ability of SBI to detect red pixels was affected by color contrast, especially in conditions of similar color saturation. We found that the detection rate of red spots was 42.7% for a very pale magenta color, significantly decreasing to 3.3% for dark brown and 10.7% for very pale yellow. A decreased detection rate of 12% was observed when a deep brown background was used. Therefore, significant differences in the SBI detection rates were observed for the different background colors. For colors commonly observed during CE, such as very pale magenta, yellow, and burnt sienna, the SBI sensitivity was similar to that of the clinical data. The sensitivity was decreased for background colors such as dark brown or very pale yellow, which may be infrequently observed in clinical settings. These results suggest that the SBI sensitivity may vary depending on the amount of concentrated bile, food or debris present in the small intestinal lumen and the underlying diseases of patients.

The average time of capsule passage through the intestine is 217 ± 90 min^[14]. However, this can vary from 48 min to more than eight hours depending on the underlying disease, such as diabetes, and on intestinal peristalsis. Significant differences in the sensitivity of SBI were observed at different capsule passage velocities in the experimental intestine models: the faster the capsule moved, the lower the sensitivity.

The results of our experiments suggest that SBI has low detection rates at sites that have colors that are significantly different from those of the normal intestine and in the areas where the capsule passed through relatively quickly. That is, even when the SBI technique fails to detect red pixels, a bleeding spot (*i.e.*, angiodysplasia) may exist in those regions. Physicians must examine the images from these sites to detect false-negatives. The different background colors of the screen image can be easily located by using the tissue color bar in the software.

Therefore, the results of our study may assist physicians in the interpretation of SBI results and reduce the time required for detection of bleeding sites within the small intestine.

This study may be helpful for improving the diagnostic accuracy of SBI. To improve SBI sensitivity, technical improvements should be made. Additionally, the results of this study suggest clinically correctable factors for SBI. Bowel preparation before CE will improve the SBI sensitivity by minimizing the presence of bile and debris in the small intestine. To confirm this hypothesis, further studies investigating the factors that affect SBI sensitivity in different clinical situations are necessary.

The limitation of this study is that experimental models were used. Although the clinical situations of patients vary, if the capsule passes through an average of 6-7 m of small intestine in four hours, the actual average velocity is approximately 0.04 cm/s. The velocities used in this study of 0.5 cm/s, 1 cm/s, and 2 cm/s are not typically experienced in the clinic. Because it is technically difficult to artificially replicate an average capsule passage velocity, we randomly selected a velocity that was easy to replicate. Therefore, our results are difficult to apply directly to a clinical setting. However, it was shown that the sensitivity of SBI can differ depending on the velocity of the capsule.

In summary, the SBI sensitivity was significantly lower for some background colors on CE images, and the sensitivity decreased with faster capsule passage velocities in experimental models of the small intestine. Therefore, physicians should consider these factors when using SBI in the evaluation of CE images.

COMMENTS

Background

It is relatively time consuming to examine and interpret the results of capsule endoscopy (CE). The suspected blood indicator (SBI) is used for rapid screening of gastrointestinal bleeding, and it automatically recognizes frames that include red-colored pixels. However, reports on the usefulness of a SBI generally show low and variable overall sensitivity for lesions.

Research frontiers

SBI generates false-positive and false-negative results, and its clinical usefulness has not been verified. The color of the small intestinal mucosa and luminal fluid, which are the backgrounds on which lesions are detected, and the capsule passage velocity may vary according to bowel preparation and patient factors.

Innovations and breakthroughs

The detection by SBI differed significantly according to the background colors used ($P < 0.001$). The sensitivities on very pale magenta, burnt sienna and yellow backgrounds were significantly higher than on the other colors, such as very pale yellow or dark brown. The sensitivity tended to decrease at rapid capsule velocities in experimental models of the small intestine.

Applications

The results of this study may assist physicians in the interpretation of SBI results and reduce the time required for detecting bleeding sites in the small intestine. Physicians must examine the images that contain sites that could have false negative results more carefully than other sites. Bowel preparation before CE is useful for improving SBI sensitivity by minimizing bile or debris in the small intestine.

Peer review

The paper seeks to assess the automatic diagnostic yield using the suspected

blood identification system from GIVEN Imaging Ltd., designed to reduce the time spent reviewing CE images in patients with intermediate hemorrhage. The authors developed an experimental method to assess the sensitivity of SBI in different conditions.

REFERENCES

- 1 **Ben Soussan E**, Antonietti M, Hervé S, Savoye G, Ramirez S, Leclaire S, Ducrotté P, Lerebours E. Diagnostic yield and therapeutic implications of capsule endoscopy in obscure gastrointestinal bleeding. *Gastroenterol Clin Biol* 2004; **28**: 1068-1073
- 2 **Costamagna G**, Shah SK, Riccioni ME, Foschia F, Mutignani M, Perri V, Vecchioli A, Brizi MG, Piccicchi A, Marano P. A prospective trial comparing small bowel radiographs and video capsule endoscopy for suspected small bowel disease. *Gastroenterology* 2002; **123**: 999-1005
- 3 **Eliakim R**, Fischer D, Suissa A, Yassin K, Katz D, Guttman N, Migdal M. Wireless capsule video endoscopy is a superior diagnostic tool in comparison to barium follow-through and computerized tomography in patients with suspected Crohn's disease. *Eur J Gastroenterol Hepatol* 2003; **15**: 363-367
- 4 **Eil C**, Remke S, May A, Helou L, Henrich R, Mayer G. The first prospective controlled trial comparing wireless capsule endoscopy with push enteroscopy in chronic gastrointestinal bleeding. *Endoscopy* 2002; **34**: 685-689
- 5 **Ladas SD**, Triantafyllou K, Spada C, Riccioni ME, Rey JF, Niv Y, Delvaux M, de Franchis R, Costamagna G. European Society of Gastrointestinal Endoscopy (ESGE): recommendations (2009) on clinical use of video capsule endoscopy to investigate small-bowel, esophageal and colonic diseases. *Endoscopy* 2010; **42**: 220-227
- 6 **Pennazio M**, Santucci R, Rondonotti E, Abbiati C, Beccari G, Rossini FP, De Franchis R. Outcome of patients with obscure gastrointestinal bleeding after capsule endoscopy: report of 100 consecutive cases. *Gastroenterology* 2004; **126**: 643-653
- 7 **Saurin JC**, Delvaux M, Gaudin JL, Fassler I, Villarejo J, Vahedi K, Bitoun A, Canard JM, Souquet JC, Ponchon T, Florent C, Gay G. Diagnostic value of endoscopic capsule in patients with obscure digestive bleeding: blinded comparison with video push-enteroscopy. *Endoscopy* 2003; **35**: 576-584
- 8 **Liangpunsakul S**, Mays L, Rex DK. Performance of Given suspected blood indicator. *Am J Gastroenterol* 2003; **98**: 2676-2678
- 9 **Buscaglia JM**, Giday SA, Kantsevov SV, Clarke JO, Magno P, Yong E, Mullin GE. Performance characteristics of the suspected blood indicator feature in capsule endoscopy according to indication for study. *Clin Gastroenterol Hepatol* 2008; **6**: 298-301
- 10 **D'Halluin PN**, Delvaux M, Lapalus MG, Sacher-Huvelin S, Ben Soussan E, Heyries L, Filoche B, Saurin JC, Gay G, Hersbach D. Does the "Suspected Blood Indicator" improve the detection of bleeding lesions by capsule endoscopy? *Gastrointest Endosc* 2005; **61**: 243-249
- 11 **Kim JY**, Chun HJ, Kim CY, Jang JS, Kwon YD, Park S, Keum B, Seo YS, Kim YS, Jeon YT, Lee HS, Um SH, Lee SW, Choi JH, Kim CD, Ryu HS. The Usefulness of a Suspected Blood Identification System (SBIS) in Capsule Endoscopy according to Various Small Bowel Bleeding Lesions. *Korean J Gastrointest Endosc* 2008; **37**: 253-258
- 12 **Signorelli C**, Villa F, Rondonotti E, Abbiati C, Beccari G, de Franchis R. Sensitivity and specificity of the suspected blood identification system in video capsule enteroscopy. *Endoscopy* 2005; **37**: 1170-1173
- 13 **Gerber J**, Bergwerk A, Fleischer D. A capsule endoscopy guide for the practicing clinician: technology and troubleshooting. *Gastrointest Endosc* 2007; **66**: 1188-1195
- 14 **de Franchis R, Lewis BS**. Procedure and Evaluation. In: Keuchel M, Hagenmueller F, Fleischer DE, editors. Atlas of video capsule endoscopy. 1st ed. Hamburg: Springer, 2006: 8-23
- 15 **Buscaglia JM**, Kapoor S, Clarke JO, Bucobo JC, Giday SA, Magno P, Yong E, Mullin GE. Enhanced diagnostic yield with prolonged small bowel transit time during capsule endoscopy. *Int J Med Sci* 2008; **5**: 303-308
- 16 **Kobayashi S**. The aim and method of the color image scale. *Color Res Appl* 1981; **6**: 93-107
- 17 **Bardan E**, Nadler M, Chowers Y, Fidder H, Bar-Meir S. Capsule endoscopy for the evaluation of patients with chronic abdominal pain. *Endoscopy* 2003; **35**: 688-689
- 18 **Gupta R**, Lakhtakia S, Tandan M, Banerjee R, Ramchandani M, Anuradha S, Ramji C, Rao GV, Pradeep R, Reddy DN. Capsule endoscopy in obscure gastrointestinal bleeding--an Indian experience. *Indian J Gastroenterol* 2006; **25**: 188-190
- 19 **Herrerias JM**, Caunedo A, Rodríguez-Télez M, Pellicer F, Herrerias JM. Capsule endoscopy in patients with suspected Crohn's disease and negative endoscopy. *Endoscopy* 2003; **35**: 564-568
- 20 **Adler DG**, Knipschild M, Gostout C. A prospective comparison of capsule endoscopy and push enteroscopy in patients with GI bleeding of obscure origin. *Gastrointest Endosc* 2004; **59**: 492-498
- 21 **Lewis BS**. How to read wireless capsule endoscopic images: tips of the trade. *Gastrointest Endosc Clin N Am* 2004; **14**: 11-16
- 22 **Lim YJ**, Moon JS, Chang DK, Jang BI, Chun HJ, Choi MG. Korean Society of Gastrointestinal Endoscopy (KSGE) Guidelines for Credentialing and Granting Privileges for Capsule Endoscopy. *Korean J Gastrointest Endosc* 2008; **37**: 393-402
- 23 **Fischer D**, Schreiber R, Levi D, Eliakim R. Capsule endoscopy: the localization system. *Gastrointest Endosc Clin N Am* 2004; **14**: 25-31
- 24 **Melmed GY**, Lo SK. Capsule endoscopy: practical applications. *Clin Gastroenterol Hepatol* 2005; **3**: 411-422
- 25 **Apostolopoulos P**, Papanikolaou IS, Kalantzis N. Capsule endoscopy in obscure occult vs. obscure overt GI bleeding. *Gastrointest Endosc* 2005; **61**: 187-188
- 26 **Itten J**. The Art of Color: the subjective experience and objective rationale of color. New York: John Wiley and Sons Inc, 1974

S- Editor Gou SX L- Editor A E- Editor Zhang DN

Impact of surgical volume on nationwide hospital mortality after pancreaticoduodenectomy

Chul-Gyu Kim, Sungho Jo, Jae Sun Kim

Chul-Gyu Kim, Department of Nursing, Cheongju University, Cheongju, Chungbuk 360-764, South Korea

Sungho Jo, Department of Surgery, Dankook University College of Medicine, Cheonan, Chungnam 330-714, South Korea

Jae Sun Kim, Health Insurance Review and Assessment Service, Seoul 137-706, South Korea

Author contributions: Kim CG performed the research, analyzed the data and wrote the manuscript; Jo S designed the research, analyzed the data and wrote the manuscript; Kim JS collected the data and performed the research.

Correspondence to: Dr. Sungho Jo, Department of Surgery, Dankook University College of Medicine, 119 Dandae-ro, Dongnam-gu, Cheonan, Chungnam 330-714,

South Korea. agapejsh@dankook.ac.kr

Telephone: +82-41-5503959 Fax: +82-41-5563878

Received: December 8, 2011 Revised: April 25, 2012

Accepted: May 12, 2012

Published online: August 21, 2012

Abstract

AIM: To evaluate the impact of surgical volume on nationwide hospital mortality after pancreaticoduodenectomy (PD) for periampullary tumors in South Korea.

METHODS: Periampullary cancer patients who underwent PD between 2005 and 2008 were analyzed from the database of the Health Insurance Review and Assessment Service of South Korea. A total of 126 hospitals were divided into 5 categories, each similar in terms of surgical volume for each category. We used hospital mortality as a quality indicator, which was defined as death during the hospital stay for PD, and calculated adjusted mortality through multivariate logistic models using several confounder variables.

RESULTS: A total of eligible 4975 patients were enrolled in this study. Average annual surgical volume of hospitals was markedly varied, ranging from 215 PDs in the very-high-volume hospital to < 10 PDs in the very-low-volume hospitals. Admission route, type of medical

security, and type of operation were significantly different by surgical volume. The overall hospital mortality was 2.1% and the observed hospital mortality by surgical volume showed statistical difference. Surgical volume, age, and type of operation were independent risk factors for hospital death, and adjusted hospital mortality showed a similar difference between hospitals with observed mortality. The result of the Hosmer-Lemeshow test was 5.76 ($P = 0.674$), indicating an acceptable appropriateness of our regression model.

CONCLUSION: The higher-volume hospitals showed lower hospital mortality than the lower-volume hospitals after PD in South Korea, which were clarified through the nationwide database.

© 2012 Baishideng. All rights reserved.

Key words: Hospital mortality; Pancreaticoduodenectomy; South Korea; Databases; Factual; Logistic models; Risk factors

Peer reviewers: Dr. Yasuhiro Fujino, Department of Surgery, Hyogo Cancer Center, 13-70 Kitaaji-cho, Akashi 673-8558, Japan; Dr. Tsutomu Fujii, Department of Surgery II, Nagoya University Graduate School of Medicine, 65 Tsurumai-cho, Showa-ku, Nagoya 4668550, Japan

Kim CG, Jo S, Kim JS. Impact of surgical volume on nationwide hospital mortality after pancreaticoduodenectomy. *World J Gastroenterol* 2012; 18(31): 4175-4181 Available from: URL: <http://www.wjgnet.com/1007-9327/full/v18/i31/4175.htm> DOI: <http://dx.doi.org/10.3748/wjg.v18.i31.4175>

INTRODUCTION

Nowadays pancreaticoduodenectomy (PD) is considered a common and feasibly-performed abdominal surgery for periampullary tumors, but it is still a high-risk surgical procedure with potential morbidity and mortality rates.

Reducing the morbidity and mortality of this formidable operation is therefore imperative. Although several acceptable results after PD in low-volume hospitals have been reported^[1-4], most studies on volume-outcome correlation in performing PD have purported better outcomes in high-volume hospitals, suggesting centralization or regionalization of PD^[5-13].

Centralization of PD can be affected by the national healthcare system, information on hospital quality, or patient hospital preference. The Korean healthcare system is based on compulsory insurance of the whole population and free selection of medical care and hospital under step-wise referral to tertiary hospital without regional restriction. Although we have no governmental guidelines for distribution of cancer treatment service or information on hospital quality officially provided by the government, PD tends to be centralized in the large and well-equipped hospitals in Seoul, the capital city of South Korea.

Analyzing the present state of centralization of PD and providing information on hospital quality can help facilitate the government to develop nationwide guidelines and help patients to select good-quality hospitals for themselves. Hospital quality can be representatively appraised through PD-related morbidity or mortality. However, perioperative morbidity may vary from institution to institution according to the criteria or definitions of particular complications, making it difficult to obtain reliable nationwide morbidity data. Therefore, more definitive and objective data, such as standardized or risk-adjusted mortality rates, are requisite as an indicator for hospital quality.

With the implication toward public reporting, we performed this study to evaluate the impact of surgical volume on nationwide hospital mortality after PD for periampullary tumors and to validate the utility of surgical volume as a quality indicator of hospitals in South Korea. To date, just a few nationwide studies have been carried out to assess the effect of surgical volume on outcomes after PD. We hope the present study can contribute to nationwide evidence for the volume-outcome correlation in performing PD.

MATERIALS AND METHODS

Data sources and subjects

Data were obtained from the Health Insurance Review and Assessment Service (HIRA), whose database was constructed through the process of medical fee claims. After providing medical treatment, the medical institutions submit treatment details and file medical fee claims through an electronic billing system in the form of diskettes, compact discs or electronic data interchange (EDI). The EDI system, which was developed to review medical fees electronically by converting claim information into an EDI file and automatically reviewing items such as medical and drug fees within the software, occupies 99.7% of all medical claims in South Korea. Each claim contains information on demographic data, diagnoses,

procedures, comorbidity, route of admission, length of stay, discharge status, source of payment, hospital charges, *etc.* Diagnostic data were coded using the International Classification of Diseases, 10th Revision (ICD-10), and procedural data were coded using the health insurance claims code developed by the Ministry of Health and Welfare. From the HIRA database, we obtained anonymous data on patients who underwent PD for periampullary cancers during the period from January 2005 to December 2008. Only the primary cancers were included, and cancers originating at the adjacent organs such as the colon, stomach, or gallbladder were excluded. Benign diseases, including trauma, were also excluded. Additionally, patients with other combined operations which could affect the surgical outcomes such as hepatectomy, gastrectomy, or colectomy were not analyzed.

Categorization of hospitals

A total of 126 hospitals performed at least one PD from 2005 to 2008 in South Korea. Four-year surgical volume of each hospital showed a large gap, ranging from 1 to 861. Therefore, we divided the hospitals into quintiles; very-low, low, medium, high, and very-high categories. For this fractionation, the hospitals were sorted in descending order by total surgical volume, and cut-off points were decided to categorize hospitals into five similarly-sized groups.

Assessment of outcome

For clarification of volume-outcome correlation of PD, we adopted hospital mortality as an outcome indicator, which was defined as death during the hospital stay for PD. Hospital mortality had to be calculated in the form of adjusted mortality, because the hospital and patient characteristics of each category were different. For this adjustment of hospital mortality, we selected several risk factors for death from the HIRA database and the literature; age, sex, admission route as a surrogate for patient's general condition [outpatient department *vs* emergency room (ER)], Charlson comorbidity score^[14] as an index for current comorbid status (≥ 3 *vs* < 3), type of medical security as a surrogate for socioeconomic status (medical aid for the destitute *vs* health insurance for the others), and operation type [classical pancreaticoduodenectomy (CPD) *vs* pylorus-preserving pancreaticoduodenectomy (PPPD)]. However, we were unable to obtain more detailed information on preoperative treatment, tumor node metastasis stage, PD-specific complications, or radicality of PD from the HIRA database, which was a major limitation of the nationwide data. Observed mortality was first obtained according to surgical volume and patient characteristics. Risk-adjusted mortality was then calculated through: (observed hospital deaths/predicted hospital deaths) \times overall mortality rate. The predicted mortality of each category could be produced by summing the probability of death of each patient in that category, and the probability of death was determined by adjustment with significant confounder variables validated through

Table 1 Patient and hospital characteristics by surgical volume

Characteristics	Very-low (<i>n</i> = 92)	Low (<i>n</i> = 20)	Medium (<i>n</i> = 10)	High (<i>n</i> = 3)	Very-high (<i>n</i> = 1)	<i>P</i> value
Age (mean ± SD) (yr)	62.2 ± 10.7	62.1 ± 10.2	62.1 ± 10.5	61.2 ± 9.9	59.9 ± 10.3	0.077
Sex ratio (M:F)	1.5	1.3	1.5	1.6	1.6	0.282
Admission route						< 0.001
Outpatient department (%)	803 (78.6)	774 (77.0)	788 (77.3)	901 (84.4)	593 (68.9)	
Emergency room (%)	218 (21.4)	231 (23.0)	232 (22.7)	167 (15.6)	268 (31.1)	
Charlson comorbidity score						0.193
< 3 (%)	683 (66.9)	651 (64.8)	680 (66.7)	667 (62.5)	554 (64.3)	
≥ 3 (%)	338 (33.1)	354 (35.2)	340 (33.3)	401 (37.5)	307 (35.7)	
Type of medical security						< 0.001
Health insurance (%)	919 (90.0)	925 (92.0)	955 (93.6)	1048 (98.1)	841 (97.7)	
Medical aid (%)	102 (10.0)	80 (8.0)	65 (6.4)	20 (1.9)	20 (2.3)	
Type of operation						< 0.001
CPD (%)	604 (59.2)	420 (41.8)	361 (35.4)	325 (30.4)	301 (35.0)	
PPPD (%)	417 (40.8)	585 (58.2)	659 (64.6)	743 (69.6)	560 (65.0)	
Average annual volume	< 10	10-18	19-35	54-111	215	9.9 ¹

¹Denotes average annual surgical volume of all hospitals. SD: Standard deviation; M: Male; F: Female; CPD: Classical pancreaticoduodenectomy; PPPD: Pylorus-preserving pancreaticoduodenectomy.

multivariate logistic regression.

Statistical analysis

Statistical analysis was carried out using the SAS statistical package version 9.1 (SAS System for Windows, SAS Institute, Cary, NC, United States). Descriptive statistics were used to obtain patient characteristics and hospital mortality in each surgical volume category. Continuous variables were compared with Student's *t* test for two groups and with analysis of variance for multiple groups. Categorical variables were assessed with χ^2 tests. Multivariate logistic regression was used to assess the correlation between surgical volume and hospital mortality, with risk-adjusted mortality as the dependent variable and surgical volume and other risk factors for death as covariates. The result of the Hosmer-Lemeshow test was 5.76 ($P = 0.674$), indicating an acceptable appropriateness of our regression model. Statistical significance was set at P values < 0.05.

RESULTS

Hospital and patient characteristics by surgical volume

Of the patients who underwent PD for periampullary cancers during the period from 2005 to 2008 in South Korea, a total of 4975 patients were eligible for the inclusion criteria and enrolled in this study. Pancreatic cancer (1800, 36.2%) occupied the most common indication for PD and was followed by common bile duct cancer (1433, 28.8%), ampulla of Vater cancer (1280, 25.7%), duodenal cancer (238, 4.8%), and other periampullary cancers (227, 4.5%).

PD patients of each category were arranged to be similar in number; 1021 (20.5%) in the very-low-volume hospitals, 1005 (20.2%) in the low-volume hospitals, 1020 (20.5%) in the medium-volume hospitals, 1068 (21.5%) in the high-volume hospitals and 861 (17.3%) in the very-high-volume hospitals. Only one hospital corresponded

to the very-high-volume hospital, whereas as many as 92 (73.0%) hospitals belonged to the very-low-volume hospitals. Average annual surgical volume of the total 126 participating hospitals was markedly varied; 215 PDs in the very-high-volume hospital and fewer than 10 PDs in the very-low-volume hospitals (Table 1). Even worse, 33 of the very-low-volume hospitals performed less than 1 PD per year.

The mean age of the PD patients was 61.5 years and there were 1.5 times more males than females. Admission *via* ER was significantly more frequent and the percentage of payment by medical aid was significantly lower in the higher-volume hospitals (both $P < 0.001$). However, the Charlson comorbidity score didn't show any association with the surgical volume category. PPPD was performed in 59.6% (2964/4975) and this proportion increased with an increase in surgical volume, ranging from 40.8% in the very-low-volume hospitals to 69.6% in the high-volume hospitals ($P < 0.001$, Table 1).

Observed hospital mortality

The overall hospital mortality rate after PD was 2.1% during the study period. The observed hospital mortality rates were higher in lower-volume hospitals, the medical aid group, and CPD patients ($P < 0.001$, $P = 0.015$, $P < 0.001$, respectively). The mean age of both the mortality and survival group was also significantly different (66.0 *vs* 61.4, $P < 0.001$). Other risk factors didn't affect hospital mortality (Table 2).

Adjusted hospital mortality

All the risk factors with $P < 0.25$ in univariate logistic regression were included for multivariate analysis. These were: age, sex, type of medical security and operation type. Table 3 shows the results of multivariate logistic regression. Hospital mortality had a significant correlation with surgical volume ($P < 0.001$). Although there was no statistical difference in hospital mortality between the

Table 2 Observed hospital mortality by patient characteristics

Characteristics	No. of patients	Mortality (%)	P value
Age			< 0.001
Live (%)	4869 (97.9)	61.4 (10.4) ¹	
Dead (%)	106 (2.1%)	66.0 (8.6) ¹	
Sex			0.193
Male (%)	2 989 (60.1)	1.9	
Female (%)	1 986 (39.9)	2.5	
Admission route			0.291
Outpatient department (%)	3 859 (77.6)	2.3	
Emergency room (%)	1 116 (22.4)	1.7	
Charlson comorbidity score			0.291
< 3 (%)	3 235 (65.0)	2.0	
≥ 3 (%)	1 740 (35.0)	2.4	
Type of medical security			0.015
Health insurance (%)	4 688 (94.2)	2.0	
Medical aid (%)	287 (5.8)	4.9	
Operation type			< 0.001
CPD (%)	2 011 (40.4)	3.0	
PPPD (%)	2 964 (59.6)	1.5	

¹Indicates average age (standard deviation) of survival group and mortality group. No: Number; CPD: Classical pancreaticoduodenectomy; PPPD: Pylorus-preserving pancreaticoduodenectomy.

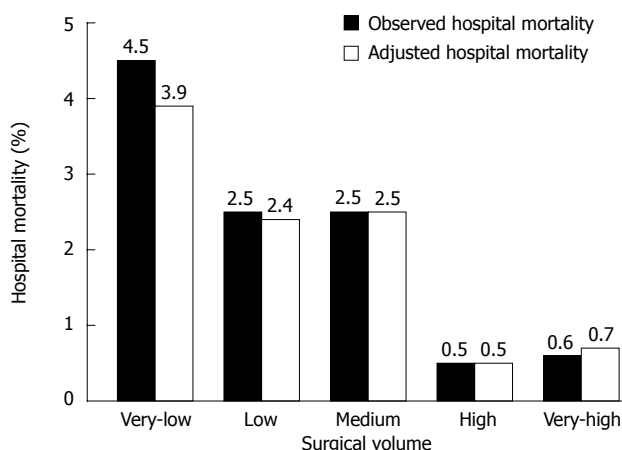


Figure 1 Observed and adjusted hospital mortality according to surgical volume. Observed hospital mortality rates showed a significant decreasing trend as surgical volume increased ($P < 0.001$). Adjusted hospital mortality rates were then calculated through multivariate logistic regression with hospital mortality rates as a dependent variable and age and operation type as significant confounder variables.

very-low-volume and medium-volume hospitals, or just a small statistical difference between the very-low-volume and low-volume hospitals, adjusted odds ratios (ORs) for hospital death of the high-volume and very-high-volume hospitals were significant lower than those of the very-low-volume hospitals (both $P < 0.001$). Age and operation type were the only significant confounder variables ($P < 0.001$ and $P = 0.025$, respectively) and were used for adjustment to produce the predicted mortality. Risk-adjusted hospital mortality rates according to surgical volume are depicted in Figure 1, ranging from 0.5% to 3.9%.

DISCUSSION

We used the nationwide database to validate the associa-

Table 3 Logistic regression for hospital mortality

Characteristics	Odds ratio (95% CI)	P value
Surgical volume		
Very-low	1.00	
Low	0.59 (0.36-0.98)	0.042
Medium	0.61 (0.37-1.01)	0.056
High	0.13 (0.05-0.32)	< 0.001
Very-high	0.16 (0.06-0.41)	< 0.001
Age ¹	1.04 (1.02-1.06)	< 0.001
Sex		0.329
Male	1.00	
Female	1.22 (0.82-1.80)	
Type of medical security		0.120
Health insurance	1.00	
Medical aid	1.60 (0.89-2.88)	
Operation type		0.025
CPD	1.00	
PPPD	0.64 (0.43-0.96)	

¹Per year increase in age. CI: Confidence Interval; CPD: Classical pancreaticoduodenectomy; PPPD: Pylorus-preserving pancreaticoduodenectomy.

tion of surgical volume and hospital mortality. Nationwide data has the power to yield reliable and objective results by itself, mainly due to a large number of subjects and the least influence of selection bias. Of the nationwide reports, however, there have been just a few studies on only PD^[5,8,10,11,13,15,16], whereas the majority included all types of pancreatic resections, including PD^[17-21]. It is known that PD is different from left-sided pancreatectomy, at least in postoperative morbidity and mortality. Nationwide hospital mortality results on PD would be reliable evidence and a base to support governmental or administrative guidelines for the establishment of policy on medical service, to select high-quality hospitals for patients, and to compare quality of care providers within and beyond South Korea.

The inverse relationship between surgical volume and hospital mortality in performing PD has been clarified in South Korea through this study. The risk-adjusted hospital mortality rates of the high-volume and very-high-volume hospitals were very low (0.5% and 0.7%) compared to those of the very-low-volume, low-volume and medium-volume hospitals (3.9%, 2.4% and 2.5%, respectively). This difference in the adjusted hospital mortality rates was found to be similar to that in the observed hospital mortality rates (0.5% and 0.6% *vs* 4.5%, 2.5% and 2.5%). In other words, the ORs for hospital mortality in the low-volume and medium-volume hospitals *vs* the very-low-volume hospitals were around 0.6 (a 40% decrease in the probability of hospital mortality), whereas the ORs in the high-volume and very-high-volume hospitals *vs* the very-low-volume hospitals were as low as 0.13 and 0.16 (a decrease of more than 80%).

The overall hospital mortality rate after PD in South Korea between 2005 and 2008 was 2.1%. This value was much lower than mortality rates from other statewide^[12,22,23] or nationwide^[5,8,10,11,13,15] databases, but a slightly higher than those from high-volume single insti-

tutions^[7,24-27]. Hospital mortality after PD is affected by many independent variables. Significant risk factors for hospital mortality, other than surgical volume as mentioned above, were age and operation type in this study. Type of medical security showed statistical significance in univariate analysis but not in multivariate analysis. Significant confounder variables for hospital mortality in PD were similar within the literature. Age, gender, body mass index, and urgent admission were advocated in other studies^[8,11,28].

Regionalization and centralization in severe medical illnesses and high-risk surgical procedures are worldwide trends which may occur naturally by patients' free selection, or intentionally by governmental policy across the world. About 40% of PDs were undertaken in the high-volume and very-high-volume hospitals, or the big 4 hospitals in South Korea. Again, more than 50% of PDs were performed only in 14 (11.1%) out of 126 hospitals. With these data, South Korea can be said to show a typical example of centralization for PD. Despite trends toward regionalization of care^[5,9,12,13,29], not a few PDs were safely performed in community hospitals by surgeons with varying degrees of experience^[28], as evidenced by a comparably low mortality rate and a high one-year survival rate^[1-4]. About 20% of patients still received PD in as many as 92 very-low-volume hospitals (73.0%) performing fewer than 10 PDs per year in South Korea. There could be several community hospitals with comparably low mortality rates, because the overall mortality rate of the very-low-volume hospitals in South Korea was not so high.

Hospital quality can be assessed with diverse outcome indicators. These are divided into short-term and long-term outcomes, with short-term outcomes including mortality, morbidity, hospital cost, and postoperative hospital stay. Survival outcome represents the long-term outcome. Considering that PD is a very complicated surgical procedure, postoperative morbidity results are very useful in comparing short-term outcomes between hospitals. However, our nationwide study didn't include morbidity results due to difficulty in data collection through the medical fee claims system of the HIRA. Additional drawbacks of this study were as follows; no long-term outcome, total hospital stay not postoperative hospital stay, no pathology-related data, or no surgeon volume. Of these drawbacks, surgeon volume is worthy of note. Surgeon volume^[19,22,28,30-32] or experience^[30], could be a more exact and detailed indicator of hospital outcome after PD than total hospital surgical volume. The HIRA database does not yet have the surgeon identifier which was used in the study by Eppsteiner *et al.*^[33]; therefore we couldn't analyze the correlation of surgeon volume and hospital outcome. In one study^[30], an experienced surgeon was defined as one performing 50 or more PDs, and experienced surgeons had comparable outcomes irrespective of annual volume. Learning curves also projected that less experienced surgeons would achieve morbidity and mortality rates equivalent to those of experienced surgeons when they reached 20 and 60 PDs, respectively. In other studies,

a high-volume surgeon was defined as having an average of 10 or more PDs per year^[28], or 5 or more PDs per year^[33]. Like stratification of hospitals by surgical volume, defining experienced or high-volume surgeons is difficult and varies according to the medical situation or surgeon training system of each country.

Quality indicators other than surgical volume have been introduced. Some researchers focused on the importance of surgery residency training programs, reporting a greater impact on outcomes after PD than hospital volume or surgeon frequency^[34]. Similarly, Joseph *et al.*^[35] put emphasis on hospital clinical resources, such as the Leapfrog Safe Practice Score, HealthGrades 5-star rating, or interventional radiology services, as well as surgical volume for lower operative mortality after PD. A pathologic indicator was also proposed by reporting that patients undergoing PD at low-volume centers were more likely to have margin-positive resections^[36].

Categorization of hospitals was carried out by two methods in the previous reports; by cut-off points of hospital similar in size in each category like our study and by cut-off points of surgical volume that were arbitrarily determined. These cutoff points of surgical volume were varying according to the medical situation and total surgical volume of states or countries. For example, Birkmeyer *et al.*^[10] defined > 5/year for high-volume hospitals in United States between 1992 and 1995, and Topal *et al.*^[5] did > 10/year for high-volume and > 20/year for very-high-volume hospitals in Belgium between 2000 and 2004, while Balzano *et al.*^[11] used a cut-off point of 14-51/year for high-volume hospitals and 89-104/year for very-high-volume hospitals in Italy in 2003. For this stratification of hospitals by surgical volume, the size of each category was uneven according to the cut-off points. In our study, the high-volume hospitals corresponded to 54-111/year and the very-high-volume hospital did 215/year between 2005 and 2008, as a result of dividing hospitals into 5 similar-sized categories. In addition, quintile division^[5,17] was rarely used in the previous studies, with the majority being performed in three or four stratifications. Accordingly it is not easy to reach an international consent on established stratification of hospitals by surgical volume.

In conclusion, the nationwide database clarified the impact of surgical volume on hospital mortality after PD in South Korea. The higher-volume hospitals had a better mortality outcome than the lower-volume hospitals. PD performance showed centralization in South Korea and the overall hospital mortality rate was comparable among countries. Further nationwide studies with surgeon volume, morbidity data, and long-term survival results after PD are warranted for more detailed information, and for a domestic and international comparison.

COMMENTS

Background

Pancreaticoduodenectomy (PD), performed for various diseases around the

duodenal ampulla, is one of the high-risk surgical procedures which tend to be centralized in high-volume hospitals across the world. Previous studies have reported that high-volume hospitals show better surgical outcomes than low-volume hospitals. Up to now, however, there have been no reports on surgical outcomes after PD, or whether surgical volume is a good quality indicator of care providers in South Korea.

Research frontiers

The correlation of surgical volume and hospital outcome after PD is well known between individual institutions or in a limited area. For research into clarifying this relationship, comprehensive results from nationwide databases are important for patients and government, as well as medical personnel.

Innovations and breakthroughs

Although there have been many studies on the relationship between surgical volume and hospital outcome after all types of pancreatic surgery from nationwide databases or after only PD from databases of institutions or states, nationwide results on only PD, which is still an operation with high morbidity and mortality rates, are very rare. Moreover, this is the first study of its type performed in South Korea and having a recent study period of four years.

Applications

With the information on the relationship between surgical volume and nationwide hospital mortality after PD in South Korea, reference guidelines for establishing medical policy and selecting good-quality hospitals could be supported.

Peer review

This is a frontier study on the relationship between surgical volume and hospital outcome after one type of major surgery in South Korea. This is a well-analyzed and clear manuscript that describes the impact of hospital volume on mortality following pancreaticoduodenectomy.

REFERENCES

- Afsari A, Zhandoug Z, Young S, Ferguson L, Silapaswan S, Mittal V. Outcome analysis of pancreaticoduodenectomy at a community hospital. *Am Surg* 2002; **68**: 281-284
- Schwartz GS, Swan RZ, Ruangvoravat L, Attiyeh FF. Morbidity and mortality after hepatic and pancreatic resections: results from one surgeon at a low-volume urban hospital over thirty years. *Am J Surg* 2011; **201**: 438-444
- Chew DK, Attiyeh FF. Experience with the Whipple procedure (pancreaticoduodenectomy) in a university-affiliated community hospital. *Am J Surg* 1997; **174**: 312-315
- Akhtar K, Perricone V, Chang D, Watson RJ. Experience of pancreaticoduodenectomy in a district general hospital *Br J Surg* 2000; **87**: 362-373
- Topal B, Van de Sande S, Fieuws S, Penninckx F. Effect of centralization of pancreaticoduodenectomy on nationwide hospital mortality and length of stay. *Br J Surg* 2007; **94**: 1377-1381
- Birkmeyer JD, Warshaw AL, Finlayson SR, Grove MR, Tosteson AN. Relationship between hospital volume and late survival after pancreaticoduodenectomy. *Surgery* 1999; **126**: 178-183
- Mukherjee S, Kocher HM, Hutchins RR, Bhattacharya S, Abraham AT. Impact of hospital volume on outcomes for pancreaticoduodenectomy: a single UK HPB centre experience. *Eur J Surg Oncol* 2009; **35**: 734-738
- Kotwall CA, Maxwell JG, Brinker CC, Koch GG, Covington DL. National estimates of mortality rates for radical pancreaticoduodenectomy in 25,000 patients. *Ann Surg Oncol* 2002; **9**: 847-854
- Gordon TA, Burleyson GP, Tielsch JM, Cameron JL. The effects of regionalization on cost and outcome for one general high-risk surgical procedure. *Ann Surg* 1995; **221**: 43-49
- Birkmeyer JD, Finlayson SR, Tosteson AN, Sharp SM, Warshaw AL, Fisher ES. Effect of hospital volume on in-hospital mortality with pancreaticoduodenectomy. *Surgery* 1999; **125**: 250-256
- Balzano G, Zerbi A, Capretti G, Rocchetti S, Capitanio V, Di Carlo V. Effect of hospital volume on outcome of pancreaticoduodenectomy in Italy. *Br J Surg* 2008; **95**: 357-362
- Gordon TA, Bowman HM, Tielsch JM, Bass EB, Burleyson GP, Cameron JL. Statewide regionalization of pancreaticoduodenectomy and its effect on in-hospital mortality. *Ann Surg* 1998; **228**: 71-78
- Gouma DJ, van Geenen RC, van Gulik TM, de Haan RJ, de Wit LT, Busch OR, Obertop H. Rates of complications and death after pancreaticoduodenectomy: risk factors and the impact of hospital volume. *Ann Surg* 2000; **232**: 786-795
- Charlson ME, Pompei P, Ales KL, MacKenzie CR. A new method of classifying prognostic comorbidity in longitudinal studies: development and validation. *J Chronic Dis* 1987; **40**: 373-383
- van Heek NT, Kuhlmann KF, Scholten RJ, de Castro SM, Busch OR, van Gulik TM, Obertop H, Gouma DJ. Hospital volume and mortality after pancreatic resection: a systematic review and an evaluation of intervention in the Netherlands. *Ann Surg* 2005; **242**: 781-788
- Nordback L, Parviainen M, Rätty S, Kuivanen H, Sand J. Resection of the head of the pancreas in Finland: effects of hospital and surgeon on short-term and long-term results. *Scand J Gastroenterol* 2002; **37**: 1454-1460
- Birkmeyer JD, Siewers AE, Finlayson EV, Stukel TA, Lucas FL, Batista I, Welch HG, Wennberg DE. Hospital volume and surgical mortality in the United States. *N Engl J Med* 2002; **346**: 1128-1137
- Finlayson EV, Goodney PP, Birkmeyer JD. Hospital volume and operative mortality in cancer surgery: a national study. *Arch Surg* 2003; **138**: 721-725; discussion 726
- Birkmeyer JD, Stukel TA, Siewers AE, Goodney PP, Wennberg DE, Lucas FL. Surgeon volume and operative mortality in the United States. *N Engl J Med* 2003; **349**: 2117-2127
- McPhee JT, Hill JS, Whalen GF, Zayaruzny M, Litwin DE, Sullivan ME, Anderson FA, Tseng JF. Perioperative mortality for pancreatectomy: a national perspective. *Ann Surg* 2007; **246**: 246-253
- Kim CG, Kwak EK, Lee SI. The relationship between hospital volume and outcome of gastrointestinal cancer surgery in Korea. *J Surg Oncol* 2011; **104**: 116-123
- Rosemurgy AS, Bloomston M, Serafini FM, Coon B, Murr MM, Carey LC. Frequency with which surgeons undertake pancreaticoduodenectomy determines length of stay, hospital charges, and in-hospital mortality. *J Gastrointest Surg* 2001; **5**: 21-26
- Ho V, Heslin MJ. Effect of hospital volume and experience on in-hospital mortality for pancreaticoduodenectomy. *Ann Surg* 2003; **237**: 509-514
- Cameron JL, Riall TS, Coleman J, Belcher KA. One thousand consecutive pancreaticoduodenectomies. *Ann Surg* 2006; **244**: 10-15
- Balcom JH, Rattner DW, Warshaw AL, Chang Y, Fernandez-del Castillo C. Ten-year experience with 733 pancreatic resections: changing indications, older patients, and decreasing length of hospitalization. *Arch Surg* 2001; **136**: 391-398
- Büchler MW, Wagner M, Schmied BM, Uhl W, Friess H, Z'graggen K. Changes in morbidity after pancreatic resection: toward the end of completion pancreatectomy. *Arch Surg* 2003; **138**: 1310-1314; discussion 1315
- Yeo CJ. The Johns Hopkins experience with pancreaticoduodenectomy with or without extended retroperitoneal lymphadenectomy for periampullary adenocarcinoma. *J Gastrointest Surg* 2000; **4**: 231-232
- Kennedy TJ, Cassera MA, Wolf R, Swanstrom LL, Hansen PD. Surgeon volume versus morbidity and cost in patients undergoing pancreaticoduodenectomy in an academic community medical center. *J Gastrointest Surg* 2010; **14**: 1990-1996
- Birkmeyer JD, Lucas FL, Wennberg DE. Potential benefits of regionalizing major surgery in Medicare patients. *Eff Clin Pract* 1999; **2**: 277-283

- 30 **Schmidt CM**, Turrini O, Parikh P, House MG, Zyromski NJ, Nakeeb A, Howard TJ, Pitt HA, Lillemoe KD. Effect of hospital volume, surgeon experience, and surgeon volume on patient outcomes after pancreaticoduodenectomy: a single-institution experience. *Arch Surg* 2010; **145**: 634-640
- 31 **Nathan H**, Cameron JL, Choti MA, Schulick RD, Pawlik TM. The volume-outcomes effect in hepato-pancreato-biliary surgery: hospital versus surgeon contributions and specificity of the relationship. *J Am Coll Surg* 2009; **208**: 528-538
- 32 **Rosemurgy A**, Cowgill S, Coe B, Thomas A, Al-Saadi S, Goldin S, Zervos E. Frequency with which surgeons undertake pancreaticoduodenectomy continues to determine length of stay, hospital charges, and in-hospital mortality. *J Gastrointest Surg* 2008; **12**: 442-449
- 33 **Eppsteiner RW**, Csikesz NG, McPhee JT, Tseng JF, Shah SA. Surgeon volume impacts hospital mortality for pancreatic resection. *Ann Surg* 2009; **249**: 635-640
- 34 **Clark W**, Hernandez J, McKeon BA, Kahn A, Morton C, Toomey P, Mullinax J, Ross S, Rosemurgy A. Surgery residency training programmes have greater impact on outcomes after pancreaticoduodenectomy than hospital volume or surgeon frequency. *HPB (Oxford)* 2010; **12**: 68-72
- 35 **Joseph B**, Morton JM, Hernandez-Boussard T, Rubinfeld I, Faraj C, Velanovich V. Relationship between hospital volume, system clinical resources, and mortality in pancreatic resection. *J Am Coll Surg* 2009; **208**: 520-527
- 36 **Bilimoria KY**, Talamonti MS, Sener SF, Bilimoria MM, Stewart AK, Winchester DP, Ko CY, Bentrem DJ. Effect of hospital volume on margin status after pancreaticoduodenectomy for cancer. *J Am Coll Surg* 2008; **207**: 510-519

S- Editor Gou SX L- Editor Rutherford A E- Editor Zhang DN

Diabetes but not insulin is associated with higher colon cancer mortality

Chin-Hsiao Tseng

Chin-Hsiao Tseng, Department of Internal Medicine, National Taiwan University College of Medicine, Taipei 100, Taiwan
Chin-Hsiao Tseng, Division of Endocrinology and Metabolism, Department of Internal Medicine, National Taiwan University Hospital, Taipei 100, Taiwan

Author contributions: Tseng CH contributed to the concept and design, data acquisition and manuscript writing.

Supported by The Department of Health of Taiwan, No. DOH97-TD-D-113-97009

Correspondence to: Chin-Hsiao Tseng, MD, PhD, Division of Endocrinology and Metabolism, Department of Internal Medicine, National Taiwan University Hospital, No. 7 Chung-Shan South Road, Taipei 100, Taiwan. ccktsh@ms6.hinet.net
Telephone: +886-2-23883578 Fax: +886-2-23883578

Received: October 14, 2011 Revised: March 30, 2012

Accepted: April 22, 2012

Published online: August 21, 2012

Abstract

AIM: To evaluate whether diabetic patients had a higher risk of colon cancer mortality and its associated risk factors.

METHODS: The sex-specific crude and age-standardized (to the 2000 World Health Organization population) mortality rates of colon cancer in the Taiwanese general population were first calculated from 1995 to 2006. The trends were evaluated by linear regression. A total of 113 347 diabetic men and 131 573 diabetic women aged ≥ 25 years at recruitment from 1995 to 1998 were followed up until the end of 2006. Age/sex-specific colon cancer mortality rate ratios were calculated comparing the mortality rates of the diabetic patients with the average mortality rates of the general population within 12 years (1995-2006). A sub-cohort of diabetic patients (42 260 men and 49 405 women) was interviewed using a baseline questionnaire and Cox's regression was used to evaluate the risk factors for colon cancer mortality in these diabetic patients.

RESULTS: The crude and age-standardized trends of colon cancer mortality from 1995 to 2006 increased significantly for both sexes in the general population. A total of 641 diabetic men and 573 diabetic women died of colon cancer, with a mortality rate of 74.4 and 54.3 per 100 000 person-years, respectively. Mortality rate ratios [95% confidence intervals (CIs)] showed a significantly higher risk of mortality from colon cancer for the diabetic patients compared to the general population, with the magnitude increasing with decreasing age: 1.65 (1.40-1.95), 2.01 (1.78-2.27), 2.75 (2.36-3.21) and 5.69 (4.65-6.96) for ≥ 75 , 65-74, 55-64 and 25-54 years old, respectively, for men; and 1.46 (1.24-1.72), 2.09 (1.84-2.38), 2.67 (2.27-3.14) and 3.05 (2.29-4.06), respectively, for women. Among the sub-cohort of diabetic patients who had been interviewed with the baseline questionnaire, including information on age, sex, diabetes duration, diabetes type, body mass index, smoking, insulin use and area of residence, age and smoking were significantly predictive for colon cancer mortality, with respective adjusted hazard ratios (HRs) (95% CIs) of 1.077 (1.066-1.088) and 1.384 (1.068-1.792). Diabetes duration became a significant factor when those who died of colon cancer within 5 years of diabetes diagnosis were excluded to minimize the possible contamination of diabetes caused by incipient colon cancer, with an adjusted hazard ratio of 1.021 (1.007-1.034). Sex, diabetes type, insulin use, body mass index and area of residence were not significant predictors for colon cancer mortality in the diabetic patients. Although insulin use was categorized into subgroups of duration of use (non-users and users < 5 years, 5-9 years and ≥ 10 years), none of the HRs for colon cancer mortality was significant with regards to different durations of insulin use.

CONCLUSION: Colon cancer mortality is increasing in Taiwan. A higher risk is observed in diabetic patients. Smoking, but not insulin use, is a modifiable risk factor.

© 2012 Baishideng. All rights reserved.

Key words: Colon cancer; Diabetes mellitus; Mortality; Secular trend

Peer reviewer: Christa Buechler, PhD, Regensburg University Medical Center, Internal Medicine I, Franz Josef Strauss Allee 11, 93042 Regensburg, Germany

Tseng CH. Diabetes but not insulin is associated with higher colon cancer mortality. *World J Gastroenterol* 2012; 18(31): 4182-4190 Available from: URL: <http://www.wjgnet.com/1007-9327/full/v18/i31/4182.htm> DOI: <http://dx.doi.org/10.3748/wjg.v18.i31.4182>

INTRODUCTION

Colorectal cancer is a major cause of death in developed countries^[1]. In Taiwan, it is the third most common cause of cancer-related death^[2], and the trend of its age-adjusted mortality showed an increase from 1971 to 1996^[3]. A meta-analysis concluded there was a 30% higher risk in diabetic patients^[4]. However, most studies were done in western countries, and the only one involving Asians in the meta-analysis was conducted in Korea, which showed a 28% higher risk of mortality in diabetic men, but not women^[5]. On the other hand, some studies showed an association in women^[6,7].

Most previous studies did not distinguish between type 1 and type 2 diabetes. A recent prospective study in the United States identified patients with type 2 diabetes and nondiabetic subjects aged 50-74 years in 1992-1993 and followed biannually by questionnaires from 1997 to 2007^[8]. Diabetes was significantly associated with colorectal cancer in men who were either insulin users or non-users; but diabetes and insulin use were not associated with a higher risk among women^[8].

Whether insulin use is associated with colon cancer mortality has rarely been studied. Furthermore, no previous studies have examined prospectively the confounding effects of diabetes duration and age; both being highly associated with insulin use. Therefore, this study evaluated: (1) the trends of colon cancer mortality in the Taiwanese general population; (2) the age/sex-specific mortality rate ratio between diabetic patients and the general population; and (3) the risk factors for colon cancer mortality in diabetic patients, including age, sex, diabetes duration, diabetes type, body mass index, smoking, insulin use/duration of insulin use and area of residence.

MATERIALS AND METHODS

Colon cancer mortality in the general population

The study was approved and supported by the Department of Health, Executive Yuan, Taiwan. In Taiwan, every resident has a unique identification number and events like birth, death, marriage or migration should be registered. If a person dies, a death certificate should be

reported to the household registration offices within 30 d as required by law. The death certificate database includes the identification number, date of birth, sex, and date and cause of death. The causes of death coded in the ninth revision of the International Classification of Diseases are used. Colon cancer has a code of 153.

The age/sex-specific population numbers are reported annually by the government. The sex-specific trends of crude and age-standardized (to the 2000 World Health Organization population) mortality rates for colon cancer in the general population were first calculated from 1995 to 2006 for all ages. Linear regression was used to evaluate whether the trends changed with regard to calendar years, where the mortality rate was the dependent variable and the calendar year the independent variable.

Colon cancer is rare in young individuals, therefore, we analyzed the data for those aged ≥ 25 years in the following groups: 25-54 years, 55-64 years, 65-74 years and ≥ 75 years old. Age/sex-specific average mortality rates during 1995-2006 were calculated by dividing the average numbers of colon cancer deaths by the average mid-year population of the specific age and sex within the period.

Colon cancer mortality in diabetic patients

Figure 1 shows a flow chart for the follow-up of diabetic patients. In March 1995, a compulsory and universal National Health Insurance (NHI) program was implemented and covered $> 96\%$ of the population. From 1995 to 1998 a cohort of 256 036 diabetic patients ("the original cohort") using the NHI was established (detailed elsewhere)^[9,10].

All patients were followed until 2006. The date and cause of death were obtained from the death certificate database. Mortality rates were computed using a person-years denominator: the duration from enrollment until the end of 2006 for those who were alive or to the date of death. The patients were categorized into age subgroups by their age at enrollment. Age/sex-specific mortality rates and mortality rate ratios were calculated. The mortality rate ratio was calculated using the average mortality rate of that subgroup within the 12 years in the general population as a reference. To reduce the aging effect on age subgroup categorization, analyses for the original cohort were also performed by splitting the follow-up duration into two periods: (1) from enrollment to the end of 2000: age categorized at enrollment and mortality followed from enrollment to 2000; and (2) from 2001 to the end of 2006: those who died before the end of 2000 were excluded, age calculated at 2001 and mortality followed from 2001-2006.

For sub-cohort analyses, we calculated the mortality rates and mortality rate ratios in the patients who had been interviewed with a baseline questionnaire (detailed elsewhere)^[11-13]. The number interviewed was 93 484 and among them 91 665 patients (42 260 men and 49 405 women) were aged ≥ 25 years ("sub-cohort diabetic patients"). To evaluate whether an association was found in

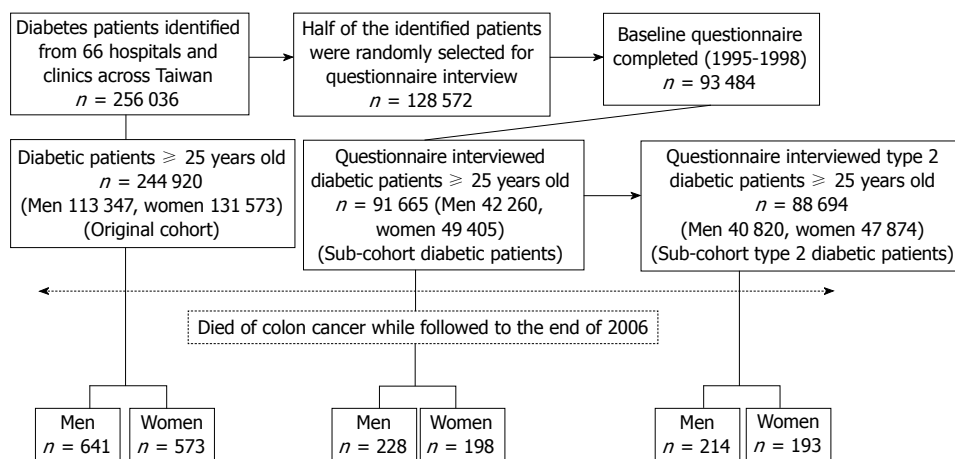


Figure 1 Flow chart showing the procedures in the calculation of colon cancer mortality in the diabetic cohorts.

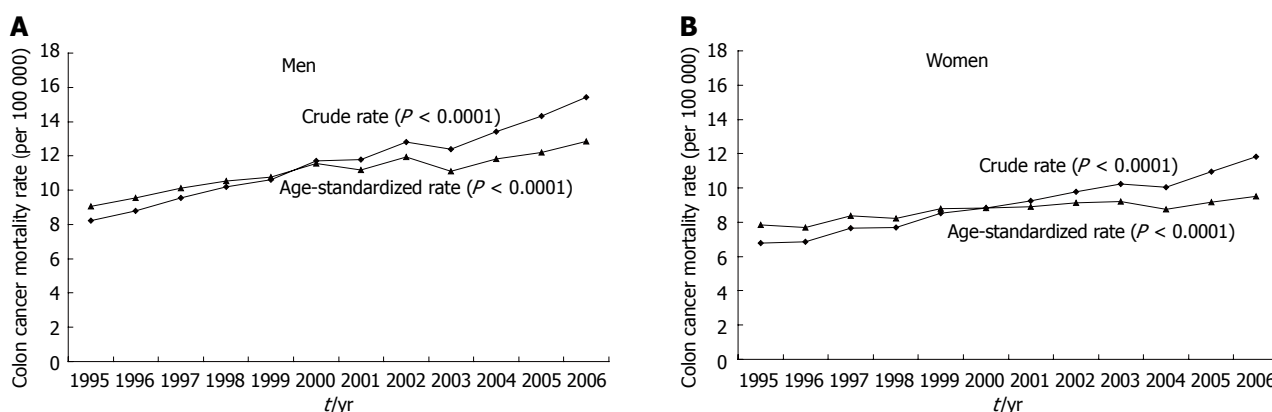


Figure 2 Secular trends of mortality from colon cancer from 1995 to 2006 in the general population of Taiwan in men (A) and women (B), respectively. The 2000 World Health Organization population was used as reference for age standardization.

patients with type 2 diabetes, mortality rates and mortality rate ratios were calculated after excluding patients with type 1 diabetes based on diabetic ketoacidosis at diabetes onset, or the need for insulin injection within 1 year after diabetes diagnosis. There were 40 820 diabetic men and 47 874 diabetic women after this exclusion (“sub-cohort type 2 diabetic patients”). Only 1440 men and 1531 women were excluded for type 1 diabetes, and among them only 14 men and five women died of colon cancer, therefore, we did not analyze the association with type 1 diabetes. To minimize the possibility that diabetes might be caused by incipient colon cancer, analyses were also done by dividing the patients into subgroups with a diabetes duration at enrollment < 10 years and ≥ 10 years.

Risk factors for colon cancer mortality in diabetic patients

The baseline characteristics of the sub-cohort diabetic patients who had been interviewed (Figure 1) were compared between men and women by either the *t* test for continuous variables or the χ^2 test for categorical variables. Cox proportional hazards models were then used to identify the risk factors for colon cancer mortality. Colon cancer mortality was the dependent variable in the models and the independent variables included age,

sex (men *vs* women), diabetes duration, diabetes type (type 2 *vs* type 1), body mass index, smoking (yes *vs* no), insulin use (yes *vs* no) and area of residence (urban *vs* rural). The area of residence was defined as urban for the Metropolitan Taipei area including Taipei City and Taipei County (New Taipei City) and other administratively named cities across Taiwan; and as rural for administratively named counties and offshore islands. To evaluate whether the duration of insulin use could be associated with colon cancer mortality, Cox models were also created by comparing insulin use at < 5 years, 5-9 years and ≥ 10 years to insulin non-users, before adjustment, at adjustment for age, sex, diabetes type, diabetes duration, body mass index, smoking and area of residence one at a time, and at adjustment for all these factors simultaneously (full model). The analyses were done before and after excluding patients who died of colon cancer within 5 years of diabetes onset, to minimize the possibility that diabetes might be caused by incipient colon cancer or might occur after the diagnosis of colon cancer.

RESULTS

The trends of crude and age-standardized colon cancer mortality showed a significant increase in both sexes in

Table 1 Age/sex-specific mortality rates (per 100 000 person-years) for colon cancer in diabetic patients and their mortality rate ratios compared to the average mortality rates in the general population of Taiwan

Age (yr)	Men					Women				
	<i>n</i>	<i>N</i>	PY	MR	MRR (95% CI)	<i>n</i>	<i>N</i>	PY	MR	MRR (95% CI)
Original diabetic cohort										
Followed from enrollment to the end of 2006										
25-54	76	42107	363948.2	20.88	5.69 (4.65, 6.96) ^a	43	43749	399556.9	10.76	3.05 (2.29, 4.06) ^a
55-64	158	28867	225706.1	70.00	2.75 (2.36, 3.21) ^a	146	37317	314033.6	46.49	2.67 (2.27, 3.14) ^a
65-74	265	30704	211811.1	125.11	2.01 (1.78, 2.27) ^a	238	35194	258155.6	92.19	2.09 (1.84, 2.38) ^a
≥ 75	142	11669	59761.6	237.61	1.65 (1.40, 1.95) ^a	146	15313	83905.5	174.01	1.46 (1.24, 1.72) ^a
Followed from enrollment to the end of 2000										
25-54	23	42107	143238.6	16.06	4.38 (3.00, 6.37) ^a	16	43749	153584.7	10.42	2.95 (1.84, 4.71) ^a
55-64	52	28867	96078	54.12	2.12 (1.62, 2.78) ^a	55	37317	129321.2	42.53	2.44 (1.88, 3.17) ^a
65-74	112	30704	94488.8	118.53	1.90 (1.58, 2.29) ^a	91	35194	113687.6	80.04	1.81 (1.48, 2.23) ^a
≥ 75	70	11669	30353.6	230.61	1.60 (1.27, 2.03) ^a	75	15313	42092.9	178.18	1.49 (1.19, 1.87) ^a
Followed from 2001 to the end of 2006										
25-54	30	32626	186021.3	16.13	4.39 (3.16, 6.11) ^a	22	34400	201514.2	10.92	3.09 (2.07, 4.60) ^a
55-64	68	22743	122446.4	55.53	2.18 (1.72, 2.76) ^a	52	29880	167205.9	31.10	1.79 (1.36, 2.34) ^a
65-74	172	26548	133463.8	128.87	2.07 (1.78, 2.40) ^a	131	33591	176023.3	74.42	1.69 (1.42, 2.00) ^a
≥ 75	114	13653	59608.3	191.25	1.33 (1.11, 1.60) ^a	131	17808	79994.6	163.76	1.37 (1.16, 1.63) ^a
Sub-cohort diabetic patients										
Diabetes of any duration at enrollment										
25-54	25	13837	100793.2	24.80	6.76 (4.81, 9.50) ^a	16	12768	95960.8	16.67	4.72 (3.02, 7.37) ^a
55-64	62	12454	84551.8	73.33	2.88 (2.26, 3.66) ^a	53	16717	118278.5	44.81	2.57 (1.98, 3.35) ^a
65-74	99	12395	76349.6	129.67	2.08 (1.71, 2.53) ^a	86	15029	96058.4	89.53	2.03 (1.64, 2.50) ^a
≥ 75	42	3574	17710.4	237.15	1.65 (1.22, 2.23) ^a	43	4891	25384.8	169.39	1.42 (1.05, 1.91) ^a
Diabetes duration < 10 yr at enrollment										
25-54	15	11631	86016.8	17.44	4.75 (3.00, 7.53) ^a	12	10389	78983.7	15.19	4.30 (2.56, 7.23) ^a
55-64	42	8892	61949.1	67.80	2.66 (1.99, 3.57) ^a	37	11636	84435.4	43.82	2.52 (1.84, 3.45) ^a
65-74	62	7887	49825.0	124.44	2.00 (1.56, 2.55) ^a	47	9246	61226.8	76.76	1.74 (1.31, 2.31) ^a
≥ 75	29	2138	10946.7	264.92	1.84 (1.29, 2.64) ^a	23	2814	15302.6	150.30	1.26 (0.84, 1.90)
Diabetes duration ≥ 10 yr at enrollment										
25-54	10	2206	14773	67.69	18.44 (11.81, 28.80) ^a	4	2379	16988.5	23.55	6.66 (2.85, 15.56) ^a
55-64	20	3562	22608.3	88.46	3.47 (2.30, 5.25) ^a	16	5081	33862.5	47.25	2.71 (1.69, 4.35) ^a
65-74	37	4508	26541.7	139.40	2.24 (1.63, 3.07) ^a	39	5783	34845.7	111.92	2.54 (1.87, 3.44) ^a
≥ 75	13	1436	6785.4	191.59	1.33 (0.77, 2.29)	20	2077	10103.5	197.95	1.66 (1.07, 2.56) ^a
Sub-cohort type 2 diabetic patients										
Diabetes of any duration at enrollment										
25-54	23	13239	96635.9	23.80	6.49 (4.54, 9.26) ^a	16	12260	92076.3	17.38	4.92 (3.16, 7.66) ^a
55-64	60	12082	82183.2	73.01	2.87 (2.24, 3.66) ^a	51	16288	115494.5	44.16	2.54 (1.94, 3.32) ^a
65-74	92	12051	74413.3	123.63	1.98 (1.62, 2.43) ^a	83	14570	93223.1	89.03	2.02 (1.63, 2.50) ^a
≥ 75	39	3448	17171.3	227.12	1.58 (1.16, 2.16) ^a	43	4756	24716.7	173.97	1.46 (1.08, 1.97) ^a
Diabetes duration < 10 yr at enrollment										
25-54	14	11248	83333.9	16.80	4.58 (2.84, 7.38) ^a	12	10082	76622.8	15.66	4.43 (2.64, 7.44) ^a
55-64	40	8730	60901.6	65.68	2.58 (1.91, 3.48) ^a	36	11453	83223.4	43.26	2.48 (1.81, 3.42) ^a
65-74	59	7742	48999.2	120.41	1.93 (1.50, 2.49) ^a	46	9068	60169.4	76.45	1.73 (1.30, 2.31) ^a
≥ 75	27	2088	10708.6	252.13	1.75 (1.21, 2.55) ^a	23	2760	15063.9	152.68	1.28 (0.85, 1.93)
Diabetes duration ≥ 10 yr at enrollment										
25-54	9	1991	13298.7	67.68	18.44 (11.53, 29.50) ^a	4	2178	15465.0	25.86	7.32 (3.17, 16.88) ^a
55-64	20	3352	21284.3	93.97	3.69 (2.45, 5.56) ^a	15	4835	32290.5	46.45	2.67 (1.64, 4.35) ^a
65-74	33	4309	25428.1	129.78	2.08 (1.49, 2.91) ^a	37	5502	33067.7	111.89	2.53 (1.85, 3.47) ^a
≥ 75	12	1360	6484.3	185.06	1.29 (0.73, 2.26)	20	1996	9674.1	206.74	1.73 (1.12, 2.67) ^a

^a*P* < 0.05 vs general population. PY: Person-years; MR: Mortality rate; MRR: Mortality rate ratio; CI: Confidence interval; *n*: Case number of colon cancer; *N*: Case number observed.

the general population during the period from 1995 to 2006 in Taiwan (Figure 2). The average mortality rates for colon cancer during the period in the general population aged 25-54 years, 55-64 years, 65-74 years and ≥ 75 years were 5.1, 24.75, 76.6 and 160.92 per 100 000 for men, respectively, and 4.51, 18.01, 46.08 and 130.90 for women.

A total of 113 347 diabetic men and 131 573 diabetic women in the original cohort were followed (Figure 1). Among them, 641 men and 573 women died of colon cancer, with mortality rates of 74.4 and 54.3 per 100 000

person-years, respectively. The age/sex-specific mortality rates in the diabetic patients and their mortality rate ratios compared to the general population are shown in Table 1. Except for those aged ≥ 75 years and with a diabetes duration of ≥ 10 years at enrollment in men, and with a diabetes duration of < 10 years at enrollment in women (Table 1), the mortality rate ratios were all significant, and especially remarkable in those aged 25-54 years. Diabetes was unlikely to be caused by colon cancer, because diabetes diagnosed ≥ 10 years before colon

Table 2 Baseline characteristics of the sub-cohort of diabetic men and women who had been interviewed with a baseline questionnaire

Variable	Men	Women	P value
n	42 260	49 405	
Age, yr	59.8 (11.7)	61.5 (10.8)	< 0.0001
Diabetes duration, yr	7.0 (6.6)	7.5 (6.6)	< 0.0001
Diabetes type, % type 1	1440 (3.4)	1531 (3.1)	0.0085
Body mass index, kg/m ²	24.4 (3.4)	24.7 (3.8)	< 0.0001
Smoking, % yes	26 522 (62.8)	1703 (3.5)	< 0.0001
Use of insulin, % yes	3717 (8.8)	5059 (10.2)	< 0.0001
Area of residence, % urban	20 231 (47.9)	22 264 (45.1)	< 0.0001
Colon cancer mortality	228 (0.5)	198 (0.4)	0.0021

Data are expressed as mean (SD) or n (%).

cancer mortality can hardly be a consequence of the carcinogenic process. The aging effect during follow-up on age subgroup categorization was also minimal because the results were similar when the long duration was split into two shorter periods in the original cohort analyses.

All baseline characteristics of the sub-cohort diabetic patients who had been interviewed with a baseline questionnaire differed significantly between the diabetic men and women (Table 2). The unadjusted and mutually-adjusted HRs for different age groups are shown in Table 3. In the adjusted models, age and smoking (especially in those aged < 65 years) were significant. When diabetic patients who died of colon cancer within 5 years of diabetes diagnosis were excluded, diabetes duration was significant (especially in those aged \geq 65 years). Sex, diabetes type, insulin use, body mass index and area of residence were not significant after adjustment.

Table 4 shows the HRs for different durations of insulin use compared to non-users in unadjusted and adjusted models. Before exclusion of patients with a duration of < 5 years between the onset of diabetes and colon cancer mortality, none of the HRs was significant. In models after exclusion, insulin use \geq 10 years might be associated with a higher risk. However, in the models after respective adjustment for age, diabetes type or diabetes duration, and in the full model, insulin use of any duration was not predictive, suggesting that the association with insulin use might be due to the effects of some confounders.

DISCUSSION

Contrary to the decreasing trend since the mid-1980s in the United States^[14], colon cancer mortality in Taiwan is increasing (Figure 2), and has been since 1971 if the observation of Chen *et al*^[3] is considered simultaneously. Although the etiology of the increasing trend remains to be explored, it may be due to the westernization of the Taiwanese lifestyle in recent decades, with increased fat intake, and the high prevalence of metabolic syndrome and diabetes. The higher risk among diabetic patients of both sexes (Table 1) was also contrary to Korean^[5] and

United States^[8] studies showing an association in men but not in women, and to others showing an association only in women^[7].

It is interesting that the increased mortality rate ratio was more remarkable at the youngest age of 25-54 years (Table 1). This has public health importance because the incidence of diabetes is increasing dramatically in the younger generation^[9]. One explanation is that age *per se* is a strong risk factor, and therefore, the impact of diabetes might not be as obvious in the elderly, resulting in a remarkably higher incidence rate ratio and a higher mortality rate ratio in the younger age group. Other explanations include that diabetes has a different impact on colon cancer mortality in different age groups, and that younger diabetic patients with colon cancer would have a poorer prognosis than non-diabetic patients. Mucin production in colorectal cancer has an inverse effect on survival among Taiwanese patients^[15]. Taiwanese patients with colon cancer and aged < 40 years also have significantly poorer 5-year survival^[16]; age is inversely associated with tumor stage at diagnosis, tumor differentiation and mucin production^[17]. In addition, the healthy survivor effect might also lead to a reduced mortality rate ratio in the elderly.

Metabolic syndrome is associated with a 35% higher risk of colon cancer in Taiwan^[18]. Similarly, a cluster of three components of the metabolic syndrome (hypertension, body mass index \geq 25 kg/m² and high-density lipoprotein cholesterol < 40 mg/dL) was associated with a 58% higher risk in a Finnish study^[19]. In Taiwan, metabolic syndrome is present in 76.2% of diabetic patients^[20], in contrast to 15% in the general population^[21]. Therefore, the higher prevalence rates of hypertension, obesity and dyslipidemia in diabetic patients might explain partly their higher risk of colon cancer.

Contrary to other studies showing an association between body mass index and distal colon adenoma^[22] or colorectal cancer^[19], body mass index was not predictive for colon cancer mortality in the present study (Table 3). One possibility is that the risk factors for incidence and mortality or for different ethnicities might be different. It is also possible that if diabetes *per se* incurred a markedly higher risk, the impact of other risk factors might be overshadowed. Therefore, risk factors in diabetic patients might not be the same as those observed in non-diabetic subjects.

The association between colorectal neoplasm and insulin use in patients with type 2 diabetes has been controversial^[8,23,24]. Although two retrospective studies suggested a positive link, a recent prospective study concluded a lack of association^[8]. A study conducted in Korea suggested a threefold higher risk of colorectal adenoma associated with insulin therapy^[23]. However, this study used a retrospective case-control design and evaluated adenoma rather than cancer. Another retrospective cohort study using the General Practice Research Database from the United Kingdom showed a significantly twofold higher risk of colorectal cancer associated with

Table 3 Cox proportional hazards models showing hazard ratios and 95% confidence intervals for colon cancer mortality in diabetic patients by age before and after exclusion of patients with a duration of < 5 years between onset of diabetes and colon cancer mortality

Variables	Interpretation	Hazard ratio (95% CI)							
		Age \geq 25 yr				Age 25-64 yr		Age \geq 65 yr	
		Unadjusted	P value	Mutually adjusted	P value	Mutually adjusted	P value	Mutually-adjusted	P value
Before exclusion									
Age	Every 1-yr increment	1.077 (1.066-1.088)	< 0.0001	1.077 (1.066-1.088)	< 0.0001	1.090 (1.062-1.119)	< 0.0001	1.072 (1.049-1.096)	< 0.0001
Sex	Men vs women	1.395 (1.150-1.691)	0.0007	1.256 (0.976-1.618)	0.0769	1.181 (0.758-1.841)	0.4622	1.288 (0.946-1.753)	0.1081
Diabetes duration	Every 1-yr increment	1.032 (1.019-1.045)	< 0.0001	1.006 (0.992-1.020)	0.3845	0.993 (0.964-1.023)	0.6652	1.009 (0.994-1.025)	0.2329
Diabetes type	Type 2 vs type 1	0.682 (0.430-1.081)	0.1036	0.750 (0.432-1.301)	0.3057	0.914 (0.345-2.425)	0.8574	0.680 (0.348-1.328)	0.2588
Body mass index	Every 1-kg/m ² increment	0.956 (0.929-0.984)	0.0021	0.976 (0.948-1.005)	0.1062	0.966 (0.920-1.014)	0.1616	0.981 (0.946-1.018)	0.3080
Smoking	Yes vs no	1.484 (1.219-1.808)	< 0.0001	1.384 (1.068-1.792)	0.0140	1.746 (1.121-2.720)	0.0136	1.215 (0.881-1.676)	0.2351
Insulin use	Yes vs no	1.344 (0.992-1.821)	0.0564	1.235 (0.843-1.809)	0.2782	1.318 (0.686-2.532)	0.4076	1.215 (0.759-1.946)	0.4168
Area of residence	Urban vs rural	0.901 (0.743-1.094)	0.2928	0.852 (0.702-1.034)	0.1046	0.734 (0.530-1.016)	0.0621	0.931 (0.731-1.187)	0.5660
After exclusion									
Age	Every 1-yr increment	1.082 (1.070-1.094)	< 0.0001	1.080 (1.068-1.092)	< 0.0001	1.096 (1.064-1.128)	< 0.0001	1.070 (1.046-1.095)	< 0.0001
Sex	Men vs women	1.454 (1.186-1.784)	0.0003	1.281 (0.980-1.676)	0.0704	1.355 (0.836-2.195)	0.2172	1.249 (0.903-1.728)	0.1787
Diabetes duration	Every 1-yr increment	1.046 (1.034-1.059)	< 0.0001	1.021 (1.007-1.034)	0.0022	1.025 (0.996-1.054)	0.0883	1.020 (1.004-1.035)	0.0120
Diabetes type	Type 2 vs type 1	0.640 (0.398-1.028)	0.0647	0.710 (0.402-1.254)	0.2386	0.637 (0.229-1.771)	0.3878	0.737 (0.371-1.465)	0.3837
Body mass index	Every 1-kg/m ² increment	0.960 (0.932-0.989)	0.0078	0.984 (0.955-1.015)	0.3034	0.983 (0.933-1.035)	0.5160	0.984 (0.948-1.022)	0.4153
Smoking	Yes vs no	1.555 (1.263-1.914)	< 0.0001	1.445 (1.099-1.899)	0.0083	1.814 (1.130-2.913)	0.0137	1.268 (0.905-1.778)	0.1672
Insulin use	Yes vs no	1.431 (1.044-1.961)	0.0258	1.159 (0.781-1.722)	0.4639	0.927 (0.440-1.954)	0.8419	1.274 (0.798-2.035)	0.3106
Area of residence	Urban vs rural	0.909 (0.741-1.116)	0.3639	0.848 (0.691-1.041)	0.1158	0.815 (0.573-1.158)	0.2536	0.876 (0.680-1.128)	0.3040

CI: Confidence interval.

insulin use^[24]. On the other hand, a prospective cohort study conducted in the United States did not suggest an association between colorectal cancer and insulin use in either men or women^[8]. The finding of the present study was in line with the United States study, suggesting a lack of association between insulin use and colon cancer mortality (Tables 3 and 4). Insulin use is essential in patients with type 1 diabetes and is always seen in older patients with type 2 diabetes who might have prolonged duration of diabetes. Therefore, it is worth mentioning that adjustments should be made simultaneously for age, diabetes duration and diabetes type in the analyses evaluating the risk of cancer associated with insulin use. The present study is probably the longest follow-up study showing that insulin use was not predictive for colon cancer mortality after adjustment for confounders, including all of these factors (Tables 3 and 4).

Consistent with some prior studies^[25,26], smoking was significantly predictive, especially in those aged < 65 years (Table 3). A recent Swedish retrospective cohort study evaluating the use of snuff and colorectal and anal cancer found no significant association^[27]. We were not able to evaluate the effect of snuff use because of a lack

of information. Although we could not evaluate the impact of socioeconomic status, this study did not show an association with area of residence (Table 3).

Incidence and mortality are two different entities, and probably linked to different factors. If diabetic patients with colon cancer had a poorer prognosis, the mortality rate ratio would not properly reflect the incidence rate ratio. A recently published prospective study (Cancer Prevention Study-II Nutrition Cohort) conducted among 2278 patients with colorectal cancer suggested that patients with type 2 diabetes had a higher risk of mortality than those without diabetes; especially a higher risk of death from cardiovascular disease^[28]. A study from Taiwan also showed that diabetic patients with colon cancer had an overall 21% higher mortality than nondiabetic patients^[29]. However, this was only observed in stage II cancer. It was believed that the 21% higher case-fatality rate could not explain the several-fold higher mortality rate ratios in the diabetic patients (Table 1).

The strengths of this study included a prospective follow-up of a large cohort of diabetic patients over a long duration; the completeness of the ascertainment of vital status by matching with the death certificate

Table 4 Cox proportional hazards models for mortality from colon cancer by duration of insulin use (reference group: diabetic patients not using insulin) before and after exclusion of patients with a duration of < 5 years between onset of diabetes and colon cancer mortality

Variables adjusted	Duration of insulin use								
	< 5 yr			5-9 yr			≥ 10 yr		
	HR	95% CI	P value	HR	95% CI	P value	HR	95% CI	P value
Before exclusion									
Unadjusted	1.128	0.734-1.735	0.5824	1.245	0.664-2.333	0.4947	1.539	0.918-2.579	0.1018
Age	1.388	0.902-2.136	0.1355	1.487	0.793-2.787	0.2163	1.441	0.860-2.416	0.1654
Sex	1.146	0.745-1.763	0.5339	1.267	0.676-2.375	0.4605	1.562	0.932-2.618	0.0907
Diabetes type	1.101	0.682-1.777	0.6931	0.817	0.362-1.843	0.6259	1.321	0.589-2.964	0.4991
Diabetes duration	1.009	0.655-1.556	0.9663	1.028	0.546-1.935	0.9330	1.018	0.590-1.756	0.9491
Body mass index	1.089	0.707-1.675	0.6995	1.210	0.645-2.268	0.5530	1.505	0.898-2.523	0.1208
Smoking	1.143	0.743-1.759	0.5416	1.263	0.674-2.367	0.4666	1.549	0.924-2.596	0.0966
Area of residence	1.122	0.729-1.726	0.6005	1.237	0.660-2.318	0.5074	1.538	0.918-2.578	0.1023
Full model ¹	1.217	0.764-1.937	0.4082	0.943	0.442-2.010	0.8788	1.003	0.454-2.212	0.9948
After exclusion									
Unadjusted	1.108	0.698-1.761	0.6630	1.416	0.755-2.656	0.2782	1.746	1.041-2.931	0.0348
Age	1.384	0.871-2.199	0.1696	1.704	0.908-3.197	0.0971	1.633	0.973-2.740	0.0635
Sex	1.129	0.710-1.793	0.6085	1.445	0.771-2.711	0.2510	1.776	1.058-2.981	0.0297
Diabetes type	1.089	0.651-1.821	0.7447	1.010	0.446-2.287	0.9807	1.700	0.770-3.757	0.1893
Diabetes duration	0.943	0.592-1.501	0.8045	1.079	0.573-2.034	0.8133	0.968	0.561-1.669	0.9057
Body mass index	1.072	0.674-1.703	0.7702	1.375	0.733-2.581	0.3215	1.710	1.019-2.870	0.0424
Smoking	1.126	0.708-1.788	0.6164	1.440	0.768-2.701	0.2557	1.760	1.049-2.954	0.0323
Area of residence	1.103	0.694-1.752	0.6786	1.409	0.751-2.643	0.2855	1.746	1.040-2.929	0.0349
Full model ¹	1.133	0.691-1.857	0.6214	1.038	0.491-2.195	0.9221	1.003	0.462-2.178	0.9949

¹Adjusted for age, sex, diabetes type, diabetes duration, body mass index, smoking and area of residence. HR: Hazard ratio; CI: Confidence interval.

database; and the consistency observed in both sexes, and in different age groups, enrollment periods and sub-cohorts of diabetic patients.

There were limitations to the study. First, diabetic patients might have visited their physicians more frequently, resulting in a higher probability of detecting cancer. However, this might only suggest a higher rate of detection of early colon cancer with a better prognosis, which might have attenuated the magnitude of the mortality rate ratios. Second, the use of cause of death on the death certificate as the only source of colon cancer diagnosis might have underestimated the mortality related to colon cancer, because some patients with colon cancer might have died without having colon cancer listed as the cause of death. Therefore the impact of this possible effect awaits further investigation. Third, multiple drug therapy in diabetic patients might have complicated the situation. For example, statin, aspirin and nonsteroidal anti-inflammatory drugs are possibly preventive for colorectal cancer^[30,31]. A higher proportion of diabetic patients might have been using these medications for the prevention of cardiovascular diseases. Different oral antidiabetic agents may have different effects on cancer development. For example, metformin has been shown to be preventive for cancer^[32], but the use of sulfonylureas may be associated with a higher risk of cancer^[33]. We could not evaluate the effects of these medications because such information was not collected. Fourth, this study did not consider confounders identified in Taiwan, including less exercise, less vegetable and fruit consumption, increased meat intake, and alcohol intake^[25]. Furthermore, we were not able to adjust for some other

confounders, as discussed below. For example, hyperhomocysteinemia has been shown to be a risk factor for type 2 diabetes and is also associated with abnormal DNA methylation, which has the potential to inactivate tumor suppressor genes leading to colorectal cancer^[31]. Family history and inflammatory bowel disease are also significant risk factors for colorectal cancer^[34-36]. None of these potential confounders were measured and could not be considered for adjustment.

In summary, we have demonstrated an increasing trend in colon cancer mortality in the Taiwanese general population from 1995 to 2006. The risk is increased in diabetic patients, with the magnitude of the mortality rate ratio becoming larger with decreasing age. Smoking is a risk factor, but insulin use is not. Given that the population is aging and the incidence of type 2 diabetes is increasing, the impact of the link between diabetes and colon cancer on the mortality of the population warrants public health attention.

COMMENTS

Background

Diabetic patients may have a higher risk of colon cancer, but whether insulin use in the diabetic patients can be a risk factor is controversial. Studies related to these issues are rarely conducted in Asian populations.

Research frontiers

A meta-analysis suggested a 30% higher risk of colorectal cancer in diabetic patients. However, most studies were done in western countries. In Korea, a 28% higher risk of mortality was observed in diabetic men, but not women. Whether insulin use is associated with colorectal cancer has rarely been studied. A recent prospective United States study showed that diabetes was significantly associated with colorectal cancer in men who were either insulin users or

non-users, but diabetes and insulin use were not associated with a higher risk among women.

Innovations and breakthroughs

The author demonstrated an increasing trend in colon cancer mortality in the Taiwanese general population from 1995 to 2006. The risk is increased in diabetic patients, with the magnitude of the mortality rate ratio becoming larger with decreasing age. In patients with diabetes, smoking is a risk factor for colon cancer mortality, but insulin use is not. The strengths of this study included a prospective follow-up of a large cohort of diabetic patients over a long duration of 12 years; the completeness of the ascertainment of vital status by matching with the national death certificate database; the consistency observed in both sexes, and in different age groups, enrollment periods and sub-cohorts of diabetic patients; and consideration of the confounding effects of diabetes duration and age - both being highly associated with insulin use.

Applications

Given that the population is aging and the incidence of diabetes is increasing, the impact of the link between diabetes and colon cancer on the mortality of the population warrants public health attention. Insulin is commonly used in diabetic patients, therefore, clarification of a lack of insulin effect on colon cancer development relieves concern about the use of insulin.

Terminology

Secular trend of mortality: a systematic change in mortality rates over a period of (calendar) time; Mortality rate ratio: ratio of two mortality rates.

Peer review

This was a well-performed study that may be published when some corrections have been done.

REFERENCES

- 1 Edwards BK, Howe HL, Ries LA, Thun MJ, Rosenberg HM, Yancik R, Wingo PA, Jemal A, Feigal EG. Annual report to the nation on the status of cancer, 1973-1999, featuring implications of age and aging on U.S. cancer burden. *Cancer* 2002; **94**: 2766-2792
- 2 Ju JH, Chang SC, Wang HS, Yang SH, Jiang JK, Chen WC, Lin TC, Hung Hsu FM, Lin JK. Changes in disease pattern and treatment outcome of colorectal cancer: a review of 5,474 cases in 20 years. *Int J Colorectal Dis* 2007; **22**: 855-862
- 3 Chen CJ, You SL, Lin LH, Hsu WL, Yang YW. Cancer epidemiology and control in Taiwan: a brief review. *Jpn J Clin Oncol* 2002; **32** Suppl: S66-S81
- 4 Larsson SC, Orsini N, Wolk A. Diabetes mellitus and risk of colorectal cancer: a meta-analysis. *J Natl Cancer Inst* 2005; **97**: 1679-1687
- 5 Jee SH, Ohrr H, Sull JW, Yun JE, Ji M, Samet JM. Fasting serum glucose level and cancer risk in Korean men and women. *JAMA* 2005; **293**: 194-202
- 6 Limburg PJ, Anderson KE, Johnson TW, Jacobs DR, Lazovich D, Hong CP, Nicodemus KK, Folsom AR. Diabetes mellitus and subsite-specific colorectal cancer risks in the Iowa Women's Health Study. *Cancer Epidemiol Biomarkers Prev* 2005; **14**: 133-137
- 7 Nilsen TI, Vatten LJ. Prospective study of colorectal cancer risk and physical activity, diabetes, blood glucose and BMI: exploring the hyperinsulinaemia hypothesis. *Br J Cancer* 2001; **84**: 417-422
- 8 Campbell PT, Deka A, Jacobs EJ, Newton CC, Hildebrand JS, McCullough ML, Limburg PJ, Gapstur SM. Prospective study reveals associations between colorectal cancer and type 2 diabetes mellitus or insulin use in men. *Gastroenterology* 2010; **139**: 1138-1146
- 9 Tseng CH, Tseng CP, Chong CK, Huang TP, Song YM, Chou CW, Lai SM, Tai TY, Cheng JC. Increasing incidence of diagnosed type 2 diabetes in Taiwan: analysis of data from a national cohort. *Diabetologia* 2006; **49**: 1755-1760
- 10 Tseng CH. Mortality and causes of death in a national sample of diabetic patients in Taiwan. *Diabetes Care* 2004; **27**: 1605-1609
- 11 Tseng CH. Diabetes conveys a higher risk of gastric cancer mortality despite an age-standardised decreasing trend in the general population in Taiwan. *Gut* 2011; **60**: 774-779
- 12 Tseng CH, Chong CK, Tai TY. Secular trend for mortality from breast cancer and the association between diabetes and breast cancer in Taiwan between 1995 and 2006. *Diabetologia* 2009; **52**: 240-246
- 13 Tseng CH. Prostate cancer mortality in Taiwanese men: increasing age-standardized trend in general population and increased risk in diabetic men. *Ann Med* 2011; **43**: 142-150
- 14 Jemal A, Siegel R, Xu J, Ward E. Cancer statistics, 2010. *CA Cancer J Clin* 2010; **60**: 277-300
- 15 You JF, Hsieh LL, Changchien CR, Chen JS, Chen JR, Chiang JM, Yeh CY, Hsieh PS, Fan CW, Liu CT, Tang R. Inverse effects of mucin on survival of matched hereditary nonpolyposis colorectal cancer and sporadic colorectal cancer patients. *Clin Cancer Res* 2006; **12**: 4244-4250
- 16 Juang YF, Huang TJ, Huang YS, Huang CJ, Hsieh JS, Chien CH, Lin HJ. Clinicopathologic characteristics in colorectal adenocarcinoma and their relationship to survival. *Gaoxiong Yixue Kexue Zazhi* 1990; **6**: 45-57
- 17 Chiang JM, Chen MC, Changchien CR, Chen JS, Tang R, Wang JY, Yeh CY, Fan CW, Tsai WS. Favorable influence of age on tumor characteristics of sporadic colorectal adenocarcinoma: patients 30 years of age or younger may be a distinct patient group. *Dis Colon Rectum* 2003; **46**: 904-910
- 18 Chiu HM, Lin JT, Shun CT, Liang JT, Lee YC, Huang SP, Wu MS. Association of metabolic syndrome with proximal and synchronous colorectal neoplasm. *Clin Gastroenterol Hepatol* 2007; **5**: 221-229; quiz 141
- 19 Bowers K, Albanes D, Limburg P, Pietinen P, Taylor PR, Virtamo J, Stolzenberg-Solomon R. A prospective study of anthropometric and clinical measurements associated with insulin resistance syndrome and colorectal cancer in male smokers. *Am J Epidemiol* 2006; **164**: 652-664
- 20 Tseng CH, Chong CK, Tseng CP, Shau WY, Tai TY. Hypertension is the most important component of metabolic syndrome in the association with ischemic heart disease in Taiwanese type 2 diabetic patients. *Circ J* 2008; **72**: 1419-1424
- 21 Hwang LC, Bai CH, Chen CJ. Prevalence of obesity and metabolic syndrome in Taiwan. *J Formos Med Assoc* 2006; **105**: 626-635
- 22 Kim MC, Kim CS, Chung TH, Park HO, Yoo CI. Metabolic syndrome, lifestyle risk factors, and distal colon adenoma: a retrospective cohort study. *World J Gastroenterol* 2011; **17**: 4031-4037
- 23 Chung YW, Han DS, Park KH, Eun CS, Yoo KS, Park CK. Insulin therapy and colorectal adenoma risk among patients with Type 2 diabetes mellitus: a case-control study in Korea. *Dis Colon Rectum* 2008; **51**: 593-597
- 24 Yang YX, Hennessy S, Lewis JD. Insulin therapy and colorectal cancer risk among type 2 diabetes mellitus patients. *Gastroenterology* 2004; **127**: 1044-1050
- 25 Yeh CC, Hsieh LL, Tang R, Chang-Chieh CR, Sung FC. Risk factors for colorectal cancer in Taiwan: a hospital-based case-control study. *J Formos Med Assoc* 2003; **102**: 305-312
- 26 Phipps AI, Baron J, Newcomb PA. Prediagnostic smoking history, alcohol consumption, and colorectal cancer survival: the Seattle Colon Cancer Family Registry. *Cancer* 2011; **117**: 4948-4957
- 27 Nordenvall C, Nilsson PJ, Ye W, Nyrén O. Smoking, snus use and risk of right- and left-sided colon, rectal and anal cancer: a 37-year follow-up study. *Int J Cancer* 2011; **128**: 157-165
- 28 Dehal AN, Newton CC, Jacobs EJ, Patel AV, Gapstur SM, Campbell PT. Impact of diabetes mellitus and insulin use on survival after colorectal cancer diagnosis: the Cancer Prevention Study-II Nutrition Cohort. *J Clin Oncol* 2012; **30**: 53-59
- 29 Huang YC, Lin JK, Chen WS, Lin TC, Yang SH, Jiang JK, Chang SC, Lan YT, Wang HS, Liu CY, Yang YW, Teng HW. Diabetes mellitus negatively impacts survival of patients

- with colon cancer, particularly in stage II disease. *J Cancer Res Clin Oncol* 2011; **137**: 211-220
- 30 **García-Rodríguez LA**, Huerta-Alvarez C. Reduced risk of colorectal cancer among long-term users of aspirin and non-aspirin nonsteroidal antiinflammatory drugs. *Epidemiology* 2001; **12**: 88-93
- 31 **Giouleme O**, Diamantidis MD, Katsaros MG. Is diabetes a causal agent for colorectal cancer? Pathophysiological and molecular mechanisms. *World J Gastroenterol* 2011; **17**: 444-448
- 32 **Aljada A**, Mousa SA. Metformin and neoplasia: implications and indications. *Pharmacol Ther* 2012; **133**: 108-115
- 33 **Bowker SL**, Majumdar SR, Veugelers P, Johnson JA. Increased cancer-related mortality for patients with type 2 diabetes who use sulfonylureas or insulin. *Diabetes Care* 2006; **29**: 254-258
- 34 **Wei YS**, Lu JC, Wang L, Lan P, Zhao HJ, Pan ZZ, Huang J, Wang JP. Risk factors for sporadic colorectal cancer in southern Chinese. *World J Gastroenterol* 2009; **15**: 2526-2530
- 35 **Ahmadi A**, Polyak S, Draganov PV. Colorectal cancer surveillance in inflammatory bowel disease: the search continues. *World J Gastroenterol* 2009; **15**: 61-66
- 36 **Xie J**, Itzkowitz SH. Cancer in inflammatory bowel disease. *World J Gastroenterol* 2008; **14**: 378-389

S-Editor Cheng JX L-Editor Kerr C E-Editor Zhang DN

Role of body mass index in colon cancer patients in Taiwan

Chih-Chien Chin, Yi-Hung Kuo, Chien-Yuh Yeh, Jinn-Shiun Chen, Reiping Tang, Chung-Rong Changchien, Jeng-Yi Wang, Wen-Shih Huang

Chih-Chien Chin, Yi-Hung Kuo, Wen-Shih Huang, Division of Colon and Rectal Surgery, Department of Surgery, Chang Gung Memorial Hospital, Chiayi 613, Taiwan

Chien-Yuh Yeh, Jinn-Shiun Chen, Reiping Tang, Chung-Rong Changchien, Jeng-Yi Wang, Division of Colon and Rectal Surgery, Department of Surgery, Chang Gung Memorial Hospital, Linko 333, Taiwan

Chih-Chien Chin, Wen-Shih Huang, Graduate Institute of Clinical Medical Science, College of Medicine, Chang Gung University, Taoyuan 333, Taiwan

Author contributions: Chin CC designed and performed most of the study and wrote the manuscript; Kuo YH helped to collect the patients' data; Yeh CY, Chen JS, Tang R, Changchien CR, Wang JY, and Huang WS provided the patients' data.

Correspondence to: Dr. Wen-Shih Huang, Division of Colon and Rectal Surgery, Department of Surgery, Chang Gung Memorial Hospital, 6 Sec. West, Chia-Pu Rd., Putz City, Chiayi 613, Taiwan. wshuang77@hotmail.com

Telephone: +886-5-3621000 Fax: +886-5-3623001

Received: May 20, 2011 Revised: April 16, 2012

Accepted: April 22, 2012

Published online: August 21, 2012

Abstract

AIM: To determine the effect of body mass index (BMI) on the characteristics and overall outcome of colon cancer in Taiwan.

METHODS: From January 1995 to July 2003, 2138 patients with colon cancer were enrolled in this study. BMI categories (in kg/m²) were established according to the classification of the Department of Health of Taiwan. Postoperative morbidities and mortality, and survival analysis including overall survival (OS), disease-free survival (DFS), and cancer-specific survival (CSS) were compared across the BMI categories.

RESULTS: There were 164 (7.7%) underweight (BMI < 18.5 kg/m²), 1109 (51.9%) normal-weight (BMI = 18.5-23.9 kg/m²), 550 (25.7%) overweight (BMI = 24.0-26.9 kg/m²), and 315 (14.7%) obese (BMI ≥

27 kg/m²) patients. Being female, apparently anemic, hypoalbuminemic, and having body weight loss was more likely among underweight patients than among the other patients ($P < 0.001$). Underweight patients had higher mortality rate ($P = 0.007$) and lower OS ($P < 0.001$) and DFS ($P = 0.002$) than the other patients. OS and DFS did not differ significantly between normal-weight, overweight, and obese patients, while CSS did not differ significantly with the BMI category.

CONCLUSION: In Taiwan, BMI does not significantly affect colon-CSS. Underweight patients had a higher rate of surgical mortality and a worse OS and DFS than the other patients. Obesity does not predict a worse survival.

© 2012 Baishideng. All rights reserved.

Key words: Body mass index; Colon cancer; Survival; Morbidity; Outcome

Peer reviewer: Fausto Catena, MD, PhD, Department of General, Emergency and Transplant Surgery, St Orsola- Malpighi University Hospital, Via Massarenti 9, 40139 Bologna, Italy

Chin CC, Kuo YH, Yeh CY, Chen JS, Tang R, Changchien CR, Wang JY, Huang WS. Role of body mass index in colon cancer patients in Taiwan. *World J Gastroenterol* 2012; 18(31): 4191-4198 Available from: URL: <http://www.wjgnet.com/1007-9327/full/v18/i31/4191.htm> DOI: <http://dx.doi.org/10.3748/wjg.v18.i31.4191>

INTRODUCTION

The prevalence of obesity and the incidence of colon cancer continue to increase in Taiwan as in other developed countries. The findings of many studies support the idea that obesity is a risk factor for the development of colon cancer^[1-3]. However, the few studies that have investigated the influence of body mass index (BMI) on the outcomes of colon cancer patients have produced

inconsistent findings^[4-7]. These previous reports were mostly from Western countries and based on clinical trial data. We investigated herein the role of BMI in general colon cancer patients in Taiwan; the population of this study may represent both Chinese people and Asians in general, in terms of the clinical characteristics, postoperative morbidities and mortalities, and long-term outcome defined by overall survival (OS), disease-free survival (DFS), and cancer-specific survival (CSS).

MATERIALS AND METHODS

Study population

From January 1995 to July 2003, 2138 patients from a total population of 2765 patients with histologically confirmed adenocarcinoma of the colon were enrolled in this study; 14 nonmetastatic patients without available BMI data and 613 patients with metastatic disease were excluded. The included patients had regular follow-up visits with a healthcare professional until December 2008 (i.e., a postoperative follow-up period of at least 5 years) or until death.

The demographic and clinicopathologic data evaluated for each patient included age, gender, body height and weight, tumor stage (as defined according to the American Joint Committee on Cancer TNM staging system, sixth edition, New York: Springer-Verlag, 2002), tumor location, degree of tumor differentiation, timing of surgery (i.e., elective or emergent), medical illness, and preoperative laboratory data.

BMI was calculated as the weight in kilograms divided by the height in meters squared. The following BMI categories were established according to the classification of the Department of Health (DOH) of Taiwan:^[8] underweight (BMI < 18.5 kg/m²), normal weight (BMI = 18.5-23.9 kg/m²), overweight (BMI = 24.0-26.9 kg/m²), and obese (BMI ≥ 27 kg/m²). For long-term outcome, BMI was also categorized according to the World Health Organization (WHO) classification^[9] as follows: underweight (BMI < 18.5 kg/m²), normal weight (BMI = 18.5-24.9 kg/m²), overweight (BMI = 25-29.9 kg/m²), and obese (BMI ≥ 30 kg/m²) to enable comparison with the Taiwanese classification, since The Expert Consultation on BMI in Asian populations recommended that the current WHO BMI cut-off points be retained as the international classification^[10].

Local recurrence or distant metastasis was confirmed histologically or radiographically, while postoperative mortality was defined as death within 30 d of the primary surgery. The patients were divided into three age groups: younger than 40 years (younger group), 40-75 years (middle age group), and older than 75 years (elderly group). The carcinoembryonic antigen (CEA) level was considered to be abnormal at > 5 ng/mL. Tumor location was categorized as right (from the cecum to the transverse colon) or left (from the splenic flexure to the sigmoid colon). Hypoalbuminemia was defined as a serum albumin level of < 35 g/L and apparent anemia was defined as a hemoglobin level of < 10 g/dL.

Table 1 Patient and tumor characteristics stratified according to body mass index category

	Percentage of patients within each BMI category				P value
	Under-weight (n = 164)	Normal weight (n = 1109)	Over-weight (n = 550)	Obese (n = 315)	
Age at diagnosis (yr)					< 0.001
≤ 40	12.8	8.7	5.8	4.8	
41-75	57.3	75.5	81.6	83.2	
> 75	29.9	15.9	12.5	12.1	
Gender (%)					
Female	65.9	47.2	44.7	48.3	< 0.001
Tumor location					
Right	47.0	41.6	35.5	29.5	< 0.001
Tumor grade					
High-to-moderate differentiation	82.9	83.7	85.6	87.9	0.239
Tumor stage					< 0.001
I	9.1	9.2	15.3	19.4	
II	48.2	50.9	44.7	45.1	
III	42.7	39.9	40.0	35.6	
Emergent operation	3.7	3.4	2.5	2.2	0.584
Body weight loss					< 0.001
CEA > 5 ng/mL	44.2	34.6	36.3	36.0	0.150
Albumin < 35 g/L	42.3	21.0	13.5	11.6	< 0.001
Hemoglobin < 10 g/dL	40.9	32.9	23.2	21.3	< 0.001
Comorbidities					
None	57.3	51.7	50.1	41.6	< 0.001
Hypertension	11.0	19.7	26.2	34.9	< 0.001
Heart disease	8.5	6.8	7.6	12.7	0.008
Previous stroke	3.0	3.4	4.5	4.8	0.527
Asthma	3.7	3.3	3.6	2.9	0.936
Diabetes mellitus	4.9	10.6	12.4	20.6	< 0.001
Peptic ulcer disease	14.0	10.8	9.1	8.9	0.229
Chronic hepatitis	1.2	4.3	3.3	4.1	0.225
Liver cirrhosis	1.8	1.4	1.1	0.6	0.650
Renal insufficiency	5.2	8.9	6.8	9.4	0.202
Others	16.6	13.8	12.0	15.1	0.555

Except where stated otherwise, data are the percentage of the particular body mass index (BMI) category population. CEA: Carcinoembryonic antigen.

Statistical analysis

Survival curves were constructed using the Kaplan-Meier method and then compared using the log-rank test. OS was calculated as the number of years from primary surgery to the date of death. DFS was calculated as the number of years from primary surgery to either the first disease recurrence or death. CSS was calculated as the number of years from primary surgery to the first of disease recurrence. The two arms were compared by Pearson χ^2 test and independent-samples *t* tests to

Table 2 Univariate analysis of survival of colon cancer patients stratified according to body mass index category (Taiwan *vs* World Health Organization)

	Underweight (<i>n</i> = 164)	Normal weight (<i>n</i> = 1109)	Overweight (<i>n</i> = 550)	Obese (<i>n</i> = 315)
BMI category in Taiwan				
Overall survival				
5-yr survival rate	60.0	73.6	78.2	75.4
HR (95% CI)	1.67 (1.31-2.13)	Reference	0.83 (0.69-0.99)	0.93 (0.74-1.16)
<i>P</i> value	< 0.001		0.046	0.500
Disease-free survival				
5-yr survival rate	57.4	70.8	73.4	71.0
HR (95% CI)	1.60 (1.26-2.04)	Reference	0.86 (0.72-1.04)	0.97 (0.79-1.20)
<i>P</i> value	< 0.001		0.103	0.807
Cancer-specific survival				
5-yr survival rate	71.6	78.5	78.9	77.3
HR (95% CI)	1.31 (0.94-1.82)	Reference	0.95 (0.77-1.19)	1.01 (0.78-1.32)
<i>P</i> value	0.107		0.657	0.932
BMI categories of WHO				
	Underweight (<i>n</i> = 164)	Normal-weight (<i>n</i> = 1331)	Overweight (<i>n</i> = 553)	Obese (<i>n</i> = 90)
Overall survival				
5-yr survival rate	60.0	74.0	78.2	75.0
HR (95% CI)	1.70 (1.34-2.15)	Reference	0.85 (0.71-1.02)	0.99 (0.66-1.39)
<i>P</i> value	< 0.001		0.072	0.833
Disease-free survival				
5-yr survival rate	57.4	71.0	73.2	70.4
HR (95% CI)	1.62 (1.28-2.06)	Reference	0.89 (0.74-1.05)	1.05 (0.73-1.49)
<i>P</i> value	< 0.001		0.169	0.808
Cancer-specific survival				
5-yr survival rate	71.6	78.2	79.5	75.0
HR (95% CI)	1.30 (0.94-1.80)	Reference	0.92 (0.74-1.13)	1.10 (0.72-1.70)
<i>P</i> value	0.113		0.418	0.661

Except where stated otherwise, data are the percentage of the particular body mass index (BMI) category population. WHO: World Health Organization; HR: Hazard ratio; CI: Confidence interval.

detect any differences in proportions and means. A Cox regression model was used for multivariate analysis. All *P* values were two-tailed, and they were considered to be statistically significant at < 0.05 .

RESULTS

Disease and patient characteristics

The study population comprised 2138 patients with colon cancer, of whom 1109 were males and 1029 were females. BMI in this study ranged from 12.2 kg/m² to 49.0 kg/m², with a mean of 23.4 kg/m². Of the 2138 patients, 164 (7.7%) were underweight, 1109 (51.9%) were normal weight, 550 (25.7%) were overweight, and 315 (14.7%) were obese.

The characteristics of the patients and tumors are presented stratified according to BMI category in Table 1. The age of the entire study population was 61.4 ± 13.9 years (mean ± SD); those of the underweight, normal-weight, overweight, and obese patients were 63.5 ± 17.3 years, 61.8 ± 14.0 years, 61.9 ± 12.4 years, and 61.7 ± 12.3 years, respectively. The mean age did not differ significantly with the BMI category (*P* = 0.828). However, the distribution of age groups differed significantly with the BMI category, with the proportions of younger and elderly patients being higher in underweight-patients group than in the other groups (*P* < 0.001). The gender distribution also differed significantly between the underweight patients and the other groups, with underweight

patients being more likely to be female. The tumor location also differed significantly, with the proportion of right colon cancer decreasing as the BMI category increased (*P* < 0.001).

With respect to the distribution of tumor stage among the BMI categories, the number of stage I tumors was lower in the underweight and normal-weight patients than in the overweight and obese patients. The obese patients had the lowest number of stage III tumors.

The proportion of emergent operations did not differ significantly with the BMI category: 3.7% of underweight, 3.4% of normal-weight, 2.5% of overweight, and 2.2% of obese patients (*P* = 0.584).

Underweight patients were the most likely to exhibit apparent anemia (hemoglobin < 10 g/dL) and have hypoalbuminemia and body weight loss (*P* < 0.001). The proportion of patients with body weight loss, hypoalbuminemia, and apparent anemia decreased as the BMI category increased. The percentage of patients with an abnormal preoperative CEA level did not differ significantly with the BMI category.

Finally, with regard to associated medical illnesses, the percentage of patients with hypertension or diabetes mellitus increased with the BMI category. Obese patients were the most likely to have heart disease. The other associated comorbidities including previous stroke, asthma, peptic ulcer disease, chronic hepatitis, renal insufficiency, and others (e.g., gall stones and thyroid disease) did not differ significantly with the BMI category.

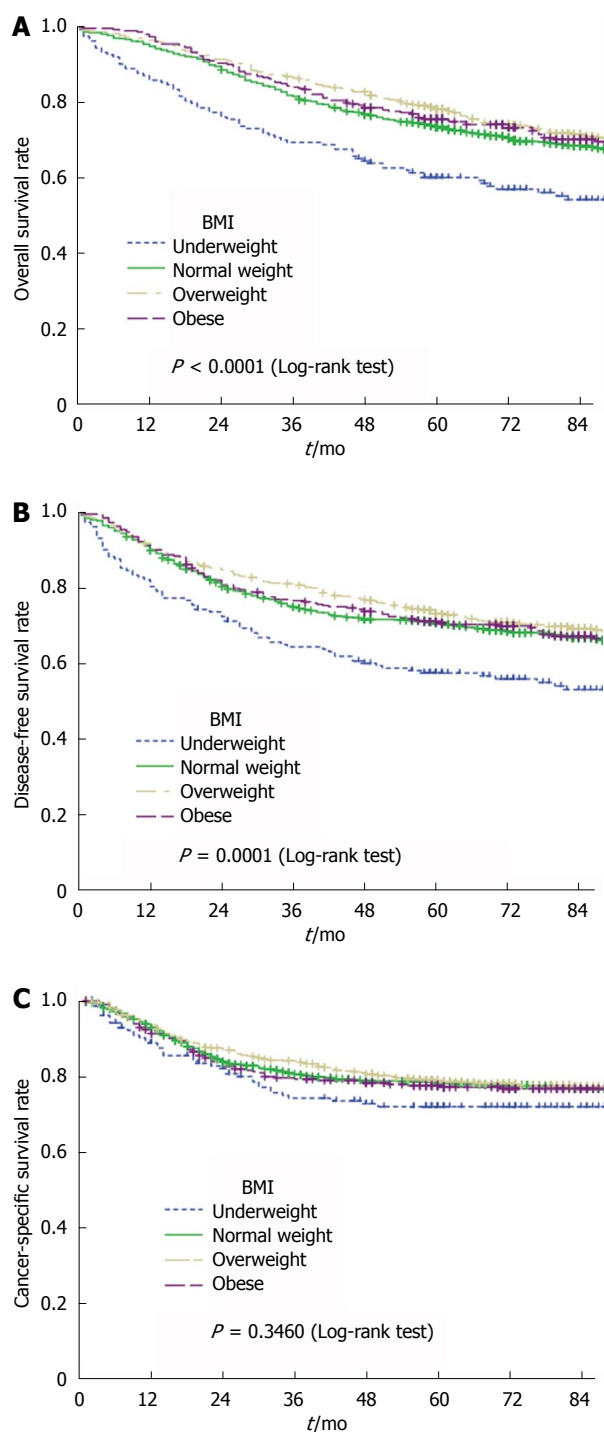


Figure 1 Overall survival curves (A), disease-free survival curves (B) and cancer-specific survival curves (C) relative to body mass index category using the Kaplan-Meier method, and comparison using the log-rank test. BMI: Body mass index.

Short-term outcome

The postoperative morbidity, anastomotic leakage, and mortality rates did not differ significantly between the underweight, normal-weight, overweight, and obese patients: 12.8%, 12.9%, 13.3% and 15.6%, respectively ($P = 0.667$); 1.2%, 1.4%, 1.6%, and 1.9%, respectively ($P = 0.880$); and 3.7%, 1.3%, 1.1%, and 0%, respectively ($P = 0.007$).

Long-term outcome

Data from all patients who received surgery were used to analyze the long-term outcome. Univariate analysis was performed using the Kaplan-Meier method, along with the log-rank test and Cox proportional-hazards model. The results of our statistical analysis are presented in Table 2, and the survival curves are shown in Figure 1A (OS), Figure 1B (DFS), and Figure 1C (CCS).

Univariate analysis revealed that OS ($P < 0.001$) and DFS ($P = 0.001$) were lowest in the underweight patients. The OS was marginally higher ($P = 0.046$) in overweight patients than in normal-weight patients, but the DFS ($P = 0.103$) did not differ significantly between the two groups. No significant difference in OS ($P = 0.500$) or DFS ($P = 0.807$) was observed between normal-weight and obese patients.

CSS did not differ significantly with the BMI category ($P = 0.346$). The results were similar when these patients were categorized according to the WHO BMI classifications.

Adjuvant chemotherapy was offered to 58.0%, 70.1%, 73.9%, and 70.8% of underweight, normal-weight, overweight, and obese patients with stage III tumors, respectively ($P = 0.096$). In total, 70.2% of patients with stage III tumors received adjuvant chemotherapy.

Since the compositions of patients and tumors differed with the BMI category, multivariate analysis was used to determine the effect of BMI along with other confounding factors on the long-term outcome. The variables of the Cox regression model included BMI, TNM stage, age group, gender, comorbidities (patients were divided into three groups: without, with one or two kinds, and with more than two kinds of comorbidity), CEA (normal *vs* abnormal), hemoglobin (< 10 g/L *vs* ≥ 10 g/L), albumin (normal *vs* hypoalbuminemia), timing of surgery (elective *vs* emergent), postoperative morbidity (with *vs* without), tumor location (right *vs* left), histologic type (adenocarcinoma *vs* mucinous *vs* signet-ring type), and histologic grade (high *vs* moderate *vs* low differentiation). The hazard ratio (HR) of each BMI category was compared with that of the normal-weight patients. The results of multivariate analysis for OS, DFS, and CSS are listed in Table 3.

As documented in Table 4, underweight patients had a significantly worse OS [HR, 1.58; 95% confidence interval (CI), 1.23-2.05; $P < 0.001$] and DFS (HR, 1.49; 95% CI, 1.16-1.93; $P = 0.002$), but their CSS did not differ significantly (HR, 1.33; 95% CI, 0.94-1.87; $P = 0.107$) when compared with the normal-weight patients. OS, DFS, or CSS did not differ significantly between the normal-weight, overweight, and obese patients.

To determine whether the prognostic effect of BMI was related to patient gender, a multivariate analysis was applied to separated data from male and female patients. The results of this statistical analysis yielded the same findings between the genders: CSS did not differ significantly with the BMI category for all patients or for male

Table 3 Multivariate analysis of colon cancer survival (overall, disease-free, and cancer-specific) by Cox regression model

Variable	Overall survival		Disease-free survival		Cancer-specific survival	
	P value	HR (95% CI)	P value	HR (95% CI)	P value	HR (95% CI)
BMI group	0.000		0.002		0.369	
Underweight <i>vs</i> normal	0.000	1.58 (1.23-2.05)	0.002	1.49 (1.16-1.93)	0.107	1.33 (0.94-1.87)
Overweight <i>vs</i> normal	0.060	0.83 (0.68-1.01)	0.123	0.86 (0.71-1.04)	0.751	0.96 (0.76-1.22)
Obese <i>vs</i> normal	0.578	0.94 (0.74-1.18)	0.972	1.00 (0.79-1.25)	0.677	1.06 (0.80-1.41)
TNM stage	0.000		0.000		0.000	
II <i>vs</i> I	0.721	1.06 (0.77-1.45)	0.981	1.00 (0.74-1.35)	0.025	1.78 (1.07-2.95)
III <i>vs</i> I	0.000	1.90 (1.39-2.60)	0.000	1.80 (1.34-2.42)	0.000	3.94 (2.39-6.48)
Age group (yr)	0.000		0.000		0.876	
41-75 <i>vs</i> ≤ 40	0.054	1.45 (0.99-2.11)	0.052	1.44 (0.99-2.09)	0.672	1.09 (0.74-1.58)
> 75 <i>vs</i> ≤ 40	0.000	3.14 (2.11-4.67)	0.000	2.88 (1.94-4.25)	0.607	1.12 (0.72-1.74)
Gender (male <i>vs</i> female)	0.329	1.08 (0.92-1.27)	0.220	1.10 (0.94-1.29)	0.734	1.03 (0.85-1.26)
Medical illness (comorbidity)	0.003		0.003		0.769	
One or two kinds <i>vs</i> none	0.358	1.09 (0.91-1.32)	0.442	1.08 (0.89-1.29)	0.927	0.99 (0.79-1.24)
> two kinds <i>vs</i> none	0.001	1.40 (1.16-1.71)	0.001	1.39 (1.15-1.68)	0.478	0.91 (0.70-1.18)
CEA (> 5 <i>vs</i> ≤ 5 ng/mL)	0.000	1.86 (1.58-2.18)	0.000	1.93 (1.65-2.25)	0.000	2.15 (1.77-2.61)
Hemoglobin (< 10 <i>vs</i> ≥ 10 g/dL)	0.913	1.01 (0.84-1.22)	0.760	1.03 (0.86-1.23)	0.835	1.03 (0.81-1.29)
Albumin (normal <i>vs</i> hypoalbuminemia)	0.000	0.65 (0.54-0.79)	0.000	0.68 (0.57-0.83)	0.297	0.87 (0.67-1.13)
Operation timing (emergent <i>vs</i> elective)	0.562	1.21 (0.64-2.26)	0.416	1.28 (0.70-2.34)	0.687	1.18 (0.53-2.66)
Morbidity (yes <i>vs</i> no)	0.000	1.55 (1.26-1.91)	0.000	1.50 (1.23-1.84)	0.279	1.17 (0.88-1.56)
Tumor location (left <i>vs</i> right)	0.785	1.03 (0.86-1.22)	0.666	1.04 (0.88-1.23)	0.583	1.06 (0.86-1.32)
Histologic type	0.079		0.144		0.055	
Signet ring cell <i>vs</i> adenocarcinoma	0.039	2.19 (1.04-4.63)	0.065	2.03 (0.96-4.30)	0.017	2.68 (1.19-6.01)
Mucinous <i>vs</i> adenocarcinoma	0.323	1.14 (0.88-1.49)	0.465	1.10 (0.85-1.43)	0.690	1.07 (0.77-1.48)
Histologic grade (differentiation)	0.282		0.213		0.173	
Moderate <i>vs</i> high	0.363	1.11 (0.89-1.37)	0.143	1.17 (0.95-1.45)	0.061	1.32 (0.99-1.76)
Low <i>vs</i> high	0.114	1.34 (0.93-1.94)	0.121	1.33 (0.93-1.92)	0.403	1.24 (0.75-2.04)

HR: Hazard ratio; CI: Confidence interval; BMI: Body mass index; TNM: Tumor, nodes, metastasis; CEA: Carcinoembryonic antigen.

or female patients.

DISCUSSION

BMI is a simple and easy-to-determine index used to classify individuals as being underweight, overweight, or obese. The classification of BMI was established to evaluate health risks such as type 2 diabetes and cardiovascular disease^[9,10]. The associations between BMI, percentage of body fat, and distribution of body fat differ across populations, which has resulted in different cut-off points for classifications being used in different countries. Furthermore, the cut-off points for certain risks vary between different Asian populations^[10]. The Expert Consultation on BMI in Asian populations recommended that the current WHO BMI cut-off points be retained as the international classification^[10]. In the present study, BMI classifications were based on the definition of the DOH, Taiwan. In addition, the WHO BMI classifications were used to evaluate the long-term outcome of colon cancer survivors and to compare with the Taiwan BMI classification system. In the present study, the prevalence rates of diabetes and hypertension increased significantly with the BMI category; this finding is highly consistent with the intended meaning of the BMI classification system. However, the risks of other comorbidities such as asthma, hepatitis, peptic ulcer disease, and renal insufficiency were not correlated with the BMI category.

Obesity is a growing problem in Taiwan and is known to increase the risk of developing colon cancer^[1-3]. It has also been reported that obese patients have a higher risk of surgical complications^[11-13]. Previous studies have produced controversial results regarding the relationship between obesity and anastomotic leakage^[14,15]. Sorensen *et al*^[14] reported that obesity is not a risk factor for anastomotic leakage in colonic resection, while Biondo *et al*^[15] reported that obesity is an independent risk factor, but is only associated with emergent procedures of the left colon. Miransky *et al*^[16] reported that obesity and a contaminated surgical procedure independently predicted surgical-site infection in colorectal procedures. Riou *et al*^[17] reported that obesity was a significant independent risk factor for wound dehiscence. Obesity has also been reported to be a risk factor for the postoperative occurrence of pulmonary complications^[18,19]. The postoperative morbidity rate and anastomotic leakage rate did not differ significantly with the BMI category in our study. However, one of the limitations of this study is that we did not examine whether the occurrence rate of the other type of complications differed with the BMI category.

In the present study, the risk of postoperative mortality was highest in underweight patients. This finding is similar to that of Hickman *et al*^[20]. Although obese patients have higher rates of comorbidities with cardiovascular disease and diabetes, the postoperative morbidity and mortality rates were comparable with the normal-weight patients. Conversely, the underweight patients had

Table 4 Results of multivariate analysis of colon cancer survival stratified according to body mass index category

	Underweight	Normal weight	Overweight	Obese
All patients (<i>n</i> = 2138)				
Overall survival				
HR (95% CI) ¹	1.58 (1.23-2.05)	Reference	0.83 (0.68-1.01)	0.94 (0.74-1.18)
<i>P</i> value ²	< 0.001		0.060	0.578
Disease-free survival				
HR (95% CI) ¹	1.49 (1.16-1.93)	Reference	0.86 (0.71-1.04)	1.00 (0.79-1.25)
<i>P</i> value ²	0.002		0.123	0.972
Cancer-specific survival				
HR (95% CI) ¹	1.33 (0.94-1.87)	Reference	0.96 (0.76-1.22)	1.06 (0.80-1.41)
<i>P</i> value ²	0.107		0.751	0.677
Males (<i>n</i> = 1109)				
Overall survival				
HR (95% CI) ¹	1.55 (1.03-2.35)	Reference	0.77 (0.58-1.01)	0.91 (0.66-1.25)
<i>P</i> value ²	0.036		0.056	0.565
Disease-free survival				
HR (95% CI) ¹	1.60 (1.04-2.44)	Reference	0.84 (0.65-1.09)	1.01 (0.75-1.37)
<i>P</i> value ²	0.031		0.192	0.937
Cancer-specific survival				
HR (95% CI) ¹	1.46 (0.84-2.52)	Reference	0.96 (0.69-1.32)	1.21 (0.83-1.77)
<i>P</i> value ²	0.179		0.789	0.328
Females (<i>n</i> = 1029)				
Overall survival				
HR (95% CI) ¹	1.55 (1.11-2.16)	Reference	0.95 (0.71-1.27)	0.99 (0.69-1.41)
<i>P</i> value ²	0.011		0.724	0.945
Disease-free survival				
HR (95% CI) ¹	1.41 (1.01-1.97)	Reference	0.91 (0.68-1.22)	1.01 (0.71-1.43)
<i>P</i> value ²	0.042		0.544	0.957
Cancer-specific survival				
HR (95% CI) ¹	1.16 (0.75-1.82)	Reference	0.96 (0.69-1.36)	0.93 (0.60-1.43)
<i>P</i> value ²	0.508		0.839	0.727

¹HR was calculated using the Cox regression model; the variables in the multivariate analysis included TNM stage, age, gender (when analyzing all patients), comorbidities, CEA, hemoglobin, albumin, operative timing, postoperative morbidity, tumor location, histologic type, and histologic grade; ²Each category compared to normal-weight patients. HR: Hazard ratio; CI: Confidence interval; BMI: Body mass index; TNM: Tumor, nodes, metastasis; CEA: Carcinoembryonic antigen.

a lower rate of comorbidities but a higher rate of postoperative mortality than did the other patients. However, a higher proportion of underweight patients in this study were hypoalbuminemic and anemic. The observed higher postoperative mortality rate may be at least partially attributed to the associated disease conditions.

Whether obese colon cancer patients have a worse long-term outcome than other patients remains a matter of controversy. Sinicrope *et al*⁷¹ reported that underweight patients had a significantly worse OS ($P = 0.0258$), and that BMI ≥ 35 kg/m² patients exhibited a trend toward a worse DFS ($P = 0.0725$) and OS ($P = 0.0805$) compared with normal-weight patients, but there was no significant difference. When they analyzed the data according to patient gender, males with BMI ≥ 35 kg/m² exhibited a reduced OS, and females with obesity (BMI = 30-34 kg/m²) had a reduced OS when compared with their normal-weight counterparts. BMI category was significantly associated with both DFS and OS in multivariate analysis in their study. Meyerhardt *et al*⁶¹ reported that neither BMI nor weight change was significantly associated with colon cancer patient survival indicators,

including the OS, DFS, and recurrence-free survival, even for underweight patients. Dignam *et al*⁵¹ reported that OS and DFS were significantly worse for underweight patients (BMI < 18.5 kg/m²) and very obese patients (BMI ≥ 35 kg/m²) than for normal-weight patients. Very obese patients had a greater risk of cancer recurrence or secondary primary tumors. In the present study, we found that BMI by itself was not a significant factor of CSS in colon cancer, but OS and DFS did tend to be worse for underweight patients than for the other patients. We found no differential effect of gender on either BMI or obesity. Compared with other patients, underweight patients had a worse OS but a similar CSS. This implies that many underweight patients died from noncancer events. It would have been reasonable to conclude that underlying comorbidities caused the higher mortality risk among the underweight patients, but in the present study this group actually had the smallest number of comorbidities. Further research should be conducted to establish the mechanisms responsible for the observed higher mortality risk in underweight patients. Furthermore, previous studies have shown that highly

obese patients (BMI ≥ 35 kg/m²) or males may have a worse long-term outcome than normal-weight patients, but the obese cohort of the present study was not large enough to allow analysis of the difference.

In this study, tumor location was found to be correlated with BMI, such that the proportion of patients with right colon cancer increased as the BMI category decreased. Whether patients with a lower BMI tend to have right-side colon cancer is not well known or studied. However, since the lumen is larger for the right than the left colon, symptoms related to the tumor such as small-caliber or bloody stool need more time to be sensed by patients with right colon cancer, resulting in a longer period of nutrition depletion and body weight loss. Minoo *et al.*^[21] reported that proximally located tumors are significantly larger than those found in the distal colon. We have shown previously that the prevalence of malnutrition (hypoalbuminemia) is higher for right colon tumors than for left colon tumors^[22]. Moreover, body weight loss is more common in right colon cancer than in left colon cancer (48.8% and 33.5%, respectively; $P < 0.001$). BMI is reduced in patients with body weight loss, and more patients with right colon tumors have body weight loss resulting in a lower BMI, which may partly explain the greater number of left-side tumors in the groups with a higher BMI.

The findings of this study suggest that a low BMI is a marker of weight loss, blood loss, nutrition depletion, and more-advanced disease, all of which are associated with a worse DFS and OS^[22-24]. This could be the reason why the low-BMI group had a lower DFS and OS.

This study was subject to some limitations. It lacked data regarding changes in body weight before and after surgery, measurement of central obesity, physical activity, and diet changes after surgery, and involved a smaller sample than did previous studies. However, the study's cohort came from a single medical institution with a standard collection of patients' data, and so there was no selection bias as might be expected in a clinical trial. The results of this study pertain to patients from Taiwan and hence may not be generalizable to other populations.

For the population of Taiwan, which represents both Chinese people and Asians in general, BMI does not appear to be a significant factor of colon-CSS, but underweight patients appear to have a higher postoperative mortality and worse OS, and are less likely to experience DFS than those in the other BMI categories. The obese patients had a higher wound complication rate, but exhibited a similar survival rate when compared to the normal-weight patients.

COMMENTS

Background

The prevalence of obesity and the incidence of colon cancer continue to increase in Taiwan as in other developed countries. Studies that have investigated the influence of body mass index (BMI) on the outcomes of colon cancer patients have produced inconsistent findings. These previous reports were mostly from Western countries, and lacked data regarding Asian people. The authors

therefore investigated the role of BMI in general colon cancer patients of Taiwan, in terms of the clinical characteristics and short- and long-term outcomes.

Research frontiers

BMI is a simple index that is used to classify individuals as being underweight, overweight, or obese. The cut-off points of BMI for classifications vary in different countries. The World Health Organization BMI classifications were used to evaluate the long-term outcome of colon cancer survivors and were compared with those determined using the Taiwan BMI classification system.

Innovations and breakthroughs

The findings of the present study demonstrate that a low BMI could be a marker of weight loss, blood loss, nutrition depletion, and more-advanced disease. For the population of Taiwan, which represents both Chinese people and other Asians in general, BMI does not appear to significantly affect the colon-cancer-specific survival, although underweight patients do appear to have a higher postoperative mortality and worse overall survival, and are less likely to experience disease-free survival than patients in the other BMI categories.

Applications

BMI is a simple index that can be used to evaluate the likelihood of colon cancer patients developing weight loss, blood loss, nutrition depletion, and more-advanced disease.

Terminology

BMI was calculated as the weight in kilograms divided by the height in meters squared. The classification of BMI was established to evaluate health risks such as type 2 diabetes and cardiovascular disease.

Peer review

This study investigated the effect of body mass index on the characteristics and overall outcome of colon cancer in Taiwan. This manuscript addresses a highly relevant subject and could be important for the cancer field.

REFERENCES

- 1 **Pischon T**, Lahmann PH, Boeing H, Friedenreich C, Norat T, Tjønneland A, Halkjaer J, Overvad K, Clavel-Chapelon F, Boutron-Ruault MC, Guernec G, Bergmann MM, Linseisen J, Becker N, Trichopoulou A, Trichopoulos D, Sieri S, Palli D, Tumino R, Vineis P, Panico S, Peeters PH, Bueno-de-Mesquita HB, Boshuizen HC, Van Guelpen B, Palmqvist R, Berglund G, Gonzalez CA, Dorransoro M, Barricarte A, Navarro C, Martinez C, Quirós JR, Roddam A, Allen N, Bingham S, Khaw KT, Ferrari P, Kaaks R, Slimani N, Riboli E. Body size and risk of colon and rectal cancer in the European Prospective Investigation Into Cancer and Nutrition (EPIC). *J Natl Cancer Inst* 2006; **98**: 920-931
- 2 **Rapp K**, Schroeder J, Klenk J, Stoehr S, Ulmer H, Concin H, Diem G, Oberaigner W, Weiland SK. Obesity and incidence of cancer: a large cohort study of over 145,000 adults in Austria. *Br J Cancer* 2005; **93**: 1062-1067
- 3 **Larsson SC**, Wolk A. Obesity and colon and rectal cancer risk: a meta-analysis of prospective studies. *Am J Clin Nutr* 2007; **86**: 556-565
- 4 **Meyerhardt JA**, Catalano PJ, Haller DG, Mayer RJ, Benson AB, Macdonald JS, Fuchs CS. Influence of body mass index on outcomes and treatment-related toxicity in patients with colon carcinoma. *Cancer* 2003; **98**: 484-495
- 5 **Dignam JJ**, Polite BN, Yothers G, Raich P, Colangelo L, O'Connell MJ, Wolmark N. Body mass index and outcomes in patients who receive adjuvant chemotherapy for colon cancer. *J Natl Cancer Inst* 2006; **98**: 1647-1654
- 6 **Meyerhardt JA**, Niedzwiecki D, Hollis D, Saltz LB, Mayer RJ, Nelson H, Whittom R, Hantel A, Thomas J, Fuchs CS. Impact of body mass index and weight change after treatment on cancer recurrence and survival in patients with stage III colon cancer: findings from Cancer and Leukemia Group B 89803. *J Clin Oncol* 2008; **26**: 4109-4115
- 7 **Sinicrope FA**, Foster NR, Sargent DJ, O'Connell MJ, Rankin C. Obesity is an independent prognostic variable in colon cancer survivors. *Clin Cancer Res* 2010; **16**: 1884-1893

- 8 http://food.doh.gov.tw/FoodNew/health/1824/1824_102.aspx
- 9 Physical status: the use and interpretation of anthropometry. Report of a WHO Expert Committee. *World Health Organ Tech Rep Ser* 1995; **854**: 1-452
- 10 **WHO Expert Consultation.** Appropriate body-mass index for Asian populations and its implications for policy and intervention strategies. *Lancet* 2004; **363**: 157-163
- 11 **DeMaria EJ, Carmody BJ.** Perioperative management of special populations: obesity. *Surg Clin North Am* 2005; **85**: 1283-1289, xii
- 12 **Benoist S, Panis Y, Alves A, Valleur P.** Impact of obesity on surgical outcomes after colorectal resection. *Am J Surg* 2000; **179**: 275-281
- 13 **Gendall KA, Raniga S, Kennedy R, Frizelle FA.** The impact of obesity on outcome after major colorectal surgery. *Dis Colon Rectum* 2007; **50**: 2223-2237
- 14 **Sørensen LT, Jørgensen T, Kirkeby LT, Skovdal J, Vennits B, Wille-Jørgensen P.** Smoking and alcohol abuse are major risk factors for anastomotic leakage in colorectal surgery. *Br J Surg* 1999; **86**: 927-931
- 15 **Biondo S, Parés D, Kreisler E, Ragué JM, Fracalvieri D, Ruiz AG, Jaurrieta E.** Anastomotic dehiscence after resection and primary anastomosis in left-sided colonic emergencies. *Dis Colon Rectum* 2005; **48**: 2272-2280
- 16 **Miransky J, Ruo L, Nicoletta S, Eagan J, Sepkowitz K, Margetson N, Thaler H, Cohen AM, Guillem JG.** Impact of a surgeon-trained observer on accuracy of colorectal surgical site infection rates. *Dis Colon Rectum* 2001; **44**: 1100-1105
- 17 **Riou JP, Cohen JR, Johnson H.** Factors influencing wound dehiscence. *Am J Surg* 1992; **163**: 324-330
- 18 **Brooks-Brunn JA.** Predictors of postoperative pulmonary complications following abdominal surgery. *Chest* 1997; **111**: 564-571
- 19 **Eichenberger A, Proietti S, Wicky S, Frascarolo P, Suter M, Spahn DR, Magnusson L.** Morbid obesity and postoperative pulmonary atelectasis: an underestimated problem. *Anesth Analg* 2002; **95**: 1788-1792
- 20 **Hickman DM, Miller RA, Rombeau JL, Twomey PL, Frey CF.** Serum albumin and body weight as predictors of postoperative course in colorectal cancer. *JPEN J Parenter Enteral Nutr* 1980; **4**: 314-316
- 21 **Minoo P, Zlobec I, Peterson M, Terracciano L, Lugli A.** Characterization of rectal, proximal and distal colon cancers based on clinicopathological, molecular and protein profiles. *Int J Oncol* 2010; **37**: 707-718
- 22 **Lai CC, You JF, Yeh CY, Chen JS, Tang R, Wang JY, Chin CC.** Low preoperative serum albumin in colon cancer: a risk factor for poor outcome. *Int J Colorectal Dis* 2011; **26**: 473-481
- 23 **Diculescu M, Iacob R, Iacob S, Croitoru A, Becheanu G, Popeneciu V.** The importance of histopathological and clinical variables in predicting the evolution of colon cancer. *Rom J Gastroenterol* 2002; **11**: 183-189
- 24 **Knight K, Wade S, Balducci L.** Prevalence and outcomes of anemia in cancer: a systematic review of the literature. *Am J Med* 2004; **116** Suppl 7A: 11S-26S

S- Editor Cheng JX L- Editor A E- Editor Zhang DN

Oxymatrine liposome attenuates hepatic fibrosis *via* targeting hepatic stellate cells

Ning-Li Chai, Qiang Fu, Hui Shi, Chang-Hao Cai, Jun Wan, Shi-Ping Xu, Ben-Yan Wu

Ning-Li Chai, Hui Shi, Chang-Hao Cai, Jun Wan, Shi-Ping Xu, Ben-Yan Wu, Department of Gastroenterology, South Building of Chinese People's Liberation Army General Hospital, Beijing 100853, China

Qiang Fu, Department of Gastroenterology, Xi'an Children's Hospital, Xi'an 710002, Shaanxi Province, China

Author contributions: Chai NL and Fu Q performed the majority of experiments; Cai CH, Wan J and Xu SP provided vital reagents and analytical tools and were also involved in editing the manuscript; Chai NL and Wu BY designed the study; Chai NL and Shi H wrote the manuscript.

Supported by National Natural Science Foundation of China, No. 30600848

Correspondence to: Ben-Yan Wu, MD, Department of Gastroenterology, South Building of Chinese People's Liberation Army General Hospital, No. 28 Fuxing Road, Beijing 100853, China. csxlily@163.com

Telephone: +86-10-66876225 Fax: +86-10-68295664

Received: May 13, 2012 Revised: June 26, 2012

Accepted: June 28, 2012

Published online: August 21, 2012

Abstract

AIM: To investigate the potential mechanism of Arg-Gly-Asp (RGD) peptide-labeled liposome loading oxymatrine (OM) therapy in CCl₄-induced hepatic fibrosis in rats.

METHODS: We constructed a rat model of CCl₄-induced hepatic fibrosis and treated the rats with different formulations of OM. To evaluate the antifibrotic effect of OM, we detected levels of alkaline phosphatase, hepatic histopathology (hematoxylin and eosin stain and Masson staining) and fibrosis-related gene expression of matrix metalloproteinase (MMP)-2, tissue inhibitor of metalloproteinase (TIMP)-1 as well as type I procollagen *via* quantitative real-time polymerase chain reaction. To detect cell viability and apoptosis of hepatic stellate cells (HSCs), we performed 3-(4,5)-dimethylthiazoliazolo(2-yl)-2,5-diphenyltetrazolium bromide assay and flow cytometry. To reinforce the

combination of oxymatrine with HSCs, we constructed fluorescein-isothiocyanate-conjugated Arg-Gly-Asp peptide-labeled liposomes loading OM, and its targeting of HSCs was examined by fluorescent microscopy.

RESULTS: OM attenuated CCl₄-induced hepatic fibrosis, as defined by reducing serum alkaline phosphatase (344.47 ± 27.52 U/L *vs* 550.69 ± 43.78 U/L, $P < 0.05$), attenuating liver injury and improving collagen deposits ($2.36\% \pm 0.09\%$ *vs* $7.70\% \pm 0.60\%$, $P < 0.05$) and downregulating fibrosis-related gene expression, that is, MMP-2, TIMP-1 and type I procollagen ($P < 0.05$). OM inhibited cell viability and induced apoptosis of HSCs *in vitro*. RGD promoted OM targeting of HSCs and enhanced the therapeutic effect of OM in terms of serum alkaline phosphatase (272.51 ± 19.55 U/L *vs* 344.47 ± 27.52 U/L, $P < 0.05$), liver injury, collagen deposits ($0.26\% \pm 0.09\%$ *vs* $2.36\% \pm 0.09\%$, $P < 0.05$) and downregulating fibrosis-related gene expression, that is, MMP-2, TIMP-1 and type I procollagen ($P < 0.05$). Moreover, *in vitro* assay demonstrated that RGD enhanced the effect of OM on HSC viability and apoptosis.

CONCLUSION: OM attenuated hepatic fibrosis by inhibiting viability and inducing apoptosis of HSCs. The RGD-labeled formulation enhanced the targeting efficiency for HSCs and the therapeutic effect.

© 2012 Baishideng. All rights reserved.

Key words: Oxymatrine; Arg-Gly-Asp peptide; Hepatic stellate cell; Hepatic fibrosis; Target therapy

Peer reviewer: Javier Gonzalez-Gallego, Professor, Institute of Biomedicine, University of Leon, 24071 Leon, Spain

Chai NL, Fu Q, Shi H, Cai CH, Wan J, Xu SP, Wu BY. Oxymatrine liposome attenuates hepatic fibrosis *via* targeting hepatic stellate cells. *World J Gastroenterol* 2012; 18(31): 4199-4206 Available from: URL: <http://www.wjgnet.com/1007-9327/full/v18/i31/4199.htm> DOI: <http://dx.doi.org/10.3748/wjg.v18.i31.4199>

INTRODUCTION

Hepatic fibrosis is characterized by excessive deposition of extracellular matrix (ECM) components in the interstitial space of the liver^[1,2]. The fibrogenesis is triggered by a variety of events that lead to chronic injury, including viral infection, drug or alcoholic toxicity, autoimmune disorders and metabolic diseases. As a consequence of liver damage, nonparenchymal cells are activated by a concert of mediators released from injured hepatocytes. A population of nonparenchymal cells, the hepatic stellate cells (HSCs), have been identified and recognized for their contributing role in the fibrotic process after transformation towards myofibroblasts^[3]. Thus, HSCs represent an attractive target for the development of antifibrotic strategies incorporating a selective targeting approach for hepatic fibrosis^[4]. Recently, several therapeutic strategies have been developed by means of targeting hepatic fibrosis, including inhibition of collagen synthesis^[5], interruption of matrix deposition^[6], stimulation of matrix degradation, modulation of HSC activation^[7], or induction of HSC death^[8]. Despite advance in understanding hepatic fibrogenesis, therapeutic repertoire for hepatic fibrosis treatment is still limited.

Oxymatrine (OM), an alkaloid extracted from the medicinal plant *Sophora alopecuroides* L, has received increasing attention for its multiple pharmacological functions. OM has been demonstrated to exert an inhibitory effect on the replication of hepatitis B^[9] and C^[10] viruses *in vitro*. Preclinical and clinical studies have shown that OM effectively inhibited infection with hepatitis B virus^[11]. In addition to antiviral effects, OM has been reported to have a beneficial effect on progression of CCl₄-induced hepatic fibrosis in rats. Recent studies have demonstrated that OM induces apoptosis in a variety of cells; mainly malignant cells^[12]. Apoptosis-inducing activity of OM makes it an attractive antifibrotic agent. However, there is limited evidence for the efficacy of OM in hepatic fibrosis and the underlying mechanism.

In the present study we aimed to investigate whether Arg-Gly-Asp (RGD)-mediated targeting delivery of OM exerted antifibrogenic action with improved efficiency of fibrogenic liver^[13]. *In vitro* experiments showed that uptake of OM in HSCs was enhanced and the apoptotic process was induced. In CCl₄-induced rats, delivery of OM to HSCs with this formulation strategy improved the efficacy of this medication in the treatment of hepatic fibrosis.

MATERIALS AND METHODS

Preparation of OM-RGD liposomes

The lipid phase consisting of a mixture of lecithin and cholesterol in a ratio of 2:1 was dissolved in CHCl₃-MeOH (1:1) followed by evaporation and addition of pleic acid and polysorbate. Lipids were mixed with the aqueous solution containing OM and polyvinylpyrrolidone in phosphate-buffered saline (PBS; pH 7.4).

The mixture was sonicated for 5 min at 50% amplifying strength resulting in a water-in-oil emulsion. After removal of the organic solvent with a rotary evaporator under vacuum, the dispersion of liposomes was formed.

RGD peptide was synthesized by the Chinese Peptide Company (Hangzhou, China). RGD peptide coupling was performed as described previously^[14]. In brief, 4 nmol cyclo-Arg-Gly-Asp (cRGD) peptide per mmol total lipid was added after deacetylation of the peptide in 0.5 mol hydroxylamine solution, and incubated for 1 h at room temperature. Unloaded liposomes and unbound RGD were separated by CL-4B column (Amersham, Piscataway, NJ, United States).

HSC preparation

HSCs were isolated by collagenase perfusion through the portal vein in Sprague-Dawley rats, followed by Nycomed gradient centrifugation. Cells were incubated in Dulbecco's Modified Eagle's Medium (DMEM) supplemented with 10% fetal bovine serum (v/v) and 100 U/mL penicillin and streptomycin, and maintained at 37 °C in a humidified incubator (90% humidity) containing 50 mL/L CO₂. HSCs seeded at a density of 10⁴ cells/cm² attained confluence in 6 d and formed a monolayer of closely apposed polygonal cells. The morphology and growth of HSCs were confirmed and evaluated by microscopy.

Cell viability assay

Cell viability was determined through 3-(4,5)-dimethyl thiaziazol(-z-y1)-3,5-diphenyltetrazolium bromide (MTT) assay. The MTT assay depends on the extent to which viable cells convert MTT bromide to an insoluble colored formazan product that can be determined spectrophotometrically. After treatment, cells were harvested and washed in PBS, and 200 mL DMEM without phenol red, containing 5 mg/mL MTT, was added to each cell. Three hours later, the medium was aspirated, and the converted dye was solubilized with isopropanol (0.1 mol/L HCl in isopropanol). The resulting absorbance from each cell was measured at a wavelength of 570 nm with background subtraction at 630 nm.

Flow cytometry

HSCs were treated with different concentration of OM-RGD liposomes for 48 h at a cell density of 2 × 10⁵ cells/mL, and then stained with annexin V-fluorescein isothiocyanate (FITC) and propidium iodide (PI) (Sigma, St Louis, MO, United States). Annexin V-FITC-positive and PI-negative cells were considered to be apoptotic cells.

Transmission electron microscopy

HSCs were cultured with different formulation of OM at 37 °C for 24 h and then harvested by trypsinization and centrifugation for 10 min at 3500 rpm at room temperature. Cells were fixed in 4% (v/v) glutaraldehyde for 4 h at 4 °C. The specimens were washed with sodium

Table 1 Serum level of alkaline phosphatase and ratio of collagen area to liver tissue in rats with CCl₄-induced hepatic fibrosis

Group	n	ALP (U/L)
Normal	10	73.91 ± 5.97
CCl ₄ -induced hepatic fibrosis	10	550.69 ± 43.80 ^a
OM-RGD liposomes	10	272.51 ± 19.55 ^{a,c}
OM liposomes	10	344.47 ± 27.52 ^c
RGD liposomes	10	562.78 ± 40.22
		Collagen area (%)
CCl ₄ -induced hepatic fibrosis	5	7.70 ± 0.60
RGD liposomes	5	8.32 ± 0.42
OM liposomes	5	2.36 ± 0.09 ^e
OM-RGD liposomes	5	0.26 ± 0.09 ^e

^a*P* < 0.05 vs normal; ^c*P* < 0.05 vs CCl₄-induced hepatic fibrosis group; ^e*P* < 0.05 vs oxymatrine (OM) liposomes. ALP: Alkaline phosphatase; RGD: Arg-Gly-Asp.

cacodylate buffer (pH 7.4) followed by post-fixation in 1% osmium tetroxide at 4 °C. Cells were then washed with cacodylate buffer (pH 7.4) and dehydrated with a graded series of acetone. The cells were embedded with 100% resin in a beam capsule. A sample block was sectioned using an ultramicrotome. The sections were placed into a grid and stained with uranyl acetate for 10 min followed by 50% filtered acetone, and finally stained with lead. The stained samples were then viewed under a transmission electron microscope (Phillips, Eindhoven, The Netherlands).

Real-time PCR

Total RNA was extracted from cells using the TRIzol reagent. The amount of each RNA sample was determined by Qubit fluorometer. Reverse transcription was performed in a 20-μL reaction system with 200 ng total RNA using high capacity cDNA reverse transcription kits. Relative quantification of designated genes including *MMP-2*, *TIMP* and type I procollagen were assessed by real-time PCR through the ABI 7900HT system. A housekeeping gene glyceraldehyde-3-phosphate dehydrogenase (*GAPDH*) was used as an internal control. Primer sequences used are shown as follows: type I procollagen, 5'-CCTGGCAGAACGGAGATGAT-3', 5'-ACCA CAGCACCATCGTTACC-3'; *MMP-2*, 5'-CTATTCTGT CAGCACTT TGG-3', 5'-CAGACTTTGGTTCTC-CA ACTT-3'; *TIMP-1*, 5'-ACA GCTTT CTGCA ACTCG-3', 5'-CTATAGGTCTTT ACGAAGGCC-3'; *GADPH*, 5'-AC CCCC AATGTATCCGTGT-3', 5'-TA CTCCTTGGAGGCCATGTA-3'. The relative abundance of target mRNA was determined with the comparative cycle threshold method.

Animals and experimental design

Male Sprague-Dawley rats came from the Experimental Animal Center of Beijing Medical University (Beijing, China) and were caged in an environment with regulated temperature (21 ± 1.6 °C), humidity (45% ± 10%), and an alternating 12-h light and dark cycle. The animals had

free access to water and diet throughout the study.

For the chronic liver injury model, animals were injected intraperitoneally with 50% CCl₄ (CCl₄:vegetable oil = 1:1) at a dose of 0.15 mL/100 g body weight and were also divided into four groups: Group A (administered with OM-loaded liposome); Group B (administered with OM-RGD liposome); Group C (hepatic fibrosis); and Group D (blank vector). Injections were given three times weekly for 8 wk. After treatment, the rats received an intravenous injection according to their subgrouping. Groups A and B were given OM liposomes and OM-RGD liposomes, respectively. The rats in Group D were administered with 0.5 mL blank liposomes. The rats were sacrificed 8 wk after injection, and the livers and blood samples were collected for further assessments.

For HSC targeting, CCl₄-treated animals were injected with FITC-labeled OM liposomes and OM-RGD liposomes *via* the tail vein. Hepatocytes and HSCs were isolated from each individual rat 24 h post-injection, as described previously^[15].

Histological analysis

Animals were sacrificed 8 wk after treatment. Liver samples from each group were harvested, fixed with 10% formaldehyde, embedded in olefin, and stained with hematoxylin and eosin (HE) as well as Masson collagen staining.

Statistical analysis

The data are expressed as mean ± SD. Student's *t*-test or Dunnett's *t*-test was used to compare the differences between treated and control groups, and differences were considered significant at *P* < 0.05.

RESULTS

Antifibrogenic effect of OM-RGD liposomes in CCl₄-induced fibrotic liver

We evaluated the therapeutic effect of OM-RGD liposomes on CCl₄-induced liver injury in rats. As shown in Table 1, elevated levels of alkaline phosphatase were reduced by OM. Histopathological analysis revealed that CCl₄-induced hepatic fibrosis was ameliorated by OM (Figure 1A). Excessive collagen deposited in response to CCl₄-induced liver injury was ameliorated by OM (Table 1, Figure 1B). Moreover, the RGD-labeled liposomal formulation exerted a more aggressive therapeutic effect in hepatic fibrosis than did OM in terms of alkaline phosphatase (Table 1), histopathology (Figure 1A), and collagen deposits (Table 1, Figure 1B).

OM-RGD liposomes induced apoptosis in HSCs in vitro

The inhibitory effect of OM-RGD liposomes on the viability of primary HSCs was determined by MTT assay. As shown in Figure 2A, OM-RGD liposomes significantly inhibited the viability of HSCs, whereas OM liposomes exhibited low cytotoxicity in HSCs. The ultrastructure of HSCs treated with different formulation of OM was

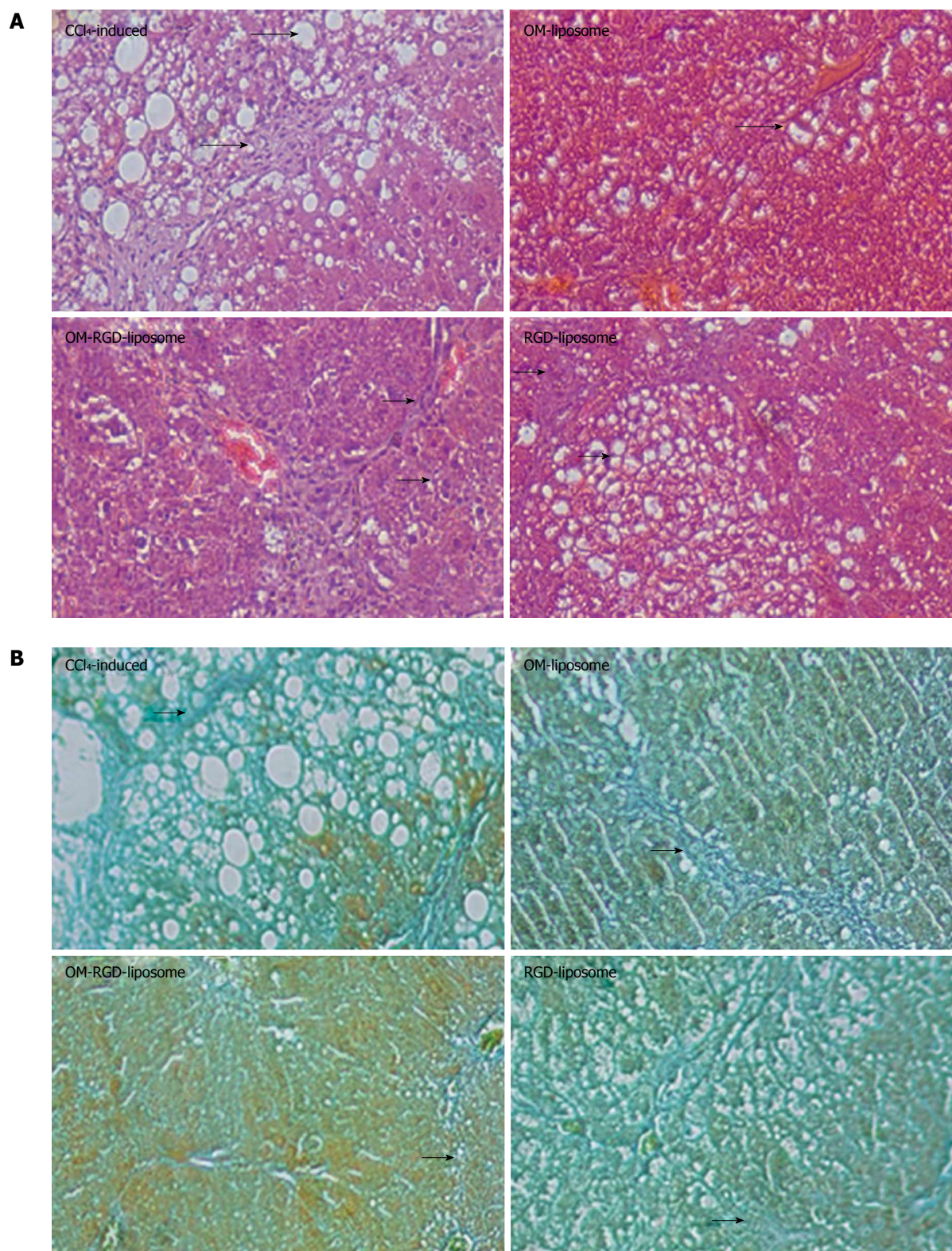


Figure 1 Oxymatrine liposomes attenuated hepatic fibrosis and improved collagen deposition. A: Representative images of liver treated with oxymatrine (OM) in different liposomal formulations in rats with CCl₄-induced hepatic fibrosis. Liver tissues were obtained at 4 wk after treatment and stained with HE; B: Representative histological images of liver treated with OM in different liposomal formulations in rats with CCl₄-induced hepatic fibrosis. Liver tissues were obtained at 4 wk after treatment and stained with Masson stain (original magnification × 100). HE: Hematoxylin and eosin.

examined by transmission electron microscopy (TEM). TEM revealed that treatment with OM-RGD liposomes resulted in typical morphological sign of apoptosis, including cell shrinkage, increased cellular granularity, and

formation of apoptotic bodies (Figure 2B). The apoptotic effect of different formulations of OM was determined by using flow cytometry. Cell cycle analysis revealed that incubation with OM-RGD liposomes resulted

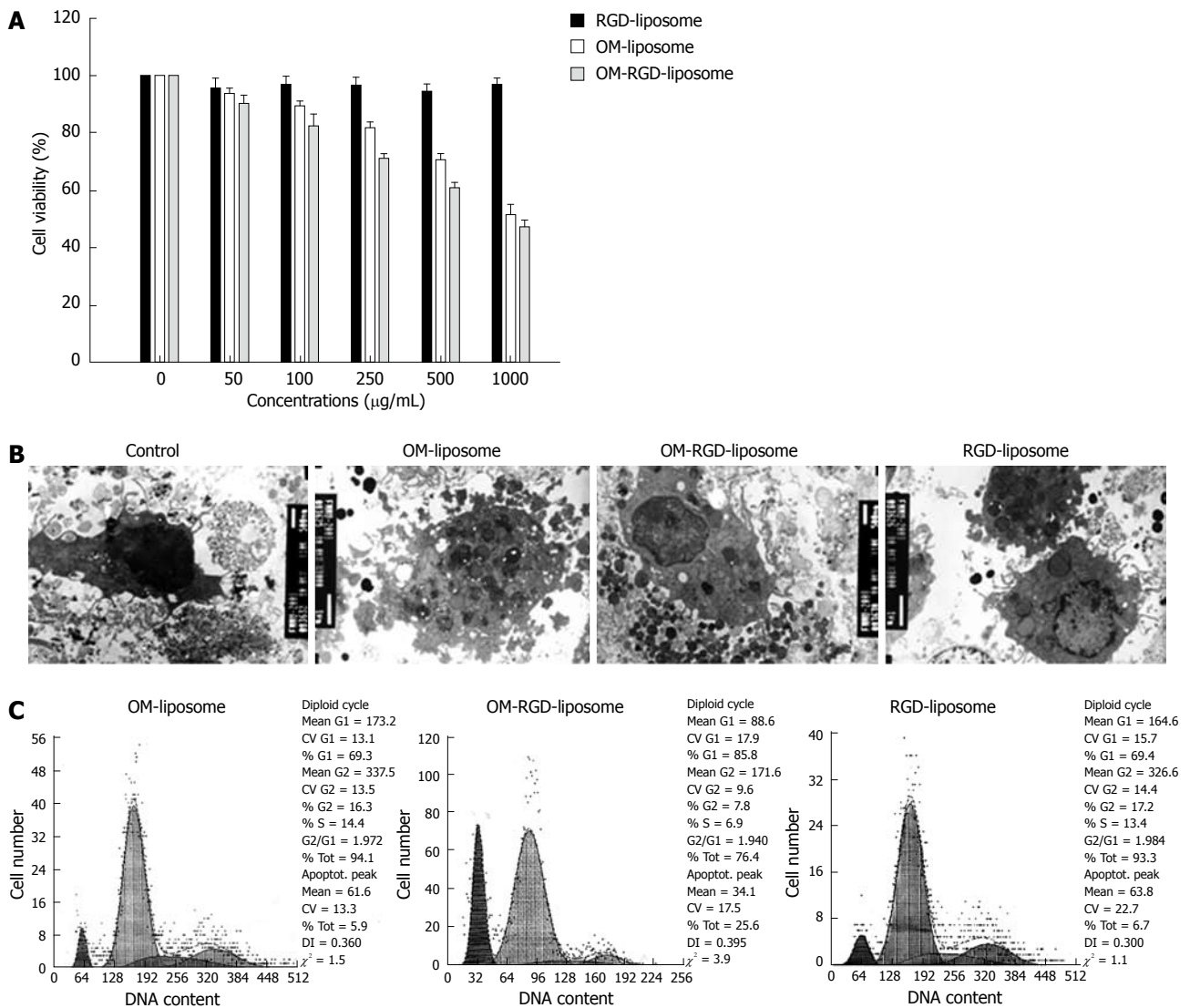


Figure 2 Oxymatrine liposomes induced apoptosis in hepatic stellate cells *in vitro*. A: Inhibitory effect of oxymatrine (OM) on hepatic stellate cell (HSC) viability *in vitro*. HSCs were isolated and treated with OM in different liposomal formulations. Cell viability was determined using MTT assay; B: Electron micrograph of untreated HSCs demonstrates the normal structure of HSCs. OM-liposome-treated (24 h) HSCs had morphological features of apoptosis: cell shrinkage and apoptotic body formation. OM-RGD-liposome-treated HSCs showed typical morphological features of apoptosis: cell shrinkage and apoptotic body formation. RGD-liposome-treated HSCs showed normal structure; C: Cell cycle analysis after induction of apoptosis in HSCs by OM *via* flow cytometry. The cells were incubated with different formulation of OM for 24 h, and stained with PI. MTT: 3-(4,5)-dimethylthiazolozol-2-yl-2,5-diphenyltetrazolium bromide; RGD: Arg-Gly-Asp; PI: Propidium iodide; DI: DNA grading index.

in a significant increase in sub-G₁ phase accumulation that was recognized as a biomarker of apoptosis (Figure 2C). Moreover, the RGD-labeled liposomal formulation had a more aggressive effect on HSCs than that of OM in terms of cell viability (Figure 2) and apoptosis (Figures 3 and 4)

OM-RGD liposomes inhibited fibrosis-related gene expression in CCl₄-induced fibrotic liver injury

We also examined the change in mRNA expression of fibrosis-related genes upon treatment with OM in different liposomal formulations. As shown in Figure 3, mRNA expression of MMP-2, TIMP-1 and type I procollagen was considerably elevated upon CCl₄ induction (*vs* normal, *P* < 0.05). Treatment with OM resulted in significant decreases in mRNA expression of these designated fibro-

sis-related genes and fibrosis-related gene expression (*vs* CCl₄-induced group, *P* < 0.05). Moreover, RGD-labeled liposomal formulation had a more aggressive downregulation of fibrosis-related gene expression than that of OM (*vs* CCl₄-induced hepatic fibrosis group, *P* < 0.05; as compared to OM liposomes, *P* < 0.05).

RGD enhanced OM targeting of HSCs in fibrotic rats

To evaluate the specificity of binding to HSCs in fibrotic liver, OM-RGD liposomes were conjugated with FITC and injected intravenously to rats with CCl₄-induced hepatic fibrosis. HSCs were isolated and examined by fluorescence microscopy. As shown in Figure 4, a significantly high number of FITC-positive HSCs was found in the OM-RGD liposome group compared with the OM liposome group.

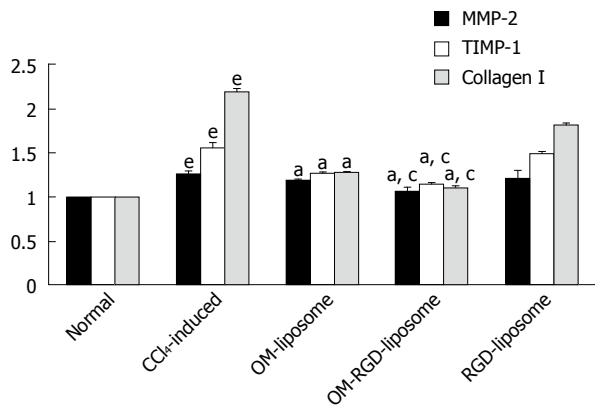


Figure 3 Oxymatrine liposomes inhibited fibrosis-related gene expression. The expression of fibrosis-related gene, such as MMP-2, TIMP-1 and collagen I was evaluated by real-time polymerase chain reaction. ^a*P* < 0.05 vs normal; ^c*P* < 0.05 vs CCl₄-induced hepatic fibrosis; ^{a, c}*P* < 0.05 vs oxymatrine liposomes. MMP: Matrix metalloproteinase; TIMP: Tissue inhibitor of metalloproteinase; OM: Oxymatrine; RGD: Arg-Gly-Asp.

DISCUSSION

Increased understanding of the pathogenesis of hepatic fibrosis has led to drug discovery for its treatment. Pre-clinical and clinical studies have reported that hepatic fibrosis is dynamic and possibly reversible^[16,17]. During recent decades, antifibrotic strategies have predominantly focused on eradication of causative factors, for example, clearance of virus^[18]. Since the pathogenesis of fibrosis was clarified recently^[19], researches have focused on agents that could prevent or reverse fibrosis. OM has been reported for its pharmacological potential to treat liver disorders, particularly inhibiting viral infection^[10,11,20,21]. It has been demonstrated to exert antifibrotic action^[22]. In our study, we confirmed that OM could attenuate CCl₄-induced hepatic fibrosis in a rat model, as defined by a significant decrease in the serum level of alkaline phosphatase and improvement of histopathological change.

OM was recently referred to as an antifibrosis agent in clinical and preclinical studies. However, its mechanisms of action were still puzzling. In preclinical studies, it was proved that OM showed prophylactic and therapeutic effects in D-galactosamine-induced rat hepatic fibrosis, partly by protecting hepatocytes and suppressing fibrosis accumulation through acting against lipid peroxidation^[23]. Another study also demonstrated that OM was effective in reducing the production and deposition of collagen in the liver tissue of experimental rats in ways that relate to modulating the fibrogenic signal transduction *via* the p38 mitogen-activated protein kinase signaling pathway^[24]. Moreover, OM could promote the expression of Smad 7 and inhibit the expression of Smad 3 and cAMP-response element binding protein-binding protein in CCl₄-induced hepatic fibrosis in rats, and modulate the fibrogenic signal transduction of the transforming growth factor (TGF)- β -Smad pathway^[25]. Clinical studies have proved that the effect of OM against hepatic fibrosis is

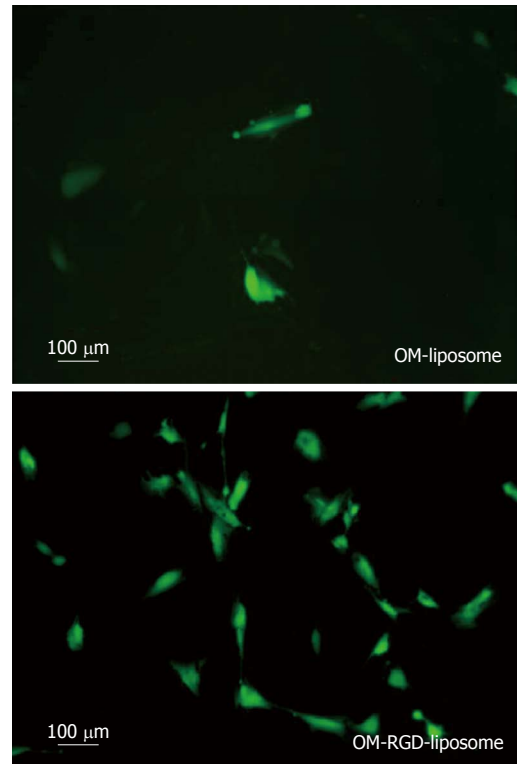


Figure 4 Representative fluorescein isothiocyanate hepatic stellate cells in rat hepatic tissue treated with oxymatrine liposomes and oxymatrine-Arg-Gly-Asp liposomes (original magnification \times 200). OM: Oxymatrine; RGD: Arg-Gly-Asp.

mediated by lowering the levels of TGF- β 1 and tumor necrosis factor- α and increasing the level of interleukin-10 in chronic hepatitis B patients^[26]. OM could also target directly fibrogenic effector cells, which has received much attention^[27]. Various cells are involved in the fibrogenic process. HSCs, the most important fibrogenic cells, are activated during injury and contribute to excessive synthesis of ECM, resulting in deposition of scar or fibrous tissue^[28-31]. OM has been demonstrated to prevent pig-serum-induced liver fibrosis in rats by inhibiting the activation of HSCs and synthesis of collagen^[32]. However, how OM inhibits HSC activation was not determined in that study^[32].

We explored the effect of OM on HSCs *in vitro*. OM inhibited viability and induced apoptosis of HSCs. This might be the underlying mechanism involved in OM therapy of hepatic fibrosis. Furthermore, we also detected fibrosis-related gene expression after OM administration. MMP-2, produced by HSCs, plays an important role in liver fibrogenesis^[33]. TIMPs, especially TIMP-1 and -2 expression and activity, were significantly increased at 8 wk in a rat porcine-serum-induced hepatic fibrosis model^[34]. Furthermore, inhibition of cell viability and type I procollagen expression in rat HSCs could improve recovery from CCl₄-induced liver fibrogenesis in rats^[35]. As shown in our study, mRNA expression of MMP-2, TIMP-1 and type I procollagen was considerably elevated upon CCl₄ induction. Treatment with OM resulted

in significant decreases in mRNA expression of these designated fibrosis-related genes. All the data indicated that OM could attenuate hepatic fibrosis *via* its effect on HSCs, such as inhibiting cell viability, inducing apoptosis and downregulation of fibrosis-related gene expression.

Since OM therapy was dependent on its interaction with HSCs, binding to HSCs became a key factor for its function. Due to a relatively small population of HSCs in the liver and lack of specific membrane receptors, HSC-specific targeting therapy has remained unavailable. Several studies have attempted to use different formulation approaches for targeting HSCs. Beljaars *et al.*^[36] have reported that human serum albumin (HSA) modified with mannose 6-phosphate (M6P) accumulated in HSCs by binding to the M6P-insulin-like growth factor II receptors found on activated HSCs. Modification of HSA with a cyclic peptide that recognizes the collagen type VI receptor has been demonstrated to enhance effectiveness and tissue specificity of antifibrogenic drugs^[37]. Moreover, the affinity of a cyclic peptide, cRGD, for collagen type VI receptor on HSCs was confirmed in both *in vitro* and *in vivo* experiments^[13]. In our study, in order to facilitate OM binding to HSCs, we conjugated liposomes targeted to HSCs in rats with CCl₄-induced hepatic fibrosis. Fluorescence microscopy showed more FITC-positive HSCs in the OM-RGD-liposome group compared with the OM-liposome group. We compared the difference in therapeutic effect of the alternative formulations of OM on liver fibrosis. We demonstrated better results in the OM-RGD-liposome group, as demonstrated by significant decreases in serum alkaline phosphatase and improvement of histopathological changes, compared with the OM-liposome group. Moreover, OM-RGD liposomes showed a more aggressive effect on viability, apoptosis and fibrosis-related gene expression of HSCs, compared with the OM liposomes. The results showed that specific binding of this liposomal formulation to HSCs enhanced the liver protective effect of OM.

In conclusion, we conjugated OM with RGD liposomes and confirmed that this formulation could enhance OM binding to HSCs and the therapeutic effect on hepatic fibrosis induced by CCl₄. We also demonstrated that the therapeutic effects of OM on hepatic fibrosis were partly dependent on inhibiting cell viability, inducing apoptosis, and downregulating fibrosis-related gene expression of HSCs, thus highlighting OM-RGD liposomes as an attractive novel therapy in liver fibrosis.

COMMENTS

Background

Oxymatrine (OM) has been reported to have a beneficial effect on progression of CCl₄-induced hepatic fibrosis in rats, however, its mechanism of action is still uncertain. Hepatic stellate cells (HSCs) have been identified as an important factor in the hepatic fibrotic process. Drugs that could induce HSC apoptosis or death might be the potential strategy for treatment of hepatic fibrosis. Recent studies have demonstrated that OM induces apoptosis in a variety of cells; mainly malignant cells. Thus, the authors performed an assay to demonstrate whether OM could attenuate hepatic fibrosis *via* inducing HSC apoptosis.

Research frontiers

OM was demonstrated to attenuate hepatic fibrosis but its mechanisms of action were still uncertain. Moreover, targeting of HSCs might facilitate the therapeutic effect of OM. The research hotspot is to clarify the mechanism of action of OM in attenuating hepatic fibrosis and how to enhance OM binding to HSCs.

Innovations and breakthroughs

Apoptosis-inducing activity of OM makes it an attractive antifibrotic agent. However, there is limited evidence for the efficacy of OM in hepatic fibrosis and the underlying mechanism of action. The authors demonstrated for the first time that OM could attenuate hepatic fibrosis *via* inhibiting viability and inducing apoptosis of HSCs. Moreover, Arg-Gly-Asp (RGD) could promote OM targeting to HSCs and enhance its effect on hepatic fibrosis.

Peer review

This study aimed to analyze the effects of RGD-peptide-labeled liposomes on CCl₄-induced hepatic fibrosis in rats. This is an interesting approach that clearly improves the efficacy of treatment. The research combined *in vitro* and *in vivo* studies, and data are clear and well presented.

REFERENCES

- 1 Friedman SL. Molecular regulation of hepatic fibrosis, an integrated cellular response to tissue injury. *J Biol Chem* 2000; **275**: 2247-2250
- 2 Mormone E, George J, Nieto N. Molecular pathogenesis of hepatic fibrosis and current therapeutic approaches. *Chem Biol Interact* 2011; **193**: 225-231
- 3 Kastanis GJ, Hernandez-Nazara Z, Nieto N, Rincón-Sánchez AR, Popratiloff A, Dominguez-Rosales JA, Lechuga CG, Rojkind M. The role of dystroglycan in PDGF-BB-dependent migration of activated hepatic stellate cells/myofibroblasts. *Am J Physiol Gastrointest Liver Physiol* 2011; **301**: G464-G474
- 4 Kim MR, Kim HS, Lee MS, Lee MJ, Jang JJ. Cell cycle protein profile of the hepatic stellate cells(HSCs)in dimethylnitrosamine-induced rat hepatic fibrosis. *Exp Mol Med* 2005; **37**: 335-342
- 5 Zhang Y, Liu P, Gao X, Qian W, Xu K. rAAV2-TGF- β (3) decreases collagen synthesis and deposition in the liver of experimental hepatic fibrosis rat. *Dig Dis Sci* 2010; **55**: 2821-2830
- 6 Baroni GS, D'Ambrosio L, Curto P, Casini A, Mancini R, Jezequel AM, Benedetti A. Interferon gamma decreases hepatic stellate cell activation and extracellular matrix deposition in rat liver fibrosis. *Hepatology* 1996; **23**: 1189-1199
- 7 Rosenberg P, Sjöström M, Söderberg C, Kinnman N, Stål P, Hultcrantz R. Attenuated liver fibrosis after bile duct ligation and defective hepatic stellate cell activation in neural cell adhesion molecule knockout mice. *Liver Int* 2011; **31**: 630-641
- 8 Li J, Liu P, Zhang R, Cao L, Qian H, Liao J, Xu W, Wu M, Yin Z. Icaritin induces cell death in activated hepatic stellate cells through mitochondrial activated apoptosis and ameliorates the development of liver fibrosis in rats. *J Ethnopharmacol* 2011; **137**: 714-723
- 9 Wang YP, Zhao W, Xue R, Zhou ZX, Liu F, Han YX, Ren G, Peng ZG, Cen S, Chen HS, Li YH, Jiang JD. Oxymatrine inhibits hepatitis B infection with an advantage of overcoming drug-resistance. *Antiviral Res* 2011; **89**: 227-231
- 10 Wu XN, Wang GJ. Experimental studies of oxymatrine and its mechanisms of action in hepatitis B and C viral infections. *Chin J Dig Dis* 2004; **5**: 12-16
- 11 Chen XS, Wang GJ, Cai X, Yu HY, Hu YP. Inhibition of hepatitis B virus by oxymatrine *in vivo*. *World J Gastroenterol* 2001; **7**: 49-52
- 12 Ling Q, Xu X, Wei X, Wang W, Zhou B, Wang B, Zheng S. Oxymatrine induces human pancreatic cancer PANC-1 cells apoptosis via regulating expression of Bcl-2 and IAP families, and releasing of cytochrome c. *J Exp Clin Cancer Res* 2011; **30**: 66
- 13 Du SL, Pan H, Lu WY, Wang J, Wu J, Wang JY. Cyclic Arg-

- Gly-Asp peptide-labeled liposomes for targeting drug therapy of hepatic fibrosis in rats. *J Pharmacol Exp Ther* 2007; **322**: 560-568
- 14 **Schiffelers RM**, Koning GA, ten Hagen TL, Fens MH, Schraa AJ, Janssen AP, Kok RJ, Molema G, Storm G. Anti-tumor efficacy of tumor vasculature-targeted liposomal doxorubicin. *J Control Release* 2003; **91**: 115-122
 - 15 **Li Q**, Yan Z, Li F, Lu W, Wang J, Guo C. The improving effects on hepatic fibrosis of interferon- γ liposomes targeted to hepatic stellate cells. *Nanotechnology* 2012; **23**: 265101
 - 16 **Hoefs JC**, Shiffman ML, Goodman ZD, Kleiner DE, Dienstag JL, Stoddard AM. Rate of progression of hepatic fibrosis in patients with chronic hepatitis C: results from the HALT-C Trial. *Gastroenterology* 2011; **141**: 900-908.e1-2
 - 17 **Hemmann S**, Graf J, Roderfeld M, Roeb E. Expression of MMPs and TIMPs in liver fibrosis - a systematic review with special emphasis on anti-fibrotic strategies. *J Hepatol* 2007; **46**: 955-975
 - 18 **Ricchi P**, Lanza AG, Ammirabile M, Costantini S, Cinque P, Spasiano A, Di Matola T, Di Costanzo GG, Pagano L, Prossomariti L. Hepatitis C virus distribution and clearance following interferon-monotherapy among thalassaemia major and intermedia patients. *Br J Haematol* 2011; **155**: 524-527
 - 19 **Fallowfield J**, Hayes P. Pathogenesis and treatment of hepatic fibrosis: is cirrhosis reversible? *Clin Med* 2011; **11**: 179-183
 - 20 **Lin M**, Yang LY, Li WY, Peng YP, Zheng JK. Inhibition of the replication of hepatitis B virus in vitro by oxymatrine. *J Int Med Res* 2009; **37**: 1411-1419
 - 21 **Lu LG**, Zeng MD, Mao YM, Li JQ, Wan MB, Li CZ, Chen CW, Fu QC, Wang JY, She WM, Cai X, Ye J, Zhou XQ, Wang H, Wu SM, Tang MF, Zhu JS, Chen WX, Zhang HQ. Oxymatrine therapy for chronic hepatitis B: a randomized double-blind and placebo-controlled multi-center trial. *World J Gastroenterol* 2003; **9**: 2480-2483
 - 22 **Shi GF**, Li Q, Weng XH, Wu XH. [Effects of Oxymatrine on the expression of tissue inhibitor of metalloproteinase-1 and alpha-smooth muscle actin in the livers of rats with hepatic fibrosis]. *Zhonghua Gan Zang Bing Zazhi* 2004; **12**: 56
 - 23 **Yang W**, Zeng M, Fan Z, Mao Y, Song Y, Jia Y, Lu L, Chen CW, Peng YS, Zhu HY. [Prophylactic and therapeutic effect of oxymatrine on D-galactosamine-induced rat liver fibrosis]. *Zhonghua Gan Zang Bing Zazhi* 2002; **10**: 193-196
 - 24 **Deng ZY**, Li J, Jin Y, Chen XL, Lü XW. Effect of oxymatrine on the p38 mitogen-activated protein kinases signalling pathway in rats with CCl4 induced hepatic fibrosis. *Chin Med J (Engl)* 2009; **122**: 1449-1454
 - 25 **Wu XL**, Zeng WZ, Jiang MD, Qin JP, Xu H. Effect of Oxymatrine on the TGFbeta-Smad signaling pathway in rats with CCl4-induced hepatic fibrosis. *World J Gastroenterol* 2008; **14**: 2100-2105
 - 26 **Shen BS**, Song XW. [Effects of oxymatrine on serum cytokines and hepatic fibrotic indexes in patients with chronic hepatitis B]. *Zhongguo Zhong Xi Yi Jie He Zazhi* 2008; **28**: 17-19
 - 27 **Xiang X**, Wang G, Cai X, Li Y. Effect of oxymatrine on murine fulminant hepatitis and hepatocyte apoptosis. *Chin Med J (Engl)* 2002; **115**: 593-596
 - 28 **Moreira RK**. Hepatic stellate cells and liver fibrosis. *Arch Pathol Lab Med* 2007; **131**: 1728-1734
 - 29 **Reeves HL**, Friedman SL. Activation of hepatic stellate cells - a key issue in liver fibrosis. *Front Biosci* 2002; **7**: d808-d826
 - 30 **Kisseleva T**, Brenner DA. Hepatic stellate cells and the reversal of fibrosis. *J Gastroenterol Hepatol* 2006; **21** Suppl 3: S84-S87
 - 31 **Gäbele E**, Mühlbauer M, Dorn C, Weiss TS, Froh M, Schnabl B, Wiest R, Schölmerich J, Obermeier F, Hellerbrand C. Role of TLR9 in hepatic stellate cells and experimental liver fibrosis. *Biochem Biophys Res Commun* 2008; **376**: 271-276
 - 32 **Shi GF**, Li Q. Effects of oxymatrine on experimental hepatic fibrosis and its mechanism in vivo. *World J Gastroenterol* 2005; **11**: 268-271
 - 33 **Li J**, Fan R, Zhao S, Liu L, Guo S, Wu N, Zhang W, Chen P. Reactive Oxygen Species Released from Hypoxic Hepatocytes Regulates MMP-2 Expression in Hepatic Stellate Cells. *Int J Mol Sci* 2011; **12**: 2434-2447
 - 34 **Hasegawa-Baba Y**, Doi K. Changes in TIMP-1 and -2 expression in the early stage of porcine serum-induced liver fibrosis in rats. *Exp Toxicol Pathol* 2011; **63**: 357-361
 - 35 **Chen MH**, Wang QF, Chen LG, Shee JJ, Chen JC, Chen KY, Chen SH, Su JG, Liu YW. The inhibitory effect of *Gynostemma pentaphyllum* on MCP-1 and type I procollagen expression in rat hepatic stellate cells. *J Ethnopharmacol* 2009; **126**: 42-49
 - 36 **Beljaars L**, Molema G, Weert B, Bonnema H, Olinga P, Groothuis GM, Meijer DK, Poelstra K. Albumin modified with mannose 6-phosphate: A potential carrier for selective delivery of antifibrotic drugs to rat and human hepatic stellate cells. *Hepatology* 1999; **29**: 1486-1493
 - 37 **Beljaars L**, Molema G, Schuppan D, Geerts A, De Bleser PJ, Weert B, Meijer DK, Poelstra K. Successful targeting to rat hepatic stellate cells using albumin modified with cyclic peptides that recognize the collagen type VI receptor. *J Biol Chem* 2000; **275**: 12743-12751

S- Editor Gou SX L- Editor Kerr C E- Editor Zhang DN

X-ray repair cross-complementing group 1 polymorphisms and hepatocellular carcinoma: A meta-analysis

Tian Xie, Zhen-Guang Wang, Jing-Lei Zhang, Hui Liu

Tian Xie, Department of Hepatic Surgery, National Hepatobiliary and Enteric Surgery Research Center, Ministry of Health, Central South University, Changsha 410008, Hunan Province, China
Zhen-Guang Wang, Jing-Lei Zhang, Hui Liu, Department of Hepatic Surgery, Eastern Hepatobiliary Surgery Hospital, Second Military Medical University, Shanghai 200438, China
Author contributions: Xie T and Wang ZG contributed equally to this work; Liu H designed research; Xie T and Wang ZG performed the data search and meta-analysis; Zhang JL and Liu H wrote the paper.

Supported by International Science and Technology Cooperation Program of the Ministry of Science and Technology, No. 010S2012ZR0058; the National Basic Research Program of China, No. 2012CB526706; the Innovation Program of Shanghai Municipal Education Commission, No. 13ZZ060; the Fund of Shanghai Municipal Health Bureau, No. 2008Y077; and the Special Program for Military Medicine, No. 2010JS15

Correspondence to: Hui Liu, Associate Professor, Eastern Hepatobiliary Surgery Hospital, Second Military Medical University, Shanghai 200438 China. happyehbh@163.com
Telephone: +86-21-65389998 Fax: +86-21-65562400
Received: March 20, 2012 Revised: May 14, 2012
Accepted: June 8, 2012

Published online: August 21, 2012

Abstract

AIM: To perform a systematic meta-analysis to investigate the association between X-ray repair cross-complementing group 1 (*XRCC1*) polymorphisms and hepatocellular carcinoma (HCC) risk.

METHODS: Relevant studies extracted from PubMed, Embase, Wanfang, VIP and the Chinese National Knowledge Infrastructure databases up to March 2012 were included in the study. Stata software, version 11.0, was used for the statistical analysis. The odds ratios (ORs) and 95% confidence interval (CI) of the *XRCC1* polymorphisms in HCC patients were analyzed and compared with healthy controls. The meta-analysis was performed using fixed-effect or random-effect

methods, depending on the absence or presence of significant heterogeneity.

RESULTS: Eleven studies with 2075 HCC cases and 2604 controls met our eligibility criteria (four studies, 888 cases and 938 controls for Arg194Trp, four studies, 858 cases and 880 controls for Arg280His, and nine studies, 1845 cases and 2401 controls for Arg399Gln). The meta-analysis revealed no associations between the Arg194Trp and Arg399Gln polymorphisms of the *XRCC1* gene and HCC risk under all contrast models (codominant, dominant and recessive models) in the overall analysis and sensitivity analysis (the studies with controls not in the Hardy-Weinberg equilibrium were excluded). For *XRCC1* Arg280His polymorphism, the overall analysis revealed the significant association between the His/His genotype and the increased risk of HCC (His/His vs Arg/Arg model, OR: 1.96, 95% CI: 1.03-3.75, $P = 0.04$). However, sensitivity analysis showed an altered pattern of result and non-significant association (OR: 2.06, 95% CI: 0.67-6.25, $P = 0.20$). The heterogeneity hypothesis test did not reveal any heterogeneity, and Begg's and Egger's tests did not find any obvious publication bias.

CONCLUSION: The *XRCC1* Arg194Trp and Arg399Gln polymorphisms are not associated with HCC risk. More rigorous association studies are needed to verify the involvement of *XRCC1* Arg280His polymorphism in HCC susceptibility.

© 2012 Baishideng. All rights reserved.

Key words: X-ray repair cross-complementing group 1; Polymorphism; Hepatocellular carcinoma; Meta-analysis

Peer reviewers: Dr. Sang Min Park, Department of Family Medicine, Seoul National University Hospital, 101 Daehangno, Jongno-gu, Seoul 110-744, South Korea; Yoshiharu Motoo, Professor, Department of Medical Oncology, Kanazawa Medical University, 1-1 Daigaku, Uchinada, Ishikawa 920-0293, Japan

Xie T, Wang ZG, Zhang JL, Liu H. X-ray repair cross-complementing group 1 polymorphisms and hepatocellular carcinoma: A meta-analysis. *World J Gastroenterol* 2012; 18(31): 4207-4214 Available from: URL: <http://www.wjgnet.com/1007-9327/full/v18/i31/4207.htm> DOI: <http://dx.doi.org/10.3748/wjg.v18.i31.4207>

INTRODUCTION

Hepatocellular carcinoma (HCC) is the fifth most common malignancy worldwide^[1]. It is accepted that the carcinogenesis of HCC is a multistep process, and multiple factors are involved in this complex process^[2]. Epidemiological studies have indicated that chronic hepatitis B virus (HBV), chronic hepatitis C virus (HCV), heavy cigarette smoking, and alcohol abuse are associated with the risk of HCC^[1]. The progression of HCC might result from a complex interaction of both environmental (including HBV or HCV infection) and genetic factors^[2]. Loss of genomic stability and the gene alterations resulting from endogenous and/or exogenous damage appear to be crucial molecular and pathogenic steps that occur early in the carcinogenesis process of HCC^[2]. Various enzymes and proteins involved in the DNA repair system play a pivotal role in maintaining the genome integrity in cells through the reversal of DNA damage^[3]. The mutations and single-nucleotide polymorphisms (SNPs) in corresponding DNA repair genes may impair their repair or reversal capacity and increase the risk of cancer^[4].

The X-ray repair cross-complementing group 1 (*XRCC1*) gene, located on chromosome 19 (19q13.2), encodes a crucial scaffold protein that is closely associated with the base excision repair (BER) pathway^[5]. The *XRCC1* protein is responsible for the repair of oxidative DNA damage and single-strand breaks through interacting with DNA ligase 3 and the complexes with DNA polymerase and poly (adenosine diphosphate-ribose) polymerase (PARP)^[6,7]. Although more than 300 validated SNPs have been identified and described in the *XRCC1* gene, only three common SNPs have been extensively studied: Arg194Trp (rs1799782, C/T substitution at position 26304 on exon 6), Arg280His (rs25489, G/A substitution at position 27466 on exon 9), and Arg399Gln (rs25487, G/A substitution at position 28152 on exon 10)^[8]. Numerous studies have focused on the association between these *XRCC1* polymorphisms and development of cancer in humans^[9-16]. *XRCC1* SNPs have been shown in the previous meta-analyses to be significantly associated with risk of gastric^[9], breast^[12] and lung^[16] cancer.

Over the past decade, a considerable number of epidemiological studies have focused on the association between *XRCC1* polymorphisms and HCC risk. However, the results remain either controversial or inconclusive. To address these issues, we carried out a systematic review and meta-analysis of all eligible case-control studies

to estimate the risk of HCC associated with the *XRCC1* polymorphisms.

MATERIALS AND METHODS

Literature search

To identify the studies eligible for inclusion in the systematic review and meta-analysis, the following electronic databases were searched: PubMed, Embase, Wanfang (Chinese), VIP (Chinese) and the Chinese National Knowledge Infrastructure (CNKI) (up to March 1, 2012). The following keywords were used: “X-ray repair cross-complementing group 1” or “XRCC1 and haplotype or polymorphism” and “liver cancer” or “hepatocellular carcinoma”. The search was performed without restriction on language and all studies on human subjects were included. Additional studies were identified by a manual search of the references of the original studies. Of the studies with overlapping data published by the same investigators, only the most recent or complete study was included in this meta-analysis.

Inclusion/exclusion criteria

The included studies had to meet all the following criteria: (1) evaluated *XRCC1* polymorphisms and HCC risk; (2) case-control or cohort studies; and (3) contained sufficient published data for estimating an odds ratio (OR) with a 95% confidence interval (CI). The polymorphisms, for which eligible data were reported in at least three published studies, were included into the meta-analysis.

Data extraction

Information was carefully extracted independently by two investigators according to the inclusion criteria. The following data were collected: the first author's surname, year of publication, country of origin, ethnicity, mean age and type of cases and controls, and the number of cases and controls for each genotype of *XRCC1* polymorphisms. Ethnic origins were categorized as Caucasian, Asian, and African. If a study did not present the ethnic origin, or if it was not possible to separate the participants into a mono-ethnic group according to the phenotypes, the group reported was termed “mixed”.

Statistical analysis

The Hardy-Weinberg equilibrium (HWE) in the control groups was calculated in our meta-analysis to determine selective bias in the control population. The χ^2 goodness-of-fit test was used to identify deviation from HWE ($P < 0.05$ was considered significant).

Associations between HCC risk and SNPs in Arg194-Trp, Arg280His, and Arg399Gln were estimated by ORs and 95% CI. The statistical significance of the summary OR was determined with the Z test according to Thakkinian's method^[17] ($P < 0.05$). For each polymorphism, the wild-type allele was set as A and the risk allele as B. The

Table 1 Characteristics of eligible studies included in this study

Ref.	Country (ethnicity)	Genotyping method	Cases/controls	Source of controls	Type of controls	Polymorphisms of <i>XRCC1</i> gene
Tang <i>et al.</i> ^[26]	China (Asian)	PCR-RFLP	150/150	Hospital	Age matched, male and healthy	Arg194Trp, Arg280His, Arg399Gln
Bo <i>et al.</i> ^[30]	China (Asian)	PCR-RFLP	130/130	Hospital	Age matched and healthy	Arg194Trp
Zeng <i>et al.</i> ^[29]	China (Asian)	TaqMan SNP Genotyping	545/515	Hospital	Age, sex and residence matched and without cancer	Arg194Trp, Arg280His, Arg399Gln
Kiran <i>et al.</i> ^[22]	India (Asian)	PCR-RFLP	63/155	Hospital	HBsAg (-), anti-HCV (-), and without renal or hepatic disease	Arg194Trp, Arg280His, Arg399Gln
Wu <i>et al.</i> ^[27]	China (Asian)	PCR-RFLP	100/60	Hospital	Age and sex matched, healthy and HBsAg (-)	Arg280His
Ren <i>et al.</i> ^[25]	China (Asian)	PCR-RFLP	50/92	Hospital	Healthy and HBsAg (-)	Arg399Gln
Borentain <i>et al.</i> ^[20]	France (Caucasian)	Sequencing	56/89	Population	Healthy and without chronic liver disease	Arg399Gln
Kirk <i>et al.</i> ^[23]	Gambia (African)	PCR-RFLP	195/352	Hospital	Age and sex matched, normal α -fetoprotein levels, and without clinical evidence of liver disease	Arg399Gln
Long <i>et al.</i> ^[24]	China (Asian)	PCR-RFLP	140/536	Hospital	Age, sex and ethnicity matched and without cancer	Arg399Gln
Han <i>et al.</i> ^[21]	China (Asian)	PCR-RFLP	69/136	Population	Age, sex and residence matched	Arg399Gln
Yu <i>et al.</i> ^[28]	China (Asian)	PCR-RFLP	577/389	Population	Age and sex matched, HBsAg (+), and without HCC	Arg399Gln

XRCC1: X-ray repair cross-complementing group 1; PCR-RFLP: Polymerase chain reaction-restriction fragment length polymorphism; SNP: Single nucleotide polymorphism; HBsAg: Hepatitis B surface antigen; HCV: Hepatitis C virus; HCC: Hepatocellular carcinoma.

A and B allele frequencies were first compared between the case and the control groups. Then, we evaluated the multiple comparisons including BB *vs* AA (codominant model), AB *vs* AA (codominant model), BB *vs* AB, (BB + AB) *vs* AA (dominant model), BB *vs* (AB + AA) (recessive model), and (BB + AA) *vs* AB (complete overdominant model).

The χ^2 -based Q statistic was used to test for the between-study heterogeneity^[18]. When $P < 0.1$ or $I^2 > 50\%$, the heterogeneity was considered statistically significant^[19]. The data were analyzed using a random-effects model if heterogeneity existed. In the absence of heterogeneity, a fixed-effects model was used. Sensitivity analysis was performed to examine the effect of excluded specific studies, such as studies with controls that were not in HWE. The statistical significance of the summary OR was determined with the Z test ($P < 0.05$).

The publication bias was assessed qualitatively by the Begg's rank correlation method and the Egger's weighted regression method ($P < 0.05$). All statistical analyses were performed with Stata software (version 11.0; Stata Corporation, College Station, TX) using two-sided P values.

RESULTS

With the retrieval strategy, 60 potentially relevant papers were extracted (12 from PubMed, 15 from Embase, 16 from Wanfang, 3 from VIP and 14 from CNKI). Forty-seven studies were subjected to a full-text review and excluded according to the selection criteria stated above. Eleven studies were identified that examined the association between the *XRCC1* polymorphisms and HCC risk^[20-30]. Table 1 summarizes the data from these studies,

which included 2075 HCC patients and 2604 control subjects. The HCC was defined according to the clinical pathological examinations. Those with no clinical evidence of HCC served as controls.

These studies focused on three identified polymorphisms of the *XRCC1* gene: Arg194Trp, Arg280His, and Arg399Gln. The genotypes and allelic frequencies of these three *XRCC1* polymorphisms in the eligible studies are listed in Table 2. Three studies which respectively analyzed the Arg194Trp^[30], the Arg280His^[22], and the Arg399Gln polymorphisms^[29] significantly deviated from the HWE ($P < 0.05$).

Arg194Trp

The Arg194Trp polymorphism is located on exon 6 of the *XRCC1* gene and has been investigated in association studies in patients with HCC. A positive association was initially noted by Kiran *et al.*^[22] who reported an excess frequency of the Arg/Trp genotype in an Indian sample of HCC patients *vs* controls. Furthermore, Bo *et al.*^[30] reported significant associations among a Chinese population between HCC and the Arg/Trp and Trp/Trp genotypes. However, another two studies of a Chinese population reported no association between the Arg194Trp polymorphism of the *XRCC1* gene and HCC^[26,31].

In this meta-analysis, four studies focused on the Arg194Trp polymorphism of *XRCC1* gene in an Asian population, including 888 HCC cases and 938 controls. An evaluation of the association between the Arg194Trp polymorphism and HCC risk is presented in Table 3. No significant association was detected between HCC and the Arg/Trp or Trp/Trp genotype (the Arg/Trp *vs* the Arg/Arg model, fixed-effects OR: 1.30, 95% CI:

Table 2 Genotype distribution of X-ray repair cross-complementing group 1 polymorphisms used in this study

Polymorphism	Ref.	Ethnicity	Case			Control			HWE
Arg194Trp			Arg/Arg	Arg/Trp	Trp/Trp	Arg/Arg	Arg/Trp	Trp/Trp	
	Tang <i>et al.</i> ^[26]	Asian	94	41	15	81	58	11	0.88
	Bo <i>et al.</i> ^[30]	Asian	94	31	5	116	12	2	0.02
	Zeng <i>et al.</i> ^[29]	Asian	305	200	40	275	202	38	0.91
	Kiran <i>et al.</i> ^[22]	Asian	8	43	12	27	64	52	0.35
Arg280His			Arg/Arg	Arg/His	His/His	Arg/Arg	Arg/His	His/His	
	Tang <i>et al.</i> ^[26]	Asian	138	11	1	123	26	1	0.76
	Zeng <i>et al.</i> ^[29]	Asian	451	86	8	423	89	3	0.46
	Wu <i>et al.</i> ^[27]	Asian	76	23	1	47	13	0	0.34
	Kiran <i>et al.</i> ^[22]	Asian	19	30	14	91	29	35	0.00
Arg399Gln			Arg/Arg	Arg/Gln	Gln/Gln	Arg/Arg	Arg/Gln	Gln/Gln	
	Tang <i>et al.</i> ^[26]	Asian	41	94	15	84	54	12	0.43
	Zeng <i>et al.</i> ^[29]	Asian	312	196	37	309	169	37	0.04
	Kiran <i>et al.</i> ^[22]	Asian	25	33	5	45	70	27	0.98
	Ren <i>et al.</i> ^[25]	Asian	32	14	4	46	41	5	0.28
	Borentain <i>et al.</i> ^[20]	Caucasian	27	21	8	27	43	19	0.80
	Kirk <i>et al.</i> ^[23]	African	160	31	4	300	48	4	0.19
	Long <i>et al.</i> ^[24]	Asian	72	63	5	362	159	15	0.62
	Han <i>et al.</i> ^[21]	Asian	34	28	7	58	63	15	0.73
	Yu <i>et al.</i> ^[28]	Asian	301	223	53	218	143	28	0.49

HWE: Hardy-Weinberg equilibrium.

0.68-2.48, $P = 0.42$; the Trp/Trp *vs* the Arg/Arg model, fixed-effects OR: 1.03, 95% CI: 0.71-1.49, $P = 0.86$). Furthermore, no significant results were observed in any other genetic models. Sensitivity analysis was performed after excluding the study conducted by Bo *et al.*^[30], because the controls were not in HWE.

Arg280His

The Arg280His allele is located on exon 9 of the XRCC1 gene. A study by Kiran *et al.*^[22] in an Indian population showed that the Arg280His polymorphism of the XRCC1 gene was positively associated with HCC. The Arg/His genotype was associated with a significantly increased risk of HCC. However, three studies in Chinese populations reported no association between the Arg280His polymorphism of the XRCC1 gene and HCC^[28,29,31].

In this study, the four studies on the Arg280His polymorphism of the XRCC1 gene among Asian populations, included 858 HCC cases and 880 controls. Overall, significant association was found for the His/His *vs* Arg/Arg model (fixed-effects OR: 1.96, 95% CI: 1.03-3.75, $P = 0.04$) (Table 3). However, sensitivity analysis after exclusion of the study^[22] with controls not in HWE did not suggest the association (the His/His *vs* Arg/Arg model, fixed-effects OR: 2.06, 95% CI: 0.67-6.25, $P = 0.20$). No significant results were observed in any other genetic models in the overall analysis and sensitivity analysis.

Arg399Gln

The Arg399Gln allele is located on the exon 10 of the XRCC1 gene. Studies by Long *et al.*^[24] and Tang *et al.*^[26] reported an excess frequency of the Arg/Gln genotype of the XRCC1 gene in HCC patients *vs* controls in Chinese populations. However, this observation was not replicated in four other studies^[21,25,30,31] of the Chinese population. A positive association between the Arg/Gln

genotype and a significantly increased risk of HCC in the African population was reported by Kirk *et al.*^[23]. The study by Borentain *et al.*^[20] in a Caucasian population showed an increased frequency of the Arg/Arg genotype in HCC patients *vs* controls. Moreover, Kiran *et al.*^[22] reported significant associations among an Indian population between HCC and the Gln/Gln genotype acting as a protective genotype for HCC.

We retrieved nine studies involving 1845 HCC cases and 2401 controls of different populations (one Caucasian, one African, and seven Asian) reporting detailed allele frequencies^[20-26,28,29]. The overall meta-analysis did not suggest any association between the XRCC1 Arg399Gln polymorphism and HCC susceptibility in all genetic models (Table 3). For example, the ORs of the HCC risks associated with the Arg399Gln polymorphism were 1.07 (random-effects, 95% CI: 0.84-1.34, $P = 0.56$) for the comparison of Arg allele *vs* Gln allele, 1.05 (random-effects, 95% CI: 0.71-1.56, $P = 0.77$) for the comparison of Gln/Gln *vs* Arg/Arg genotype, and 1.13 (random-effects, 95% CI: 0.80-1.57, $P = 0.71$) for the comparison of Arg/Gln *vs* Arg/Arg. The results were consistent after we excluded one study^[29] with controls not in HWE.

By stratifying the meta-analysis by ethnicity, no significant association between XRCC1 Arg399Gln polymorphism and HCC risk was observed in the Asian subgroup, which included 1594 HCC cases and 1960 controls. Sensitivity analysis was performed after one study was excluded^[29]. This did not alter the pattern of the results.

Publication bias

The Begg's rank correlation method and Egger's weighted regression method were used to assess publication

Table 3 Associations between Arg194Trp, Arg280His and Arg399Gln polymorphisms of X-ray repair cross-complementing group 1 gene and hepatocellular carcinoma risk shown in the meta-analysis

	<i>n</i> ¹	Cases/controls	OR (95% CI)	Significance (<i>Z</i> test) ²		Heterogeneity (<i>Q</i> test)		
				<i>Z</i>	<i>P</i>	<i>Q</i>	<i>I</i> ² (%)	<i>P</i>
Arg194Trp								
All	4	888/938						
Trp vs Arg			1.08 (0.73-1.60)	0.39	0.69	13.64	78.0	0.00
Trp/Trp vs Arg/Arg			1.03 (0.71-1.49)	0.17	0.86	2.18	0.0	0.53
Arg/Trp vs Arg/Arg			1.30 (0.68-2.48)	0.79	0.42	17.86	83.2	0.00
Trp/Trp vs Arg/Trp			0.88 (0.41-1.89)	0.31	0.75	9.95	69.9	0.01
Arg/Trp + Trp/Trp vs Arg/Arg			1.24 (0.70-2.20)	0.76	0.44	15.45	80.6	0.00
Trp/Trp vs Arg/Trp + Arg/Arg			0.93 (0.50-1.74)	0.21	0.83	7.45	59.7	0.05
Trp/Trp + Arg/Arg vs Arg/Trp			0.72 (0.36-1.43)	0.92	0.36	23.78	87.4	0.00
All HWE	3	758/808						
Trp vs Arg			0.89 (0.76-1.05)	1.32	0.18	0.55	0.0	0.76
Trp/Trp vs Arg/Arg			0.96 (0.66-1.43)	0.18	0.85	0.39	0.0	0.82
Arg/Trp vs Arg/Arg			0.94 (0.56-1.60)	0.20	0.84	6.57	69.6	0.03
Trp/Trp vs Arg/Trp			0.87 (0.36-2.13)	0.29	0.77	9.95	79.9	0.00
Arg/Trp + Trp/Trp vs Arg/Arg			0.88 (0.72-1.09)	1.12	0.26	2.88	30.6	0.23
Trp/Trp vs Arg/Trp + Arg/Arg			0.83 (0.43-1.58)	0.56	0.57	5.86	65.9	0.05
Trp/Trp + Arg/Arg vs Arg/Trp			0.92 (0.47-1.81)	0.23	0.81	14.09	85.8	0.00
Arg280His								
All	4	858/880						
His vs Arg			1.03 (0.62-1.70)	0.11	0.90	12.73	76.4	0.00
His/His vs Arg/Arg			1.96 (1.03-3.75)	2.06	0.04	0.44	0.0	0.93
Arg/His vs Arg/Arg			1.16 (0.47-2.86)	0.33	0.74	26.36	88.6	0.00
His/His vs Arg/His			1.13 (0.30-4.22)	0.19	0.85	7.01	57.2	0.07
Arg/His + His/His vs Arg/Arg			1.10 (0.52-2.33)	0.25	0.80	20.16	85.1	0.00
His/His vs Arg/His + Arg/Arg			1.23 (0.69-2.21)	0.73	0.46	1.63	0.0	0.65
His/His + Arg/Arg vs Arg/His			0.90 (0.38-2.11)	0.23	0.81	24.71	87.9	0.00
All HWE	3	795/725						
His vs Arg			0.83 (0.49-1.41)	0.67	0.50	5.44	63.2	0.06
His/His vs Arg/Arg			2.06 (0.67-6.25)	1.28	0.20	0.43	0.0	0.80
Arg/His vs Arg/Arg			0.74 (0.43-1.30)	1.03	0.30	5.08	60.6	0.07
His/His vs Arg/His			2.54 (0.80-8.04)	1.59	0.11	0.07	0.0	0.96
Arg/His + His/His vs Arg/Arg			0.78 (0.44-1.36)	0.86	0.39	5.40	63.0	0.06
His/His vs Arg/His + Arg/Arg			2.11 (0.69-6.43)	1.32	0.18	0.36	0.0	0.83
His/His + Arg/Arg vs Arg/His			1.34 (0.78-2.31)	1.07	0.28	4.95	59.6	0.08
Arg399Gln								
All	9	1845/2401						
Gln vs Arg			1.07 (0.84-1.34)	0.57	0.56	33.12	75.8	0.00
Gln/Gln vs Arg/Arg			1.05 (0.71-1.56)	0.29	0.77	14.84	46.1	0.06
Arg/Gln vs Arg/Arg			1.13 (0.80-1.57)	0.71	0.47	39.18	79.6	0.00
Gln/Gln vs Arg/Gln			0.93 (0.71-1.21)	0.52	0.60	6.32	0.0	0.61
Arg/Gln + Gln/Gln vs Arg/Arg			1.11 (0.80-1.54)	0.63	0.52	41.34	80.6	0.00
Gln/Gln vs Arg/Gln + Arg/Arg			1.00 (0.78-1.28)	0.03	0.97	7.87	0.0	0.44
Gln/Gln + Arg/Arg vs Arg/Gln			0.85 (0.63-1.15)	1.02	0.30	32.13	75.1	0.00
All HWE	8	1300/1886						
Gln vs Arg			1.06 (0.79-1.41)	0.40	0.69	32.61	78.5	0.00
Gln/Gln vs Arg/Arg			1.06 (0.65-1.73)	0.25	0.80	14.61	52.1	0.04
Arg/Gln vs Arg/Arg			1.10 (0.73-1.68)	0.49	0.62	38.85	82.0	0.00
Gln/Gln vs Arg/Gln			0.96 (0.70-1.30)	0.25	0.79	6.15	0.0	0.52
Arg/Gln + Gln/Gln vs Arg/Arg			1.09 (0.72-1.64)	0.43	0.66	40.82	82.9	0.00
Gln/Gln vs Arg/Gln + Arg/Arg			1.02 (0.77-1.37)	0.19	0.84	7.72	9.3	0.35
Gln/Gln + Arg/Arg vs Arg/Gln			0.86 (0.60-1.24)	0.77	0.44	31.84	78.0	0.00
Asian	7	1594/1960						
Gln vs Arg			1.12 (0.87-1.44)	0.89	0.37	25.85	76.8	0.00
Gln/Gln vs Arg/Arg			1.13 (0.86-1.48)	0.92	0.35	10.48	42.7	0.10
Arg/Gln vs Arg/Arg			1.22 (0.83-1.78)	1.04	0.29	33.10	81.9	0.00
Gln/Gln vs Arg/Gln			0.92 (0.69-1.21)	0.58	0.56	5.83	0.0	0.44
Arg/Gln + Gln/Gln vs Arg/Arg			1.20 (0.83-1.73)	0.98	0.32	33.84	82.3	0.00
Gln/Gln vs Arg/Gln + Arg/Arg			1.02 (0.79-1.33)	0.20	0.83	5.96	0.0	0.42
Gln/Gln + Arg/Arg vs Arg/Gln			0.81 (0.57-1.13)	1.21	0.22	28.55	79.0	0.00
Asian HWE	6	1049/1445						
Gln vs Arg			1.12 (0.81-1.54)	0.69	0.49	24.80	79.8	0.00
Gln/Gln vs Arg/Arg			1.16 (0.69-1.97)	0.59	0.55	9.89	49.4	0.07
Arg/Gln vs Arg/Arg			1.22 (0.74-2.00)	0.78	0.43	32.23	84.5	0.00
Gln/Gln vs Arg/Gln			0.95 (0.68-1.32)	0.31	0.76	5.70	12.3	0.33

Arg/Gln + Gln/Gln <i>vs</i> Arg/Arg	1.20 (0.74-1.94)	0.75	0.45	32.66	84.7	0.00
Gln/Gln <i>vs</i> Arg/Gln + Arg/Arg	1.06 (0.78-1.46)	0.41	0.67	5.69	12.1	0.33
Gln/Gln + Arg/Arg <i>vs</i> Arg/Gln	0.80 (0.51-1.26)	0.93	0.35	27.84	82.0	0.00

¹Number of studies; ²Random-effects model was used when *P* value for heterogeneity test $P < 0.1$ or $I^2 > 50\%$; otherwise, fixed-effects model was used. HWE: Hardy-Weinberg equilibrium; OR: Odds ratio.

bias. There was no evidence of publication bias for these polymorphisms.

DISCUSSION

The *XRCC1* protein is a key molecule of BER in the DNA repair process, which plays a key role in the integrity and stability of the genome and the pathogenesis and progression of human cancers^[31]. Polymorphisms that can alter *XRCC1* expression and function may contribute to the risk of cancers. Several studies have been conducted in recent years to evaluate the association between the *XRCC1* SNPs and HCC risk predisposition in different ethnic populations, but the results have been conflicting^[20-30].

In the present study, we performed a systematic review and meta-analysis to examine the association between three *XRCC1* gene polymorphisms and HCC risk. These three polymorphisms of the *XRCC1* gene result in nonconservative amino-acid changes at evolutionary conserved regions: a C to T substitution in codon 194 of exon 6 (Arg to Trp), a G to A substitution in codon 280 of exon 9 (Arg to His), and a G to A substitution in codon 399 of exon 10 (Arg to Gln)^[32]. Although the functional effects of these nonsynonymous polymorphisms in *XRCC1* are not well known, the nature of the amino acid substitutions may cause functional changes in the *XRCC1* protein and impair DNA repair efficiency or accuracy, which could be implicated in the risk of cancer. However, previous meta-analysis showed inconsistent results in the association between the polymorphisms of the *XRCC1* gene and the risk of cancers.

These previous meta-analysis found that the carriers of homozygous Trp/Trp variant genotype of the Arg-194Trp polymorphism had an increased risk of gastric cancer^[9] and other cancers, especially lung cancer and esophageal cancer, in the Chinese mainland population^[11]. However, no associations were observed between the Arg194Trp polymorphism with skin^[15], colorectal^[33], and prostate cancer^[34], and nasopharyngeal carcinoma^[10]. The Arg280His polymorphism was associated with an approximate 3.5-fold increase in skin cancer risk in homozygote codominant and recessive models^[15]. However, the Arg280His polymorphism was not found to be a statistically significant risk factor for gastric cancer^[9] and nasopharyngeal carcinoma^[10]. The Gln/Gln genotype of the Arg399Gln polymorphism was associated with an increased risk of prostate cancer^[34] and nasopharyngeal carcinoma^[10], but was not correlated with skin^[15], gastric^[9], and colorectal^[33] cancer susceptibility for all genetic models. For prostate cancer, Wei *et al.*^[34] concluded that the Gln allele of the Arg399Gln polymorphism might be a low-

penetrant risk factor for prostate cancer only in Asian men, but was not related to overall prostate cancer risk.

It is difficult to interpret the reasons for these inconsistent results; nonetheless, several factors may influence the function of these polymorphisms of the *XRCC1* gene in various ways, including variation in the exposure of different populations to carcinogens and variation in different types of DNA damage associated with the initiation of different cancers. Further research is needed to clarify this inconsistency.

There has been no previous meta-analysis of the effect of the Arg194Trp and Arg280His polymorphisms of the *XRCC1* gene on the risk of HCC. Our data suggested that the Arg194Trp polymorphism might not be a risk factor for HCC. For the *XRCC1* Arg280His polymorphism, our meta-analysis on the available studies showed that the His/His genotype was significantly associated with increased HCC risk. However, the sensitivity analysis after exclusion of the study with controls not in HWE did not suggest this association. Our meta-analysis does not strongly support the association between the His/His genotype of the *XRCC1* Arg280His polymorphism and the increased risk in HCC. Although there is some evidence of association between the *XRCC1* Arg280His polymorphism and HCC, the above finding deserves further and more rigorous association studies. A previous meta-analysis study found that the Arg399Gln polymorphism had no association with HCC^[13], which is similar to our current finding. Recently, another variant in the *XRCC1* gene located in the 5'-untranslated region, -77 T to C, was identified^[35] and indicated as a genetic determinant for developing breast cancer^[14]. However, there is a lack of association study between the -77 T/C polymorphism of the *XRCC1* gene and HCC risk.

Similar to other systematic reviews and meta-analyses, there were some limitations in this study. Firstly, the sample sizes in the overall and subgroup analyses were small. Secondly, only two published studies included in this meta-analysis focused on the Arg399Gln polymorphism and its relationship with HCC in Caucasian and African populations. Thirdly, the sources of heterogeneity that existed among the studies for most polymorphisms were not addressed. Finally, this meta-analysis was based on unadjusted data, whereas a more precise analysis could be performed if individual data were available. Additional well-designed, more-detailed studies with larger populations and different ethnicities are needed to further evaluate the associations.

In conclusion, The *XRCC1* Arg194Trp and Arg399Gln polymorphisms are not associated with HCC risk. More rigorous association studies are needed to clarify the involvement of *XRCC1* Arg280His polymorphism in

HCC susceptibility. No publication biases regarding these three evaluated polymorphisms were found in this meta-analysis.

COMMENTS

Background

Hepatocellular carcinoma (HCC) is the fifth most common malignancy worldwide. The X-ray repair cross-complementing group 1 (XRCC1) gene encodes a crucial scaffold protein that is responsible for the repair of oxidative DNA damage and single-strand breaks. Many studies have explored the association between the XRCC1 polymorphisms and HCC risk, but the results remain either controversial or inconclusive. To address these issues, the authors carried out a systematic review and meta-analysis of all eligible case-control studies to estimate the association between the XRCC1 polymorphisms and the risk of HCC.

Research frontiers

To date, a number of studies have assessed the association between the XRCC1 polymorphisms and HCC risk among different populations; however, the results have been inconsistent and inconclusive.

Innovations and breakthroughs

This meta-analysis suggested that none of the Arg194Trp and Arg399Gln polymorphisms of XRCC1 were significantly associated with a risk of HCC. More rigorous association studies are needed to verify the involvement of XRCC1 Arg280His polymorphism in HCC susceptibility.

Applications

This meta-analysis showed that the Arg399Gln and Arg194Trp polymorphisms of the XRCC1 gene did not alter the susceptibility to HCC. The findings may provide valuable information about the etiology of HCC for both researchers and clinicians.

Peer review

This manuscript was a meta-analysis to analyze the association between X-ray repair cross-complementing group 1 polymorphisms and HCC. This is a scientifically interesting topic. Although the results show that this is a negative study, it is very important to systematically review these relevant reports.

REFERENCES

- Caldwell S, Park SH. The epidemiology of hepatocellular cancer: from the perspectives of public health problem to tumor biology. *J Gastroenterol* 2009; **44** Suppl 19: 96-101
- Sato K, Mori M. Evolving molecular mechanism-based strategies for control of hepatocellular carcinoma. *Curr Med Chem* 2011; **18**: 4375-4388
- Lahtz C, Pfeifer GP. Epigenetic changes of DNA repair genes in cancer. *J Mol Cell Biol* 2011; **3**: 51-58
- Jiang J, Zhang X, Yang H, Wang W. Polymorphisms of DNA repair genes: ADPRT, XRCC1, and XPD and cancer risk in genetic epidemiology. *Methods Mol Biol* 2009; **471**: 305-333
- Thompson LH, Bachinski LL, Stallings RL, Dolf G, Weber CA, Westerveld A, Siciliano MJ. Complementation of repair gene mutations on the hemizygous chromosome 9 in CHO: a third repair gene on human chromosome 19. *Genomics* 1989; **5**: 670-679
- Dianov GL, Sleeth KM, Dianova II, Allinson SL. Repair of abasic sites in DNA. *Mutat Res* 2003; **531**: 157-163
- Thompson LH, West MG. XRCC1 keeps DNA from getting stranded. *Mutat Res* 2000; **459**: 1-18
- Whitehouse CJ, Taylor RM, Thistlethwaite A, Zhang H, Karimi-Busheri F, Lasko DD, Weinfeld M, Caldecott KW. XRCC1 stimulates human polynucleotide kinase activity at damaged DNA termini and accelerates DNA single-strand break repair. *Cell* 2001; **104**: 107-117
- Chen B, Zhou Y, Yang P, Wu XT. Polymorphisms of XRCC1 and gastric cancer susceptibility: a meta-analysis. *Mol Biol Rep* 2012; **39**: 1305-1313
- Huang GL, Guo HQ, Yu CY, Liu XY, Li BB, Wu JJ, He ZW. XRCC1 polymorphisms and risk of nasopharyngeal carcinoma: a meta-analysis. *Asian Pac J Cancer Prev* 2011; **12**: 2329-2333
- Huang J, Zhang J, Zhao Y, Liao B, Liu J, Li L, Liao M, Wang L. The Arg194Trp polymorphism in the XRCC1 gene and cancer risk in Chinese Mainland population: a meta-analysis. *Mol Biol Rep* 2011; **38**: 4565-4573
- Huang Y, Li L, Yu L. XRCC1 Arg399Gln, Arg194Trp and Arg280His polymorphisms in breast cancer risk: a meta-analysis. *Mutagenesis* 2009; **24**: 331-339
- Liu F, Li B, Wei Y, Yan L, Wen T, Zhao J, Xu M. XRCC1 genetic polymorphism Arg399Gln and hepatocellular carcinoma risk: a meta-analysis. *Liver Int* 2011; **31**: 802-809
- Liu L, Yuan P, Liu L, Wu C, Zhang X, Guo H, Zhong R, Xu Y, Wu J, Duan S, Rui R, Wu T, Nie S, Miao X, Lin D. A functional -771 G>C polymorphism in XRCC1 is associated with risk of breast cancer. *Breast Cancer Res Treat* 2011; **125**: 479-487
- Zhang H, Li W, Franklin MJ, Dudek AZ. Polymorphisms in DNA repair gene XRCC1 and skin cancer risk: a meta-analysis. *Anticancer Res* 2011; **31**: 3945-3952
- Zheng H, Wang Z, Shi X, Wang Z. XRCC1 polymorphisms and lung cancer risk in Chinese populations: a meta-analysis. *Lung Cancer* 2009; **65**: 268-273
- Thakkinstian A, McElduff P, D'Este C, Duffy D, Attia J. A method for meta-analysis of molecular association studies. *Stat Med* 2005; **24**: 1291-1306
- Zintzaras E, Ioannidis JP. Heterogeneity testing in meta-analysis of genome searches. *Genet Epidemiol* 2005; **28**: 123-137
- Higgins JP, Thompson SG. Quantifying heterogeneity in a meta-analysis. *Stat Med* 2002; **21**: 1539-1558
- Borentain P, Gérolami V, Ananian P, Garcia S, Noundou A, Botta-Fridlund D, Le Treut YP, Bergé-Lefranc JL, Gérolami R. DNA-repair and carcinogen-metabolising enzymes genetic polymorphisms as an independent risk factor for hepatocellular carcinoma in Caucasian liver-transplanted patients. *Eur J Cancer* 2007; **43**: 2479-2486
- Han YN, Yang JL, Zeng SG, Wu YQ. Study on the association of human XRCC1-399 single nucleotide polymorphism and primary hepatocytic carcinoma. *Ganzang* 2004; **9**: 235-237
- Kiran M, Saxena R, Chawla YK, Kaur J. Polymorphism of DNA repair gene XRCC1 and hepatitis-related hepatocellular carcinoma risk in Indian population. *Mol Cell Biochem* 2009; **327**: 7-13
- Kirk GD, Turner PC, Gong Y, Lesi OA, Mendy M, Goedert JJ, Hall AJ, Whittle H, Hainaut P, Montesano R, Wild CP. Hepatocellular carcinoma and polymorphisms in carcinogen-metabolizing and DNA repair enzymes in a population with aflatoxin exposure and hepatitis B virus endemicity. *Cancer Epidemiol Biomarkers Prev* 2005; **14**: 373-379
- Long XD, Ma Y, Wei YP, Deng ZL. Polymorphism of DNA repair gene XRCC1 and risk of hepatocellular carcinoma. *Guangxi Yike Daxue Xuebao* 2004; **21**: 313-315
- Ren Y, Wang D, Li Z, Xin Y, Yin J, Zhang B, Ding H, Li N. Study on the Relationship between Gene XRCC1 Codon 399 Single Nucleotide Polymorphisms and Primary Hepatic Carcinoma in Han Nationality. *Linchuang Ganzangbing Zazhi* 2008; **24**: 361-364
- Tang Y, Li X, Liu T, Yang J, Luo J, Liang Z. Genetic polymorphisms of DNA repair genes in patients with hepatocellular carcinoma. *Shandong Yiyao* 2011; **51**: 19-20
- Wu H, Yang Z, Xie Y, Kuang Z, Luo X, Liang A, Luo J. Correlation between DNA repair gene XRCC1 Arg280His polymorphism and susceptibility to hepatocellular carcinoma in Fusui county of Guangxi. *Zhongguo Xiandai Yixue Zazhi* 2009; **19**: 2737-2740, 2743
- Yu MW, Yang SY, Pan JJ, Lin CL, Liu CJ, Liaw YF, Lin SM, Chen PJ, Lee SD, Chen CJ. Polymorphisms in XRCC1 and glutathione S-transferase genes and hepatitis B-related hepatocellular carcinoma. *J Natl Cancer Inst* 2003; **95**: 1485-1488

- 29 **Zeng X**, Yu H, Qiu X, Ji L, Li L. A case-control study of polymorphism of XRCC1 gene and the risk of hepatocellular carcinoma. *Zhongguo Jibing Kongzhi Zazhi* 2010; **14**: 760-763
- 30 **Bo W**, Zhang G, Li D, Wang X, Liang T. Polymorphisms of DNA repair gene XRCC1 and susceptibility to hepatic cancer. *Xiandai Zhongliu Yixue* 2011; **19**: 1724-1726
- 31 **Poehlmann A**, Roessner A. Importance of DNA damage checkpoints in the pathogenesis of human cancers. *Pathol Res Pract* 2010; **206**: 591-601
- 32 **Shen MR**, Jones IM, Mohrenweiser H. Nonconservative amino acid substitution variants exist at polymorphic frequency in DNA repair genes in healthy humans. *Cancer Res* 1998; **58**: 604-608
- 33 **Gsur A**, Bernhart K, Baierl A, Feik E, Führlinger G, Hofer P, Leeb G, Mach K, Micksche M. No association of XRCC1 polymorphisms Arg194Trp and Arg399Gln with colorectal cancer risk. *Cancer Epidemiol* 2011; **35**: e38-e41
- 34 **Wei B**, Zhou Y, Xu Z, Ruan J, Zhu M, Jin K, Zhou D, Hu Q, Wang Q, Wang Z, Yan Z. XRCC1 Arg399Gln and Arg194Trp polymorphisms in prostate cancer risk: a meta-analysis. *Prostate Cancer Prostatic Dis* 2011; **14**: 225-231
- 35 **Hao B**, Wang H, Zhou K, Li Y, Chen X, Zhou G, Zhu Y, Miao X, Tan W, Wei Q, Lin D, He F. Identification of genetic variants in base excision repair pathway and their associations with risk of esophageal squamous cell carcinoma. *Cancer Res* 2004; **64**: 4378-4384

S- Editor Gou SX L- Editor Ma JY E- Editor Li JY

Metabolic syndrome and gallstone disease

Li-Ying Chen, Qiao-Hua Qiao, Shan-Chun Zhang, Yu-Hao Chen, Guan-Qun Chao, Li-Zheng Fang

Li-Ying Chen, Qiao-Hua Qiao, Yu-Hao Chen, Guan-Qun Chao, Li-Zheng Fang, Department of Family Medicine, Sir Run Run Shaw Hospital, Zhejiang University, Hangzhou 310016, Zhejiang Province, China

Shan-Chun Zhang, Department of Epidemiology and Biostatistics, School of Public Health, Zhejiang University, Hangzhou 310058, Zhejiang Province, China

Author contributions: All the authors have made substantial contributions to the conception and design, acquisition of data, or analysis and interpretation of data, and the manuscript preparation or critical revision of important intellectual content; and all have read and approved the final version to be published.

Correspondence to: Li-Zheng Fang, MD, Professor, Department of Family Medicine, Sir Run Run Shaw Hospital, Zhejiang University, Hangzhou 310016, Zhejiang Province, China. hsh0906@163.com

Telephone: +86-571-86002116 Fax: +86-571-88984828

Received: February 25, 2012 Revised: May 18, 2012

Accepted: May 26, 2012

Published online: August 21, 2012

Abstract

AIM: To investigate the association between metabolic syndrome (MetS) and the development of gallstone disease (GSD).

METHODS: A cross-sectional study was conducted in 7570 subjects (4978 men aged 45.0 ± 8.8 years, and 2592 women aged 45.3 ± 9.5 years) enrolled from the physical check-up center of the hospital. The subjects included 918 patients with gallstones (653 men and 265 women) and 6652 healthy controls (4325 men and 2327 women) without gallstones. Body mass index (BMI), waist circumference, blood pressure, fasting plasma glucose (FPG) and serum lipids and lipoproteins levels were measured. Colorimetric method was used to measure cholesterol, high-density lipoprotein cholesterol (HDL-C) and low-density lipoprotein cholesterol (LDL-C). Dextrose oxidizing enzyme method was used to measure FPG. Subjects were asked to complete a questionnaire that enquired about the information on

demographic data, age, gender, histories of diabetes mellitus, hypertension, and chronic liver disease and so on. Metabolic syndrome was diagnosed according to the Adult Treatment Panel III (ATP III) criteria. Gallstones were defined by the presence of strong intraluminal echoes that were gravity-dependent or attenuated ultrasound transmission.

RESULTS: Among the 7570 subjects, the prevalence of the gallstone disease was 12.1% (13.1% in men and 10.2% in women). BMI, waist circumference, systolic blood pressure, diastolic blood pressure, fasting blood glucose and serum triglyceride (TG) in cases group were higher than in controls, while serum high-density lipid was lower than in controls. There were significant differences in the waist circumference, blood pressure, FPG and TG between cases and controls. In an age-adjusted logistic regression model, metabolic syndrome was associated with gallstone disease. The age-adjusted odds ratio of MetS for GSD in men was 1.29 [95% confidence interval (CI), 1.09-1.52; $P = 0.0030$], and 1.68 (95% CI, 1.26-2.25; $P = 0.0004$) in women; the overall age-adjusted odds ratio of MetS for GSD was 1.42 (95% CI, 1.23-1.64; $P < 0.0001$). The men with more metabolic disorders had a higher prevalence of gallstone disease, the trend had statistical significance ($P < 0.0001$). The presence of 5 components of the MetS increased the risk of gallstone disease by 3.4 times ($P < 0.0001$). The prevalence of GSD in women who had 5 components of MetS was 5 times higher than in those without MetS. The more the components of MetS, the higher the prevalence of GSD ($P < 0.0001$). The presence of 5 components of the MetS increased the risk of gallstone disease by 4.0 times.

CONCLUSION: GSD appears to be strongly associated with MetS, and the more the components of MetS, the higher the prevalence of GSD.

© 2012 Baishideng. All rights reserved.

Key words: Gallstone disease; Obesity; Hypertension;

Dyslipidemia; Metabolic syndrome

Peer reviewers: Vasily I Reshetnyak, MD, PhD, Professor, Scientist Secretary of the Scientific Research Institute of General Reanimatology, 25-2, Petrovka str., 107031 Moscow, Russia; Wen Xie, MD, PhD, Assistant Professor, Center for Pharmacogenetics, University of Pittsburgh School of Pharmacy, 656 Salk Hall, 3501 Terrace Street, Pittsburgh, PA 15261, United States

Chen LY, Qiao QH, Zhang SC, Chen YH, Chao GQ, Fang LZ. Metabolic syndrome and gallstone disease. *World J Gastroenterol* 2012; 18(31): 4215-4220 Available from: URL: <http://www.wjgnet.com/1007-9327/full/v18/i31/4215.htm> DOI: <http://dx.doi.org/10.3748/wjg.v18.i31.4215>

INTRODUCTION

China is one of the fastest developing countries. Rapid economic development and industrialization have brought about changes in traditional diets and increasingly sedentary lifestyles. Metabolic syndrome (MetS) is defined as a cluster of multiple cardiovascular risk factors, including central obesity, elevated fasting plasma glucose, high blood pressure, lower high-density lipid (HDL), and higher serum triglyceride (TG) levels. The prevalence of MetS has been increasing gradually in China. In 1992, the overall prevalence of MetS in China was 13.3% (12.7% in men and 14.2% in women)^[1]. By 2000, the prevalence of MetS had elevated to 15.1%; 13.6% in men and 16.6% in women^[2]. In 2009, a population-based cross-sectional survey in China showed that the crude and age-standardized prevalence of MetS was 31.5% and 30.5%, respectively^[3]. Numerous studies have indicated that MetS is closely associated with some common diseases, such as diabetes, hypertension, cardiovascular diseases, cancer, and gallstone disease. Consequently, the increasing prevalence of MetS may potentially associate with the increased prevalence of these diseases. Studies about the association between gallstone disease and MetS suggested that MetS is a risk factor for gallstone disease (GSD)^[4], and some studies concluded that GSD might be a component of MetS^[4,5] although it needs to be validated by more evidences.

GSD represents a significant burden for health care worldwide^[6] and is one of the most common disorders among the patients admitted to the emergency rooms with abdominal discomfort, epigastric pain, nausea, vomiting, loss of appetite, *etc*^[7]. Ethnicity and family traits are recognized as contributing factors^[8]. GSD is known to affect 60%-70% of native Americans and a proportionately smaller number of individuals of mixed hispanic/native American origin^[9]. The incidence of GSD is at least 10% among white adults in Western countries^[10], but it is lower in African Americans and East Asians^[9]. GSD is also on the rise and becoming a major health problem in China^[11,12]; according to the reported estimates that the prevalence of GSD increased from 4.3% in 1989 to as high as 10.7% in 1995^[12]. Risk factors associated with

cholelithiasis include female gender, age, obesity, diabetes, hyperlipidemia, rapid appetite loss, hepatitis C, cirrhosis, and high caloric intake^[9,13,14]. The association between GSD and MetS has been a focus of some recent studies. To the best of our knowledge, the prevalence of the disease and the association between the development of GSD and MetS are not fully elucidated. Moreover, there is currently only minimal data regarding the relationship between GSD and MetS in apparently healthy Asian people. This study aimed to establish if there is an association between the presence of MetS and the development of GSD. MetS is known to be strongly associated with lifestyle, and if MetS is proved to be related to gallstone, we may reduce the prevalence of gallstones through lifestyle interventions.

MATERIALS AND METHODS

Data resource and data collection

We conducted a cross-sectional study in 7570 subjects enrolled from the Physical Check-Up Center of the Sir Run Run Shaw Hospital. Among them, there were 4978 men, aged 45.0 ± 8.8 years, and 2592 women, aged 45.3 ± 9.5 years. The study protocol was approved by the Ethics Committee of the hospital. All the subjects signed the informed consent. And 918 (653 men and 265 women) subjects were found to have gallstones. The gallstone cases and controls consisted of a series of consecutive asymptomatic subjects. Exclusion criteria included histories of cholecystectomy, pancreatitis, sequela of clonorchis sinensis infection, gallbladder polyps, silt, dimly disease or gallbladder wall thickening, chronic kidney disease, pregnancy, and major gastrointestinal surgeries. Blood samples were collected via venipuncture from the study participants after they had fasted overnight for laboratory tests. Fasting plasma glucose (FPG), TG, total cholesterol, high-density lipoprotein cholesterol (HDL-C), and low-density lipoprotein cholesterol (LDL-C) concentrations were measured using the AEROSET analyze system (ADDO™, America). Colorimetric method was used to measure cholesterol, HDL-C and LDL-C. Dextrose oxidizing enzyme method was used to measure FPG. Ultrasonographic examinations were also done.

Questionnaire

Subjects were asked to complete a questionnaire that enquired for information on demographic data, age, gender, marital status, address, telephone, histories of diabetes mellitus, hypertension, chronic liver disease, hyperlipidemia, systemic diseases, gastrointestinal surgery (vagotomy gastrectomy for peptic ulcer, ileal resection for inflammatory bowel disease, or any other disease or cause), gravidity, and the use of oral contraceptives, any other medications, and family history.

Physical examination

Body weight of the subjects, dressed in light clothing

Table 1 Demographic and clinical characteristics of the study subjects (mean \pm SD) *n* (%)

Variables	Cases (<i>n</i> = 918)	Controls (<i>n</i> = 6652)	<i>P</i> values
Age (yr)	48.5 \pm 9.1	44.7 \pm 9.0	< 0.0001
Height (cm)	165.6 \pm 7.9	165.6 \pm 7.7	0.2791
Weight (kg)	72.6 \pm 11.3	69.4 \pm 12.2	< 0.0001
Body mass index (kg/m ²)	26.3 \pm 3.0	25.2 \pm 3.4	< 0.0001
Waist circumference (cm)	91.6 \pm 9.4	87.8 \pm 10.7	< 0.0001
Systolic blood pressure (mmHg)	123.6 \pm 14.3	119.8 \pm 14.5	< 0.0001
Diastolic blood pressure (mmHg)	74.1 \pm 9.8	72.2 \pm 10.4	< 0.0001
Fasting blood glucose (mmol/L)	5.39 \pm 1.37	5.11 \pm 1.04	< 0.0001
High density lipid (mg/L)	44.6 \pm 10.9	46.0 \pm 0.58	0.0004
Triglyceride (mg/L)	201.1 \pm 183.3	183.7 \pm 182.7	0.0069
Male	653 (71.1)	4325 (65.0)	0.0003
Larger waist circumference	673 (73.3)	3918 (58.9)	< 0.0001
Higher blood pressure	401 (43.7)	2072 (31.2)	< 0.0001
Higher FPG	146 (15.9)	600 (9.0)	< 0.0001
Lower high-density lipid	407 (44.3)	2842 (42.8)	0.3551
Higher triglyceride	473 (51.5)	3044 (45.8)	0.0010

Student *t* test was applied to compare the differences between cases and controls for all continuous variables. Larger waist circumference denotes waist circumference \geq 80 cm for females or \geq 90 cm for males; higher blood pressure denotes systolic blood pressure \geq 130 or diastolic blood pressure \geq 85 mmHg or drug treatment; raised fasting plasma glucose (FPG) denotes FPG \geq 5.6 mmol/L or drug treatment; raised triglyceride denotes triglyceride \geq 1.70 mmol/L or drug treatment; lower HDL-C denotes HDL < 1.29 mmol/L for females or < 1.03 mmol/L for males or drug treatment. χ^2 test was used to compare the differences between cases and controls for all category variables. HDL: High blood pressure; HDL-C: High-density lipoprotein cholesterol.

and without shoes, was measured to the nearest 0.10 kg. Height was measured to the nearest 0.5 cm. Body mass index (BMI) was calculated as weight (kg) divided by height (m) squared (kg/m²). Waist circumference (at the nearest 0.1 cm) was measured at the midpoint between the lower border of the rib cage and the iliac crest. Three blood pressure readings were obtained at 1-min intervals, and the second and third systolic and diastolic pressure readings were averaged and used in the analyses.

Diagnostic criteria

MetS was diagnosed using the Adult Treatment Panel III (ATP III) criteria. According to the ATP III criteria, MetS was defined as the presence of any three of the following five traits: (1) Abdominal obesity, defined as a waist circumference in men \geq 90 cm and in women \geq 80 cm; (2) Serum triglycerides \geq 150 mg/dL (1.7 mmol/L) or medicinal treatment for elevated TG; (3) Serum HDL cholesterol < 40 mg/dL (1.03 mmol/L) in men and < 50 mg/dL (1.29 mmol/L) in women or medication for low HDL-C; (4) Blood pressure \geq 130/85 mmHg or medication for high blood pressure; and (5) Fasting plasma glucose (FPG) \geq 100 mg/dL (5.6 mmol/L) or

Table 2 Association of metabolic syndrome with human gallstone *n* (%)

MetS status	Gallstone status		OR (95% CI)	<i>P</i> values
	Cases	Controls		
Male				
Non-MetS	343 (11.6)	2600 (88.4)	1.29 (1.09-1.52)	0.0030
MetS	310 (15.2)	1725 (84.8)		
Female				
Non-MetS	169 (8.4)	1852 (91.6)	1.68 (1.26-2.25)	0.0004
MetS	96 (16.8)	475 (82.2)		
Total				
Non-MetS	512 (10.3)	4452 (89.7)	1.42 (1.23-1.64)	< 0.0001
MetS	406 (15.6)	2200 (84.4)		

Age-adjusted logistic regression model was used to test the associations between metabolic syndrome (MetS) and human gallstone. OR: Odds ratio; CI: Confidence interval.

medication for elevated blood glucose^[15].

The diagnosis of GSD was established on the basis of the results of abdominal ultrasound (US) using a 3.5-MHz transducer. US was conducted by an experienced radiologist, who was unaware of the objectives of the study and blinded to laboratory values. Gallstones were defined by the presence of strong intraluminal echoes that were gravity-dependent or that attenuated ultrasound transmission (acoustic shadowing)^[16].

Statistical analysis

All statistical analyses were conducted using SPSS version 13.0 (SPSS Inc, Chicago, Ill). The results were expressed as the mean \pm SD. Binary variables were summarized by N and percentage. Student *t* test was applied to compare the differences between cases and controls for all continuous variables. χ^2 test was used to compare the differences between cases and controls for all category variables. Age-adjusted logistic regression model was used to test the association between MetS and human gallstones.

RESULTS

Of the 7570 examined subjects, the prevalence of the GSD was 12.1% (13.1% in men and 10.2% in women). The results of univariate analysis of various factors and its relationship with GSD are shown in Table 1. In comparison with subjects without GSD, those with GSD were significantly older and had a higher waist circumference (WC), BMI, systolic blood pressure, diastolic blood pressure, fasting blood glucose and TG. Moreover, subjects with GSD had a significantly lower HDL cholesterol level than those without GSD. The incidence of larger waist circumference, higher blood pressure, increased FPG and TG was obviously higher in cases group than in the controls.

In age-adjusted logistic regression analyses (Table 2), MetS was significantly associated with the risk of GSD irrespective of the sex of the subjects. The age-adjusted odds ratio of MetS for GSD was 1.29 [95% Confidence

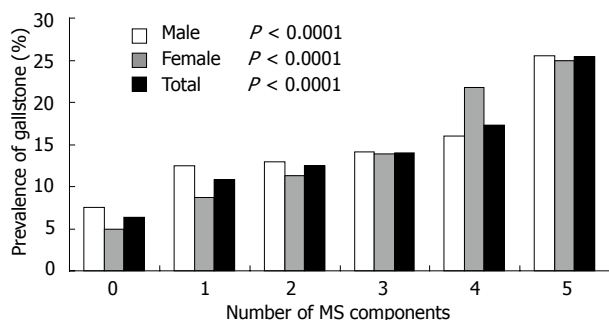


Figure 1 Trend test of the prevalence of gallstone disease and the number of metabolic syndrome components in males, females and total study subjects respectively. Trend test of the prevalence of gallstone disease and the number of metabolic syndrome components in males, in females and in total study subjects. MS: Metabolic syndrome.

interval (CI), 1.09-1.52; $P = 0.0030$] in men, and 1.68 (95% CI, 1.26-2.25; $P = 0.0004$) in women; and the overall age-adjusted odds ratio of MetS for GSD was 1.42 (95% CI, 1.23-1.64; $P < 0.0001$).

We also analyzed the association between the prevalence of GSD and the number of MetS components. Figure 1 shows that the more the components of MetS, the higher the prevalence of GSD in men, and the trend was significant ($P < 0.0001$). The presence of 5 components of the MetS increased the risk of gallstone disease by 3.4 times ($P < 0.0001$). We found the same trend in the women. The prevalence of GSD in women who had 5 components of MetS, was 5 times that of those without MetS component. The overall prevalence of GSD, and the trend was also significant ($P < 0.0001$).

DISCUSSION

In China, the study about the prevalence of GSD is rare, and the available studies are not sufficient in sample size or lack of appropriate statistical methods. We designed the cross-sectional study with a large sample of Chinese population. We found that the prevalence of the GSD was 12.1% (13.1% in men and 10.2% in women), which was slightly higher than the figure presented in a previous hospital-based study conducted at the West China Hospital, Sichuan University, which was reported to be 10.7% (9.9% in men and 11.6% in women)^[17]. A population-based screening study conducted in Taiwan in 2006 reported that the overall prevalence of GSD was 5.0% (4.6% in men, 5.4% in women), without significant gender differences^[18]. The apparently higher prevalence rate in our study may contribute to the Westernized lifestyle of our subjects who were of middle-to-high income class.

According to most of the previous epidemiologic studies, women have a higher prevalence of GSD than men in the Western world, and estrogen is considered to be an obvious factor for the gender difference^[19]. However, our findings showed that the prevalence of GSD was higher in men than in women. Actually, gender as a risk factor for cholelithiasis still remains controversial. While the majority of studies conducted in the West have

concluded that women are more likely to develop cholelithiasis^[20,21] than men, studies among Asian patients have failed to identify a gender-related difference^[22,23]. In fact, Liu *et al.*^[24] found a higher incidence of cholelithiasis in men than in women below 50 years of age, but a higher incidence in women than in men in age groups above 50 years. And Hung *et al.*^[25] indicated that menopause is a risk factor for cholelithiasis in women. Moreover, female predominance is less evident in Asia where the pigmented stone diseases are more common^[26]. So the male predominance with GSD in our study may be attributed to the fact that our subjects were of Asian ethnicity and most of them were aged below 50 years, meanwhile most of our female subjects were premenopausal women.

Older age is another significant risk factor for GSD^[27,28], so we used age-adjusted logistic regression model to test the associations between MetS and human gallstone. It has been reported that the presence of MetS as an insulin resistance phenotype was associated with an increased prevalence of gallstones^[29]. In our age-adjusted logistic regression analysis, MetS was associated with an increased risk of GSD.

Obesity is a major cornerstone of MetS, in our study, the presence of a high waist circumference was common in patients with GSD. A population-based follow-up study on GSD in Kinmen also showed that greater waist circumference was associated with the development of GSD among type 2 diabetics^[30]. Cojocar *et al.*^[29] found that waist circumference and BMI were significantly associated with a higher risk of cholesterol gallstone. Obesity is a major risk factor for developing GSD because it can increase hepatic secretion of cholesterol^[31].

Although dyslipidemia is very common in MetS, no conclusive evidence links dyslipidemia and GSD. A Korean study demonstrated that HDL cholesterol level was significantly lower in subjects with GSD; however, they did not find any component of dyslipidemia related to MetS that could be correlated with GSD formation^[19]. A cross-sectional study in a check-up unit in a university hospital in Mexico City described the influence of low HDL cholesterol on developing GSD (OR = 2.32)^[4]. In our study, subjects with GSD had lower HDL cholesterol and higher TG, but there was only difference in the incidence of higher TG between cases and controls. The relationship between HDL and GSD remains unclear. In most patients with higher TG, an association with overweight and insulin resistance is often observed based on the supersaturated (cholesterol) bile and diminished gallbladder motility, both contributing to gallstone formation^[14]. Phase separation of cholesterol crystals from supersaturated bile is considered the key event in cholesterol gallstone formation. It is a basal framework of the interactions between the sterol, bile salts and phospholipids in aqueous solutions. Biliary bile acid and phospholipids are important to solubilize cholesterol^[32]. Phospholipid transfer protein (PLTP) transfers lipids from low-density lipoproteins to high-density lipoproteins. It was found that an inhibitory effect of haptoglobin over PLTP activ-

ity in hyperlipidemic plasma may contribute to the regulation of reverse cholesterol transport^[33]. Huang *et al.*^[34] revealed a hitherto unrecognized role of protein kinase C β (PKC β) in the fine tuning diet-induced cholesterol and bile acid homeostasis, thus identifying PKC β as a major physiological regulator of both triglyceride and cholesterol homeostasis. Moreover, polymorphisms in the gene encoding are also found to increase the gallstone risk. Such as the cholesterol transporter ABCG5-G8 and phospholipid floppase ABCB4^[32].

Considering the obvious association between gallstone disease and MetS in this study, the fact that higher blood pressure was associated with MetS and GSD appears reasonable. Systolic blood pressure and diastolic blood pressure were higher in patients with GSD as compared with the controls. A study in Taiwan documented that cholelithiasis in Asian obese patients is significantly associated with increased diastolic blood pressure^[35]. Blood pressure $\geq 130/85$ mmHg was significantly associated with a higher risk of cholesterol gallstone^[36]. The mechanism why higher blood pressure increased the risk of GSD still remains unclear. Some scholars considered that this association could be explained by the action of insulin in hypertension. To validate the mechanism, we will further study the relationship between hypertension and GSD. We have designed a study to investigate the association between BP and GSD, as well as the impact of medication for hypertension on GSD.

Previous studies indicated that diabetes mellitus was a risk factor for GSD^[37-39]. GSD appeared strongly associated with fasting glycemia^[29]. We noted that there was a positive correlation between prevalence of gallstone with higher FPG. The possible mechanisms for this association may be as follows: hyperglycemia inhibits bile secretion from the liver and disturbs gallbladder contraction^[40]; hyperglycemia may affect gallbladder motility^[41]; or some factors modifying the crystal nucleation and mucous secretion in bile^[42].

Finally, GSD appears to be strongly associated with MetS. The result is consistent with the hypothesis that insulin resistance plays an important role in the pathogenesis of GSD. Animal experiments demonstrated that mice with isolated hepatic insulin resistance created by liver-specific disruption of the insulin receptor [Liver insulin receptor knockout (LIRKO) mice] are markedly predisposed towards cholesterol gallstone formation. After only one week on a lithogenic diet, 36% of LIRKO mice developed gallstones and 100% had gallstones by 12 wk^[43]. Chang *et al.*^[6], showed that insulin resistance was positively associated with gallstones in non-diabetic Korean men, and this occurred regardless of obesity. Taking into account this association, some authors raised the question whether administration of lipid-lowering drug is a therapeutic option for GSD? Ezetimibe was shown to have a beneficial effect against cholelithiasis in both animal and humans^[44], it is, therefore, possible to suggest that a clinical trial designed to investigate the potential efficiency of ezetimibe for reducing biliary cholesterol

saturation and insulin resistance in populations with a predisposition to cholelithiasis should be now warranted.

In conclusion, GSD is common in China, and the present study shows an obvious association between MetS and GSD, and the more the metabolic components of MetS, the higher the prevalence of the GSD. But the mechanism for the association remains unclear, further research is needed to clarify how BP influences the formation of GSD, whether medication for dyslipidemia benefits the GSD patients, and whether we can reduce the prevalence of GSD through lifestyle interventions.

COMMENTS

Background

China is one of the fastest developing countries. The rapid economic growth and industrialization has brought about changes in traditional diets and lifestyles. The prevalence of metabolic syndrome (MetS) is increasing. But there have been few studies about the prevalence of gallstone disease (GSD), and the association between the development of GSD and MetS is not fully elucidated.

Research frontiers

The authors designed a cross-sectional study with a large sample of Chinese subjects to evaluate the association between MetS and the development of GSD. They concluded that GSD is strongly associated with MetS.

Innovations and breakthroughs

This study demonstrated a strong association between GSD and MetS, but the prevalence of GSD was higher in men than in women. This finding is not consistent with the results from most previous epidemiologic studies. The reason for the discrepancy may be that the subjects in this study are of Asian ethnicity and most of the subjects are below 50 years of age, meanwhile most of the female subjects are premenopausal women.

Applications

There is only minimal data regarding the relationship between GSD and MetS in apparently healthy Asian population. The findings of this study will make it possible to reduce the prevalence of gallstones with appropriate administration of medication and/or lifestyle interventions.

Peer review

This article is well written. This study demonstrated a strong association between GSD and MetS. The presentation of results is logic and the discussion is comprehensive.

REFERENCES

- 1 Further Study of Risk Factors for Stroke and Coronary Heart Disease Cooperation Group. The prevalence of metabolic syndrome in a 11 provinces cohort in China. *Zhonghua Yufang Yixue Zazhi* 2002; **36**: 298-300
- 2 Gu D, Gupta A, Muntner P, Hu S, Duan X, Chen J, Reynolds RF, Whelton PK, He J. Prevalence of cardiovascular disease risk factor clustering among the adult population of China: results from the International Collaborative Study of Cardiovascular Disease in Asia (InterAsia). *Circulation* 2005; **112**: 658-665
- 3 Zuo H, Shi Z, Hu X, Wu M, Guo Z, Hussain A. Prevalence of metabolic syndrome and factors associated with its components in Chinese adults. *Metabolism* 2009; **58**: 1102-1108
- 4 Méndez-Sánchez N, Chavez-Tapia NC, Motola-Kuba D, Sanchez-Lara K, Ponciano-Rodríguez G, Baptista H, Ramos MH, Uribe M. Metabolic syndrome as a risk factor for gallstone disease. *World J Gastroenterol* 2005; **11**: 1653-1657
- 5 Nervi F, Miquel JF, Alvarez M, Ferreccio C, García-Zattera MJ, González R, Pérez-Ayuso RM, Rigotti A, Villarreal L. Gallbladder disease is associated with insulin resistance in a high risk Hispanic population. *J Hepatol* 2006; **45**: 299-305
- 6 Bodmer M, Brauchli YB, Krähenbühl S, Jick SS, Meier CR.

- Statin use and risk of gallstone disease followed by cholecystectomy. *JAMA* 2009; **302**: 2001-2007
- 7 **Marschall HU**, Einarsson C. Gallstone disease. *J Intern Med* 2007; **261**: 529-542
 - 8 **Wittenburg H**, Lammert F. Genetic predisposition to gallbladder stones. *Semin Liver Dis* 2007; **27**: 109-121
 - 9 **Shaffer EA**. Gallstone disease: Epidemiology of gallbladder stone disease. *Best Pract Res Clin Gastroenterol* 2006; **20**: 981-996
 - 10 **Shaffer EA**. Epidemiology and risk factors for gallstone disease: has the paradigm changed in the 21st century? *Curr Gastroenterol Rep* 2005; **7**: 132-140
 - 11 **Huang J**, Chang CH, Wang JL, Kuo HK, Lin JW, Shau WY, Lee PH. Nationwide epidemiological study of severe gallstone disease in Taiwan. *BMC Gastroenterol* 2009; **9**: 63
 - 12 **Liu CM**, Tung TH, Liu JH, Lee WL, Chou P. A community-based epidemiologic study on gallstone disease among type 2 diabetics in Kinmen, Taiwan. *Dig Dis* 2004; **22**: 87-91
 - 13 **Acalovschi M**, Buzas C, Radu C, Grigorescu M. Hepatitis C virus infection is a risk factor for gallstone disease: a prospective hospital-based study of patients with chronic viral C hepatitis. *J Viral Hepat* 2009; **16**: 860-866
 - 14 **Smelt AH**. Triglycerides and gallstone formation. *Clin Chim Acta* 2010; **411**: 1625-1631
 - 15 **Heng D**, Ma S, Lee JJ, Tai BC, Mak KH, Hughes K, Chew SK, Chia KS, Tan CE, Tai ES. Modification of the NCEP ATP III definitions of the metabolic syndrome for use in Asians identifies individuals at risk of ischemic heart disease. *Atherosclerosis* 2006; **186**: 367-373
 - 16 **Chang Y**, Sung E, Ryu S, Park YW, Jang YM, Park M. Insulin resistance is associated with gallstones even in non-obese, non-diabetic Korean men. *J Korean Med Sci* 2008; **23**: 644-650
 - 17 **Sun H**, Tang H, Jiang S, Zeng L, Chen EQ, Zhou TY, Wang YJ. Gender and metabolic differences of gallstone diseases. *World J Gastroenterol* 2009; **15**: 1886-1891
 - 18 **Chen CH**, Huang MH, Yang JC, Nien CK, Etheredge GD, Yang CC, Yeh YH, Wu HS, Chou DA, Yueh SK. Prevalence and risk factors of gallstone disease in an adult population of Taiwan: an epidemiological survey. *J Gastroenterol Hepatol* 2006; **21**: 1737-1743
 - 19 **Kim SS**, Lee JG, Kim DW, Kim BH, Jeon YK, Kim MR, Huh JE, Mok JY, Kim SJ, Kim YK, Kim IJ. Insulin resistance as a risk factor for gallbladder stone formation in Korean post-menopausal women. *Korean J Intern Med* 2011; **26**: 285-293
 - 20 **Tazuma S**. Gallstone disease: Epidemiology, pathogenesis, and classification of biliary stones (common bile duct and intrahepatic). *Best Pract Res Clin Gastroenterol* 2006; **20**: 1075-1083
 - 21 **Völzke H**, Baumeister SE, Alte D, Hoffmann W, Schwahn C, Simon P, John U, Lerch MM. Independent risk factors for gallstone formation in a region with high cholelithiasis prevalence. *Digestion* 2005; **71**: 97-105
 - 22 **Lai SW**, Muo CH, Liao KF, Sung FC, Chen PC. Risk of acute pancreatitis in type 2 diabetes and risk reduction on anti-diabetic drugs: a population-based cohort study in Taiwan. *Am J Gastroenterol* 2011; **106**: 1697-1704
 - 23 **Novacek G**. Gender and gallstone disease. *Wien Med Wochenschr* 2006; **156**: 527-533
 - 24 **Liu CM**, Tung TH, Chou P, Chen VT, Hsu CT, Chien WS, Lin YT, Lu HF, Shih HC, Liu JH. Clinical correlation of gallstone disease in a Chinese population in Taiwan: experience at Cheng Hsin General Hospital. *World J Gastroenterol* 2006; **12**: 1281-1286
 - 25 **Hung SC**, Liao KF, Lai SW, Li CI, Chen WC. Risk factors associated with symptomatic cholelithiasis in Taiwan: a population-based study. *BMC Gastroenterol* 2011; **11**: 111
 - 26 **Stinton LM**, Myers RP, Shaffer EA. Epidemiology of gallstones. *Gastroenterol Clin North Am* 2010; **39**: 157-169, vii
 - 27 **Liew PL**, Lee WJ, Wang W, Lee YC, Chen WY, Fang CL, Huang MT. Fatty liver disease: predictors of nonalcoholic steatohepatitis and gallbladder disease in morbid obesity. *Obes Surg* 2008; **18**: 847-853
 - 28 **Festi D**, Dormi A, Capodicasa S, Staniscia T, Attili AF, Loria P, Pazzi P, Mazzella G, Sama C, Roda E, Colecchia A. Incidence of gallstone disease in Italy: results from a multicenter, population-based Italian study (the MICOL project). *World J Gastroenterol* 2008; **14**: 5282-5289
 - 29 **Cojocaru C**, Pandele GI. [Metabolic profile of patients with cholesterol gallstone disease.] *Rev Med Chir Soc Med Nat Iasi* 2010; **114**: 677-682
 - 30 **Tung TH**, Ho HM, Shih HC, Chou P, Liu JH, Chen VT, Chan DC, Liu CM. A population-based follow-up study on gallstone disease among type 2 diabetics in Kinmen, Taiwan. *World J Gastroenterol* 2006; **12**: 4536-4540
 - 31 **Chen CH**, Huang MH, Yang JC, Nien CK, Yang CC, Yeh YH, Yueh SK. Prevalence and risk factors of nonalcoholic fatty liver disease in an adult population of Taiwan: metabolic significance of nonalcoholic fatty liver disease in nonobese adults. *J Clin Gastroenterol* 2006; **40**: 745-752
 - 32 **Van Erpecum KJ**. Pathogenesis of cholesterol and pigment gallstones: an update. *Clin Res Hepatol Gastroenterol* 2011; **35**: 281-287
 - 33 **Henderson RJ**, Wasan KM, Leon CG. Haptoglobin inhibits phospholipid transfer protein activity in hyperlipidemic human plasma. *Lipids Health Dis* 2009; **8**: 27
 - 34 **Huang W**, Bansode RR, Xie Y, Rowland L, Mehta M, Davidson NO, Mehta KD. Disruption of the murine protein kinase Cbeta gene promotes gallstone formation and alters biliary lipid and hepatic cholesterol metabolism. *J Biol Chem* 2011; **286**: 22795-22805
 - 35 **Liew PL**, Wang W, Lee YC, Huang MT, Lin YC, Lee WJ. Gallbladder disease among obese patients in Taiwan. *Obes Surg* 2007; **17**: 383-390
 - 36 **Misciagna G**, Guerra V, Di Leo A, Correale M, Trevisan M. Insulin and gall stones: a population case control study in southern Italy. *Gut* 2000; **47**: 144-147
 - 37 **Nakeeb A**, Comuzzie AG, Al-Azzawi H, Sonnenberg GE, Kissebah AH, Pitt HA. Insulin resistance causes human gallbladder dysmotility. *J Gastrointest Surg* 2006; **10**: 940-948; discussion 948-949
 - 38 **Shebl FM**, Andreotti G, Meyer TE, Gao YT, Rashid A, Yu K, Shen MC, Wang BS, Han TQ, Zhang BH, Stanczyk FZ, Hsing AW. Metabolic syndrome and insulin resistance in relation to biliary tract cancer and stone risks: a population-based study in Shanghai, China. *Br J Cancer* 2011; **105**: 1424-1429
 - 39 **Lioudaki E**, Ganotakis ES, Mikhailidis DP. Lipid lowering drugs and gallstones: a therapeutic option? *Curr Pharm Des* 2011; **17**: 3622-3631
 - 40 **Chen CY**, Lu CL, Huang YS, Tam TN, Chao Y, Chang FY, Lee SD. Age is one of the risk factors in developing gallstone disease in Taiwan. *Age Ageing* 1998; **27**: 437-441
 - 41 **Misciagna G**, Leoci C, Guerra V, Chiloiro M, Elba S, Petruzzi J, Mossa A, Noviello MR, Coviello A, Minutolo MC, Mangini V, Messa C, Cavallini A, De Michele G, Giorgio I. Epidemiology of cholelithiasis in southern Italy. Part II: Risk factors. *Eur J Gastroenterol Hepatol* 1996; **8**: 585-593
 - 42 **Kim JM**, Lee HL, Moon W, Koh DH, Lee OY, Yoon BC, Choi HS, Hahm JS, Lee MH, Lee DH, Ahn YH. [Association between insulin, insulin resistance, and gallstone disease in Korean general population.] *Korean J Gastroenterol* 2007; **50**: 183-187
 - 43 **Zhao YD**, Springall DR, Hamid Q, Yacoub MH, Levene M, Polak JM. Localization and characterization of endothelin-1 binding sites in the transplanted human lung. *J Cardiovasc Pharmacol* 1995; **26** Suppl 3: S336-S340
 - 44 **Wang HH**, Portincasa P, Mendez-Sanchez N, Uribe M, Wang DQ. Effect of ezetimibe on the prevention and dissolution of cholesterol gallstones. *Gastroenterology* 2008; **134**: 2101-2110

Eosinophilic esophagitis-endoscopic distinguishing findings

Ana Célia Caetano, Raquel Gonçalves, Carla Rolanda

Ana Célia Caetano, Raquel Gonçalves, Carla Rolanda, Department of Gastroenterology, Braga Hospital, 4710243 Braga, Portugal

Ana Célia Caetano, Carla Rolanda, Life and Health Sciences Research Institute, School of Health Sciences, University of Minho, 4710057 Braga, Portugal

Ana Célia Caetano, Carla Rolanda, Life and Health Sciences Research Institute/3Bs-PT Government Associate Laboratory, 4710057 Braga, Portugal

Author contributions: Caetano AC contributed to the analysis, interpretation of data and bibliographic review; Gonçalves R and Rolanda C contributed to the critical revision and final approval of the version to be published.

Correspondence to: Ana Célia Caetano, MD, Department of Gastroenterology, Braga Hospital, Sete Fontes-São Victor, 4710243 Braga, Portugal. anaceliacaetanocs@gmail.com

Telephone: +35-191-5303019 Fax: +35-125-3027999

Received: February 22, 2012 Revised: May 2, 2012

Accepted: May 26, 2012

Published online: August 21, 2012

Abstract

Eosinophilic esophagitis (EE) is the most frequent condition found in a group of gastrointestinal disorders called eosinophilic gastrointestinal diseases. The hypothetical pathophysiological mechanism is related to a hypersensitivity reaction. Gastroesophageal reflux disease-like complaints not ameliorated by acid blockade or occasional symptoms of dysphagia or food impaction are likely presentations of EE. Due to its unclear pathogenesis and unspecific symptoms, it is difficult to diagnose EE without a strong suspicion. Although histological criteria are necessary to diagnosis EE, there are some characteristic endoscopic features. We present the case of a healthy 55-year-old woman with dysphagia and several episodes of esophageal food impaction over the last six months. This case report stresses the most distinguishing endoscopic findings-mucosa rings, white exudative plaques and linear furrows-that can help in the prompt recognition of this condition.

© 2012 Baishideng. All rights reserved.

Key words: Distinguishing findings; Dysphagia; Eosinophilic esophagitis; Gastro esophageal reflux disease; Histological criteria

Peer reviewer: Dr. Xiaoyun Liao, Department of Medical Oncology, Dana-Farber Cancer Institute, 450 Brookline Avenue, Room JF-208E, Boston, MA 02215, United States

Caetano AC, Gonçalves R, Rolanda C. Eosinophilic esophagitis-endoscopic distinguishing findings. *World J Gastroenterol* 2012; 18(31): 4221-4223 Available from: URL: <http://www.wjgnet.com/1007-9327/full/v18/i31/4221.htm> DOI: <http://dx.doi.org/10.3748/wjg.v18.i31.4221>

INTRODUCTION

Eosinophilic gastrointestinal diseases (EGD) are rare conditions of growing interest due to their increasing diagnostic frequency in well developed countries^[1]. Eosinophilic esophagitis (EE) is the most common EGD, and its clinical presentation varies extensively making the diagnosis difficult and clinical suspicion fundamental. Although not entirely clear, given that EE correlates with other atopic disorders and has a good response to corticoid treatment, it seems that its pathophysiological mechanism is related to a hypersensitivity reaction^[1].

In this case report, through several expressive images, we highlight the set of endoscopic features which helped in the early recognition of EE.

CASE REPORT

A 55-year-old woman with no previous medical history presented with dysphagia and several episodes of esophageal food impaction over the last six months. Upper gastrointestinal (GI) endoscopy revealed scattered white plaques in the proximal esophagus (Figure 1A), a whitish exudate coating the mucosa in the distal part of the esophagus (Figure 1B), and characteristic images of concentric transient rings and linear furrows (Figure 1C).

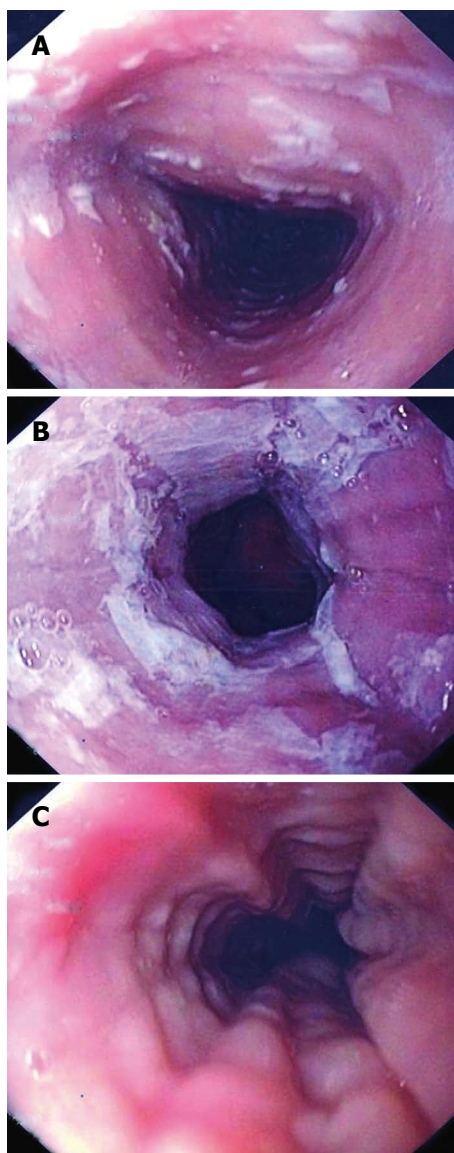


Figure 1 A 55-year-old woman presented with dysphagia and several episodes of esophageal food impaction over the last six months. A: Scattered white plaques in the proximal esophagus; B: Whitish exudate coating the mucosa in the distal part of the esophagus; C: Concentric transient rings and linear furrows on esophagoscopy.

Biopsy specimens showed dense eosinophilic infiltrates, > 20 eosinophils/high power field (HPF) and microabscesses (Figure 2A and B). Gastroesophageal reflux disease (GERD) was excluded when no improvement was observed following the administration of a proton pump inhibitor (PPI). The patient started treatment with a budesonide inhaler twice daily (instructions to swallow) and experienced symptom relief.

DISCUSSION

EE is part of a group of disease known as the eosinophilic gastrointestinal disorders. The pathogenesis of EE is not yet understood, although it appears to be related

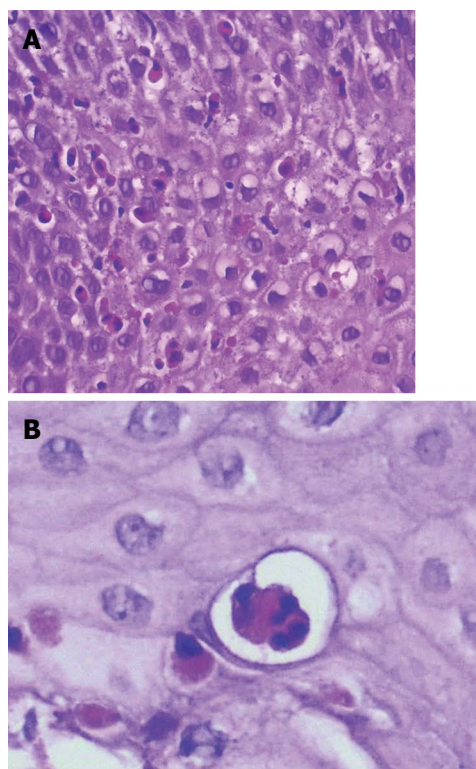


Figure 2 Histological findings in esophageal biopsy specimen. A: Dense eosinophilic infiltrates; B: Microabscesses on esophageal microscopy.

to a hypersensitivity reaction. Some studies suggest that increased mucosa permeability allows contact with potential allergenic digestion products leading to a consequent immunologic response^[2]. EE tends to be a chronic disorder with intermittent or persistent symptoms, usually GERD-like complaints which are not ameliorated by acid blockade with PPI. Additionally, patients may present with symptoms of dysphagia or food impaction. Due to its unspecific esophageal symptoms, clinical suspicion is critical in the diagnosis of EE. Although endoscopy may be normal in one third of cases, images of mucosal rings, white exudative plaques and esophageal strictures are characteristic findings of this pathology. Nevertheless, multiple biopsies should be performed in different esophageal locations, as well as in the stomach and duodenum as the diagnosis of EE relies on histological criteria-one HPF must contain, at least, 15 intraepithelial eosinophils. Additional histological features include eosinophilic microabscesses^[1,3].

To date, there are no large randomized controlled trials on EGD treatment. The majority of data are from smaller studies where corticosteroids play a role in the treatment of these disorders. Generally, oral or topical corticoid therapy is given to the patient for at least eight weeks followed by a gradual taper. The symptoms usually recur, suggesting the need for continuous therapy. Some case reports show evidence of better symptom control following maintenance treatment with mast cell inhibitors or leukotriene receptor antagonists, however,

larger trials are needed^[2,3].

REFERENCES

- 1 **Furuta GT**, Liacouras CA, Collins MH, Gupta SK, Justinich C, Putnam PE, Bonis P, Hassall E, Straumann A, Rothenberg ME. Eosinophilic esophagitis in children and adults: a systematic review and consensus recommendations for diagnosis and treatment. *Gastroenterology* 2007; **133**: 1342-1363
- 2 **Shifflet A**, Forouhar F, Wu GY. Eosinophilic digestive diseases: eosinophilic esophagitis, gastroenteritis, and colitis. *J Formos Med Assoc* 2009; **108**: 834-843
- 3 **Dellon ES**. Diagnosis of eosinophilic esophagitis: current approach and future directions. *Curr Gastroenterol Rep* 2011; **13**: 240-246

S- Editor Gou SX **L- Editor** Webster JR **E- Editor** Zhang DN

Dehiscence following successful endoscopic closure of gastric perforation during endoscopic submucosal dissection

Masau Sekiguchi, Haruhisa Suzuki, Ichiro Oda, Shigetaka Yoshinaga, Satoru Nonaka, Makoto Saka, Hitoshi Katai, Hirokazu Taniguchi, Ryoji Kushima, Yutaka Saito

Masau Sekiguchi, Haruhisa Suzuki, Ichiro Oda, Shigetaka Yoshinaga, Satoru Nonaka, Yutaka Saito, Endoscopy Division, National Cancer Center Hospital, Tokyo 104-0045, Japan
Makoto Saka, Hitoshi Katai, Gastric Surgery Division, National Cancer Center Hospital, Tokyo 104-0045, Japan

Hirokazu Taniguchi, Ryoji Kushima, Pathology Division, National Cancer Center Hospital, Tokyo 104-0045, Japan

Author contributions: Sekiguchi M, Suzuki H, and Oda I designed the study, analyzed and interpreted the data, and drafted the article; Yoshinaga S, Nonaka S, Saka M, Katai H, Taniguchi H, Kushima R, and Saito Y contributed to the discussion and reviewed the manuscript; all the authors had final approval of the article.

Correspondence to: Haruhisa Suzuki, MD, Endoscopy Division, National Cancer Center Hospital, 5-1-1 Tsukiji, Chuo-ku, Tokyo 104-0045, Japan. harusuzu@ncc.go.jp

Telephone: +81-3-35422511 Fax: +81-3-35423815

Received: March 1, 2012 Revised: April 17, 2012

Accepted: April 20, 2012

Published online: August 21, 2012

in an *en-bloc* resection. Intensive conservative management was conducted following ESD, however, an endoscopic examination five days after ESD revealed dehiscence of the perforation requiring an emergency laparotomy.

© 2012 Baishideng. All rights reserved.

Key words: Early gastric cancer; Endoscopic closure; Endoscopic submucosal dissection; Gastric perforation; Laparotomy

Peer reviewer: Dr. Antonello Trecca, Digestive Endoscopy, Usi Group, Via Machiavelli 22, 00184 Rome, Italy

Sekiguchi M, Suzuki H, Oda I, Yoshinaga S, Nonaka S, Saka M, Katai H, Taniguchi H, Kushima R, Saito Y. Dehiscence following successful endoscopic closure of gastric perforation during endoscopic submucosal dissection. *World J Gastroenterol* 2012; 18(31): 4224-4227 Available from: URL: <http://www.wjgnet.com/1007-9327/full/v18/i31/4224.htm> DOI: <http://dx.doi.org/10.3748/wjg.v18.i31.4224>

Abstract

Gastric perforation is one of the most serious complications that can occur during endoscopic submucosal dissection (ESD). In terms of the treatment of such perforations, we previously reported that perforations immediately observed and successfully closed with endoclips during endoscopic resection could be managed conservatively. We now report the first case in our medical facility of a gastric perforation during ESD that was ineffectively treated conservatively even after successful endoscopic closure. In December 2006, we performed ESD on a recurrent early gastric cancer in an 81-year-old man with a medical history of laparotomy for cholelithiasis. A perforation occurred during ESD that was immediately observed and successfully closed with endoclips so that ESD could be continued resulting

INTRODUCTION

Endoscopic submucosal dissection (ESD) is now an accepted therapy for node-negative early gastric cancer (EGC). Compared to endoscopic mucosal resection (EMR), ESD is often preferred because this technique provides a higher rate of successful *en-bloc* resections^[1-7], however, the risk of complications, particularly perforations, is also higher with ESD. The incidence of perforations occurring during ESD has been reported to range from 3.5% to 6.1%^[2-8]. In terms of the treatment of gastric perforations during endoscopic resection, we previously reported that perforations immediately observed

and successfully closed with endoclips during endoscopic resection could be treated conservatively without the need for an emergency laparotomy^[8]. We now report the first case in our medical facility of a gastric perforation during ESD of EGC which was ineffectively treated conservatively, even though it was immediately detected and successfully closed with endoclips. Laparotomy was performed five days after ESD due to dehiscence following endoscopic closure.

CASE REPORT

An 81-year-old man with a medical history of laparotomy for cholelithiasis performed in 1987 was admitted to our hospital in December 2006 for the endoscopic treatment of a recurrent EGC. He had previously undergone an initial ESD for EGC at the lesser curvature of the lower gastric body in 1999. Pathological findings revealed a well-differentiated mucosal adenocarcinoma without lymphovascular involvement. The lateral margin could not be properly evaluated, however, because an incision had inadvertently been made in the lesion during ESD. After the initial ESD, endoscopic examinations were performed periodically and a recurrent tumor 20 mm in size was detected at the site of the ESD scar in October 2006 (Figure 1A).

In December 2006, ESD was performed on the recurrent tumor and an oval perforation 5 mm in length occurred during the procedure at the site of extensive fibrosis from the initial ESD scar (Figure 1B). The perforation was immediately observed and successfully closed with endoclips (HX-610-090; Olympus Medical Systems Corp., Tokyo, Japan) (Figure 1C) so that the ESD could then be continued resulting in an *en-bloc* resection. Pathological examination revealed a well to moderately differentiated mucosal adenocarcinoma with ulcer scar from the initial ESD without lymphovascular involvement (Figure 1D, E and F). The lateral and vertical margins were negative. Following ESD, the patient was intensively managed with nasogastric suction, fasting and intravenous antibiotic therapy. The patient's abdominal symptoms were unremarkable with no physical indications of diffuse peritonitis observed, although the patient had a fever and high C-reactive peptide level during the observation period. Despite intensive conservative management, the patient's fever persisted and his C-reactive peptide level remained elevated at 20 mg/dL, thus we performed an endoscopic examination five days after ESD which revealed that the perforation site previously closed with endoclips had split open (Figure 2A). Since the open perforation site could not be closed endoscopically, an emergent laparotomy was performed on the same day. Surgical findings indicated that the perforation of the gastric wall extending to the omental bursa was 30 mm × 10 mm in length and the perforation site was not covered with adipose tissue (Figure 2B). Pigmentation from bile and localized findings of inflammation were observed in the omental bursa probably caused by adhesions from the previous laparotomy for cholelithiasis performed in 1987. Distal gastrectomy was performed instead of omental implantation because

the gastric wall at the perforation site was fragile and the split-open perforation was relatively large in size. The patient recovered well postoperatively and was discharged 11 d after surgery with no recurrence detected as of December 2010.

DISCUSSION

We previously reported that gastric perforations which occurred during endoscopic resection could be managed conservatively with complete endoscopic closure based on the analysis of 117 patients with such perforations at our facility^[8]. In our analysis, endoscopic closure with endoclips was successful in 115 of the 117 patients (98.3%) and conservative management for those 115 patients was uneventful. That is, none of the patients with successful endoscopic closure required an emergency laparotomy. In the present case, however, conservative management proved to be ineffective despite the fact that successful endoscopic closure was performed during ESD. An endoscopic examination conducted five days after ESD revealed that the perforation site previously closed successfully with endoclips had split open necessitating an emergency laparotomy.

The gastric lesion in our patient was a recurrent tumor following an initial ESD, and the existence of fibrosis at the site of ESD scar was considered to be one of the factors associated with incomplete healing of the perforation. However, on referring to our previous analysis of 46 patients who received ESDs for locally recurrent EGCs after prior endoscopic resections, perforations occurred during ESD in four patients (8.7%) with all four patients fully recovering following successful endoscopic closure with endoclips^[9]. Therefore, based on those earlier reported results, we cannot conclude that the existence of fibrosis in connection with local recurrence was the only reason for failure of the healing process in the present perforation case. We speculate that there may have been another contributing cause, specifically the patient's medical history of laparotomy for cholelithiasis. It is thought that the reason the perforation site did not heal after successful endoscopic closure was related to the adhesions resulting from the previous laparotomy. Adipose tissue did not cover the perforation site after endoscopic closure due to these adhesions, thus the perforation site was unable to heal properly. We believe that the patient's unremarkable abdominal symptoms were also related to these adhesions as they created a closed space in the abdominal cavity thus localizing the peritonitis resulting from the gastric perforation.

Our experience in this case indicates that gastric perforations which occur during ESD cannot always be treated conservatively even after successful endoscopic closure using endoclips, particularly if the patient has a medical history of laparotomy. Consequently, we must keep this possibility in mind when performing ESD on an EGC patient with a medical history of laparotomy. In addition, we need to remember that perforation patients with a medical history of laparotomy do not always show

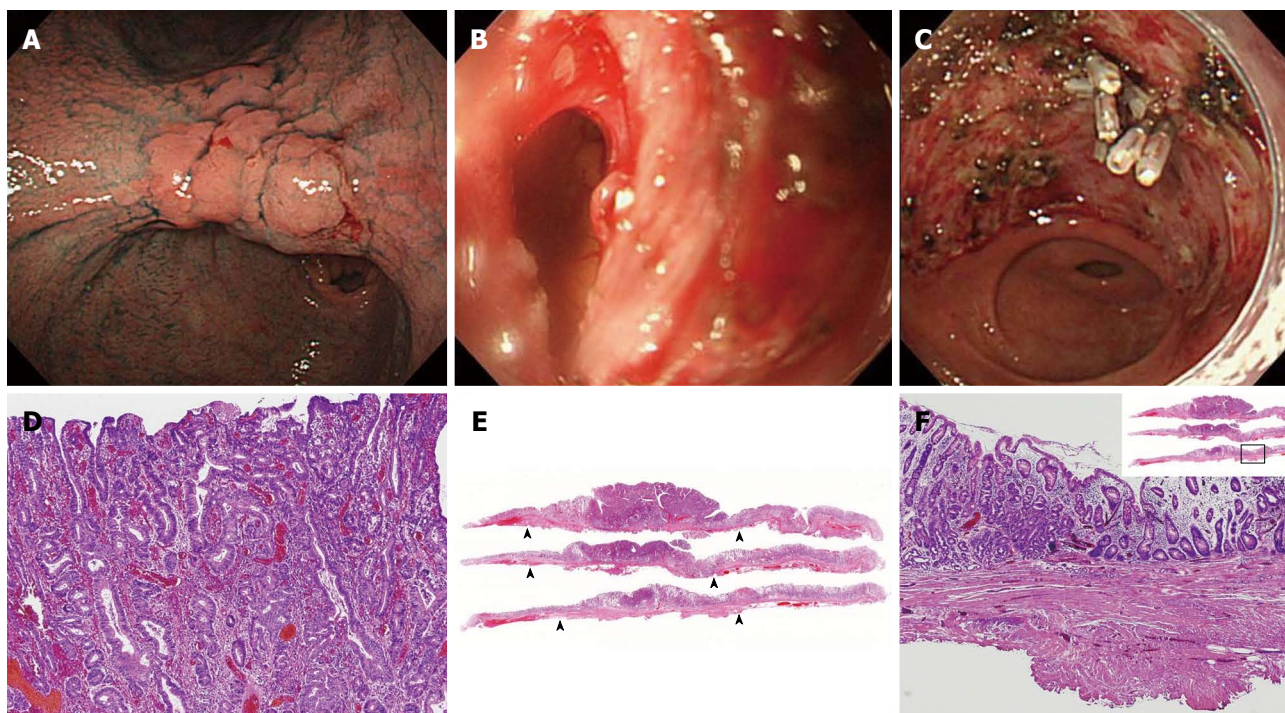


Figure 1 Endoscopic submucosal dissection of a recurrent tumor in December 2006. A: Pre-treatment endoscopy. A recurrent tumor 20 mm in size was detected at the site of the initial endoscopic submucosal dissection (ESD) scar by surveillance endoscopy; B: Endoscopic treatment. ESD was performed on the recurrent tumor, and an oval perforation 5 mm in length occurred at the site of extensive fibrosis during ESD; C: Endoscopic closure of the gastric perforation. The perforation was immediately observed and successfully closed with endoclips so that ESD could be continued resulting in *en-bloc* resection; D: Microscopic examination. A well to moderately differentiated mucosal adenocarcinoma without lymphovascular involvement was shown (hematoxylin and eosin stain, $\times 40$); E, F: Histopathologically, an ulcer scar from the initial ESD (UI-III) was also shown [between arrowheads (E)] [hematoxylin and eosin stain, $\times 1$ (E), $\times 20$ (F)].

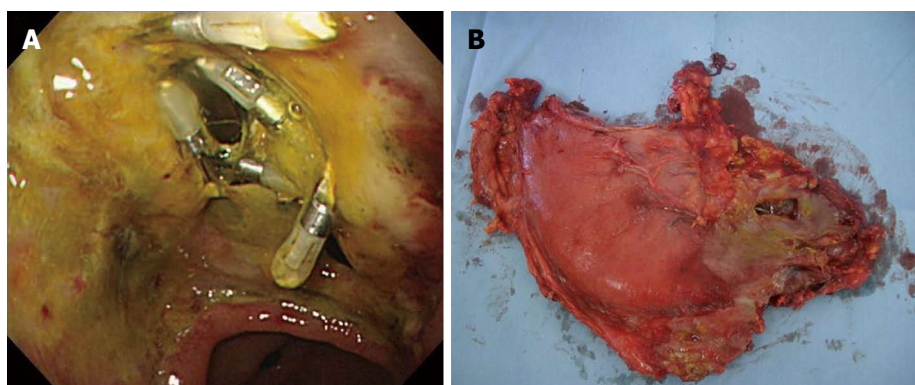


Figure 2 Dehiscence following successful endoscopic closure of the gastric perforation. A: Endoscopy five days after endoscopic submucosal dissection (ESD). The split-open perforation previously closed successfully with endoclips during ESD was revealed; B: Surgical findings. A perforation of the gastric wall extending to the omental bursa 30 mm \times 10 mm in length was seen. The perforation site was not covered with adipose tissue.

remarkable abdominal symptoms and physical findings of diffuse peritonitis.

ACKNOWLEDGMENTS

We wish to express our appreciation to Christopher Dix for his assistance in editing this manuscript.

REFERENCES

- 1 Gotoda T, Yamamoto H, Soetikno RM. Endoscopic submucosal dissection of early gastric cancer. *J Gastroenterol* 2006; **41**: 929-942
- 2 Oda I, Gotoda T, Hamanaka H, Eguchi T, Saito Y, Matsuda T, Bhandari P, Emura F, Saito D, Ono H. Endoscopic submucosal dissection for early gastric cancer: technical feasibility, operation time and complications from a large consecutive series. *Dig Endosc* 2005; **17**: 54-58
- 3 Onozato Y, Ishihara H, Iizuka H, Sohara N, Kakizaki S, Okamura S, Mori M. Endoscopic submucosal dissection for early gastric cancers and large flat adenomas. *Endoscopy* 2006; **38**: 980-986
- 4 Imagawa A, Okada H, Kawahara Y, Takenaka R, Kato J, Kawamoto H, Fujiki S, Takata R, Yoshino T, Shiratori Y.

- Endoscopic submucosal dissection for early gastric cancer: results and degrees of technical difficulty as well as success. *Endoscopy* 2006; **38**: 987-990
- 5 **Kakushima N**, Fujishiro M, Kodashima S, Muraki Y, Tateishi A, Omata M. A learning curve for endoscopic submucosal dissection of gastric epithelial neoplasms. *Endoscopy* 2006; **38**: 991-995
- 6 **Oda I**, Saito D, Tada M, Iishi H, Tanabe S, Oyama T, Doi T, Otani Y, Fujisaki J, Ajioka Y, Hamada T, Inoue H, Gotoda T, Yoshida S. A multicenter retrospective study of endoscopic resection for early gastric cancer. *Gastric Cancer* 2006; **9**: 262-270
- 7 **Isomoto H**, Shikuwa S, Yamaguchi N, Fukuda E, Ikeda K, Nishiyama H, Ohnita K, Mizuta Y, Shiozawa J, Kohno S. Endoscopic submucosal dissection for early gastric cancer: a large-scale feasibility study. *Gut* 2009; **58**: 331-336
- 8 **Minami S**, Gotoda T, Ono H, Oda I, Hamanaka H. Complete endoscopic closure of gastric perforation induced by endoscopic resection of early gastric cancer using endoclips can prevent surgery (with video). *Gastrointest Endosc* 2006; **63**: 596-601
- 9 **Yokoi C**, Gotoda T, Hamanaka H, Oda I. Endoscopic submucosal dissection allows curative resection of locally recurrent early gastric cancer after prior endoscopic mucosal resection. *Gastrointest Endosc* 2006; **64**: 212-218

S- Editor Gou SX L- Editor Webster JR E- Editor Zhang DN

Autoimmune pancreatitis complicated by gastric varices: A report of 3 cases

Norihiro Goto, Jun Mimura, Toshinao Itani, Motohito Hayashi, Yukari Shimada, Tomoaki Matsumori

Norihiro Goto, Jun Mimura, Toshinao Itani, Motohito Hayashi, Yukari Shimada, Tomoaki Matsumori, Department of Gastroenterology, Nishi-Kobe Medical Center, Hyogo 651-2273, Japan

Author contributions: Goto N and Mimura J designed the research study; Goto N, Mimura J, Itani T, Hayashi M, Shimada Y, and Matsumori T performed the esophagogastroduodenoscopies and clinical follow-ups; Goto N analyzed the data and wrote the manuscript.

Correspondence to: Norihiro Goto, MD, Department of Gastroenterology, Nishi-Kobe Medical Center, 5-7-1 Kojidai Nishiku, Kobe, Hyogo 651-2273, Japan. marshall_prs@nmc-kobe.org
Telephone: +81-78-9972200 Fax: +81-78-9972220

Received: January 22, 2012 Revised: April 17, 2012

Accepted: April 20, 2012

Published online: August 21, 2012

Key words: Autoimmune; Pancreatitis; Gastric varices

Peer reviewers: Dr. Terumi Kamisawa, Department of Internal Medicine, Tokyo Metropolitan Komagome Hospital, Honkomagome, Bunkyo-ku 31822, Tokyo; Kazuichi Okazaki, Professor, The Third Department of Internal Medicine, Kansai Medical University, 2-3-1 Shinmachi, Hirakata, Osaka 573-1191, Japan

Goto N, Mimura J, Itani T, Hayashi M, Shimada Y, Matsumori T. Autoimmune pancreatitis complicated by gastric varices: A report of 3 cases. *World J Gastroenterol* 2012; 18(31): 4228-4232 Available from: URL: <http://www.wjgnet.com/1007-9327/full/v18/i31/4228.htm> DOI: <http://dx.doi.org/10.3748/wjg.v18.i31.4228>

Abstract

We present three cases of autoimmune pancreatitis (AIP) complicated by gastric varices. Case 1: A 57-year-old man was diagnosed with AIP complicated by gastric varices and splenic vein obstruction. Splenomegaly was not detected at the time of the diagnosis. The AIP improved using steroid therapy, the splenic vein was reperfused, and the gastric varices disappeared; case 2: A 55-year-old man was diagnosed with AIP complicated by gastric varices, splenic vein obstruction, and splenomegaly. Although the AIP improved using steroid therapy, the gastric varices and splenic vein obstruction did not resolve; case 3: A 68-year-old man was diagnosed with AIP complicated by gastric varices, splenic vein obstruction, and splenomegaly. The gastric varices, splenic vein obstruction, and AIP did not improve using steroid therapy. These three cases suggest that gastric varices or splenic vein obstruction without splenomegaly may be an indication for steroid therapy in patients with AIP because the complications will likely become irreversible over time.

© 2012 Baishideng. All rights reserved.

INTRODUCTION

Autoimmune pancreatitis (AIP) is accepted worldwide as a distinctive type of pancreatitis, and the number of patients with AIP is increasing^[1-5]. However, there are few reports of AIP complicated by gastric varices, and the effect of steroid therapy on the gastric varices is unknown. We present three cases of autoimmune pancreatitis complicated by gastric varices.

CASE REPORT

Case 1

A 57-year-old man was admitted to the hospital due to back pain and jaundice. He had a history of diabetes mellitus and no history of habitual alcohol consumption. Laboratory studies revealed liver dysfunction (total bilirubin 3.1 mg/dL, aspartate aminotransferase 275 IU/L, alanine aminotransferase 557 IU/L, and alkaline phosphatase 2822 IU/L), hyperglycemia (236 mg/dL), elevated hemoglobin A1c (7.9%), and elevated IgG4 (176.4 mg/dL). Tumor markers, a complete blood count, electrolyte plasma levels, coagulation tests, amylase levels, lipase levels, and kidney function were all within the nor-

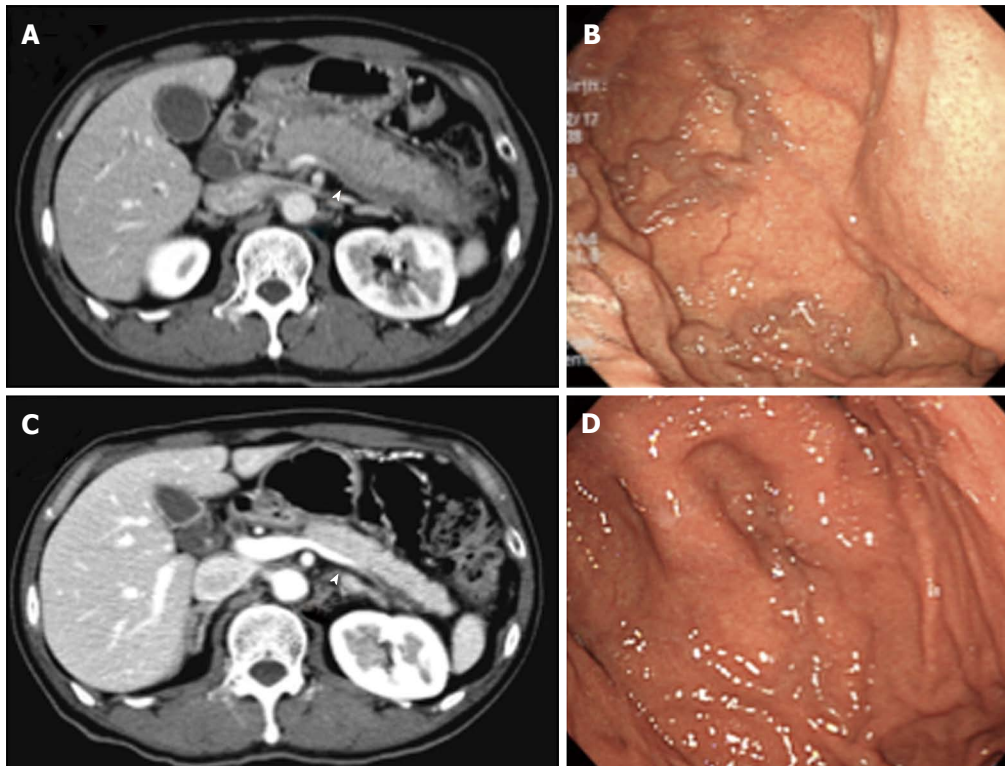


Figure 1 Disappearance of gastric varices following steroid therapy. A: Computed tomography showed a diffusely enlarged pancreas with a capsule-like rim, obstructed splenic vein (arrowhead), and dilated common bile duct; B: Esophagogastroduodenoscopy showed gastric varices in the fundus of the stomach; C: The splenic vein was reperused (arrowhead), and autoimmune pancreatitis improved following steroid therapy; D: Gastric varices disappeared following steroid therapy.

mal limits. Computed tomography (CT) of the abdomen revealed a diffusely enlarged pancreas with a capsule-like rim, an obstructed splenic vein, and a dilated common bile duct (Figure 1A). Endoscopic retrograde cholangiopancreatography (ERCP) revealed irregular narrowing of the main pancreatic duct and stricture of the lower common bile duct. Esophagogastroduodenoscopy (EGD) revealed gastric varices in the fundus of the stomach (Figure 1B).

According to the 2006 Clinical Diagnostic Criteria of The Japan Pancreas Society, the patient was diagnosed with AIP complicated by splenic vein obstruction and gastric varices. Endoscopic biliary drainage by stent placement was performed to alleviate the obstructive jaundice, followed by the oral administration of 30 mg/d prednisolone for 2 wk. The dose was tapered by 5 mg every 2 wk to a maintenance dose of 5 mg/d. Two weeks after the initial treatment, a CT scan showed that the enlarged pancreas had improved and that the splenic vein was reperused (Figure 1C). Six mo after the initial therapy, EGD showed that the gastric varices had disappeared (Figure 1D). Twenty-one mo after admission to the hospital, the patient was followed in the clinic with a maintenance dose of 5 mg/d prednisolone.

Case 2

A 55-year-old man was admitted to the hospital following the incidental detection of gastric fundal varices on EGD during a complete physical examination (Figure 2A). He

had no previous illnesses and no history of habitual alcohol consumption. The patient was asymptomatic, and nothing abnormal was detected on physical examination. A CT scan revealed a locally enlarged pancreatic tail with a capsule-like rim around the lesion, an obstructed splenic vein, and splenomegaly (Figure 2B). ERCP was performed, revealing irregular narrowing of the main pancreatic duct in the pancreatic tail (Figure 2C). Laboratory studies showed an elevated IgG4 (239.1 mg/dL). Tumor markers, a complete blood count, electrolyte plasma levels, coagulation tests, amylase levels, lipase levels, and kidney and liver functions were all within the normal limits.

According to the 2006 Clinical Diagnostic Criteria, the patient was diagnosed with AIP complicated by splenic vein obstruction, gastric varices, and splenomegaly. Oral administration of 30 mg/d prednisolone for 4 wk was used to induce remission, and the dose was tapered by 5 mg every 2 wk to a maintenance dose of 5 mg/d. Two weeks after the initial treatment, a CT scan showed that the enlarged pancreas tail had improved and that the capsule-like rim had disappeared (Figure 2D). However, the splenic vein was not reperused. Ten mo after the initial therapy, EGD showed no improvement of the gastric varices. One year after hospital admission, the patient was followed in the clinic with a maintenance dose of 5 mg/d prednisolone.

Case 3

A 68-year-old man was admitted to the hospital due

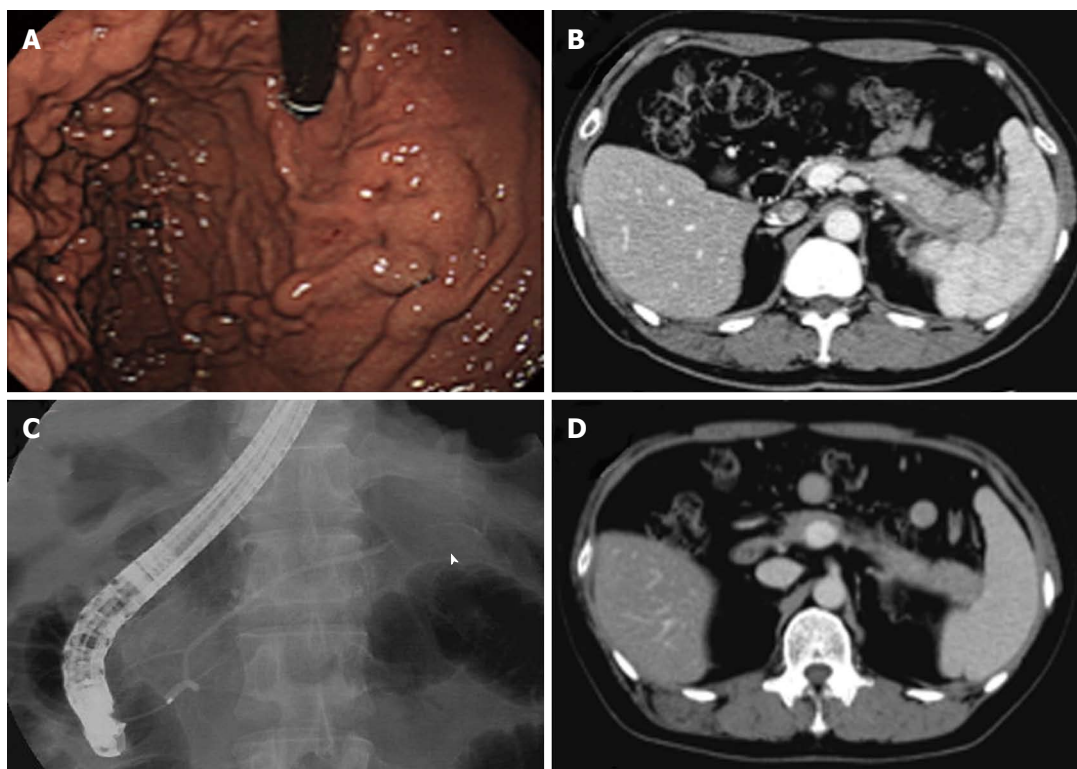


Figure 2 The splenic vein was not reperfused, although the autoimmune pancreatitis improved. A: Esophagogastroduodenoscopy showed gastric varices in the fundus of the stomach; B: Computed tomography showed a locally enlarged pancreatic tail with a capsule-like rim, an obstructed splenic vein, and splenomegaly; C: Endoscopic retrograde cholangiopancreatography showed irregular narrowing of the main pancreatic duct in the pancreatic tail (arrowhead); D: Autoimmune pancreatitis improved following steroid therapy, but the splenic vein was not reperfused.

to hematemesis. An emergency EGD was performed, revealing gastric ulcer bleeding at the gastric notch and incidentally detected gastric varices in the fundus of the stomach (Figure 3A). The gastric ulcer was successfully treated with endoscopic coagulation and administration of a proton pump inhibitor. Additional investigations were performed to ascertain the cause of the gastric varices. The patient had a past history of diabetes mellitus and no history of habitual alcohol consumption. A CT scan revealed a slightly enlarged pancreas with a capsule-like rim around the lesion, a pancreatic stone in the pancreatic tail, an obstructed splenic vein, and splenomegaly (Figure 3B and C). Magnetic resonance cholangiopancreatography (MRCP) revealed irregular narrowing of the main pancreatic duct in the pancreatic head and body, slight dilation of the main pancreatic duct in the pancreatic tail, stricture of the hilar bile duct and lower bile duct, and dilation of the right intra-hepatic bile duct (Figure 3D). ERCP showed the same findings as MRCP. Laboratory studies revealed elevated levels of IgG4 (186 mg/dL), hemoglobin A1c (8.0%), carcinoembryonic antigen (8.2 ng/mL), CA19-9 (38.7 U/mL), and alkaline phosphatase (345 IU/L). The complete blood count, electrolyte plasma levels, coagulation tests, amylase levels, lipase levels, and kidney function were all within the normal limits.

Although the slight dilation of the distal main pancreatic duct was atypical of AIP, the slightly enlarged pancreas, the irregular narrowing of the main pancreatic duct in

the pancreatic head and body, and the elevated levels of IgG4 met the 2006 Clinical Diagnostic Criteria. The patient was diagnosed with AIP complicated by splenic vein obstruction, gastric varices, splenomegaly, and sclerosing cholangitis. Oral administration of 30 mg/d prednisolone for 4 wk was used to induce remission, and the dose was tapered by 5 mg every 2 wk to a maintenance dose of 5 mg/d. However, a CT scan showed no improvement of the pancreatic lesion, and EGD showed no improvement of the gastric varices. Because steroid therapy was not effective, maintenance therapy was discontinued 5 mo after the initial treatment. One year after hospital admission, the patient was followed in the clinic without treatment.

DISCUSSION

There are few reports of autoimmune pancreatitis complicated by gastric varices. The effects of steroid therapy on the varices is unknown^[6]. However, the reported 8%^[7] frequency of splenic vein obstruction in patients with chronic pancreatitis indicates that it is not a rare complication. Splenic vein obstruction causes a localized form of portal hypertension, known as sinistral portal hypertension, which leads to the formation of gastric varices along the fundus and the greater curvature of the stomach due to increased blood flow through the short gastric veins or the gastroepiploic vein^[8]. From 1999 to 2011, our hospital treated 20 consecutive patients with AIP who fulfilled either the 2006 Clinical Diagnostic Criteria

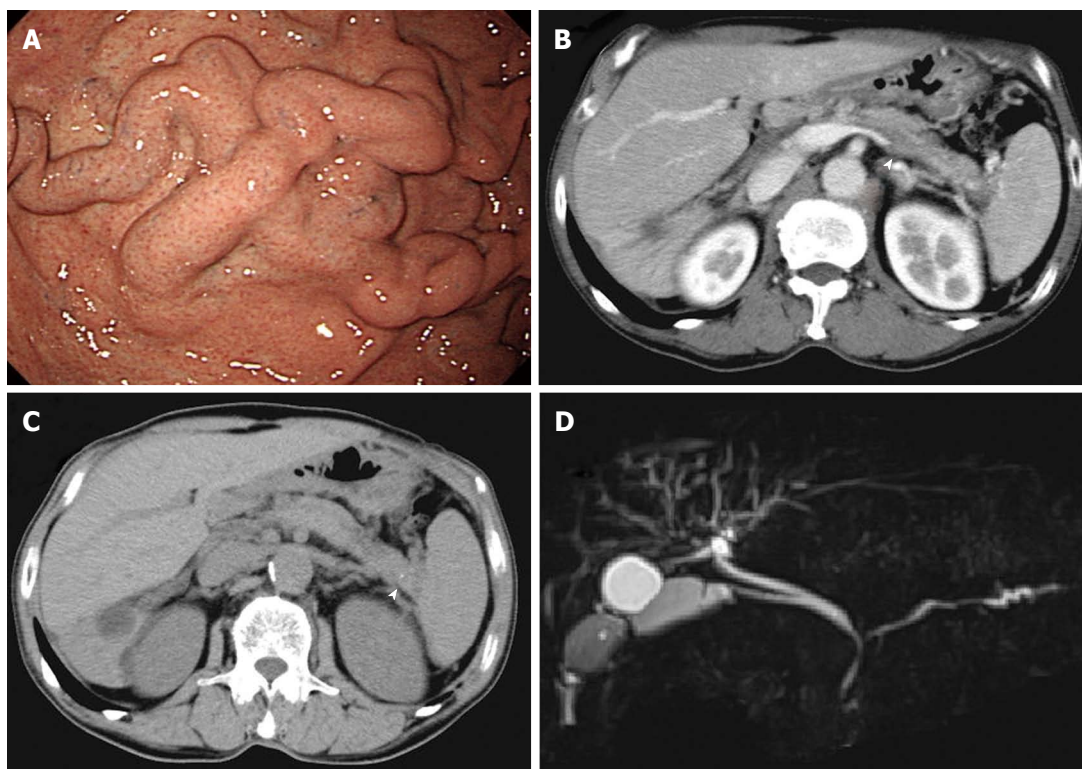


Figure 3 Autoimmune pancreatitis that did not improve with steroid therapy. A: Esophagogastroduodenoscopy showed gastric varices in the fundus of the stomach; B: Computed tomography (CT) showed a slightly enlarged pancreas with a capsule-like rim, an obstructed splenic vein (arrowhead), and splenomegaly; C: CT showed a pancreatic stone in the pancreatic tail (arrowhead); D: Magnetic resonance cholangiopancreatography showed irregular narrowing of the main pancreatic duct in the pancreatic head and body, slight dilation of the main pancreatic duct in the pancreatic tail, stricture of the hilar bile duct and lower bile duct, and dilation of the right intra-hepatic bile duct.

of The Japan Pancreas Society or the Asia diagnostic criteria. Splenic vein obstruction was confirmed in 4 of the patients (20%) using CT, and 3 of the 4 patients (15%) had gastric varices.

The clinical course of these three cases varied depending on the presence of splenomegaly. In case 1, splenomegaly was not detected at the time of diagnosis. Gastric varices disappeared as the AIP improved using steroid therapy; In case 2, splenomegaly was detected at the time of diagnosis. The gastric varices did not improve, although the AIP improved using steroid therapy; In case 3, splenomegaly was detected at the time of diagnosis. Neither the gastric varices nor the AIP improved with steroid therapy. These three cases suggest that gastric varices complicating AIP without splenomegaly may improve using steroid therapy.

The pathogenetic hypothesis of splenic vein obstruction has been related to many factors: compression by a pseudocyst or an enlarged pancreatic parenchyma and secondary involvement of the vein by surrounding edema, cellular infiltration, and the fibroinflammatory process^[9]. Whether the splenic vein obstruction is formed by mechanical force or inflammatory infiltration, the obstruction will become an irreversible thrombosis over time. Although the AIP improved in case 2, the splenic vein obstruction, which had likely progressed into a thrombosis, was irreversible. A gastrosplenic shunt or other collateral veins that drain into the systemic circulation

were not detected on CT scans in any of the three cases. Development of congestive splenomegaly may have been dependent on the length of time the patients had been affected with sinistral portal hypertension. These three cases indicate the need to reperfuse the obstructed splenic vein before the development of splenomegaly, otherwise the obstruction becomes irreversible. According to a nationwide survey by the Research Committee of Intractable Pancreatic Diseases conducted by the Ministry of Health, Labor and Welfare of Japan, the remission rate of steroid-treated AIP is 98%^[10]. However, rare cases of steroid-refractory AIP can occur. Kamisawa *et al*^[11] reported the development of pancreatic atrophy in 5 out of 23 patients with AIP. Takayama *et al*^[12] reported that AIP has the potential to be a progressive disease with pancreatic stones. These reports suggest that recurrent cases of AIP can turn into chronic pancreatitis-like lesions during long-term follow-up and become refractory to steroid therapy. In case 3, the AIP was refractory to steroid therapy. Because the enlargement of the pancreas was not prominent and a pancreatic stone was detected, the lesion was likely the result of recurrent inflammation of AIP.

The role of a prophylactic splenectomy in asymptomatic patients with splenic vein obstruction and gastric varices remains controversial. Badley concluded that the benefit of preventing possible bleeding of the varices outweighs the risk of postsplenectomy sepsis^[13], although

Bernades *et al*^[7] reported that the risk of variceal bleeding is lower than previously reported. In cases 2 and 3, we did not perform a prophylactic splenectomy or partial splenic embolization because the patients opted for a watchful waiting approach.

The indications for steroid therapy in patients with AIP are symptoms such as obstructive jaundice, abdominal pain, back pain and the presence of symptomatic extrapancreatic lesions^[1]. However, some patients with AIP improve spontaneously^[1,14]. The treatment of asymptomatic patients with AIP remains controversial. Based on the potential risk and benefits, these three cases suggest that patients with AIP and gastric varices or splenic vein obstruction without splenomegaly should be treated with steroids before pancreatic lesions or splenic vein obstructions become irreversible. Because this study only included three cases, it is necessary to collect data on more patients with AIP complicated by gastric varices to effectively evaluate this hypothesis.

In conclusion, we treated 3 cases of autoimmune pancreatitis complicated with gastric varices. Gastric varices or splenic vein obstruction without splenomegaly may be an indication for steroid therapy in patients with AIP.

REFERENCES

- 1 **Kamisawa T**, Okazaki K, Kawa S, Shimosegawa T, Tanaka M. Japanese consensus guidelines for management of autoimmune pancreatitis: III. Treatment and prognosis of AIP. *J Gastroenterol* 2010; **45**: 471-477
- 2 **Yoshida K**, Toki F, Takeuchi T, Watanabe S, Shiratori K, Hayashi N. Chronic pancreatitis caused by an autoimmune abnormality. Proposal of the concept of autoimmune pancreatitis. *Dig Dis Sci* 1995; **40**: 1561-1568
- 3 **Okazaki K**, Chiba T. Autoimmune related pancreatitis. *Gut* 2002; **51**: 1-4
- 4 **Pickartz T**, Mayerle J, Lerch MM. Autoimmune pancreatitis. *Nat Clin Pract Gastroenterol Hepatol* 2007; **4**: 314-323
- 5 **Gardner TB**, Chari ST. Autoimmune pancreatitis. *Gastroenterol Clin North Am* 2008; **37**: 439-460, vii
- 6 **Fuke H**, Shimizu A, Shiraki K. Gastric varix associated with autoimmune pancreatitis. *Clin Gastroenterol Hepatol* 2006; **4**: xxxii
- 7 **Bernades P**, Baetz A, Lévy P, Belghiti J, Menu Y, Fékété F. Splenic and portal venous obstruction in chronic pancreatitis. A prospective longitudinal study of a medical-surgical series of 266 patients. *Dig Dis Sci* 1992; **37**: 340-346
- 8 **Sakorafas GH**, Tsiotou AG. Splenic-vein thrombosis complicating chronic pancreatitis. *Scand J Gastroenterol* 1999; **34**: 1171-1177
- 9 **Lillemoe KD**, Yeo CJ. Management of complications of pancreatitis. *Curr Probl Surg* 1998; **35**: 1-98
- 10 **Nishimori I**, Okazaki K, Kawa S, Otsuki M. Treatment for autoimmune pancreatitis. *J Biliary Tract Pancreas* 2007; **28**: 961-966
- 11 **Kamisawa T**, Yoshiike M, Egawa N, Nakajima H, Tsuruta K, Okamoto A. Treating patients with autoimmune pancreatitis: results from a long-term follow-up study. *Pancreatol* 2005; **5**: 234-238; discussion 238-240
- 12 **Takayama M**, Hamano H, Ochi Y, Saegusa H, Komatsu K, Muraki T, Arakura N, Imai Y, Hasebe O, Kawa S. Recurrent attacks of autoimmune pancreatitis result in pancreatic stone formation. *Am J Gastroenterol* 2004; **99**: 932-937
- 13 **Bradley EL**. The natural history of splenic vein thrombosis due to chronic pancreatitis: indications for surgery. *Int J Pancreatol* 1987; **2**: 87-92
- 14 **Wakabayashi T**, Kawaura Y, Satomura Y, Watanabe H, Motoo Y, Sawabu N. Long-term prognosis of duct-narrowing chronic pancreatitis: strategy for steroid treatment. *Pancreas* 2005; **30**: 31-39

S- Editor Gou SX L- Editor A E- Editor Zhang DN

Ischemic colitis during interferon-ribavirin therapy for chronic hepatitis C: A case report

Su Jung Baik, Tae Hun Kim, Kwon Yoo, Il Hwan Moon, Min-Sun Cho

Su Jung Baik, Department of Gastroenterology, Health Promotion Center, Yonsei University Gangnam Severance Hospital, Seoul 158-050, South Korea

Tae Hun Kim, Kwon Yoo, Il Hwan Moon, Department of Internal Medicine, Ewha Medical Research Institute, Ewha University Mokdong Hospital, Ewha Womans University School of Medicine, Seoul 158-710, South Korea

Min-Sun Cho, Department of Pathology, Ewha University Mokdong Hospital, Ewha Womans University School of Medicine, Seoul 158-710, South Korea

Author contributions: Baik SJ drafted and edited the manuscript; Kim TH treated the patient and contributed both to manuscript revision and final approval; Yoo K and Moon IH contributed to the literature review; Cho MS contributed to the pathological analysis.

Correspondence to: Tae Hun Kim, MD, Professor, Department of Internal Medicine, Ewha Medical Research Institute, Ewha University Mokdong Hospital, Ewha Womans University School of Medicine, 911-1 Mokdong, Yangcheon-gu, Seoul 158-710, South Korea. thkm@ewha.ac.kr

Telephone: +82-2-26502724 Fax: +82-2-26552076

Received: December 8, 2011 Revised: February 10, 2012

Accepted: May 6, 2012

Published online: August 21, 2012

Abstract

Ischemic colitis is a rare complication of interferon administration. Only 9 cases in 6 reports have been described to-date. This report describes a case of ischemic colitis during pegylated interferon and ribavirin treatment for chronic hepatitis C, and includes a review of the relevant literature. A 48-year-old woman was treated with pegylated interferon α -2a and ribavirin for chronic hepatitis C, genotype 1b. After 19 wk of treatment, the patient complained of severe afebrile abdominal pain with hematochezia. Vital signs were stable and serum white blood cell count was within the normal range. Abdominal computed tomography showed diffuse colonic wall thickening from the splenic flexure to the proximal sigmoid colon, which is the most vulnerable area for the development of ischemic

colitis. Colonoscopy revealed an acute mucosal hyperemic change, with edema and ulcerations extending from the proximal descending colon to the sigmoid colon. Colonic mucosal biopsy revealed acute exudative colitis. Polymerase chain reaction and culture for *Mycobacterium tuberculosis* were negative and the cultures for cytomegalovirus, *Salmonella* and *Shigella* species were negative. After discontinuation of interferon and ribavirin therapy, abdominal pain and hematochezia subsided and, following colonoscopy showed improvement of the mucosal ulcerations. Ischemic colitis cases during interferon therapy in patients with chronic hepatitis C reported so far have all involved the descending colon. Ischemic colitis is a rarely encountered complication of interferon administration in patients with chronic hepatitis C and should be considered when a patient complains of abdominal pain and hematochezia.

© 2012 Baishideng. All rights reserved.

Key words: Ischemia; Hepatitis C; Interferon

Peer reviewers: Ole Haagen Nielsen, Professor, Department of Gastroenterology, Herlev Hospital, University of Copenhagen, Herlev Ringvej 75, DK-2730 Herlev, Denmark; Dr. Giuseppe Chiarioni, Division of Gastrointestinal Rehabilitation, Azienda Ospedaliera di Verona, Ospedale di Valeggio s/M, 37067 Valeggio, Italy

Baik SJ, Kim TH, Yoo K, Moon IH, Cho MS. Ischemic colitis during interferon-ribavirin therapy for chronic hepatitis C: A case report. *World J Gastroenterol* 2012; 18(31): 4233-4236 Available from: URL: <http://www.wjgnet.com/1007-9327/full/v18/i31/4233.htm> DOI: <http://dx.doi.org/10.3748/wjg.v18.i31.4233>

INTRODUCTION

Pegylated interferon (IFN) combined with ribavirin is currently the standard treatment for chronic hepatitis C (CHC) and can achieve sustained virological response

in approximately 55% of genotype-I hepatitis C virus (HCV) infections^[1]. The side effects of this combination treatment result in premature treatment termination in 10%-15% and dose adjustment in 32%-42% of patients^[1]. Therefore, physicians need to be well aware of both the common and uncommon side effects of treatment. Ischemic colitis is a rare complication of interferon administration^[2]. Only 9 cases in 6 reports (one in Japanese^[3] and 5 in English^[2,4-7]) have been described to date. This report describes a case of ischemic colitis during pegylated interferon and ribavirin treatment for CHC and includes a review of the relevant literatures.

CASE REPORT

A 48-year-old woman was admitted for the evaluation of acute abdominal pain and hematochezia. The patient had been treated with combination therapy of pegylated IFN- α 2a (180 μ g/wk) (Pegasys; Roche, Basel, Switzerland) and ribavirin (1000 mg/d) (LG Ribavirin; LG Life Sciences, Seoul, Korea) for CHC, genotype Ib. A qualitative HCV test was initially obtained using reverse transcription-polymerase chain reaction (RT-PCR) (Abbott Laboratories, Abbott Park, IL, United States), and the serum HCV viral load was 1.67×10^6 viral copies/mL. The serum HCV RNA level decreased to undetectable levels after 12 wk of treatment. The treatment process was uneventful until 16 wk of therapy. At week 16, the patient complained of mild epigastric discomfort and nausea, which resolved spontaneously a few days later. Three weeks later, at week 19 of therapy, the patient complained of severe abdominal pain with hematochezia, but she remained afebrile. Small amounts of bloody stool were passed 2-3 times per day. The patient denied recent travel or additional medications such as antibiotics or non-steroidal anti-inflammatory drugs. The patient had no history of diabetes mellitus, hypertension, inflammatory bowel disease, atrial fibrillation, valvular heart disease, coronary artery disease, or hypercoagulable conditions. She was a non-smoker, and her family history was unremarkable.

Physical examination revealed direct tenderness on the left lower quadrant of the abdomen. Blood pressure was 114/76 mmHg, pulse 80 beats/min, respiration rate 20/min, and body temperature 37.9 °C. Complete blood count revealed a hematocrit of 26.9%, hemoglobin 8.7 gm/dL, platelets 115 000/ μ L, and white blood cell count 4700/ μ L with differential counts within the normal range. C-reactive protein was slightly elevated at 0.7 mg/dL (normal < 0.4 mg/dL). Serum electrolytes, liver profile, renal function tests, amylase, and lipase were within normal limits. The coagulation profile was within the normal range, with a prothrombin time of 11.2 s and an activated partial thromboplastin time of 23.9 s. Upper endoscopy was performed 6 mo prior to admission, which documented a healing stage small gastric ulceration at the antrum. *Helicobacter pylori* infection was documented by histological examination and was successfully eradicated

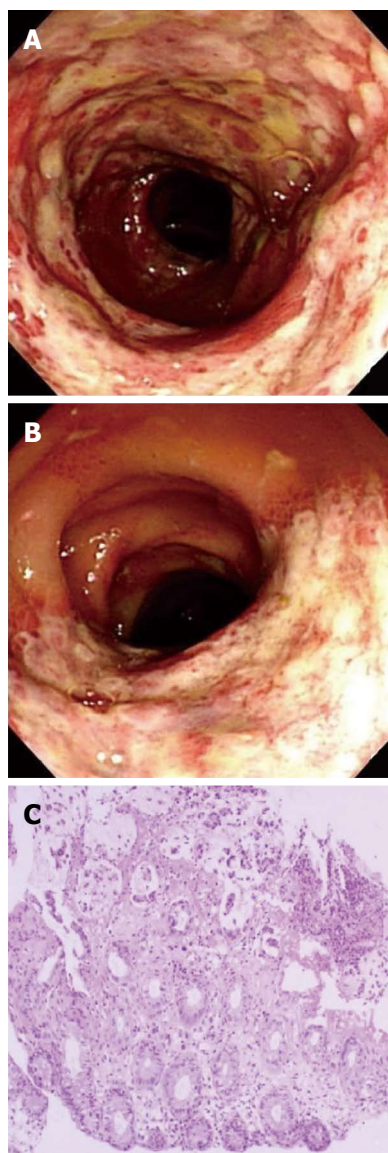


Figure 1 Colonoscopy images and pathology. A: Mucosal hyperemic change with edema, erosion, and ulcerations and hemorrhagic friable mucosa on the sigmoid colon; B: Segmental ulceration was seen on the proximal descending colon; C: Pathological examination of the descending colon showed acute exudative colitis. Epithelial detachment was observed (hematoxylin and eosin stain, $\times 40$).

with antibiotic therapy at that time. At admission, upper endoscopy was negative for an active bleeding source, and colonoscopic examination revealed acute hyperemic mucosal changes with edema, erosion, and ulcerations. Acute inflamed, friable mucosal changes extended from the sigmoid colon (Figure 1A) to the proximal descending colon (Figure 1B). The rectum showed relatively normal mucosa. Colonic mucosal biopsy revealed acute exudative colitis compatible with a diagnosis of ischemic colitis (Figure 1C). On the biopsy specimen, staining for cytomegalovirus showed no positive cells, and staining for acid-fast bacilli was negative. Tuberculous nucleic acid was undetectable by polymerase chain reaction. A serum anti-Streptolysin O test was negative. Bacteriologic culture studies of stool and colonic fluid were negative

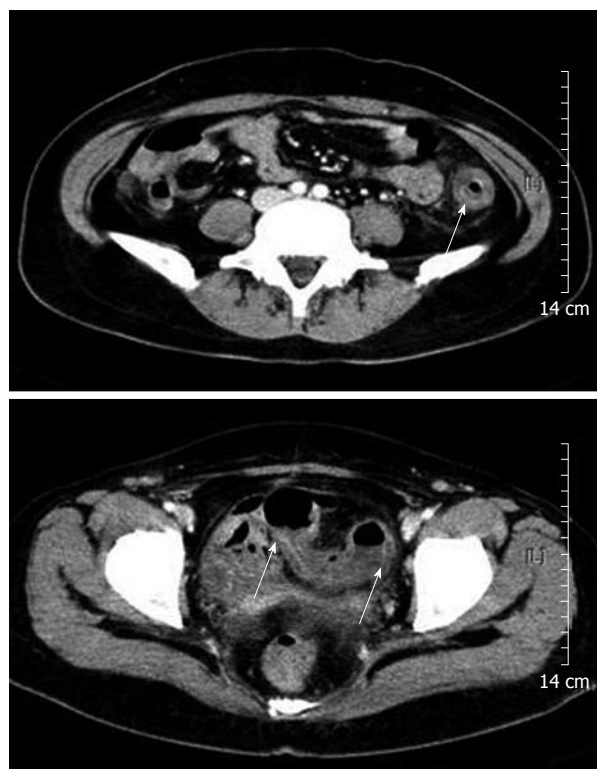


Figure 2 Abdominal computed tomography. A: Circumferentially layered wall thickening and pericolic fat infiltration at the descending colon (arrow); B: Circumferential wall thickening and pericolic fat infiltration at the proximal sigmoid colon (arrows).

for *Mycobacterium*, *Salmonella*, and *Shigella* species. Abdominal computed tomography showed circumferential wall thickening and pericolic fat infiltration from the descending colon to the proximal sigmoid colon, a well-known predisposing area for the development of ischemic colitis (Figure 2). The findings from colonoscopy, computed tomography, and pathology were all compatible with the diagnosis of ischemic colitis.

After IFN and ribavirin treatment were discontinued, the patient's abdominal pain decreased and hematochezia resolved. One week later, subsequent colonoscopy showed marked improvement in ulceration and mucosal edema. Serum HCV RNA remained undetectable for up to 3 mo after cessation of treatment, but reappeared 1 year later. The reappearance of serum HCV RNA suggests that the antiviral treatment for CHC was not successful.

DISCUSSION

In current standard combination therapy of pegylated IFN and ribavirin in CHC patients, more than 50% of sustained virological response is expected. However, a large proportion of the patients are not eligible for the treatment or drop out early during the treatment due to side effects.

The side effects of IFN and ribavirin combination therapy are mostly associated with IFN administration, while hemolytic anemia is attributable to ribavirin^[1]. Side

Table 1 Characteristics of ischemic colitis associated with interferon treatment in chronic hepatitis C patients

Ref.	Age/gender, diagnosis	Treatment and duration	Location of ischemic colitis
Okanoue <i>et al</i> ^[2]	47/F, CHC	IFN- α , 4 wk	Rectum to descending colon
	55/F, CHC	IFN, 23 wk	Rectum to descending colon
	65/M, CHC	IFN, 5 wk	Rectum to descending colon
Horigome <i>et al</i> ^[3]	53/M, CHC	IFN- α , 12 wk	Sigmoid colon to descending colon
Tada <i>et al</i> ^[6]	65/M, CHC	IFN- α , 4 wk	Descending colon
	55/F, CHC	IFN- α , 24 wk	Descending colon
Leung <i>et al</i> ^[7]	44/M, CHC	Pegylated IFN- α , 34 wk	Sigmoid colon to splenic flexure
Wenner <i>et al</i> ^[4]	7/F, CHC with CRF	IFN- α , 7 wk	Descending colon
Punnam <i>et al</i> ^[5]	51/M, CHC	Pegylated IFN- α , 12 wk	Mid-transverse to proximal descending colon

CHC: Chronic hepatitis C; CRF: Chronic renal failure; IFN- α : Interferon- α ; F: Female; M: Male.

effects associated with IFN treatment have been described not only in CHC, but also in chronic hepatitis B^[8], chronic myeloid leukemia^[9], metastatic renal cell carcinoma^[10], and multiple myeloma^[11]. Flu-like symptoms such as general malaise, fever, arthralgia, headache, and hematologic abnormalities such as leukopenia and thrombocytopenia are frequently observed early adverse effects of IFN- α administration^[2]. Although the severity of these symptoms is directly related to the dose and frequency of IFN administration, remarkable individual variation has been observed^[2]. Among the various gastrointestinal side effects of IFN- α , ischemic colitis is rarely reported during treatment of CHC, occurring in less than 1% of patients^[12]. Other than ischemic colitis, microscopic colitis^[7] and ulcerative colitis^[13] have also been reported.

Nine cases of ischemic colitis related to IFN therapy in CHC have been reported in 6 studies, and the most common symptoms were abdominal pain and lower gastrointestinal bleeding such as melena and hematochezia^[2-7]. The descending colon was most frequently involved in all ischemic colitis cases associated with CHC (Table 1). In reported cases, hematochezia and melena appeared between week 4 and 34 of IFN treatment, and the mean duration of IFN treatment before the occurrence of ischemic colitis was 14 wk. The characteristics of this case correspond well with those of previously reported cases in terms of symptoms, location, and period of duration.

The etiology of ischemic colitis is not yet clearly elucidated. The mechanism of IFN-induced ischemic colitis is thought to be associated with immune modulation of cytokine networks. Sparano *et al*^[10] documented the role of interleukin-2 (IL-2) and IFN- α in the development of colonic ischemia. They suggested that a disordered coagulation cascade played a role in the pathogenesis of colonic ischemia, assuming that derangement of coagulation is

mediated by tumor necrosis factor or its interactions with other cytokines^[10]. IFN therapy also induces an increase in plasma-activated complement C5a, a potent intravascular aggregator of granulocytes, favoring the development of microthrombi in small vessels. IFN-induced vasculitic reactions, mediated by the deposition of immune complexes in the vasculature, may also play a pathogenic role in ischemia of various organs^[14,15]. Thrombogenic effects of activated cytokines and immune complex-mediated vasculitic reactions may play a role in the pathogenesis of IFN-induced ischemic colitis^[14]. The potential role of cytokines for the development of IFN induced ischemic colitis needs to be investigated further.

In conclusion, physicians should be vigilant of the various common and uncommon complications of both pegylated IFN and ribavirin. Ischemic colitis is a rarely encountered complication of pegylated IFN administration but it should be considered when a patient complains of abdominal pain and hematochezia.

REFERENCES

- 1 **Sung H**, Chang M, Saab S. Management of Hepatitis C Antiviral Therapy Adverse Effects. *Curr Hepat Rep* 2011; **10**: 33-40
- 2 **Okanoue T**, Sakamoto S, Itoh Y, Minami M, Yasui K, Sakamoto M, Nishioji K, Katagishi T, Nakagawa Y, Tada H, Sawa Y, Mizuno M, Kagawa K, Kashima K. Side effects of high-dose interferon therapy for chronic hepatitis C. *J Hepatol* 1996; **25**: 283-291
- 3 **Horigome H**, Takezono Y, Fujino N, Uchida A, Murasaki G. [A case of ischemic colitis associated with interferon treatment]. *Nihon Shokakibyō Gakkai Zasshi* 1996; **93**: 181-184
- 4 **Wenner WJ**, Piccoli DA. Colitis associated with alpha interferon? *J Clin Gastroenterol* 1997; **25**: 398-399
- 5 **Punnam SR**, Pothula VR, Gourineni N, Punnam A, Ranganathan V. Interferon-ribavirin-associated ischemic colitis. *J Clin Gastroenterol* 2008; **42**: 323-325
- 6 **Tada H**, Saitoh S, Nakagawa Y, Hirana H, Morimoto M, Shima T, Shimamoto K, Okanoue T, Kashima K. Ischemic colitis during interferon-alpha treatment for chronic active hepatitis C. *J Gastroenterol* 1996; **31**: 582-584
- 7 **Leung Y**, Urbanski SJ, Schindel L, Myers RP. Ischemic colitis during pegylated interferon-alpha and ribavirin therapy for chronic hepatitis C. *Can J Gastroenterol* 2006; **20**: 661-663
- 8 **Gish RG**, Lau DT, Schmid P, Perrillo R. A pilot study of extended duration peginterferon alfa-2a for patients with hepatitis B e antigen-negative chronic hepatitis B. *Am J Gastroenterol* 2007; **102**: 2718-2723
- 9 **Hehlmann R**, Hochhaus A, Baccarani M. Chronic myeloid leukaemia. *Lancet* 2007; **370**: 342-350
- 10 **Sparano JA**, Dutcher JP, Kaleya R, Caliendo G, Fiorito J, Mitsudo S, Shechner R, Boley SJ, Gucalp R, Ciobanu N. Colonic ischemia complicating immunotherapy with interleukin-2 and interferon-alpha. *Cancer* 1991; **68**: 1538-1544
- 11 **Ludwig H**, Fritz E. Interferon in multiple myeloma--summary of treatment results and clinical implications. *Acta Oncol* 2000; **39**: 815-821
- 12 **Fried MW**. Side effects of therapy of hepatitis C and their management. *Hepatology* 2002; **36**: S237-S244
- 13 **Sprengrer R**, Sagmeister M, Offner F. Acute ulcerative colitis during successful interferon/ribavirin treatment for chronic hepatitis. *Gut* 2005; **54**: 438-439; author reply 439
- 14 **Guyer DR**, Tiedeman J, Yannuzzi LA, Slakter JS, Parke D, Kelley J, Tang RA, Marmor M, Abrams G, Miller JW. Interferon-associated retinopathy. *Arch Ophthalmol* 1993; **111**: 350-356
- 15 **Nadir A**, Amin A, Chalisa N, van Thiel DH. Retinal vein thrombosis associated with chronic hepatitis C: a case series and review of the literature. *J Viral Hepat* 2000; **7**: 466-470

S- Editor Gou SX L- Editor Rutherford A E- Editor Zhang DN

Spontaneous hemoperitoneum from hepatic metastatic trophoblastic tumor

Ya-Hui Liu, Hong-Xi Ma, Bai Ji, Dian-Bo Cao

Ya-Hui Liu, Bai Ji, Department of Surgery, The First Hospital of Jilin University, Changchun 130021, Jilin Province, China
Hong-Xi Ma, Department of Pathology, The First Hospital of Jilin University, Changchun 130021, Jilin Province, China
Dian-Bo Cao, Department of Radiology, The First Hospital of Jilin University, Changchun 130021, Jilin Province, China

Author contributions: Liu YH, Bai J made substantial contributions to the research design and patient treatment; Ma HX performed the histopathological analysis; Cao DB contributed to radiological imaging examination and diagnosis, and drafted the paper; and all authors have read and approved the final version to be published.

Correspondence to: Dian-Bo Cao, MD, PhD, Assistant Professor, Department of Radiology, The First Hospital of Jilin University, No. 71 Xinmin Street, Changchun 130021, Jilin Province, China. caotian1970@yeah.net

Telephone: +86-431-88782911 Fax: +86-431-85654528

Received: March 12, 2012 Revised: April 25, 2012

Accepted: May 26, 2012

Published online: August 21, 2012

common appearances of hepatic metastases. For SP resulting from hepatic metastatic tumors, surgical intervention is still the predominant therapeutic method, but the prognosis is very poor.

© 2012 Baishideng. All rights reserved.

Key words: Hemoperitoneum; Hepatic metastases; Trophoblastic tumor; Computed tomography; Treatment

Peer reviewer: Dr. Guideng Li, Department of Biological Chemistry, University of California, Irvine, CA 92697-4120, United States

Liu YH, Ma HX, Ji B, Cao DB. Spontaneous hemoperitoneum from hepatic metastatic trophoblastic tumor. *World J Gastroenterol* 2012; 18(31): 4237-4240 Available from: URL: <http://www.wjgnet.com/1007-9327/full/v18/i31/4237.htm> DOI: <http://dx.doi.org/10.3748/wjg.v18.i31.4237>

Abstract

Spontaneous hemoperitoneum (SP) is defined as the presence of blood within the peritoneal cavity that is unrelated to trauma. Although there is a vast array of etiologies for SP, primary hepatocellular carcinoma and hepatic adenoma are considered to be the most common causes. Hepatic metastatic tumor associated with spontaneous rupture is rare. SP from hepatic metastatic trophoblastic tumor may initially present with a sudden onset of abdominal pain. Abdominal computed tomography (CT) plays an important role in establishing the diagnosis of SP, indicating its origin and etiology, and determining subsequent management. Herein, we report an uncommon case of hemoperitoneum from spontaneous rupture of a hepatic metastatic trophoblastic tumor in a young female patient. Interestingly, the contrast-enhanced CT findings demonstrated hypervascular hepatic masses with persistent enhancement at all phases, which were completely different from the

INTRODUCTION

Spontaneous hemoperitoneum (SP) is defined as the presence of blood within the peritoneal cavity that is unrelated to trauma. Primary hepatocellular carcinoma (HCC) and hepatic adenoma are considered to be the most common causes; however, hepatic metastatic tumors associated with SP are rare. Those metastatic tumors may include colon, lung, renal cell and testicular neoplasms, and Wilm's tumor, but few cases of metastatic trophoblastic tumor responsible for HP have been reported, especially in the absent evidence of primary malignant tumor. Computed tomography (CT) plays an important role in establishing the diagnosis of SP. Metastatic liver tumors display variant appearances in routine CT scan and are often classified as hypervascular, hypovascular and nonvascular metastases on dynamic contrast-enhanced CT scan. Most of the hepatic metastatic tumors present with hypovascular appearances, namely mild enhancement in both the portal

phase and delayed phase. But in our patient with hepatic trophoblastic tumor, there were typically unusual presentations, which showed almost identical enhancement patterns with abdominal aorta in all phases. To our knowledge, there are few reports of similar cases focusing on uncommon CT manifestations in hepatic metastatic trophoblastic tumor. We report an uncommon case of hemoperitoneum from spontaneous rupture of a hepatic metastatic trophoblastic tumor in a young female patient below.

CASE REPORT

A 24-year-old girl was admitted to our emergency department because of sudden onset of abdominal pain, and emergent non-enhanced CT scan showed intrahepatic multiple lesions associated with rupture and bleeding into the peritoneal cavity (Figure 1). Three months ago, she underwent splenic repair, and her family could not tell about the specific cause even after she was discharged from the hospital. She had a history of pregnancy and abortion two years ago. Physical examination on admission was unremarkable except for mild epigastric tenderness and longitudinal abdominal scar. At exploratory laparotomy, there was dark red blood in the abdominal cavity. After cleaning of the blood, multiple cystic masses bulging from the surface of the liver were found, one of which was ruptured and then removed for pathological analysis. Her serum beta human chorionic gonadotropin (β -HCG), alpha-fetoprotein (AFP) and cancer antigen-125 (CA-125) levels were 94 mIU/mL (reference range: 0-6 mIU/mL), 1.01 ng/mL (reference range: < 7.0 ng/mL) and 46.86 ng/mL (reference range: < 3.4 ng/mL), respectively. Post-operative contrast-enhanced CT of abdomen showed multiple hepatic hypervascular masses keeping the similar enhancement with abdominal aorta in all phases (the diameter of the masses ranged from 0.8 cm to 2.8 cm) and arteriportal shunts (Figures 2, 3A and B). CT scan of the chest and pelvis revealed no abnormalities. Histopathological examination confirmed the tumor to be predominantly composed of mononuclear epithelioid cells with pink cytoplasm and large, irregularly shaped nuclei with prominent nucleoid (Figure 4). Immunostaining was positive for placental alkaline phosphatase (Figure 5), while negative for HepPar-1, smooth muscle actin. Hepatic metastatic trophoblastic tumor was diagnosed by histopathological examination and immunohistochemical analyses. No abnormality was found in the all-round gynecological checkup, especially in the uterus. The patient refused to chemotherapy and died a month later despite of receiving supportive treatment. Her family refused the autopsy.

DISCUSSION

SP, an uncommon cause of acute abdominal pain, is defined as the presence of blood within the peritoneal cavity that is unrelated to trauma. Its occurrence may



Figure 1 Axial computed tomography showing multiple hypodense nodules in the liver and hemoperitoneum around the liver and spleen.



Figure 2 Contrast-enhanced computed tomography scan showing multiple hypervascular nodules similar to the enhancement of abdominal aorta in the arterial phase.

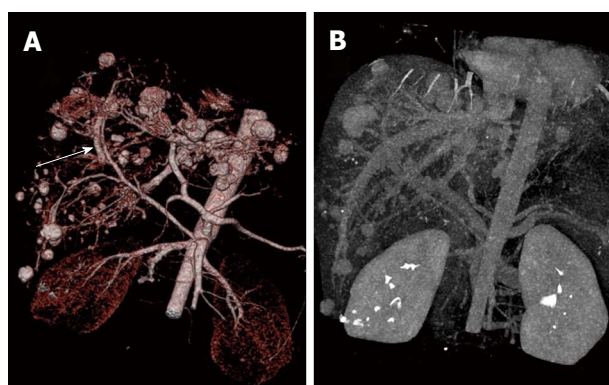


Figure 3 Volume rendering images showing multiple hypervascular nodules similar to saccular aneurysmal dilation and the presence of arteriportal shunts (white arrow). A: Multiple hypervascular nodules similar to saccular aneurysmal dilation; B: Presence of arteriportal shunts.

be catastrophic. There are various causes for SP, such as hepatic, splenic, gynecological and vascular involvement, and altered coagulation status^[1,2]. Therefore, underlying causes must be identified if the patient survives the initial events. As for hepatic causes, previously undetected liver lesion may be a relatively common cause of spontaneous rupture leading to hemoperitoneum, and unnoticeable

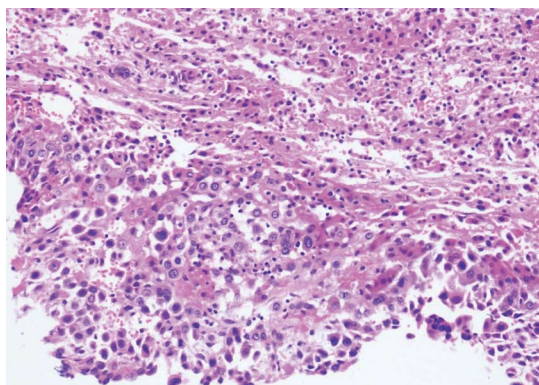


Figure 4 Histopathology showing the tumor composed of mononuclear epithelioid cells with large, irregularly shaped nuclei (hematoxylin and eosin stain × 200).

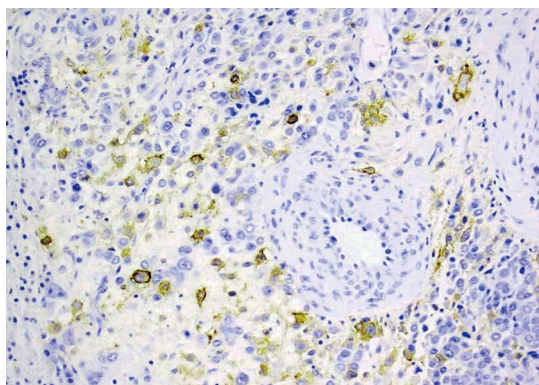


Figure 5 Immunohistochemical analysis was positive for placental alkaline phosphatase (× 200).

minor trauma may be the precipitating factor. Hepatic adenoma and HCC developed from cirrhosis are the most common causes for SP^[3,4], however, hepatic metastatic tumor associated with SP is rare, as most of them tend to be less invasive, and have less blood vessels and less propensities to penetrate the liver capsule as compared with HCC. In our case, hepatic metastatic tumor associated with SP was due to the rupture of hepatic metastasis of a trophoblastic tumor with hypervascularity, which was seldom found responsible for SP in clinical practice.

The mechanism for the rupture of hepatic metastasis remains unclear, but the large lesion adjacent to the liver capsule is at the greatest risk due to direct pressure against the capsular surface, especially in increased intra-abdominal pressure. Acute hemoperitoneum as a result of hemorrhage from liver metastasis is an uncommon but a terminal event. In a large report of 70 patients with SP, metastatic disease was only found responsible for one case^[5]. Those metastatic lesions may include colon, lung, renal cell, testicular tumors, and Wilm's tumor^[6-8]. So, a thorough search should be made for evidence of a primary tumor that may have metastasized to the liver. However, hepatic involvement from trophoblastic tumor accounts for only 10% of the patients and occurs in the late course of the disease. Regression of a primary tumor

after it has metastasized is not uncommon, and one-third of cases manifests as complications of metastatic diseases^[9].

The available imaging modalities used for the diagnosis of SP include sonography, CT and magnetic resonance imaging. Meticulous imaging technique and careful observation of key imaging features are important for accurate characterization of the organ origin of the spontaneous bleeding. Currently, CT scan is the most frequently used modality in evaluating the patients with suspected hemoperitoneum^[2,10,11]. Emphasis should be laid on detecting hemoperitoneum, then localizing the source of bleeding and finally detecting the primary cause. On CT imaging, the appearance of blood within the peritoneum varies depending on the site and the extent of bleeding, and the age of blood. If the time interval between bleeding and imaging is several hours, high attenuation clot may be seen. Over the next few days, the attenuation of the blood decreases, which becomes similar to simple fluid after 2-3 wk. High attenuation clots may appear at the site of the bleeding and suggest a clue as to the site of the bleeding origin. Once the presence of hemoperitoneum has been identified or active bleeding is controlled, a comprehensive search should be made further for an underlying cause. This may start with a careful evaluation of the liver and spleen, because they are the most common organs responsible for spontaneous bleeding. If the SP is derived from a hepatic or splenic cause, the peritoneal blood may be centered around the responsible lesion^[12,13], as described in our case. Although hepatic metastases can come from many locations of the body, SP secondary to metastases exhibit similar findings on non-enhanced CT scan.

Dramatic advance in multi-detector technology has significantly improved the accuracy of CT and dynamic contrast-enhanced CT scan which can identify imaging characteristics of intrahepatic lesions, especially the rare appearances from uncommon disease entity. Metastatic tumors of liver present with intra-liver occupied lesions on unenhanced CT scan, including multi-nodules similar to the "bull's eye" sign, homogenized low-density mononodule, equal- or high-density mass and cystic lesion. Appearances of dynamic contrast-enhanced CT scan for these disease entities may have variant enhancement patterns according to the vascularity of the primary tumor and are often classified as hypervascular, hypovascular and nonvascular metastases. Most of hepatic metastatic tumors show mild enhancement in the portal phase and delayed phase consistent with hypovascular lesions, while there were typically unusual presentations in our patient, which showed the synchronized enhancement with abdominal aorta in all phases. The similar case is extremely rare in the reported literature. Therefore, for a female patient in child-bearing age who presents with SP and unusual contrast-enhanced CT findings similar to our patient's, we should be alert to the possibility of the spontaneous rupture of metastatic trophoblastic disease in the liver, even though the primary lesion is not found on that

occasion.

Prognosis of patients with rupture hepatic metastasis of trophoblastic disease is extremely poor, and the choice of treatment depends on the tumor size, tumor location, severity of bleeding and the general condition of the patient. Surgery and embolisation with or without chemotherapy are the mandatory therapeutic choices^[14,15]. Because of the severe condition of our patient, transcatheter arterial chemotherapeutic embolization is abortive.

In conclusion, we described the CT findings of SP secondary to rupture of hepatic metastatic trophoblastic disease in a female patient. Unusual enhancement patterns on contrast-enhanced CT scan will further enhance our recognition of the SP from hepatic metastatic trophoblastic disease and help differentiate it from other hypervascular hepatic masses.

REFERENCES

- 1 **Lucey BC**, Varghese JC, Anderson SW, Soto JA. Spontaneous hemoperitoneum: a bloody mess. *Emerg Radiol* 2007; **14**: 65-75
- 2 **Lucey BC**, Varghese JC, Soto JA. Spontaneous hemoperitoneum: causes and significance. *Curr Probl Diagn Radiol* 2005; **34**: 182-195
- 3 **da Fonseca CR**, Duarte FP. [Hemoperitoneum as the form of presentation of hepatocellular carcinoma. The contribution of computed tomography to the diagnosis]. *Acta Med Port* 1999; **12**: 223-226
- 4 **Erdogan D**, Busch OR, van Delden OM, Ten Kate FJ, Gouma DJ, van Gulik TM. Management of spontaneous haemorrhage and rupture of hepatocellular adenomas. A single centre experience. *Liver Int* 2006; **26**: 433-438
- 5 **Chen ZY**, Qi QH, Dong ZL. Etiology and management of hemorrhage in spontaneous liver rupture: a report of 70 cases. *World J Gastroenterol* 2002; **8**: 1063-1066
- 6 **Gulati A**, Vyas S, Lal A, Harsha T S, Gupta V, Nijhawan R, Khandelwal N. Spontaneous rupture of hepatic metastasis from choriocarcinoma: a review of imaging and management. *Ann Hepatol* 2009; **8**: 384-387
- 7 **Kadowaki T**, Hamada H, Yokoyama A, Ito R, Ishimaru S, Ohnishi H, Katayama H, Oshima M, Okura T, Kito K, Higaki J. Hemoperitoneum secondary to spontaneous rupture of hepatic metastasis from lung cancer. *Intern Med* 2005; **44**: 290-293
- 8 **Tung CF**, Chang CS, Chow WK, Peng YC, Hwang JI, Wen MC. Hemoperitoneum secondary to spontaneous rupture of metastatic epidermoid carcinoma of liver: case report and review of the literature. *Hepatogastroenterology* 2002; **49**: 1415-1417
- 9 **Heaton GE**, Matthews TH, Christopherson WM. Malignant trophoblastic tumors with massive hemorrhage presenting as liver primary. A report of two cases. *Am J Surg Pathol* 1986; **10**: 342-347
- 10 **Mortelet KJ**, Cantisani V, Brown DL, Ros PR. Spontaneous intraperitoneal hemorrhage: imaging features. *Radiol Clin North Am* 2003; **41**: 1183-1201
- 11 **Lubner M**, Menias C, Rucker C, Bhalla S, Peterson CM, Wang L, Gratz B. Blood in the belly: CT findings of hemoperitoneum. *Radiographics* 2007; **27**: 109-125
- 12 **Pombo F**, Arrojo L, Perez-Fontan J. Haemoperitoneum secondary to spontaneous rupture of hepatocellular carcinoma: CT diagnosis. *Clin Radiol* 1991; **43**: 321-322
- 13 **Becker CD**, Mentha G, Terrier F. Blunt abdominal trauma in adults: role of CT in the diagnosis and management of visceral injuries. Part 1: liver and spleen. *Eur Radiol* 1998; **8**: 553-562
- 14 **Tarantino L**, Sordelli I, Calise F, Ripa C, Perrotta M, Sperlongano P. Prognosis of patients with spontaneous rupture of hepatocellular carcinoma in cirrhosis. *Updates Surg* 2011; **63**: 25-30
- 15 **Lazaridis G**, Pentheroudakis G, Fountzilias G, Pavlidis N. Liver metastases from cancer of unknown primary (CUPL): a retrospective analysis of presentation, management and prognosis in 49 patients and systematic review of the literature. *Cancer Treat Rev* 2008; **34**: 693-700

S- Editor Gou SX L- Editor A E- Editor Zhang DN

Non-steroidal anti-inflammatory drugs-induced small intestinal injury and probiotic agents

Mario Guslandi

Mario Guslandi, Gastroenterology Unit, S. Raffaele University Hospital, 20132 Milan, Italy

Author contributions: Guslandi M contributed solely to this work.

Correspondence to: Mario Guslandi, Professor, Gastroenterology Unit, S. Raffaele Hospital, Via Olgettina 60, 20132 Milano, Italy. guslandi.mario@hsr.it

Telephone: +39-2-26431 Fax: +39-2-26433491

Received: December 2, 2011 Revised: March 8, 2012

Accepted: April 21, 2012

Published online: August 21, 2012

Abstract

Intestinal bacteria play a role in the development of non-steroidal anti-inflammatory drugs (NSAID)-induced small intestinal injury. Agents such as probiotics, able to modify the gut ecology, might theoretically be useful in preventing small intestinal damage induced by NSAIDs. The clinical studies available so far do suggest that some probiotic agents can be effective in this respect.

© 2012 Baishideng. All rights reserved.

Key words: Non-steroidal anti-inflammatory drugs; Small intestine; Intestinal bacteria; Probiotics

Peer reviewers: Marcela Kopacova, Professor, MD, PhD, 2nd Department of Internal Medicine, Charles University in Praha, Faculty of Medicine at Hradec Král, Sokolska 581, Hradec Kralove 50005, Czech; Shardul S Wagh, University Department of Biochemistry, RTM Nagpur University, L.I.T. Premises, Aravati Road, Nagpur 440033, India; Nageshwar Duvvuru Reddy, Professor, Gastroenterology, Asian Institute of Gastroenterology, A-27, Journalist Colony, Jubilee Hillshyderabad, Hyderabad 500033, India

Guslandi M. Non-steroidal anti-inflammatory drugs-induced small intestinal injury and probiotic agents. *World J Gastroenterol* 2012; 18(31): 4241-4242 Available from: URL: <http://www.wjgnet.com/1007-9327/full/v18/i31/4241.htm> DOI: <http://dx.doi.org/10.3748/wjg.v18.i31.4241>

TO THE EDITOR

Park *et al*^[1,2] in their interesting editorial^[1] about small intestinal injury induced by non-steroidal anti-inflammatory drugs (NSAIDs), discussed the possible role of the intestinal flora in the pathogenesis of the enteric damage, but, oddly enough, when listing the pharmacological agents theoretically useful as protective or therapeutic medicines, they omitted to mention probiotics. Live micro-organisms could prevent NSAID-induced small intestinal damage by both modifying intestinal microbial ecology and modulating the local immune function.

Various studies have addressed the issue. While a pilot study in human volunteers failed to demonstrate any effect of *Lactobacillus GG* in preventing indomethacin-induced alterations of intestinal permeability^[3], a subsequent experimental study demonstrated that in rats pretreated with *Lactobacillus casei*, strain Shirota significantly prevents the development of indomethacin-induced enteropathy^[4], although the mechanism responsible for this phenomenon remains not completely clear.

In a recent trial, patients treated for three months with low-dose enteric-coated aspirin (100 mg daily) were randomized to receive either co-administration of *Lactobacillus casei* or no additional treatment^[5]. Capsule endoscopy, performed before and after treatment, showed a significant decrease ($P = 0.039$) in the number of mucosal breaks and in the endoscopic score in the probiotic group as compared with controls.

In a randomized, double-blind, cross-over placebo-controlled study in healthy volunteers, the probiotic mixture VSL # 3 was found to prevent the increase in faecal concentration of the inflammatory marker calprotectin during intake of indomethacin 50 mg daily^[6].

The role of bacteria in the development of small intestinal lesions during NSAID administration seems indirectly confirmed, but the recent experimental observations showed that proton pump inhibitors significantly worsen intestinal ulcerations and bleeding in naproxen- and celecoxib-treated rats and this is related to substantial

shifts in enteric microbial population (e.g., a marked reduction in *Actinobacteria* and *Bifidobacteria*)^[7].

All in all, it appears that probiotics can represent promising agents in the prevention of NSAID-induced small intestine injury, although additional studies are needed to better clarify this point. However, the efficacy of any single probiotic strain should be evaluated separately, due to the differences in the biological effects and mode of actions of the various agents currently available.

REFERENCES

- 1 **Park SC**, Chun HJ, Kang CD, Sul D. Prevention and management of non-steroidal anti-inflammatory drugs-induced small intestinal injury. *World J Gastroenterol* 2011; **17**: 4647-4653
- 2 **Scarpignato C**. NSAID-induced intestinal damage: are luminal bacteria the therapeutic target? *Gut* 2008; **57**: 145-148
- 3 **Gotteland M**, Cruchet S, Verbeke S. Effect of Lactobacillus ingestion on the gastrointestinal mucosal barrier alterations induced by indometacin in humans. *Aliment Pharmacol Ther* 2001; **15**: 11-17
- 4 **Watanabe T**, Nishio H, Tanigawa T, Yamagami H, Okazaki H, Watanabe K, Tominaga K, Fujiwara Y, Oshitani N, Asahara T, Nomoto K, Higuchi K, Takeuchi K, Arakawa T. Probiotic Lactobacillus casei strain Shirota prevents indomethacin-induced small intestinal injury: involvement of lactic acid. *Am J Physiol Gastrointest Liver Physiol* 2009; **297**: G506-G513
- 5 **Endo H**, Higurashi T, Hosono K, Sakai E, Sekino Y, Iida H, Sakamoto Y, Koide T, Takahashi H, Yoneda M, Tokoro C, Inamori M, Abe Y, Nakajima A. Efficacy of Lactobacillus casei treatment on small bowel injury in chronic low-dose aspirin users: a pilot randomized controlled study. *J Gastroenterol* 2011; **46**: 894-905
- 6 **Montalto M**, Gallo A, Curigliano V, D'Onofrio F, Santoro L, Covino M, Dalvai S, Gasbarrini A, Gasbarrini G. Clinical trial: the effects of a probiotic mixture on non-steroidal anti-inflammatory drug enteropathy - a randomized, double-blind, cross-over, placebo-controlled study. *Aliment Pharmacol Ther* 2010; **32**: 209-214
- 7 **Wallace JL**, Syer S, Denou E, de Palma G, Vong L, McKnight W, Jury J, Bolla M, Bercik P, Collins SM, Verdu E, Ongini E. Proton pump inhibitors exacerbate NSAID-induced small intestinal injury by inducing dysbiosis. *Gastroenterology* 2011; **141**: 1314-1322

S- Editor Gou SX L- Editor Ma JY E- Editor Zhang DN

Acknowledgments to reviewers of World Journal of Gastroenterology

Many reviewers have contributed their expertise and time to the peer review, a critical process to ensure the quality of *World Journal of Gastroenterology*. The editors and authors of the articles submitted to the journal are grateful to the following reviewers for evaluating the articles (including those published in this issue and those rejected for this issue) during the last editing time period.

Deepak N Amarapurkar, MD, DM, DNB, FACS, FICP, D 401 Ameya, New Prabhadevi Road, Prabhadevi, Mumbai 400025, India

Mark Bloomston, MD, FACS, Assistant Professor of Surgery, Division of Surgical Oncology, N924 Doan Hall, 410W. 10th Avenue, Columbus, Ohio 43082, United States

Carla W Brady, MD, MHS, Duke University Medical Center, Division of Gastroenterology, DUMC Box 3913, Durham, NC 27705, United States

Christopher Christophi, Professor and Head of The University of Melbourne, Department of Surgery, Austin Hospital, Melbourne, 145 Studley Road, Victoria 3084, Australia

Edward J Ciaccio, PhD, Research Scientist, Department of Medicine, HP 804, Columbia University, 180 Fort Washington Avenue, New York, NY 10032, United States

Itaru Endo, MD, PhD, Professor and Chairman, Department of Gastroenterological Surgery, Yokohama City University, Graduate School of Medicine, 3-9 Fukuura, Kanazawa-ku, Yokohama 236-0004, Japan

Dr. Mukaddes Esrefoglu, Professor, Department of Histology and Embryology, Inonu University, 44280 Malatya, Turkey

Glenn T Furuta, Associate Professor, Director of the Gastrointestinal Eosinophil Disease Program, Department of Pediatrics, The Children's Hospital Denver, University of Colorado Denver, School of Medicine, 13123 East 16th Ave. B290, Aurora, CO 80045, United States

Grigoriy E Gurvits, MD, Department of Gastroenterology, St. Vincent's Hospital and Medical Center, New York Medical College, 153 West 11th Street, Smith 2, New York, NY 10011, United States

Nayoung Kim, MD, PhD, Associate Professor, Department of Internal Medicine, Seoul National University Bundang Hospital, 300, Gumi-dong, Bundang-gu, Gyeonggi-do, Seongnam-si 463-707, South Korea

Yasuhiro Kodera, MD, PhD, FACS, Associate Professor, Department of Surgery II, Nagoya University Graduate School of Medicine, 65 Tsurumai-cho, Showa-ku, Nagoya, Aichi 466-8550, Japan

Anastasios Koulaouzidis, MD, MRCP (UK), Day Case and Endoscopy Unit, Centre of Liver and Digestive Disorders, Royal Infirmary of Edinburgh, 51 Little France Crescent, Edinburgh EH16 4SA, Scottish, United Kingdom

Javier San Martín, Chief, Gastroenterology and Endoscopy, Sanatorio Cantegril, Av. Roosevelt y P 13, Punta del Este 20100, Uruguay

Toshihiro Mitaka, MD, PhD, Professor, Department of Pathophysiology, Cancer Research Institute, Sapporo Medical University School of Medicine, South-1, West-17, Chuo-ku, Sapporo 060-8556, Japan

Emiko Mizoguchi, MD, PhD, Department of Medicine, Gastrointestinal Unit, GRJ 702, Massachusetts General Hospital, Boston, MA 02114, United States

Zenichi Morise, MD, PhD, Professor and Chairman, Department of Surgery Banbuntane Houtokukai Hospital, Fujita Health University School of Medicine, 3-6-10 Otobashi Nakagawa-ku, Nagoya, AICHI 454-8509, Japan

Susumu Ohwada, Associate Professor, Department of Surgery, Gunma University Graduate School of Medicine, 3-39-15 Shoma-Machi, Maebashi 371-8511, Japan

Giuseppe Orlando, MD, PhD, MCF, Nuffield Department of Surgery, University of Oxford, Radcliffe Hospital, Headley Way, Headington, Oxford OX3 9DU, United Kingdom

Carlos J Pirola, PhD, FAHA, Medical Research Institute A Lanari, Combatientes de Malvinas 3150, Buenos Aires 1427, Argentina

Tor C Savidge, PhD, Associate Professor, Department of Gastroenterology and Hepatology, Galveston, TX 77555, United States

Vincenzo Stanghellini, MD, Professor of Medicine, Department of Internal Medicine and Gastroenterology, Policlinico S. Orsola-Malpighi, University of Bologna, Via Massarenti 9, Bologna I 40138, Italy

Bao-Ting Zhu, MD, PhD, Professor, Department of Pharmacology, Toxicology and Therapeutics, School of Medicine, University of Kansas Medical Center, MS-1018, room-KLSIC 4061, 2146 W. 39th Ave, Kansas City, KS 66160, United States

Events Calendar 2012

January 13-15, 2012
Asian Pacific *Helicobacter pylori*
Meeting 2012
Kuala Lumpur, Malaysia

January 19-21, 2012
American Society of Clinical
Oncology 2012 Gastrointestinal
Cancers Symposium
San Francisco, CA 3000,
United States

January 19-21, 2012
2012 Gastrointestinal Cancers
Symposium
San Francisco, CA 94103,
United States

January 20-21, 2012
American Gastroenterological
Association Clinical Congress of
Gastroenterology and Hepatology
Miami Beach, FL 33141,
United States

February 3, 2012
The Future of Obesity Treatment
London, United Kingdom

February 16-17, 2012
4th United Kingdom Swallowing
Research Group Conference
London, United Kingdom

February 23, 2012
Management of Barretts
Oesophagus: Everything you need
to know
Cambridge, United Kingdom

February 24-27, 2012
Canadian Digestive Diseases Week
2012
Montreal, Canada

March 1-3, 2012
International Conference on
Nutrition and Growth 2012
Paris, France

March 7-10, 2012
Society of American Gastrointestinal
and Endoscopic Surgeons Annual
Meeting
San Diego, CA 92121, United States

March 12-14, 2012
World Congress on
Gastroenterology and Urology
Omaha, NE 68197, United States

March 17-20, 2012
Mayo Clinic Gastroenterology and
Hepatology
Orlando, FL 32808, United States

March 26-27, 2012
26th Annual New Treatments in
Chronic Liver Disease
San Diego, CA 92121, United States

March 30-April 2, 2012
Mayo Clinic Gastroenterology and
Hepatology
San Antonio, TX 78249,
United States

March 31-April 1, 2012
27th Annual New Treatments in
Chronic Liver Disease
San Diego, CA 92121, United States

April 8-10, 2012
9th International Symposium on
Functional GI Disorders
Milwaukee, WI 53202, United States

April 13-15, 2012
Asian Oncology Summit 2012
Singapore, Singapore

April 15-17, 2012
European Multidisciplinary
Colorectal Cancer Congress 2012
Prague, Czech

April 18-20, 2012
The International Liver Congress
2012
Barcelona, Spain

April 19-21, 2012
Internal Medicine 2012
New Orleans, LA 70166,
United States

April 20-22, 2012
Diffuse Small Bowel and Liver
Diseases
Melbourne, Australia

April 22-24, 2012
EUROSON 2012 EFSUMB Annual

Meeting
Madrid, Spain

April 28, 2012
Issues in Pediatric Oncology
Kiev, Ukraine

May 3-5, 2012
9th Congress of The Jordanian
Society of Gastroenterology
Amman, Jordan

May 7-10, 2012
Digestive Diseases Week
Chicago, IL 60601, United States

May 17-21, 2012
2012 ASCRS Annual Meeting-
American Society of Colon and
Rectal Surgeons
Hollywood, FL 1300, United States

May 18-19, 2012
Pancreas Club Meeting
San Diego, CA 92101, United States

May 18-23, 2012
SGNA: Society of Gastroenterology
Nurses and Associates Annual
Course
Phoenix, AZ 85001, United States

May 19-22, 2012
2012-Digestive Disease Week
San Diego, CA 92121, United States

June 2-6, 2012
American Society of Colon and
Rectal Surgeons Annual Meeting
San Antonio, TX 78249,
United States

June 18-21, 2012
Pancreatic Cancer: Progress and
Challenges
Lake Tahoe, NV 89101, United States

July 25-26, 2012
PancreasFest 2012
Pittsburgh, PA 15260, United States

September 1-4, 2012
OESO 11th World Conference
Como, Italy

September 6-8, 2012
2012 Joint International

Neurogastroenterology and Motility
Meeting
Bologna, Italy

September 7-9, 2012
The Viral Hepatitis Congress
Frankfurt, Germany

September 8-9, 2012
New Advances in Inflammatory
Bowel Disease
La Jolla, CA 92093, United States

September 8-9, 2012
Florida Gastroenterologic Society
2012 Annual Meeting
Boca Raton, FL 33498, United States

September 15-16, 2012
Current Problems of
Gastroenterology and Abdominal
Surgery
Kiev, Ukraine

September 20-22, 2012
1st World Congress on Controversies
in the Management of Viral Hepatitis
Prague, Czech

October 19-24, 2012
American College of
Gastroenterology 77th Annual
Scientific Meeting and Postgraduate
Course
Las Vegas, NV 89085, United States

November 3-4, 2012
Modern Technologies in
Diagnosis and Treatment of
Gastroenterological Patients
Dnepropetrovsk, Ukraine

November 4-8, 2012
The Liver Meeting
San Francisco, CA 94101,
United States

November 9-13, 2012
American Association for the Study
of Liver Diseases
Boston, MA 02298, United States

December 1-4, 2012
Advances in Inflammatory Bowel
Diseases
Hollywood, FL 33028, United States

GENERAL INFORMATION

World Journal of Gastroenterology (*World J Gastroenterol*, *WJG*, print ISSN 1007-9327, online ISSN 2219-2840, DOI: 10.3748) is a weekly, open-access (OA), peer-reviewed journal supported by an editorial board of 1352 experts in gastroenterology and hepatology from 64 countries.

The biggest advantage of the OA model is that it provides free, full-text articles in PDF and other formats for experts and the public without registration, which eliminates the obstacle that traditional journals possess and usually delays the speed of the propagation and communication of scientific research results. The open access model has been proven to be a true approach that may achieve the ultimate goal of the journals, i.e. the maximization of the value to the readers, authors and society.

Maximization of personal benefits

The role of academic journals is to exhibit the scientific levels of a country, a university, a center, a department, and even a scientist, and build an important bridge for communication between scientists and the public. As we all know, the significance of the publication of scientific articles lies not only in disseminating and communicating innovative scientific achievements and academic views, as well as promoting the application of scientific achievements, but also in formally recognizing the “priority” and “copy-right” of innovative achievements published, as well as evaluating research performance and academic levels. So, to realize these desired attributes of *WJG* and create a well-recognized journal, the following four types of personal benefits should be maximized. The maximization of personal benefits refers to the pursuit of the maximum personal benefits in a well-considered optimal manner without violation of the laws, ethical rules and the benefits of others. (1) Maximization of the benefits of editorial board members: The primary task of editorial board members is to give a peer review of an unpublished scientific article via online office system to evaluate its innovativeness, scientific and practical values and determine whether it should be published or not. During peer review, editorial board members can also obtain cutting-edge information in that field at first hand. As leaders in their field, they have priority to be invited to write articles and publish commentary articles. We will put peer reviewers’ names and affiliations along with the article they reviewed in the journal to acknowledge their contribution; (2) Maximization of the benefits of authors: Since *WJG* is an open-access journal, readers around the world can immediately download and read, free of charge, high-quality, peer-reviewed articles from *WJG* official website, thereby realizing the goals and significance of the communication between authors and peers as well as public reading; (3) Maximization of the benefits of readers: Readers can read or use, free of charge, high-quality peer-reviewed articles without any limits, and cite the arguments, viewpoints, concepts, theories, methods, results, conclusion or facts and data of pertinent literature so as to validate the innovativeness, scientific and practical values of their own research achievements, thus ensuring that their articles have novel arguments or viewpoints, solid

evidence and correct conclusion; and (4) Maximization of the benefits of employees: It is an iron law that a first-class journal is unable to exist without first-class editors, and only first-class editors can create a first-class academic journal. We insist on strengthening our team cultivation and construction so that every employee, in an open, fair and transparent environment, could contribute their wisdom to edit and publish high-quality articles, thereby realizing the maximization of the personal benefits of editorial board members, authors and readers, and yielding the greatest social and economic benefits.

Aims and scope

The major task of *WJG* is to report rapidly the most recent results in basic and clinical research on esophageal, gastrointestinal, liver, pancreas and biliary tract diseases, *Helicobacter pylori*, endoscopy and gastrointestinal surgery, including: gastroesophageal reflux disease, gastrointestinal bleeding, infection and tumors; gastric and duodenal disorders; intestinal inflammation, microflora and immunity; celiac disease, dyspepsia and nutrition; viral hepatitis, portal hypertension, liver fibrosis, liver cirrhosis, liver transplantation, and metabolic liver disease; molecular and cell biology; geriatric and pediatric gastroenterology; diagnosis and screening, imaging and advanced technology.

Columns

The columns in the issues of *WJG* will include: (1) Editorial: To introduce and comment on major advances and developments in the field; (2) Frontier: To review representative achievements, comment on the state of current research, and propose directions for future research; (3) Topic Highlight: This column consists of three formats, including (A) 10 invited review articles on a hot topic, (B) a commentary on common issues of this hot topic, and (C) a commentary on the 10 individual articles; (4) Observation: To update the development of old and new questions, highlight unsolved problems, and provide strategies on how to solve the questions; (5) Guidelines for Basic Research: To provide guidelines for basic research; (6) Guidelines for Clinical Practice: To provide guidelines for clinical diagnosis and treatment; (7) Review: To review systematically progress and unresolved problems in the field, comment on the state of current research, and make suggestions for future work; (8) Original Article: To report innovative and original findings in gastroenterology; (9) Brief Article: To briefly report the novel and innovative findings in gastroenterology and hepatology; (10) Case Report: To report a rare or typical case; (11) Letters to the Editor: To discuss and make reply to the contributions published in *WJG*, or to introduce and comment on a controversial issue of general interest; (12) Book Reviews: To introduce and comment on quality monographs of gastroenterology and hepatology; and (13) Guidelines: To introduce consensus and guidelines reached by international and national academic authorities worldwide on basic research and clinical practice gastroenterology and hepatology.

Name of journal

World Journal of Gastroenterology

Instructions to authors

ISSN and EISSN

ISSN 1007-9327 (print)
ISSN 2219-2840 (online)

Editor-in-chief

Ferruccio Bonino, MD, PhD, Professor of Gastroenterology, Director of Liver and Digestive Disease Division, Department of Internal Medicine, University of Pisa, Director of General Medicine 2 Unit University Hospital of Pisa, Via Roma 67, 56124 Pisa, Italy

Myung-Hwan Kim, MD, PhD, Professor, Head, Department of Gastroenterology, Director, Center for Biliary Diseases, University of Ulsan College of Medicine, Asan Medical Center, 388-1 Pungnap-2dong, Songpa-gu, Seoul 138-736, South Korea

Kjell Öberg, MD, PhD, Professor, Department of Endocrine Oncology, Uppsala University Hospital, SE-751 85 Uppsala, Sweden

Matt D Rutter, MBBS, MD, FRCP, Consultant Gastroenterologist, Senior Lecturer, Director, Tees Bowel Cancer Screening Centre, University Hospital of North Tees, Durham University, Stockton-on-Tees, Cleveland TS19 8PE, United Kingdom

Andrzej S Tarnawski, MD, PhD, DSc (Med), Professor of Medicine, Chief Gastroenterology, VA Long Beach Health Care System, University of California, Irvine, CA, 5901 E. Seventh Str., Long Beach, CA 90822, United States

Editorial office

World Journal of Gastroenterology
Editorial Department: Room 903, Building D,
Ocean International Center,
No. 62 Dongsihuan Zhonglu,
Chaoyang District, Beijing 100025, China
E-mail: wjg@wjgnet.com
<http://www.wjgnet.com>
Telephone: +86-10-59080039
Fax: +86-10-85381893

Indexed and abstracted in

Current Contents®/Clinical Medicine, Science Citation Index Expanded (also known as SciSearch®), Journal Citation Reports®, Index Medicus, MEDLINE, PubMed, PubMed Central, Digital Object Identifier, and Directory of Open Access Journals. ISI, Thomson Reuters, 2011 Impact Factor: 2.471 (32/74 Gastroenterology and Hepatology).

Published by

Baishideng Publishing Group Co., Limited

SPECIAL STATEMENT

All articles published in this journal represent the viewpoints of the authors except where indicated otherwise.

Biostatistical editing

Statistical review is performed after peer review. We invite an expert in Biomedical Statistics to evaluate the statistical method used in the paper, including *t*-test (group or paired comparisons), chi-squared test, Redit, probit, logit, regression (linear, curvilinear, or stepwise), correlation, analysis of variance, analysis of covariance, *etc.* The reviewing points include: (1) Statistical methods should be described when they are used to verify the results; (2) Whether the statistical techniques are suitable or correct; (3) Only homoge-

neous data can be averaged. Standard deviations are preferred to standard errors. Give the number of observations and subjects (*n*). Losses in observations, such as drop-outs from the study should be reported; (4) Values such as ED50, LD50, IC50 should have their 95% confidence limits calculated and compared by weighted probit analysis (Bliss and Finney); and (5) The word 'significantly' should be replaced by its synonyms (if it indicates extent) or the *P* value (if it indicates statistical significance).

Conflict-of-interest statement

In the interests of transparency and to help reviewers assess any potential bias, *WJG* requires authors of all papers to declare any competing commercial, personal, political, intellectual, or religious interests in relation to the submitted work. Referees are also asked to indicate any potential conflict they might have reviewing a particular paper. Before submitting, authors are suggested to read "Uniform Requirements for Manuscripts Submitted to Biomedical Journals: Ethical Considerations in the Conduct and Reporting of Research: Conflicts of Interest" from International Committee of Medical Journal Editors (ICMJE), which is available at: http://www.icmje.org/ethical_4conflicts.html.

Sample wording: [Name of individual] has received fees for serving as a speaker, a consultant and an advisory board member for [names of organizations], and has received research funding from [names of organization]. [Name of individual] is an employee of [name of organization]. [Name of individual] owns stocks and shares in [name of organization]. [Name of individual] owns patent [patent identification and brief description].

Statement of informed consent

Manuscripts should contain a statement to the effect that all human studies have been reviewed by the appropriate ethics committee or it should be stated clearly in the text that all persons gave their informed consent prior to their inclusion in the study. Details that might disclose the identity of the subjects under study should be omitted. Authors should also draw attention to the Code of Ethics of the World Medical Association (Declaration of Helsinki, 1964, as revised in 2004).

Statement of human and animal rights

When reporting the results from experiments, authors should follow the highest standards and the trial should conform to Good Clinical Practice (for example, US Food and Drug Administration Good Clinical Practice in FDA-Regulated Clinical Trials; UK Medicines Research Council Guidelines for Good Clinical Practice in Clinical Trials) and/or the World Medical Association Declaration of Helsinki. Generally, we suggest authors follow the lead investigator's national standard. If doubt exists whether the research was conducted in accordance with the above standards, the authors must explain the rationale for their approach and demonstrate that the institutional review body explicitly approved the doubtful aspects of the study.

Before submitting, authors should make their study approved by the relevant research ethics committee or institutional review board. If human participants were involved, manuscripts must be accompanied by a statement that the experiments were undertaken with the understanding and appropriate informed consent of each. Any personal item or information will not be published without explicit consents from the involved patients. If experimental animals were used, the materials and methods (experimental procedures) section must clearly indicate that appropriate measures were taken to minimize pain or discomfort, and details of animal care should be provided.

SUBMISSION OF MANUSCRIPTS

Manuscripts should be typed in 1.5 line spacing and 12 pt. Book Antiqua with ample margins. Number all pages consecutively, and start each of the following sections on a new page: Title Page, Abstract, Introduction, Materials and Methods, Results, Discussion, Acknowledgements, References, Tables, Figures, and Figure Legends. Neither the editors nor the publisher are responsible for the opinions expressed by contributors. Manuscripts formally accepted for publication become the permanent property of Baishideng Publishing Group Co., Limited, and may not be reproduced by any means, in whole or in part, without the written permission of both the authors and the publisher. We reserve the right to copy-edit and put onto our website accepted manuscripts. Authors should follow the relevant guidelines for the care and use of laboratory animals of their institution or national animal welfare committee. For the sake of transparency in regard to the performance and reporting of clinical trials, we endorse the policy of the ICMJE to refuse to publish papers on clinical trial results if the trial was not recorded in a publicly-accessible registry at its outset. The only register now available, to our knowledge, is <http://www.clinicaltrials.gov> sponsored by the United States National Library of Medicine and we encourage all potential contributors to register with it. However, in the case that other registers become available you will be duly notified. A letter of recommendation from each author's organization should be provided with the contributed article to ensure the privacy and secrecy of research is protected.

Authors should retain one copy of the text, tables, photographs and illustrations because rejected manuscripts will not be returned to the author(s) and the editors will not be responsible for loss or damage to photographs and illustrations sustained during mailing.

Online submissions

Manuscripts should be submitted through the Online Submission System at: <http://www.wjgnet.com/esps/>. Authors are highly recommended to consult the ONLINE INSTRUCTIONS TO AUTHORS (http://www.wjgnet.com/1007-9327/g_info_20100315215714.htm) before attempting to submit online. For assistance, authors encountering problems with the Online Submission System may send an email describing the problem to wjg@wjgnet.com, or by telephone: +86-10-5908-0039. If you submit your manuscript online, do not make a postal contribution. Repeated online submission for the same manuscript is strictly prohibited.

MANUSCRIPT PREPARATION

All contributions should be written in English. All articles must be submitted using word-processing software. All submissions must be typed in 1.5 line spacing and 12 pt. Book Antiqua with ample margins. Style should conform to our house format. Required information for each of the manuscript sections is as follows:

Title page

Title: Title should be less than 12 words.

Running title: A short running title of less than 6 words should be provided.

Authorship: Authorship credit should be in accordance with the standard proposed by ICMJE, based on (1) substantial contributions to conception and design, acquisition of data, or analysis and interpretation of data; (2) drafting the article or revising it critically

for important intellectual content; and (3) final approval of the version to be published. Authors should meet conditions 1, 2, and 3.

Institution: Author names should be given first, then the complete name of institution, city, province and postcode. For example, Xu-Chen Zhang, Li-Xin Mei, Department of Pathology, Chengde Medical College, Chengde 067000, Hebei Province, China. One author may be represented from two institutions, for example, George Sgourakis, Department of General, Visceral, and Transplantation Surgery, Essen 45122, Germany; George Sgourakis, 2nd Surgical Department, Korgialenio-Benakio Red Cross Hospital, Athens 15451, Greece.

Author contributions: The format of this section should be: Author contributions: Wang CL and Liang L contributed equally to this work; Wang CL, Liang L, Fu JF, Zou CC, Hong F and Wu XM designed the research; Wang CL, Zou CC, Hong F and Wu XM performed the research; Xue JZ and Lu JR contributed new reagents/analytic tools; Wang CL, Liang L and Fu JF analyzed the data; and Wang CL, Liang L and Fu JF wrote the paper.

Supportive foundations: The complete name and number of supportive foundations should be provided, e.g. Supported by National Natural Science Foundation of China, No. 30224801

Correspondence to: Only one corresponding address should be provided. Author names should be given first, then author title, affiliation, the complete name of institution, city, postcode, province, country, and email. All the letters in the email should be in lower case. A space interval should be inserted between country name and email address. For example, Montgomery Bissell, MD, Professor of Medicine, Chief, Liver Center, Gastroenterology Division, University of California, Box 0538, San Francisco, CA 94143, United States. montgomery.bissell@ucsf.edu

Telephone and fax: Telephone and fax should consist of +, country number, district number and telephone or fax number, e.g. Telephone: +86-10-59080039 Fax: +86-10-85381893

Peer reviewers: All articles received are subject to peer review. Normally, three experts are invited for each article. Decision for acceptance is made only when at least two experts recommend an article for publication. Reviewers for accepted manuscripts are acknowledged in each manuscript, and reviewers of articles which were not accepted will be acknowledged at the end of each issue. To ensure the quality of the articles published in *WJG*, reviewers of accepted manuscripts will be announced by publishing the name, title/position and institution of the reviewer in the footnote accompanying the printed article. For example, reviewers: Professor Jing-Yuan Fang, Shanghai Institute of Digestive Disease, Shanghai, Affiliated Renji Hospital, Medical Faculty, Shanghai Jiaotong University, Shanghai, China; Professor Xin-Wei Han, Department of Radiology, The First Affiliated Hospital, Zhengzhou University, Zhengzhou, Henan Province, China; and Professor Anren Kuang, Department of Nuclear Medicine, Huaxi Hospital, Sichuan University, Chengdu, Sichuan Province, China.

Abstract

There are unstructured abstracts (no less than 256 words) and structured abstracts (no less than 480). The specific requirements for structured abstracts are as follows:

An informative, structured abstracts of no less than 480 words should accompany each manuscript. Abstracts for original contributions should be structured into the following sections.

Instructions to authors

AIM (no more than 20 words): Only the purpose should be included. Please write the aim as the form of “To investigate/study/...”; MATERIALS AND METHODS (no less than 140 words); RESULTS (no less than 294 words): You should present *P* values where appropriate and must provide relevant data to illustrate how they were obtained, e.g. 6.92 ± 3.86 vs 3.61 ± 1.67 , $P < 0.001$; CONCLUSION (no more than 26 words).

Key words

Please list 5-10 key words, selected mainly from *Index Medicus*, which reflect the content of the study.

Text

For articles of these sections, original articles and brief articles, the main text should be structured into the following sections: INTRODUCTION, MATERIALS AND METHODS, RESULTS and DISCUSSION, and should include appropriate Figures and Tables. Data should be presented in the main text or in Figures and Tables, but not in both. The main text format of these sections, editorial, topic highlight, case report, letters to the editors, can be found at: http://www.wjgnet.com/1007-9327/g_info_20100315215714.htm.

Illustrations

Figures should be numbered as 1, 2, 3, etc., and mentioned clearly in the main text. Provide a brief title for each figure on a separate page. Detailed legends should not be provided under the figures. This part should be added into the text where the figures are applicable. Figures should be either Photoshop or Illustrator files (in tiff, eps, jpeg formats) at high-resolution. Examples can be found at: <http://www.wjgnet.com/1007-9327/13/4520.pdf>; <http://www.wjgnet.com/1007-9327/13/4554.pdf>; <http://www.wjgnet.com/1007-9327/13/4891.pdf>; <http://www.wjgnet.com/1007-9327/13/4986.pdf>; <http://www.wjgnet.com/1007-9327/13/4498.pdf>. Keeping all elements compiled is necessary in line-art image. Scale bars should be used rather than magnification factors, with the length of the bar defined in the legend rather than on the bar itself. File names should identify the figure and panel. Avoid layering type directly over shaded or textured areas. Please use uniform legends for the same subjects. For example: Figure 1 Pathological changes in atrophic gastritis after treatment. A:...; B:...; C:...; D:...; E:...; F:...; G: ...etc. It is our principle to publish high resolution-figures for the printed and E-versions.

Tables

Three-line tables should be numbered 1, 2, 3, etc., and mentioned clearly in the main text. Provide a brief title for each table. Detailed legends should not be included under tables, but rather added into the text where applicable. The information should complement, but not duplicate the text. Use one horizontal line under the title, a second under column heads, and a third below the Table, above any footnotes. Vertical and italic lines should be omitted.

Notes in tables and illustrations

Data that are not statistically significant should not be noted. ^a $P < 0.05$, ^b $P < 0.01$ should be noted ($P > 0.05$ should not be noted). If there are other series of *P* values, ^c $P < 0.05$ and ^d $P < 0.01$ are used. A third series of *P* values can be expressed as ^e $P < 0.05$ and ^f $P < 0.01$. Other notes in tables or under illustrations should be expressed as ¹F, ²F, ³F; or sometimes as other symbols with a superscript (Arabic numerals) in the upper left corner. In a multi-curve illustration, each curve should be la-

beled with ●, ○, ■, □, ▲, △, etc., in a certain sequence.

Acknowledgments

Brief acknowledgments of persons who have made genuine contributions to the manuscript and who endorse the data and conclusions should be included. Authors are responsible for obtaining written permission to use any copyrighted text and/or illustrations.

REFERENCES

Coding system

The author should number the references in Arabic numerals according to the citation order in the text. Put reference numbers in square brackets in superscript at the end of citation content or after the cited author's name. For citation content which is part of the narration, the coding number and square brackets should be typeset normally. For example, “Crohn's disease (CD) is associated with increased intestinal permeability^[1,2]”. If references are cited directly in the text, they should be put together within the text, for example, “From references^[19,22-24], we know that...”.

When the authors write the references, please ensure that the order in text is the same as in the references section, and also ensure the spelling accuracy of the first author's name. Do not list the same citation twice.

PMID and DOI

Please provide PubMed citation numbers to the reference list, e.g. PMID and DOI, which can be found at <http://www.ncbi.nlm.nih.gov/sites/entrez?db=pubmed> and <http://www.crossref.org/SimpleTextQuery/>, respectively. The numbers will be used in E-version of this journal.

Style for journal references

Authors: the name of the first author should be typed in bold-faced letters. The family name of all authors should be typed with the initial letter capitalized, followed by their abbreviated first and middle initials. (For example, Lian-Sheng Ma is abbreviated as Ma LS, Bo-Rong Pan as Pan BR). The title of the cited article and italicized journal title (journal title should be in its abbreviated form as shown in PubMed), publication date, volume number (in black), start page, and end page [PMID: 11819634 DOI: 10.3748/wjg.13.5396].

Style for book references

Authors: the name of the first author should be typed in bold-faced letters. The surname of all authors should be typed with the initial letter capitalized, followed by their abbreviated middle and first initials. (For example, Lian-Sheng Ma is abbreviated as Ma LS, Bo-Rong Pan as Pan BR) Book title. Publication number. Publication place: Publication press, Year: start page and end page.

Format

Journals

English journal article (list all authors and include the PMID where applicable)

- 1 **Jung EM**, Clevert DA, Schreyer AG, Schmitt S, Rennert J, Kubale R, Feuerbach S, Jung F. Evaluation of quantitative contrast harmonic imaging to assess malignancy of liver tumors: A prospective controlled two-center study. *World J Gastroenterol* 2007; **13**: 6356-6364 [PMID: 18081224 DOI: 10.3748/wjg.13.6356]

Chinese journal article (list all authors and include the PMID where applicable)

- 2 **Lin GZ**, Wang XZ, Wang P, Lin J, Yang FD. Immunolog-

ic effect of Jianpi Yishen decoction in treatment of Pixu-diarrhoea. *Shijie Huaren Xiaobua Zazhi* 1999; **7**: 285-287

In press

- 3 **Tian D**, Araki H, Stahl E, Bergelson J, Kreitman M. Signature of balancing selection in Arabidopsis. *Proc Natl Acad Sci USA* 2006; In press

Organization as author

- 4 **Diabetes Prevention Program Research Group**. Hypertension, insulin, and proinsulin in participants with impaired glucose tolerance. *Hypertension* 2002; **40**: 679-686 [PMID: 12411462 PMID:2516377 DOI:10.1161/01.HYP.0000035706.28494.09]

Both personal authors and an organization as author

- 5 **Vallancien G**, Emberton M, Harving N, van Moorseelaar RJ, Alf-One Study Group. Sexual dysfunction in 1, 274 European men suffering from lower urinary tract symptoms. *J Urol* 2003; **169**: 2257-2261 [PMID: 12771764 DOI:10.1097/01.ju.0000067940.76090.73]

No author given

- 6 21st century heart solution may have a sting in the tail. *BMJ* 2002; **325**: 184 [PMID: 12142303 DOI:10.1136/bmj.325.7357.184]

Volume with supplement

- 7 **Geraud G**, Spierings EL, Keywood C. Tolerability and safety of frovatriptan with short- and long-term use for treatment of migraine and in comparison with sumatriptan. *Headache* 2002; **42** Suppl 2: S93-99 [PMID: 12028325 DOI:10.1046/j.1526-4610.42.s2.7.x]

Issue with no volume

- 8 **Banit DM**, Kaufer H, Hartford JM. Intraoperative frozen section analysis in revision total joint arthroplasty. *Clin Orthop Relat Res* 2002; (**401**): 230-238 [PMID: 12151900 DOI:10.1097/00003086-200208000-00026]

No volume or issue

- 9 Outreach: Bringing HIV-positive individuals into care. *HRSA Careaction* 2002; 1-6 [PMID: 12154804]

Books

Personal author(s)

- 10 **Sherlock S**, Dooley J. Diseases of the liver and biliary system. 9th ed. Oxford: Blackwell Sci Pub, 1993: 258-296

Chapter in a book (list all authors)

- 11 **Lam SK**. Academic investigator's perspectives of medical treatment for peptic ulcer. In: Swabb EA, Azabo S. Ulcer disease: investigation and basis for therapy. New York: Marcel Dekker, 1991: 431-450

Author(s) and editor(s)

- 12 **Breedlove GK**, Schorfheide AM. Adolescent pregnancy. 2nd ed. Wiczorek RR, editor. White Plains (NY): March of Dimes Education Services, 2001: 20-34

Conference proceedings

- 13 **Harnden P**, Joffe JK, Jones WG, editors. Germ cell tumours V. Proceedings of the 5th Germ cell tumours Conference; 2001 Sep 13-15; Leeds, UK. New York: Springer, 2002: 30-56

Conference paper

- 14 **Christensen S**, Oppacher F. An analysis of Koza's computational effort statistic for genetic programming. In: Foster JA, Lutton E, Miller J, Ryan C, Tettamanzi AG, editors. Genetic programming. EuroGP 2002: Proceedings of the 5th European Conference on Genetic Programming; 2002 Apr 3-5; Kinsdale, Ireland. Berlin: Springer, 2002: 182-191

Electronic journal (list all authors)

- 15 Morse SS. Factors in the emergence of infectious dis-

eases. *Emerg Infect Dis* serial online, 1995-01-03, cited 1996-06-05; 1(1): 24 screens. Available from: URL: <http://www.cdc.gov/ncidod/eid/index.htm>

Patent (list all authors)

- 16 **Pagedas AC**, inventor; Ancel Surgical R&D Inc., assignee. Flexible endoscopic grasping and cutting device and positioning tool assembly. United States patent US 20020103498. 2002 Aug 1

Statistical data

Write as mean \pm SD or mean \pm SE.

Statistical expression

Express *t* test as *t* (in italics), *F* test as *F* (in italics), chi square test as χ^2 (in Greek), related coefficient as *r* (in italics), degree of freedom as *v* (in Greek), sample number as *n* (in italics), and probability as *P* (in italics).

Units

Use SI units. For example: body mass, *m* (B) = 78 kg; blood pressure, *p* (B) = 16.2/12.3 kPa; incubation time, *t* (incubation) = 96 h, blood glucose concentration, *c* (glucose) 6.4 ± 2.1 mmol/L; blood CEA mass concentration, *p* (CEA) = 8.6 24.5 μ g/L; CO₂ volume fraction, 50 mL/L CO₂, not 5% CO₂; likewise for 40 g/L formaldehyde, not 10% formalin; and mass fraction, 8 ng/g, etc. Arabic numerals such as 23, 243, 641 should be read 23 243 641.

The format for how to accurately write common units and quantum numbers can be found at: http://www.wjgnet.com/1007-9327/g_info_20100315223018.htm.

Abbreviations

Standard abbreviations should be defined in the abstract and on first mention in the text. In general, terms should not be abbreviated unless they are used repeatedly and the abbreviation is helpful to the reader. Permissible abbreviations are listed in Units, Symbols and Abbreviations: A Guide for Biological and Medical Editors and Authors (Ed. Baron DN, 1988) published by The Royal Society of Medicine, London. Certain commonly used abbreviations, such as DNA, RNA, HIV, LD50, PCR, HBV, ECG, WBC, RBC, CT, ESR, CSF, IgG, ELISA, PBS, ATP, EDTA, mAb, can be used directly without further explanation.

Italics

Quantities: *t* time or temperature, *c* concentration, *A* area, *l* length, *m* mass, *V* volume.

Genotypes: *gyrA*, *arg 1*, *c myc*, *c fos*, etc.

Restriction enzymes: *EcoRI*, *HindI*, *BamHI*, *Kbo I*, *Kpn I*, etc.

Biology: *H. pylori*, *E. coli*, etc.

Examples for paper writing

Editorial: http://www.wjgnet.com/1007-9327/g_info_20100315220036.htm

Frontier: http://www.wjgnet.com/1007-9327/g_info_20100315220305.htm

Topic highlight: http://www.wjgnet.com/1007-9327/g_info_20100315220601.htm

Observation: http://www.wjgnet.com/1007-9327/g_info_20100312232427.htm

Guidelines for basic research: http://www.wjgnet.com/1007-9327/g_info_20100315220730.htm

Instructions to authors

Guidelines for clinical practice: http://www.wjgnet.com/1007-9327/g_info_20100315221301.htm

Review: http://www.wjgnet.com/1007-9327/g_info_20100315221554.htm

Original articles: http://www.wjgnet.com/1007-9327/g_info_20100315221814.htm

Brief articles: http://www.wjgnet.com/1007-9327/g_info_20100312231400.htm

Case report: http://www.wjgnet.com/1007-9327/g_info_20100315221946.htm

Letters to the editor: http://www.wjgnet.com/1007-9327/g_info_20100315222254.htm

Book reviews: http://www.wjgnet.com/1007-9327/g_info_20100312231947.htm

Guidelines: http://www.wjgnet.com/1007-9327/g_info_20100312232134.htm

RESUBMISSION OF THE REVISED MANUSCRIPTS

Please revise your article according to the revision policies of *WJG*. The revised version including manuscript and high-resolution image figures (if any) should be re-submitted online (<http://www.wjgnet.com/esps/>). The author should send the copyright transfer letter, responses to the reviewers, English language Grade B certificate (for non-native speakers of English) and final manuscript checklist to wjg@wjgnet.com.

Language evaluation

The language of a manuscript will be graded before it is sent for revision. (1) Grade A: priority publishing; (2) Grade B: minor language polishing; (3) Grade C: a great deal of language polishing needed; and (4) Grade D: rejected. Revised articles should reach Grade A or B.

Copyright assignment form

Please download a Copyright assignment form from http://www.wjgnet.com/1007-9327/g_info_20100315222818.htm.

www.wjgnet.com/1007-9327/g_info_20100315222818.htm.

Responses to reviewers

Please revise your article according to the comments/suggestions provided by the reviewers. The format for responses to the reviewers' comments can be found at: http://www.wjgnet.com/1007-9327/g_info_20100315222607.htm.

Proof of financial support

For paper supported by a foundation, authors should provide a copy of the document and serial number of the foundation.

Links to documents related to the manuscript

WJG will be initiating a platform to promote dynamic interactions between the editors, peer reviewers, readers and authors. After a manuscript is published online, links to the PDF version of the submitted manuscript, the peer-reviewers' report and the revised manuscript will be put on-line. Readers can make comments on the peer reviewer's report, authors' responses to peer reviewers, and the revised manuscript. We hope that authors will benefit from this feedback and be able to revise the manuscript accordingly in a timely manner.

Science news releases

Authors of accepted manuscripts are suggested to write a science news item to promote their articles. The news will be released rapidly at EurekAlert/AAAS (<http://www.eurekalert.org>). The title for news items should be less than 90 characters; the summary should be less than 75 words; and main body less than 500 words. Science news items should be lawful, ethical, and strictly based on your original content with an attractive title and interesting pictures.

Publication fee

WJG is an international, peer-reviewed, Open-Access, online journal. Articles published by this journal are distributed under the terms of the Creative Commons Attribution Non-commercial License, which permits use, distribution, and reproduction in any medium, provided the original work is properly cited, the use is non commercial and is otherwise in compliance with the license. Authors of accepted articles must pay a publication fee. The related standards are as follows. Publication fee: 1365 USD per article. Editorial, topic highlights, book reviews and letters to the editor are published free of charge.

World Journal of Gastroenterology®

Volume 18 Number 31
August 21, 2012



Published by Baishideng Publishing Group Co., Limited
Room 1701, 17/F, Henan Building,
No. 90 Jaffe Road, Wanchai, Hong Kong, China
Fax: +852-31158812
Telephone: +852-58042046
E-mail: bpg@baishideng.com
<http://www.wjgnet.com>

ISSN 1007-9327

